OPTIMIZING MISCANTHUS FOR THE SUSTAINABLE BIOECONOMY: FROM GENES TO PRODUCTS

EDITED BY: Kerrie Farrar, Emily A. Heaton and Luisa M. Trindade
PUBLISHED IN: Frontiers in Plant Science

frontiers Research Topics

About Frontiers

Frontiers is more than just an open-access publisher of scholarly articles: it is a pioneering approach to the world of academia, radically improving the way scholarly research is managed. The grand vision of Frontiers is a world where all people have an equal opportunity to seek, share and generate knowledge. Frontiers provides immediate and permanent online open access to all its publications, but this alone is not enough to realize our grand goals.

Frontiers Journal Series

The Frontiers Journal Series is a multi-tier and interdisciplinary set of open-access, online journals, promising a paradigm shift from the current review, selection and dissemination processes in academic publishing. All Frontiers journals are driven by researchers for researchers; therefore, they constitute a service to the scholarly community. At the same time, the Frontiers Journal Series operates on a revolutionary invention, the tiered publishing system, initially addressing specific communities of scholars, and gradually climbing up to broader public understanding, thus serving the interests of the lay society, too.

Dedication to Quality

Each Frontiers article is a landmark of the highest quality, thanks to genuinely collaborative interactions between authors and review editors, who include some of the world's best academicians. Research must be certified by peers before entering a stream of knowledge that may eventually reach the public - and shape society; therefore, Frontiers only applies the most rigorous and unbiased reviews.
Frontiers revolutionizes research publishing by freely delivering the most outstanding research, evaluated with no bias from both the academic and social point of view. By applying the most advanced information technologies, Frontiers is catapulting scholarly publishing into a new generation.

What are Frontiers Research Topics?

Frontiers Research Topics are very popular trademarks of the Frontiers Journals Series: they are collections of at least ten articles, all centered on a particular subject. With their unique mix of varied contributions from Original Research to Review Articles, Frontiers Research Topics unify the most influential researchers, the latest key findings and historical advances in a hot research area! Find out more on how to host your own Frontiers Research Topic or contribute to one as an author by contacting the Frontiers Editorial Office: researchtopics@frontiersin.org

OPTIMIZING MISCANTHUS FOR THE SUSTAINABLE BIOECONOMY: FROM GENES TO PRODUCTS

Topic Editors:
Kerrie Farrar, Aberystwyth University, United Kingdom
Emily A. Heaton, Iowa State University, United States
Luisa M. Trindade, Wageningen University, Netherlands

Cover image: Rattanapon Ninlapoom/Shutterstock.com

In this Research Topic we report advances in fundamental and applied aspects of the perennial C4 bioenergy crop Miscanthus (Miscanthus spp.) and its role in mitigating climate change as part of the bioeconomy. Miscanthus is extremely well suited for bioenergy, biofuel and bioproduct production over a wide geographic area including Europe and North America as well as its native Asia.

Miscanthus offers a unique perspective within plant science: the challenge is to domesticate this novel crop for diverse environments and uses while simultaneously developing sustainable value chains to displace fossil fuels and contribute to climate change mitigation. Contributions to this Research Topic were offered from leading Miscanthus researchers from different parts of the world. We accepted 16 articles from 95 authors, which have generated 21,161 views at March 26 2018. Nine of the articles are the output of the European FP7 OPTIMISC project and describe multiple experiments investigating a common set of Miscanthus genotypes in Europe and Asia. These papers are complemented by 7 additional articles from global authors, providing a comprehensive analysis of the state of the art of Miscanthus research and application.

Table of Contents

frontiers
in Plant Science

Editorial: Optimizing Miscanthus for the Sustainable Bioeconomy: From Genes to Products

Kerrie Farrar [1†], Emily A. Heaton [2†] and Luisa M. Trindade [3*†]

[1] Institute of Biological, Environmental and Rural Sciences, Aberystwyth University, Aberystwyth, United Kingdom,
[2] Department of Agronomy, Iowa State University, Ames, IA, United States, [3] Department of Plant Breeding, Wageningen University, Wageningen, Netherlands

Editorial on the Research Topic

Optimizing Miscanthus for the Sustainable Bioeconomy: From Genes to Products

In this Research Topic we report advances in fundamental and applied aspects of the perennial C4 bioenergy crop miscanthus (*Miscanthus* spp.) and its role in mitigating climate change as part of the bioeconomy. Miscanthus is a high yielding C4 perennial grass with great potential for sustainable biomass production in temperate climates, including Europe and North America as well as its native Asia. With high resource use efficiency and good biomass quality, miscanthus is a well-suited feedstock for a plethora of applications including bioenergy, biofuels and biomaterials (van der Weijde et al.).

Miscanthus offers a unique perspective within plant science: the challenge is to domesticate this novel crop for diverse environments and uses while simultaneously developing sustainable value chains to displace fossil fuels and contribute to climate change mitigation. Contributions to this Research Topic were offered from leading miscanthus researchers from different parts of the world. We accepted 16 articles from 95 authors, which have generated 21,161 views at March 26, 2018. Nine of the articles are the output of the European FP7 OPTIMISC project and describe multiple experiments investigating a common set of miscanthus genotypes in Europe and Asia. These papers are complemented by seven additional articles from global authors, providing a comprehensive analysis of the state of the art of miscanthus research and application.

Efficient **Establishment and Crop Management** are essential for this perennial crop that typically takes at least two growing seasons to reach commercial maturity, has an expected life span of over 10 annual commercial harvests, and receives minimal inputs after the planting phase. Within the OPTIMISC project, 15 miscanthus genotypes including *M. sinensis, M. sacchariflorus* and their hybrids, including the commercial clone *M. × giganteus* (*Mxg*), were planted in 6 locations across Europe and into Asia to determine the factors limiting to miscanthus production. Strong species x environment effects on biomass yield were observed, with the hybrids outperforming parental species in all locations except Turkey, where all types performed well. In the four Central/Southern locations, tested cultivars typically reached commercial yield in year two (Kalinina et al.). While temperature and rainfall were primary drivers of yield, soil fertility is also known to be important, especially as the crop matures.

An important consideration when establishing a non-native plant as a crop is the impact on native diversity. In the US, two miscanthus genotypes were introduced into different types of minimally managed landscapes and their invasive potential assessed over the following 5 years. Although there is concern that miscanthus has the potential to become invasive, only weak

community impacts were observed. Furthermore, eradication can readily be achieved at early stages, emphasizing the requirement for early monitoring and management of this fast growing crop (West et al.).

Plant genotype and environment interact to impact **Crop Yield and Phenology**. Plant growth stages are coded systematically using systems such as the BBCH-scale which has been widely-adapted for a range of mono- and dicotyledonous plant species. Combining descriptions of close relatives with field observations Tejera and Heaton developed a simple BBCH scale for *Mxg* and related species, in which summary statistics can readily be estimated for a multi-stemmed plant. This enables improved comparisons between miscanthus and other species, and between miscanthus genotypes grown in different environments. The multilocation OPTIMISC trial comparing diverse miscanthus germplasm grown in six locations across Europe was used by Nunn et al. to determine the climatic limitations on biomass accumulation and inform the selection of trait combinations required to extend the boundaries of miscanthus cultivation. In panel analysis, biomass yield was assessed in 138 *Miscanthus sinensis* accessions collected in Southwest China and *M. sinensis* genotypes identified that matched or exceeded the biomass yield of *Mxg*. These corresponded generally to genotypes with high tiller numbers and plant height (Nie et al.). Together these studies provide insight into strategies for improving yield and resilience to stresses in miscanthus.

There have been conflicting reports on the effect of N fertilization on *Mxg* but Lee et al. determined that both biomass yield and the majority of yield component traits increased in value with N fertilization, and that the effect increased as the stands aged. In a separate experiment, N management was varied over two growing seasons, resulting in enhanced growth of above- and belowground tissues in the fertilized treatments with respect to the unfertilized control. Regular sampling of above and below ground organs was performed to observe the N dynamics throughout the growing season of the crop, and between growing years (Dierking et al.). Conversely, Jezowski et al. demonstrated the ability of *Mxg* to grow on degraded coal mine soils with or without high rates of sewage sludge and mineral fertilizer, indicating that $M \times g$ shows great growth potential for application on land that is unsuitable for other agricultural uses.

Similarly, the limitations imposed by soil or water salinity, an increasingly common abiotic stress globally, were assessed by collecting and assessing miscanthus from saline environments. Seventy genotypes of *M. sinensis*, *M. sacchariflorus* and interspecific hybrids, including the core genotypes from the OPTIMISC multilocation trial, were tested for growth under 150 mM saline in a hydroponic system. A range of responses was observed among the genotypes. Some of the relatively tolerant types accumulated little Na^+ in the leaves, indicating an active Na^+ exclusion mechanism while other genotypes showed reduced leaf growth, potentially demonstrating osmotic tolerance (Chen et al.). Taken together these studies provide insight into strategies for optimizing biomass production in miscanthus across a wide range of locations, encompassing climatic variation and land unsuitable for food production.

Three manuscripts describe the **Biomass Quality** of the 15 core OPTIMISC genotypes evaluated at six sites for three consecutive years for different end uses. Results highlight the great impact genotypic differences can have on the quality of biomass for bioenergy production, and interactions with the growth environment. In studies of biomass quality, this interaction was substantial and the authors concluded that it should be taken into account in breeding programs (Van der Weijde et al.). A subset of the OPTIMISC accessions, the five highest yielding genotypes in three locations, were further tested for combustion quality in different locations at different harvest times. he results showed that a delay in harvesting time improves combustion quality but at the expense of yield (Iqbal et al.). Kiesel et al. showed with another subset of the OPTIMISC accessions the effect of effect of the genotype, location and harvest date on energy yields of anaerobic digestion and combustion. In an independent experiment, Belmokhtar et al. studied the biomass yield and quality of five mature genotypes of *Mxg* and *M. sinensis* for three consecutive years (from years 3 to 5). They analyzed cell wall composition and saccharification efficiency using a miniaturized assay and revealed that more digestible genotypes contain a higher amount of hemicellulosic polysaccharides and lower amounts of lignin and cellulose.

For an energy, crop analysis of both the **Environmental impact and Bioeconomy** are critical as the energy produced must be commercially competitive with fossil fuels or other energy sources, yet more sustainable, particularly in terms of greenhouse gas emissions over the life cycle of the crop and conversion.

Ten field trials in different locations with various propagation and harvesting methods were compared for economic and environmental assessment of seed and rhizome propagated miscanthus in the UK. It was concluded that new hybrid seed propagation significantly reduces establishment costs with a breakeven yield of about half average UK typical yield for *Mxg*. Different harvesting and processing options are optimal for different end uses (Hastings et al.).

Understanding the environmental impact of miscanthus across a range of both value chains (e.g., heat and power, biomaterials) and hazard categories (e.g., human toxicity, marine toxicity) was advanced by the work of Wagner et al. who used results from the OPTIMISC multilocation trial to assess 36 growing site × pathway combinations. This is most holistic life-cycle assessment yet conducted on miscanthus. The place where miscanthus drove differences in environmental performance through biomass yield. While some miscanthus value chains showed large net environmental benefits, particularly to water toxicity and eutrophication, others could have net negative effects, particularly dependent on choice of reference scenarios and credits given for co-products. OPTIMISC accomplishments are summarized by Lewandowski et al . with many highlights, including data describing where and why miscanthus hybrids out yield *Mxg*; how to select and grow miscanthus for improved biomass quality, even under abiotic stress; advances in seed propagation and harvest; and end-user needs including life-cycle assessment.

This issue provides new insights in the understanding of miscanthus as a crop, including crop establishment and

management, yield and crop phenology; the environmental impact of this crop and the suitability of biomass for biobased products.

AUTHOR CONTRIBUTIONS

All authors listed have made a substantial, direct and intellectual contribution to the work, and approved it for publication.

FUNDING

Extending *Miscanthus* Cultivation with Novel Germplasm at Six Contrasting Sites

Olena Kalinina[1]*, Christopher Nunn[2], Ruth Sanderson[2], Astley F. S. Hastings[3], Tim van der Weijde[4], Mensure Özgüven[5], Ivan Tarakanov[6], Heinrich Schüle[7], Luisa M. Trindade[4], Oene Dolstra[4], Kai-Uwe Schwarz[8], Yasir Iqbal[1], Andreas Kiesel[1], Michal Mos[9], Iris Lewandowski[1] and John C. Clifton-Brown[2]

[1] Department of Biobased Products and Energy Crops, Institute of Crop Science, University of Hohenheim, Stuttgart, Germany, [2] Institute of Biological, Environmental and Rural Sciences, Aberystwyth University, Aberystwyth, UK, [3] The Institute of Biological and Environmental Sciences, University of Aberdeen, Aberdeen, UK, [4] Department of Plant Breeding, Wageningen University, Wageningen, Netherlands, [5] Faculty of Agriculture and Natural Sciences, Konya Food and Agriculture University, Konya, Turkey, [6] Department of Plant Physiology, Russian State Agrarian University - Moscow Timiryazev Agricultural Academy, Moscow, Russia, [7] German Agrarian Centre, Potash, Ukraine, [8] Schwarz, Braunschweig, Germany, [9] Blankney Estates, Blankney, UK

Miscanthus is a genus of perennial rhizomatous grasses with C4 photosynthesis which is indigenous in a wide geographic range of Asian climates. The sterile clone, *Miscanthus × giganteus (M. × giganteus)*, is a naturally occurring interspecific hybrid that has been used commercially in Europe for biomass production for over a decade. Although, *M. × giganteus* has many outstanding performance characteristics including high yields and low nutrient offtakes, commercial expansion is limited by cloning rates, slow establishment to a mature yield, frost, and drought resistance. In this paper, we evaluate the performance of 13 novel germplasm types alongside *M. × giganteus* and horticultural "Goliath" in trials in six sites (in Germany, Russia, The Netherlands, Turkey, UK, and Ukraine). Mean annual yields across all the sites and genotypes increased from 2.3 ± 0.2 t dry matter ha^{-1} following the first year of growth, to 7.3 ± 0.3, 9.5 ± 0.3, and 10.5 ± 0.2 t dry matter ha^{-1} following the second, third, and fourth years, respectively. The highest average annual yields across locations and four growth seasons were observed for *M. × giganteus* (9.9 ± 0.7 t dry matter ha^{-1}) and interspecies hybrid OPM-6 (9.4 ± 0.6 t dry matter ha^{-1}). The best of the new hybrid genotypes yielded similarly to *M. × giganteus* at most of the locations. Significant effects of the year of growth, location, species, genotype, and interplay between these factors have been observed demonstrating strong genotype × environment interactions. The highest yields were recorded in Ukraine. Time needed for the crop establishment varied depending on climate: in colder climates such as Russia the crop has not achieved its peak yield by the fourth year, whereas in the hot climate of Turkey and under irrigation the yields were already high in the first growing season. We have identified several alternatives to *M. × giganteus* which have provided stable yields across wide climatic ranges, mostly interspecies hybrids, and also *Miscanthus* genotypes providing high biomass yields at specific geographic locations. Seed-propagated interspecific and intraspecific hybrids, with high stable yields and cheaper reliable scalable establishment remain a key strategic objective for breeders.

Keywords: *Miscanthus*, novel hybrids, multi-location field trials, establishment, productivity, marginal land

INTRODUCTION

There is an increasing demand for sustainably produced biomass in the growing European bioeconomy but its material and energetic use should not compete with food supply (Lewandowski et al., 2016). Therefore, the additionally required biomass should not be grown on good agricultural land but on land that is economically or bio-physically marginal for food production. According to Allen et al. (2014), there are an estimated 1,350,000 hectares (ha) of such land in Europe that is abandoned from or unsuitable for food crop production and could be preferentially exploited for growing biomass crops.

Miscanthus is a genus of high-yielding perennial rhizomatous grasses with C4 photosynthesis. It is considered a promising candidate bioeconomy crop due to the combination of high yields, low input demand, good environmental performance, multiple biomass use options, and the potential to grow on land that is considered marginal for food production (Dohleman and Long, 2009; McCalmont et al., 2015; Lewandowski et al., 2016). *Miscanthus* demonstrates a broad genetic variability in the area of its origin, namely East-Asia (Clifton-Brown et al., 2016). However, this theoretical potential cannot yet be exploited fully in Europe. Currently the industrial use of this crop in Europe is limited to one standard clone *Miscanthus* × *giganteus* (*M.* × *giganteus*; Hodkinson and Renvoize, 2001), a sterile interspecific hybrid propagated vegetatively. Cultivation and yields of *M.* × *giganteus* can be limited by low temperatures in the northern European regions (Clifton-Brown and Lewandowski, 2000) and drought in the southern regions (Hastings et al., 2009a,b). Another limitation to the broader distribution of miscanthus are the high production costs for *M.* × *giganteus* (Lewandowski et al., 2016). Vegetative propagation is an expensive way of establishing the plantations (Xue et al., 2015). Introducing new germplasm from the wild collections is needed to extend the geographical range in which *Miscanthus* can be cultivated and overcome some of the current limitations, and some early selections from European breeding programs should create invaluable knowledge of the "Genotype × Environment" interactions.

Germplasm used in European breeding programs belong mainly to the species *M. sacchariflorus* and *M. sinensis*. To date, their interspecific hybrids, such as *M.* × *giganteus*, are generally higher yielding than the pure species (Davey et al., 2017) in temperate zones. A cold tolerance test with five genotypes showed that certain *M. sinensis* types could withstand lower winter temperatures than *M.* × *giganteus* and *M. sacchariflorus* (Clifton-Brown et al., 2000). In general, *M. sinensis* interspecific hybrids have thinner and shorter stems than *M. sacchariflorus* and their hybrids, which combined lead to lower yields in trials with the scientific standard planting density of 20,000 plants ha^{-1} (Iqbal and Lewandowski, 2014). In the UK and Germany, the miscanthus breeding program led by Aberystwyth over the past decade has focussed on producing interspecific *M. sinensis* × *M. sacchariflorus* hybrids with high yield, cold or other stress tolerance and seed production (Clifton-Brown et al., 2016). As high seed production in interspecific hybrids

does not occur naturally in Northern Europe, breeders in the Netherlands have focussed on the genetic improvement of intraspecific hybrids of *M. sinensis* types. Scientific field trials have shown the potential for other *M. sinensis* intraspecies hybrids in drought prone areas (Clifton-Brown et al., 2002). During the past decade, the breadth of *Miscanthus* germplasm available in Europe has been expanded through plant collection trips (Clifton-Brown J. C. et al., 2011; Clifton-Brown J. et al., 2011; Hodkinson et al., 2016). There is tremendous diversity available within the *Miscanthus* genus to exploit, particularly within *M. sinensis* which occurs in the widest climatic range of all *Miscanthus* species. *M. sinensis* types are known to senesce earlier than many tall *M. sacchariflorus* types (Robson et al., 2012). *M. sinensis* generally flowers in North European climates (Jensen et al., 2011), while most *M. sacchariflorus* needs warmer climates to flower before winter (Jensen et al., 2013). Although flowering in the production area potentially increases the invasive risk, this can be mitigated by the manipulation of ploidy to produce sterile triploids (Anderson et al., 2006).

In this paper, we report on a multi-location field plot experiment, where we have tested a range of selected diverse germplasm from the different *Miscanthus* species on a wide climatic gradient spanning Atlantic, continental, and Mediterranean climates. All the germplasm entries for this experiment were selected from breeding nurseries in Northern Europe. Four wild "tall *M. sacchariflorus*" types were selected in Aberystwyth from spaced plants trials planted from the accessions collected in 2006/7 from Eastern Asia. Four *M. sinensis* populations were selected: two from Wageningen University and two from open-pollinated "strong" *M. sinensis* parents selected in Northern Germany. Five interspecies hybrids of *M. sinensis* and *M. sacchariflorus* were selected in a spaced plant breeding nursery in Braunschweig, Germany from progeny of different crosses in 2011.

The overarching objective of this study was to create the understanding needed to extend the range for *Miscanthus* production in Eurasia. We were particularly interested in understanding if *Miscanthus* selected in UK, Netherlands, and Germany could both establish, over-winter and produce an economically viable yield with relatively low temperatures and rainfall in Eastern areas. There is a known opportunity for miscanthus cultivation in Eastern European countries such as Ukraine and Russia where both significant amounts of underused land and a strong local market for the biomass for heat exist. Our expectation was that best performers in terms of yield could be identified in each of the six sites due to environmental specificity: both at level of the germplasm groups and at the level of specific genotypes or populations. It was expected that the performance of some of the novel interspecies and intraspecies hybrids would match or exceed *M.* × *giganteus*, thus providing potential growers and end users with new options. We also believed that the knowledge generated by a multi-location trial approach, containing a wide selection of "relevant" germplasm types, would identify environmental specificity for both the parents and progeny of *M. sinensis* and *M. sacchariflorus*. This G × E information can be used to assist breeders to develop better

future hybrids. For the purposes of examining G × E interactions we felt it is was necessary to reduce the number of variables by using a high proportion of clonal selections (genotypes) for 11 of the 15 selections rather than individuals from populations derived from "seed." If any of these clones proved outstanding, then breeding of seed propagated equivalents would be the logical next step. The four seeded entries (of *M. sinensis* type) would be used to explore if phenotypic variation within a population cross was a significant issue for the future expansion of a crop based on seeded *M. sinensis* hybrids.

Our first hypothesis was that, under the wide range of climate and soil conditions between Stuttgart (Germany), Moscow (Russia), Wageningen (The Netherlands), Adana (Turkey), Aberystwyth (UK), and Potash (Ukraine), significant differences would exist in establishment rate and yield performance of the novel germplasm types. The abiotic stress tolerance traits observed would be used to inform further breeding of future seeded hybrids.

Our second hypothesis was that new selections, heretofore only tested in spaced plant nurseries, could perform as well or better than *M. × giganteus* in competitive plot trials in sites with more extreme climates and poorer soils than have been tested to date.

MATERIALS AND METHODS

Plant Material

Germplasm to evaluate was selected by the breeders at Aberystwyth and Wageningen Universities. The fifteen selections included four genotypes of wild *M. sacchariflorus*, five interspecies hybrids of *M. sacchariflorus* × *M. sinensis*, four *M. sinensis* seed-based population hybrids (two of which were paired crosses, and two open-pollinated) and two triploid standard clones: *M. × giganteus* (between *M. sinensis* and *M. sacchariflorus*; Greef and Deuter, 1993) and *M. sinensis* "Goliath" (*M. sinensis* × *sinensis*; **Table 1**). The origins of the germplasm types or their parents, where known, ranged from 23 to 45 N (Supplementary Table 1). The wild *M. sacchariflorus* type collection sites ranged from 31 to 37 N. Growing season rainfall (April–September) at the known locations of germplasm collection range from 500 to 2000 mm p.a. The mean minimum monthly winter temperatures in these areas ranged from −16 to 12°C. The hybrids OPM-6, 7, 8, and 10 and the *M. sinensis* OPM-11, 12 and 15 were provided by Aberystwyth University and the *M. sinensis* genotypes OPM-13 and 14 were provided by Wageningen University. All hybrids and *M. sinensis* were diploid. Some of the wild *M. sacchariflorus* genotypes were tetraploid (see Supplementary Table 1).

In vitro propagation was used to produce "plug" plants in modular trays (Quick Pot 96 38 × 38 × 78 mm, HerkuPlast, Kubern, GmbH, Ering/Inn, Germany) from clones OPM 1–11. Seeded entries (OPM-12–15) were sown in similar trays. OPM-13 and OPM-14 were raised in the Netherlands. OPM-12 and OPM-15 were raised in the UK. All were grown in the glasshouse before hardening off, transportation to and transplantation at the six field trial locations. Hereafter, all the germplasm types are referred to as "genotypes."

TABLE 1 | Germplasm selected for the multi-location trials.

Genotype ID	Species	Accession details	Propagation method
OPM-1	Sac	Wild Sac	*In vitro*
OPM-2	Sac	Wild Sac	*In vitro*
OPM-3	Sac	Wild Sac	*In vitro*
OPM-4	Sac	Wild Sac	*In vitro*
OPM-5	Hybrid	Wild Sin × Wild Sac hybrid	*In vitro*
OPM-6	Hybrid	Wild Sac × Wild Sin	*In vitro*
OPM-7	Hybrid	Wild Sac × Wild Sin	*In vitro*
OPM-8	Hybrid	Wild Sac × Wild Sin	*In vitro*
OPM-9	Hybrid (Gig)	Wild Sac × Wild Sin	*In vitro*
OPM-10	Hybrid	Wild Sac × Wild Sin	*In vitro*
OPM-11	Sin (Goliath)	Wild Sin × open	*In vitro*
OPM-12	Sin	Wild Sin × open	Seeds
OPM-13	Sin	Sin × Sin	Seeds
OPM-14	Sin	Sin × Sin	Seeds
OPM-15	Sac × Sin × open Sin (open-pollinated hybrid with dominating Sin phenotype and high morphological variability)	(Sac × Sin) × open Sin	Seeds

Sac, M. sacchariflorus; Sin, M. sinensis; Hybrid, M. sinensis × M. sacchariflorus hybrid. Common clone names added where these exist [e.g., Gig = M. × giganteus, Sin (Goliath) = M. sinensis Goliath].

Field Trials

Between April and May 2012, 15 genotypes (**Table 1**) were established at six field locations (**Figure 1**) covering a wide range of environmental conditions (Supplementary Table 2): in Turkey near Adana, in Germany near Stuttgart, in Ukraine near Potash, in the Netherlands at Wageningen, in the United Kingdom near Aberystwyth and in Russia near Moscow. For the remainder of this paper, the sites are referred to by the name of the nearest town.

The field trials were established on arable or horticultural land except in Aberystwyth, where the trial was planted on marginal (low quality) grassland (Supplementary Table 2). At each site soil preparations suitable for the planting of cereals were made, removing the previous crop/vegetation and associated weeds. At each location the trial was planted as a randomized complete block design comprising three replicate blocks each containing a single plot of each of the 15 genotypes. Each plot measured 5 × 5 m and contained 49 plants in a 7 × 7 grid with a planting density of 1.96 plants m^{-2}. The total trial area at each site was 75 × 43 m.

In 2012, soil samples were taken before planting and fertilization from two randomly selected plots in each replicate block at each location. Soil samples were collected at the 0–30, 30–60, 60–90 cm layers where there was sufficient profile depth. Samples were analyzed for pH, plant available nitrogen (N$_{min}$) and total potassium (K), phosphorous (P), and magnesium (Mg) (Supplementary Table 3). The plant available nitrogen

FIGURE 1 | Location of the field trials established in May 2012: Aberystwyth (Aber; United Kingdom), Wageningen (Wagen; The Netherlands), Stuttgart (Germany), Adana (Turkey), Potash (Ukraine), and Moscow (Russia), and historical summer rainfall map (average of equinox to equinox rainfall from 2010 to 2014 from CRU TS v. 3.24).
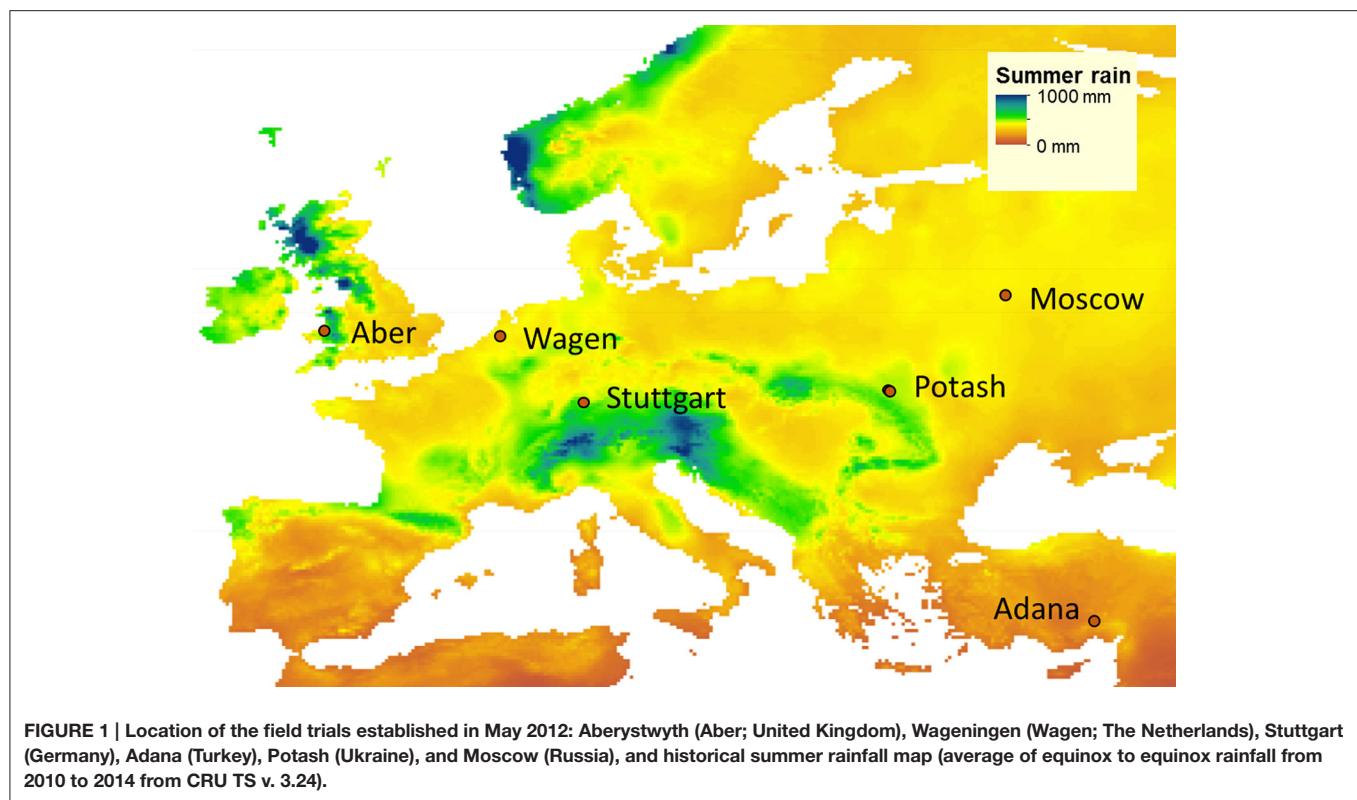
was determined by using $CaCl_2$ extraction followed by FIA measurement (DIN ISO 14255:1998-11). Determination of soil P and K was carried out by using CAL extraction followed by flame photometer or FIA measurement (OENORM L 1087:2012-12-01). Soil pH was determined by using a glass electrode after $CaCl_2$ extraction (DIN ISO 10390:2005; Ehmann et al., 2017). Further inter-row soil cores were taken from each plot in October 2012 using a soil column cylinder auger (Eijelkamp, Giesbeek, Netherlands) to determine soil bulk density, soil depth, and stone content (Supplementary Table 3).

Trial Management and Climatic Conditions

Miscanthus plugs were planted by hand in May 2012 except in Adana where the trial was established earlier, in mid-April, to avoid dry and hot weather whilst planting. In spring 2012, fertilizer was applied at all the sites at rates 44 and 110 kg ha^{-1} year^{-1} P and K, respectively, which, combined with residual soil nutrients, designed to match crop requirements (Lewandowski et al., 2000). No nitrogen fertilizer was applied in the first year to minimize weed growth. From year 2 fertilizer was applied at the rate of 140 kg ha^{-1} K, 100 kg ha^{-1} P, and 60 kg ha^{-1} N applied once per season in spring, rates designed to ensure non-limiting crop nutrition at all sites.

From 2013, continuous drip irrigation was applied in Adana to compensate for lack of rainfall and to maintain the trial during prolonged drought periods. Irrigation was applied more often and in larger volumes in 2013 to ensure crop establishment and then reduced in 2014 and 2015 to identify genotypes suited to arid and hot climatic conditions. Volumes of water applied

were recorded. Emerging weeds were removed regularly by hand during the growing seasons 2012–2014 at all sites.

Climate data (rainfall, air, and soil temperature and radiation) were obtained from the weather stations at the study sites. Supplementary Table 4 summarizes climatic conditions during each growing season at each location and the irrigation applied in Adana.

Measurements

Plant survival was recorded in May 2013 as the number of plants producing new shoots in spring. Plant loss was calculated as the number of non-shooting plants expressed as a percentage of the total plants planted per plot. Any gaps occurring due to overwinter mortality in the first winter were filled in using plants from the adjacent replacement plots planted for this purpose at each corresponding site in 2012.

At the end of the third growing season (autumn 2014) canopy height was measured and stem number per plant (only stems reaching at least 60% of canopy height) was recorded on 3–5 central plants per plot.

Each year biomass was harvested from the core square (9 plants; middle 2 m^2) of the plots in February–April depending upon location and when the crop was dry. Cutting height for yield determination was 5 cm above the soil surface. Harvested plant material was dried to constant weight at 60°C. Dry matter yield was calculated as tons of dry matter (DM) ha^{-1}. Total DM yield was calculated as the sum of the plot yields over four growing seasons.

Statistical Analyses

All statistical analyses were performed with the aid of GenStat (Version 18.2; VSN International Ltd., Hemel Hempstead, UK; Payne et al., 2015). Within location, effects of species group on total 4-year biomass yield were assessed by analysis of variance according to the randomized block design. Yields of OPM-5–10 in seasons 3 and 4 were compared by analysis of variance as split plot in time. Effects of genotype and location and their interaction on biomass yield, plot mean values for canopy height and stem count in year 3 were assessed by residual maximum likelihood analysis and using a separate residual variance at each location. Where necessary, multiple pairwise comparisons within tables of means were accounted for by Bonferroni-adjustment of the comparison-wise type I error rate. Sensitivity of biomass yield, canopy height, and stem count of the genotypes to the six environments was assessed by modified joint regression analysis (Finlay and Wilkinson, 1963) as implemented in the RFINLAYWILKINSON procedure of GenStat (Payne et al., 2015). Stem counts were transformed to the square root scale prior to calculating plot means and prior to each analysis.

RESULTS

Plant Overwinter Survival

At most field sites, there were few plant losses in the first winter after planting (**Table 2**). However, in Aberystwyth the plants did not establish well in the first year and in total 43% of the plants needed to be replaced. A possible reason for high plantlet mortality at this location may have been the weather conditions viz. cool air temperatures in 2012 and flooding at the time of miscanthus planting. Aberystwyth had the highest (727 mm, which is double the long term average) total rainfall and the lowest mean air temperature (11°C, which is 2° lower than the long term average) among the sites in the first growing season (Supplementary Table 4). This location also had the lowest $DD_{(base10)}$ and PAR among the field trial sites in 2012 (see Supplementary Table 5), two important parameters known to influence miscanthus growth and yields (Clifton-Brown et al., 2000), which could result in weaker and smaller plants by winter.

At the other locations, on average only 3% of all plants needed to be replaced after winter. The highest losses were observed with OPM-15 (a seed-propagated, *Sac × Sin × Sin* open-pollinated hybrid) where on average 10% of plants needed to be replaced (Aberystwyth site not included). The seedlings of this accession were initially slightly smaller at planting due to a slightly later sowing date than the other genotypes, which may have contributed to the higher mortality rate observed.

At the more northern sites with continental climate, Moscow and Potash, higher plant mortality was observed than in Wageningen or Stuttgart. At the two former locations some losses were observed for most of the genotypes but losses never exceeded 14% for any of the genotypes concerned. Interestingly, *M. × giganteus* showed no plant losses at the warmer field locations in Adana, Stuttgart, and Wageningen, but higher losses than the new *M. sinensis × M. sacchariflorus* hybrids at colder locations in Potash and Moscow, where the lowest minimum air and soil surface temperatures were recorded (Supplementary Table 6). In Adana, significant plant losses were only observed for some of the *M. sinensis* accessions (OPM-11, 12, 13, and 15).

Biomass Yield

Annual Biomass Yield

Annual biomass (t DM ha^{-1}) yield varied depending on the growing season, trial location, and *Miscanthus* genotype. Overall, biomass yields increased with increasing crop maturity. Mean annual yields across all the sites and genotypes increased from 2.3 ± 0.2 t DM ha^{-1} from the first year of growth, to 7.3 ± 0.3, 9.5 ± 0.3, and 10.5 ± 0.2 t DM ha^{-1} from the second, third, and fourth years, respectively. The highest yielding location was Potash with the average annual yield of 9.6 ± 0.4 t DM ha^{-1}. The lowest-yielding was Aberystwyth with 4.0 ± 0.3 t DM ha^{-1} of average annual yield. The highest average yields across locations and years were observed for *M. × giganteus* (9.9 ± 0.7 t DM ha^{-1}) and interspecies hybrid OPM-6 (9.4 ± 0.6 t DM ha^{-1}). Interspecific hybrids on average produced higher yields than *M. sinensis* and *M. sacchariflorus* genotypes ($p < 0.001$ for the comparison of *M. sinensis* and *M. sacchariflorus* groups with hybrids).

At all sites except Adana annual biomass yield increased throughout the first 3 years while the crop was establishing (**Figure 2**). However, in Adana, high biomass yields were achieved in the first growing season. At this location, the average first-year yield reached 8.1 ± 0.4 t DM ha^{-1}, 7.7 times higher than

TABLE 2 | Plant losses (% of plants planted) recorded in the field during the first winter (November 2012 until March 2013) for the 15 *Miscanthus* genotypes at six field locations.

Location	Genotype (OPM) and species group														
	Sac				*Sac × Sin*						*Sin*				
	1	2	3	4	5	6	7	8	9 Gig	10	11	12	13	14	15
Adana	0	0	0	2	1	0	1	1	0	1	34	16	12	0	18
Stuttgart	4	1	0	3	2	2	0	1	0	0	0	3	2	3	4
Potash	3	3	1	2	0	3	2	1	13	2	1	8	1	4	14
Wageningen	1	0	1	0	2	0	0	0	0	1	0	0	0	0	1
Aberystwyth	59	82	45	55	44	28	29	27	32	35	35	31	50	57	39
Moscow	3	13	0	5	0	1	6	1	11	5	7	13	4	4	11
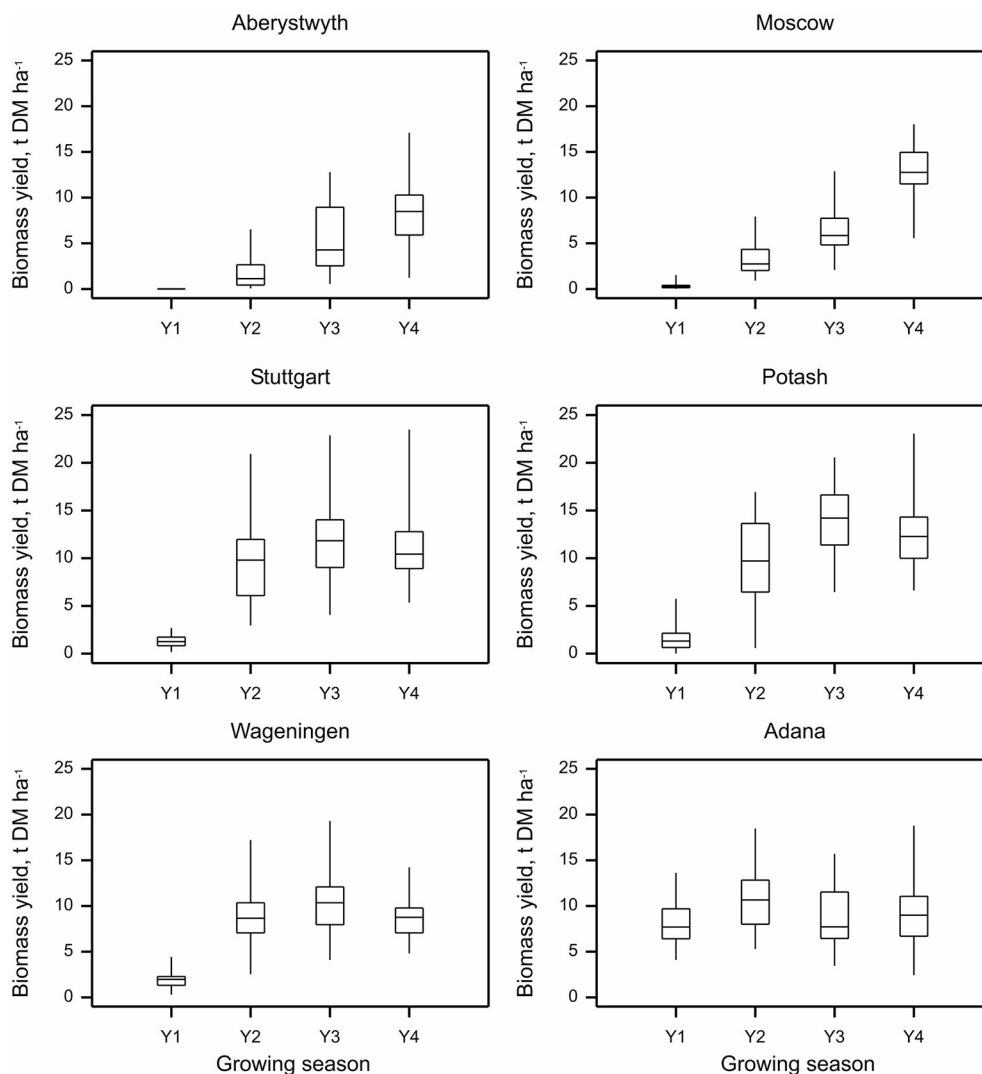
FIGURE 2 | Annual biomass yield of *Miscanthus* (15 genotypes pooled) at six trial locations over four growing seasons 2012–2015 (Y1–Y4). Whiskers denote the overall range at each location within each year, boxes denote interquartile ranges and within this the horizontal bar denotes the median.

at the other sites. It increased further to 10.7 ± 0.4 t DM ha^{-1} in the second growing season and although dropping slightly in the following growing season remained relatively stable throughout seasons 3 and 4 (8.7 ± 0.5 and 9.4 ± 0.5 t DM ha^{-1} in 2014 and 2015, respectively). Interestingly, at Moscow and Aberystwyth, locations where the crop apparently took longer to establish, the yields steadily increased throughout the 4 years and possibly had not achieved their peak by year 4. At Stuttgart and Potash, good yields were achieved in the second year (9.5 ± 0.6 and 9.5 ± 0.7 t DM ha^{-1}, respectively), there was however high within-site variation at these locations (**Figure 2**). At Stuttgart, highly variable soil depth within the site (40–100 cm) could be responsible for this variation in yield. At Wageningen and Potash, biomass yield was generally lower in year 4 than year 3 (14.1 ± 0.5 v 12.6 ± 0.5 at Potash, and 10.4 ± 0.4 v 8.7 ± 0.3 t DM ha^{-1} at Wageningen in 2014 and 2015, respectively), which was possibly

due to lower rainfall in 2015 (in particular at Potash, rainfall in 2015 was almost half that in 2014; Supplementary Table 4).

In terms of biomass yield, genotypes ranked differently by year and by location. The higher-yielding genotypes were different at the six sites (see also yield ranking in Lewandowski et al., 2016). The best-yielding genotype across locations from the first growing season was *M.* × *giganteus* (OPM-9) producing on average 3.4 ± 1.0 t DM ha^{-1} and after the second and third seasons, the *sac* × *sin* hybrid OPM-6 with 10.6 ± 1 and 12.4 ± 0.9 t DM ha^{-1}, respectively. In the fourth growing season, *M.* × *giganteus* showed again the highest average yield of 13.8 ± 0.7 t DM ha^{-1} across locations. Overall these two genotypes were the highest biomass producers showing either the first or the second best yield depending on the year (**Table 3**).

At Adana, *M.* × *giganteus* was the highest-yielding genotype in the first three seasons whilst in 2015, the best yield was

TABLE 3 | Annual biomass yield (t DM ha^{-1}) of 15 *Miscanthus* genotypes at six trial locations in 2014 (Y3) analyzed by REML using separate residual variances for each location.

Location	Genotype (OPM)															
	1	2	3	4	5	6	7	8	9	10	11	12	13	14	15	Mean
Aberystwyth	1.5	2.9	6.4	3.3	5.6	10.6	4.7	11.3	8.3	10.8	3.0	2.9	3.0	2.2	4.8	5.4
Moscow	3.4	5.5	4.7	2.9	7.2	10.4	6.8	7.6	7.8	8.5	6.2	6.0	5.6	5.7	4.3	6.2
Stuttgart	8.3	12.9	14.6	6.1	13.7	16.3	12.7	14.2	13.6	13.6	11.8	12.5	10.2	9.5	7.9	11.9
Potash	14.1	18.0	15.4	13.3	17.3	17.0	14.3	13.3	16.7	15.7	15.3	10.5	9.2	11.7	10.3	14.1
Wageningen	5.9	10.3	9.8	8.3	9.4	10.8	9.5	14.5	14.3	12.1	12.8	9.8	9.3	9.1	9.5	10.4
Adana	6.3	6.3	5.2	4.5	7.3	9.4	7.0	7.3	13.0	6.8	12.4	12.5	12.1	9.8	10.4	8.7
Mean	6.6	9.3	9.4	6.4	10.1	12.4	9.2	11.4	12.3	11.3	10.2	9.0	8.2	8.0	7.9	

Statistical significance of effects of genotype p < 0.001 (average s.e. 0.61), location p < 0.001 (average s.e. 0.59) and interaction p < 0.001 (average s.e. 1.45).

recorded for *M. sinensis* OPM-12. At Aberystwyth, hybrid OPM-8 consistently yielded the highest of all the genotypes in the first three seasons but in year 4 it was outperformed by *M. × giganteus* although not significantly so. At the other locations the best-yielding genotypes varied depending on the year (see also Lewandowski et al., 2016).

Total Biomass Yield over Four Growing Seasons

The highest total biomass yield of 37.9 ± 1.8 t DM ha^{-1} (location mean for all genotypes) was observed at Potash, Ukraine and the second highest in Adana, Turkey (36.9 ± 1.3 t DM ha^{-1}). The lowest-yielding locations were Aberystwyth with a total yield of 15.4 ± 1.3 t DM ha^{-1} and Moscow with 22.5 ± 0.9 t DM ha^{-1}.

Significant differences ($p < 0.01$) between the species groups (i.e., between "*M. sacchariflorus*," "*M. sinensis*," "Hybrids," and "*M. × giganteus* control clone") in total four year yield were observed at each location (**Figure 3**). The total yield of the new interspecies hybrids did not differ ($p > 0.05$) from that of *M. × giganteus* at all the locations, except Adana (the only location with additional irrigation applied), where *M. × giganteus* outperformed hybrids ($p < 0.05$). In particular, the hybrids OPM-6, 8, 10 achieved the same 4-year yield as *M. × giganteus* (locations pooled), but also one of the *M. sacchariflorus* types, OPM-2, had total yield similar to that of *M. × giganteus* clone. However, there was still evidence of significant differences between genotypes within species group at Aberystwyth ($p < 0.021$), Stuttgart ($p < 0.023$), and Potash ($p < 0.01$).

The *M. sinensis* types on average produced significantly less biomass than interspecies hybrids, except in Adana, where *M. sinensis* types OPM-11 and 12 produced the highest yields, and Wageningen where these two groups yielded similarly. *M. sinensis* types had on average similar total yields to *M. sacchariflorus* genotypes at all trial locations, except in Potash where *M. sacchariflorus* genotypes produced a higher total yield than *M. sinensis* types ($p < 0.05$; **Figure 3**). *M. sacchariflorus* on average (four genotypes pooled) produced similar to *M. × giganteus* yields at Potash and Stuttgart and had lower total yields than *M. giganteus* at the other locations. Over a period of 4 years, OPM-2 (*M. sacchariflorus*) and hybrid genotypes OPM-6,

8, and 10 showed similar total yields to *M. × giganteus* (locations pooled).

Total biomass DM yield over 4 years was linearly correlated ($p < 0.001$) with the annual yields achieved in each of the growing seasons. Over all locations the correlation increased from 0.49 in the year 1–0.90 in the second, 0.86 in the third growing seasons and 0.62 in the year 4.

Genotype Differences in Yield in an Established Crop (2014–2015)

Figure 4 shows the yields of the individual interspecies hybrid genotypes and *M. × giganteus* in years 3 and 4, when the crop reached or approached maturity and yields stabilized. In these growing seasons there was no genotype effect on annual yield at any location except Adana, i.e., biomass yields for *M. × giganteus* and *Sac × Sin* hybrids were similar ($p > 0.05$). At Adana, *M. × giganteus* showed higher biomass yield than OPM-7, 8, and 10 ($p < 0.05$) while OPM-5 and 6 produced biomass yields comparable to *M. × giganteus*. At Potash and Wageningen year 3 biomass yields were greater than in year 4 ($p < 0.001$), which reflect differences in the weather conditions (specifically significantly decreased summer rainfall in 2015) between the years at these sites (Supplementary Table 4). At Moscow and Aberystwyth, overall mean biomass yield was affected by year ($p < 0.001$ and $p = 0.002$, respectively) and increased from year 3 to 4 indicating further crop maturation at these sites. However, at Aberystwyth the effect of year was not consistent across all genotypes with only *M. × giganteus* showing a significant yield increase ($p < 0.05$) between years 3 and 4. All other genotypes showed similar yield in years 3 and 4. In Stuttgart, there were no effects ($p > 0.05$) of genotype, year or of an interaction between the two.

Canopy Height and Stem Number

Canopy height in autumn (**Table 4**) was affected by site, genotype and their interaction ($p < 0.001$). On average, the tallest plants were observed in Stuttgart, Potash, and Wageningen (mean canopy height 198.5 ± 7.7, 194.4 ± 6.5, and 191.7 ± 5.0 cm, respectively) and the shortest were in Moscow (122.1 ± 3.1 cm). The genotypes of *M. sacchariflorus*, OPM-1 and 3 in particular, and *M. × giganteus* (OPM-9) had the highest canopy heights
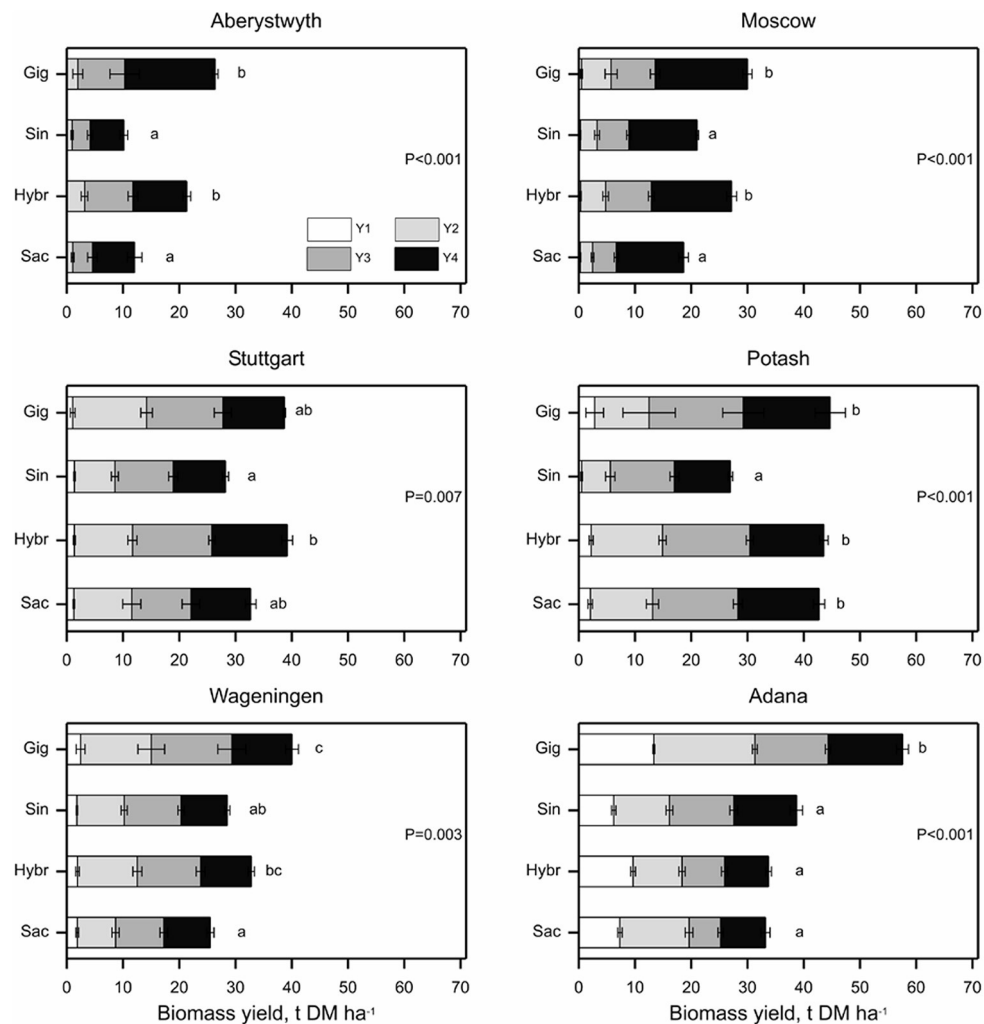
FIGURE 3 | Cumulative biomass yield over four growing seasons (Y1–Y4) at six trial locations. *Miscanthus* genotypes were categorized as: Gig = *Miscanthus* × *giganteus*, Sin = *M. sinensis*, Hybr = *M. sinensis* × *M. sacchariflorus* hybrids or Sac = *M. sacchariflorus* genotypes. Error bars represent ± standard error of the mean for corresponding growing season. Probabilities indicate the overall effect of species group on total cumulative biomass yield within each site and differing letters indicate species group means differ ($p < 0.05$) based on bonferroni adjusted multiple comparisons.

among all the genotypes (204.1 ± 15.6, 194.2 ± 14.8, and 212.8 ± 11.1 cm, respectively).

Stem number in growing season 3 (**Table 5**) was also significantly affected by site and genotype with an interaction ($p < 0.001$). Highest average stem number was observed at Wageningen (60.5 stems plant^{-1}) and the lowest at Aberystwyth (27.8 stems plant^{-1}). Across locations, the highest average stem number was observed for the hybrid genotypes OPM-6, 7, and 10, with 74.1, 71.2, and 68.7 stems plant^{-1}, respectively. The lowest average stem numbers were observed in *M.* × *giganteus* (OPM-9; 29.1 stems plant^{-1}) and OPM-2, 1, 12, and 11 (33.6, 35.1, 35.5, and 37.3 stems plant^{-1}, respectively). *M. sacchariflorus* genotypes tended to have lower stem numbers than *M. sinensis* types.

There was also a site × genotype interaction observed for stem number ($p < 0.001$). Based on analysis of variance within each location, genotypes differed in stem number at the field sites

in Moscow, Potash, Stuttgart, and Wageningen ($p = 0.01$, $p = 0.001$, $p < 0.001$, and $p < 0.001$, respectively). At Wageningen and Moscow, OPM-6 had the highest stem numbers among the genotypes tested (**Table 5**). At Stuttgart, OPM-6 and 7 were the genotypes with the highest stem numbers. At Potash, stem number was highest in OPM-7. OPM-6, a high-yielding genotype, showed a higher ($p < 0.05$) number of stems compared to *M.* × *giganteus* at three locations: in Stuttgart, Wageningen, and Moscow. At two sites, Aberystwyth and Adana, no significant differences ($p = 0.517$ and $p = 0.877$, respectively) in stem number between genotypes were detected.

In the combined data set over all locations there was a positive linear correlation between biomass yield (t DM ha^{-1}) and both autumn canopy height (cm) and stem number (stems plant^{-1}) in the third growing season (2014). Canopy height was more strongly associated (Pearson $r = 0.55$, $p < 0.001$) with yield than
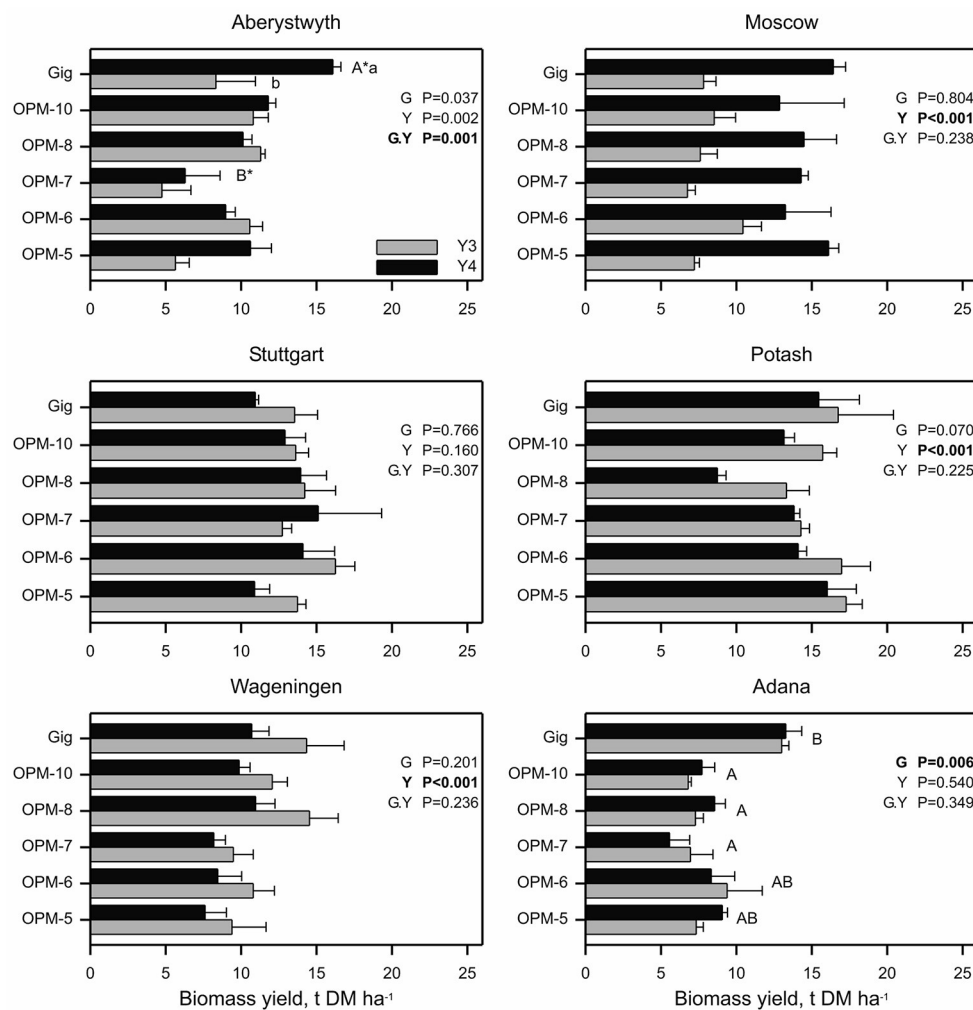
FIGURE 4 | Biomass yield of *Miscanthus* × *giganteus* and *M. sinensis* × *M. sacchariflorus* hybrids in 2014 (Y3) and 2015 (Y4) within six field trial locations. Error bars represent the standard error of the mean. Effects of genotype, year and interaction (genotype.year) are denoted by G, Y and G.Y, respectively. At Adana, differing capital letters indicate genotype means differ ($p < 0.05$) based on bonferroni adjusted multiple comparisons. At Aberystwyth, differing capital letters (A*, B*) indicate genotype means within a year and differing lower case letters within a genotype indicate means differ between years ($p < 0.05$).

TABLE 4 | Season-end canopy height (cm) of 15 *Miscanthus* genotypes at six trial locations in 2014 (Y3) analyzed by REML using separate residual variances for each location.

Location	Genotype (OPM)															
	1	2	3	4	5	6	7	8	9	10	11	12	13	14	15	Mean
Aberystwyth	168.0	112.0	173.7	141.3	146.7	161.3	139.3	186.0	180.3	142.3	111.7	151.7	103.0	107.0	114.3	142.6
Moscow	136.4	114.6	126.9	97.8	116.8	116.1	111.3	116.2	180.4	126.7	127.6	118.8	114.4	120.1	100.3	121.6
Stuttgart	253.0	228.0	246.0	190.7	162.0	173.3	207.0	173.7	234.7	243.0	175.3	220.3	170.7	152.3	147.3	198.5
Potash	286.7	250.0	261.7	191.7	181.7	165.0	176.7	175.0	221.7	185.0	198.3	161.7	161.7	163.3	136.7	194.4
Wageningen	231.7	216.7	220.0	193.3	166.7	143.3	155.0	195.0	261.7	186.7	196.7	193.3	166.7	176.7	171.7	191.7
Adana	149.0	126.0	137.0	157.3	152.0	116.3	104.7	97.3	198.0	112.7	138.0	146.3	150.0	123.3	93.3	133.4
Mean	204.1	174.5	194.2	162.0	154.3	145.9	149.0	157.2	212.8	166.1	157.9	165.4	144.4	140.5	127.3	

Statistical significance of effects of genotype $p < 0.001$ (average s.e. 6.22), location $p < 0.001$ (average s.e. 3.95) and interaction $p < 0.001$ (average s.e. 13.68).

TABLE 5 | Season-end stem count (stems plant^{-1}) of 15 *Miscanthus* genotypes at six trial locations in 2014 (Y3) analyzed by REML using separate residual variances for each location.

Location	Genotype (OPM)															
	1	2	3	4	5	6	7	8	9	10	11	12	13	14	15	Mean
Aberystwyth	29.2	12.6	26.5	35.5	32.1	58.6	47.8	33.8	22.0	33.8	11.2	31.4	12.7	19.7	30.2	27.8
Moscow	57.6	34.7	39.4	40.1	58.7	99.3	72.8	64.7	35.1	81.3	42.0	43.1	48.9	53.3	44.9	53.1
Stuttgart	26.1	42.6	34.6	73.8	63.3	105.9	93.8	71.5	29.8	70.1	43.2	33.5	59.9	60.5	74.6	56.6
Potash	31.4	34.9	38.0	35.7	45.3	40.7	77.6	48.3	23.9	73.2	21.3	13.5	21.4	30.8	19.9	35.1
Wageningen	23.3	32.0	38.6	54.2	39.6	116.1	93.3	66.9	25.0	91.3	68.0	44.3	102.9	67.5	98.3	60.5
Adana	49.5	52.5	54.1	42.7	39.6	43.5	49.6	36.5	41.2	70.9	54.7	55.8	43.2	36.6	32.0	46.4
Mean	35.1	33.6	38.1	46.1	45.8	74.1	71.2	52.5	29.1	68.7	37.3	35.5	43.6	43.0	46.4	

Statistical significance of effects of genotype p < 0.001 (average s.e. 0.27; s.e. applies to means on square root scale), location p < 0.001 (average s.e. 0.31) and interaction p < 0.001 (average s.e. 0.66).

stem number ($r = 0.21$, $p < 0.001$). Stem number and canopy height showed no association ($r = 0.03$, $p = 0.649$). But there were also exceptions within the genotype, in particular, OPM-6, one of the highest yielding genotypes in years 3 and 4, had a low canopy height but a high stem count.

Phenotype Sensitivity to Location

Both canopy height and stem number measured in year 3 showed significant differences in sensitivities across the six locations ($p = 0.007$ and $p = 0.01$, respectively).

In terms of canopy height genotypes OPM-2 and 1 were most sensitive, i.e., less stable across locations than overall mean sensitivity in the data set (**Figure 5A**), followed closely by OPM-3 (all three belong to *M. sacchariflorus* species). The lowest sensitivities were observed for OPM-6 and 5, *Sac × Sin* hybrids, i.e., these genotypes had the most consistent canopy heights irrespective of the environment they were planted in.

For stem number, OPM-6, with the highest overall mean stem count, showed a higher than average sensitivity to location (tended to be less stable) than *M. × giganteus* and other genotypes with lower stem counts, e.g., OPM-1–4 *M. sacchariflorus* genotypes (**Figure 5B**). These tended to be the most stable. OPM-13 (*M. sinensis*) and OPM-15 (an open-pollinated *Sac × Sin × Sin* hybrid), showed the least stable stem counts across locations, whereas for all the *M. sacchariflorus* genotypes rather low sensitivity values have been obtained. Among the hybrids OPM-5 and among the *M. sinensis* types OPM-12 showed lower sensitivities.

Biomass yield estimated in year 3 showed no significant difference in sensitivity across the six locations ($p = 0.269$). Overall, OPM-2 tended to be the least stable and OPM-8 the most stable genotype (**Figure 5C**). The high-yielding *Sac × Sin* hybrids OPM-6 and 7 showed higher than average yield sensitivity and this tended to be higher than that of *M. × giganteus*. Overall, all the *M. sacchariflorus* genotypes showed higher than average sensitivity, whereas most of the *M. sinensis* types tended to have lower than average sensitivity in yield to the locations studied. OPM-8, 13, and 15 had a similarly low yield sensitivity to *M. × giganteus*.

DISCUSSION

Establishment and Survival

In our experiment, the small plugs produced by *in vitro* tillering and seed were shipped to all the sites in boxes and were watered at planting. Several liters of water were applied to wet the soil in the immediate vicinity of the plug plant. This helps establish the hydraulic contact needed to prevent plug dehydration in the first 10 days while roots grow out of the plug into the soil. In most of the locations, transplanting success rates were close to 100%. The exception was Aberystwyth, where the shallow soils (Supplementary Table 2) were too damp to create a fine tilth and the soil tilth was too "lumpy" to ensure a good hydraulic contact. Further, immediately after planting in Aberystwyth, there was a 2 week period of fine weather which dried the soil surface. This was followed by an exceptionally wet (double normal rainfall) weather conditions, cold (temperatures < 16°C) and overcast in June-September (half normal radiation). This combination of conditions was highly unfavorable for *Miscanthus* establishment from delicate plugs, and resulted in high establishment plant losses. It was not our intention to make an in depth study of the agronomy of plant plug establishment as this was the task for the upscaling trials within the same OPTIMISC project (Lewandowski et al., 2016). The lessons learnt from the Aberystwyth site in the first year are nonetheless important for the subsequent agronomic trials on the establishment of *Miscanthus* from plugs in the cool wet climates and have been taken into account in the development of commercially relevant establishment protocols where safe reliable establishment of the crop is a pre-requisite to an industry based on *Miscanthus* biomass (Michal Mos and Chris Ashman, personal communication). In Aberystwyth, the lost plants were replaced with spare plants in June 2013. Weather conditions for growth in 2013 were more favorable than 2012, and no further plant losses occurred, allowing the G × E experiment to continue with measurements from the site in Aberystwyth.

It was expected that there would be differences in overwintering in the first winter following planting, particularly in the highly continental climates of Potash in Ukraine and Moscow in Russia. In Moscow, overwinter mortality was slightly

FIGURE 5 | Sensitivity of (A) canopy height, **(B)** stem count, and **(C)** biomass yield of 15 *Miscanthus* genotypes to location in 2014 (Y3) based on joint regression analysis (Finlay and Wilkinson, 1963). Labels 1–8, Gig, 9–15 denote OPM-1 to OPM-15, respectively, vertical bars denote 95% simultaneous confidence intervals for each sensitivity estimate and the horizontal dotted line denotes the overall mean sensitivity of all 15 genotypes.

higher than at most other locations (except Aberystwyth), which could be related to shorter growing season, spring frosts, and earlier low temperatures in autumn at this location. Earlier work indicated that there is a threshold (in terms of lethal temperature to kill 50% of the rhizomes, LT_{50}) for overwinter freezing tolerance of the rhizomes of approximately $-3.5°C$ for *M. sacchariflorus* and *M. × giganteus* (Clifton-Brown and Lewandowski, 2000). Interestingly, a repeat of an earlier freezing experiment within OPTIMISC project by partners in

Belgium confirmed the $-3.5°C$ LT_{50} (Fonteyne et al., 2016a,b). Unexpectedly, *M. × giganteus* survived in all sites, even in Moscow and Ukraine, where winter soil temperatures would normally have fallen below $-3.5°C$ sometime within the 4 year trial period (between 2012 and 2015). In fact soil temperatures did not fall below $-3.5°C$ at any of the sites, and consequently only low overwinter losses were recorded in Moscow and Potash. Some of the plant losses in Aberystwyth did occur overwinter, despite the fact that winter soil temperatures at 5 cm depth remained above freezing. The high establishment losses in Aberystwyth were more likely to be caused by the poor first season summer growing conditions which resulted in insufficient rhizome growth to overwinter, a problem seen in trials in Ireland over a decade ago (Clifton-Brown et al., 2015). In the OPTIMISC multi-location trial we did not measure the rhizome mass after the first growing season as we had done in an earlier trial (Clifton-Brown and Lewandowski, 2000) because this would have left unwanted gaps in the plots.

Adana (Turkey) provided the most exceptional environment in this experiment for early establishment. Here, without irrigation *Miscanthus* could not establish. However, with the application of irrigation amounts to almost completely cover potential evapotranspiration in the first year, the establishment rate was so rapid that many genotypes almost reached mature "ceiling" yields in a single growing season. In the Netherlands, where the soil has a light sandy texture, mature ceiling yields appear to have been reached by the end of the second year. In contrast, despite the favorable growing season temperatures and rainfall in Stuttgart, the mature yields were only attained by year 3. We believe this slower establishment is partly due to the heavy clay soil and highly variable soil depth (40–100 cm) across the site which impede rapid root and rhizome growth, In Ukraine, where the soil conditions were the best of all sites, and summer temperatures are favorable, yields increased consecutively until the third year but were reduced slightly in year 4, due to significantly decreased summer rainfall. In contrast, yields in the Aberystwyth and Moscow sites rose slowly in the first and second years, but by the third and fourth year the difference in annual productivity between sites that established most quickly (Adana and Netherlands) had begun to narrow. It will require a further year or two to ascertain if indeed the ceiling yield was reached in fourth year in Aberystwyth and Moscow.

Interestingly, as the annual productive differences between the slower and faster establishing sites reduced with stand age, the yield differences between the sites over the crops lifespan of 12–20 years (Lesur et al., 2013) would be expected to narrow. We would expect significant differences in long-term yields of the different germplasm types would be detected if yield measurements could continue.

Yield Performance and Environment

The continental climate with warm summers, combined with nutrient-rich deep soils ensuring a good water supply throughout the growing season in Ukraine resulted in the highest ranked productivity of all the six sites over the first 4 years.

At Adana in Turkey, high yields could be achieved already in the first growing season and further yield increase was rather

slow. A number of factors could contribute to high yields at this site. The trial in Adana was irrigated, evidently providing sufficient soil moisture content to allow successful and quick plant establishment. The Adana site had the highest PAR and degree-days (DD$_{base0}$, $_{base10}$) over the first growing season, and also the highest air and deep soil (over 2 m depth) temperatures among all the locations (**Table 2**; Supplementary Tables 2–6). The warm climate and long vegetation period seem to be advantageous for miscanthus yields at this site, when sufficient water supply was ensured. The literature sources report that *M. × giganteus* is providing higher yields in warmer, wetter areas with moderately heavy soils (Beale and Long, 1995; Lewandowski et al., 2000).

At two locations, in Aberystwyth and in Moscow, the yields were low in the first year after planting but continued gradually increasing over all the 4 years. The crop has possibly not yet achieved its peak yields at these two locations. As mentioned above, in Aberystwyth the weather in the first growing season directly after planting was most probably the key factor affecting the establishment and the first-year biomass yield. The total yield achieved at this location over 4 years was also the lowest among the trials. It is worth mentioning that the field trial at Aberystwyth was established on marginal, shallow soil poor on nutrients (Supplementary Tables 2, 3), on a former grassland, whereas the other trials were placed on arable or horticultural land.

The yields at Moscow site were comparable to the other sites and improved significantly in the years following establishment, reaching 16 t DM ha^{-1} for some genotypes (e.g., *M. × giganteus*) in year 4. Lower than expected overwinter mortality and good mature biomass yields at this site might be related to relatively mild winter soil temperatures in the years of assessment and deep snow cover preventing rhizome damage overwinter. Although air temperatures at this site (as well as in Potash in Ukraine) sometimes went lower than −20°C, soil temperature did not fall lower than 0.7°C at 20 cm depth in the first winter (**Table 2**). Deep soil and good plant available nitrogen supply at this site could also be advantageous for biomass production (Supplementary Tables 2, 3).

M. × giganteus gave its best yields at the sites with rich deep soil, such as Potash, or in a warm climate under sufficient irrigation, such as in Adana. *M. sinensis* genotypes on average showed their best yields in Adana, possibly profiting from a long vegetation period. Earlier, Robson et al. (2012) reported that *M. sinensis* genotypes may remain green for longer period than *M. sacchariflorus* genotypes.

Biomass yields were lower at Wageningen and Potash in the fourth growth season compared to the third. This could be a result of lower precipitation at these sites in the year 4, but also the other climate factors could play a role. Precipitation during the growing period is mentioned as the key factor for high miscanthus yields in the literature (Ercoli et al., 1999; Richter et al., 2008; Gauder et al., 2012). Some other factors, such as heat sum during the growing period, soil moisture and PAR, are also known to be important for biomass production (Gauder et al., 2012; Larsen et al., 2016). At Adana, the biomass yields dropped slightly in the last two growing seasons compared to

the second which most probably was caused by the reduction in irrigation.

Genetic Variation and Performance of the Genotypes across Sites

Across all sites over 4 years, the rankings of the most productive genotypes/hybrids were quite similar and we found less environmental specificity than expected despite the wide climatic range of the six sites. Unexpectedly, *M. × giganteus* survived in all sites and by the third and fourth years was amongst the highest yielding types and is a key "generic high performing genotype" with wide climatic adaptability.

The interspecies hybrid group produced more biomass than both the *M. sacchariflorus* and *M. sinensis* groups. This confirms the importance of interspecies crosses to achieve the highest yields. Overall, *M. × giganteus* was the highest yielding clone and OPM-6 hybrid came a close second. The low environmental specificity was a surprising result, since we expected that there would be a greater requirement for matching germplasm types to cope with environmental extremes of overwinter cold in Ukraine and Moscow and drought and heat in Adana. The relatively early senescing clone, OPM-10, was a consistent "performer" across all sites, but never the highest yielding type in any location. OPM-10's environmental resilience is noteworthy because resilience is key to production and survival in marginal land types where extremes of drought, sometimes combined with low temperatures in and out of the growing season, limit the production of food crops.

When we set up the multi-location trial in 2012, we expected the warm summers in Adana would cause similar stunting effects to those observed in Texas (Charlie Rodgers, personal communication). In fact *M. × giganteus* performed much better than expected. From this we conclude that *Miscanthus × giganteus* is still within its range of thermal adaptation in Adana and that the growing season water availability is the main constraint for production in southern Mediterranean climate, rather than heat stress. Interestingly, with reduced irrigation levels in the third and fourth growing seasons in Adana, the water saving strategies of the *M. sinensis* types detected in earlier experiments (Clifton-Brown et al., 2002), were confirmed by the significant jump in yield rank (in particular OPM-13). As irrigation water is expensive, maximizing the biomass production through improved water use efficiency is very important and a subject of intense research in several interrelated research projects, of which EU FP7's WATBIO (Taylor et al., 2016) is one of the most comprehensive including genomics for breeding.

The relatively low environment sensitivity in many selections, have both advantages and disadvantages for further breeding. A key advantage is that leading selections made in plot trials in "central" locations such as Braunschweig in Germany (with cold continental winters, warm summers with regular water deficits) have wide relevance for the selection of novel germplasm for much of Europe.

Yield Traits

Across all sites and all genotypes in 2014, there were significant positive correlations between harvested yield and autumn canopy

height and stem number. For this set of germplasm, canopy height ($r = 0.55$) appeared to be more predictive for the biomass yield than stem number ($r = 0.21$). Although, these correlations were statistically significant they explained only a minor part of the observed variation in yield. In particular, OPM-6 hybrid, one of the highest yielding genotypes, had a low canopy height but a high stem count compared to the other genotypes.

A number of studies have reported correlations between yield and various morphological and physiological parameters in miscanthus (Jeżowski, 2008; Gauder et al., 2012; Robson et al., 2013; Maddison et al., 2017). Several earlier studies showed that tillering is among the most important traits influencing biomass yield (Jeżowski, 2008; Nie et al., 2016). Our results have only shown a weak association between the stem number and yield for the set of germplasm evaluated. The higher stem numbers are often associated with thinner stems (Robson et al., 2013). In the same field trial we found that germplasm types with higher stem counts have lower moisture contents at harvest ($r = -0.43$, $p < 0.001$; data not shown in this manuscript). These thinner stemmed types are easier to cut and bale at harvest than those with thicker stems (Hastings et al., 2017). They however have the disadvantage that leaf shares are higher than in the tallest genotypes (such as OPM-1 and 9), which can increase the ash content (Iqbal et al., 2017). Here, it is worth mentioning that since only stems reaching at least 60% of the canopy height were counted, this measurement may underestimate the total shoot number for the *M. sinensis* genotypes (which tend to produce multiple short stems).

To date morphological characterization has largely been carried out in "spaced plant" breeding nurseries. While spaced plant nurseries are needed to handle the large numbers of genotypes to be screened in breeding, yield may or may not correlate to in plot yield performance where the individual plants are tested in "competitive" plant stands with full canopy closure. Planting densities have a very important role to play in yield determination. In our multi-location trial we decided to standardize the planting density at two plants m^{-2} for all germplasm types based on prior experience (Clifton-Brown et al., 2001). There are many complex interactions between planting density and the germplasm morphological characteristics such as height, shoot density and growing environment. Since such trials are resource intensive these experiments should only be attempted on a very few highly promising novel hybrids.

The new data from this multi-location trial confounds our efforts to identify simple ideotypes for high yield. Both short and tall morphotypes can be effective strategies. This points us back to the importance of work on whole season photosynthetic efficiency where we know interspecies hybrids such as *M. × giganteus* have proved outstanding at low temperatures (Beale and Long, 1995; Davey et al., 2017). This is further complicated by environmental plasticity. For example under extremely hot climate, the morphology of *M. × giganteus,* which expresses a dominant phenotype associated with its tall *M. sacchariflorus* parent when grown in temperate climates (with a canopy height over 3 m), changes to a more *M. sinensis* phenotype with a multitude of short thin stems and a canopy height of about 1 m.

CONCLUSIONS

Performance of the 15 genotypes of miscanthus has been assessed across a wide range of environments in the European countries, Russia and Turkey. A number of genotypes, in particular interspecies hybrids of *M. sinensis* and *M. sacchariflorus* showed good yield potential to be used in parallel or as a replacement to *M. × giganteus* standard clone. In particular, *Sac × Sin* hybrids were high-yielding. Two of these, OPM-6 and 7 provided similar to *M. × giganteus* biomass yields at most locations.

Environment-sensitive genotypes, which showed high yields but low yield stability across geographic sites, such as e.g., OPM-2 (*M. sacchariflorus*) can be recommended for use in particular locations, where they are the most productive. Whereas, the genotypes providing stable yields in different environments, such as OPM-8 or 13, can be valuable for breeding programs of miscanthus. Interestingly, *M. × giganteus* produced high biomass yields at multiple sites and showed a high yield stability in the Finlay Wilkinson analysis. *M. sacchariflorus* germplasm types showed high yields but the yields were more vulnerable to the environmental conditions and varied among the locations. The *M. sinensis* genotypes had overall lower yields (with some exceptions) but the yields were more stable across the locations.

This multi-location trial showed that the range of miscanthus cultivation can be extended into the Eastern areas, also for the standard clone *M. × giganteus* which showed good overwintering in this study. Climate changes are reducing the severity of winters, and it appears to be safe to plant *Miscanthus* further eastwards than earlier predicted, e.g., Hastings et al. (2009a,b).

AUTHOR CONTRIBUTIONS

OK, JC, IL designed and planned the experiments; OK, CN, TV, MÖ, IT, HS performed the experiments; OK, RS analyzed the data; OK drafted the manuscript; CN, RS, IL, JC, AH, LT critically revised the manuscript draft; all the authors revised and approved the final version to be published.

FUNDING

ACKNOWLEDGMENTS

SUPPLEMENTARY MATERIAL

The Supplementary Material for this article can be found online at: http://journal.frontiersin.org/article/10.3389/fpls.2017.00563/full#supplementary-material

REFERENCES

Allen, B., Kretschmer, B., Baldock, D., Menadue, H., Nanni, S., and Tucker, G. (2014). *Space for Energy Crops – Assessing the Potential Contribution to Europe's Energy Future*. Report produced for BirdLife Europe, European Environmental Bureau and Transport & Environment. Institute for European Environmental Policy (IEEP), London. Available online at: http://www.eeb.org/EEB/?LinkServID =F6E6DA60-5056-B741-DBD250D05D441B53

Anderson, N. O., Gomez, N., and Galatowitsch, S. M. (2006). A non-invasive crop ideotype to reduce invasive potential. *Euphytica* 148, 185–202. doi: 10.1007/s10681-006-5936-6

Beale, C. V., and Long, S. P. (1995). Can perennial C4 grasses attain high efficiencies of radiant energy conversion in cool climates? *Plant Cell Environ.* 18, 641–650. doi: 10.1111/j.1365-3040.1995.tb00565.x

Clifton-Brown, J. C., Lewandowski, I., Andersson, B., Basch, G., Christian, D. G., Kjeldsen, J. B., et al. (2001). Performance of 15 Miscanthus genotypes at five sites in Europe. *Agron. J.* 93, 1013–1019. doi: 10.2134/agronj2001.9351013x

Clifton-Brown, J. C., Lewandowski, I., Bangerth, F., and Jones, M. B. (2002). Comparative responses to water stress in stay-green, rapid- and slow senescing genotypes of the biomass crop, Miscanthus. *New Phytol.* 154, 335–345. doi: 10.1046/j.1469-8137.2002.00381.x

Clifton-Brown, J. C., Renvoize, S. A., Chiang, Y.-C., Ibaragi, Y., Flavell, R., Greef, J. M., et al. (2011). "Developing Miscanthus for Bioenergy," in *Energy Crops*, eds N. G. Halford and A. Karp (London: Royal Society of Chemistry), 301–321.

Clifton-Brown, J., and Lewandowski, I. (2000). Overwintering problems of newly established Miscanthus plantations can be overcome by identifying genotypes with improved rhizome cold tolerance. *New Phytol.* 148, 287–294. doi: 10.1046/j.1469-8137.2000.00764.x

Clifton-Brown, J., Hastings, A., Mos, M., McCalmont, J. P., Ashman, C., Awty-Carroll, D., et al. (2016). Progress in upscaling Miscanthus biomass production for the European bio-economy with seed-based hybrids. *GCB Bioenergy* 9, 6–17. doi: 10.1111/gcbb.12357

Clifton-Brown, J., Neilson, B., Lewandowski, I., and Jones, M. B. (2000). The modelled productivity of Miscanthus× giganteus (GREEF et DEU) in Ireland. *Ind. Crops Prod.* 12, 97–109. doi: 10.1016/S0926-6690(00)00042-X

Clifton-Brown, J., Robson, P., Sanderson, R., Hastings, A., Valentine, J., and Donnison, I. (2011). Thermal requirements for seed germination in Miscanthus compared with switchgrass (*Panicum virgatum*), reed canary grass (*Phalaris arundinaceae*), maize (*Zea mays*) and perennial ryegrass (*Lolium perenne*). *GCB Bioenergy* 3, 375–386. doi: 10.1111/j.1757-1707.2011.01094.x

Clifton-Brown, J., Schwarz, K. U., and Hastings, A. (2015). History of the development of miscanthus as a bioenergy crop: from small beginnings to potential realisation. *Biol. Environ. Proc. R. Ir. Acad.* 115B, 45–57. doi: 10.3318/bioe.2015.05

Davey, C. J., Jones, L. E., Laurence, E. J., Squance, M., Purdy, S., Maddison, A., et al. (2017). Radiation capture and conversion efficiencies of Miscanthus saccariflorus, *M. sinensis* and their naturally occurring hybrid M. × giganteus. *GCB Bioenergy* 9, 385–399. doi: 10.1111/gcbb.12331

Dohleman, F. G., and Long, S. P. (2009). More productive than maize in the Midwest: how does Miscanthus do it? *Plant Physiol.* 150, 2104–2115. doi: 10.1104/pp.109.139162

Ehmann, A., Bach, I. M., Laopeamthong, S., Bilbao, J., and Lewandowski, I. (2017). Can phosphate salts recovered from manure replace conventional phosphate fertilizer? *Agriculture* 7:1. doi: 10.3390/agriculture7010001

Ercoli, L., Mariotti, M., Masoni, A., and Bonari, E. (1999). Effect of irrigation and nitrogen fertilization on biomass yield and efficiency of energy use in crop production of Miscanthus. *Field Crops Res.* 63, 3–11. doi: 10.1016/S0378-4290(99)00022-2

Finlay, K. W., and Wilkinson, G. N. (1963). The analysis of adaptation in a plant-breeding programme. *Aust. J. Agric. Res.* 14, 742–754. doi: 10.1071/AR9630742

Fonteyne, S., Lootens, P., Muylle, H., Van den Ende, W., De Swaef, T., Reheul, D., et al. (2016b). Chilling tolerance and early vigour related characteristics evaluated in two Miscanthus genotypes. *Photosynthetica* 54, 295–306. doi: 10.1007/s11099-016-0193-y

Fonteyne, S., Muylle, H., De Swaef, T., Reheul, D., Roldán-Ruiz, I., and Lootens, P. (2016a). How low can you go? Rhizome and shoot frost tolerance in miscanthus germplasm. *Ind. Crops Prod.* 89, 323–331. doi: 10.1016/j.indcrop.2016. 05.031

Gauder, M., Graeff-Hönninger, S., Lewandowski, I., and Claupein, W. (2012). Long-term yield and performance of 15 different Miscanthus genotypes in southwest Germany. *Ann. Appl. Biol.* 160, 126–136. doi: 10.1111/j.1744-7348.2011.00526.x

Greef, J. M., and Deuter, M. (1993). Syntaxonomy of Miscanthus × giganteus GREEF et DEU. *Angew. Bot.* 67, 87–90.

Hastings, A., Clifton-Brown, J., Wattenbach, M., Mitchell, C. P., Stampfl, P., and Smith, P. (2009a). Future energy potential of Miscanthus in Europe. *GCB Bioenergy* 1, 180–196. doi: 10.1111/j.1757-1707.2009.01012.x

Hastings, A., Clifton-Brown, J., Wattenbach, M., Mitchell, C., and Smith, P. (2009b). The development of MISCANFOR, a new Miscanthus crop growth model: towards more robust yield predictions under different climatic and soil conditions. *GCB Bioenergy* 1, 154–170. doi: 10.1111/j.1757-1707.2009.01007.x

Hastings, A., Mos, M., Yesufu, J. A., McCalmont, J., Ashman, C., Nunn, C., et al. (2017). Economic and environmental assessment of seed and rhizome propagated Miscanthus in the UK. *Front. Plant Sci.*

Hodkinson, T. R., and Renvoize, S. (2001). Nomenclature of Miscanthus × giganteus (Poaceae). *Kew Bull* 56, 759–760. doi: 10.2307/4117709

Hodkinson, T. R., Petrunenko, E., Klaas, M., Münnich, C., Barth, S., Shekhovtsov, S. V., et al. (2016). "New breeding collections of *Miscanthus sinensis*, *M. saccariflorus* and hybrids from *Primorsky Krai*, Far Eastern Russia," in *Perennial Biomass Crops for a Resource-Constrained World*, eds S. Barth, D. Murphy-Bokern, O. Kalinina, G. Taylor, and M. Jones (Cham: Springer International Publishing), 105–118. doi: 10.1007/978-3-319-44530-4

Iqbal, Y., and Lewandowski, I. (2014). Inter-annual variation in biomass combustion quality traits over five years in fifteen Miscanthus genotypes in south Germany. *Fuel Process Technol.* 121, 47–55. doi: 10.1016/j.fuproc.2014.01.003

Iqbal, Y., Nunn, C., Hastings, A., Kalinina, O., Khokhlov, N., Kiesel, A., et al. (2017). Harvest time optimisation of miscanthus genotypes for different biomass end uses. *Front. Plant Sci.* (Accepted with minor revision).

Jensen, E., Farrar, K., Thomas-Jones, S., Hastings, A., Donnison, I., and Clifton-Brown, J. (2011). Characterization of flowering time diversity in Miscanthus species. *GCB Bioenergy* 3, 387–400. doi: 10.1111/j.1757-1707.2011.01097.x

Jensen, E., Robson, P., Norris, J., Cookson, A., Farrar, K., Donnison, I., et al. (2013). Flowering induction in the bioenergy grass *Miscanthus saccariflorus* is a quantitative short-day response, whilst delayed flowering under long days increases biomass accumulation. *J. Exp. Bot.* 64, 541–552. doi: 10.1093/jxb/ers346

Jeżowski, S. (2008). Yield traits of six clones of Miscanthus in the first 3 years following planting in Poland. *Ind. Crops Prod.* 27.1, 65–68. doi: 10.1016/j.indcrop.2007.07.013

Larsen, S., Jaiswal, D., Bentsen, N. S., Wang, D., and Long, S. P. (2016). Comparing predicted yield and yield stability of willow and Miscanthus across Denmark. *GCB Bioenergy* 8, 1061–1070. doi: 10.1111/gcbb.12318

Lesur, C., Jeuffroy, M. H., Makowski, D., Riche, A. B., Shield, I., Yates, N., et al. (2013). Modeling long-term yield trends of Miscanthus × giganteus using experimental data from across Europe. *Field Crops Res.* 149, 252–260. doi: 10.1016/j.fcr.2013.05.004

Lewandowski, I., Clifton-Brown, J. C., Scurlock, J. M. O., and Huisman, W. (2000). Miscanthus: European experience with a novel energy crop. *Biomass Bioenergy* 19, 209–227. doi: 10.1016/S0961-9534(00)00032-5

Lewandowski, I., Clifton-Brown, J., Trindade, L. M., van der Linden, G. C., Schwarz, K.-U., Müller-Sämann, K., et al. (2016). Progress on optimizing Miscanthus biomass production for the European bioeconomy: results of the EU FP7 project OPTIMISC. *Front. Plant Sci.* 7:1620. doi: 10.3389/fpls.2016.01620

Maddison, A. L., Camargo-Rodriguez, A., Scott, I. M., Jones, C. M., Elias, D. M. O., Hawkins, S., et al. (2017). Predicting future biomass yield in *Miscanthus* using the carbohydrate metabolic profile as a biomarker. *GCB Bioenergy* doi: 10.1111/gcbb.12418

McCalmont, J. P., Hastings, A., McNamara, N. P., Richter, G. M., Robson, P., Donnison, I. S., et al. (2015). Environmental costs and benefits of growing Miscanthus for bioenergy in the UK. *GCB Bioenergy* 9, 489–507. doi: 10.1111/gcbb.12294

Nie, G., Huang, L., Zhang, X., Taylor, M., Jiang, Y., Yu, X., et al. (2016). Marker-trait association for biomass yield of potential bio-fuel feedstock *Miscanthus sinensis* from Southwest China. *Front. Plant Sci.* 7:802. doi: 10.3389/fpls.2016.00802

Payne, R. W., Murray, D. A., Harding, S. A., Baird, D. B., and Soutar, D. M. (2015). *Introduction to Genstat® for Windows^{TM}, 18th Edn*. Hemel Hempstead: VSN International.

Richter, G. M., Riche, A. B., Dailey, A. G., Gezan, S. A., and Powlson, D. S. (2008). Is UK biofuel supply from Miscanthus water-limited? *Soil Use Manag.* 24, 235–245. doi: 10.1111/j.1475-2743.2008.00156.x

Robson, P., Jensen, E., Hawkins, S., White, S. R., Kenobi, K., Clifton-Brown, J., et al. (2013). Accelerating the domestication of a bioenergy crop: identifying and modelling morphological targets for sustainable yield increase in Miscanthus. *J. Exp. Bot.* 64, 4143–4155. doi: 10.1093/jxb/ert225

Robson, P., Mos, M., Clifton-Brown, J., and Donnison, I. (2012). Phenotypic variation in senescence in Miscanthus: towards optimising biomass quality and quantity. *Bioenergy Res.* 5, 95–105. doi: 10.1007/s12155-011-9118-6

Taylor, G., Allwright, M. R., Smith, H. K., Polle, A., Wildhagen, H., Hertzberg, M., et al. (2016). "Bioenergy trees: genetic and genomic strategies to improve yield," in *Perennial Biomass Crops for a Resource-Constrained World*, eds S. Barth, D. Murphy-Bokern, O. Kalinina, G. Taylor, and M. Jones (Cham: Springer International Publishing), 167–190.

Xue, S., Kalinina, O., and Lewandowski, I. (2015). Present and future options for Miscanthus propagation and establishment. *Renew. Sustain. Energy Rev.* 49, 1233–1246. doi: 10.1016/j.rser.2015.04.168

Lack of Impacts during Early Establishment Highlights a Short-Term Management Window for Minimizing Invasions from Perennial Biomass Crops

Natalie M. West[1,2]*, David P. Matlaga[2,3], Ranjan Muthukrishnan[4], Greg Spyreas[5], Nicholas R. Jordan[6], James D. Forester[4] and Adam S. Davis[2]

[1] Pest Management Research Unit, United States Department of Agriculture – Agricultural Research Service, Sidney, MT, USA, [2] Global Change and Photosynthesis Research Unit, United States Department of Agriculture – Agricultural Research Service, Urbana, IL, USA, [3] Department of Biology, Susquehanna University, Selinsgrove, PA, USA, [4] Department of Fisheries, Wildlife, and Conservation Biology, University of Minnesota, St. Paul, MN, USA, [5] Prairie Research Institute, Illinois Natural History Survey, Champaign, IL, USA, [6] Department of Agronomy and Plant Genetics, University of Minnesota, St. Paul, MN, USA

Managing intentional species introductions requires evaluating potential ecological risks. However, it is difficult to weigh costs and benefits when data about interactions between novel species and the communities they are introduced to are scarce. In anticipation of expanded cultivation of perennial biomass crops, we experimentally introduced *Miscanthus sinensis* and *Miscanthus* × *giganteus* (two non-native candidate biomass crops) into two different non-crop habitats (old field and flood-plain forest) to evaluate their establishment success and impact on ambient local communities. We followed these controlled introductions and the composition dynamics of the receiving communities over a 5-year period. Habitats differed widely in adult *Miscanthus* survival and reproduction potential between species, although seed persistence and seedling emergence were similar in the two biomass crops in both habitats. Few introductions survived in the floodplain forest habitat, and this mortality precluded analyses of their potential impacts there. In old field habitats, proportional survival ranged from 0.3 to 0.4, and plant survival and growth increased with age. However, there was no evidence of biomass crop species effects on community richness or evenness or strong impacts on the resident old field constituents across 5 years. These results suggest that *Miscanthus* species could establish outside of cultivated fields, but there will likely be a lag in any impacts on the receiving communities. Local North American invasions by *M. sinensis* and *M. sacchariflorus* display the potential for *Miscanthus* species to develop aggressively expanding populations. However, the weak short-term community-level impacts demonstrated in the current study indicate a clear management window in which eradicating species footholds is easily achieved, if they can be detected early enough. Diligent long-term monitoring, detection, and eradication plans are needed to successfully minimize harmful invasions from these biomass crops.

Keywords: biomass crops, *Miscanthus*, impacts, controlled invasions, agroecosystems

INTRODUCTION

Evaluating ecological risks associated with intentional plant introductions requires understanding species colonization and establishment success as well as potentially negative impacts on the recipient community (Theoharides and Dukes, 2007; Barney et al., 2013). For agricultural introductions, the disadvantages of a high escape probability may be mitigated by low potential impacts of that species on surrounding communities (Yokomizo et al., 2012; Grechi et al., 2014). However, stochasticity, agricultural breeding, and novel selection pressures in response to new interactions and environments can complicate predictions about the relative benefits versus threat potential of novel introductions (Mack, 2000; Moles et al., 2012; Richardson, 2013; Driscoll et al., 2014). Therefore, estimated responses may not be directly comparable across systems. Species traits and invasion history can provide a preliminary indication of how an introduction will fare (Davis et al., 2010), but species success and consequences depend on the spatial and temporal context and interactions with the receiving community (Hulme et al., 2013; Kumschick et al., 2015). To better predict potential costs associated with the cultivation and introduction of novel species, we need *in situ* empirical information on the establishment likelihood and community impacts associated with introductions (Flory et al., 2012; Scasta et al., 2015).

We measured the establishment success and impact (measureable change in ecological properties or processes, i.e., Simberloff et al., 2013; Blackburn et al., 2014) of *Miscanthus* introductions in two common non-agronomic habitats in central Illinois, USA. *Miscanthus* sp. have been widely introduced for horticulture, and more recently as biomass feedstocks, in the US and Europe since at least the 19th century. Escaped patches already present in the landscape tend to be small (<1 m^2), but there are locally extensive populations (Quinn et al., 2010; Dougherty et al., 2014; Schnitzler and Essl, 2015). We chose old field and floodplain forest habitats for two main reasons. First, these are dominant non-agricultural plant habitats in central Illinois. Forested floodplain areas have remained largely uncultivated, whereas old field sites are often located on farmland too unproductive to remain in cultivation. Second, both habitat types are commonly found adjacent to production areas, and for this reason are likely to be receptor habitats for *Miscanthus* escaping from production fields. Quantifying the likelihood of escapes surviving and reproducing in these receptor habitats provides a context for identifying potential costs and management associated with introducing *Miscanthus* production into the central Illinois landscape.

We know that many traits attractive for biomass crops are also associated with successful invasive species (Raghu et al., 2011; Flory et al., 2012; Schnitzler and Essl, 2015). *Miscanthus* taxa display a range of characteristics associated with invaders, such as rapid biomass accumulation, tall stature, allelopathic properties, and wide ecological tolerances and dispersal capabilities (Chou, 2009; Quinn et al., 2012; Matlaga and Davis, 2013; Hager et al., 2014; Hedìnec et al., 2014), suggesting the possibility of negative impacts once plants are established. However, whether such traits will allow *Miscanthus* to establish, and significantly change the

composition or functioning of receptor communities, requires evaluation (Drenovsky et al., 2012; Barney et al., 2013; Blackburn et al., 2014; Dick et al., 2014).

Impacts from non-native species are strongly context dependent and variable in magnitude and direction, which complicates assessments of new introductions (Byers and Noonburg, 2003; Pyšek et al., 2012; Hulme et al., 2013; Blackburn et al., 2014; Grechi et al., 2014). It can be difficult to distinguish invader impacts from other concurrent and potentially synergistic stressors (Dick et al., 2014; Kumschick et al., 2015). For instance, invader density likely influences variation in community interactions and impacts, but ecological impacts do not necessarily increase linearly with the density or perceived competitive dominance of the invader (Thiele et al., 2010; Jackson et al., 2015). Assessing multiple measures of introduction consequences in different environmental contexts is therefore vital for predicting the likelihood and impacts of invasion success.

We experimentally examined the establishment and impact of *Miscanthus* introduced at different densities into old fields and floodplain forest sites to: (1) quantify the viability of escapes into these habitats; (2) identify potential limitations and catalysts to *Miscanthus* establishment in non-crop habitats; and (3) evaluate the impacts of *Miscanthus* introduction on resident plant communities. We followed the long-term persistence of both clonal, seed-infertile, *Miscanthus × giganteus* "Illinois" clone (low risk, i.e., Quinn et al., 2015) and feral, seed-fertile, *Miscanthus sinensis* (high risk) to represent a spectrum of the potential invasiveness in *Miscanthus* germplasm being improved for biomass production. Escape viability and potential ecological limitations were evaluated by tracking recruitment, persistence, and growth of introduced plants over time. Impacts were assessed as measureable differences in species richness and evenness (components of diversity), as well as shifts in species and functional group abundance (measures of biotic interaction), between plots with and without *Miscanthus* introduced at different densities. Assessing the viability and negative impacts of non-native species introductions is important to inform prioritization and implementation of control strategies (Lewis and Porter, 2014). Our study is one of only a few to track metrics of community change over multiple years in response to controlled invasions into natural areas.

MATERIALS AND METHODS

Study Species

Miscanthus sinensis Andress. is a seed-fertile crop introduced from Japan for horticultural use in the 1800s. It became naturalized in the eastern U.S. by the mid-20th century, and is locally invasive (Quinn et al., 2010). *M. sinensis* is both a candidate biomass crop as well as a parent species to other candidate varieties (e.g., Arnoult and Brancourt-Hulmel, 2015). We collected *M. sinensis* root-stock and seeds from roadside and forest opening patches in Daniel Boone National Forest, Powell County, KY, USA, in September 2009. *Miscanthus × giganteus* 'Illinois' clone (hereafter, *M. giganteus*) J.M. Greef & Deuter

ex Hodkinson & Renvoize is a seed infertile hybrid of *M. sinensis* and *M. saccchariflorus* (Christian and Haase, 2001), and is one of the most widely planted cellulosic biofeedstock in the U.S. (Anderson et al., 2015). We obtained *M. giganteus* root stock for experimental plantings from the Chicago Botanic Garden. Utilizing plugs rather than seeds allowed us to evaluate plant survival and provide an estimate of long-term persistence once plants were introduced, while controlling accidental seed introductions into our study communities. We also estimated seed-based recruitment and overwintering persistence within our plots. Because the 'Illinois' clone is seed-infertile, we obtained seeds harvested from a pilot plantation of a pre-release, seed-fertile, tetraploid *M. giganteus* cultivar ('PowerCane,' Mendel Biotechnology, Hayward, CA, USA; see references in Bonin et al., 2017) to evaluate the potential for seed-based recruitment into study areas. Multiple studies have examined the seed and seedling viability and persistence of both 'PowerCane' and *M. sinensis* under various conditions and in various habitats (e.g., Smith and Barney, 2014; West et al., 2014a; Hager et al., 2015a; Smith et al., 2015; Bonin et al., 2017); these studies provide an understanding of the demographic contributions of seed to *Miscanthus* invasion potential. For our purposes, seed-based recruitment provides an additional measure of habitat suitability for escapes.

Experimental Plantings

We established *Miscanthus* in three old field and three floodplain forest sites. Our old field habitats, Phillips and Trelease Prairies and the Vermillion River Observatory, and two floodplain forest sites, Nanney and Richter Tracts, are owned and managed by the University of Illinois Urbana–Champaign. The last floodplain forest habitat, Homer Lake, is part of the Champaign County, IL Park District. Consistent with management practices in our region, old field sites were mowed annually in the spring to a height of 7.5–10 cm to inhibit woody encroachment. Floodplain forests were unmanaged and subject to frequent and occasionally prolonged flooding.

Both *Miscanthus* species were propagated in the greenhouse prior to planting. We divided potted *Miscanthus* into approximately 10-cm diameter plugs with 10 to 15-cm long shoots. We hardened them off for a week and then transported them to the field. We introduced plugs into eight 10-m × 10-m single-species plots per site (four plots per species) in a split-split plot design (Supplement Figure 1A). Main single-species plots were divided into four 5-m × 5-m subplots that were each randomly assigned one of four density treatments: high ($n = 16$ plants with 1-m spacing, 1 plant/m^2); medium ($n = 9$ plants with 1.25-m spacing, 0.56 plant/m^2); low ($n = 4$ plants with 1.67-m spacing, 0.25 plant/m^2); or control ($n = 0$ plants/m^2). Plantings were positioned a minimum of 1-m from the subplot edge, and planting layouts were centered within the subplots (Supplement Figure 1B).

Introductions were initiated in April 2010. Plugs were planted into 25 cm deep holes and covered with a 25-cm × 25-cm heavy-gauge plastic mesh secured with sod staples to prevent movement due to flooding or animals. To maintain density treatments, plants that did not resprout by the spring census in 2011 and 2012 were removed and replaced. Nearly 75% of plugs (1037 out of 1392) were replanted in 2011 due to mortality; only 27% (379 out of 1392) were replanted in 2012. To control for effects of planting disturbance on community comparisons, we did sham plantings, which consisted of digging similar sized holes within the control subplots and then replacing the soil. The number of sham plantings was set as the median number of plantings (or replantings) out of all densities within that plot. We minimized soil disturbance during introduction, and any excess soil remaining after planting was transported out of the plot. Because *Miscanthus* establishment is sensitive to water limitation (Zub and Brancourt-Hulmel, 2010; Anderson et al., 2015), plugs were watered at the time of planting (or replanting), and periodically for the following month. Therefore, our data on establishment reflect a best-case scenario in terms of moisture conditions.

Habitat Characteristics and Establishment

We measured a combination of soil fertility and soil water conditions to represent abiotic habitat differences. To quantify soil fertility, we collected soil samples to a depth of 10 cm from the center of each subplot with a 10 cm diameter soil corer in summer 2011. These samples were dried and sieved to remove non-soil particles, and analyzed by A&L Great Lakes Laboratories for plant macro- and micronutrients (P, K, Mg, Ca, S, Zn Mn, Fe, Cu, NO_3^-, NH_4^+, and B), pH, soil organic matter, and cation exchange capacity (CEC). We measured soil redox potential as an integrated measure of saturated soil water conditions over the growing season using the Indicator of Reduction in Soil (IRIS) procedure (Castenson and Rabenhorst, 2006; Jenkinson and Franzmeier, 2006). We left IRIS tubes in the control subplot of each plot from April to August 2014, and recorded the amount of ferrihydrite paint lost from the tube surface at the end of the season. To quantify surface area exposed, we took digital images of each plane of the tube surface, and combined the multiple views into a single image. We then adjusted combined images to a consistent size (2745 × 675 pixels), and counted the number of pixels that lacked paint using MATLAB (Mathworks, Natick, MA, USA). We used these counts to calculate the percent paint surface area lost to redox reactions. Additionally, we did a pulse measurement of soil water content by sampling two 10-cm soil cores per sub-subplot 24–36 h after a rain of more than 2.5 cm in July 2013. We weighed wet samples, dried them for 72 h, took the dry weight, and subtracted the difference to estimate gravimetric soil moisture. These two measurements allowed us to compare relative differences in soil water status among plots.

To simplify the inclusion of soil nutrient conditions in the examination of habitat differences, and to account for strong covariance among the soil nutrients, we created a composite soil variable. We identified the optimal group of uncorrelated soil variables necessary to adequately distinguish habitats using a linear discriminant analysis (*subselect* R package: *ldaHmat* and *eleaps* functions). Improvement in correlation with a first canonical axis peaked with four soil factors (Mg, CEC, Fe, and B), and these variables successfully predicted habitat membership with less than a 5% error. Therefore, we combined them into

a composite soil fertility variable quantified as the first axis scores from a principal components analysis of the four identified variables.

To represent relative differences associated with light availability within our two habitats, we evaluated light conditions both above and below understory vegetation (vegetation cover below any existing tree canopy). We measured photosynthetically active radiation above the understory canopy (approximately 1.5 m from the ground, in μmol m^{-2} s^{-1}, PARA) and light transmittance (% PARA). These factors were quantified at the subplot level, and then averaged for analysis at the plot level. We measured both above and below understory canopy PAR with a linear ceptometer (LP-80 Accu-PAR, Decagon Devices, Court Pullman, WA, USA) as the average PAR at four points around each subplot. We quantified transmittance (the amount of above understory PAR penetrating to ground level) as below understory PAR/above understory PAR.

Miscanthus Recruitment

To test habitat type effects on seedling emergence, we established caged plots (to deter herbivory and seed predation) in one randomly selected corner of each plot in late fall 2011 (Supplement Figure 1B). Seeds were planted in 10 cm × 10 cm seed trays filled to a depth of 5 cm with soil from the receiving site. Each tray was placed in a cylindrical 1-mm mesh cage 40 cm in diameter and 30 cm high, which was additionally filled with site-collected soil to allow the seed tray to lie flush with the surrounding soil surface. The base of each cage was buried approximately 10 cm and secured in place. Because of site-use and material transfer agreement restrictions, we were unable to plant the seed-fertile *M. giganteus* in the field. However, previous work on the regeneration niche of this pre-release cultivar indicates fertile *M. giganteus* seed performs similarly to *M. sinensis* (Smith and Barney, 2014; West et al., 2014a). We monitored seedling emergence monthly March–November 2012, and seedlings were removed after each count to avoid confounding measures of emergence and survival.

To examine habitat type effects on seed viability after overwintering, additional seeds were cold-stratified *in situ* within stainless steel mesh packets buried in the field next to seedling plots in November 2012 (Supplement Figure 1B). Because it did not require field germination, we were able to use both species of *Miscanthus* for this test. We staked each 20 cm × 20 cm 0.5-mm wire mesh bag containing 100 seeds of the appropriate species in each corresponding subplot in November 2012. Bags were placed on bare ground, and any detritus moved to accommodate the bag was replaced to emulate site conditions. Bags remained in place until late April 2013, when they were collected and germinable seed fraction determined by counting the number of overwintered seeds that germinated under greenhouse conditions.

Miscanthus Performance

We recorded plant survival and tiller number twice annually from spring 2010 to 2014 to quantify plant performance and the integrity of density treatments over time. Census timing during the year was variable due to phenological fluctuation; thus, spring

measurements occurred in April–May, and fall in October–November. Per year plant measurements, such as growth and survival, involved the period from spring to spring each year. In 2014, the second census was conducted in late July to optimize eradication efforts.

In 2014, we also quantified *Miscanthus* biomass within plots. We clipped and weighed all aboveground *Miscanthus* biomass per individual plant in the field. A subset of these plants were taken back to the lab, dried for 48 h at 45 degrees Celsius, and weighed to determine the relationship between field and dry weights (see footnote to **Table 1**). Additionally, we measured the area covered by each plant by measuring the widest axis of tiller extent and the one perpendicular to it, and calculating the area as an ellipse. Any flowering panicles produced in 2013 were collected, and the number of caryopses produced by habitat and by plant were quantified by weight relative to a 100 caryopsis weight standard. Viable seed production by *M. giganteus* 'Illinois' clone is inhibited by incomplete gametophyte development that results in sterility (Słomka et al., 2012). Therefore, these estimates merely represent a quantification of potential seed production within these habitats given the possibility of fertile genotypes being introduced for agronomic purposes (i.e., Bonin et al., 2017). Because our management agreements required panicle collection before dehiscence (to avoid unintentional spread and naturalization at the study sites), we were unable to reliably quantify viable seed produced for *M. sinensis*, and can only present relative differences in reproductive effort.

Miscanthus Impacts on the Local Plant Community

Plant community data were obtained by randomly sampling a total of 2 m^2 within each density subplot in late June-early July 2011–2014. Each year, we quantified the total number and percent cover of species in eight 25 cm × 25 cm quadrats along four randomly placed transects within each density subplot, and combined these 32 small-scale estimates of plant cover to represent community metrics at the density subplot level. Species richness (S) was the total number of unique species recorded within the density subplot. We calculated Pielou's species evenness (J), where P_i is the relative contribution of ith species to total cover, and S is species richness [$J = -\Sigma (P_i * \ln(P_i)/\ln (S)$], i.e., Maron et al., 2014). Abundance observations were combined for the density subplot by converting cover estimates to area approximations (e.g., 80% of a 25 cm × 25 cm quadrat = 5 cm^2) and summing them for each species.

DATA ANALYSIS

We used R v.3.3.1 (R Core Team, 2016) for all analyses. Inconsistent *Miscanthus* survival through time and among plots precluded an exact maintenance of original planting densities. Thus, *Miscanthus* density in analyses was represented as the average number of *Miscanthus* plants per m^2 from 2011 to 2014 within the 4 m × 4 m density subplot. Although many plots had fewer individuals than originally planted by the end of

TABLE 1 | *Miscanthus* recruitment and establishment: Mean ± SD, as well as the range (in parentheses, minimum–maximum) of measurements in old field and floodplain forest plots.

	M. giganteus		*M. sinensis*	
	Old field	**Floodplain**	**Old field**	**Floodplain**
(A) Recruitment				
(Proportion seeds to seedlings)				
Overwintering	0.23 ± 0.08[1]	0.23 ± 0.09[1]	0.32 ± 0.08	0.36 ± 0.1
	(0.03 − 0.34)	(0.08 − 0.39)	(0.18 − 0.41)	(0.20 − 0.49)
Field emergence	*	*	0.12 ± 0.07	0.26 ± 0.15
	*	*	(0 − 0.28)	(0 − 0.56)
(B) Establishment				
Per plot				
Survival	0.29 ± 0.13	0.04 ± 0.05	0.38 ± 0.17	0.02 ± 0.04
	(0.11 − 0.48)	(0 − 0.18)	(0.05 − 0.65)	(0 − 0.11)
# Surviving plants[2,3]	17.8 ± 6.8	3.9 ± 2.3	19.3 ± 7.2	4 ± 2.6
	(8 − 27)	(2 − 8)	(3 − 27)	(1 − 6)
Biomass (g)[4,5]	326.8 ± 288.4	24.8 ± 21.4	168.5 ± 131.8	5.7 ± 5.6
	(1.51 − 3540)	(0.20 − 81.0)	(1 − 2160)	(0.32 − 27.1)
Area occupied by *Miscanthus* (m^2)	7.2 ± 4.6	1.0 ± 0.7	5.3 ± 4.1	0.53 ± 1.0
	(2.4 − 18.2)	(0 − 2.0)	(0.9 − 13.8)	(0 − 2.4)
# Flowering plants	5.1 ± 2.8	*	12.3 ± 6.4	*
	(1 − 10)		(1 − 25)	
Per plant				
Area (m^2)	0.33 ± 0.2	0.37 ± 0.2	0.24 ± 0.2	0.35 ± 0.2
	(<0.01 − 1.61)	(0.02 − 0.91)	(<0.01 − 1.2)	(0.04 − 1.3)
# Tillers	7.8 ± 4.5	2.6 ± 1.3	12.4 ± 6.8	3.3 ± 1.9
	(1 − 47)	(1 − 6)	(1 − 96)	(1 − 9)
# Inflorescences	2.2 ± 0.7	*	5.2 ± 3.0	*
	(1 − 8)		(1 − 37)	
# Caryopses	5552.9 ± 3605.1	*	7890.9 ± 6864.8	*
	(482 − 37949)		(67 − 108767)	

*Indicates metrics for which data are unavailable. Recruitment was measured over a 1 year period between 2012 and 2013; we quantified Establishment in 2014. [1]Estimates reported for seed-fertile M. giganteus 'PowerCane,' as the 'Illinois' clone is seed-infertile. [2]# Plots with surviving plants: M. giganteus: n = 12 (field) and 7 (floodplain); M. sinensis: n = 12 (field) and 3 (Floodplain). [3]# Live plants total: M. giganteus: n = 213 (field) and 27 (floodplain); M. sinensis: n = 230 (field) and 12 (floodplain). [4]M. giganteus dry weight (g) = 0.29*field weight + 0.39; p < 0.001; r^2 = 0.98. [5]M. sinensis dry weight (g) = 0.31*field weight − 0.30; p < 0.001; r^2 = 0.99.*

the experiment, a significant difference in average plant density persisted among the different treatment subplots ($p < 0.001$ for mean density and pairwise comparisons, Supplement Figure 2). We incorporated replants into survival estimates as additional plants included in the summation of the total number of individuals planted per plot.

Habitat Characteristics

We used non-metric multidimensional scaling (NMDS) to display the range of site variation in environmental variables (function *metaMDS*, *vegan* package, with Gower metric dissimilarities to account for variables measured at different scales), and its relation to plant survival per single species plot (overlaid using *ordisurf* function, see below for calculation). We evaluated the correlation strength of five environmental parameters (PARA, gravimetric soil moisture, soil redox potential, transmittance, and composite soil fertility) with the NMDS axis scores (*envfit* function), and plotted the significant habitat vectors with an r^2 greater than 0.5. Because these data

were analyzed at the plot level, density was not included as a factor.

Recruitment

We quantified potential recruitment differences between habitats as: (1) overwintering seed viability (*M. sinensis and M. giganteus*); and (2) field emergence (*M. sinensis*). We analyzed mean recruitment differences between habitats separately for each species using linear mixed effects models (function *lme* in the *nlme* package) with plot nested within site as a random effect.

Demographic Performance of *Miscanthus*

We quantified overall survival as the proportion of total individuals planted per plot that were alive in 2014. This total number of individuals planted per plot includes the initial 29 plants established in 2010, as well as any replants introduced in 2011 or 2012. Because these data were analyzed at the plot level, density was not included as a factor. We evaluated the influence

of plant density on the resultant area occupied by *Miscanthus* in subplots by the end of the experiment (2014) using a linear model with pairwise Tukey tests to evaluate treatment differences.

To evaluate individual survival and growth, we analyzed differences in: (1) age-related survival probability [i.e., *g(x)* in Gotelli, 2008] and growth; and (2) plant performance between habitats. Because density had no significant effects on growth and survival parameters (see Results), it was excluded as a factor from these analyses.

(1) Age – Related Survival Probability and Growth

We calculated the survival probability (p_s) for each plot at each successive age as:

$$p_s(x) = s(x)/s(x-1) \qquad (1)$$

where $s(x)$ is the cumulative survivorship at age x, calculated as:

$$s(x) = N(x)/N(x_0) \qquad (2)$$

where N is the number of individuals. Year 1 and 2 estimates include data from the initial planting as well as the 2011 and 2012 replantings, whereas year 3 included plants from the 2010 and 2011 cohorts. We quantified growth as the change in the maximum tiller number per plant recorded between springs each year. To avoid confounding growth estimates (which were often negative) with mortality, we only included plants that survived the full year (had non-zero tiller numbers in two successive springs, *M. giganteus*: $n = 595$; *M. sinensis*: $n = 440$).

We analyzed survival and growth at different ages with linear mixed effects models (function *lme* from R *nlme* package). Survival probability (p_s) at different ages was compared at the plot level between habitat and species with plot and then year nested within site as random effects. Growth (change in tiller number) was compared at the plant level between habitat and species with random effects nested as year:plant ID:subplot:plot:site.

(2) Plant Performance

We intended to examine final plant tiller count, biomass in grams per surviving individual, area in m^2, flower number and potential seed production to compare overall plant performance between habitats. However, low plant survival and lack of flowering in the floodplain forest rendered statistical habitat comparisons impossible. Therefore, we merely present the data available for differences between habitats.

Miscanthus Impacts on Old Field Community Structure

Because plant survival was extremely low in floodplain forest habitats (see Results below), we limited our analysis of community impacts to the old field sites. We used a linear mixed effects model (*lme* in R *nlme* package) to examine relative impact of *Miscanthus* presence and density on community evenness and richness after 5 years (that is, in 2014). *Miscanthus* density × *Miscanthus* species were entered as fixed effects, and plot was nested within site as a random effect in the model.

We calculated the relative impact of *Miscanthus* on evenness and richness (two components of diversity) within each subplot using the relative impact (RI) equation from Vilà et al. (2006) (adapted from Armas et al., 2004).

$$\text{RI} = \frac{(V_{\text{control}} - V_{\text{treatment}})}{(V_{\text{control}} + V_{\text{treatment}})} \qquad (3)$$

A negative RI value indicates an increase of the dependent variable (V, e.g., richness or evenness) associated with invader presence (positive impact of invasion). Conversely, a positive value means that invader presence decreases V (negative impact of invasion). A zero value indicates that the invader presence does not have a significant effect on the parameter (Vilà et al., 2006). The RI for each *Miscanthus* introduction subplot was computed using values from the control subplot within the same plot. To further determine whether *Miscanthus* presence significantly affected overall evenness or richness of the plant community, we performed a single sample *t*-test of the relative impact on each of these metrics within *Miscanthus* subplots with a null hypothesis of $\mu = 0$ (i.e., RI = 0). In other words, if the mean RI value is significantly different than 0, there is a significant impact of the invader, relative to the control, for the variable measured. Further, if the RI is significant, positive values indicate greater declines in the measured variable (negative impacts) associated with invader presence. Negative RI values indicate potential increases in the variable associated with invader presence.

Miscanthus Impacts on Community Composition

We examined the influence of *Miscanthus* introduction and density on community dynamics to evaluate potential implications for old field community composition and structure over time. We determined annual species turnover (shifts in community constituents) and change in species rank abundances (shifts in species hierarchies) from 2011 to 2014. Two species (*Festuca arundinacea* and *Solidago canadensis*) present in all old field plots formed the dominant matrix vegetation (>50% cover in most old field plots). We excluded these two from community dynamics analyses to maximize our ability to detect initial short term impacts on species composition.

Species annual turnover was quantified as both the proportion of species dropping out of plot censuses between 1 year and the next ('− species') and species added between 1 year and the next ('+ species') (*turnover* in R *codyn* package). Mean change in species rank was quantified as the average difference in species rank abundance between consecutive years among species that were present across the entire measurement period, and represents community shifts in relative abundance over time (Hallett et al., 2016, *rank_shift* in R package *codyn*). To account for the possibility of changes in functional group abundance over time with *Miscanthus* introduction, we examined the effect of *Miscanthus* density on the relative prevalence of four functional groups (grasses, forbs, legumes, shrub/woody species) over time (*adonis* in R *vegan* package, strata = site). We also evaluated each variable for overall impacts (RI) from *Miscanthus* presence (single sample *t*-test with null hypothesis of RI = 0).

RESULTS

Habitat Characteristics

PARA, soil moisture, and soil fertility were strongly associated with the NMDS axis scores [$r^2 = 0.92$ (PARA); 0.66 (soil moisture); 0.84 (soil fertility), $p < 0.01$ for all]. These variables also provide good separation between the two habitat types (**Figure 1**). Although redox potential and transmittance also significantly separated between NMDS axes, their association was weaker [$r^2 = 0.22$ (redox); 0.32 (transmittance), $p < 0.01$ for both]. After the third year, we did not detect any *Miscanthus* in one floodplain site (Richter), and only two individuals of *M. giganteus* in another (Nanney). Several plants of both species did persist in the third floodplain site (Homer Lake). In contrast, all old field plots had many surviving individuals. Any small scale differences in how habitat characters within sites might have affected survival were obscured by the overwhelming survival difference between habitats (see below). Therefore, habitat characteristics associated with plant survival could not be statistically compared.

Miscanthus Recruitment

We tested the effect of overwintering on seed germination for both *Miscanthus* species. Seed germination after overwintering differed between *Miscanthus* species; however, there was no significant effect of habitat type ($t = -2.82; df = 4, 40; p = 0.007$, **Table 1A**). Although, we could not test *M. giganteus* for habitat differences in seedling emergence, *M. sinensis* did not differ in seedling emergence between habitats ($t = 2.12; df = 4, 42; p = 0.1$, **Table 1A**).

Miscanthus Demographic Performance

Miscanthus sinensis had both higher survival in old fields, and lower survival in floodplains, compared to *M. giganteus* ($p_{interaction} < 0.01$, df.residual $= 42$, $z = -3.5$, **Table 1**). *M. giganteus* survival was reduced nearly 85%, and *M. sinensis* survival over 90%, in floodplain forests compared to old fields (**Table 1B**). Overall, survival differed substantially between habitats for both species (**Figure 1**; df.residual $= 20$, *M. giganteus*: $p < 0.01$, $z = -3.1$; *M. sinensis*: $p < 0.01$, $z = -3.8$).

Increased planting density did increase the area of the plot occupied by *Miscanthus* species by 2014 (**Figure 2**). There was a significant difference in *Miscanthus* area with density treatment ($p < 0.001$, $F = 5.44$ on 5 and 64 *df*); however, the low and medium treatments were not significantly different from each other in final *Miscanthus* area ($p > 0.01$ for high versus low and medium; $p = 0.18$ for low versus medium) by 2014. Additionally, there was no difference between *Miscanthus* species ($p = 0.28$). There was also no significant effect of plant population density on either growth or survival (e.g., **Figure 3**; $p > 0.1$ for interactions of density with habitat, survival probability, and number of tillers). Density was therefore excluded from subsequent growth and survival analyses, and we present growth and survival at the whole plot level (out of 29 individuals, plus replants, planted in each single species plot).
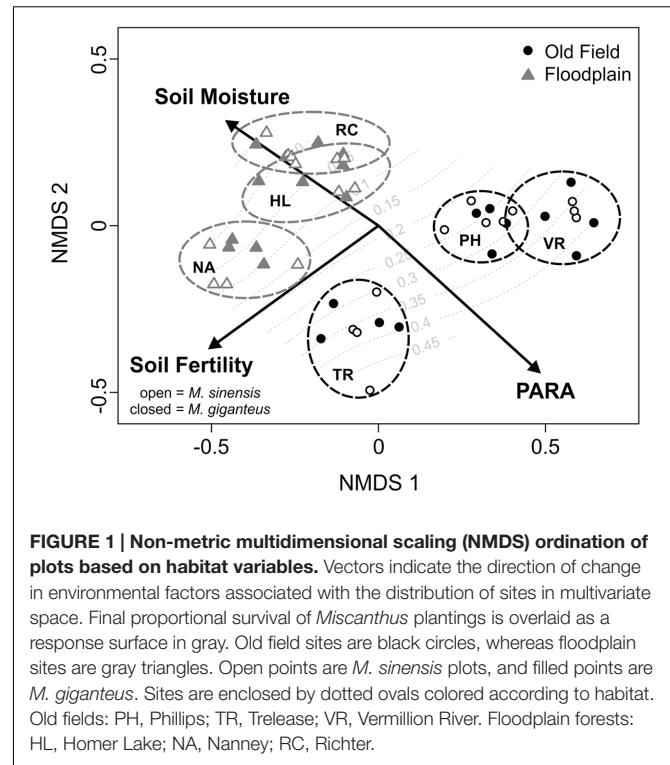
FIGURE 1 | Non-metric multidimensional scaling (NMDS) ordination of plots based on habitat variables. Vectors indicate the direction of change in environmental factors associated with the distribution of sites in multivariate space. Final proportional survival of *Miscanthus* plantings is overlaid as a response surface in gray. Old field sites are black circles, whereas floodplain sites are gray triangles. Open points are *M. sinensis* plots, and filled points are *M. giganteus*. Sites are enclosed by dotted ovals colored according to habitat. Old fields: PH, Phillips; TR, Trelease; VR, Vermillion River. Floodplain forests: HL, Homer Lake; NA, Nanney; RC, Richter.
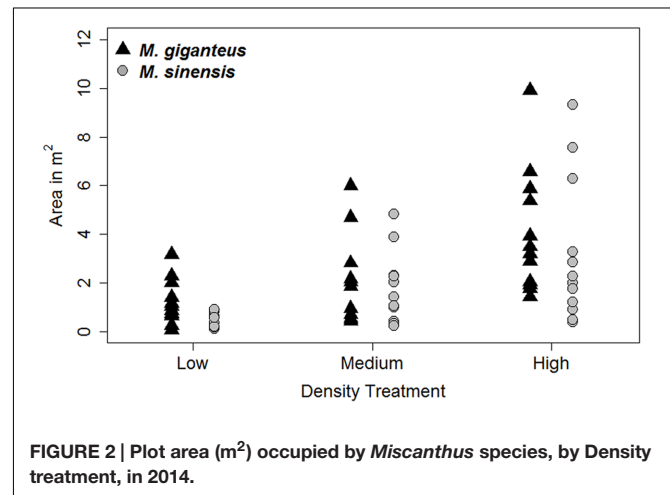
FIGURE 2 | Plot area (m^2) occupied by *Miscanthus* species, by Density treatment, in 2014.

Age – Related Survival Probability and Growth

Miscanthus survival probability with age and habitat did not differ between species (age: $p = 0.08$, $t = -1.8$, 92 *df*; habitat: $p = 0.24$, $t = -1.4$, 4 *df*). However, age-related survival did differ between habitats ($p_{habitat*age} = 0.02$, $t = -2.4$, 92 *df*; **Figures 3A,B**). Survival probability for both species increased with age in old fields, but not floodplain forests.

Growth displayed a similar pattern. Both the number of tillers and change in tiller number tended to increase with age in old fields, but not floodplain forests ($p < 0.01$, $z = -5.1$, 282 *df*; **Figures 3C,D**).
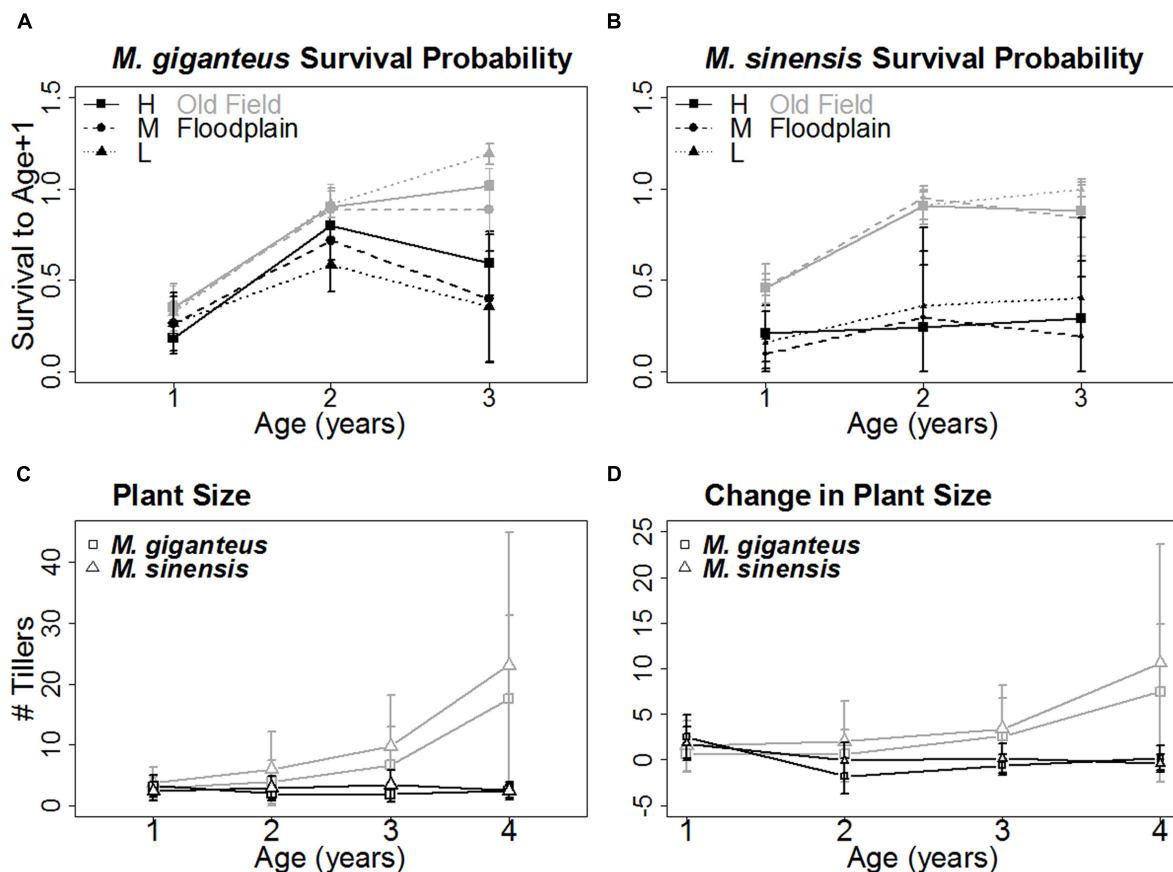
FIGURE 3 | Age-related survival and growth of each species (Mean ± SD). The probability of surviving to the next year increased similarly with age for both *M. giganteus* **(A)** and *M. sinensis* **(B)** in old field (gray) but not floodplain (black) habitats. Size, represented by tiller number **(C)** and growth, represented by change in tiller number **(D)**, with age followed a similar pattern. Both increased with age in old field but not floodplains for both *M. giganteus* (squares) and *M. sinensis* (triangles). The *x*-axis for **(A)** and **(B)** represents the three yearly age transitions. The *x*-axis for **(C)** and **(D)** represents years of age.

TABLE 2 | Richness (A, # of species) and Evenness (B, J) for control (no *Miscanthus*) and Treatment (*M. giganteus* or *M. sinensis* addition) plots in each of the three old field sites.

Site	(A) Richness			(B) Evenness		
	Control	*M. giganteus*	*M. sinensis*	Control	*M. giganteus*	*M. sinensis*
Phillips Tract	7.1 ± 1.3	7.0 ± 0.3	8.6 ± 1.0	0.49 ± 0.03	0.5 ± 0.03	0.5 ± 0.03
Trelease Prairie	14.5 ± 1.3	18.6 ± 1.7	17.3 ± 0.7	0.64 ± 0.03	0.7 ± 0.02	0.6 ± 0.03
Vermillion River	18.0 ± 1.0	18.3 ± 0.6	19.8 ± 1.1	0.66 ± 0.03	0.6 ± 0.02	0.7 ± 0.01

Final Plant Performance

Performance of surviving plants also varied significantly between habitats (**Table 1B**). Biomass and final tiller numbers were both greater in old field habitats relative to floodplain forests. However, on average, individual plant area was not. Within years, plants detected in the spring were consistently present (though sometimes with fewer tillers) in the fall. Most mortality occurred from fall to spring: for instance, there were no live plants recorded in the Richter (floodplain) site after fall 2012. Estimated reproduction did vary between species, but no plants flowered in the floodplain habitat. Therefore, old field habitats not only supported plant persistence, but also greater plant size

and reproductive biomass through time compared to floodplain forests.

Miscanthus Impacts on Community Structure

Miscanthus presence was associated with marginal increases in richness relative to control plots ($p < 0.001$, $t = -3.90$, 71 *df*, **Table 2A**). Excluding *Miscanthus* additions, introduction plots had 1.8 (±0.4 SE) species more than control plots. Relative richness impacts (RI) were unrelated to *Miscanthus* species identity ($p = 0.46$, $t = -0.74$, 46 *df*) or average density within
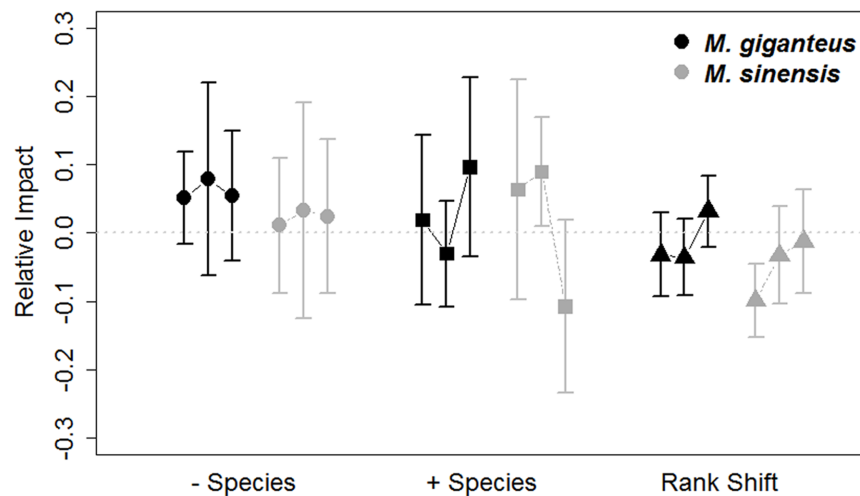
FIGURE 4 | Relative impacts (RI, Mean ± SE) on species turnover and species ranks in *M. giganteus* (black) and *M. sinensis* (gray) plots each year from 2011 to 2014. The values for each of the three consecutive year-to-year transitions are connected by lines for each species. The gray dotted line indicates RI value of 0, indicating no impact. Positive RI values indicate greater declines in measured variables relative to gain and can be interpreted as negative associations with *Miscanthus* addition. Species turnover differed from year-to-year [+ species (appearances) = triangles, − species (disappearances) = circles], but mean shifts in species rank (squares) did not. *Miscanthus* introduction did not influence these community metrics, regardless of species.

the subplots ($p = 0.57$, $t = -0.56$, 46 df) compared to controls. Similarly, *Miscanthus* presence did not affect evenness ($p = 0.98$, $t = -0.03$, 71 df), regardless of *Miscanthus* species ($p = 0.83$, $t = 0.21$, 46 df, **Table 2B**) or density ($p = 0.06$, $t = -1.9$, 46 df). Overall, we did not detect strong impacts of *Miscanthus* introduction on community structure metrics.

Miscanthus Impacts on Community Composition

Species turnover did vary by year (− species: $p < 0.001$, $t = -3.8$; + species: $p = 0.002$, $t = 3.1$; 189 df). Additionally, turnover was unaffected by *Miscanthus* species identity (− species: $p = 0.9$, $t = -0.2$; + species: $p = 0.2$, $t = -0.1$; 92 df) or density (− species: $p = 0.4$, $t = 0.8$; + species: $p = 0.2$, $t = -1.2$; 189 df). *Miscanthus* introduction in general did not appear to exclude species (RI − species: $p = 0.12$, $t = 1.55$, 215 df), or increase new species occurrences (RI + species: $p = 0.4$, $t = 0.8$, 215 df; **Figure 4**) relative to control plots.

Miscanthus introduction did increase species rank shifts relative to control plots overall (RI rank shift: $p = 0.03$, $t = -2.1$, 215 df). However, mean species rank shift did not differ between years, species or with *Miscanthus* densities (linear model: Year: $p = 0.6$, $t = 0.5$, 189 df; Species: $p = 0.2$, $t = 1.4$, 92 df; Density: $p = 0.3$, $t = 1.0$, 189 df). The abundance of functional groups within plots varied by year and between *Miscanthus* species (Year: $p = 0.006$, $F = 2.5$, 1 df; Species: $p = 0.004$, $F = 4.3$, 1 df; **Figure 5**), but did not vary with *Miscanthus* density ($p = 0.4$, $F = 4.3$, 1 df). Overall, *Miscanthus* had some association with relative abundance of species and functional groups in the community. In addition to *Miscanthus*, introduction subplots had around two species more relative to control subplots, and RI varied by year and

species. *Miscanthus* did not appear to exclude species from the community.

DISCUSSION

Miscanthus will likely escape and establish in habitats surrounding biomass production fields, but whether these introductions lead to negative community impacts remains uncertain given the limited short term empirical data available. Both floodplain and old field habitats studied were susceptible to early invasion (e.g., successful emergence and seed persistence), but differed greatly in persistence of established plants. We did observe some shifts in relative species and functional group abundances associated with *Miscanthus* presence in old field habitats. However, there is not a clear pattern indicating whether these shifts may eventually drive emergent impacts such as competitive exclusion with increasing *Miscanthus* dominance (i.e., MacDougall and Turkington, 2005; Gaertner et al., 2014).

We implemented controlled introductions of various *Miscanthus* densities in different sites and habitats to consider potential invasion success under a range of conditions. Successful establishment and increase in survivorship with age suggests *Miscanthus* can become community constituents in old field habitats. Surveys of naturalized *M. sinensis* and congener *M. sacchariflorus* (the two parent species of *M. giganteus*) in the US and Canada have associated these species with open and disturbed habitats, such as roadsides, agricultural field margins, and forest and residential property edges (Bonin et al., 2014; Dougherty et al., 2014; Hager et al., 2015b; Smith et al., 2015). Similarly, our sites were mowed annually, which likely improved conditions for establishment and growth. We found that species and functional group abundances in the resident
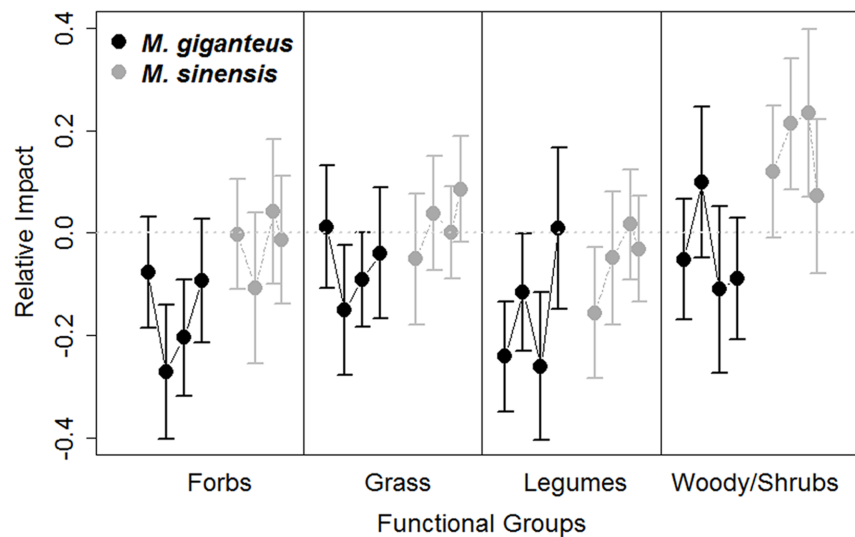
FIGURE 5 | Relative impact (RI, Mean ± SE) of *Miscanthus* introduction on the proportion abundance of functional group cover in *M. giganteus* (black) and *M. sinensis* (gray) plots each year from 2011 to 2014. Each dot represents consecutive single year values, connected by lines for each species. The gray dotted line indicates RI value of 0, indicating no impact. Positive RI values indicate increasingly negative effects of the invader. Functional abundance did vary among years and between *Miscanthus* species, with *M. sinensis* displaying slightly stronger RI.

community were affected by *Miscanthus* introductions into old fields. However, relative impacts on these community variables were not strong. This may be due in part to the site history of our old field communities. Previous invasions or disturbances can remove sensitive species and create a 'hardier' community that is resistant to the effects of subsequent, functionally similar invaders (i.e., Ricciardi et al., 2013). All three of our old field sites are heavily dominated by a matrix of *Festuca arundinacea* and *Solidago canadensis*, and were mowed annually, which likely improved conditions for the dominant species and establishment and growth of *Miscanthus*. This combination of dominance and disturbance could have already imposed limitations on the subdominant species assemblage present.

We noted that species richness was slightly higher when *Miscanthus* was added, and that there were some shifts in functional groups. This observation may illustrate the complexity of potential community impacts of *Miscanthus*. It is possible that *Miscanthus* can eventually reduce local dominance by key matrix species, thus opening spaces for other less frequent species. Such complex dynamics might result from allelopathic effects that *Miscanthus* can exert in some systems (Chou, 2009; Hedìnec et al., 2014; Hager et al., 2015b). More broadly, novel species introductions have been found to be both positively and negatively associated with community richness patterns, and this inconsistency has been attributed to characters such as measurement scale (i.e., Shea and Chesson, 2002; Chen et al., 2010), biotic resistance (i.e., Levine et al., 2004), resource availability and disturbance (i.e., Davis et al., 2000), and community interaction strength (i.e., MacDougall and Turkington, 2005). Whether our observed impact on species and functional group abundance represents a driving interaction (as opposed to 'passive,' MacDougall and Turkington, 2005) requires

further study. There was a great deal of variation in the direction and strength of response over time. Although the two *Miscanthus* species were not statistically different in their relative impacts, *M. sinensis* impact values did tend to be more positive (greater negative impact) compared to *M. giganteus*, and there was a complete reversal of this pattern for species appearances (+ species) from year 3 to 4 (**Figures 4**, **5**). More replicated plots along a greater diversity or disturbance gradient might show whether these contingencies reflect real differences in community impacts related to *Miscanthus* invasions.

Density of plantings had no significant influence on any of the variables measured. We expected higher colonization pressure to increase establishment and impact strength (Ricciardi et al., 2013). Planting greater numbers of *Miscanthus* did increase the population size (number of surviving individuals), and area occupied by *Miscanthus*, in higher density subplots, but did not increase individual plant survival or the likelihood of impacts. *Miscanthus* species can form dense, monotypic stands in both the native and non-native range, and in addition to high biomass accumulation, litter accumulation is extensive (Stewart et al., 2009; Dougherty et al., 2014; Hager et al., 2015b). It may be that the higher density of individuals would have led to greater effects over time. Additionally, because early planting mortality was high and required replanting to preserve initial density treatments, plant ages varied by up to 2 years within some plots by the end of the experiment. As such, our ability to detect the impact of increased *Miscanthus* density on plant community dynamics was likely somewhat obscured by this difference in times available for biomass accumulation and, thus, plant size, within plots of similar density. It was only in the last year of the experiment that plantings, particularly of *M. giganteus*, had expanded enough spatially to grow together. Our plantings

are on par with agronomic studies that suggest *Miscanthus* can take up to 4 years to reach peak biomass and canopy closure (Anderson et al., 2011; Arundale et al., 2014), though our stands were relatively diffuse compared to agronomic situations. A longer time period than our 5-year experiment would be required to fully address community consequences of *Miscanthus* introduction. Previous studies have shown that *Miscanthus* species can form dense patches outside of cultivation (e.g., Quinn et al., 2010). This lag in *Miscanthus* development provides an opportunity to eradicate escapes before their potential impacts are maximized.

Because of the potential for *Miscanthus* rhizome fragmentation and dispersal (Mann et al., 2013; West et al., 2014b), we were particularly concerned about invasive *Miscanthus* populations in floodplain forests as hidden engines of invasion. However, floodplain forests were more resistant to *Miscanthus* invasion than old field sites, inflicting greater mortality and supporting less growth over time. This difference between habitats is in contrast to previous studies in California, where *M. giganteus* established and persisted well in riparian areas and wet conditions, but declined post-establishment in drier upland sites (Barney et al., 2012; Mann et al., 2013). This discrepency is probably partially due to different ranges of moisture stress variation, as *Miscanthus* is climatically suited to broader areas of eastern compared to western North America (see Hager et al., 2014). Two of our three floodplain sites were heavily dominated by particular species before *Miscanthus* introduction (Nanney site: *Phalaris arundinacea* [reed canary grass]; Richter site: *Urtica dioica* [stinging nettle]), which likely drove microclimate variables such as light availability. This *in situ* competitive pressure may have influenced the lack of (Richter site) or very low (Nanney site) long term *Miscanthus* establishment. For instance, Hager et al. (2015a) found stronger *Miscanthus* seedling establishment limitation within forests compared to forest margins in central Illinois. However, our third floodplain site (Homer Lake) also had low *Miscanthus* persistence and no flowering over time without dominating understory species. Additionally, although *Miscanthus* performed worse in the shadier floodplain environments, previous studies have found introduced *Miscanthus* species to be relatively shade tolerant (Matlaga et al., 2012; Quinn et al., 2012). Although we lack specific site-level data on flooding frequency, spring floods in our sites resulted in high silt deposition and extended periods of standing water and saturated soils, which may have further decreased the viability of introductions. For example, 11 USGS gauging stations along waterways within an 80 km radius of our field sites recorded over-bankfull averages of 0.63–148.5 days/year between 1993 and 2012 (see Supplementary Material in West et al., 2014b). Shade and persistent flooding are likely limiting factors to *Miscanthus* establishment in this habitat, especially where apparent ground layer plant competition was low.

There are major gaps in our understanding of how species traits and characteristics of the recipient environments interact to affect community consequences from species introductions. The likelihood that an alien plant introduction will lead to community impacts depends largely on the combination of species traits and response variables measured, but whether there is an increase or decrease in the variable examined depends on environmental context (Hulme et al., 2013; Fried et al., 2014). Establishment studies alone cannot adequately identify factors that produce variation in invader impact at the community level, or their importance in predicting the impact of a plant introduction in a given community. Species invasiveness and community or habitat invasibility are often treated independently in invasion biology, and their interaction lends uncertainty to predictions about new invasions (Bennett et al., 2012; Rejmánek et al., 2013). Linking habitat context to the establishment and persistence of biomass species allow us to refine and optimize model predictions and best practices to limit invasions. Although regulations within the Renewable Fuel Standard to minimize the risk of spread from bioenergy cropping systems (US Environmental Protection Agency [EPA], 2013) do not currently apply to *Miscanthus*, large scale production of *Miscanthus* species will benefit from recommendations for proactive control. Assessing the emergent community impacts facilitates prioritization and implementation of species management. Recent models examining *Miscanthus* spread based on species characters and landscape configurations suggest spread could be rapid and extensive, and that passive management options such as buffers are insufficient to curtail dispersal (West et al., 2014b; Muthukrishnan et al., 2015; Pittman et al., 2015). Further, both *Miscanthus* species we studied can add biomass quickly and increase survivorship with age, and have a seedbank of at least 1 year (Hager et al., 2015a). Our study suggests there is a temporal window of at least 5 years in duration, and possibly longer, in which active management to monitor escapes and reduce establishment outside of cultivation (early detection and rapid response) will minimize invasion risks and community impacts associated with *Miscanthus* cultivation in the landscape. Active management, applied to passive measures such as buffers, might provide adequate control of *Miscanthus* invasion, but such combined strategies have not been modeled, to our knowledge.

The time required for escapes to accumulate in the landscape depends on the degree of active management. Thus, management cost and efficiency can indirectly drive time to escape, and the length of the escape time lag influences the relative costs and benefits of introduction (Yokomizo et al., 2012). However, lack of consistent long-term evidence of *in situ* invasiveness makes it difficult to distinguish whether a species is unlikely to be invasive, or is a future invader building toward future problems (Davis et al., 2010; Flory et al., 2012; Larkin, 2012). Field studies such as ours that evaluate establishment likelihood and consequences are vital to informing long term risk assessment and costs associated with introduction decisions. *Miscanthus* species can form nearly monotypic stands in North America, and current climate matching (Miguez et al., 2012; Hager et al., 2014; Evans et al., 2015) and landscape models (Muthukrishnan et al., 2015; Pittman et al., 2015) suggest there are few barriers to their further spread. Managing *Miscanthus* escapes in the short-term by containing or eradicating escapes will reduce the likelihood of local impacts that expand to larger-scale effects over time, which

would improve the long-term benefits of perennial *Miscanthus* crops.

AUTHOR CONTRIBUTIONS

FUNDING

ACKNOWLEDGMENTS

SUPPLEMENTARY MATERIAL

The Supplementary Material for this article can be found online at: http://journal.frontiersin.org/article/10.3389/fpls.2017.00767/full#supplementary-material

REFERENCES

Anderson, E., Arundale, R., Maughan, M., Oladeinde, A., Wycislo, A., and Voigt, T. (2011). Growth and agronomy of *Miscanthus x giganteus* for biomass production. *Biofuels* 2, 167–183. doi: 10.4155/bfs.10.80

Anderson, E. K., Lee, D., Allen, D. J., and Voigt, T. B. (2015). Agronomic factors in the establishment of tetraploid seeded *Miscanthus x giganteus*. *GCB Bioenergy* 7, 1075–1083. doi: 10.1111/gcbb.12192

Armas, C., Ordiales, R., and Pugnaire, F. I. (2004). Measuring plant interactions: a new comparative index. *Ecology* 85, 2682–2686. doi: 10.1890/03-0650

Arnoult, S., and Brancourt-Hulmel, M. (2015). A review on *Miscanthus* biomass production and composition for bioenergy use: genotypic and environmental variability and implications for breeding. *Bioenergy Res.* 8, 502–526. doi: 10.1007/s12155-014-9524-7

Arundale, R. A., Dohleman, F. G., Heaton, E. A., McGrath, J. M., Voigt, T. B., and Long, S. P. (2014). Yields of *Miscanthus x giganteus* and *Panicum virgatum* decline with stand age in the Midwestern USA. *GCB Bioenergy* 6, 1–13. doi: 10.1111/gcbb.12077

Barney, J. N., Mann, J. J., Kyser, G. B., and DiTomaso, J. M. (2012). Assessing habitat susceptibility and resistance to invasion by the bioenergy crops switchgrass and *Miscanthus x giganteus* in California. *Biomass Bioenergy* 40, 143–154. doi: 10.1016/j.biombioe.2012.02.013

Barney, J. N., Tekiela, D. R., Dollete, E. S. J., and Tomasek, B. J. (2013). What is the "real" impact of invasive plant species? *Front. Ecol. Environ.* 11, 322–329. doi: 10.1890/120120

Bennett, J. R., Dunwiddie, P. W., Giblin, D. E., and Arcese, P. (2012). Native versus exotic community patterns across three scales: roles of competition, environment and incomplete invasion. *Perspect. Plant Ecol. Evol. Syst.* 14, 381–392. doi: 10.1016/j.ppees.2012.10.001

Blackburn, T. M., Essl, F., Evans, T., Hulme, P. E., Jeschke, J. M., Kühn, I., et al. (2014). A unified classification of alien species based on the magnitude of their environmental impacts. *PLoS Biol.* 12:e1001850. doi: 10.1371/journal.pbio.1001850

Bonin, C. L., Heaton, E. A., and Barb, J. (2014). *Miscanthus sacchariflorus* – biofuel parent or new weed? *GCB Bioenergy* 6, 629–636. doi: 10.1111/gcbb.12098

Bonin, C. L., Mutegi, E., Snow, A. A., Miriti, M., Chang, H., and Heaton, E. A. (2017). Improved feedstock option or invasive risk? Comparing establishment and productivity of fertile *Miscanthus × giganteus* to *Miscanthus sinensis*. *Bioenergy Res.* 10, 317–328. doi: 10.1007/s12155-016-9808-1

Byers, J. E., and Noonburg, E. G. (2003). Scale dependent effects of biotic resistance to biological invasion. *Ecology* 84, 1428–1433. doi: 10.1890/02-3131

Castenson, K. L., and Rabenhorst, M. C. (2006). Indicator of reduction in soil (IRIS). *Soil Sci. Soc. Am. J.* 70, 1222–1226. doi: 10.2136/sssaj2005.0130

Chen, H., Qjan, H., Spyreas, G., and Crossland, M. (2010). Native-exotic species richness relationship across spatial scales and biotic homogenization in wetland plant communities of Illinois, USA. *Divers. Distrib.* 16, 737–743. doi: 10.1111/j.1472-4642.2010.00679.x

Chou, C.-H. (2009). *Miscanthus* plants used as an alternative biofuel material: the basic studies on ecology and molecular evolution. *Renew. Energy* 34, 1908–1912. doi: 10.1016/j.renene.2008.12.027

Christian, D. G., and Haase, E. (2001). "Agronomy of *Miscanthus*," in *Miscanthus for Energy and Fibre*, eds M. B. Jones and M. Walsh (London: James and James Ltd), 21–45.

Davis, A. S., Cousens, R. D., Hill, J., Mack, R. N., Simberloff, D., and Raghu, S. (2010). Screening bioenergy feedstock crops to mitigate invasion risk. *Front. Ecol. Environ.* 8:533–539. doi: 10.1890/090030

Davis, M. A., Grime, J. P., and Thompson, K. (2000). Fluctuating resources in plant communities: a general theory of invasibility. *J. Ecol.* 88, 528–534. doi: 10.1046/j.1365-2745.2000.00473.x

Dick, J. T. A., Alexander, M. E., Jeschke, J. M., Ricciardi, A., MacIsaac, H. J., Robinson, T. B., et al. (2014). Advancing impact prediction and hypothesis testing in invasion ecology using a comparative functional response approach. *Biol. Invasions* 16, 735–753. doi: 10.1007/s10530-013-0550-8

Dougherty, R. F., Quinn, L. D., Endres, A. B., Voigt, T. B., and Barney, J. N. (2014). Natural history survey of the ornamental grass *Miscanthus sinensis* in the introduced range. *Invasive Plant Sci. Manage.* 7, 113–120. doi: 10.1614/IPSM-D-13-00037.1

Drenovsky, R. E., Grewell, B. J., D'Antonio, C. M., Funk, J. L., James, J. J., Molinari, N., et al. (2012). A functional trait perspective on plant invasion. *Ann. Bot.* 110, 141–153. doi: 10.1093/aob/mcs100

Driscoll, D. A., Catford, J. A., Barney, J. N., Hulme, P. E., Inderjit, Martin, T. G., et al. (2014). New pasture plants intensify invasive species risk. *Proc. Natl. Acad. Sci. U.S.A.* 111, 16622–16627. doi: 10.1073/pnas.1409347111

Evans, S. G., Kelley, L. C., and Potts, M. D. (2015). The potential impact of second-generation biofuel landscapes on at-risk species in the US. *GCB Bioenergy* 7, 337–348. doi: 10.1111/gcbb.12131

Flory, S. L., Lorentz, K. A., Gordon, D. R., and Sollenberger, L. E. (2012). Experimental approaches for evaluating the invasion risk of biofuel crops. *Environ. Res. Lett.* 7, 45904–45907. doi: 10.1088/1748-9326/7/4/045904

Fried, G., Laitung, B., Pierre, C., Chagué, N., and Panetta, F. D. (2014). Impact of invasive plants in Mediterranean habitats: disentangling the effects of characteristics of invaders and recipient communities. *Biol. Invasions* 16, 1639–1658. doi: 10.1007/s10530-013-0597-6

Gaertner, M., Biggs, R., Te Beest, M., Hui, C., Molofsky, J., and Richardson, D. M. (2014). Invasive plants as drivers of regime shifts: identifying high-priority invaders that alter feedback relationships. *Divers. Distrib.* 20, 733–744. doi: 10.1111/ddi.12182

Gotelli, N. J. (2008). *A Primer of Ecology*. Sunderland, MA: Sinauer Associates.

Grechi, I., Chadès, I., Buckley, Y. M., Friedel, M. H., Grice, A. C., Possingham, H. P., et al. (2014). A decision framework for management of conflicting production and biodiversity goals for a commercially valuable invasive species. *Agric. Syst.* 125, 1–11. doi: 10.1016/j.agsy.2013.11.005

Hager, H. A., Quinn, L. D., Barney, J. N., Voigt, T. B., and Newman, J. A. (2015a). Germination and establishment of bioenergy grasses outside cultivation:

a multi-region seed addition experiment. *Plant Ecol.* 216, 1385–1399. doi: 10.1007/s11258-015-0516-2

Hager, H. A., Rupert, R., Quinn, L. D., and Newman, J. A. (2015b). Escaped *Miscanthus sacchariflorus* reduces the richness and diversity of vegetation and the soil seed bank. *Biol. Invasions* 17, 1833–1847. doi: 10.1007/s10530-014-0839-2

Hager, H. A., Sinasac, S. E., Gedalof, Z. E., and Newman, J. A. (2014). Predicting potential global distributions of two *Miscanthus* grasses: implications for horticulture, biofuel production, and biological invasions. *PLoS ONE* 9:e100032. doi: 10.1371/journal.pone.0100032

Hallett, L. M., Jones, S. K., MacDonald, A. A. M., Jones, M. B., Flynn, D. F. B., Ripplinger, J., et al. (2016). codyn: an R package of community dynamics metrics. *Methods Ecol. Evol.* 7, 1146–1151. doi: 10.1111/2041-210x.12569

Hedìnec, P., Novotnι, D., Usťak, S., Honzík, R., Kováǎová, M., Šimáèková, H., et al. (2014). Allelopathic effect of new introduced biofuel crops on the soil biota: a comparative study. *Eur. J. Soil Biol.* 63, 14–20. doi: 10.1016/j.ejsobi.2014.05.002

Hulme, P. E., Pyšek, P., Jarošík, V., Pergl, J., Schaffner, U., and Vilà, M. (2013). Bias and error in understanding plant invasion impacts. *Trends Ecol. Evol.* 28, 212–218. doi: 10.1016/j.tree.2012.10.010

Jackson, M. C., Ruiz-Navarro, A., and Britton, J. R. (2015). Population density modifies the ecological impacts of invasive species. *Oikos* 124, 880–887. doi: 10.1111/oik.01661

Jenkinson, B. J., and Franzmeier, D. P. (2006). Development and evaluation of iron-coated tubes that indicate reduction in soils. *Soil Sci. Soc. Am. J.* 70, 183–191. doi: 10.2136/sssaj2004.0323

Kumschick, S., Gaertner, M., Vilà, M., Essl, F., Jeschke, J. M., Pyšek, P., et al. (2015). Ecological impacts of alien species: quantification, scope, caveats, and recommendations. *BioScience* 65, 55–63. doi: 10.1093/biosci/biu193

Larkin, D. J. (2012). Lengths and correlates of lag phases in upper-Midwest plant invasions. *Biol. Invasions* 14, 827–838. doi: 10.1007/s10530-011-0119-3

Levine, J. M., Adler, P. B., and Yelenik, S. G. (2004). A meta-analysis of biotic resistance to exotic plant invasions. *Ecol. Lett.* 7, 975–989. doi: 10.1111/j.1461-0248.2004.00657.x

Lewis, K. C., and Porter, R. D. (2014). Global approaches to addressing biofuel-related invasive species risks and incorporation into U.S. laws and policies. *Ecol. Monogr.* 84, 171–201. doi: 10.1890/13-1625.1

MacDougall, A. S., and Turkington, R. (2005). Are invasive species the drivers or passengers of change in degraded ecosystems? *Ecology* 86, 42–55. doi: 10.1890/04-0669

Mack, R. N. (2000). Cultivation fosters plant naturalization by reducing environmental stochasticity. *Biol. Invasions* 2, 111–122. doi: 10.1023/A:1010088422771

Mann, J. J., Kyser, G. B., Barney, J. N., and DiTomaso, J. M. (2013). Assessment of aboveground and belowground vegetative fragments as propagules in the bioenergy crops *Arundo donax* and *Miscanthus x giganteus*. *Bioenergy Res.* 6, 688–698. doi: 10.1007/s12155-012-9286-z

Maron, J. L., Auge, H., Pearson, D. E., Korell, L., Hensen, I., Suding, K. N., et al. (2014). Staged invasions across disparate grasslands: effects of seed provenance, consumers and disturbance on productivity and species richness. *Ecol. Lett.* 17, 499–507. doi: 10.1111/ele.12250

Matlaga, D. P., and Davis, A. S. (2013). Minimizing invasive potential of *Miscanthus x giganteus* grown for bioenergy: identifying demographic thresholds for population growth and spread. *J. Appl. Ecol.* 50, 479–487. doi: 10.1111/1365-2664.12057

Matlaga, D. P., Quinn, L. D., Davis, A. S., and Stewart, J. R. (2012). Light response of native and introduced *Miscanthus sinensis* seedlings. *Invasive Plant Sci. Manage.* 5, 363–374. doi: 10.1614/IPSM-D-11-00056.1

Miguez, F. E., Maughan, M., Bollero, G. A., and Long, S. P. (2012). Modeling spatial and dynamic variation in growth, yield, and yield stability of the bioenergy crops *Miscanthus x giganteus*. *GCB Bioenergy* 4, 509–520. doi: 10.1111/j.1757-1707.2011.01150.x

Moles, A. T., Flores-Moreno, H., Bonser, S. P., Warton, D. I., Helm, A., Warman, L., et al. (2012). Invasions: the trail behind, the path ahead, and a test of a disturbing idea. *J. Ecol.* 100, 116–127. doi: 10.1111/j.1365-2745.2011.01915.x

Muthukrishnan, R., West, N. M., Davis, A. S., Jordan, N. R., and Forester, J. D. (2015). Evaluating the role of landscape in the spread of invasive species: the case of the biomass crop *Miscanthus x giganteus*. *Ecol. Model.* 317, 6–15. doi: 10.1016/j.ecolmodel.2015.08.022

Pittman, S. E., Muthukrishnan, R., West, N. M., Davis, A. S., Jordan, N. R., and Forester, J. D. (2015). Mitigating the potential for invasive spread of the exotic biofuel crop, *Miscanthus x giganteus*. *Biol. Invasions* 17, 3247–3261. doi: 10.1007/s10530-015-0950-z

Pyšek, P., Jarošík, V., Hulme, P. E., Pergl, J., Hejda, M., Schaffner, U., et al. (2012). A global assessment of invasive plant impacts on resident species, communities and ecosystems: the interaction of impact measures, invading species' traits and environment. *Glob. Change Biol.* 18, 1725–1737. doi: 10.1111/j.1365-2486.2011.02636.x

Quinn, L. D., Allen, D. J., and Stewart, J. R. (2010). Invasiveness potential of *Miscanthus sinensis*: implications for bioenergy production in the United States. *Glob. Change Biol. Bioenergy* 2, 310–320. doi: 10.1111/j.1757-1707.2010.01062.x

Quinn, L. D., Gordon, D. R., Glaser, A., Lieurance, D., and Flory, S. L. (2015). Bioenergy feedstocks at low risk for invasion in the USA: a "White List" approach. *Bioenergy Res.* 8, 471–481. doi: 10.1007/s12155-014-9503-z

Quinn, L. D., Stewart, J. R., Yamada, T., Toma, Y., Saito, M., Shimoda, K., et al. (2012). Environmental tolerances of *Miscanthus sinensis* in invasive and native populations. *Bioenergy Res.* 5, 139–148. doi: 10.1007/s12155-011-9163-1

R Core Team (2016). *R: A Language and Environment for Statistical Computing*. Vienna: R Foundation for Statistical Computing. doi: 10.1016/j.cosust.2010.11.005

Raghu, S., Spencer, J. L., Davis, A. S., and Widenmann, R. N. (2011). Ecological considerations in the sustainable development of terrestrial biofuel crops. *Curr. Opin. Environ. Sustain.* 3, 15–23.

Rejmánek, M., Richardson, D. M., and Pyšek, P. (2013). "Plant invasions and invasibility of plant communities," in *Vegetation Ecology*, 2 Edn, eds E. van der Maarel and J. Franklin (Hoboken, NJ: Wiley-Blackwell), 572.

Ricciardi, A., Hoopes, M. F., Marchetti, M. P., and Lockwood, J. L. (2013). Progress toward understanding the ecological impacts of nonnative species. *Ecol. Monogr.* 83, 263–282. doi: 10.1890/13-0183.1

Richardson, D. M. (2013). Lessons learned: How can we manage the invasion risk from biofuels? *Biofuels* 4, 455–457.

Scasta, J. D., Engle, D. M., Fuhlendorf, S. D., Redfearn, D. D., and Bidwell, T. G. (2015). Meta-analysis of exotic forages as invasive plants in complex multi-functioning landscapes. *Invasive Plant Sci. Manage.* 8, 292–306. doi: 10.1614/ipsm-d-14-00076.1

Schnitzler, A., and Essl, F. (2015). From horticulture and biofuel to invasion: the spread of *Miscanthus* taxa in the USA and Europe. *Weed Res.* 55, 221–225. doi: 10.1111/wre.12141

Shea, K., and Chesson, P. (2002). Community ecology theory as a framework for biological invasions. *Trends Ecol. Evol.* 17, 170–176. doi: 10.1016/S0169-5347(02)02495-3

Simberloff, D., Martin, J.-L., Genovesi, P., Maris, V., Wardle, D. A., Aronson, J., et al. (2013). Impacts of biological invasions: what's what and the way forward. *Trends Ecol. Evol.* 28, 56–66. doi: 10.1016/j.tree.2012.07.013

Słomka, A., Kuta, E., Płażek, A., Dubert, F., Żur, I., Dubas, E., et al. (2012). Sterility of *Miscanthus × giganteus* results from hybrid incompatibility. *Acta Biol. Cracov. Ser. Bot.* 54, 113–120. doi: 10.2478/v10182-012-0011-1

Smith, L. L., and Barney, J. N. (2014). The relative risk of invasion: evaluation of *Miscanthus x giganteus* seed establishment. *Invasive Plant Sci. Manage.* 7, 93–106. doi: 10.1614/IPSM-D-13-00051.1

Smith, L. L., Tekiela, D. R., and Barney, J. N. (2015). Predicting biofuel invasiveness: a relative comparison to crops and weeds. *Invasive Plant Sci. Manage.* 8, 323–333. doi: 10.1614/ipsm-d-15-00001.1

Stewart, J. R., Toma, Y., Fernández, F. G., Nishiwaki, A., Yamada, T., and Bollero, G. (2009). The ecology and agronomy of *Miscanthus sinensis*, a species important to bioenergy crop development, in its native range in Japan: a review. *Glob. Change Biol. Bioenergy* 1, 126–153. doi: 10.1111/j.1757-1707.2009.01010.x

Theoharides, K. A., and Dukes, J. S. (2007). Plant invasion across space and time: factors affecting non indigenous species success during four stages of invasion. *New Phytol.* 176, 256–273. doi: 10.1111/j.1469-8137.2007.02207.x

Thiele, J., Kollmann, J., Markussen, B., and Otte, A. (2010). Impact assessment revisited: improving the theoretical basis for management of invasive alien species. *Biol. Invasions* 12, 2025–2035. doi: 10.1007/s10530-009-9605-2

US Environmental Protection Agency [EPA] (2013). *Office of Transportation and Air Quality. EPA Issues Supplemental Final Rule for New Qualifying Renewable Fuels Under the RFS Program*. Available at: https://www.epa.gov/sites/production/files/2015-08/documents/420f13040_5.pdf

Vilà, M., Tessier, M., Suehs, C. M., Brundu, G., Carta, L., Galanidis, A., et al. (2006). Local and regional assessments of the impacts of plant invaders on vegetation structure and soil properties of Mediterranean islands. *J. Biogeogr.* 33, 853–861. doi: 10.1111/j.1365-2699.2005.01430.x

West, N. M., Matlaga, D. P., and Davis, A. S. (2014a). Quantifying targets to manage invasion risk: light gradients dominate the early regeneration niche of naturalized and pre-commercial *Miscanthus* populations. *Biol. Invasions* 16, 1991–2001. doi: 10.1007/s10530-014-0643-zx

West, N. M., Matlaga, D. P., and Davis, A. S. (2014b). Managing spread from rhizome fragments is key to reducing invasiveness in *Miscanthus x giganteus*. *Invasive Plant Sci. Manage.* 7, 517–525. doi: 10.1614/IPSM-D-14-00018.1

Yokomizo, H., Possingham, H. P., Hulme, P. E., Grice, A. C., and Buckley, Y. M. (2012). Cost-benefit analysis for intentional plant introductions under uncertainty. *Biol. Invasions* 14, 839–849. doi: 10.1007/s10530-011-0120-x

Zub, H. W., and Brancourt-Hulmel, M. (2010). Agronomic and physiological performances of different species of *Miscanthus*, a major energy crop. A review. *Agron. Sustain. Dev.* 30, 201–214. doi: 10.1051/agro/2009034

Check for updates

Description and Codification of *Miscanthus × giganteus* Growth Stages for Phenological Assessment

Mauricio D. Tejera and Emily A. Heaton *

Department of Agronomy, Iowa State University, Ames, IA, United States

Triploid *Miscanthus × giganteus* (Greef et Deu. ex Hodkinson et Renvoize) is a sterile, perennial grass used for biomass production in temperate environments. While *M. × giganteus* has been intensively researched, a scale standardizing description of *M. × giganteus* morphological stages has not been developed. Here we provide such a scale by adapting the widely-used Biologische Bundesanstalt, Bundessortenamt, CHemische Industrie (BBCH) scale and its corresponding numerical code to describe stages of morphological development in *M. × giganteus* using observations of the "Freedom" and "Illinois" clone in Iowa, USA. Descriptive keys with images are also presented. Because *M. × giganteus* plants overlap in the field, the scale was first applied to individual stems and then scaled up to assess plants or communities. Of the 10 principal growth stages in the BBCH system, eight were observed in *M. × giganteus*. Each principal stage was subdivided into secondary stages to enable a detailed description of developmental progression. While *M. × giganteus* does not have seed development stages, descriptions of those stages are provided to extend the scale to other *Miscanthus* genotypes. We present methods to use morphological development data to assess phenology by calculating the onset, duration, and abundance of each developmental stage. This scale has potential to harmonize previously described study-specific scales and standardize results across studies. Use of the precise staging presented here should more tightly constrain estimates of developmental parameters in crop models and increase the efficacy of timing-sensitive crop management practices like pest control and harvest.

Keywords: BBCH, morphology, phenology, phenophase, phyllochron, perennial C4 grass, bioenergy, senescence

INTRODUCTION

Miscanthus × giganteus is an interspecific hybrid of *M. sacchariflorus* and *M. sinensis* (Greef et al., 1997; Hodkinson and Renvoize, 2001) with C_4 photosynthesis and a perennial growth habit. It is native to East Asia but sterile triploid clones are now used as biomass crops in temperate environments around the globe, where they are typically characterized by relatively high biomass yields, moderate cold tolerance and low input requirements (Clifton-Brown et al., 2007; Christian et al., 2008; Heaton et al., 2008; Arnoult and Brancourt-Hulmel, 2015). Triploid *M. × giganteus* has these characteristics in part because it produces an annual crop of harvestable stems from a perennial root/rhizome complex that enables efficient inter-annual nutrient cycling (Cadoux et al., 2012; Dohleman et al., 2012).

A major target of perennial grass improvement programs is to develop genotypes with variant plant morphology and phenology that allow more efficient resource capture or improved

feedstock quality (Jones et al., 2015). To advance understanding of phenology in *Miscanthus* and related species, we propose using a common morphological development scale based on triploid *M.* × *giganteus,* since it is both a commercial crop and a frequently used control species. Adopting common, numerical naming conventions for morphological stages would allow unambiguous and quantitative characterization of *M.* × *giganteus* development, as well as its seasonal timing i.e., phenology (Sanderson et al., 1997), as has been done in other major crops. Clearly describing when a plant goes through a particular developmental stage is beneficial because it lets researchers track and compare factors influencing that timing, such as, temperature, rainfall, photoperiod, genetics, or stress. Morphological development descriptions are also crucial to practitioners who need to manage the crop at physiologically important times (e.g., for pest control and harvest) that are better described by a development stage than a substitute metric like Julian day or thermal time.

There are several commonly used morphological development scales able to characterize plant principal growth stages but they differ in the precision with which they describe intermediate growth stages. For example, the widely used scales of Feekes (Feekes, 1941; Large, 1954) and Haun (1973) could be used to assess *Miscanthus* spp., but only in a limited way. Because these scales were developed for cereals they lack detail needed to describe the entire growth cycle of perennial grasses, and have coarse resolution in the vegetative stages (see Landes and Porter, 1989 for further comparison between scales). By contrast, Moore et al. (1991) developed a scale for forage grasses that emphasizes vegetative stages, but does not provide fine resolution of reproductive stages, limiting the scale's utility for some traits of interest, such as, flowering time and seed development.

To date, the *Miscanthus* community has opted to develop entirely new morphological development scales to meet particular research needs (e.g., Hastings et al., 2009; Miguez et al., 2009; Jensen et al., 2011; Robson et al., 2012; Zub et al., 2012; da Costa et al., 2014; Purdy et al., 2015; Trybula et al., 2015). These scales function well in a specific study or research area, but do not translate well for broader use. For example, none of them provide a complete description of all plant developmental stages, nor enough detail within each stage to accurately track development through a growing season. Therefore, *Miscanthus* spp. morphological development descriptions extant in the literature today represent stand-alone descriptions which are difficult to apply more broadly.

The Biologische Bundesantalt, Bundessortenamt and CHemische Industrie (BBCH) is another widely used scale that has been adapted for more than 50 species (Meier et al., 2009; Martínez-Nicolás et al., 2016) including the commercially used C$_4$ grasses sugarcane (*Saccharum officinarum* L.; Bonnett, 2013), switchgrass (*Panicum virgatum* L.; Sanderson et al., 1997), sweet sorghum (*Sorghum bicolor* L. Moench; Dalla Marta et al., 2014), and maize (*Zea mays* L.; Lancashire et al., 1991). The BBCH system has been adopted around the globe because it has a flexible but consistent framework that facilitates comparison across diverse plant types, an especially useful feature for assessing bioenergy genera with very different features, e.g., *Cynara* (Archontoulis et al., 2010) and *Miscanthus.*

The BBCH framework consists of a two digit decimal code based on Zadoks et al. (1974) decimal code for cereals (Lancashire et al., 1991). The first digit corresponds to a *principal growth stage* (0–9) and subdivides the developmental cycle of the plant into 10 clearly recognizable and distinguishable stages (Hess et al., 1997). The second digit corresponds to a *secondary growth stage* (0–9) and describes the intermediate stages within a principal growth stage and progression through those stages. Depending on the principal stage, secondary stages correspond to either ordinal or percentage values. The two digit code consists of a combination of the principal growth stage code (tens place) and secondary stage code (ones place). In cases where further precision is needed, secondary stages can be subdivided by incorporating mesostages and extending the code to a three digit code. Characterizing morphological development of *Miscanthus* spp. with the BBCH scale would allow comparison of *Miscanthus* spp. development with that of other species for which the BBCH scale has been adapted and provide clear developmental benchmarks by which to assess and compare phenology.

The purpose of this paper is to modify the BBCH scale to describe the morphological development of *M.* × *giganteus.* Here, we (1) modify the BBCH scale to describe and codify *M.* × *giganteus* growth stages; and (2) describe and demonstrate use of the modified BBCH scale to assess phenology, specifically the onset, duration and abundance of phenological events. We hope this scale will be used by the *Miscanthus* research community to characterize development and phenology, and facilitate transparency and comparison between studies. We further hope this scale will assist management decisions for *M.* × *giganteus* producers.

MATERIALS AND METHODS

To modify the BBCH scale for *M.* × *giganteus* we first developed a draft scale from similar scales in the literature. We then refined that draft scale to a robust, functioning scale using targeted *M.* × *giganteus* field observations from 2 years and three locations in Iowa, USA. We next demonstrated how the scale can be used to perform phenology assessments. We did that by adapting published practices to collect morphological data, spatially upscale phenological stages, and model developmental progression to assess phenology. This allows calculation of the date at which a given stage was reached, i.e., the onset date (Cornelius et al., 2011), and measures of developmental progression. i.e., stage duration and abundance. To clarify these procedures, we present an explanatory dataset containing biweekly measurements of *M.* × *giganteus* development over one growing season. This explanatory dataset is not meant to provide a full phenological assessment of *M.* × *giganteus,* but instead demonstrate the procedures needed to do such assessments.

Modifying the BBCH Scale to
M. × *giganteus*

First, we developed a draft *M.* × *giganteus* scale using published descriptions for the closely related species sugarcane (Bonnett, 2013) and switchgrass (Sanderson et al., 1997). Typically the

BBCH scale only considers development of the main stem (Meier et al., 2009), but *M.* × *giganteus* does not have a clear main stem, nor is it easy to distinguish individual *M.* × *giganteus* plants in the field. Therefore, terminology and images were adjusted to consider development of individual stems.

Second, we adjusted the draft scale to allow for both sterile and fertile *Miscanthus* genotypes. Since *Miscanthus* crops are dominantly rhizomatous, seed germination stages were replaced by rhizome growth and emergence stages. Similarly, while today's commercially available *M.* × *giganteus* clones are sterile triploids that do not sexually reproduce, the scale has stages related to seed development, enabling assessment of seeded genotypes (Clifton-Brown et al., 2017). Grain filling stages (e.g., milk and dough) were described based on generic grass descriptions (Meier, 2001) as modified for perennial grasses (i.e., *P. virgatum*) by Sanderson et al. (1997) (see **Tables 1, 3**).

Third, we presented mesostages as tenths of the secondary stage instead of extending the code to a whole-number three digit code. This facilitates arithmetic operations and comparison within and between studies by keeping values between 0 and 99.

Refining the BBCH Scale with *M.* × *giganteus* Field Observations

To refine the literature-based draft scale for real-world application, we supplemented it with information from field observations. Observations were made of *M.* × *giganteus* clone "Freedom" grown in three locations across Iowa, USA and clone "Illinois" grown only at the Sorenson farm in central Iowa, over two growing seasons (**Table 1**). These observations spanned two degrees of latitude, three degrees of longitude, two plant ages (juvenile and mature), and a range of soil, climate, and fertility conditions. At each of the three locations, rhizomes of *M.* × *giganteus* clone "Freedom" (sourced from Repreve Renewables, now AgGrow Tech, Greensboro, NC, USA) were planted in both 2015 and 2016 as part of a larger study that included five nitrogen fertilization rates (0, 112, 224, 336, and 448 kg ha^{-1}). Additionally, at the Sorenson farm, rhizomes of *M.* × *giganteus* clone "Illinois" (sourced from Caveny Farm, Monticello, IL, USA) had been planted in 2009. All stands were planted with 0.6 m spacing between rows and approximately 0.4 m spacing between plants within the row. During the 2015 and 2016 growing seasons, stands at the Sorenson farm (with both clones and stand ages) were used to gather observations,

descriptions, images, and explanatory data. The other two locations were then used to identify gaps in the morphological description and ensure broad transferability of the scale. Stands were healthy without disease or stress symptoms during the period of study.

Morphological development information used to characterize, supplement, and refine descriptions of *M.* × *giganteus* developmental stages was collected biweekly at the Sorenson farm beginning in early spring at planting/emergence and continued until mid-winter when stems had senesced. While morphological descriptors of aboveground biomass were developed using both clones, rhizome bud development was assessed using only "Freedom" rhizomes. These stages describe morphological growth of two structures (i.e., bud swelling, first lamina expansion), and no discernible differences from the "Illinois" clone were observed based on our previous work with that clone (Heaton et al., 2008; Boersma and Heaton, 2014). To facilitate observations, rhizomes used for rhizome bud development characterization were kept unplanted under temperature and moisture conditions favorable for growth (∼25°C and <2 kPa water vapor pressure deficit).

At each biweekly observation, a random sample of stems was collected from the observation stands and described according to the draft scale. The draft scale was then iteratively adjusted as needed to match field observations, and supporting images taken. In total, the complete morphological characterization was based on at least 200 randomly selected stems per morphological development stage. Descriptions of principal and secondary growth stages were organized to match existing BBCH scale descriptions, creating a working *M.* × *giganteus* scale.

Assessing Phenology Using Modified BBCH Scale

To demonstrate assessment of *M.* × *giganteus* phenology, we collected a time series of morphological development data additional to those used in developing the *M.* × *giganteus* BBCH scale (section Refining the BBCH Scale with *M.* × *giganteus* Field Observations). We compiled these explanatory data by recording all the morphological development stages present in a random sample of ten stems of 2-year old *M.* × *giganteus* at Sorenson farm biweekly from late spring to late fall 2016. We adapted the following methodological guidelines presented by the USA National Phenology Network (Denny et al., 2014) to standardize phenological data collection.

TABLE 1 | Overview of locations and plant material used to refine *Miscanthus* × *giganteus* morphological development descriptions for the BBCH scale.

Sites in Iowa, USA	Location (lat., long.)	Clone	Planting year	Soil class	Mean air temperature (°C)	Precipitation (mm)
Allee farm	42.586, −95.012	Freedom	2015, 2016	Typic endoaquoll	10.0 ± 11.4	908.2 ± 19.6
Sorenson farm	42.013, −93.744	Freedom Illinois	2015, 2016 2009	Typic endoaquoll	11.1 ± 11.3	940.8 ± 14.7
South East Research Farm	41.201, −91.488	Freedom	2015, 2016	Aquic argiudoll	12.0 ± 11.1	865.6 ± 15.7

Annual temperature and annual precipitation were averaged over observation years (2015–2016).

TABLE 2 | *Miscanthus × giganteus* morphological development stages according to the BBCH scale.

Code	Description
PRINCIPAL GROWTH STAGE 0: BUD DEVELOPMENT	
00	Dormant rhizome
01	Beginning of bud swelling
03	End of bud swelling
05	Bud breaking: rolled leaves growing towards the surface
07	Elongation of chlorotic laminae
09	Emergence of rolled leaves through soil surface
PRINCIPAL GROWTH STAGE 1: LEAF DEVELOPMENT	
10	First visible leaf laminae
11	2 Fully expanded leaves
12	4 Fully expanded leaves
13	6 Fully expanded leaves continues until
…continues until…	
19	18+ Fully expanded leaves
PRINCIPAL GROWTH STAGE 2: TILLERING‡	
20	No tillers on main shoot
20.1	Partially swollen axillary bud (~2mm)
20.5	Swollen axillary bud (~8-1.0mm)
20.9	Bud breaking
21	1 Tiller on main shoot
22	2 Tillers on main shoot
…continues until…	
29	9 Tillers on main shoot
PRINCIPAL GROWTH STAGE 3: STEM ELONGATION	
30	Pseudo stem elongation
31	2 Palpable nodes
32	4 Palpable nodes
33	6 Palpable nodes
…continues until…	
39	18+ Palpable nodes
PRINCIPAL GROWTH STAGE 4: BOOTING	
40	Flag leaf visible but still rolled
41	Flag leaf is fully expanded
43	Inflorescence occupies 25% of flag leaf sheath
45	Inflorescence occupies 50% of flag leaf sheath
47	Inflorescence occupies 75% of flag leaf sheath
49	Inflorescence fills flag leaf sheath but no florets are exposed
PRINCIPAL GROWTH STAGE 5: INFLORESCENCE EMERGENCE	
51	First florets just visible through flag leaf collar
53	Inflorescence upper branches exposure
56	Inflorescence lower branches exposure
59	Inflorescence fully exposed and peduncle exposure
PRINCIPAL GROWTH STAGE 6: FLOWERING	
60	Sporadic open florets
61	10% of florets open
62	20% of florets open
63	30% of florets open
… continues until…	
69	90 to 100% of florets open

(Continued)

TABLE 2 | Continued

Code	Description
PRINCIPAL GROWTH STAGE 7: SEED DEVELOPMENT‡	
71	Watery ripe
73	Early milk
75	Medium milk
77	Late milk
PRINCIPAL GROWTH STAGE 8: RIPENING‡	
81	Early dough
83	Soft dough
85	Hard dough
87	Fully ripe
89	Over-ripe
PRINCIPAL GROWTH STAGE 9: SENESCENCE	
90	Partial leaf yellowing
91	Stems 10% senesced
92	Stems 20% senesced
93	Stems 30% senesced
…continues until…	
99	Stems 90 to 100% senesced

The two digit code consists of a combination of the principal growth stage code (tens place) and secondary stage code (ones place).
See Figure 1 for corresponding images. Stages are assessed on individual stems.
‡Stages never or rarely observed in commercial M. × giganteus clones. Based on Meier, (2001) general grass descriptions and adapted to perennial grasses using by Sanderson et al. (1997).

(1) *Make repeated observations of the stage status.* This provides temporal information on the presence/absence and duration of the developmental stage.

(2) *Make multiple observations per location.* Multiple random stems should be observed on each date. This helps quantify temporal and spatial variation and allows scaling to larger areas like a field or population. Additionally, it gives information about stage abundance and commonality, allowing better characterization of phenological patterns. Repeated observations in space and time also enable identification of cohort emergence across the growing season. Sampling can be targeted to the cohort of interest, or used to characterize variability across the population.

(3) *Independently track multiple stages occurring in parallel.* This is of special interest since morphological stages occur at the same time during the *Miscanthus* growing cycle, e.g., leaf growth and stem elongation. Typically users of morphological development scales stop tracking one stage once the next begins, but users should be able to measure progression through parallel stages if desired.

Estimating Growth Stage Progression

We next used our morphological development time series data to demonstrate how growth stage progression can be determined using two metrics: cumulative abundance of a stage and development rates between stages. For the former, we followed and recommend the method developed by Schirone et al. (1991) to estimate onset duration and abundance of morphological

TABLE 3 | Raw explanatory data showing number of stems of *Miscanthus* × *giganteus* BBCH stage 15 or higher as measured during the 2016 growing season in Sorenson farm, Iowa.

BBCH stage	Jun-29	Jul-11	Jul-25	Aug-9	Aug-23	Sep-6	Sep-21
Number of stems at a given stage							
15	0	2	0	0	0	0	0
15.5	1	2	0	0	1	0	0
16	0	0	6	0	0	0	0
16.5	0	0	1	2	0	1	0
17	0	0	2	4	2	1	0
17.5	0	0	0	1	1	0	0
18	0	0	0	3	3	4	0
18.5	0	0	0	0	1	2	4
19	0	0	0	0	0	1	3
19.5	0	0	0	0	1	0	1
Cumulative sum of stems at a given stage or higher							
15	1	4	9	10	9	9	8
18	0	0	0	3	5	7	8
Cumulative proportion of stem							
15	0.1	0.4	0.9	1	1	1	1
18	0	0	0	0.2	0.56	0.78	1

Sample size was 10 stems for all sampling dates but for 23-Aug, 6-Sept and 21-Sep with 9, 9, and 8 stems, respectively.

growth stages. Cumulative abundance is calculated as the number of stems that have passed a defined developmental threshold, and presents abundance as a proportion of the total stems measured. At each sampling date, the cumulative abundance of a considered stage is estimated as the number of stems at the threshold stage or higher, divided by the sample size. When graphed, this temporal series describes a sigmoid curve, which can be modeled with a logistic function. The onset date is estimated by modeling a curve through the measured data points, then identifying the point in time at which the frequency of individuals at the threshold stage equals 50%. Onset dates for each secondary growth stage should be calculated separately within each principal growth stage to elucidate overlapping *M.* × *giganteus* stages.

Principal growth stage development rate (PGSDR) was calculated as the rate of appearance of new secondary stages over time. This rate specifies the time required to develop morphologic structures (e.g., leaves, nodes). If the relationship of development to time is linear, PGSDR is the slope of the linear regression between secondary growth stage progression and time. In case of a non-constant rate during the growing season, multiple linear regressions for multiple constant rates or non-linear models can be used. In the latter case, the derivate of the function may be more informative.

In principal growth stage 1, PGSDR corresponds to leaf appearance rate and its inverse is equivalent to the phyllochron, or accumulated time (in days or thermal time) required for the appearance of successive leaves on a stem (Xue et al., 2004). Leaf appearance rate and phyllochron have direct application to crop modeling, crop management, assessment of abiotic stress, and cultivar selection.

Leaf duration, defined as the time between leaf emergence and senescence, is another important parameter in plant phenology, crop management and modeling. When principal growth stage senescence is described in terms of number of senesced leaves and secondary growth stages attributed in the same mode as in leaf development (one every two senesced leaves), leaf duration can be estimated as the difference in onset dates for same secondary growth stage between principal growth stage 1 and 9.

We used our explanatory data set to demonstrate calculation of leaf appearance rate and phyllochron as a function of both calendar days and thermal time. Thermal time was measured in growing degree days (GDD, °C day) as:

$$GDD = \left[\frac{T_{max} - T_{min}}{2} \right] - T_b$$

Where T_{max} and T_{min} are daily maximum and minimum air temperature, respectively, and T_b is the base temperature below which development does not occur. We used 6°C as the base temperature for leaf expansion (Farrell et al., 2006) and considered $[(T_{max} - T_{min})/2] = T_b$ when $[(T_{max} - T_{min})/2] < 0$ [see McMaster and Wilhelm, 1997, for further detail on the importance of clarifying how to deal with $[(T_{max} - T_{min})/2] < 0]$. Cumulative degree days were calculated as the sum of daily GDD across the growing season.

For a complete and concise description of principal growth stage progression, the cumulative thermal time should be reported for each principal stage. This could be calculated as the difference between first and last secondary growth stage onset dates. Also, using the development rate approach, it can be estimated as the difference between time at the last secondary growth stage and the first one. This approach has the advantage that it allows estimation of the beginning of the principal growth stage as the root of the describing polynomial.

Calculating Growth Stage and Summary Statistics

Summary statistics allow the scaling of stem-based observations to the field or population level. The method presented here has been modified from Kalu and Fick (1981) and Moore et al. (1991). Since *M.* × *giganteus* may have multiple principal growth stages running in parallel, summary statistics can be calculated separately for each stage (Equations 1, 2). Based on a sample of *N* stems, the average morphological stage at growth stage *i* ($\overline{BBCH_i}$) is calculated as:

$$\overline{BBCH_i} = \frac{\sum_{j=1}^{N} BBCH_{ij}}{N} \tag{1}$$

Where $BBCH_{ij}$ represents the BBCH code for the *j*th stem in the *i*th principal growth stage. Essentially, $\overline{BBCH_i}$ estimates the average BBCH code for each individual principal stage. The complete developmental stage ($BBCH_{complete}$) would be presented as all the average codes for each stage separated by oblique strokes. Alternatively, if users stop tracking one stage once the next begins, the complete code is the two digit code associated with most developed stage.

The variability across samples is determined for each principal growth stage individually as the standard deviation for principal growth stage i (S_{BBCHi}), calculated as:

$$S_{BBCHi} = \sqrt{\frac{\sum_{j=1}^{N} \left(\overline{BBCH_i} - BBCH_{ij}\right)^2}{N}} \qquad (2)$$

S_{BBCHi} is useful to estimate the variability that exists within an $M. \times giganteus$ stand at each principal growth stage and help to compare the progression of each stage. A small S_{BBCHi} indicates the majority of stems are at similar level of progression within a given principal growth stage, while a large S_{BBCHi} indicates that there is a wide range of maturity within a growth stage.

RESULTS

We modified the BBCH scale to describe morphological development stages of $M. \times giganteus$ using peer-reviewed literature supplemented by field observations made over a range of plant age and growth conditions. Below we present descriptions of $M. \times giganteus$ principal growth stages (**Table 2**) and use morphological development data to demonstrate the calculation of stage summary statistics as well stage onset, duration, and abundance for phenology assessment.

BBCH Scale Description and Codification for $M. \times giganteus$

Principal Growth Stage 0: Bud Development

Stage 0 describes plant development beginning with rhizome buds. It is also applicable to axillary buds growing from aerial stems, which have also been proposed as propagules (Boersma and Heaton, 2014), as in sugarcane. Rhizome bud development goes from beginning of bud swelling (stage 01) through emergence when leaves break through the soil surface (stage 09). Bud swelling ends (stage 03, **Figure 1**) as buds break (stage 05), the first true leaves elongate past protective bud scales (**Figure 1**), and leaf laminae grow toward the soil surface (**Table 2**). In the establishment year, bud development typically begins in late spring, depending on planting date and weather conditions. In older stands, stem emergence typically begins when soil temperatures are consistently above 10°C or cumulative degree days above 0°C are higher than 650 (Hastings et al., 2009).

Principal Growth Stage 1: Leaf Development

This principal stage is based on the total number of leaves present on the stem and does not differentiate between green or senesced leaves. Observers can choose to assess only green leaves or include senesced leaves, depending on their goals. The proportion of senesced leaves present at a given point is presented in stage 9, senescence. New leaves are not counted until fully expanded as indicated by a visible ligule. New leaves continue to emerge until the stem fully flowers and senesces, or is winter-killed. $M. \times giganteus$ typically has less than 20 leaves on a stem; therefore, we suggest here that secondary stages advance by every two leaves (**Table 2**). For example, a stem with two fully expanded leaves would be at growth stage 11, where the principal growth stage 1 (leaf development) is given in the tens place and the secondary growth stage is given in the ones place as 2 leaves/2 = 1. Similarly, a stem with 8 leaves would be at growth stage 14 (**Figure 1**). Should a stem have 15 leaves, a mesostage can be added using a decimal point, and the stem would be at growth stage 17.5. Although uncommon, especially if only following green leaves, stems that produce more than 19 leaves would be staged as 19.5, the maximal value for this growth stage.

Principal Growth Stage 2: Tillering

Because this scale is applied to individual stems coming from a belowground rhizome network, tillering in this sense refers to new stems developed from axillary buds on the monitored stem. $M. \times giganteus$ stems are unbranched and rarely produce tillers, however, some swollen axillary buds could appear on the base of the stem, especially if the stem is damaged (e.g., from hail or herbivory). Rarely, these buds will produce new stems and it is even more seldom that these stems will reach the canopy level. Secondary stages in this case correspond to the number of tillers produced per stem. The norm is no tillers on a stem (stage: 20) though infrequently one or two tillers may be present (stage 21 or 22).

Presence of swollen buds could be recorded within this principal growth stage since it could have impacts on phenology and plant physiology. These stages would be included as decimal points; 20.1: presence of partially swollen axillary bud (∼2 mm), 20.5: axillary bud fully swollen (∼8–1.0 mm, **Figure 1**), 20.9: Bud breaking. Finally, in the case of tillering, the scale continues to be applied to the main stem (**Table 2**).

Principal Growth Stage 3: Stem Elongation

In $M. \times giganteus$, stem elongation occurs soon after emergence and continues until the culm flowers or is winter-killed. This stage is of prime importance since it tracks the development of the principal harvestable structure. Stem elongation is addressed by counting the number of aboveground palpable nodes present on the stem, that is, the number of nodes that can be felt by gently pressing along the stem. We suggest that, as in leaves, secondary stages progress every two nodes (**Table 2**). For example, a stem with eight fully expanded leaves and four palpable nodes would be coded as 14/32 (**Figure 1**), indicating 4 * 2 = 8 leaves in principal growth stage 1 (leaf development) and 2 * 2 = 4 palpable nodes in principal growth stage 3 (stem elongation). If more detail is needed, odd number of nodes could be coded as mesostages using the tenths place. For example, if a stem has seven nodes it should be staged as 33.5, indicating 3 * 2 = 6 nodes and 0.5 indicating the presence of another node (giving a total of seven nodes). As in leaf development, stems with more than 19 nodes (biologically rare, Uwatoko et al., 2016) will all be staged as 39.5.

Principal Growth Stage 4: Booting

This principal stage refers to the progression of the inflorescence through the appearance of the flag leaf sheath. It starts when flag leaf is visible but lamina still rolled (stage 40). Stage 41 occurs when the flag leaf is fully expanded (**Figure 1**), indicating the end of leaf development. Booting ends when the inflorescence fills the
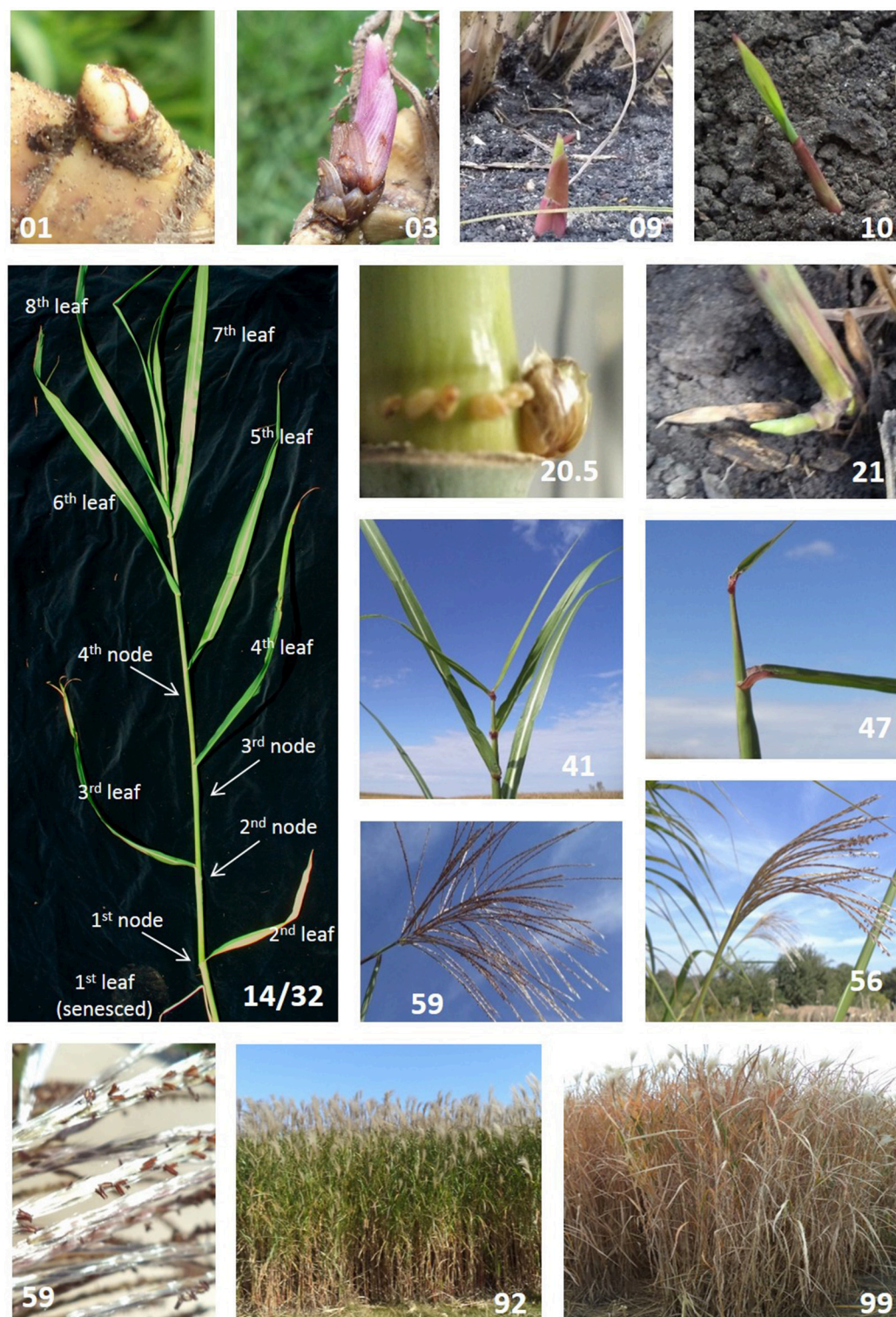
FIGURE 1 | Select *Miscanthus × giganteus* morphological development stages as described using the BBCH scale (**Table 2**). Each picture highlights a single developmental stage: 01 beginning of bud swelling; 03 end of bud swelling; 09 emergence through soil surface; 10 first visible leaf lamina; 14/32 stem with eight fully expanded leaves (14) and 4 nodes (32); 20.5 swollen axillary bud (~8–10 mm); 21 one tiller on main shoot; 41 flag leaf is fully expanded; 47 inflorescence occupies 75% of flag leaf sheath; 56 inflorescence lower branches exposed; 59 inflorescence fully exposed and peduncle exposure; 59 showing anther details; 92 stems 20% senesced; 99 stems 90–100% senesced.

entire flag leaf sheath and no florets are yet exposed (stage 49). Intermediate secondary stages distinguish the proportion of the sheath occupied by the inflorescence. Since this could be hard to identify and track we recommend using generic landmarks and assigning them in 25% increments. In consequence, only three secondary growth stages are required to allocate these morphological changes evenly: 43, 45, and 47 (**Table 2**, **Figure 1**). For instance, stage 43 occurs when the inflorescence fills 25% of the sheath, stage 45 when the inflorescence occupies 50% and so on. First florets may not appear through the collar of the flag leaf and may grow instead through the sheath. In this case the stem will still be staged as 49.

Principal Growth Stage 5: Inflorescence Emergence

The $M. \times$ *giganteus* inflorescence is a panicle of racemose branches with paired and pedicellate spikelets (Hodkinson and Renvoize, 2001). This stage starts with upper spikelets coming out of the flag leaf collar (stage 51) and ends once the panicle is fully exposed and the peduncle is visible (stage 59). In general terms, secondary stages could be characterized by: upper branch exposure (borne on the upper half of the main axis, stage 53), lower branch exposure (borne on the lower half of the main axis lower branches, stage 56, **Figure 1**) and peduncle exposure (stage 59, **Table 2**, **Figure 1**). If more detail is required, secondary growth stages could be expressed as the exposed percentage of the panicle. This requires a trained observer to estimate the relative proportion of a partially exposed panicle. Note that stage 59 may not occur in environments where the growing season is not long enough or hard frost events are frequent in middle to late fall. In this case inflorescence emergence may stop before the panicle is fully exposed. Exposed florets may continue to open.

Principal Growth Stage 6: Flowering

This stage is defined as the proportion of exposed florets with emerged anthers. It starts with sporadic exposed anthers (stage 60) until full flowering (stage 69) when anthers are present throughout the entire inflorescence; secondary stages are attributed in 10 percent increments (e.g., stage 65: 50% of anthers are exposed, **Table 2**, **Figure 1**). Flowering proceeds basipetally through the inflorescence. Anther exposure can occur while the inflorescence is still emerging and, consequently, the inflorescence could fully flower even though the inflorescence is not fully exposed.

$M. \times$ *giganteus* is a sterile clone and no seed is produced so flowering represents the last reproductive stage. In order to expand the scope of this scale to other varieties and *Miscanthus* spp., grain maturity stages were included. These stages were based on general grass descriptions from Meier (2001) as adapted to perennial grasses (e.g., *P. virgatum*) by Sanderson et al. (1997).

Principal Growth Stage 7: Seed Development

At the beginning of seed development (stage 71) the total number of cells in the endosperm is established and grains have a watery ripe consistency; first grains may have reached half their final size. Gradually, seeds increase solid (e.g., starch, protein) concentrations and reach their final size at medium milk stage (75). Seed development ends at late milk stage (77).

Principal Growth Stage 8: Ripening

Most of the seed dry weight is accumulated during the ripening stage. Along with the continued increment in starch and protein concentration, water content decreases, increasing grain hardness. Secondary stages are characterized by pressing the grain with a fingernail. Stage 83 is when grain content is soft and the fingernail impression is not held; 85 is when a fingernail impression remains after the test. Stage 87 represents when the grain is hard and difficult to break with a thumbnail and finally stage 89 is when the grain cannot be dented.

Principal Growth Stage 9: Senescence

This stage describes the senescence progression of the stem during a growing season and it is based on leaf senescence without differentiating between possible causes, e.g., stress or seasonal cues. In order to provide a better approach for comparative purposes it should be reported as the proportion of the total number of leaves present at any given point. A leaf is consider senesced once 50% or more of the laminae has senesced. For simplicity, it could also be quantified as a visual estimate of the senesced proportion of the entire plant. For instance, a plant with five senesced leaves out of a total of 25 could be considered 20% senesced and coded as 92 (**Figure 1**). Stages 91–99 represent the progressive senescence of leaves on the stem, from 10 to 90%, respectively, at 10% increments (**Table 2**, **Figure 1**). This stage could start very early in the growing season once the stand reaches canopy closure and low light quality triggers senescence in lower canopy leaves.

Using Morphological Data to Assess Phenology

Estimating Growth Stage Progression

In 2016, morphological development was observed biweekly in 2-year-old $M. \times$ *giganteus*. Data were used to illustrate the steps required to estimate progression of morphological development stages using the cumulative abundance of a given stage (**Table 3**). For example on July 11 there were four stems at stage 15 or higher (2 at 15 and 2 at 15.5) and 0 stems at stage 18. By September 6 all sampled stems were at stage 15 or higher, and seven were at stage 18 or higher (4 at 18, 2 at 18.5 and 1 at 19). Note that abundance is expressed as a proportion and thus is not dependent on equal sample sizes between dates. Graphing cumulative abundance of growth stages 15 and 18 over time produced sigmoid curves that were used to derive the onset date of each stage (**Figure 2**). The onset date of stage 15 was July 13 (5282 GDD) and the onset date of stage 18 was August 19 (7963 GDD).

We also estimated PGSDR for principal growth stage 1 (leaf development; $PGSDR_1$) and 3 (stem elongation; $PGSDR_3$) as the slope of the linear regression between average principal growth stage per sampling date and thermal time in GDD (**Figure 3**). For example, $PGSDR_1 = 0.00094$ means that almost a thousandth of a secondary growth stage is developed per GDD. Its inverse (1053) represents the number of GDD required to complete a secondary growth stage. Given that secondary growth stages advance every two leaves, leaf appearance rate is double $PGSDR_1$ (0.00188 leaf GDD^{-1}) and the phyllochron is half of $PGSDR_1$ (526.5 GDD leaf $^{-1}$).
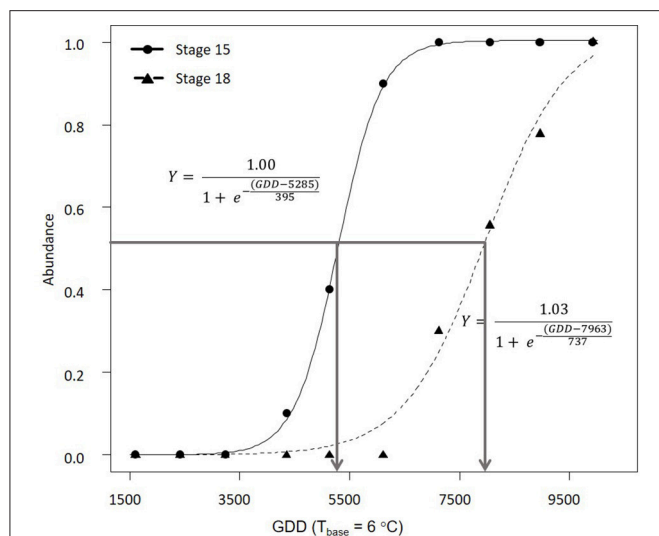
FIGURE 2 | Progression of 2-year-old *Miscanthus × giganteus* through BBCH developmental stages 15 and 18 in 2016. The horizontal line indicates 50% of stems at certain stage or higher and the arrows indicate the estimated onset date for each stage. Logistic equation for each progression is also presented.
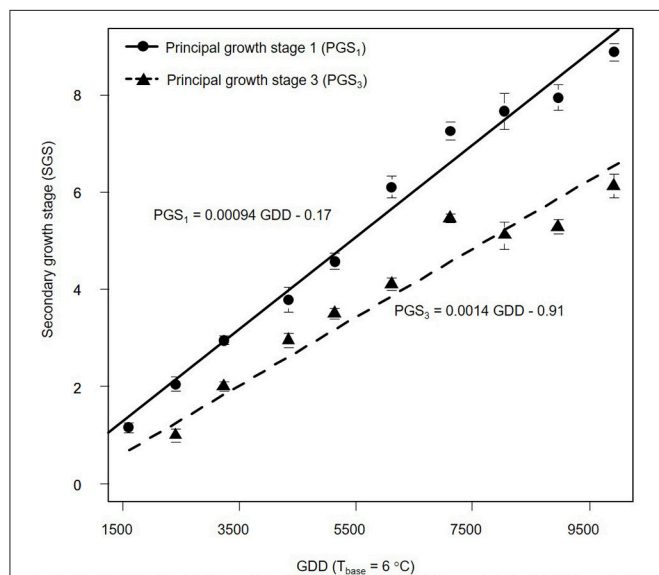
FIGURE 3 | Progression of *Miscanthus × giganteus* principal growth stage 1 (leaf development) and 3 (stem elongation) over growing degree days (GDD). Stages were based on the BBCH scale developmental scale. Each observation is the average of 10 stems. Vertical lines represent ± 1 standard error; see text for details on the summary statistic methods. Linear equations for each principal growth stage are provided and principal growth stage developmental rate corresponds to the slope of each equation.

Growth Stage and Summary Statistics

The *M. × giganteus* morphological development data collected over the 2016 growing season was also used to demonstrate the calculation of the average and standard deviation of principal growth stages 1 and 3 (**Table 4**).

TABLE 4 | Explanatory data showing the principal growth stages (1 = leaf development and 3 = stem elongation) and secondary growth stages of five *Miscanthus × giganteus* stems over four sampling dates in 2016 in Sorenson farm, Iowa.

Principal Growth Stage	May-19	Jun-13	Jul-11	Sep-6
1: LEAF DEVELOPMENT				
	11.5	12.5	14	18.5
	11.5	12.5	15.5	18
	11	13.5	15	18.5
	11.5	13	15.5	16.5
	11	13	14.5	18
$BBCH_1$	$\frac{56.5}{5}=11.3$	$\frac{64.5}{5}=12.9$	$\frac{74.5}{5}=14.9$	$\frac{89.5}{5}=17.9$
S_{BBCH1}	$\sqrt{\frac{0.3}{5}}=0.24$	$\sqrt{\frac{0.7}{5}}=0.37$	$\sqrt{\frac{1.7}{5}}=0.58$	$\sqrt{\frac{2.7}{5}}=0.74$
3: STEM ELONGATION				
	30	32	33.5	36
	30	31.5	34	35.5
	30	31.5	34	35.5
	30	32	33.5	35
	30	32.5	33.5	35.5
$BBCH_3$	$\frac{150}{5}=30$	$\frac{159.5}{5}=31.9$	$\frac{168.5}{5}=33.7$	$\frac{177.5}{5}=35.5$
S_{BBCH3}	$\sqrt{\frac{0}{5}}=0$	$\sqrt{\frac{0.7}{5}}=0.37$	$\sqrt{\frac{0.3}{5}}=0.24$	$\sqrt{\frac{0.5}{5}}=0.31$
$BBCH_{complete}$	11.3	12.9/31.9	14.9/33.7	17.9/35.5

Average stage, standard deviation at principal growth stage i (BBCH_i), and the complete growth stage for each sampling date are presented.

DISCUSSION

We used peer-reviewed literature and field observations to modify the BBCH morphological development scale (Lancashire et al., 1991) for *M. × giganteus* and related species. The inclusion of principal growth stages related to seed development, absent today in commercial clones, allows easy adaption and application of the scale to other species including new seeded hybrids with higher adaptability and stress tolerance (Clifton-Brown et al., 2017). The detailed, yet flexible scale framework should enable inter-comparison of *M. × giganteus* studies, and facilitate phenological research and crop management.

Comparison with Other Scales

The simplicity of the *Miscanthus* BBCH scale permits conversion of previous phenological descriptions into a standardized form regardless of the specific research topic, allowing comparison of results from multiple study-specific scales. For example, the five-point scale (1 = 80–100% green, 2 = 60–80% green, 3 = 40–60% green, 4 = 20–40% green, 5 = <20% green) used by Purdy et al. (2015) to characterize *Miscanthus* spp. seasonal carbohydrate dynamics corresponds to stages 90 through 99 in our BBCH scale. Similarly, in the scale Fonteyne et al. (2016) used (0 = no flowering, 1 = flag leaf formed, 2 = panicle emergence, 3 = anthesis, 4 = end of anthesis) to study rhizome and shoot frost tolerance, stages 1, 2, 3, and 4 correspond to BBCH stages 41, 59, principal stage 6, and 69, respectively. However, Fonteyne's (2016) stage 3 (anthesis) does not provide

enough detail about anthesis progression through the panicle to allow for a secondary BBCH stage to be attributed. Additionally, "no-flowering" (Fonteyne's stage 0) is not specific enough to link to any BBCH stage.

While the above scales were used to assess plant physiology with implications for plant breeding, phenology is also widely used in ecosystem modeling assessments. The phenological description used by Miguez et al. (2009) to parameterize the eco-physiological model WIMOVAC for $M. \times giganteus$ is different than the one used in MISCANFOR (Hastings et al., 2009), however, they could both be coded consistently using the BBCH scale reported here. Likewise, the scale Hastings et al. (2009) used to describe $M. \times giganteus$ growth and development counting GDD using a base temperature of above 0°C (GDD_0) could be expressed using our BBCH code system in the following ways: shoot emergence (BBCH stage 09) starts at $GDD_0 > 650$, mean air temperature > 10°C, and when the photoperiod is longer than 12 h. Leaf development (BBCH stage 10) starts at $GDD_0 > 850$ and ends (BBCH stage 19) when leaf area index < 8, 3 days below 10°C, 3 days below the wilting point, or $GDD_0 = 2,200$. Finally, plant senescence starts (BBCH stage 90) when there are 6 days below 10°C, one frost day, or 30 wilting days. Similarly, phenology assessment can also be expressed using our BBCH scale in the Agricultural Production Systems Simulator (APSIM) re-parametrization for $M. \times giganteus$ developed by Ojeda et al. (2017) based on Trybula et al. (2015). They used GDD = 1,000 from emergence to stem elongation. This equates to stage 09 through principal growth stage 3 in our scale. Similarly, GDD = 800 from stem elongation to flowering, is from principal growth stage 3 to principal growth stage 5, and GDD = 300 from flowering to full senescence, corresponds to principal growth stage 5 to stage 99 in our scale.

Scale Uses and Applications

In addition to interoperability, another important advantage of our BBCH scale is its scalability, made possible by the arithmetically meaningful nature of its numerical indices and coding. Scalability allows measurement on a practical scale, i.e., on individual stems, rather than depending on sampling non-discreet plants or undertaking the sampling of an entire population. The method presented here to estimate summary statistics from a multiple-stem sample has been modified from Kalu and Fick (1981) and Moore et al. (1991) to incorporate multiple development states of $M. \times giganteus$ in parallel. This is a crucial attribute of our coding system because not only do individual stems experience multiple stages in parallel notably leaf development (1) and stem elongation (3), but it is a virtual certainty that multiple stages would be observed among stems at a field scale, and not considering parallel stages could produce misleading estimates. Take, for example, a sample of stems where one has only four leaves (stage 12) and the other already two palpable nodes (stage 31). The calculated mean growth stage for the sample would be 22, indicating the average stem has two tillers, which is completely erroneous, and biologically unlikely since tillering in $M. \times giganteus$ is rare. In contrast, estimating summary statistics per principal growth stage and presenting them together separated by oblique strokes provides a more accurate description.

Repeated observations reveal progression of morphological stages and enable calculation of important $M. \times giganteus$ phenology parameters. For example, onset dates are useful to coordinate agronomic practices and help characterize the effect of environmental and management factors on the growth cycle. We presented a regression-based method to model phenological progression over time estimating onset and duration of stages. This method, adapted from Schirone et al. (1991), is flexible enough to use with other nonlinear models. For example, an asymptotic exponential curve could be used if the initial lag phase is very short; see Archontoulis and Miguez (2013) for a complete review of other possible nonlinear models. Another convenient feature is that it allows use of different thresholds to define onset dates. However, sigmoidal curve interpolation errors are larger at the beginning and end of the curve so, for a better estimation of onset dates, thresholds should be within the linear section of the curve (Cornelius et al., 2011). Moreover, this method is not restricted to calendar date as a measure of time, but can be used for estimations using accumulated thermal time or light interception to further parameterize ecosystem models. Principal growth stage developmental rate also describes progression of morphological stages. While calculation of onset dates provides a better description of the progression of an individual secondary growth stage, PGSDR estimates the rate of progression of the entire principal growth stage and requires fewer observations to be estimated. If PGSDR is constant for all secondary growth stages, the difference between onset dates of two sequential stages is equivalent to PGSDR.

In conclusion, the proposed extended BBCH scale provides a detailed and accurate description of $M. \times giganteus$ morphological stages, using a simple and intuitive two-digit code method. Overall, the proposed modified BBCH scale will enhance effective communication by presenting a precise and uniform framework of terminology and quantitative metrics that enable analytical assessment. The scale takes into account special features of $M. \times giganteus$ such as, its perennial life cycle, lack of seed production, rhizomatous growing habit and indiscreet plants. Moreover, it easily accommodates the development of the large number of leaves and nodes produced by $M. \times giganteus$ stems. Used together with methods presented here to spatially upscale and assess phenology, this coding system provides support to the entire $M. \times giganteus$ community by enabling intercomparison across scientific studies and providing growers with developmentally appropriate crop management guidance.

AUTHOR CONTRIBUTIONS

MT collected all data required for the research, developed the current scale and was the main author of the paper. EH supervised MT and provided substantial contributions to the conception and writing of the paper.

ACKNOWLEDGMENTS

REFERENCES

Archontoulis, S. V., and Miguez, F. E. (2013). Nonlinear regression models and applications in agricultural research. *Agron. J.* 105, 1–13. doi: 10.2134/agronj2012.0506

Archontoulis, S. V., Struik, P. C., Vos, J., and Danalatos, N. G. (2010). Phenological growth stages of *Cynara cardunculus* : codification and description according to the BBCH scale. *Ann. Appl. Biol.* 156, 253–270. doi: 10.1111/j.1744-7348.2009.00384.x

Arnoult, S., and Brancourt-Hulmel, M. (2015). A review on miscanthus biomass production and composition for bioenergy use: genotypic and environmental variability and implications for breeding. *Bioenergy Res.* 8, 502–526. doi: 10.1007/s12155-014-9524-7

Boersma, N. N., and Heaton, E. A. (2014). Does propagation method affect yield and survival? The potential of *Miscanthus×giganteus* in Iowa, USA. *Ind. Crops Prod.* 57, 43–51. doi: 10.1016/j.indcrop.2014.01.058

Bonnett, G. D. (2013). "Developmental stages (Phenology)," in *Sugarcane: Physiology, Biochemistry, and Functional Biology*, eds A. M. Tronsmo and H. Fykse (Chichester: John Wiley & Sons Ltd), 35–53.

Cadoux, S., Riche, A. B., Yates, N. E., and Machet, J. M. (2012). Nutrient requirements of *Miscanthus x giganteus*: conclusions from a review of published studies. *Biomass Bioenergy* 38, 14–22. doi: 10.1016/j.biombioe.2011.01.015

Christian, D. G., Riche, A. B., and Yates, N. E. (2008). Growth, yield and mineral content of *Miscanthus x giganteus* grown as a biofuel for 14 successive harvests. *Ind. Crops Prod.* 28, 320–327. doi: 10.1016/j.indcrop.2008.02.009

Clifton-Brown, J. C., Breuer, J., and Jones, M. B. (2007). Carbon mitigation by the energy crop, *Miscanthus*. *Glob. Change Biol.* 13, 2296–2307. doi: 10.1111/j.1365-2486.2007.01438.x

Clifton-Brown, J., Hastings, A., Mos, M., McCalmont, J. P., Ashman, C., Awty-Carroll, D., et al. (2017). Progress in upscaling *Miscanthus* biomass production for the European bio-economy with seed-based hybrids. *GCB Bioenergy* 9, 6–17. doi: 10.1111/gcbb.12357

Cornelius, C., Petermeier, H., Estrella, N., and Menzel, A. (2011). A comparison of methods to estimate seasonal phenological development from BBCH scale recording. *Int. J. Biometeorol.* 55, 867–877. doi: 10.1007/s00484-011-0421-x

da Costa, R. M., Lee, S. J., Allison, G. G., Hazen, S. P., Winters, A., and Bosch, M. (2014). Genotype, development and tissue-derived variation of cell-wall properties in the lignocellulosic energy crop *Miscanthus*. *Ann. Bot.* 114, 1265–1277. doi: 10.1093/aob/mcu054

Dalla Marta, A., Mancini, M., Orlando, F., Natali, F., Capecchi, L., and Orlandini, S. (2014). Sweet sorghum for bioethanol production: crop responses to different water stress levels. *Biomass Bioenergy* 64, 211–219. doi: 10.1016/j.biombioe.2014.03.033

Denny, E. G., Gerst, K. L., Miller-Rushing, A. J., Tierney, G. L., Crimmins, T. M., Enquist, C. A., et al. (2014). Standardized phenology monitoring methods to track plant and animal activity for science and resource management applications. *Int. J. Biometeorol.* 58, 591–601. doi: 10.1007/s00484-014-0789-5

Dohleman, F. G., Heaton, E. A., Arundale, R. A., and Long, S. P. (2012). Seasonal dynamics of above- and below-ground biomass and nitrogen partitioning in *Miscanthus* × giganteus and *Panicum virgatum* across three growing seasons. *GCB Bioenergy* 4, 534–544. doi: 10.1111/j.1757-1707.2011.01153.x

Farrell, A. D., Clifton-Brown, J. C., Lewandowski, I., and Jones, M. B. (2006). Genotypic variation in cold tolerance influences the yield of *Miscanthus*. *Ann. Appl. Biol.* 149, 337–345. doi: 10.1111/j.1744-7348.2006.00099.x

Feekes, W. (1941). *De Tarwe en Haar Milieu*. Groningen: Tarwe Commission.

Fonteyne, S., Muylle, H., De Swaef, T., Reheul, D., Roldán-Ruiz, I., and Lootens, P. (2016). How low can you go?-Rhizome and shoot frost tolerance in *Miscanthus* germplasm. *Ind. Crops Prod.* 89, 323–331. doi: 10.1016/j.indcrop.2016.05.031

Greef, J. M., Deuter, M., Jung, C., and Schondelmaier, J. (1997). Genetic diversity of European *Miscanthus* species revealed by AFLP fingerprinting. *Genet. Resour. Crop Evol.* 44, 185–195. doi: 10.1023/A:1008693214629

Hastings, A., Clifton-Brown, J., Wattenbach, M., Mitchell, C. P., and Smith, P. (2009). The development of MISCANFOR, a new *Miscanthus* crop growth model: towards more robust yield predictions under different climatic and soil conditions. *Glob. Change Biol. Bioenergy* 1, 154–170. doi: 10.1111/j.1757-1707.2009.01007.x

Haun, J. R. (1973). Visual quantification of wheat development. *Agron. J.* 65, 116. doi: 10.2134/agronj1973.00021962006500010035x

Heaton, E. A., Dohleman, F. G., and Long, S. P. (2008). Meeting US biofuel goals with less land: the potential of *Miscanthus*. *Glob. Change Biol.* 14, 2000–2014. doi: 10.1111/j.1365-2486.2008.01662.x

Hess, M., Barralis, G., Bleiholder, H., Buhr, L., Eggers, T. H., Stauss, H., et al. (1997). Use of the extended BBCH-scale - general for the description of the growth stages of mono- and dicotyledonous weed species. *Weed Res.* 37, 433–441. doi: 10.1046/j.1365-3180.1997.d01-70.x

Hodkinson, T. R., and Renvoize, S. (2001). Nomenclature of *Miscanthus x giganteus* (Poaceae). *Kew Bull.* 56, 759–760. doi: 10.2307/4117709

Jensen, E., Farrar, K., Thomas-Jones, S., Hastings, A., Donnison, I., and Clifton-Brown, J. (2011). Characterization of flowering time diversity in *Miscanthus* species. *GCB Bioenergy* 3, 387–400. doi: 10.1111/j.1757-1707.2011.01097.x

Jones, M. B., Finnan, J., and Hodkinson, T. R. (2015). Morphological and physiological traits for higher biomass production in perennial rhizomatous grasses grown on marginal land. *GCB Bioenergy* 7, 375–385. doi: 10.1111/gcbb.12203

Kalu, B. A., and Fick, G. W. (1981). Quantifying morphological development of alfalfa for studies of herbage quality. *Crop Sci.* 21, 267–271. doi: 10.2135/cropsci1981.0011183X002100020016x

Lancashire, P. D., Bleiholder, H., Van Den Boom, T., LangelÜDdeke, P., Stauss, R., Weber, E., et al. (1991). A uniform decimal code for growth stages of crops and weeds. *Ann. Appl. Biol.* 119, 561–601. doi: 10.1111/j.1744-7348.1991.tb04895.x

Landes, A., and Porter, J. R. (1989). Comparison of scales used for categorising the development of wheat, barley, rye and oats. *Ann. Appl. Biol.* 115, 343–360. doi: 10.1111/j.1744-7348.1989.tb03393.x

Large, E. C. (1954). Growth stages in cereals illustration of the feekes scale. *Plant Pathol.* 3, 128–129. doi: 10.1111/j.1365-3059.1954.tb00716.x

Martínez-Nicolás, J. J., Legua, P., Melgarejo, P., Martínez, R., and Hernández, F. (2016). Phenological growth stages of nashi tree (*Pyrus pyrifolia*): codification and description according to the BBCH scale. *Ann. Appl. Biol.* 168, 255–263. doi: 10.1111/aab.12261

McMaster, G. S., and Wilhelm, W. W. (1997). Growing degree-days: one equation, two interpretations. *Agric. For. Meteorol.* 87, 291–300. doi: 10.1016/S0168-1923(97)00027-0

Meier, U. (2001). Growth stages of mono-and dicotyledonous plants. *BBCH Monogr. Agric* 12, 141–147. doi: 10.5073/bbch0515

Meier, U., Bleiholder, H., Buhr, L., Feller, C., Hack, H., Heß, M., et al. (2009). The BBCH system to coding the phenological growth stages of plants-history and publications. *J. für Kult.* 61, 41–52. Available online at: https://www.journal-kulturpflanzen.de/artikel.dll/meier- et-al_OTAyMjUy.PDF

Miguez, F. E., Zhu, X., Humphries, S., Bollero, G. A., and Long, S. P. (2009). A semimechanistic model predicting the growth and production of the bioenergy crop *Miscanthus×giganteus*: description, parameterization and validation. *GCB Bioenergy* 1, 282–296. doi: 10.1111/j.1757-1707.2009.01019.x

Moore, K. J., Moser, L. E., Vogel, K. P., Waller, S. S., Johnson, B. E., and Pedersen, J. F. (1991). Describing and quantifying growth stages of perennial forage grasses. *Agron. J.* 83, 1073. doi: 10.2134/agronj1991.00021962008300060027x

Ojeda, J. J., Volenec, J. J., Brouder, S. M., Caviglia, O. P., and Agnusdei, M. G. (2017). Evaluation of agricultural production systems simulator as yield predictor of *Panicum virgatum* and *Miscanthus x giganteus* in several US environments. *GCB Bioenergy* 9, 796–816. doi: 10.1111/gcbb.12384

Purdy, S. J., Cunniff, J., Maddison, A. L., Jones, L. E., Barraclough, T., Castle, M., et al. (2015). Seasonal carbohydrate dynamics and climatic regulation

of senescence in the perennial grass, *Miscanthus. Bioenergy Res.* 8, 28–41. doi: 10.1007/s12155-014-9500-2

Robson, P., Mos, M., Clifton-Brown, J., and Donnison, I. (2012). Phenotypic variation in senescence in *Miscanthus*: towards optimising biomass quality and quantity. *Bioenergy Res.* 5, 95–105. doi: 10.1007/s12155-011-9118-6

Sanderson, M. A., West, C. P., Moore, K. J., Stroup, J., and Moravec, J. (1997). Comparison of morphological development indexes for switchgrass and bermudagrass. *Crop Sci.* 37, 871. doi: 10.2135/cropsci1997.0011183X003700030029x

Schirone, B., Leone, A., Mazzoleni, S., and Spada, F. (1991). A new method of survey and data analysis in phenology. *J. Veg. Sci.* 2, 27–34. doi: 10.2307/3235895

Trybula, E. M., Cibin, R., Burks, J. L., Chaubey, I., Brouder, S. M., and Volenec, J. J. (2015). Perennial rhizomatous grasses as bioenergy feedstock in SWAT: parameter development and model improvement. *GCB Bioenergy* 7, 1185–1202. doi: 10.1111/gcbb.12210

Uwatoko, N., Tamura, K., Yamashita, H., and Gau, M. (2016). Naturally occurring triploid hybrids between *Miscanthus sacchariflorus* and *M. sinensis* in Southern Japan, show phenotypic variation in agronomic and morphological traits. *Euphytica* 212, 355–370. doi: 10.1007/s10681-016-1760-9

Xue, Q., Weiss, A., and Baenziger, P. S. (2004). Predicting leaf appearance in field-grown winter wheat: evaluating linear and non-linear models. *Ecol. Modell.* 175, 261–270. doi: 10.1016/j.ecolmodel.2003.10.018

Zadoks, J. C., Chang, T. T., and Konzak, C. F. (1974). A decimal code for the growth stages of cereals. *Weed Res.* 14, 415–421. doi: 10.1111/j.1365-3180.1974.tb01084.x

Zub, H. W., Arnoult, S., Younous, J., Lejeune-Hénaut, I., and Brancourt-Hulmel, M. (2012). The frost tolerance of *Miscanthus* at the juvenile stage: differences between clones are influenced by leaf-stage and acclimation. *Eur. J. Agron.* 36, 32–40. doi: 10.1016/j.eja.2011.08.001

Environmental Influences on the Growing Season Duration and Ripening of Diverse *Miscanthus* Germplasm Grown in Six Countries

Christopher Nunn[1]*, Astley Francis St. John Hastings[2], Olena Kalinina[3],
Mensure Özgüven[4], Heinrich Schüle[5], Ivan G. Tarakanov[6], Tim Van Der Weijde[7],
Aleksander A. Anisimov[6], Yasir Iqbal[3], Andreas Kiesel[3], Nikolay F. Khokhlov[6],
Jon P. McCalmont[1], Heike Meyer[8], Michal Mos[9], Kai-Uwe Schwarz[8], Luisa M. Trindade[7],
Iris Lewandowski[3] and John C. Clifton-Brown[1]

[1] Institute of Biological, Environmental and Rural Sciences, Aberystwyth University, Aberystwyth, United Kingdom, [2] School of
Biological and Environmental Sciences, University of Aberdeen, Aberdeen, United Kingdom, [3] Department of Biobased
Products and Energy Crops, Institute of Crop Science, University of Hohenheim, Stuttgart, Germany, [4] Field Crops
Department, Konya Food and Agriculture University, Konya, Turkey, [5] German Agrarian Centre, Potash, Ukraine, [6] Moscow
Timiryazev Agricultural Academy, Russian State Agrarian University, Moscow, Russia, [7] Department of Plant Breeding,
Wageningen University, Wageningen, Netherlands, [8] Schwarz, Braunschweig, Germany, [9] Blankney Estates, Blankney,
United Kingdom

The development of models to predict yield potential and quality of a Miscanthus crop must consider climatic limitations and the duration of growing season. As a biomass crop, yield and quality are impacted by the timing of plant developmental transitions such as flowering and senescence. Growth models are available for the commercially grown clone *Miscanthus x giganteus* (*Mxg*), but breeding programs have been working to expand the germplasm available, including development of interspecies hybrids. The aim of this study was to assess the performance of diverse germplasm beyond the range of environments considered suitable for a Miscanthus crop to be grown. To achieve this, six field sites were planted as part of the EU OPTIMISC project in 2012 in a longitudinal gradient from West to East: Wales—Aberystwyth, Netherlands—Wageningen, Stuttgart—Germany, Ukraine—Potash, Turkey—Adana, and Russia—Moscow. Each field trial contained three replicated plots of the same 15 Miscanthus germplasm types. Through the 2014 growing season, phenotypic traits were measured to determine the timing of developmental stages key to ripening; the tradeoff between growth (yield) and quality (biomass ash and moisture content). The hottest site (Adana) showed an accelerated growing season, with emergence, flowering and senescence occurring before the other sites. However, the highest yields were produced at Potash, where emergence was delayed by frost and the growing season was shortest. Flowering triggers varied with species and only in *Mxg* was strongly linked to accumulated thermal time. Our results show that a prolonged growing season is not essential to achieve high yields if climatic conditions are favorable and in regions where the growing season is bordered by frost, delaying harvest can improve quality of the harvested biomass.

Keywords: miscanthus, ripening, senescence, modeling, multi-location

INTRODUCTION

Miscanthus is a rhizomatous perennial grass of Eastern Asian origin that is cultivated in the USA and Europe for its stem biomass (Clifton-Brown et al., 2001; Heaton et al., 2010). The senesced stems are currently mainly used for heat generation through combustion. *Miscanthus* shows exceptional productivity in temperate zones partly owing to its lower temperature tolerance than other C_4 species such as *Zea mays* (maize) (Wang et al., 2008).

The seasonal pattern of growth of Miscanthus follows a cycle of: spring emergence, leaf expansion, flowering, senescence, and dormancy. The ability of *Miscanthus* to emerge early in spring has been shown to be a key determinant of final yield in the UK (Davey et al., 2016). It was projected using simulation modeling that decreasing the base temperature (T_b) for spring emergence from $10°$ to $9°C$ would result in a 12% increase in intercepted photosynthetically active radiation (iPAR) (Davey et al., 2016). Flowering time has also been shown to influence final yield as early flowering genotypes produce lower yields than those that flower late or not at all (Clifton-Brown et al., 2001; Jensen et al., 2011). Flowering has also been linked to senescence (Wingler et al., 2008, 2010) which marks the end of biomass accumulation for that year. The timing of senescence is critically important for the remobilization of mineral nutrients and carbohydrates back to the rhizome for storage over winter and to drive shoot re-growth in spring. If this process occurs too early yield is reduced but if it occurs too late and the still-active stems are killed by a frost, the nutrients are not all remobilized and the long-term sustainability of the crop may be negatively affected (Robson et al., 2012; Purdy et al., 2014). The timing of the onset of senescence and the rate of its progression also determines the quality of the final biomass. If the timing is late or rate too slow then the crop does not dry-down (ripen) completely before harvest which results in moisture and nutrients being present in the harvested material. This has major impacts on post-harvest microbial spoilage before utilization, transport, and impairs thermal conversion efficiency (Lewandowski et al., 2003; Robson et al., 2012).

Miscanthus is generally harvested at the end of winter after senescence is complete and before emergence of new shoots (January–March). This means that the yield potential is determined by environmental conditions through the growing season combined with the environmental conditions from the end of the growing season until harvest. Temperature has been shown to control growth-rate in grass, over-riding the effects of light and circadian rhythms (Matos et al., 2014). In *Miscanthus*, cold spring temperatures limit the leaf elongation rate and cold autumn night-time temperatures can accelerate senescence and over-ride favorable warm day-time temperatures (Farrell et al., 2006; Purdy et al., 2014). A greater understanding of the effects of regional climate on plant development would help identify the optimal genotype to grow in a particular location.

Most of the research on *Miscanthus* has been carried out on a single genotype, the sterile hybrid, *M. x giganteus*. However, enormous diversity exists in the species and breeding programs are generating new elite varieties to expand the European market

(Clifton-Brown et al., 2008) and the ability to predict the yield performance of diverse genotypes in a range of climatic regions would accelerate the release of new varieties tailored to specific locations.

Process based models for traits such as leaf expansion, radiation use efficiency (RUE) and the ability of the canopy to intercept light [the canopy extinction coefficient (k)] have previously been developed for *Miscanthus* (Clifton-Brown et al., 2000, 2004; Hastings et al., 2008, 2009; Davey et al., 2016). However, the genotypes used to parameterize the existing models are clonal, wild-type germplasm whereas breeding research is focused on the production of elite seed propagated varieties (Clifton-Brown et al., 2016). To address this gap in the modeling data we have built on the existing MiscanFor (Hastings et al., 2009) model that predicts biomass accumulation using all the trait models described above and including the principles of Monteith (1978). This model uses thermal time as a driver for plant development and cumulative radiation intercepted to calculate biomass accumulation. Cumulative degree days above a threshold base temperature (T_b), determine the beginning and end of the growing season, constrained by the first autumn frost and soil moisture (Hastings et al., 2009). The cumulative degree day calculation (DDc) is a measure of the accumulation of temperature units from stem emergence to each developmental stage. It is used to derive the physical status of plant development in the model (Hastings et al., 2009) and is particularly useful for comparing *Mxg* performance at different sites as it accounts for the faster growth in warmer climates. However, the senescence and ripening processes have been poorly characterized in experiments in the past and thus the current model process descriptions of the plant dieback and biomass ripening are rather crude.

The objective of this study is the investigation of parameters used in existing *Miscanthus* models, such as MiscanFor, to extend their use to new hybrids in different climatic and soil environments by providing an improved description of the timing of key developmental stages and growth and ripening rates. This was achieved in instrumented and replicated field trials that were established at six sites in a longitudinal and latitudinal gradient across Europe planted with 15 new genotypes developed by *Miscanthus* breeding programs located in Aberystwyth (UK), Wageningen (Netherlands), and Braunschweig (Germany). Soil at each site was characterized by coring down to 1 m to determine soil texture, profile depth, and calculated plant available water. The climatic conditions and soil temperatures were monitored by on-site weather stations for 4 years from planting and phenotypic and yield measurements were taken over 2 years (Kalinina et al., 2017). Statistical analysis indicated that there was a strong interaction between genotype and environment (including soil and climatic conditions; Kalinina et al., 2017).

We hypothesized that novel germplasm that could extend the growing season duration, either by early emergence or later senescence, would lead to a greater yield without a sacrifice in biomass quality (through increased moisture content). Further to this, we anticipated matching germplasm best suited to the diverse environments of the six widely distributed trial locations.

There was large variation in the progression of ripening and the traits leading to the end of the growing season with species type and location with some genotypes not flowering at all and growth continuing in others after the initiation of flowering. In locations with significant periods of sub-zero temperatures, the time between thawing and harvest did affect the harvest quality. The yields were produced at the location with the shortest growing season from emergence to peak yield.

MATERIALS AND METHODS

Field Trials

In spring 2012, a multi-location, replicated plot trial was established at six sites around Europe. The full details of the plot establishment, agronomics and yields are reported in Kalinina et al. (2017). The sites were selected to provide a wide range of climatic conditions in Turkey near Adana, in Germany near Stuttgart, in Ukraine near Potash, in the Netherlands at Wageningen, in the United Kingdom near Aberystwyth and in Russia near Moscow (**Table 1**). For the remainder of this paper, the sites will be referred to by the name of the nearest town; Adana, Stuttgart, Potash, Wageningen (abbreviated to "Wagen"), Aberystwyth (abbreviated to "Aber"), and Moscow. The field trials were established on arable or horticultural land except in Aberystwyth, where the trial was planted on marginal (low quality) grassland. The trial was planted as a randomized block design (generated with Genstat 14th edition) consisting of three blocks each containing a single replicate plot of each of the 15 germplasm types (**Table 2**). Each 5×5 m plot contained 49 plants, giving a resultant planted density of just under 2 plants m^{-2}.

Plant Material

Clonal genotypes and seeded types were selected from the different genetic collections of *Miscanthus* spp. in United Kingdom, The Netherlands and Germany. They were provided by Aberystwyth University, Wageningen University and SCHWARZ consulting (Kalinina et al., 2017). The 15 germplasm types included four selected genotypes of wild *M. sacchariflorus* collected from 31° to 37° latitude, five interspecies hybrids of *M. sacchariflorus* and *M. sinensis*, four *M. sinensis* seed based population hybrids (two of which were paired crosses, and two open pollinated) and two triploid standard clones: *M. x giganteus* [between *M. sinensis* and *M. sacchariflorus*, (Greef and Deuter, 1993)] and *M. sinensis* "Goliath" [*sinensis x sinensis*, (Purdy et al., 2013)] (**Table 2**).

Weather Data

Weather data was taken from a meteorological station at or within 1 km of each experimental site collecting the following data in daily time steps: daily maximum and minimum air temperature (at 2 m height), soil temperatures (at 5 cm depth), daily rainfall, daily wind run, relative humidity, and cumulative daily solar radiation. This data was recorded from the planting date to the end of the 4 year duration of the experiment. Prior long term monthly average data was available for at least 5 years at each site (**Table 1**). Photosynthetically active radiation was estimated as half the incident solar radiation (Jones, 1992) and potential evapotranspiration (PET) was calculated as from the Penman-Monteith (P-M) equations (Monteith, 1965).

To ensure sufficient moisture for good root establishment, during planting approximately 2 liters per plant irrigation was applied at all sites. Adana used drip irrigation to supplement rainfall during each year as required for plant health in the Mediterranean climate. Each irrigation event timing and quantity was recorded.

Soil Moisture

The soil plant available water holding capacity at each site was characterized by a comprehensive soil coring and analysis program. Soil cores were taken across the trial plots in a regular pattern using a 8.54 cm diameter cylinder corer (Eijkelkamp) driven into the ground with tractor mounted hydraulics until bed rock was reached or 1 m depth. The depth of soil was recorded and soil profile photographed. The texture along the profile was determined using the Fitzpatrick hand method (Fitztpatrick, 1992) and the stone content and bulk density measured. These physical parameters were used to calculate the wilt point and soil water holding capacity in mm using the (Campbell, 1985) method as modified by Hastings et al. (2014). The difference between the wilt point and field capacity is the plant available water in mm (PAW) (**Table 1**).

The drought stress through the growing year was estimated by calculating the soil moisture deficit (SMD) at each day from

TABLE 1 | Site locations for the multi-location plot trials with long-term growing season (spring to autumn equinox) mean air Temperature (°C) and Rainfall (mm).

Location	Latitude	Longitude	Altitude (m)	Air temperature (°C)	Total rainfall (mm)	Soil plant available water (mm)			
						Mean	sd	Max	Min
Adana	37	35	27	26.1	75	233	34	266	126
Stuttgart	48.74	8.93	463	16.4	378	144	54	268	56
Potash	48.89	30.44	237	18.5	300	260	4	262	241
Wageningen	51.59	5.39	10	15.8	376	141	17	176	95
Aberystwyth	52.43	−4.01	39	13.8	401	55	15	84	15
Moscow	55	37	140	14.8	347	202	16	251	160

The range of soil water holding capacity (PAW, mm) across each site is shown with a mean and standard deviation for the 45 plots.

the date of planting. This was calculated using the daily potential evapotranspiration modified by the ratio between the daily soil water balance and the PAW using the method proposed by (Aslyng, 1965) to give an actual evapotranspiration (AET). The PAW was used as the soil water capacity which was increased by the rainfall and irrigation and decreased by the AET to calculate daily soil water balance. On days where the SMD fell below 80% of the PAW the plants were considered to be suffering from drought stress.

Plant Development Measurements

During the growing season of 2014 detailed growth measurements were taken from three to five plants in the central measurement area of nine plants. The *Mx. sacchariflorus* genotypes (OPM-1 to OPM-4) have a more spreading rhizome making individual plants more difficult to distinguish. For these genotypes, all plant specific measurements used a marked area of 0.5 m^2 centerd on the original planting location. Plant height measurements were taken regularly from emergence to the end of the year. The initial height (e_hgt) was measured from ground to the tip of the newest leaf. Emergence date was determined by a linear regression of the e_hgt measurements up to 40 cm. After the formation of the first ligule, stem height (s_hgt) was measured bi-monthly from ground to the highest ligule on the tallest stem of the plant. After canopy formation, an additional canopy height measurement was taken weekly for each plot to provide better detection of temporal changes in growth rate.

Annual Harvest Yield

Harvest was performed annually in spring following the growing season between February and April depending on local climatic conditions (**Table 3**). The nine plants (4.59 m^2) in the central area of each plot were cut manually with a hedge trimmer to a target cutting height of 5 cm above the soil surface. Harvested plant material was dried to constant weight at 80°C and moisture content was determined. Dry matter yield was calculated as tones of dry matter per hectare. Stem density and plant height were recorded at the end of the growing season (in October–November) on the marked plants in the middle of the plot.

Serial Harvests to Estimate Standing Crop During Growth

To measure biomass accumulation and leaf:stem ratios, stem samples were harvested monthly from each plot. To minimize damage to the plots, the stem samples were taken from the row between the border and central measurement area. For each plot, eight stems were harvested, two from each of four plants. The stems were selected from one side of the plot, alternating with each month so that each plant was only sampled once every 4 months. The selection was randomized using a marked stick placed through the row of plants, with the closest stem to each of the eight marks selected. Only stems with a height >60% of the canopy height were included; this excluded any newly emerging stems which would have distorted the leaf stem ratios and stem weights (Davey et al., 2016). The samples were then separated into leaf and stem material, and weighed. The leaf length and maximum leaf width were measured, as was the total leaf area

TABLE 2 | Germplasm selected for the multi-location trials.

Genotype ID	Species	Accession details	Propagation method
OPM-1	Sac	Wild Sac	*in vitro*
OPM-2	Sac	Wild Sac	*in vitro*
OPM-3	Sac	Wild Sac	*in vitro*
OPM-4	Sac	Wild Sac	*in vitro*
OPM-5	Hybrid	Wild Sin × Wild Sac	*in vitro*
OPM-6	Hybrid	Wild Sac × Wild Sin	*in vitro*
OPM-7	Hybrid	Wild Sac × Wild Sin	*in vitro*
OPM-8	Hybrid	Wild Sac × Wild Sin	*in vitro*
OPM-9	Hybrid (*Mxg*)	Wild Sac × Wild Sin	*in vitro*
OPM-10	Hybrid	Wild Sac × Wild Sin	*in vitro*
OPM-11	Sin (Goliath)	Wild Sin × open	*in vitro*
OPM-12	Sin	Wild Sin × open	seeds
OPM-13	Sin	Sin × Sin	seeds
OPM-14	Sin	Sin × Sin	seeds
OPM-15	Hybrid	Sac × Sin × open Sin (open-pollinated hybrid with dominating Sin phenotype and high morphological variability)	seeds

Sac, M. sacchariflorus; Sin, M. sinensis; hybrid, M. sinensis × M. sacchariflorus hybrid. Common clone names added where these exist [e.g., Mxg, M. x giganteus; Sin (Goliath), M. sinensis Goliath].

TABLE 3 | Date of the yield harvest at each of the six OPMTIMISC sites after the 2014 growing season.

Location	Harvest date
Adana	14/02/2015
Stuttgart	18/03/2015
Potash	23/02/2015
Wagen	04/03/2015
Aber	03/02/2015
Moscow	13/03/2015

where equipment was available. The leaf and stem material was oven dried to constant weight to determine the moisture content.

Serial cut dry weights were used to estimate the harvestable above ground biomass for each plot through the growing season. The ratio of the eight stem weight at each serial cut date and the eight stem weight at the final harvest was used to back calculate the standing crop biomass for each sampling date from emergence to harvest.

Flowering

The plots were examined regularly for evidence of the transition from vegetative growth to flowering. Flowering and seed set were classified with four stages to determine the initiation of flowering, panicle emergence and the duration of anthesis; with a score given for the plot as a whole and also for the individual measurement plants to give detail on when flowering began and also how consistent this flowering was between plants within a

plot. The score system recorded first emergence of a flag leaf (1), panicle emergence >1 cm (2), panicles present on >50% mature stems in a plot (3), and flowering complete on all plots (4).

Senescence

To monitor the onset of senescence, each plot was visually assessed and assigned a score from 0 to 10 (Robson et al., 2012). This score was based on the ratio of the green to brown plant material in a plot, with a score of 0 indicating all green and a score of 10 indicating complete senescence. To ensure consistency, measurements were taken from the same direction for each plot and photographs were used to calibrate scoring between locations. This score was measured approximately fortnightly from the start of autumn until hard frost or completion of senescence.

Data Analysis

Data analysis was performed using the statistical programming software R (R Core Team, 2016). To assess the ripening of the crop, three key stages were identified: the date of peak above ground biomass, the initiation of flowering and the initiation of senescence. While all sites followed the same phenotyping protocol, there was variation in the measurement dates between sites. To synchronize measurements between locations the progression of each of the key ripening indicators (peak yield, flowering and senescence) was modeled with a curve fitting regression to predict the value for each day of the year (DOY).

Model fitting and prediction for the growth curve was performed using the base stats package in the statistical programming software R (R Core Team, 2016). The serial cut stem weight measurements for the three replicate plots for each genotype at each location were used to generate a loess curve regression analysis (span = 0.7 degree = 2). The date of the maximum value of this growth curve was used to define the date of peak yield.

Model fitting and prediction for the progression of flowering was performed using the dose response model package for R, drc (Ritz et al., 2015). For each genotype at each location, a two parameter log-logistic function was fitted to the flowering score (minimum = 0, maximum = 4) against day of year. This regression model was then used to predict a day of year for each flowering stage (1–3). Because of the nature of the logistic curve, this model could not be used to predict the date for end of flowering.

To summarize the progression of senescence, a similar system to that reported in Robson et al. (2012) was used. This defined two measurements; a mean senescence score and the time to reach a given threshold value. The mean score was calculated from 1st September until the harvest date. As senescence was not measured in late winter and spring, this average does not include the browning effect of frost events. To include this effect, a second summary value was included for sites which experienced a hard frost. For these sites, the senescence score was set to 100% after a frost event below $-3°C$. The threshold values of interest were 20, 50, and 80% senescence and the time to reach these

thresholds were calculated in number of days and thermal time from emergence.

To prevent distortion of these summary values due to the effect of variation in the frequency and number of measurements between locations, a two parameter log-logistic function was fitted to the senescence scores for each genotype at each location, using the dose response model package for R, drc (Ritz et al., 2015).

To compare the progression of flowering and senescence to biomass accumulation, the scores were normalized. The flowering score (0–4) was divided by four and the senescence score (0–10) was divided by ten. The estimated dry matter for each plot was divided by the equivalent dry matter at harvest giving a value for the proportion of the final harvest weight standing in the field through the year.

To compare plant development between sites thermal time was calculated based on the air temperature measurements of the accumulation of degree days from emergence to each of the development stages. Many studies (Snyder et al., 1999; Cesaraccio et al., 2001; Hastings et al., 2009) have found a T_b of 0°C suitable, and this was used to report thermal time values in this paper.

Statistical comparison of the species and location main effects have been were performed using the HSD (honest significant difference) function of the agricolae package for R (De Mendiburu, 2016)

RESULTS

Weather Data

This study focussed on the third year of growth (2014), when at most locations the plants are physiologically mature and canopy closure occurs in most genotypes at most sites within the growing season. While all locations showed some variation from the long term average, especially in rainfall; of interest to this study was the response of the crop to the six different growing conditions in 2014.

In 2014, the average "growing season" temperature gradient, from high to low, followed an East-West trend. The coldest winter temperatures (mean minimum air temperature) showed a West-East trend with the exception of Adana, which is over 11° further south than Stuttgart, the next most southerly of the six test sites. This also created a gradient of annual temperature range, where the difference between summer and winter increased from West to East, as the site climates became more continental.

For five out of the six sites, growing season temperatures in 2014 were similar to the long term averages. In Moscow, summer temperatures were significantly higher than long term averages (**Figure 1A**, **Table 1**). Overwinter temperatures fell below freezing at all locations; however, only at Potash and Moscow was there extended periods with a mean air temperature below 0°C. Minimum air temperatures at Adana did not fall below $-2°C$ and at Aberystwyth did not fall below $-3°C$ until mid-January.

Rainfall varied in 2014 compared to the long term average at all locations in this trial (**Figure 1B**, **Table 1**). Adana had a drier winter and wetter summer than usual, with high rainfall in June 2014. Stuttgart also had a much wetter summer than
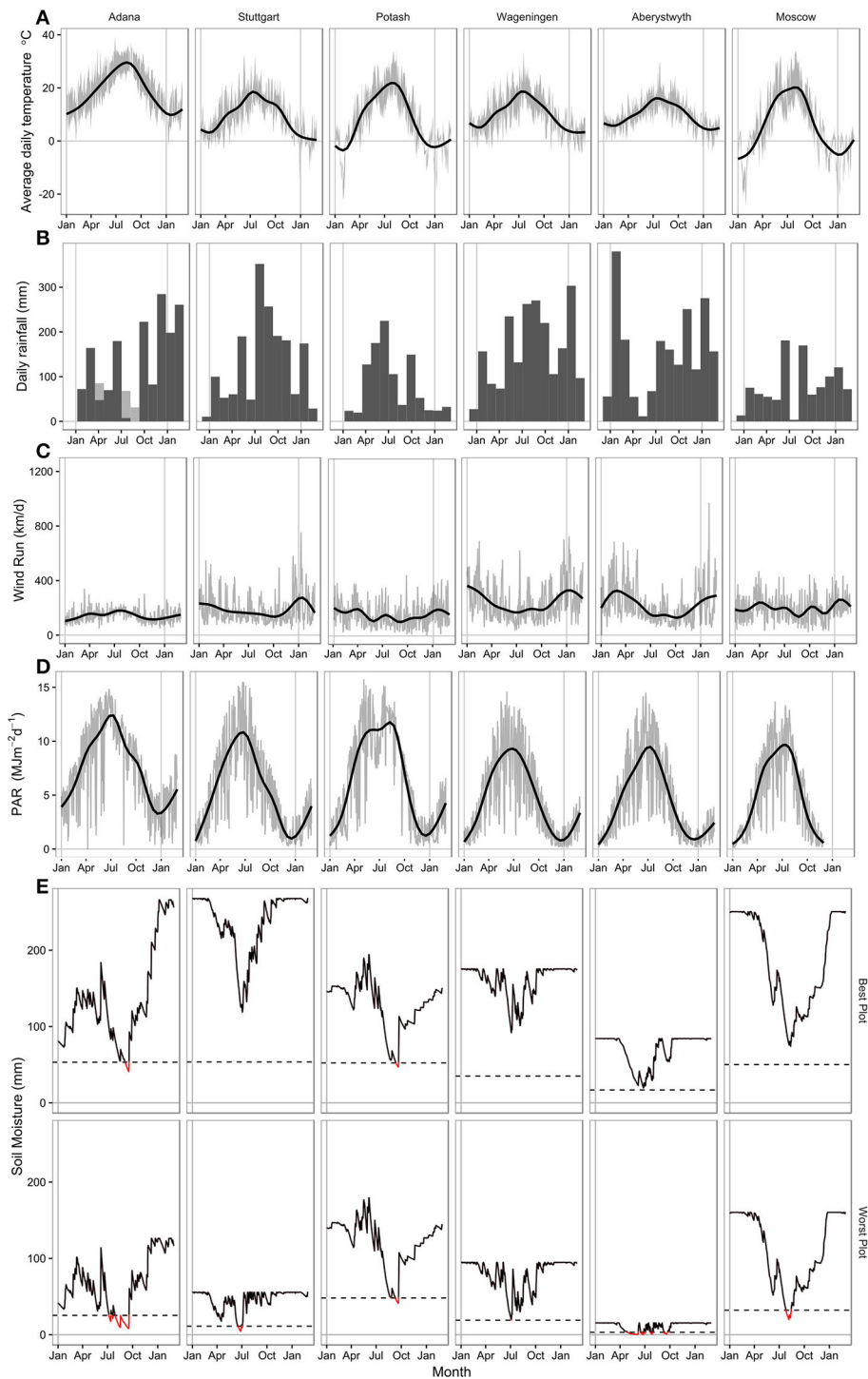
FIGURE 1 | Climate data at each location for the 2014 growing season from 1st January 2014 to 1st April 2015. **(A)** Smoothed daily mean air temperature (2 m height) with a gray ribbon showing daily maximum and minimum air temperatures. **(B)** Total monthly rainfall (mm) with irrigation shown with hatched bars at Adana. **(C)** Smoothed daily wind run (km/d) with gray line showing daily values. **(D)** Smoothed photosynthetically active radiation (MJm^{-2}d^{-1}) with gray line showing daily values. **(E)** Modeled daily soil moisture (mm) at the plot with the best and worst water holding capacity (PAW) at each location. The dashed line shows 20% PAW, below which the crop is considered to be water stressed.

normal, with heavy rainfall in July and August. Potash had a drier winter and much wetter April and May than the average. Total growing season rainfall at Wageningen was fairly normal, although May, July and August were wetter than normal. Spring through to summer was dry at both Aberystwyth and Moscow with lower than average growing season rainfall amounts in both sites. From April to October rainfall exceeded 50 mm every month at only two sites; Stuttgart and Wageningen (**Figure 1B**). At all other sites rainfall dropped below this value for at least 1 month leading to some water deficits at different times during the growing season. In Adana and Moscow, rainfall dropped to <10 mm in late summer, whereas in Aberystwyth rainfall dropped below 10 mm near the beginning of the growing season in May.

Incident photosynthetically active radiation (PAR, MJ m-2 d-1), which was estimated from 50% of global radiation at some sites, was highest in Adana throughout the year (**Figure 1D**). In Potash a drop in PAR was observed in June that corresponded with a period of high rainfall.

Most locations suffered some soil water deficits (mm) in the 2014 growing season (**Figure 1E**) which approached the plant available water (PAW, mm) holding capacity of the soil profile. In Adana, despite irrigation, calculated soil moisture deficits exceeded 80% of the plant available water (PAW) from June to October. In Stuttgart there was sufficient summer rainfall to ensure that water was non-limiting throughout most of the growing season in plots with soil depths >60 cm. Across the Stuttgart field site, soil depth varied markedly (from 30 to 100 cm) resulting a large variation in calculated soil PAW. Soil moisture deficit below 80% of the PAW occurred in June and July in the shallower plots.

At Potash, warm growing season temperatures and high atmospheric vapor pressure deficits caused by lower summer relative humidities than at the other sites led to large soil moisture deficits. However, as the soil is a high quality chernozem, which is highly water retentive, water supply in Potash was unlimited for most of the 2014 growing season and soil moisture deficits only exceeded the estimated PAW in September and October (**Figure 1E**). At Wageningen, where there was good distribution of rainfall throughout the growing season, the sandy soil textures meant that we predict there was mild water deficit in June in some of the poorer plots though these don't appear to have produced detectable changes in growth rate (**Figure 1E**). The site in Aberystwyth has the poorest soils of all the six locations. Soils varied from 30 to 60 cm depth across the site, with PAW's from 16 to 84 (mm). The spring of 2014 was dry; with total rainfall between March and May of 127 mm. SMD exceeded 80% of the PAW from June to October, severely restricting the water available for growth. In comparison to Aberystwyth, Moscow has generally good quality and deep soils. However, during a dry and hot period in August 2014, SMD fell rapidly and exceeded 80% PAW in the shallowest plots significantly reducing late summer season growth rates.

Plant Development
Emergence
In all species, spring emergence date, flowering time, the date of peak biomass and senescence all occurred earliest at Adana (**Figure 2**, **Table 4**). Emergence at Adana occurred in early February, at least 40 days before any other location and before the predicted date used by MISCANMOD. Emergence at Aberystwyth, Stuttgart and Wageningen occurred around the spring equinox (day 78) as expected (**Table 4A**); although some of the hybrid and *Mx. sinensis* genotypes emerged earlier. Emergence dates at Potash and Moscow were significantly later than in all other sites (day 102 and 106 respectively). Generally the thermal time was similar between locations at between 350 and 450 DD_0. The thermal time to emergence was highest at Wageningen ($609DD_0$ for *Mxg*) and lowest at Moscow ($191DD_0$ for hybrids). Thermal time to emergence was much lower at Moscow despite the late emergence date.

Flowering
All hybrid genotypes flowered at all sites, with one unexpected exception; OPM-8 did not flower at Adana, although flowering was earliest at this site for all other genotypes. *Mxg* flowered in four out of the six sites. Three of the four "pure" *Mx. sacchariflorus* genotypes did not flower at any location. The only *Mx. sacchariflorus* which flowered was OPM-4 at the hottest site (Adana). All *Mx. sinensis* germplasm types flowered at all locations (**Table 4B**), but not all flowering plants completed flowering before the end of the growing season.

At all sites except Moscow, the *Mx. sinensis* types flowered earliest, ranging from DOY 121–185, followed by the hybrids (DOY 126–220) (**Table 4B**). At Moscow the hybrids and *Mx. sinensis* genotypes flowered at almost the same time (DOY 240 and DOY 243), respectively. At all the four sites where *Mxg* flowered; Adana, Stuttgart, Wageningen and Aberystwyth, it was the last species to do so (**Table 4B**).

In the novel hybrids, the daylength at the initiation of flowering ranged from 14 to 16 h. *Mxg* started flowering over a much greater range of photoperiods than the novel hybrids, with flowering occurring in mid-summer in Adana at 15 h, and in late autumn in Aberystwyth at 10 h (**Table 4B**). The *Mx. sinensis* species generally flowered at the same photoperiod or slightly longer than the novel hybrids. The greatest difference was at Aberystwyth where the *Mx. sinensis* flowered in mid-summer, when the photoperiod was 17 h and the new hybrids flowered later, when photoperiod was 15 h.

Flowering occurred much earlier in the year at Adana than any of the other locations, on average 88–98 days earlier for the hybrid and *Mx. sinensis* genotypes and 102 days earlier for *Mxg*. Using the early emergence date at Adana to calculate a number of days to flowering by subtracting the day of emergence from the day of flowering, this difference was reduced to 33 days for *Mx. sinensis,* 44 days for the novel hybrids and 54 days for *Mxg* (**Table 4**).

Senescence
The DOY to reach 50% senescence varied between locations, with the mean values ranging between DOY 201 for *Mxg* at Adana compared to 297 at Aberystwyth (**Table 4C**). The earliest site to reach 50% senescence for all species was Adana and the location that showed the latest senescence was Aberystwyth. The novel hybrids generally senesced earlier than the other species
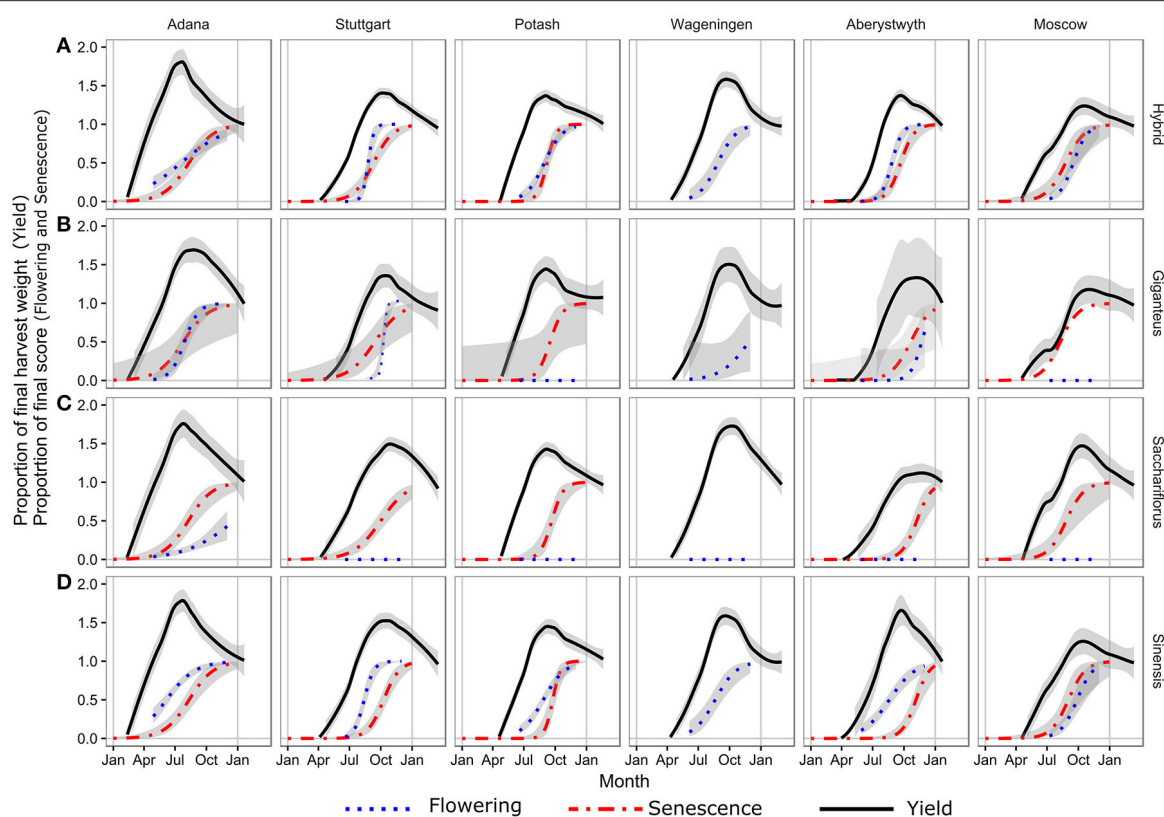
FIGURE 2 | Regression curves for the three ripening traits. Fitted curve to the serial cut yield estimates normalized to the final harvest in spring as a black line. Fitted curve for senescence scored at plot level based on weekly to monthly measurements as red line. Fitted curve to the flowering score as blue line. The gray shading is 1 standard error on the curve fits (n varies). Flowering score 0–4 (5 steps) has been normalized to 0–1.

but during a period of large soil moisture deficit in Adana and Moscow, *Mxg* senesced earlier than all other genotypes (**Table 4C**). The novel hybrids showed the least variation in senescence date between sites, with the minimum and maximum DOY for 50% senescence being 222 (Adana) and 265 (Aber), respectively, giving a range of 43 days. For *Mx. sinensis* and *Mx. sacchariflorus* there was >90 days variation in senescence time within the groups and between the sites (**Table 4C**).

When the growing season length was adjusted to factor in emergence date, Aberystwyth remained the site with the latest senescence for all species, but although Adana had the earliest senescence, Moscow was found to have the shortest growing season measured in terms of days between emergence to senescence in all species (**Table 4**).

The thermal time taken to reach 50% senescence also showed large variation between sites. The hybrids showed the greatest variability, with 50% senescence at Adana corresponding to thermal time of 3,985 DD compared to 2,327 DD at Moscow, a range of 1,658 DD.

Growing Season Length

As was observed for the senescence scores, across all genotypes and sites, peak biomass was attained earliest in Adana and latest in Aberystwyth (**Table 4D**). Peak biomass was reached

earliest in the hybrid genotypes, followed by the *Mx. sinensis* group, *Mxg* and the *Mx. sacchariflorus* group. In contrast to the senescence scores, the greatest difference between sites was observed in the novel interspecies hybrids with a range of 111 days between the earliest and latest to reach peak biomass in Adana (DOY 180) and Moscow (DOY 291). The length of the effective growing season to peak biomass varied significantly between locations (**Table 4D**) as expected. The longest growing season at 200–220 days was at Stuttgart where emergence occurred at day 80 and growth was not cut short by frost. The shortest growing seasons were at Potash and Adana; however the timing of growing season dates were very different with an early emergence and very early end of growth at Adana compared to a late emergence and early end of growth at Potash. These were the sites with the highest cumulative degree days. The completion of the growing season at an earlier DOY at Adana corresponds to the early flowering of the hybrids and *Mx. sinensis*, which shortened the growing season compared to the later flowering Mx. sacchariflorus genotypes and *Mxg* (**Table 4**).

The shortest growing season from emergence to 50% senescence was at Moscow, where emergence was delayed and senescence was accelerated due to drought. The shortest growing season duration from emergence to maximum yield was at Potash

TABLE 4 | Ripening traits in 2014 growing season by location and species group (hybrid, *M. sinensis* × *M. sacchariflorus* hybrid; *Mxg, M. x giganteus*; *Sac, M. sacchariflorus*; *Sin, M. sinensis*).

A

Location	Day of year—emergence				HSD group	Thermal time—emergence				HSD group	Daylength—emergence				HSD group
	Hybrid	*Mxg*	*sac*	*sin*		Hybrid	*Mxg*	*Sac*	*Sin*		Hybrid	*Mxg*	*Sac*	*Sin*	
Adana	36	38	36	36	e	450	460	450	450	a	11	11	11	11	e
Stuttgart	77	81	81	76	d	350	393	393	339	b	12	12	12	12	d
Potash	104	103	104	97	b	359	350	359	303	c	14	14	14	13	b
Wagen	84	92	86	83	cd	530	609	528	514	c	13	13	13	12	cd
Aber	75	82	83	83	c	464	520	525	525	a	12	12	12	12	c
Moscow	101	104	108	106	a	191	211	246	230	c	14	14	14	14	a
HSD group	b	a	a	b		a	a	a	a		b	a	a	ab	

B

Location	Day of year—Flowering score = 1				HSD group	Days from emergence—Fscore = 1				HSD group	Thermal Time—Fscore = 1				HSD group
	Hybrid	*Mxg*	*sac*	*sin*		Hybrid	*Mxg*	*Sac*	*Sin*		Hybrid	*Mxg*	*Sac*	*Sin*	
Adana	126	182	171	121	d	90	144	134	85	d	1507	2813	2508	1396	c
Stuttgart	231	283		210	b	154	202		133	a	2159	2897		1787	a
Potash	216			205	c	112			108	c	2000			1718	ab
Wagen	211	268		198	c	127	176		114	b	1583	2641		1431	bc
Aber	220	300		185	c	145	218		102	b	1770	2816		1159	d
Moscow	240			243	a	139			137	c	2376			2380	bc
HSD group	b	a	c	c		b	a	b	c		b	a	a	c	

C

Location	Day of year—Senescence = 5				HSD group	Days from emergence—Senescence = 5				HSD group	Thermal time—Senescence = 5				HSD group
	Hybrid	*Mxg*	*Sac*	*Sin*		Hybrid	*Mxg*	*Sac*	*Sin*		Hybrid	*Mxg*	*Sac*	*Sin*	
Adana	222	201	219	222	d	184	162	181	186	c	3,985	3365	3891	4005	a
Stuttgart	256	257	277	287	b	175	173	191	207	b	2,514	2506	2781	2969	b
Potash	252	264	268	269	c	147	160	163	171	d	2,710	2925	2949	2930	b
Wagen	–	–	–	–	–	–	–	–	–	–	–	–	–	–	–
Aber	265	297	316	313	a	190	215	233	230	a	2,457	2809	3006	2968	c
Moscow	239	220	242	250	d	138	116	134	144	e	2,327	1991	2325	2459	d
HSD group	c	bc	b	a		b	b	b	a		C	c	b	a	

D

Location	Day of year—Peak				HSD group	Days from emergence—Peak				HSD group	Thermal time—Peak				HSD group
	hybrid	*Mxg*	*Sac*	*Sin*		hybrid	*Mxg*	*Sac*	*Sin*		hybrid	*Mxg*	*Sac*	*Sin*	
Adana	180	236	223	190	e	143	197	186	153	d	2,461	4,282	3,877	2,697	a
Stuttgart	282	285	310	303	a	201	201	225	223	a	2,910	2,667	3,112	2,957	a
Potash	246	244	245	254	d	141	140	140	156	e	2,428	2,676	2,588	2,544	c
Wagen	269	268	277	263	c	187	202	205	186	c	2,326	2,677	2,559	2,562	b
Aber	264	263	280	261	b	189	181	197	178	b	2,491	2,495	2,823	2,706	cd
Moscow	291	291	291	291	c	190	187	183	185	de	2,740	2,764	2,670	2,665	d
HSD group	b	a	a	b		b	a	a	b		C	A	B	Bc	

E

Location	Peak yield (t ha^{-1})				HSD group	Harvest yield (t ha^{-1})				HSD group	Percentage biomass loss				HSD group
	Hybrid	*Mxg*	*Sac*	*Sin*		Hybrid	*Mxg*	*Sac*	*Sin*		Hybrid	*Mxg*	*Sac*	*Sin*	
Adana	16.61	22.03	10.68	24.14	a	7.55	13	5.6	11.43	c	55	41	48	53	a
Stuttgart	19.9	18.52	16.35	16.46	a	14.11	13.55	10.49	10.38	b	29	27	36	37	bc
Potash	21.6	24.35	21.4	16.74	a	15.51	16.75	15.19	11.4	a	28	31	29	32	bc
Wagen	17.75	22.82	14.84	15.97	a	11.26	14.34	8.58	10.1	bc	37	37	42	37	b
Aber	12.17	12.15	5.22	6.8	b	8.61	8.33	3.52	3.18	d	29	31	33	53	b
Moscow	10.63	9.51	6.65	7.77	b	8.11	7.82	4.23	5.66	d	24	18	36	27	c
HSD group	a	a	b	ab		a	a	b	b		a	a	a	a	

*Pairwise comparisons use the TUKEY HSD test to assign grouping. **(A)** Timing for modeled emergence day of year, with the thermal time (Tb = 0) and daylength. **(B)** Modeled start of flowering (Fscore = 1) showing day of year (DOY), number of days from emergence and thermal time after emergence. **(C)** Timing to reach 50% senescence (Sscore = 5) showing DOY, days after emergence and thermal time after emergence. **(D)** Timing to reach peak biomass as DOY, days after emergence and thermal time from emergence. Peak yield date in Moscow is cut off where a < −3oC frost occurs on day 291. **(E)** Modeled peak yield, harvestable yield in spring and% overwinter loss.*

except in the *Mx. sinensis* types where the growing season was slightly shorter at Adana (**Table 4D**).

At the Moscow site, the growing season to 50% senescence is very short but the fitted curve from the serial cuts indicate that the biomass was still increasing at the final serial cut. However, a hard frost at day 291 would have killed any plant above ground and ended any further growth and active senescence. This gives a growing season length of 163–166 days, which is comparable to the number of days from emergence to 50% senescence at the other locations (147–236).

The longest growing seasons were generally at Stuttgart, whereas Aberystwyth had the longest duration to reach 50% senescence (**Table 4C**). This result demonstrates that there is no direct relationship between reaching a score of 50% senescence and peak biomass. *Mxg* and *Mx. sacchariflorus* genotypes had continued growing longer than the novel hybrids and the *Mx. sinensis* types but generally reached 50% senescence before the *Mx. sinensis*.

In the hybrids the timing of flowering and senescence was closely linked, whereas in *Mxg*, senescence tended to precede flowering (**Figures 2A,B**). This was in contrast to *Mx. sinensis* where the opposite was observed and flowering preceded senescence (**Figure 2D**). Comparing the flowering and senescence scores to the date of peak yield indicated that the biomass accumulation had peaked for all genotypes by the date the senescence score reached 0.5.

The flowering score at peak biomass was more variable, depending on species type, with the hybrid and *Mx. sinensis* genotypes in mid flowering (score of ~3) at the peak yield and just starting (score of ~1) for *Mxg* (**Figure 2**).

Yield

The highest peak yielding group on average was *Mxg* with a maximum of 24.35 t ha^{-1} at Potash (**Table 4E**), but the hybrids performed best at Stuttgart, Aberystwyth, and Moscow with a maximum yield of 19.9 t ha^{-1} at Stuttgart. The *Mx. sacchariflorus* genotypes were the poorest yielding at all sites except Potash where the *Mx. sinensis* species were lower yielding. Yields for all species were highest at Potash and lowest at Aberystwyth and Moscow. This demonstrates that yield was not compromised by a short growing season duration as Potash had the shortest growing season but the highest yields and the opposite was true of Aberystwyth. There was generally a positive correlation between peak and harvestable yield with the order largely remaining the same; *Mxg* was the highest yielding species and Potash the highest yielding site. Overwinter losses ranged on average between 30 and 40% for the four species. The hybrids had the greatest range between sites with 55% loss at Adana compared to 24% loss at Moscow. In the *Mx. sinensis* genotypes more than 50% of biomass was lost over winter at two sites, Adana and Aberystwyth. The site that generally experienced the greatest over-winter decline for all species was Adana and losses were lowest at Moscow.

Moisture Content

The moisture content of the above ground plant material reduced through the year, starting at around 80% in all genotypes at all locations (**Figure 3**). In general, the pattern of change showed a decrease through the growing season, as the material changed from young green shoots to full stems. As the plant actively senesced, this decrease in moisture content continued, although the rate gradually decreased, with the moisture content stabilizing at between 40 and 50% at most locations through autumn. The greater spread of data observed at Adana and Moscow may correspond to periods of low rainfall during the growing period resulting in accelerated drying (**Figures 1, 3**). At the end of the year moisture contents tended to have remained higher at Potash and Aberystwyth with a maximum ~50% moisture in *Mxg* at both sites. The driest site was Stuttgart at which every genotype contained <25% water by January (**Figure 3**). Over winter, the rate of drying tended to increase again, due to the passive senescence effects of the environment however, this trend was not observed for germplasm grown at Potash which generally showed a plateau in drying between the first frost to −3°C and spring harvest (**Figure 3**). Although climatic conditions between Potash and Moscow were quite similar (**Figure 1**) this same trend was not observed at Moscow where all genotypes had dried down to ≤25% by the spring harvest.

To further investigate why quality, in terms of drying, was compromised at Potash compared to Moscow, the climatic conditions around the final harvest were investigated (**Figure 4**). At both sites, the average daily temperature before 20 February 2015 was frequently sub-zero but after this date the averages were consistently 0–10°C until the end of March with very few deviations (**Figure 4**). However, the harvest at Potash took place within the first week of this spring thaw (23 February 2015), whereas at Moscow it was carried out nearly 3 weeks later (13 March 2015).

DISCUSSION

Emergence and Plant Growth

The MiscanFor model for *Mxg* uses the date of the spring equinox, where the daylength exceeds 12 h at all latitudes, as a trigger for emergence date (Hastings et al., 2009). In this study, the wide variation in environmental conditions, especially over winter, provided useful new data on the triggers of emergence. At two of the trial sites (Adana and Aberystwyth) there was a lack of significant over-winter frost and at both of these locations emergence occurred before the date defined by Hastings et al. (2009). However, emergence occurred remarkably close to this date at Stuttgart, Wageningen and Aberystwyth, in all species groups. While thermal time may provide an indicator of the speed of development of new shoots, it is not a good indicator for the date of emergence as it does not easily account for frost damage. In this study, as emergence date was calculated from a regression of height measurements, any shoots killed by a frost event would not be recorded, which accounts for the delayed emergence date at Potash and Moscow.

Miscanthus is reportedly a facultative short day flowering species, though it will flower if given enough heat, even without shortening days (Jensen et al., 2013). Of the *sacchariflorus* genotypes, only OPM-4 flowered and this was only at Adana;
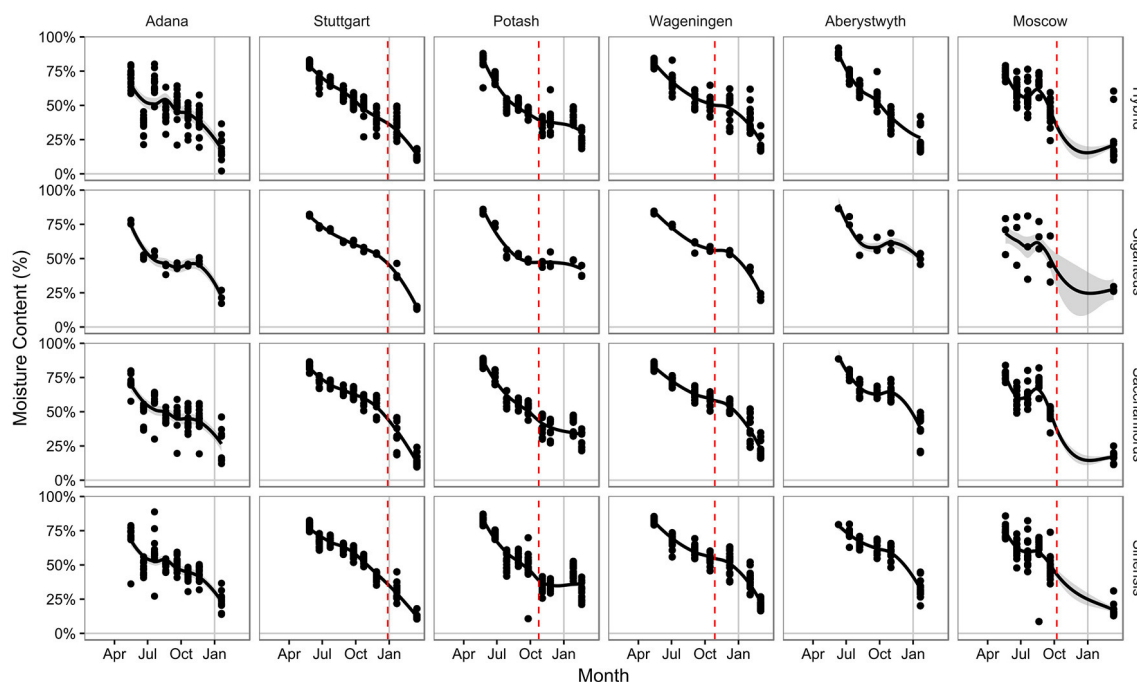
FIGURE 3 | Moisture content of harvested serial cut material by location and species groups. Data points show the measured moisture content for each plot. Gray area shows one standard error from fitted curve. Red dashed line indicates the first −3°C frost of winter
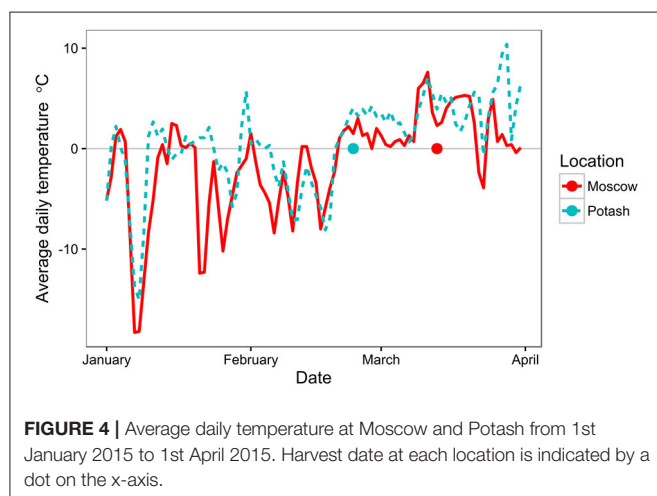
FIGURE 4 | Average daily temperature at Moscow and Potash from 1st January 2015 to 1st April 2015. Harvest date at each location is indicated by a dot on the x-axis.

the hottest site. This supports the findings of Jensen et al. (2013). However, the lack of flowering in the other sacchariflorus genotypes was probably due to insufficient water triggering accelerated rate of senescence. At Adana, senescence had generally passed 50% by early August which meant that when the shortening photoperiods should have induced flowering, the plants had already senesced.

The lack of correlation between thermal time and flowering date across the six sites for the hybrid and *Mx. sinensis* genotypes is consistent with previous reports and indicates that thermal time cannot be the dominant trigger for flowering (Jensen et al.,

2011). However, an additional possibility is that a thermal time trigger is present for flowering, but that there is a lag involved before flowering is measurable on the plant. This would be extremely difficult to determine as the length of this lag could be variable, based on temperature, genotype, photoperiod and water deficit (Jensen et al., 2011). In several genotypes at several sites, flowering was triggered but did not complete before winter, demonstrating that the conditions experienced in the period from flag leaf to anthesis are also critical for determining whether the plant completes its life-cycle or not. This requirement adds another level of complexity to the development of models to predict flowering time.

Mxg does seem to require a minimum thermal time to flower; and also a minimum number of calendar days as in Moscow and Potash, *Mxg* does not flower, even though there are sufficient thermal units (>2,800 DD_0). The growing seasons are cut short at both of these locations by frost, indicating that *Mxg* does require a minimum number of days to develop before flowering. The daylength does not seem to determine flowering at all.

In *sinensis*, flowering generally occurred earlier in the west and latest in the east, with the exception of Adana, where flowering occurred at the lowest thermal time. This latter finding is in contrast to previous reports in which flowering at a hot, southern site in Portugal occurred at a higher thermal time than the more northern sites (Clifton-Brown et al., 2001). However, the long-term average temperatures at Adana were 7°C warmer than those reported in Portugal and correspondingly flowering in *sinensis* still occurred in summer in Portugal (Clifton-Brown et al., 2001), whereas flowering was triggered in spring at Adana.

The effect of water deficit on flowering in *miscanthus* is not understood in detail and this paper has not been able to improve this. At Adana, where there were significant water deficits, flowering occurred early in the year, and at a low thermal time. However, flowering was delayed at Moscow, where there were also water deficits in the mid-summer. The other location where drought stress was significant was at Aberystwyth, and here the flowering of the *sinensis* genotypes was earlier than expected, with a very low thermal time from emergence. This would indicate that drought stress can accelerate the onset of flowering in *sinensis*, but there is not sufficient data to indicate that the hybrids follow this trend, especially as the next lowest thermal time for hybrid flowering was at Wageningen, where there was very little water deficit.

Flowering was expected to be an important trait for ripening and to mark the end of the growing season (Robson et al., 2012). However, for the hybrid and *sinensis* germplasm used in this trial, there was a period of continued growth and biomass gain after flowering. Also, genotypes which did not flower, such as the *sacchariflorus* types, did stop growing and senesced before winter.

Senescence and the End of Growth

The key definition of ripening in a biomass crop is when the rate of biomass accumulation stops, which in this paper has been termed the peak yield date. In *miscanthus*, especially when used for combustion, the end of growth also marks the beginning of an improvement in quality (Lewandowski and Heinz, 2003; Iqbal et al., 2017). However, the flowering types (hybrid and sin) lost the highest proportion of peak biomass at Adana, where flowering was early in the year and so there was an extended senescence (active and passive) period before harvest.

As with flowering, the rate of senescence was distinctive between genotypes and locations. Due to drought stress effects and general browning of leaves below the canopy, it is more difficult to determine the start of senescence. It could be reasoned that the absence of flowering in Sac and *Mxg*, at some sites, may be the cause of the extended growing season in these genotypes but in *Mxg* the longest growing season was observed at Stuttgart and Wageningen (∼200 days) where flowering was observed, whereas the growing season was ∼60 days shorter at Potash where flowering was not observed.

While there is a period of drought stress at Moscow which leads to a browning of the crop, growth continued in September, after rainfall and then continued until halted by frost. Clifton-Brown et al. (2002) found that with a stay green variety, photosynthesis restarted after water stress was relieved which matches the results in Moscow.

The growing season at Moscow did not start until the final frost (day 100) and flowering and senescence had not completed when growth was cut short by autumn frosts (day 291). It does not appear that a shortened growing season led to reduced yields, as the shortest growing season was at Potash, where the highest yields were recorded, and at Adana, which had the highest *sinensis* yields. The *sinensis* harvest would have been higher at Adana, however the extended period between peak yield and harvest led to large yield loses.

These results demonstrate that the relationship between flowering time, growing season duration and yield is not as deterministic as previously thought. It has previously been reported that an extended canopy duration, from earlier emergence in spring rather than delayed senescence, was critical to achieving high yields at Aberystwyth (Davey et al., 2016). However, our findings have shown the opposite; that Potash, with the shortest growing season, achieved the highest yields and Aberystwyth with the one of the longest growing seasons had the lowest yields. This indicates that the ideotype required to produce optimum yields in a temperate oceanic climate such as Wales is different to that required in a temperate continental climate like Ukraine. In Wales, where summer conditions remain comparatively cool with low PAR, a plant must capitalize on the long spring-summer daylength to achieve high biomass. However, in Ukraine where summer temperatures and PAR are high, the rate of growth is more rapid and the importance of growing season duration is minimized. These are important considerations when considering both a location specific and more generalized breeding strategy.

Generally, the pattern of change of moisture content was the same for all genotypes at a specific location, indicating that environmental conditions had a greater influence than plant morphology and senescence. This study did not find a strong link between early senescence and low moisture at harvest, except at Aberystwyth, which is the same location as a previous study (Robson et al., 2012) which found a strong link. This is a temperate oceanic environment, with mild winters and rare frosts. These findings indicate that the hardness and duration of winter frost has an effect on the above ground material, with extended periods of below freezing temperatures preventing the plants from drying out.

In future studies we will pay closer attention to the dynamics of moisture content of the crop by increasing the frequency of measurements over from monthly to bi-monthly to get smoother fits. In Moscow the snow cover detracts from the practicality of frequent sampling, but had it been done, we would have better understood the ripening profiles of different genotypes in another extreme environment which would have added to our knowledge of genotype × environment responses.

Multi-Location Trials

The establishment and measurement of six trials in very different environments did pose some problems. Some measurements—such as greenness and canopy height—were based on a subjective judgment by the onsite operator; additionally even the most objective measurements such as stem height and weight could be affected by location specific practices and conditions. For example, the fresh weight of the stems collected at each serial cut will potentially by affected by the time from cut to weighing; and the environmental conditions at the time. Even the shape of the plots and space between the measurement plants can be affected by the path taken by the operator. These differences were anticipated as much as possible and prescribed in the measurement protocols. Additionally, regular meetings and in field training along with videos of measurements being taken provided examples for comparison; as did pictures of the

progression of the different sites for comparison of the more subjective measurements.

CONCLUSIONS

In this paper, we have characterized the timing of emergence from the overwintering rhizome, rate of canopy development and in season growth, flowering and senescence time, and overwinter ripening prior to harvest for 13 wild and hybrid germplasm types alongside the standard genotypes Mxg and *M. sinensis* "Goliath."

While there was a wide "within and between site" variation in growth traits, there were several germplasm types that were generic high performers in most of the environments tested. In general, the highest yielding types were the interspecies hybrids including Mxg.

Biomass quality as expressed by moisture content at harvest was not determined by senescence and was more affected by the overwintering conditions and the time period between complete senescence and harvest. In locations with extended freezing temperatures a delay between thawing and harvest may be necessary to improve biomass quality.

Water balance calculations performed for all sites for the third growing season after planting showed the germplasm was exposed to a wide range of "in growing season" partial and severe water deficits. *M. sinensis* types were more drought resilient than the interspecies hybrids, but as these flowered earlier, they were often lower yielding. The complex germplasm responses to these dynamic water deficits can partly explain the lack of simple correlations in thermal time and photoperiod with flowering and senescence time. More work is needed to unravel these complex processes using side by side irrigated and rainfed trials with a smaller set of key germplasm types.

In temperate climates, such as the UK, strong correlations between growing season length and yield have been found in many diverse *Miscanthus* genotypes. Consequently, early leaf emergence in spring time and late flowering / senescence have long been target traits for breeders attempting to increase biomass yield. In this "EU-OPTIMISC" multi-location field experiment, which included two *Miscanthus* trial locations

in strong continental climates (Moscow and Potash), simple correlations with these traits and yield were not detected. Our results indicate that, for these strong continental climates with short sharp growing seasons, breeding selections should focus high net photosynthetic rates and water use efficiency rather than the triggers and brakes determining the beginning and end of the effective growing season.

The results of this study advance science by extending our understanding of the boundaries of the cultivatable area of *Miscanthus* to the North and East of geographical Europe. The wide diversity of germplasm from *M. sinensis*, *M. sacchariflorus* and several of their hybrids used in this experiment had informed breeders of the trait combinations needed to maximize biomass production in these regions with diverse environmental conditions.

AUTHOR CONTRIBUTIONS

CN: corresponding author; AH: data analysis and manuscript editing; OK, MÖ, HS, IT, TV, AA, NK, JM, MM, and LT: data collection; YI: data analysis; AK: data analysis and manuscript editing; HM and KS: germplasm supply; IL: project leader; JC: project coordinator and manuscript editing.

REFERENCES

Aslyng, H. C. (1965). Evaporation, evapotranspiration and water balance investigations at copenhagen 1955–64. *Acta Agric. Scand.* 15, 284–300. doi: 10.1080/00015126509433124

Campbell, G. (1985). *Soil Physics with BASIC: Transport Models for Soil-Plant Systems, Developments in Soil Science.* Elsevier.

Cesaraccio, C., Spano, D., Duce, P., and Snyder, R. L. (2001). An improved model for determining degree- day values from daily temperature data. *Int. J. Biometeorol.* 45, 161–169. doi: 10.2307/210739

Clifton-Brown, J. C., Lewandowski, I., Andersson, B., Basch, G., Christian, D. G., Kjeldsen, U., et al. (2001). Performance of 15 Miscanthus genotypes at five sites in Europe. *Agron. J.* 93, 1013–1019. doi: 10.2134/agronj2001.935 1013x

Clifton-Brown, J. C., Lewandowski, I., Bangerth, F., and Jones, M. B. (2002). Comparative responses to water stress in stay-green, rapid- and slow senescing genotypes of the biomass crop, Miscanthus. *New Phytol.* 154, 335–345. doi: 10.1046/j.1469-8137.2002.00381.x

Clifton-Brown, J. C., Neilson, B., Lewandowski, I., and Jones, M. B. (2000). The modelled productivity of *Miscanthus x giganteus* (GREEF et DEU) in Ireland. *Ind. Crops Prod.* 2, 97–109. doi: 10.1016/s0926-6690(00)00042-x

Clifton-Brown, J. C., Stampfl, P. F., and Jones, M. B. (2004). Miscanthus biomass production for energy in Europe and its potential contribution to decreasing fossil fuel carbon emissions. *Glob. Change Biol.* 10, 509–518. doi: 10.1111/j.1529-8817.2003.00749.x

Clifton-Brown, J., Hastings, A., Mos, M., McCalmont, J. P., Ashman, C., Awty-Carroll, J., et al. (2016). Progress in upscaling Miscanthus biomass production for the European bio-economy with seed-based hybrids. *GCB Bioenergy* 9, 6–17. doi: 10.1111/gcbb.12357

Clifton-Brown, J., Robson, P., Allison, G. G., Lister, S. J., Sanderson, R., Morris, E., et al. (2008). Miscanthus: breeding our way to a better future. *Aspects Appl. Biol.* 90, 199–206.

Davey, C. L., Jones, L. E., Squance, M., Purdy, S. J., Maddison, A. L., Cunniff, I., et al. (2016). Radiation capture and conversion efficiencies of *Miscanthus sacchariflorus*, *M. sinensis* and their naturally occurring hybrid *M. giganteus*. *Glob. Change Biol. Bioenergy* 9, 385–399. doi: 10.1111/gcbb.12331

De Mendiburu, F. (2016). *Agricolae: Statistical Procedures for Agricultural Research.* Available online at: http://tarwi.lamolina.edu.pe/~fmendiburu

Farrell, A. D., Clifton-Brown, J. C., Lewandowski, I., and Jones, M. B. (2006). Genotypic variation in cold tolerance influences the yield of Miscanthus. *Ann. Appl. Biol.* 149, 337–345. doi: 10.1111/j.1744-7348.2006.00099.x

Fittzpatrick, E. A. (1992). *Soil Description.* Aberdeen: Department of Soil Science Department, University of Aberdeen 28–34.

Greef, J. M., and Deuter, M. (1993). Syntaxonomy of *Miscanthus x giganteus* Greef et Deu. *Angew. Bot.* 67, 87–90.

Hastings, A., Clifton-Brown, J., Wattenbach, M., Stampfl, P., Mitchell, C. P., and Smith, P. (2008). Potential of Miscanthus grasses to provide energy and hence reduce greenhouse gas emissions. *Agron. Sus. Dev.* 28, 465–472. doi: 10.1051/agro:2008030

Hastings, A., Clifton-brown, J., Wattenbach, M., Mitchell, C. P., and Smith, P. (2009). The development of MISCANFOR, a new Miscanthus crop growth model: towards more robust yield predictions under different climatic and soil conditions. *GCB Bioenergy* 1, 154–170. doi: 10.1111/j.1757-1707.2009.01007.x

Hastings, A., Tallis, M., Casella, E., Matthews, R., W., Henshall, P. A., Milner, S., et al. (2014). The technical potential of Great Britain to produce ligno-cellulosic biomass for bioenergy in current and future climates. *Glob. Change Biol. Bioenergy* 6, 108–122. doi: 10.1111/gcbb.12103

Heaton, E. A., Dohleman, F. G., Miguez, A. F., Juvik, J. A., Lozovaya, V., Widholm, J., et al. (2010). Miscanthus: a promising biomass crop. *Adv. Bot. Res.* 56, 75–137. doi: 10.1016/b978-0-12-381518-7.00003-0

Iqbal, Y., Nunn, C., Hastings, A., Kalinina, O., Khokhlov, N., Kiesel, A., et al. (2017). Harvest time optimisation of miscanthus genotypes for different biomass end uses. *Front. Plant Sci.* 8:727. doi: 10.3389/fpls.2017.00727

Jensen, E., Farrar, K., Thomas-Jones, S., Hastings, A., Donnison, I., and Clifton-Brown, J. (2011). Characterization of flowering time diversity in *Miscanthus* species. *Glob. Change Biol. Bioenergy* 3, 387–400. doi: 10.1111/j.1757-1707.2011.01097.x

Jensen, E., Robson, P., Norris, J., Cookson, A., Farrar, K., Donnison, I., et al. (2013). Flowering induction in the bioenergy grass is a quantitative short- day response, whilst delayed flowering under long days increases biomass accumulation. *J. Exp. Bot.* 64, 541–552. doi: 10.1093/jxb/ers346

Jones, H. G. (1992). *Plants and Microclimate: A Quantitative Approach to Environmental Plant Physiology.* Cambridge University Press.

Kalinina, O., Nunn, C., Hastings, A., Khokhlov, N., McCalmont, J., Meyer, H., et al. (2017). Performance of 15 Miscanthus genotypes at six field sites in Europe, Turkey and Russia. *Front. Plant Sci.* 7:1620. doi: 10.3389/fpls.2016.01620

Lewandowski, I., Clifton-Brown, J. C., Andersson, B., Basch, G., Christian, D. G., Jorgensen, U., et al. (2003). Environment and harvest time affects the combustion qualities of Miscanthus genotypes. *Agron. J.* 95, 1274–1280. doi: 10.2134/agronj2003.1274

Lewandowski, I., and Heinz, A. (2003). Delayed harvest of miscanthus - influences on biomass quantity and quality and environmental impacts of energy production. *Eur. J. Agron.* 19, 45–63. doi: 10.1016/s1161-0301(02)00018-7

Matos, D. A., Cole, B. J., Whitney, I. P., MacKinnon, K. J. M., Kay, S. A., and Hazen, S. P. (2014). Daily changes in temperature, not the circadian

clock, regulate growth rate in *Brachypodium distachyon. PLoS ONE* 9:100072. doi: 10.1371/journal.pone.0100072

Monteith, J. (1965). Evaporation and environment. *Symp. Soc. Exp. Biol.* 19, 205–234.

Monteith, J. L. (1978). Reassessment of maximum growth-rates for C3 and C4 crops. *Exp. Agric.* 14, 1–5. doi: 10.1017/s0014479700008255

Purdy, S. J., Cunniff, J., Maddison, A. L., Jones, L. E., Barraclough, T., Castle, M., et al. (2014). Seasonal carbohydrate dynamics and climatic regulation of senescence in the perennial grass, Miscanthus. *Bioenergy Res.* 8, 28–41. doi: 10.1007/s12155-014-9500-2

Purdy, S. J., Maddison, A. L., Jones, L. E., Webster, R. J., Andralojc, J., et al. (2013). Characterization of chilling-shock responses in four genotypes of Miscanthus reveals the superior tolerance of *M. x giganteus* compared with *M. sinensis* and *M. sacchariflorus. Ann. Bot.* 111, 999–1013. doi: 10.1093/aob/mct059

R Core Team (2016). *R: A Language and Environment for Statistical Computing*, R Foundation for Statistical Computing.

Ritz, C., Baty, F., Streibig, J. C., and Gerhard, D. (2015). Dose-response analysis using R. *PLoS ONE* 10:e0146021. doi: 10.1371/journal.pone.0146021

Robson, P., Mos, M., Clifton-Brown, J., and Donnison, I. (2012). Phenotypic variation in senescence in Miscanthus: towards optimising biomass quality and quantity. *BioEnergy Res.* 5, 95–105. doi: 10.1007/s12155-011-9118-6

Snyder, R. L., Spano, D., Cesaraccio, C., and Duce, P. (1999). Determining degree- day thresholds from field observations. *Int. J. Biometeorol.* 42, 177–183. doi: 10.1007/s004840050102

Wang, D., Naidu, S. L., Portis, A. R., Moose, S. P., and Long, S. P. (2008). Can the cold tolerance of C(4) photosynthesis in *Miscanthusxgiganteus* relative to Zea mays be explained by differences in activities and thermal properties of Rubisco? *J. Exp. Bot.* 59, 1779–1787. doi: 10.1093/jxb/ern074

Wingler, A., Purdy, S., Chardon, F., and Masclaux-Daubresse, C. (2008). Genetic basis of the link between senescence regulation and flowering time control. *Comp. Biochem. Physiol. Mol. Integr. Physiol.* 150, S188–S188. doi: 10.1016/j.cbpa.2008.04.510

Wingler, A., Purdy, S. J., Edwards, S. A., Chardon, F., and Masclaux-Daubresse, C. (2010). QTL analysis for sugar-regulated leaf senescence supports flowering-dependent and -independent senescence pathways. *New Phytol.* 185, 420–433. doi: 10.1111/j.1469-8137.2009.03072.x

Marker-Trait Association for Biomass Yield of Potential Bio-fuel Feedstock *Miscanthus sinensis* from Southwest China

Gang Nie[1], Linkai Huang[1], Xinquan Zhang[1]*, Megan Taylor[2], Yiwei Jiang[2], Xiaoqing Yu[3], Xinchun Liu[4], Xinyu Wang[1] and Yajie Zhang[1]

[1] Department of Grassland Science, Animal Science and Technology College, Sichuan Agricultural University, Chengdu, China, [2] Department of Agronomy, Purdue University, West Lafayette, IN, USA, [3] Department of Agronomy, Iowa State University, Ames, IA, USA, [4] Department of Plant Genetics and Breeding, Agricultural College, Sichuan Agricultural University, Chengdu, China

As a great potential bio-fuel feedstock, the genus *Miscanthus* has been widely studied around the world, especially *Miscanthus* × *giganteus* owing to its high biomass yield in Europe and North America. However, the narrow genetic basis and sterile characteristics of *M.* × *giganteus* have become a limitation for utilization and adaptation to extreme climate conditions. In this study, we focused on one of the progenitors of *M.* × *giganteus*, *Miscanthus sinensis*, which was originally distributed in East Asia with abundant genetic resources and comparable biomass yield potential to *M.* × *giganteus* in some areas. A collection of 138 individuals was selected for conducting a 3-year trial of biomass production and analyzed by using 104 pairs of SRAP, ISAP, and SSR primers for genetic diversity as well as marker-trait association. Significant differences in biomass yield and related traits were observed among individuals. Tiller number, fresh biomass yield per plant and dry biomass yield per plant had a high level of phenotypic variation among individuals and the coefficient of variation were all above 40% in 2011, 2012, and 2013. The majority of the traits had a significant correlation with the biomass yield except for the length and width of flag leaves. Plant height was a highly stable trait correlated with biomass yield. A total of 1059 discernible loci were detected by markers across individuals. The population structure (Q) and cluster analyses identified three subpopulations in the collection and family relative kinship (K) represented high gene flow among *M. sinensis* populations from Southwest China. Model testing identified that Q+K was the best model for describing the associations between the markers and traits, compared to the simple linear, Q or K model. Using the Q+K model, 12 significant associations ($P < 0.001$) were identified including four markers with plant height and one with biomass yield. Such associations would serve an efficient tool for an early selection of *M. sinensis* and facilitate a genetic improvement of biomass yield for this species.

Keywords: bio-fuel, biomass yield, molecular markers, association analysis, *Miscanthus sinensis*

INTRODUCTION

The growing use of fossil fuel has contributed to increasing global warming, but the uses of renewable energy resources such as bio-fuels could be an efficient approach to solve the energy challenge (Kim et al., 2014). The genus *Miscanthus*, comprising of C4 perennial warm-season rhizomatous grasses (Lewandowski et al., 2003b), is a promising non-food bio-energy crop for cellulosic bio-fuel production due to its broad adaptation, potential high biomass productivity, low-nutrient input, and the ability to sequester carbon (Lewandowski et al., 2000; Clifton-Brown et al., 2001; Stewart et al., 2009; Dwiyanti et al., 2014; Anzoua et al., 2015). *Miscanthus × giganteus* is a hybrid generated from a cross between tetraploid *Miscanthus sacchariflorus* and diploid *Miscanthus sinensis*. It has been considered as a candidate for bio-fuel production within the genus.

It is generally known that biomass yield is a critical trait for potential bio-energy crops. Extensive research works of biomass yield in *Miscanthus* have been completed in Europe and North America (Greef et al., 1997; Hodkinson et al., 2002a,b; Heaton et al., 2008, 2009; Hastings et al., 2009). *M. × giganteus* performs well on biomass yield and is the only hybrid genotype currently available for use in most countries (Nishiwaki et al., 2011; Dwiyanti et al., 2014), but it is time and labor consuming to propagate the plants through rhizome division or tissue culture. Furthermore, it is highly risky and genetically difficult to improve *M. × giganteus* through breeding due to the narrow genetic basis and triploid nature of this species, posing limitations to its biomass productivity, climatic adaptation and overwintering survival under some extreme conditions (Lewandowski et al., 2003a; Clark et al., 2014; Anzoua et al., 2015). As a progenitor of *M. × giganteus*, diploid *M. sinensis* is a kind of cross-pollination plant which can be propagated by seeds and potentially provides a comparable biomass yield to that of *M. × giganteus* in some areas (Zhao et al., 2013; Anzoua et al., 2015; Gifford et al., 2015). Originally distributed in East Asia throughout China, Korea, and Japan, collection of *M. sinensis* has been made and utilized by many research groups for phenotypic characterization and genetic evaluation (Xu et al., 2013; Nie et al., 2014; Yook et al., 2014; Anzoua et al., 2015). Nevertheless, further works for evaluation of domestication and improvement of *M. sinensis* as a new valuable genetic resource need to be conducted, especially in areas of its origin (Yook et al., 2014).

Because *Miscanthus* requires a lengthy establishment phase and there are some challenges in collecting phenotypic data for a large number of individuals, development of genetic markers associated with a trait of interest would be an efficient approach to enhance *Miscanthus* breeding programs (Clifton-Brown and Lewandowski, 2000; Gifford et al., 2015). Prior to the development of a marker-assisted selection program, quantitative trait locus (QTL) mapping using a population derived from a biparental cross would have been performed to establish associations between traits and genetic markers. However, the process of constructing a mapping population for QTL analysis can be lengthy, especially for perennial grasses.

Association mapping, also known as linkage disequilibrium (LD) mapping, has been proved to be useful and powerful for genetic dissection of complex traits (Yu et al., 2011). Compared to linkage mapping in traditional biparental populations, association mapping results in higher mapping resolution and evaluates a wide range of alleles rapidly (Yu and Buckler, 2006). This technique has been successfully applied for investigating some important agronomic traits in model plant and crop species (Aranzana et al., 2005; Breseghello and Sorrells, 2006; Skøt et al., 2007; Eleuch et al., 2008; Harjes et al., 2008; Wang et al., 2008). There were only a few reports on *Miscanthus* association mapping (Zhao et al., 2013; Slavov et al., 2014); meanwhile, QTL studies were conducted on limited genetic maps and population (Atienza et al., 2003a,b,c,d; Gifford et al., 2015; Liu et al., 2015).

The unavailable genome sequence and lack of reliable molecular markers limit *Miscanthus* genetic research. However, the *Miscanthus* genus belongs to the Tribe Andropogoneae (Poaceae) which contains many important C4 crops including maize (*Zea mays* L.), sorghum (*Sorghum bicolor* L. Moench), and sugarcane (*Saccharum officinarum* L.) with rich genomic databases, and a large number of SSRs have been proven to have high transferability to *M. sinensis* (Hernandez et al., 2001; Lu et al., 2012; Xu et al., 2013; Zhao et al., 2013; Chae et al., 2014; Yook et al., 2014). In addition, new PCR-based markers can be developed for amplifying different regions of DNA segment targets without needing prior knowledge of target sequences and they can be used for studying *M. sinensis* genetic diversity, QTL and association mapping.

Southwest China is the major distribution area or diversity center for *M. sinensis*. As one of the new leading candidates to meet biomass demand for future power generation and bio-fuels production, *M. sinensis* needs further genetic improvement using both conventional breeding and modern biotechnical approaches. In previous studies, we used different molecular markers and chloroplast DNA (trnL-F and rpl20-rps12) sequence to detect the genetic diversity and differentiate the collected *M. sinensis* population from southwest China (Xu et al., 2013; Nie et al., 2014; Yan et al., 2015). Although, different population size was used in these studies before, the similar results demonstrated that the population had high gene flow and fairly weak genetic differentiation, which would increase power to detect marker-trait associations. Building on previous studies, we extended the number of PCR-based markers by using simple sequence repeats (SSRs) developed from *M. sinensis* (Hung et al., 2009; Ho et al., 2011; Zhou et al., 2011), maize (Zhong et al., 2009; Lu et al., 2012), sorghum (Wang et al., 2005; Xu et al., 2013), sugarcane (Lu et al., 2012), and SSR developed from conserved expressed sequence tags (ESTs) databases on grass species (Kantety et al., 2002), as well as intron splice position amplified markers of intron sequence amplified polymorphism (ISAP) and parts of sequence related amplified polymorphism (SRAP) markers used in Nie et al. (2014) on 138 diverse *M. sinensis* varieties selected from previous population according to the geographic information (Xu et al., 2013; Nie et al., 2014). We also conducted a 3-year replicated field trail for phenotypic evaluation of the population and combined with genotype data for marker-trait association analysis to identify key loci associated with phenotypic traits related to biomass yield. The research results would be useful

for Miscanthus breeding aimed at improvement of biomass and related traits.

MATERIALS AND METHODS

Plant Material Collection and DNA Extraction

A total of 138 *M. sinensis* individuals used in this study were selected from previous studies (Xu et al., 2013; Nie et al., 2014) collected from Sichuan, Chongqing, Guizhou, and Yunnan provinces, located in Southwest China. The individual geographic information were listed in **Table 1** (The distribution map could see Nie et al., 2014, **Figure 3**). Briefly, each of the genotypes was cloned to three individuals using rhizome division and planted following a complete randomized block design, with one replicate per genotype in each of three blocks. Prior to transplanting, plant leaves were cut back to 8–10 cm with 6–10 tillers. All the individuals were transplanted to the Sichuan Agriculture University farm (Ya' an, Sichuan, China; *N 30°08', E 103°14'*) in May of 2010, with an average annual precipitation of 1774 mm. The soil pH at the experimental site ranged from 5.3 to 5.5, and soil type was purplish loam with 1.46% organic qualitative content. Plants were well watered immediately after transplanting and no fertilizer or water was applied to the plants afterwards.

Fresh young leaves from each individual were collected for genomic DNA extraction using the Plant Genomic DNA kit (Tiangen®, China) according to the manufacturer's protocol. The quality and concentration of the DNA were determined by comparing the sample with known standards of lambda DNA on 0.8% (w/v) agarose gels and NanoDrop ND-1000 spectrophotometer (NanoDrop Technologies Inc., Rockland, DE, USA). The isolated genomic DNA was diluted to 20 ng/μL for PCR amplification.

Primer Selection and PCR Amplification

In this study, we selected part of SRAP primers published previously (Li and Quiros, 2001; Nie et al., 2014) to conduct the association analysis. In addition, six individuals of *M. sinensis* that varied in morphology and geographic locations were selected for screening other markers based on Nie et al. (2014), including 72 ISAP primer combinations (Lu et al., 2008) and 117 SSR primer combinations (Kantety et al., 2002; Wang et al., 2005; Hung et al., 2009; Zhong et al., 2009; Ho et al., 2011; Zhou et al., 2011; Lu et al., 2012). All the primers used in this study were synthesized by Nanjing GenScript Biological Technology & Service (China).

For PCR amplification, the total volume of each PCR reaction system was 20 μl, containing 3 μL template DNA (20 ng/μL), 10 μL of Mix (10 × reaction buffer, 2.0 mM Mg^{2+}, 0.6 mM of each dNTP, Tiangen®, China), 0.8 μL primers (10 pmol/μL), 0.4 μL Golden DNA Polymerase (2.5 U/μL, Tiangen®, China) and 5 μL of ddH$_2$O. Amplification was performed on a Peltier Thermal Cycler (DNA Engine®, Bio-Rad, USA) under the following conditions: for SRAP and ISAP amplification, 5 min at 94°C for 1 cycle, followed by 5 cycles at 94°C for 1 min, 35°C for 1 min, and 72°C for 1 min, and then 35 cycles at 94°C for 1 min,

TABLE 1 | Geographic information for 138 *M. sinensis* individuals in this study.

Identity	Source	Habital	Altitude (m)	Latitude (N)
1	Ya'an	Hillside	623.3	29°58′40.2″
2	Laoban Mountain	Forest	633.8	29°58′51.5″
3	Laoban Mountain	Forest	650.7	29°58′42.2″
4	Laoban Mountain	Forest	644.1	29°58′39.3″
5	Laoban Mountain	Fores	644.1	29°58′39.3″
6	Ya'an	Orangery	657.8	29°58′39.1″
7	Bi Feng Xia	Bamboo grove	681.1	30°04′28.5″
8	Bi Feng Xia	Forest	1018	30°04′49.0″
9	Bi Feng Xia	Forest	1018	30°04′49.0″
10	Bi Feng Xia	Hillside	989	30°05′01.9″
11	Bi Feng Xia	Hillside	989	30°05′01.9″
12	Bi Feng Xia	Hillside	904.6	30°05′18.0″
13	Bao Xing	Riverside	1253	30°28′51.0″
14	Bao Xing	Riverside	1253	30°28′51.0″
15	Bao Xing	Riverside	1253	30°28′51.0″
16	Bao Xing	River Valley	1179	32°21′11.3″
17	Bao Xing	River Valley	1179	32°21′11.3″
18	Bao Xing	River Valley	1179	32°21′11.3″
19	Bao Xing	Highway side	924	30°20′32.7″
20	Erlang Mountain	Forest	2091	29°52′55.0″
21	Erlang Mountain	Forest	2091	29°52′55.0″
22	Erlang Mountain	Hillside	1650	29°53′25.0″
23	Erlang Mountain	Hillside	1650	29°53′25.0″
24	Erlang Mountain	Hillside	1605	29°53′44.5″
25	Erlang Mountain	Hillside	1605	29°53′44.5″
26	Erlang Mountain	Hillside	1419	29°56′43.1″
27	Tuowu Mountain	Forest	1630	29°02′41.52″
28	Tuowu Mountain	Forest	1630	29°02′41.52″
29	Tuowu Mountain	Forest	1630	29°02′41.52″
30	Tuowu Mountain	Forest	1630	29°02′41.52″
31	Tuowu Mountain	Forest	1630	29°02′41.52″
32	Niba Mountain	Forest	1626	29°42′47.5″
33	Niba Mountain	Forest	1626	29°42′47.5″
34	Niba Mountain	Hillside	1594	29°43′07.7″
35	Niba Mountain	Hillside	1594	29°43′07.7″
36	Renshou	Highway	432.2	30°00′26.6″
37	Renshou	Highway	432.2	30°00′26.6″
38	Renshou	Highway	432.9	30°00′06.6″
39	Renshou	Highway	432.9	30°00′06.6″
40	Renshou	Bushes	471.8	30°00′16.6″
41	Renshou	Bushes	471.8	30°00′16.6″
42	Hongya	Bushes	483.5	29°53′22.6″
43	Hongya	Bushes	520.8	29°49′48.7″
44	Hongya	Dam side slope	487.4	29°50′26.8″
45	Hongya	Dam side slope	493.1	29°50′26.6″
46	Hongya	Dam side slope	501	29°53′12.6″
47	Zizhong	Orangery	350.1	29°49′03.4″
48	Zizhong	Orangery	350.1	29°49′03.4″
49	Zizhong	Orangery	350.1	29°49′03.4″
50	Zizhong	Orangery	350.1	29°49′03.4″

(Continued)

TABLE 1 | Continued

Identity	Source	Habital	Altitude (m)	Latitude (N)
51	Zizhong	Bushes	348.2	29°49′06.0″
52	Luzhou	Rice ridge	318.7	28°52′44.9″
53	Luzhou	Rice ridge	318.7	28°52′44.9″
54	Luzhou	Rice ridge	318.7	28°52′44.9″
55	Luzhou	Rice ridge	321	28°52′42.7″
56	Luzhou	Bushes	241.6	28°49′01.7″
57	Luzhou	Bushes	241.6	28°49′01.7″
58	Luzhou	Bushes	241.6	28°49′01.7″
59	Luzhou	Bushes	241.6	28°49′01.7″
60	Yibin	Cityside	500	28°45′08.8″
61	Yibin	Cityside	500	28°45′08.8″
62	Yibin	Cityside	500	28°45′08.8″
63	Yibin	Riverside	317.5	28°45′31.0″
64	Yibin	Riverside	342.4	28°50′42.0″
65	Zigong	Grass Bushes	353.5	29°26′37.4″
66	Zigong	Grass Bushes	353.5	29°26′37.4″
67	Jiangyou	Roadside	564.4	31°56′59.5″
68	Jiangyou	Roadside	564.4	31°56′59.5″
69	Jiangyou	Roadside	564.4	31°56′59.5″
70	Jiangyou	Highway	616.8	31°59′45.6″
71	Jiangyou	Highway	616.8	31°59′45.6″
72	Jiangyou	Highway	641.2	32°03′04.4″
73	Jiangyou	Highway	641.2	32°03′04.4″
74	Jiangyou	Highway	641.2	32°03′04.4″
75	Jiangyou	Highway	687.8	32°04′26.4″
76	Jiangyou	Highway	687.8	32°04′26.4″
77	Jian'ge	Hillside	611	32°13′58.3″
78	Jian'ge	Hillside	611	32°13′58.3″
79	Guangyuan	Hillside	612.1	32°38′16.9″
80	Guangyuan	Hillside	612.1	32°38′16.9″
81	Guangyuan	Hillside	612.1	32°38′16.9″
82	Guangyuan	Hillside	612.1	32°38′16.9″
83	Guangyuan	Hillside	612.1	32°38′16.9″
84	Guangyuan	Hillside	612.1	32°38′16.9″
85	Guangyuan	Bushes	644.8	32°38′57.9″
86	Guangyuan	Bushes	644.8	32°38′57.9″
87	Guangyuan	Bushes	644.8	32°38′57.9″
88	Daying	Highway	327.8	30°36′36.7″
89	Daying	Highway	327.8	30°36′36.7″
90	Daying	Highway	327.8	30°36′36.7″
91	Daying	Highway	327.8	30°36′36.7″
92	Daying	Highway	327.8	30°36′36.7″
93	Daying	Highway	327.8	30°36′36.7″
94	Shapingba	Riverside	255.3	29°39′39.9″
95	Shapingba	Riverside	255.3	29°39′39.9″
96	Banan	Hillside	476.5	29°31′10.7″
97	Banan	Hillside	476.5	29°31′10.7″
98	Banan	Forest edge	476.5	29°31′10.7″
99	Banan	Forest edgean	476.5	29°31′10.7″
100	Banan	Forest edge	476.5	29°31′10.7″
101	Banan	Forest edge	476.5	29°31′10.7″

(Continued)

TABLE 1 | Continued

Identity	Source	Habital	Altitude (m)	Latitude (N)
102	Banan	Forest edge	476.5	29°31′10.7″
103	Banan	Forest edge	476.5	29°31′10.7″
104	Nanchuan	Bushes	579.4	29°09′25.9″
105	Nanchuan	Bushes	579.4	29°09′25.9″
106	Nanchuan	Bushes	579.4	29°09′25.9″
107	Nanchuan	Hillside	579.4	29°09′25.9″
108	Nanchuan	Hillside	579.4	29°09′25.9″
109	Nanchuan	Hillside	579.4	29°09′25.9″
110	Nanchuan	Hillside	579.4	29°09′25.9″
111	Dabai	Hill foot	455.9	28°29′26.1″
112	Dabai	Hill foot	455.9	28°29′26.1″
113	Dabai	Hill foot	455.9	28°29′26.1″
114	Dabai	Hill foot	455.9	28°29′26.1″
115	Zunyi	Conifer forest	914.7	27°46′18.8″
116	Zunyi	Conifer forest	914.7	27°46′18.8″
117	Zunyi	Conifer forest	914.7	27°46′18.8″
118	Zunyi	Conifer forest	914.7	27°46′18.8″
119	Zunyi	Conifer forest	914.7	27°46′18.8″
120	Zunyi	Conifer forest	914.7	27°46′18.8″
121	Guiyang	Field ridge	1286	27°42′52.1″
122	Guiyang	Field ridge	1286	27°42′52.1″
123	Guiyang	Field ridge	1286	27°42′52.1″
124	Guiyang	Field ridge	1287	26°42′20.1″
125	Guiyang	Dam side slope	1268	26°30′20.2″
126	Guiyang	Dam side slope	1268	26°30′20.2″
127	Guiyang	Dam side slope	1268	26°30′20.2″
128	Zhenning	Hillside	1284	26°02′35.6″
129	Zhenning	Hillside	1284	26°02′35.6″
130	Zhenning	Hillside	1284	26°02′35.6″
131	Zhenning	Hillside	1284	26°02′35.6″
132	Huangguoshu	Forest edge	946.5	25°58′22.5″
133	Huangguoshu	Forest edge	946.5	25°58′22.5″
134	Huangguoshu	Forest edge	946.5	25°58′22.5″
135	Huangguoshu	Forest edge	946.5	25°58′22.5″
136	Huangguoshu	Forest edge	946.5	25°58′22.5″
137	Yuxi	Bushes	1721	24°12′15.9″
138	Yuxi	Bushes	1721	24°12′15.9″

50°C for 1 min, and 72°C for 1 min, extended at 72°C for 10 min, then stored at 4°C; for SSR, 5 min at 94°C for 1 cycle, followed by 10 cycles at 94°C for 1 min, 55°C for 30 s, and 72°C for 40 s, decreased 0.5°C for annealing with each cycle, and then 35 cycles at 94°C for 1 min, 50°C for 30 s, and 72°C for 40 s, extended at 72°C for 10 min, then stored at 4°C. Electrophoresis was performed in a denaturing 6% polyacrylamide gel (acrylamide: bis-acrylamide 19:1, 1 × TBE) to separate allele sizes. The gel was stained by AgNO$_3$ solutions.

Phenotypic Data Collection and Analysis

Three morphological traits were measured at early harvest season in 2011. Plant height (H) was measured at the ground level to the top of the plant. The total number of tillers in each plant (TN) was

counted after harvest. The fresh biomass yield of per plant (fresh weight, FW) was evaluated with autumn harvest in October. In 2012 and 2013, in addition to H, TN, and FW, several other morphological traits associated with biomass were measured. The main tiller diameter (TD) was measured approximately 10–15 cm from the base of the plant on three randomly chosen tillers. Number of main stem internodes (NI) was counted and the length of the main internode (LI) was measured. The length of flag leaf (LF) and length of longest leaf (LL) were measured from the ligule to the tip along the central vein of the leaf. The width of flag leaf (WF) and width of longest leaf (WL) were measured for the width of the blade at half-leaf length for the leaf which was recorded for measuring the length. Plants were harvested about 20 cm above the soil surface, and the whole above-ground biomass was weighed as FW in October. The harvested tissue were then dried in an oven at 105°C for 1 h, followed by 70°C for 3 days, for determining dry biomass yield per plant (dry weight, DW). All the plants in the field were cut about 20 cm to avoid rhizome damage and facilitate quick re-growth in the following season.

Analysis of variance (ANOVA) and correlation analysis of morphological traits were performed using SPSS 17.0 software (IBM, Armonk, New York, USA). Effects of both environment (different measurement year) and individuals on various traits were determined using the Least Significant Difference test model. Pearson correlation coefficients were calculated for correlation analysis. The coefficient of variation (CV) was calculated using the following model—CV = SD/Mean * 100%—for detecting the discrete level of the data.

Genetic Diversity and Population Structure

The alleles of molecular markers were scored manually for the population as band presence (1) or absence (0), and each of them was treated as an independent character regardless of its intensity. A present/absent data matrix was constructed to analyze the genetic diversity and population structure. The discriminatory power of different primers was evaluated by means of polymorphic information content (*PIC*), calculated by the following model $PIC_i = 2f_i(1 - f_i)$ (Roldan-Ruiz et al., 2000). In the model, PIC_i is the polymorphic information content of marker "I," f_i is the frequency of the amplified allele (band present), and $1 - f_i$ is the frequency of the null allele.

Population structure (Q) of 138 *M. sinensis* individuals was confirmed using the model-based clustering approach implemented in STRUCTURE v2.3.4 software (Pritchard et al., 2000) with the "admixture model," burn-in period of 100,000 iterations and a run of 100,000 replications of Markov Chain Monte Carlo (MCMC) after burn in. For each run, 20 independent runs of STRUCTURE were performed with the number of clusters (K) varying from 1 to 10. Maximum likelihood and delta K ($\triangle$K) tests were used to determine the optimum number of subgroups (Evanno et al., 2005). For clustering analysis, the similarity coefficients were used to construct an unweighted pair group method with arithmetic means (UPGMA) dendogram using sequential agglomerative hierarchical and nested clustering (SAHN) module in the NTSYS-pc version2.10 software. Analysis of molecular variance (AMOVA) was used to

calculate variation among and within populations using GenAlEx ver. 6.41 (Peakall and Smouse, 2012).

All genetic diversity indices were calculated using PopGen32 v.1.31, assuming Hardy-Weinberg equilibrium; the genetic diversity was evaluated with parameters: Nei's (1973) gene diversity (H) and Shannon's Information Index of Diversity (I). The total gene diversity (H_T) was divided into gene diversity within populations (H_S) and the gene diversity among populations (D_{ST}). These parameters were calculated according to the equation $H_T = H_S + D_{ST}$. The genetic differentiation coefficient (G_{ST}) was calculated as a ratio of D_{ST}/H_T and was used to measure population differentiation. Gene flow was calculated as $N_m = 0.5(1 - G_{ST})/G_{ST}$ to estimate the level of gene drift among the populations (Slatkin and Barton, 1989).

Marker-Trait Association Analysis

The markers with minor allele frequency less than 5% were removed in order to reduce false positive associations. Relative kinship (K) among samples was calculated by TASSEL 2.1 software. The marker-trait association analysis was conducted to reveal associations between the interest traits and marker alleles using TASSEL 2.1 software along with the General Linear Model (GLM) and Mixed Linear Model (MLM) procedure (Bradbury et al., 2007) to control for population structure and relative kinship. The simple linear model, Q (population structure results included as fixed effects generating from STRUCTURE software) model, K (relative kinship results included as fixed effects generating from TASSEL software) model, and Q+K models were tested to identify the best model fitting biomass related traits using Quantile-quantile (QQ) plots for association mapping in the *M. sinensis* populations. Two thresholds for significant associations were tested in our study. First, the significance threshold for associations between loci and traits was set at $P < 0.001$. Second, the Bonferroni correction of multiple testing ($P < 0.05/934 \sim 5.35 \times 10^{-5}$) was performed based on q-value using false discovery rate (FDR, $\alpha_c = 0.05$). The phenotypic variation explained by the single associated marker (R^2) indicated the fixed marker effects.

Genome-Wide Prediction

The genome-wide prediction was carried out by using the R package rrBLUP (Endelman, 2011) with ridge regression. The average correlation between the predicted phenotypic values from marker data and the original phenotypic values directly from field trail was used as the criteria of genome prediction accuracy. The accuracy (Pearson's correlation coefficient) was calculated with recommended 10-fold cross-validation and was repeated 100 times (Slavov et al., 2014). The adjusted prediction accuracy was calculated by dividing accuracy by the square root of the broad-sense heritability (h^2), where h^2 was calculated by using PROC MIXED (SAS Institute, Version 9.1, Cary, NC, USA). The h^2 was calculated as follows: $h^2 = \sigma_g^2/(\sigma_g^2 + \sigma_e^2/re + \sigma_{ge}^2/e)$, where σ_g^2, σ_e^2, σ_{ge}^2 represent Type III SS (sums of squares) for genotype (G), environment (E), and G × E, respectively. The "e" is the degree of freedom of environment and "re" is the degree of freedom of G × E.

RESULTS

Phenotypic Variation and Correlation

Significant differences among individuals were observed through ANOVA analysis for all measured traits (**Table 2**). In addition, the biomass yield per plant was increased year by year after establishment. Significant increases were noted in the mean of fresh biomass yield per plant—498.7 g in 2011, 770.8 g in 2012 and 1001.9 g in 2013, with the highest individual increased from 1350 g in 2011 to 2225 g in 2013. The results showed that TN, FW, and DW had a high level of phenotypic variation with CV of above 40% in 2011, 2012, and 2013.

Significant positive correlations of biomass yield (both fresh and dry) with TN, H, TD, NI, LI, LL, and WL were found, while no correlations were seen in with LF and WF (**Table 3**). The higher correlation coefficients indicated that *M. sinensis* biomass yield in the field was largely influenced by TN and H. On the other hand, TN had a significant negative correlation with tiller diameter ($r = -0.185$, $P < 0.05$) and leaf length ($r = -0.287$, $P < 0.01$), indicating that a *M. sinensis* plant with a high number of tillers always followed with small tiller diameter and low leaf length. Plant height had a significant positive correlation with the main internode length ($r = 0.522$, $P < 0.01$). Significant positive correlations were also found between leaf width and tiller diameter and between flag leaf length and flag leaf width.

Genotypic Variation and Population Structure

A total of 104 pairs of primers (Supplementary Table 1) were screened for genotyping the collections of 138 *M. sinensis* individuals while the other primers failed to amplify or did not produce clear bands. In total, 1059 bands were produced and 993 (93.8%) were polymorphic. For the SSR primers developed from *M. sinensis*, sorghum, sugarcane, maize, and conserved ESTs in grasses, the average of bands produced per primer was 7.8, 8.9, 5.8, 7.2, and 8.0, respectively. The production of ISAP primers had a similar result (6.5) with SSR, while the SRAP had a higher productive capacity (19.8). The mean of polymorphic information content ranged from 26.7% (SSR-4) to 39.0% (SSR-5), demonstrating a different discriminatory capacity for each kind of primer (**Table 4**).

Population structure of the 138 individuals was estimated under the Hardy-Weinberg Equilibrium by using STRUCTURE V2.3.3 software. After dropping the markers with minor allele frequency less than 5%, the total number of marker loci retained for structure and association analysis was 934. Based on maximum likelihood and delta K ($\triangle$K) values, the number of optimum subgroups was three (**Figure 1**). Accordingly, the 138 individuals were assigned into these three groups. Among them, 34 individuals were assigned to G1, 66 individuals to G2, and 38 individuals to G3 (**Figure 2**). By using a membership probability threshold (*Q*-value) of 0.60, the majority of the individuals were clearly assigned to the specific groups while admixture between groups referred to 18 individuals with $Q < 0.6$ (data not shown).

The genetic similarities coefficient (GS) values of 138 individuals ranged from 0.59 to 0.95 with an average of 0.67. The UPGMA dendrogram based on GS data obviously revealed three

TABLE 2 | The mean, range, standard deviation (SD), coefficient of variation (CV) and *F*-value of plant height (H), tiller number (TN), fresh biomass yield each plant (FW), dry biomass yield each plant (DW), the main tiller diameter (TD), the number of main stem internodes (NI), the length of main internode (LI), the length of flag leaf (LF), the width of flag leaf (WF), the length of longest leaf (LL), and the width of longest leaf (WL) in *Miscanthus sinensis* population in 2011, 2012, and 2013.

Trait	Year	Mean	Range	SD	CV (%)	*F*
H (cm)	2011	203.67	125.31–330.58	41.46	21.98	4.24***
	2012	205.18	120.63–307.14	37.58	18.45	
	2013	188.61	111.00–313.62	30.95	15.08	
TN	2011	29.30	4–73	15.18	51.81	6.61***
	2012	38.21	5–138	25.94	67.87	
	2013	43.38	9–92	19.04	43.88	
FW (g)	2011	498.7	50–1350	250.98	50.32	6.08***
	2012	770.8	85–2045	444.64	57.69	
	2013	1001.9	200–2225	474.35	47.35	
DW (g)	2012	363.8	55–1170	220.49	60.61	8.923***
	2013	399.0	105–875	180.47	45.23	
TD (cm)	2012	0.535	0.277–0.859	0.10	19.62	9.346***
	2013	0.579	0.193–0841	0.12	20.67	
NI	2012	10.50	6–16	2.30	21.93	3.952***
	2013	12.34	7–17	2.22	17.95	
LI (cm)	2012	9.07	4.32–15.68	2.33	25.74	3.785***
	2013	10.97	5.49–20.63	2.47	22.52	
LF(cm)	2012	32.13	7.03–77.53	14.07	43.80	9.626***
	2013	35.10	11.33–70.33	11.89	33.88	
WF (cm)	2012	0.87	0.33–1.87	0.30	34.46	6.009***
	2013	0.97	0.52–2.43	0.37	38.07	
LL (cm)	2012	77.63	35.21–121.78	14.89	19.19	6.756***
	2013	82.36	53.97–119.78	12.47	15.14	
WL (cm)	2012	1.59	0.72–2.47	0.36	22.40	12.213***
	2013	1.83	1.10–3.12	0.41	22.53	

***Significant differences at $P < 0.001$.

major clusters similar to the result from the population structure analysis when the GS value was equal to 0.67 (Supplementary Figure 1).

The three groups comprised of 138 individuals had a relatively high genetic diversity reflected by Nei's (1973) gene diversity (H) and Shannon's Information Index of Diversity (I) (**Table 5**). Total gene diversity (H_T) was 0.35 ± 0.015, while gene diversity within groups (H_S) was 0.33 ± 0.014 and gene diversity among groups (D_{ST}) was 0.016. The total Shannon's Information Index of Diversity (SII) among 138 individuals was 0.52 ± 0.015 with the average of SII within groups was 0.50. The mean genetic differentiation coefficient (G_{ST}) was estimated from the 933 bands with a value of 0.046. A higher level of genetic variation

TABLE 3 | Pearson correlation coefficients among TN, H, FW, TD, NI, LI, LF, WF, LL, WL, and DW[§] in *M. sinensis* population[‡].

	TN	H	FW	TD	NI	LI	LF	WF	LL	WL	DW
TN	1										
H	−0.028	1									
FW	0.610**	0.408**	1								
TD	−0.185*	0.204*	0.364**	1							
NI	−0.030	0.391**	0.285**	0.218*	1						
LI	−0.011	0.522**	0.223**	0.002	0.301**	1					
LF	−0.125	0.246**	0.042	0.095	−0.131	0.062	1				
WF	−0.138	0.283**	0.110	0.229**	0.117	0.181*	0.525**	1			
LL	−0.136	0.380**	0.264**	0.386**	0.085	0.212*	0.427**	0.208*	1		
WL	−0.287**	0.331**	0.285**	0.527**	0.360**	0.195*	0.053	0.406**	0.360**	1	
DW	0.527**	0.392**	0.897**	0.334**	0.386**	0.251**	−0.006	0.131	0.170*	0.364**	1

[§]*TN, tiller number; H, plant height; FW, fresh biomass yield each plant; TD, the main tiller diameter; NI, the number of main stem internode; LI, the length of main internode; LF, the length of flag leaf; WF, the width of flag leaf; LL, the length of longest leaf; WL, the width of longest leaf; and DW, dry biomass yield each plant.*

[‡]*Correlation calculated using mean of 3 years.*

*Correlation is significant at P < 0.05.

**Correlation is significant at P < 0.01.

TABLE 4 | The amplification results of each primer and the comparison of productive capacity among seven primers.

Primer kind	NPC	TB	TPB	ANB	PPB (%)	PIC (%)	Origin developed
SSR-1	25	195	193	7.8	99.0	0.343	*M. sinensis*
SSR-2	7	62	60	8.9	96.8	0.350	*Sorghum*
SSR-3	9	52	45	5.8	86.5	0.282	*Saccharum*
SSR-4	9	65	56	7.2	86.2	0.267	*Zea mays*
SSR-5	10	80	78	8.0	97.5	0.390	*Conserved grass ESTs*
SRAP	24	475	442	19.8	93.1	0.341	\
ISAP	20	130	119	6.5	91.5	0.275	\
Total	104	1059	933	\	\	\	\

NPC, Number of primer combinations; TB, Total number of bands produced; TPB, Total number of polymorphic bands produced; ANB, The average number of bands produced; PPB (%), Percentage of polymorphic bands; PIC (%), Polymorphic information content.

within the populations than among them suggested a high frequency of gene flow ($Nm = 10.32$) between the groups. The AMOVA analysis of the *M. sinensis* populations showed similar results, and both the genetic variations within (96.0%) and among (4.0%) groups were significant ($P < 0.05$) (**Table 6**).

Marker-Trait Association Analysis

Marker-based relative kinship estimates have proven useful for quantitative inheritance studies in different populations. For the 138 *M. sinensis* individuals, the pair-wise relative kinship (K) estimates represented a normal distribution with approximately 98% of individuals from 0 to 0.5 (**Figure 3**). The results agreed that a high gene flow existed among samples. Quantile-quantile (QQ) plot is a probability plot, which is a graphical method of comparing two probability distributions (observed vs. expected). In this study, Q and K were detected among samples. Therefore, the association analysis was performed by taking Q and K into account using GLM and MLM approaches in the software TASSEL 2.1. Biomass yield and related traits were used to test the model with Q only matrix, K only matrix, Q+K matrix and

simple linear model (S) excluding the Q and K in QQ plots (**Figure 4**).

In most cases, the Q+K model and the K model had similar power and demonstrated the best approximation to the excepted cumulative distribution of *P*-values, followed by the Q and S model. The results from the Q+K and K models showed a significant improvement in goodness of fit compared with the other models, except that the fresh biomass and dry biomass yields in the Q+K model had a slightly higher power than the K model. At last, the Q+K model was selected as the best fitting model for association analysis.

A total of 21 significant associations were detected using a simple linear model, 18 using Q model, 15 using K model and 12 using Q+K model ($P < 0.001$). The averages of the phenotypic variations explained by the model for significant associations were 9.2% (S), 10.9% (Q), 46.8% (K), and 47.1% (Q+K), which was consistent with the model test results. For the significant associations detected by Q+K model, 4 markers were associated with plant height, 3 markers with flag leaf width, 1 marker with internode number, and 1 marker with fresh biomass yield (**Table 7**). In addition, marker "494" was associated with tiller diameter, leaf length and leaf width simultaneously. When comparing the significant associations detected by the Q+K model and the K model, 3 biomass yields related associations were filtered out ($P > 0.001$) in the Q+K model while they significant in the K model. The results were consistent with the model test above that the Q+K and K models had nearly the same capacity to detect the associations but the Q+K model seems a little better fit for biomass to control false positive associations. Specifically, one of associations (marker "793" for flag leaf width) reached genome-wide significant after Bonferroni correction for multiple testing ($P < 0.05/934 \sim 5.35 \times 10^{-5}$), with an estimated false discovery rate (FDR) < 0.05.

For an overall measure of quality of the genotype and phenotype data, genome-wide prediction was conducted in this study (**Table 8**). Most of measured traits were moderately heritable with the total average of broad-sense heritability (h^2) equal to 0.56. Furthermore, the average of prediction
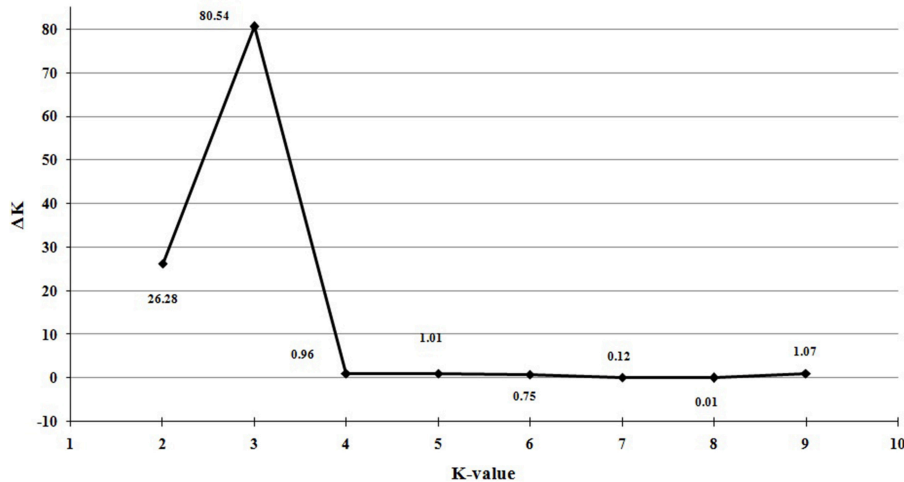
FIGURE 1 | Optimal value of K determined by delta K (△K).
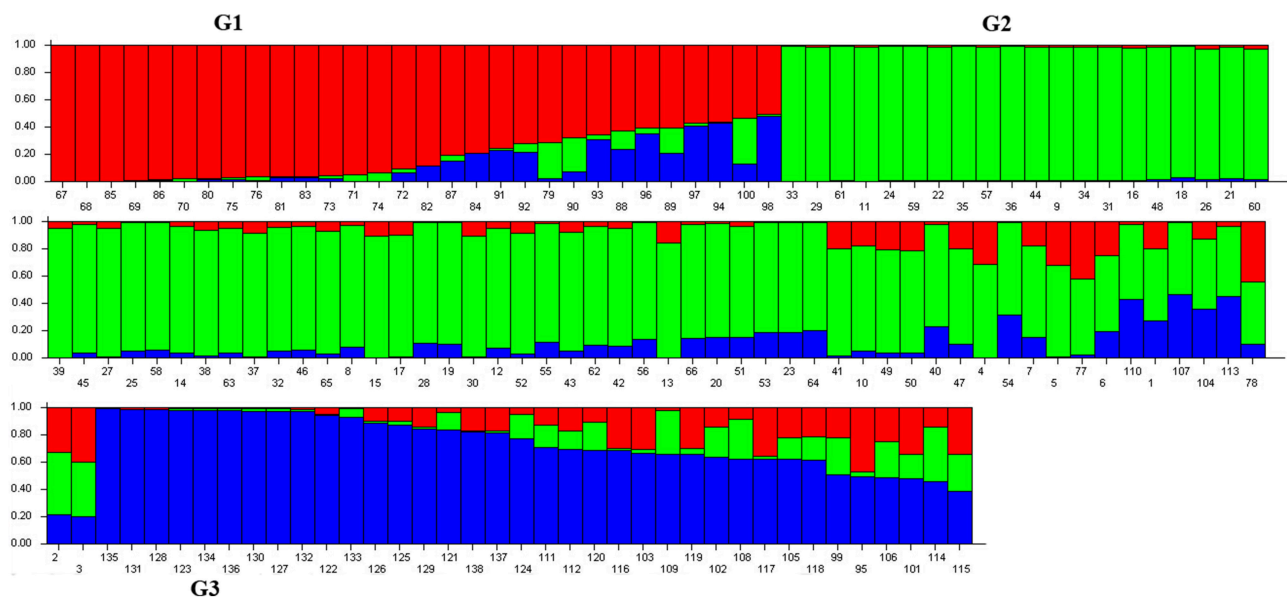
FIGURE 2 | Population structure analysis of 138 *M. sinensis* individuals from southwest China. Numbers on the x-axis indicate the individual and numbers on the y-axis show the group membership. G1, G2, and G3 represent the identified structure groups.

accuracy and adjust prediction accuracy was 0.24 and 0.33, respectively. Although, the values of prediction accuracy seem lower, the adjust accuracy of genome-wide prediction for flag leaf width had moderate predictive ability (0.59). Interestingly, association analysis also showed that one marker was highly associated with flag leaf width on genome-wide significant level.

DISCUSSION

Miscanthus is a typical perennial grass species that requires a long period of time for establishment after transplanting clonal

replicates prior to reaching the maximum growth for optimum and stable productivity (Clifton-Brown and Lewandowski, 2000; Anzoua et al., 2015). *M. sinensis* grows slowly at the initial phase of establishment due to uneven splitting of the rhizome, the differences in growing conditions prior to transplanting, and variable adaptive capacity to the new environment. Since high biomass yield is the primary goal in improving *M. sinensis*, it appears that the correlation between traits and biomass yield during the establishment time may be important in *M. sinensis* breeding programs because plant biomass yield may not be always the optimum criteria for early selection (Gifford et al., 2015). Using traits that can be reliably measured in the early

years of establishment to predict future performance could help an efficient early selection to reduce the breeding time. At least, data could be used to remove the unwanted genotypes with little potential.

In this study, plants were not evaluated in the first year after transplanting. In the subsequent 3 years, *M. sinensis* individuals were examined for biomass yield and related morphological traits in Ya'an, southwest of China, an area known as having the richest rainfall but relatively less light for grass species growth. Abundant phenotypic variations of traits in the establishment phase were found in the population. Most of the traits related to biomass yield tended to reach optimum value in the third year after transplanting and were close to stable growing stage. The results were consistent with previous studies, which suggested

TABLE 5 | Genetic diversity of *M. sinensis* populations.

Population identity	Sample size	Na	Ne	H	I
G1	34	1.97	1.55	0.33	0.50
G2	66	1.99	1.57	0.34	0.51
G3	38	1.98	1.55	0.32	0.49
Mean		1.98	1.56	0.33	0.50
Within Species	138	2.00	1.58	0.35	0.52

Na, Observed number of alleles averaged across loci; Ne, Effective number of alleles averaged across loci; H, Nei's (1973) gene diversity; I, Shannon's Information index.

TABLE 6 | AMOVA analysis of *M. sinensis* groups.

Source of variation	Degree of freedom	Sum of square	Summary of matches	Percentage of (%) variation	*P*-value
Among Groups	2	897.9	448.9	4%	0.035
Within Groups	135	23235.8	172.1	96%	0.010
Total	137	24133.7		100%	

that a 3 year establishment phase was needed to achieve a stable or reliable population to collect phenotypic data in *Miscanthus* species (Clifton-Brown and Lewandowski, 2000).

Superior genotypes of *M. sinensis* with high tiller numbers and plant height could be comparable to *Miscanthus × giganteus* in terms of biomass yield potential (Heaton et al., 2004; Huang et al., 2011). Although field performance was evaluated for only 3 years (a few traits evaluated for the last 2 years) after transplanting in this study, some individuals had comparable or exceeded values relative to *Miscanthus × giganteus* in Europe and North America (Lewandowski et al., 2003a,b; Jezowski, 2008; Maughan et al., 2012; Gifford et al., 2015). The results suggested that some *M. sinensis* genotypes with vigorous growth, especially with high tillering capacity, greatly contributed to more biomass yield. Those genotypes would have the genetic potential to match or exceed the biomass yield of *Miscanthus × giganteus* in similar climate areas, although the performance of those genotypes has not been tested in colder climates or higher latitudes. In particular, plant height almost reached the optimum at the second year after transplanting and became stable the following year. The results suggested that plant height can be used as early selection criteria to develop genotypes with high biomass yield potential in *M. sinensis*. Thus, it could be possible to develop high biomass yield of *M. sinensis* by simultaneous selecting individuals with high tiller numbers and plant height. Genotypes with high biomass yield identified in this study would be useful for accelerating its domestication as an energy crop in similar areas.

As one of the 34 biodiversity hotspots around the world, southwest China has a special geographical location, climatic conditions, and abundant wild resources (Mittermeier et al., 2000). Prior studies have shown that high gene flow existed among *M. sinensis* populations from southwest China (Xu et al., 2013; Nie et al., 2014), which could be due to an introgression occurred from here to other distribution areas around China (Xiao et al., 2013). By analyzing *trnL-F* and *rpl20-rps12* sequences, Yan et al. (2015) found that the haplotypes "H2" widely distributed among populations from southwest
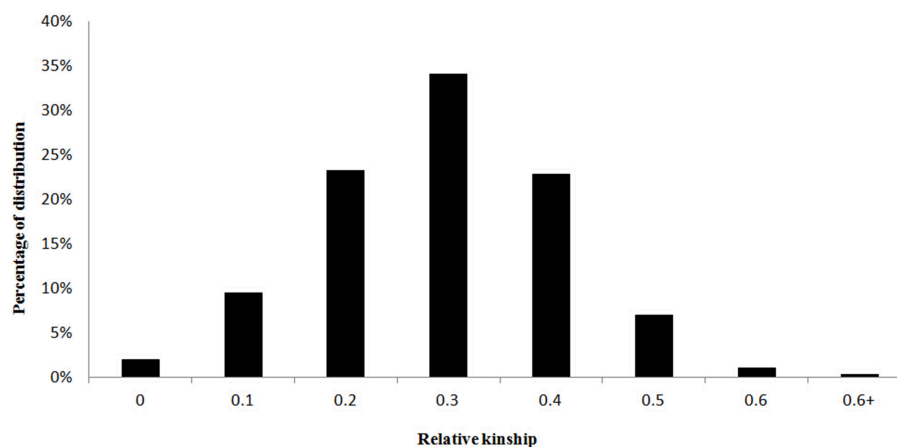

FIGURE 3 | The distributions of pair-wise kinship coefficients for 138 *M. sinensis* individuals.

FIGURE 4 | Quantile-quantile plots for model comparison with biomass yield and related traits. (A), Evaluation of model types using markers for tiller number; **(B)**, Evaluation of model types using markers for plant height; **(C)**, Evaluation of model types using markers for tiller diameter; **(D)**, Evaluation of model types using markers for internode number; **(E)**, Evaluation of model types using markers for internode length; **(F)**, Evaluation of model types using markers for leaf length; **(G)**, Evaluation of model types using markers for leaf width; **(H)**, Evaluation of model types using markers for fresh biomass yield; **(I)**, Evaluation of model types using markers for dry biomass yield. In this figure, black dots line represent the predicted value equal to the observed value; blue dots represent the simple linear model (without population structure and relative kinship); red diamond represents the Q model; blue diamond represents the K model; and red dots represent the Q+K model.

China and had a high level of similarity (99.64%) with haplotypes "A" identified in Japanese *M. sinensis* populations (Shimono et al., 2013). Furthermore, through comparison of haplotypes from NCBI, they determined that haplotypes "H1" and "H6" had relatively high similarity to the haplotypes obtained from the Liaoning and Jilin provinces located in northeast China (Jiang et al., 2013). In this study, the 138 individuals collected from *N 24°12′15.9″* to *N 32°38′57.9″* across southwest China revealed a very high level of gene flow, which is consistent with previous studies. All the results inferred that *M. sinensis* populations from southwest China have a mixed and complex ancestry owing to the complex ecotypes, random genetic drift, and the high rate of gene flow. Hence, knowing the relationship and population structure of *M. sinensis* from southwest China is important for taxonomic research and phylogenetic evaluation for their conservation and utilization.

Due to the lengthy period of establishment and the challenges in getting phenotypic data from a large population, a marker-assisted selection program would add tremendous value to a *Miscanthus* breeding program. However, different types of markers vary in amplification capacity and relationship to the traits in *Miscanthus* species. SSR regions lie within microsatellite repeats, and have a random distribution genome wide, while the target locus of SRAP is mainly located in open reading frame regions (ORFs). ISAP, as a very good complementary, is designed by using the highly conserved sequence of introns splice position as the core of the primer sequences to amplify the genes encoding areas, which could leading to a high association with expressed sequence. In this study, SRAP have a very high amplification capacity than other markers, demonstrating its values for use in the molecular marker system. The average number of alleles per loci produced in this study was similar to previous studies (Hung et al., 2009; Ho et al., 2011; Zhou et al., 2011; Lu et al., 2012; Nie et al., 2014). Furthermore, both the conserved grass EST-SSRs and ISAP markers were amplified in *M. sinensis* for the first time but proved to be highly efficient markers for *Miscanthus*. Using a large amount of molecular markers has great potential to obtain reliable and important loci for detecting the relationships between markers and traits of interest.

Molecular markers have been used to evaluate the genetic relationship of accessions in *M. sinensis* all around its distributed areas. Some genetic maps with high density and resolution have been constructed (Kim et al., 2012; Ma et al., 2012; Swaminathan et al., 2012; Liu et al., 2015). Atienza's genetic map had been sufficiently used in four QTL studies (Atienza et al., 2003a,b,c,d) in the early stage, but limitations occurred due to the low reproducibility of RAPD markers, the small population size ($N = 89$) and incomplete genetic map (28 linkage

TABLE 7 | Significant marker-trait association of *M. sinensis* individuals.

Trait	Allele number	Primer number	Locus	Allele size (bp)	R^2 (%)
Plant Height	86	N-13	ISAP-F6+R7	156	5.39***
Plant Height	737	N-89	SRAP-Me1+em8	250	4.43***
Plant Height	859	N-95	SRAP-Me10+em2	343	4.55***
Plant Height	945	N-98	SRAP-Me6+em10	137	5.06***
Tiller Diameter	494	N-70	SSR-SG26	127	6.79***
Leaf Length	494	N-70	SSR-SG26	127	5.36***
Leaf Width	494	N-70	SSR-SG26	127	5.80***
Internode Number	334	N-46	SSR-HAU-12	78	5.48***
Flag Leaf Width	14	N-2	ISAP-F1+R3	127	4.94***
Flag Leaf Width	335	N-47	SSR-HAU-58	375	5.11***
Flag Leaf Width	793	N-92	SRAP-Me6+em8	232	8.43***
Fresh Biomass yield	927	N-98	SRAP-Me6+em10	380	5.17***

***Significant association at $P < 0.001$ with FDR correction at $\alpha_c = 0.05$; R^2, Phenotypic variation explained by markers.

TABLE 8 | Performance of genome-wide prediction in 138 *Miscanthus sinensis* genotypes based on 934 markers.

Trait	Heritability	Accu[b]	SD[c]$_{Accu}$	Adjusted Accu[d]	SD[e]$_{Ad Accu}$
Plant Height	0.67	0.20	0.046	0.24	0.056
Tiller Number	0.74	0.23	0.033	0.27	0.039
Fresh Biomass yield	0.69	0.11	0.046	0.13	0.056
Dry Biomass yield	0.62	0.23	0.035	0.29	0.044
Tiller Diameter	0.62	0.10	0.039	0.13	0.050
Internode Number	0.33	0.20	0.040	0.35	0.069
Internode Length	0.42	0.28	0.031	0.44	0.048
Flag Leaf Length	0.46	0.29	0.030	0.43	0.045
Flag Leaf Width	0.47	0.41	0.024	0.59	0.035
Leaf Length	0.49	0.23	0.031	0.33	0.044
Leaf Width	0.63	0.31	0.030	0.39	0.038
Total Average[a]	0.56	0.24	0.035	0.33	0.048

[a]Total Average, overall average and standard deviation across traits.

[b]Accu, average predicted accuracy across 100 random 10-fold cross-validations based on 934 markers.

[c]SD$_{Accu}$, averagestandard deviation of predicted accuracy.

[d]Adjusted Accu, average adjusted predicted accuracy of genome-wide prediction across 100 random 10-fold cross-validations based on 934 markers.

[e]SD$_{AdAccu}$, average standard deviation of adjusted predicted accuracy.

groups detected whereas *M. sinensis* has 19 chromosomes). More recently, Gifford et al. (2015) and Liu et al. (2015) conducted QTL studies based on the high density genetic maps (Swaminathan et al., 2012; Liu et al., 2015), but identification of QTLs using the genetic map are still limited. Furthermore, the association studies were lagged than QTL research on Miscanthus, and to date, the only two studies were reported. Zhao et al. (2013) conducted marker-trait association by analyzing a *M. sinensis* population from China and using 23 SSR markers transferable from *Brachypodium distachyon* and 9 markers were significantly ($P < 0.01$) associated with heading date and biomass yield. A genome-wide association study was conducted in a 138 *M. sinensis* population by using 53,174 single-nucleotide variants (SNVs) (Slavov et al., 2014) and a total of 17 significant associations (false discovery rate $< 10^{-5}$) with phenology, morphology, and cell wall composition traits were detected.

In our study, 12 significant associations of biomass yield with related traits were identified and marker "793" associated with flag leaf width reached genome-wide significant after Bonferroni correction for multiple testing. The possible reason why we obtained a number of significant associations similar to Slavov et al. (2014) while using a much smaller number of markers could be that the PCR-based markers are more likely to be associated with traits than random SNPs (just based on their distribution in the genome). However, in our study the ability to predict phenotypes seemed lower than that obtained from genome-wide sequencing (Slavov et al., 2014). Other factors like the number of markers and the structure of the population may be equally important in influencing the power of association studies. The phenotypic data and markers result from association study could be potential candidates to supplementing the database of *Miscanthus* for improving genome-wide selection in a breeding program.

AUTHOR CONTRIBUTIONS

XZ, LH, and GN conceived the project and designed the experiments; GN, XW, and YZ performed the experiments; GN, XY, and XL analyzed the data; XZ, MT, and YJ finalized the manuscript; all authors discussed the results and reviewed the manuscript.

ACKNOWLEDGMENTS

SUPPLEMENTARY MATERIAL

The Supplementary Material for this article can be found online at: http://journal.frontiersin.org/article/10.3389/fpls.2016.00802

REFERENCES

Anzoua, K. G., Suzuki, K., Fujita, S., Toma, Y., and Yamada, T. (2015). Evaluation of morphological traits, winter survival and biomass potential in wild Japanese *Miscanthus sinensis* Anderss. populations in northern Japan. *Grassl. Sci.* 61, 83–91. doi: 10.1111/grs.12085

Aranzana, M. J., Kim, S., Zhao, K., Bakker, E., Horton, M., Jakob, K., et al. (2005). Genome-wide association mapping in Arabidopsis identifies previously known flowering time and pathogen resistance genes. *PLoS Genet.* 1:e60. doi: 10.1371/journal.pgen. 0010060

Atienza, S. G., Satovic, Z., Petersen, K. K., Dolstra, O., and Martin, A. (2003a). Identification of QTLs associated with yield and its components in *Miscanthus sinensis* Anderss. *Euphytica* 132, 353–361. doi: 10.1023/A:1025041926259

Atienza, S. G., Satovic, Z., Petersen, K. K., Dolstra, O., and Martin, A. (2003b). Identification of QTLs influencing agronomic traits in *Miscanthus sinensis* Anderss. I. Total height, flag-leaf height and stem diameter. *Theor. Appl. Genet.* 107, 123–129. doi: 10.1007/s00122-003-1220-5

Atienza, S. G., Satovic, Z., Petersen, K. K., Dolstra, O., and Martin, A. (2003c). Identification of QTLs influencing combustion quality in *Miscanthus sinensis* Anderss. II. Chlorine and potassium content. *Theor. Appl. Genet.* 107, 857–863. doi: 10.1007/s00122-003-1218-z

Atienza, S. G., Satovic, Z., Petersen, K. K., Dolstra, O., and Martin, A. (2003d). Influencing combustion quality in *Miscanthus sinensis* Anderss.: identification of QTLs for calcium, phosphorus and sulphur content. *Plant Breeding* 122, 141–145. doi: 10.1046/j.1439-0523.2003. 00826.x

Bradbury, P. J., Zhang, Z., Kroon, D. E., Casstevens, T. M., Ramdoss, Y., and Buckler, E. S. (2007). TASSEL: software for association mapping of complex traits in diverse samples. *Bioinformatics* 23, 2633–2635. doi: 10.1093/bioinformatics/btm308

Breseghello, F., and Sorrells, M. E. (2006). Association mapping of kernel size and milling quality in wheat (*Triticum aestivum* L.) cultivars. *Genetics* 172, 1165–1177. doi: 10.1534/genetics.105. 044586

Chae, W. B., Hong, S. J., Gifford, J. M., Rayburn, A. L., Sacks, E. J., and Juvik, J. A. (2014). Plant morphology, genome size, and SSR markers differentiate five distinct taxonomic groups among accessions in the genus *Miscanthus*. *Global Change Biol. Bioenergy* 6, 646–660. doi: 10.1111/gcbb.12101

Clark, L. V., Brummer, J. E., Glowacka, K., Hall, M. C., Heo, K., Peng, J., et al. (2014). A footprint of past climate change on the diversity and population structure of *Miscanthus sinensis*. *Ann. Bot.* 114, 97–107. doi: 10.1093/aob/mcu084

Clifton-Brown, J. C., and Lewandowski, I. (2000). Overwintering problems of newly established *Miscanthus* plantations can be overcome by identifying genotypes with improved rhizome cold tolerance. *New Phytol.* 148, 287–294. doi: 10.1046/j.1469-8137.2000.00764.x

Clifton-Brown, J. C., Lewandowski, I., Andersson, B., Basch, G., Christian, D. G., Kjeldsen, J. B., et al. (2001). Performance of 15 *Miscanthus* genotypes at five sites in Europe. *Agron. J.* 93, 1013–1019. doi: 10.2134/agronj2001.9351013x

Dwiyanti, M. S., Stewart, J. R., Nishiwaki, A., and Yamada, T. (2014). Natural variation in *Miscanthus sinensis* seed germination under low temperatures. *Grassl. Sci.* 60, 194–198. doi: 10.1111/grs.12051

Eleuch, L., Jilal, A., Grando, S., Ceccarelli, S., Schmising, M. V., Tsujimoto, H., et al. (2008). Genetic diversity and association analysis for salinity tolerance, heading date and plant height of barley germplasm using simple sequence repeat markers. *J. Integr. Plant Biol.* 50, 1004–1014. doi: 10.1111/j.1744-7909.2008.00670.x

Endelman, J. B. (2011). Ridge regression and other kernels for genomic selection with R package rrBLUP. *Plant Genome* 4, 250–255. doi: 10.3835/plantgenome2011.08.0024

Evanno, G., Regnaut, S., and Goudet, J. (2005). Detecting the number of clusters of individuals using the software STRUCTURE: a simulation study. *Mol. Ecol.* 14, 2611–2620. doi: 10.1111/j.1365-294X.2005.02553.x

Gifford, J. M., Chae, W. B., Swaminathan, K., Moose, S. P., and Juvik, J. A. (2015). Mapping the genome of *Miscanthus sinensis* for QTL associated with biomass productivity. *GCB Bioenergy* 7, 797–810. doi: 10.1111/gcbb.12201

Greef, J. M., Deuter, M., Jung, C., and Schondelmaier, J. (1997). Genetic diversity of European *Miscanthus* species revealed by AFLP fingerprinting. *Genet. Res. Crop Evol.* 44, 185–195. doi: 10.1023/A:1008693214629

Harjes, C. E., Rocheford, T. R., Bai, L., Brutnell, T. P., Kandianis, C. B., Sowinski, S. G., et al. (2008). Natural genetic variation in lycopene epsilon cyclase tapped for maize biofortification. *Science* 319, 330–333. doi: 10.1126/science.1150255

Hastings, A., Clifton-Brown, J., Wattenbach, M., Mitchell, P., and Smith, P. (2009). The development of MISCANFOR, a new Miscanthus crop growth model: towards more robust yield predictions under different climatic and soil conditions. *GCB Bioenergy* 1, 154–170. doi: 10.1111/j.1757-1707.2009.01007.x

Heaton, E. A., Dohleman, F. G., and Long, S. P. (2008). Meeting US biofuel goals with less land: the potential of *Miscanthus*. *GCB* 14, 2000–2014. doi: 10.1111/j.1365-2486.2008.01662.x

Heaton, E. A., Dohleman, F. G., and Long, S. P. (2009). Seasonal nitrogen dynamics of *Miscanthus × giganteus* and *Panicum virgatum*. *GCB Bioenergy* 1, 297–307. doi: 10.1111/j.1757-1707.2009.01022.x

Heaton, E., Voigt, T., and Long, S. P. (2004). A quantitative review comparing the yields of two candidate C4 perennial biomass crops in relation to nitrogen, temperature and water. *Biomass Bioenergy* 27, 21–30. doi: 10.1016/j.biombioe.2003.10.005

Hernandez, P., Dorado, G., Laurie, D. A., Martin, A., and Snape, J. W. (2001). Microsatellites and RFLP probes from maize are efficient sources of molecular markers for the biomass energy crop *Miscanthus*. *Theor. Appl. Genet.* 102, 616–622. doi: 10.1007/s001220051688

Ho, C. W., Wu, T. H., Hsu, T. W., Huang, J. C., Huang, C. C., and Chiang, T. Y. (2011). Development of 12 genic microsatellite loci for a biofuel grass, *Miscanthus sinensis* (Poaceae). *Am. J. Bot.* 98, e201–e203. doi: 10.3732/ajb.1100071

Hodkinson, T. R., Chase, M. W., Lledo, M. D., Salamin, N., and Renvoize, S. A. (2002a). Phylogenetics of *Miscanthus*, Saccharum and related genera (Saccharinae, Andropogoneae, Poaceae) based on DNA sequences from ITS nuclear ribosomal DNA and plastid trnL intron and trnL-F intergenic spacers. *J. Plant Res.* 115, 381–392. doi: 10.1007/s10265-002-0049-3

Hodkinson, T. R., Chase, M. W., Takahashi, C., Leitch, I. J., Bennett, M. D., and Renvoize, S. A. (2002b). The use of DNA sequencing (ITS and trnL-F), AFLP, and fluorescent in situ hybridization to study allopolyploid *Miscanthus* (Poaceae). *Am. J. Bot.* 89, 279–286. doi: 10.3732/Ajb.89.2.279

Huang, C. L., Liao, W. C., and Lai, Y. C. (2011). Cultivation studies of Taiwanese native *Miscanthus floridulus* lines. *Biomass Bioenergy* 35, 1873–1877. doi: 10.1016/j.biombioe.2011.01.032

Hung, K. H., Chiang, T. Y., Chiu, C. T., Hsu, T. W., and Ho, C. W. (2009). Isolation and characterization of microsatellite loci from a potential biofuel plant *Miscanthus sinensis* (Poaceae). *Conserv. Genet.* 10, 1377–1380. doi: 10.1007/s10592-008-9699-6

Jezowski, S. (2008). Yield traits of six clones of *Miscanthus* in the first 3 years following planting in Poland. *Ind. Crop Prod.* 27, 65–68. doi: 10.1016/j.indcrop.2007.07.013

Jiang, J. X., Zhu, M. D., Ai, X., Xiao, L., Deng, G. T., and Yi, Z. L. (2013). Molecular evidence for a natural diploid hybrid between *Miscanthus sinensis* (Poaceae) and *M. sacchariflorus*. *Plant Syst. Evol.* 299, 1367–1377. doi: 10.1007/s00606-013-0801-2

Kantety, R. V., La Rota, M., Matthews, D. E., and Sorrells, M. E. (2002). Data mining for simple sequence repeats in expressed sequence tags from barley, maize, rice, sorghum and wheat. *Plant Mol. Biol.* 48, 501–510. doi: 10.1023/A:1014875206165

Kim, C., Lee, T. H., Guo, H., Chung, S. J., Paterson, A. H., Kim, D. S., et al. (2014). Sequencing of transcriptomes from two *Miscanthus* species reveals functional specificity in rhizomes, and clarifies evolutionary relationships. *BMC Plant Biol.* 14, 134. doi: 10.1186/1471-2229-14-134

Kim, C., Zhang, D., Auckland, S. A., Rainville, L. K., Jakob, K., Kronmiller, B., et al. (2012). SSR-based genetic maps of *Miscanthus sinensis* and *M. sacchariflorus*, and their comparison to sorghum. *Theor. Appl. Genet.* 124, 1325–1338. doi: 10.1007/s00122-012-1790-1

Lewandowski, I., Clifton-Brown, J. C., Andersson, B., Basch, G., Christian, D. G., Jorgensen, U., et al. (2003a). Environment and harvest time affects the combustion qualities of *Miscanthus* genotypes. *Agron. J.* 95, 1274–1280. doi: 10.2134/agronj2003.1274

Lewandowski, I., Clifton-Brown, J. C., Scurlock, J. M. O., and Huisman, W. (2000). *Miscanthus*: European experience with a novel energy crop. *Biomass Bioenergy* 19, 209–227. doi: 10.1016/S0961-9534(00)00032-5

Lewandowski, I., Scurlock, J. M. O., Lindvall, E., and Christou, M. (2003b). The development and current status of perennial rhizomatous grasses as energy crops in the US and Europe. *Biomass Bioenergy* 25, 335–361. doi: 10.1016/S0961-9534(03)00030-8

Li, G., and Quiros, C. F. (2001). Sequence-related amplified polymorphism (SRAP), a new marker system based on a simple PCR reaction: its application to mapping and gene tagging in Brassica. *Theor. Appl. Genet.* 103, 455–461. doi: 10.1007/s001220100570

Liu, S., Clark, L. V., Swaminathan, K., Gifford, J. M., Juvik, J. A., and Sacks, E. J. (2015). High-density genetic map of *Miscanthus sinensis* reveals inheritance of zebra stripe. *GCB Bioenergy* 8, 616–630. doi: 10.1111/gcbb.12275

Lu, C. R., Yu, S. X., Yu, J. W., Fan, S. L., Song, M. Z., Wang, W., et al. (2008). Development and appraisement of functional molecular marker: intron sequence amplified polymorphism (ISAP). *Hereditas* 30, 1207–1216. doi: 10.3724/SP.J.1005.2008.01207

Lu, Y. F., Jiang, J. X., and Yi, Z. L. (2012). Study on the transferability of maize SSR and sugarcane EST-SSR markers to *Miscanthus* (Poaceae). *Acta Pratacul. Sin.* 21, 86–95. Available online at: http://cyxb.lzu.edu.cn/CN/abstract/abstract3412.shtml

Ma, X. F., Jensen, E., Alexandrov, N., Troukhan, M., Zhang, L., Thomas-Jones, S., et al. (2012). High resolution genetic mapping by genome sequencing reveals genome duplication and tetraploid genetic structure of the diploid *Miscanthus sinensis*. *PLoS ONE* 7:e33821. doi: 10.1371/journal.pone.0033821

Maughan, M., Bollero, G., Lee, D. K., Darmody, R., Bonos, S., Cortese, L., et al. (2012). *Miscanthus × giganteus* productivity: the effects of management in different environments. *GCB Bioenergy* 4, 253–265. doi: 10.1111/j.1757-1707.2011.01144.x

Mittermeier, R. A., Myers, N., and Mittermeier, C. G. (2000). *Hotspots: Earth's Biologically Richest and Most Endangered Terrestrial Ecoregions.* Washington, DC: Conservation International.

Nei, M. (1973). Analysis of gene diversity in subdivided population. *Proc. Natl. Acad. Sci. U.S.A.* 70, 3321–3323.

Nie, G., Zhang, X. Q., Huang, L. K., Xu, W. Z., Wang, J. P., Zhang, Y. W., et al. (2014). Genetic variability and population structure of the potential bioenergy crop *Miscanthus sinensis* (Poaceae) in Southwest China based on SRAP markers. *Molecules* 19, 12881–12897. doi: 10.3390/molecules190812881

Nishiwaki, A., Mizuguti, A., Kuwabara, S., Toma, Y., Ishigaki, G., Miyashita, T., et al. (2011). Discovery of natural *Miscanthus* (Poaceae) triploid plants in sympatric populations of *Miscanthus sacchariflorus* and *Miscanthus sinensis* in southern Japan. *Am. J. Bot.* 98, 154–159. doi: 10.3732/ajb.1000258

Peakall, R., and Smouse, P. E. (2012). GenAlEx 6.5: genetic analysis in Excel. Population genetic software for teaching and research–an update. *Bioinformatics* 28, 2537–2539. doi: 10.1093/bioinformatics/bts460

Pritchard, J. K., Stephens, M., and Donnelly, P. (2000). Inference of population structure from multilocus genotype data. *Genetics* 155, 945–959. doi: 10.1534/genetics.107.072371

Roldan-Ruiz, I., Dendauw, J., Van Bockstaele, E., Depicker, A., and De Loose, M. (2000). AFLP markers reveal high polymorphic rates in ryegrasses (*Lolium* spp.). *Mol. Breeding* 6, 125–134. doi: 10.1023/A:1009680614564

Shimono, Y., Kurokawa, S., Nishida, T., Ikeda, H., and Futagami, N. (2013). Phylogeography based on intraspecific sequence variation in chloroplast DNA of *Miscanthus sinensis* (Poaceae), a native pioneer grass in Japan. *Botany* 91, 449–456. doi: 10.1139/cjb-2012-0212

Skøt, L., Humphreys, J., Humphreys, M. O., Thorogood, D., Gallagher, J., Sanderson, R., et al. (2007). Association of candidate genes with flowering time and water-soluble carbohydrate content in *Lolium perenne* (L.). *Genetics* 177, 535–547. doi: 10.1534/genetics.107.071522

Slatkin, M., and Barton, N. H. (1989). A comparison of three indirect methods for estimating average levels of gene flow. *Evolution* 43, 1349–1368.

Slavov, G. T., Nipper, R., Robson, P., Farrar, K., Allison, G. G., Bosch, M., et al. (2014). Genome-wide association studies and prediction of 17 traits related to

phenology, biomass and cell wall composition in the energy grass *Miscanthus sinensis*. *New Phytol.* 201, 1227–1239. doi: 10.1111/nph.12621

Stewart, J. R., Toma, Y., Fernandez, F. G., Nishiwaki, A., Yamada, T., and Bollero, G. (2009). The ecology and agronomy of *Miscanthus sinensis*, a species important to bioenergy crop development, in its native range in Japan: a review. *GCB Bioenergy* 1, 126–153. doi: 10.1111/j.1757-1707.2009.01010.x

Swaminathan, K., Chae, W. B., Mitros, T., Varala, K., Xie, L., Barling, A., et al. (2012). A framework genetic map for *Miscanthus sinensis* from RNAseq-based markers shows recent tetraploidy. *BM Genomics* 13:142. doi: 10.1186/1471-2164-13-142

Wang, J., McClean, P. E., Lee, R., Goos, R. J., and Helms, T. (2008). Association mapping of iron deficiency chlorosis loci in soybean (Glycine max L. Merr.) advanced breeding lines. *Theor. Appl. Genet.* 116, 777–787. doi: 10.1007/s00122-008-0710-x

Wang, M. L., Barkley, N. A., Yu, J.-K., Dean, R. E., Newman, M. L., Sorrells, M. E., et al. (2005). Transfer of simple sequence repeat (SSR) markers from major cereal crops to minor grass species for germplasm characterization and evaluation. *Plant Genet Res* 3, 45–57. doi: 10.1079/PGR200461

Xiao, L., Xue, D., Jiang, J. X., Ai, X., Qin, J. P., Chen, Z. Y., et al. (2013). Genetic diversity in *Miscanthus sinensis* of China revealed by Simple Sequence Repeats DNA markers. *J. Plant Genet Res.* 14, 32–36. doi: 10.3969/j.issn.1672-1810.2013.01.006

Xu, W. Z., Zhang, X. Q., Huang, L. K., Nie, G., and Wang, J. P. (2013). Higher genetic diversity and gene flow in wild populations of *Miscanthus sinensis* in southwest China. *Biochem. Syst. Ecol.* 48, 174–181. doi: 10.1016/j.bse.2012.11.024

Yan, H. D., Zhang, X. Q., Fu, C., Huang, L. K., Yin, G. H., Nie, G., et al. (2015). Chloroplast DNA variation and genetic structure of *Miscanthus sinensis* in southwest China. *Biochem. Syst. Ecol.* 58, 132–138. doi: 10.1016/j.bse.2014.11.007

Yook, M. J., Lim, S. H., Song, J. S., Kim, J. W., Zhang, C. J., Lee, E. J., et al. (2014). Assessment of genetic diversity of Korean *Miscanthus* using morphological traits and SSR markers. *Biomass Bioenergy* 66, 81–92. doi: 10.1016/j.biombioe.2014.01.025

Yu, J., and Buckler, E. S. (2006). Genetic association mapping and genome organization of maize. *Curr. Opin. Biotechnol.* 17, 155–160. doi: 10.1016/j.copbio.2006.02.003

Yu, X., Bai, G., Luo, N., Chen, Z., Liu, S., Liu, J., et al. (2011). Association of simple sequence repeat (SSR) markers with submergence tolerance in diverse populations of perennial ryegrass. *Plant Sci.* 180, 391–398. doi: 10.1016/j.plantsci.2010.10.013

Zhao, H., Wang, B., He, J., Yang, J., Pan, L., Sun, D., et al. (2013). Genetic diversity and population structure of *Miscanthus sinensis* germplasm in China. *PLoS ONE* 8:e75672. doi: 10.1371/journal.pone.0075672

Zhong, Z. L., Jiang, J. X., Lang, L., and Yi, Z. L. (2009). Genetic diversity analysis of *Miscanthus* species by maize SSR primers. *Prog. Mod. Biomed.* 9, 2076–2079. doi: 10.13241/j.cnki.pmb.2009.11.001

Zhou, H. F., Li, S. S., and Ge, S. (2011). Development of microsatellite markers for *Miscanthus sinensis* (Poaceae) and cross-amplification in other related species. *Am. J. Bot.* 98, e195–e197. doi: 10.3732/ajb.1100040

Nitrogen Fertilization Effects on Biomass Production and Yield Components of *Miscanthus* × *giganteus*

Moon-Sub Lee[1], Andrew Wycislo[1,2], Jia Guo[1], D. K. Lee[1] and Thomas Voigt[1,2]*

[1] Department of Crop Sciences, University of Illinois Urbana-Champaign, Urbana, IL, USA, [2] Energy Biosciences Institute, University of Illinois Urbana-Champaign, Urbana, IL, USA

Grasses such as *Miscanthus* × *giganteus* and *Panicum virgatum* (switchgrass) can potentially be used to produce bioenergy on a large scale in the Midwestern USA. The biomass productivity of these warm-season perennial grasses, particularly *M.* × *giganteus*, can be substantial, even when grown with limited inputs. The literature, however, varies regarding the nitrogen requirements for *M.* × *giganteus* biomass production. In addition, there is a lack of information that identifies the yield-component(s) (including total tiller number, tiller weight, total tiller diameter, total tiller height, phytomer number, reproductive tiller number, vegetative tiller number, reproductive tiller height, vegetative tiller height, reproductive tiller diameter, vegetative tiller diameter, and reproductive tiller phytomer number) that contributes to *M.* × *giganteus* biomass yields. Thus, the objective of this study was to examine the effects of fertilization on biomass yield and individual *M.* × *giganteus* plant-yield components. Plots of *M.* × *giganteus* were planted in 2008 in Urbana, IL, USA, and received annual applications of 0, 60, or 120 kg N ha^{-1}. *M.* × *giganteus* productivity increased when nitrogen was applied; between 2011 and 2014, nitrogen applications of 60 or 120 kg N ha^{-1} produced average annual yields of 22.0 dry Mg ha^{-1} compared to 11.8 dry Mg ha^{-1} for unfertilized *M.* × *giganteus*. Both the total number of tillers per m^2 and the tiller weight also increased as N-application rates increased. Our results indicate that increased reproductive tiller density and tiller weight with increased N fertilization increased *M.* × *giganteus* biomass yield.

Keywords: *Miscanthus* × *giganteus*, bioenergy, biomass productivity, nitrogen fertilization, yield components

INTRODUCTION

When growing crops for cellulosic bioenergy, efficient production of high-yielding biomass feedstocks is a primary goal. In the U.S. Midwest, *Miscanthus* × *giganteus* Greef et Deu ex. Hodkinson et Renvoize (hereafter *M.* × *giganteus*), a sterile, warm-season, perennial grass, shows potential as a bioenergy crop due to its great biomass production (Heaton et al., 2008). *M.* × *giganteus* is a rhizomatous grass native to East Asia that was first cultivated as an energy crop in Europe in the early 1980s (Lewandowski et al., 2000). It is believed to be a cross between the fertile species *M. sinensis* and *M. sacchariflorus* (Hodkinson et al., 2002). As it is sterile, *M.* × *giganteus* must be propagated vegetatively using rhizome cuttings, rhizome-derived

plugs, or *in vitro* micro propagation (Lewandowski, 1998; Anderson et al., 2011). Rhizome propagation has produced more robust plants than *in vitro* propagation (Lewandowski, 1998).

M. × giganteus has high yield potential. In Europe, *M. × giganteus* has produced 25 to 30 Mg ha^{-1} (Lewandowski et al., 2000). In the U.S., *M. × giganteus* biomass productivity from University of Illinois bioenergy studies has ranged between 15 and 30 Mg ha^{-1} in several Illinois field studies (Heaton et al., 2004, 2008; Maughan et al., 2012).

Nitrogen applications to *M. × giganteus* have had variable productivity results. Two long-termed *M. × giganteus* fertility studies in Europe found no productivity response to N fertilization over many years (Himken et al., 1997; Christian et al., 2008), while a third study reported a N response of biomass as the plot aged beyond 10 years (Clifton-Brown et al., 2007). The Illinois *M. × giganteus* studies were initially designed to compare *M. × giganteus* yields with those of switchgrass (*Panicum virgatum* L.) with no added fertility (Heaton et al., 2008). As the stands aged, *M. × giganteus* yields declined (Arundale et al., 2014a). However, when nitrogen was applied to the aged plots, previously unfertilized, *M. × giganteus* productivity increased as the N rates increased (Arundale et al., 2014b).

Grass phenotypic traits such as tiller density, tiller length, the number of phytomers per tiller [phytomers are vegetative units of grass shoots that include an internode, leaf, a portion of the node at the upper end, and a vegetative bud and portion of the node at the lower end (Beard and Beard, 2005)], the reproductive-to-vegetative tiller ratio, and tiller weight all play a role in determining productivity in herbaceous bioenergy crops. To date, these yield components have been evaluated and correlated with biomass productivity in switchgrass and prairie cordgrass (*Spartina pectinata* Link).

A study of three switchgrass cultivars showed strong correlation with increasing yield and both tiller density and phytomer mass, and weak correlation with the number of phytomers per tiller (Boe and Beck, 2008). Similar studies also found that the number of reproductive tillers per m^2 and the number of phytomers per tiller were good selection criteria for increased biomass production of switchgrass (Boe, 2007). In addition, Boe (2007) also reported that switchgrass plants with greater numbers of large, reproductive stems tended toward higher yields (Boe, 2007). Das et al. (2004) reported a positive correlation between yield and tiller density. Much of the overall variation in switchgrass yield, therefore, results from genetic variability among cultivars (Boe and Beck, 2008). In prairie cordgrass, another warm-season rhizomatous perennial grass, Guo et al. (2015) found that tiller mass, tiller density, heading date, plant height, and phytomer number were all positively correlated with yield in some manner, but also found that much of the phenotypic variation was from the genetic diversity of the germplasm. With respect to the yield effect of nitrogen, Muir et al. (2001) reported that switchgrass tiller mass and tiller density responded positively to increased N fertilization and that tiller mass was more important than tiller density for biomass production. Similarly, Sanderson and Reed (2000) described that high N input increased individual switchgrass tiller weight, which increased biomass production.

There are conflicting results regarding *M. × giganteus* yield response to nitrogen fertilization, and the yield components that contribute to *M. × giganteus* biomass productivity are not well understood. Moreover, there are no reports of *M. × giganteus* yield components, N-fertilizer effects on yield components, and the yield component and N fertility roles on biomass productivity. Our central hypothesis was that N fertilization will increase one or more yield components and those components will contribute to *M. × giganteus* biomass. Therefore, the objective of this study was to examine the effects of fertilization on biomass yield and individual yield components in *M. × giganteus*.

MATERIALS AND METHODS

The study site was located near Urbana, IL, USA, at the University of Illinois Energy Farm (40.0624 N, −88.1915 W) in Dana silt loam soil (fine-silty, mixed, superactive, mesic Oxyaquic Argiudolls). Before field planting in this study, *M. × giganteus* rhizomes (approximately 25 g) were collected from a field nursery at the University of Illinois Landscape Horticulture Research Center (Urbana, IL, USA) in 2007, and planted into pots (9 cm × 9 cm × 12 cm) using Sunshine Metro-Mix950® (Sun Gro Horticulture Distribution Inc., Hadley, MA, USA) as the growing medium. The potted *M. × giganteus* plants were grown in the University of Illinois greenhouse (Urbana, IL, USA) maintained at 27°C/16°C day/night temperature with 14 h photoperiod providing 400 μmol m^{-2}s^{-1} photon flux at plant canopy level. In July 2008, potted *M. × giganteus* were planted by hand on one-meter spacing in twelve, 10 m × 10 m plots (100 plants per plot) with three nitrogen fertility treatments applied annually in early spring at or near the time of emergence at 0, 60, and 120 kg N ha^{-1} using urea as the N source (Maughan et al., 2012). Due to winterkill during the 2008–2009 winter the site was partially replanted in spring 2009 to fill plots to 100 plants each. The study was planted using a randomized complete block design with four replications, each comprised of the three N-application levels (Maughan et al., 2012).

This study reports on 2011–2014 growing-season findings. Biomass yields in 2010 were minimal (<3 Mg ha^{-1}) and data were not included in this study. From 2011 to 2014, the study was harvested post-senescence after each growing season, between mid-December and March, which is the agronomic harvest timing for *M. × giganteus* grown as a bioenergy grass in Central Illinois. Biomass was cut by hand in 1-m^2 quadrats with five replications per plot in senesced biomass harvests. Quadrats were selected throughout the plots in an attempt to produce samples representative of the plot as a whole and were not selected from border rows. Stems were cut at 10 cm and each quadrat was bundled individually. The biomass from each quadrat was measured for total plant fresh weight, subsample wet and oven-dry weights, vegetative tiller number (tiller m^{-2}) and reproductive tiller number (tiller m^{-2}). Five vegetative and five reproductive tillers were randomly selected from each of five replications per plot for yield components including tiller weight

(g tiller^{-1}), reproductive and vegetative tiller diameter (mm), reproductive and vegetative tiller height (cm), and reproductive and vegetative tiller phytomer number. Tiller diameter was measured at the midpoint of the lowest complete phytomer. Tiller height was measured to the top node of vegetative stems and to the base of the flower in reproductive stems. Dry biomass weight (PB, Mg ha^{-1}) was determined by drying a 1.0 kg of subsample to 60°C for up to 72 h until dry weight was constant. Finally, we calculated nitrogen use efficiency (NUE) according to Delogu et al. (1998) and Lewandowski and Schmidt (2006), where NUE is the ratio of yield (yield at N_x-yield at N_0) to N supply.

Weather data including precipitation and temperature was obtained from the Illinois State Climatologist and the Illinois state water survey 2015 (Illinois State Water Survey[1]). Precipitation and temperature records are shown for the location for the duration of the study (**Table 1**).

Data analysis including ANOVA, mean separation, and normality of the residuals and homogeneity of variances were performed in SAS software (SAS Institute, Cary, NC, USA).

[1]http://www.isws.illinois.edu

Biomass and yield components data were analyzed using Proc Mixed in SAS with N-rate (N), year (Y), and the interaction of N-rate and year (YN) were considered fixed effects and block as random. Tukey's studentized range test was used to compare biomass yield and phenotypic traits at $\alpha = 0.05$.

RESULTS

Monthly precipitation and temperature data for 2011–2014 are presented in **Tables 1**, **2**, respectively. June 2012 precipitation was 45% below the 30-year average at 58 mm and July 2012 precipitation was 87% below the 30-year average at 15 mm, whereas August and September 2013 were 9.1 and 9.7 mm, which are 90% less than 30-year average (**Table 1**).

During 2011–2014, the main effects of N rate and year and their interaction effects were significant for biomass yield (**Table 2**). Biomass yield increased with increased N fertilization up to 60 kg N ha^{-1}, and biomass yields between the two N fertilization rates (60 and 120 kg N ha^{-1}) were not different. As interaction effects indicate, biomass yield generally appeared

TABLE 1 | Weather conditions during 2011–2015 with 30-year average (1981–2010) for Urbana, IL, USA.

(A) Precipitation (unit: mm).

Month	2011	2012	2013	2014	30-year average
January	17	81	65	41	48
February	96	29	82	77	51
March	35	41	34	35	82
April	188	59	179	100	93
May	125	79	95	111	122
June	106	58	159	209	107
July	40	15	90	221	119
August	45	141	9	39	111
September	69	145	17	87	82
October	62	139	91	126	71
November	120	27	39	61	88
December	70	53	34	46	70
Annual total precipitation	973	867	894	1153	1044

(B) Temperature (unit: °C).

Month	2011	2012	2013	2014	30-year average	2011	2012	2013	2014	30-year average
January	−3.7	3.3	1.3	−3.6	−1.2	−11.7	−7.2	−8.8	−14.2	−10.2
February	0.8	4.6	1.3	−4.2	1.5	−7.3	−5.1	−7.3	−13.8	−8.2
March	9.0	17.8	3.8	5.8	8.3	−1.7	4.2	−3.0	−6.2	−2.8
April	16.2	17.2	14.3	16.1	15.4	4.3	4.1	2.6	3.6	3.4
May	20.6	25.4	22.3	22.2	21.3	9.3	11.7	10.2	9.9	9.2
June	26.8	27.8	26.0	26.4	26.4	15.5	13.6	14.3	15.8	14.9
July	31.4	33.5	26.1	24.8	27.8	19.4	18.9	15.6	13.8	16.6
August	29.4	29.0	27.3	26.4	27.1	15.9	14.4	15.0	16.3	15.6
September	22.2	22.7	26.4	22.7	24.0	10.2	10.4	12.1	10.1	10.7
October	18.4	14.6	17.2	15.7	16.8	4.2	3.6	4.7	5.0	4.2
November	10.8	8.9	7.2	4.9	8.7	0.8	−2.3	−3.6	−5.6	−1.7
December	4.4	4.9	−0.1	1.8	0.9	−3.8	−3.2	−9.4	−4.4	−7.7

mm, millimeter; °C, degrees celsius.

to decrease from 2011 to 2014 without N fertilization. However, biomass production was consistent throughout the years with N rate of 60 kg N ha^{-1} (**Table 3**). From 2011 to 2014, *M. × giganteus* plots fertilized at 60 kg and 120 kg N ha^{-1} produced average annual yields of 25.5 and 24.9 Mg ha^{-1}, respectively, compared to 13.0 Mg biomass ha^{-1} from the unfertilized plots (**Table 3**).

The main effects of N rate and year were significant for all biomass yield component traits except for the vegetative tiller number and vegetative tiller phytomer number, respectively, and N × year interactions were significant for total tiller number tiller weight, reproductive tiller height, reproductive tiller phytomer number, and vegetative tiller height (**Table 2**). In general, the values of all yield component traits increased with N fertilization except for the vegetative tiller number and vegetative tiller phytomer number, and differences between fertilized plots and unfertilized plots increased as the stands aged. However, no difference was observed between the two N rates (**Table 3**). In 2014, the reproductive tiller number was 24 and 42 tillers m^{-2} for 0 and 60 kg N ha^{-1}, respectively, and tiller weight was 28 and

44 g tiller^{-1} for 0 and 60 kg N ha^{-1}, respectively (**Table 4**). While the vegetative tiller number was not affected by N fertilization, total tiller number increased with N fertilization (**Table 3**). There was no difference in total tiller number among years, but total tiller number was lower in 2012, especially without N application (**Table 3**).

The correlations between yield components and biomass yield in 2012, 2013, and 2014 were highly significant, exclusive of vegetative tiller number and vegetative tiller phytomer number in 2014 (**Table 4**). In 2011, there were weak, or no, observed correlations between yield components and biomass yield. Among biomass yield components, total tiller number, reproductive tiller number, and tiller weight were positively correlated with biomass yield and were the strongest indicators for biomass yield (**Table 4**). When correlation analysis between yield components and biomass yield were performed across years, the highest correlations were observed between reproductive tiller number and biomass yield ($R^2 = 0.6831$) and tiller weight and biomass yield ($R^2 = 0.7517$) (**Figures 1A,B**, respectively).

TABLE 2 | Probability values from analysis of variance for biomass yield and yield components[†] of *Miscanthus × giganteus* affected by N rate during 2011–2014 at Urbana, IL, USA.

	PB[¶]	T-TN[†]	VTN[†]	RTN[†]	TW[†]	RTD[†]	RTHT[†]	RTPN[†]	VTD[†]	VTHT[†]	VTPN[†]
N rate	0.0004	0.0015	0.1074	0.0003	<0.0001	0.0002	<0.0001	<0.0001	0.0002	<0.0001	<0.0001
Year	0.0016	<0.0001	0.0163	0.0006	<0.0001	<0.0001	0.0074	<0.0001	<0.0001	<0.0001	0.2148
N × Y	0.0204	0.0360	0.6493	0.0539	0.0003	0.0626	<0.0001	0.0133	0.6770	<0.0001	0.1830

[¶]*PB, plant biomass (Mg ha^{-1}). [†]T-TN, total tiller number (tiller m^{-2}); VTN, vegetative tiller number (tiller m^{-2}); RTN, reproductive tiller number (tiller m^{-2}); TW, tiller weight (g tiller^{-1}); RTTD, reproductive tiller stem diameter (mm); RTHT, reproductive tiller height (cm); RTPN, reproductive tiller phytomer number; VTD, vegetative tiller diameter (mm); VTHT, vegetative tiller height (cm); VTPN, vegetative tiller phytomer number.*

TABLE 3 | *Miscanthus × giganteus* biomass yield[¶] and yield components[†] as affected by N fertilization rate during 2011–2014 at Urbana, IL, USA.

Year	N fertility	PB[¶]	T-TN[†]	VTN[†]	RTN[†]	TW[†]	RTD[†]	RTHT[†]	RTPN[†]	VTD[†]	VTHT[†]	VTPN[†]
2011	0N	15.9d[‡]	46.5d–f	20.3	26.3	36.6cd	8.8	253.0g	13.4h	7.8	225.2c	11.3
	60N	23.3c	49.0c–f	15.2	33.8	50.0a	9.8	282.3de	14.4g	8.8	262.8ab	12.6
	120N	22.1c	53.0c–e	22.1	30.9	43.8ab	10.1	273.7ef	14.7fg	8.9	247.6b	12.3
2012	0N	11.6ef	43.7f	24.3	10.9	25.9e	8.2	237.2h	13.5h	6.6	196.6d	10.4
	60N	24.5a–c	66.9a	17.7	39.3	37.1c	9.3	304.4a–c	15.3ef	7.4	266.7a	11.8
	120N	23.7bc	68.4a	25.8	32.7	34.1cd	9.0	296.8cd	15.5de	7.2	255.6ab	11.4
2013	0N	15.3ed	48.8c–f	13.8	35.1	30.8d	8.4	258.1fg	14.3g	6.1	187.4d	10.3
	60N	28.3ab	65.3ab	13.0	52.4	43.3b	9.0	303.4a–c	16.1	7.0	266.9a	12.7
	120N	28.5a	63.9ab	15.7	48.3	44.4ab	9.3	298.8b–d	17.1b	7.1	258.3ab	12.7
2014	0N	8.46f	39.5f	14.5	25.1	21.0f	8.6	229.2h	14.6g	6.4	135.7e	9.7
	60N	25.9a–c	57.8bc	15.5	42.4	44.8ab	10.0	314.5ab	16.7bc	7.1	254.3ab	11.9
	120N	25.2a–c	54.8cd	16.0	38.8	45.6ab	10.1	315.7a	17.9a	7.1	246.7b	13.2
N rate	0N	12.8B	44.6B	18.2	24.3B	28.1B	8.5B	244.4B	13.9C	6.7B	186.2B	10.4B
Mean	60N	25.5A	59.7A	15.3	42.0A	43.6A	9.5A	301.0A	15.6B	7.6A	262.7A	12.2A
	120N	24.9A	60.0A	19.9	37.6A	43.6A	9.6A	296.2A	16.3A	7.7A	252.0A	12.4A
Year	2011	20.4b	49.5b	19.2ab	30.3bc	42.4a	9.6a	270.0b	14.1d	8.5a	245.2a	12.1
Mean	2012	19.9b	59.7a	22.6a	27.6c	32.4c	8.8b	279.4a	14.8c	7.1b	239.6a	11.2
	2013	24.0a	59.3a	15.3b	45.2a	39.5b	8.9b	287.0a	15.8b	6.7c	237.5a	11.9
	2014	19.9b	50.7b	14.1b	35.4b	37.1b	9.5a	286.3a	16.4a	6.9bc	212.2b	11.6

[¶]*PB, plant biomass (Mg ha^{-1}). [†]T-TN, total tiller number (tiller m^{-2}); VTN, vegetative tiller number (tiller m^{-2}); RTN, reproductive tiller number (tiller m^{-2}); TW, tiller weight (g tiller^{-1}); RTTD, reproductive tiller stem diameter (mm); RTHT: reproductive tiller height (cm); RTPN: reproductive tiller phytomer number; VTD, vegetative tiller diameter (mm); VTHT, vegetative tiller height (cm); VTPN, vegetative tiller phytomer number. [‡]Value with the same letter with in each of interaction effect of N rate and Year, main effect of N rate, and main effect of Year are not significantly different as indicated by HSD test at P = 0.05 level.*

TABLE 4 | Correlation coefficients between biomass yield and yield components[†] of *M. × giganteus* during 2011–2014 at Urbana, IL, USA.

Year	T-TN[†]	VTN[†]	RTN[†]	TW[†]	RTD[†]	RTHT[†]	RTPN[†]	VTD[†]	VTHT[†]	VTPN[†]
2011	0.80**	0.30	0.56	0.77**	0.77**	0.41	0.33	0.80**	0.56	0.54
2012	0.94**	−0.44	0.95**	0.93**	0.86**	0.92**	0.86**	0.79**	0.90**	0.67*
2013	0.96**	0.23	0.95**	0.93**	0.89**	0.84**	0.78**	0.74**	0.87**	0.88**
2014	0.92**	0.15	0.97**	0.97**	0.63**	0.95**	0.90**	0.83**	0.96**	0.49

*Coefficient of correlation significant at $P < 0.05$. **Coefficient of correlation significant at $P < 0.01$. [†]T-TN, total tiller number (tiller m^{-2}); VTN, vegetative tiller number (tiller m^{-2}); RTN, reproductive tiller number (tiller m^{-2}); TW, tiller weight (g $tiller^{-1}$); RTTD, reproductive tiller stem diameter (mm); RTHT, reproductive tiller height (cm); RTPN, reproductive tiller phytomer number; VTD, vegetative tiller diameter (mm); VTHT, vegetative tiller height (cm); VTPN, vegetative tiller phytomer number.*
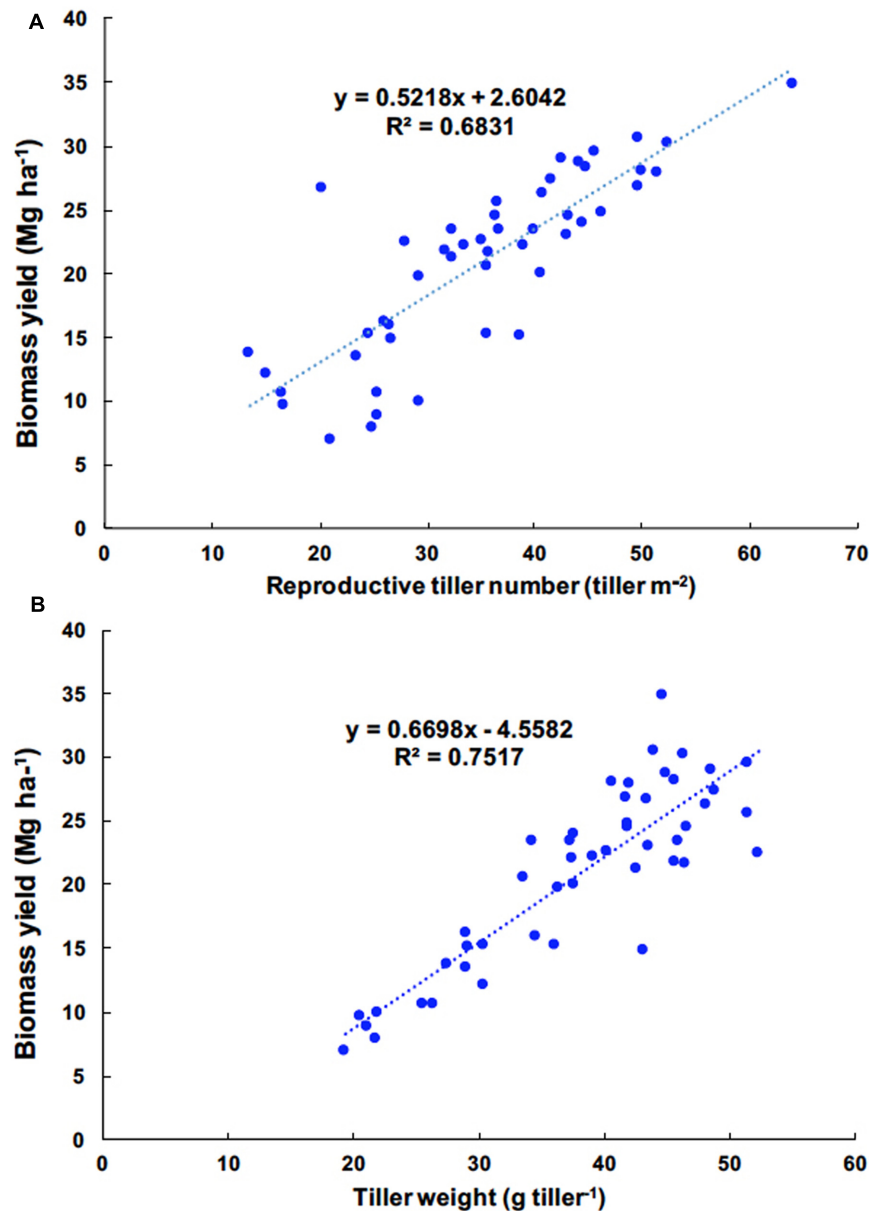
FIGURE 1 | Linear regression of reproductive tiller number and biomass yield (A) and tiller weight and biomass yield **(B)** of *Miscanthus × giganteus* fertilized by N rates, 0, 60, and 120 kg N ha^{-1} during 2011–2014 at Urbana, IL, USA.

DISCUSSION

In this experiment, nitrogen fertilization increased *M. × giganteus* productivity during 2011–2014, but there were no yield differences between plots fertilized with 60 and 120 kg N ha^{-1}. The positive responses to N fertilization are in agreement with Arundale et al. (2014b). Furthermore, N management is particularly essential for a biomass feedstock because N is associated with productivity and the cost of production (Vogel et al., 2002). The NUE was 0.3 Mg (kg N)$^{-1}$ for the 60 kg N ha^{-1} treatments and 0.1 Mg (kg N)$^{-1}$ for the 120 kg N ha^{-1} treatments. Increased N application rate led to a reduction in NUE, which is similar to the finding of Lewandowski and Schmidt (2006). However, many other studies reported that N fertilization is not required to achieve high *M. × giganteus* biomass yields (Himken et al., 1997; Lewandowski et al., 2000; Heaton et al., 2004; Christian et al., 2008). The different responses to N applications can be explained by the following: (1) Much of the *M. × giganteus* productivity research was conducted in Europe, and despite of the spatial variations, generally atmospheric N deposition rates are higher in Western Europe than in the USA (Holland et al., 2005). The topographical difference might affect soil N, which is thus related to N fertilization biomass yield response. (2) The reported absence of N fertilization effect could also be attributed to relatively short-termed experiments or to *M. × giganteus* growth during establishment years (Miguez et al., 2008). To produce 15 Mg ha^{-1} of *M. × giganteus* biomass, the N, P, and K requirements would be 92 kg N ha^{-1}, 13 kg P ha^{-1}, and 204 kg K ha^{-1} based on yearly crop off-take (Beale and Long, 1997). In addition, in Ercoli et al. (1999), it was implied that if N fertilizer was not supplied to the cropping system, there would be a reduction of biomass yield over long-termed growth. Conversely, if *M. × giganteus* is continuously harvested, there is N removal from the soil that should be compensated for by an external source of N. (3) Soil type, especially soil texture, can be an important factor for soil N availability. Even though the soil in our plots was classified as a silt loam soil by the USDA Soil Survey, based on our soil analysis (Maughan et al., 2012), this soil was a sandy loam soil with low CEC and N content. Biomass yield response to N fertilization in our study could be associated with low soil N retention as we observed no yield differences among N-fertilized plots during 2009–2010 (data not shown). Our results suggested that site-specific N management is necessary for sustainable biomass production of *M. × giganteus*.

Precipitation is the most important factor that directly and indirectly impacts aboveground biomass production in terrestrial ecosystems (Kardol et al., 2010), and roots are the primary connection between soil and soil water to plants (Clothier and Green, 1997; Xi et al., 2013). Plant biomass production positively responds to annual precipitation (Paruelo et al., 1999), and the seasonal precipitation pattern is a key factor in determining perennial grass establishment and biomass yield (Lee and Boe, 2005; Anderson et al., 2015). In addition, Richter et al. (2008) showed that growing season (April–September) precipitation and soil moisture capability are critical factors for perennial grass biomass production. Even though *M. × giganteus* is a

warm-season, C$_4$ grass with high water-use efficiency, biomass productivity can be affected by precipitation during the April–September growing season (Heaton et al., 2004). Anderson et al. (2011), found that *M. × giganteus* has little drought tolerance or the ability to cope with environments that receive limited precipitation. *M. × giganteus* roots have grown to an approximate depth of 1.8 m (Carroll and Somerville, 2009), and Neukirchen et al. (1999) reported that *M. × giganteus* produced 28% of total root biomass in the top 0.30 m soil depth with nearly 50% of the total roots growing in soil layers deeper than 0.90 m. Moreover, Chimento and Amaducci (2015) reported that roots of herbaceous crops, including giant reed, switchgrass and *M. × giganteus*, had more than 50% of the whole root biomass in the 30 cm of soil, and specifically, a substantial portion of *M. × giganteus* roots, including fine root biomass and root length density, was distributed in the upper soils. Conversely, Monti and Zatta (2009) wrote that compared to switchgrass where 35% were found in the upper 0.35 m soil, nearly 90% of total *M. × giganteus* roots were found in that soil layer.

With regard to N fertilization and water availability, Chimento and Amaducci (2015) reported that switchgrass root biomass was greater than that of giant reed, and Amaducci et al. (2017) found that switchgrass biomass production was impacted by water availability in fertilized plots, but not in unfertilized plots. Water availability affected the biomass yield of giant reed (*Arundo donax* L.) in both unfertilized and fertilized plots (Amaducci et al., 2017). Therefore, switchgrass had higher root biomass production than giant reed (Chimento and Amaducci, 2015), which resulted in less sensitivity to water availability than giant reed (Amaducci et al., 2017). On the other hand, Mann et al. (2013) wrote that switchgrass roots are likely to stretch deeply into areas of available soil moisture to overcome increasing moisture deficits that take place near the surface. In this experiment, the precipitation was variable during the 4-year time study period with much less precipitation than the 30-year average during June and July 2012 (32% of the 30-year average) and August and September 2013 (10% of 30-year average). We observed that *M. × giganteus* biomass yields declined in the unfertilized plots in 2012, while there were no yield reductions in the fertilized plots. It is possible that *M. × giganteus* tends to adopt a tolerance strategy (Lambers et al., 2008; Farooq et al., 2009) by relying on shallow rhizome production rather than mining deep wet soils. Limited rooting and root production in unfertilized *M. × giganteus* may have limited biomass production during dry growing seasons. Even though *M. × giganteus* is likely to exploit shallow rhizome production to overcome water-deficient conditions (Mann et al., 2013), applying N fertilization may help *M. × giganteus* to develop root structures, which may increase potential water uptake from the subsoil, and thereby overcome periods of low water availability in topsoil (Smika et al., 1961; Viets, 1962; Neukirchen et al., 1999). In addition, it has been reported that drought tolerance in plants could be enhanced by increased N fertilization (Halvorson and Reule, 1994; Fife and Nambiar, 1997; Van Schaik et al., 1997). For instance, N fertilization may alleviate drought stress by preventing cell membrane damage and improving osmoregulation (Saneoka et al., 2004).

Nitrogen fertilization is important for tiller, tiller density, and panicle development as well as for seed production in perennial grasses (Canode and Law, 1978; Haferkamp and Copeland, 1984; Thompson and Clark, 1989, 1993). In this study, N fertilization increased the total number of tillers and the ratio of reproductive tillers and vegetative tillers which resulted in increased tiller weight and biomass yield. This finding agrees with the results reported for switchgrass by Sanderson and Reed (2000) and Muir et al. (2001). Nitrogen fertilization increased tiller survival and N deficiency during early stages of tiller development seemed particularly unfavorable to tiller survival (Power and Alessi, 1978). For example, on average, *M.* × *giganteus* expanded vegetatively 0.15 m year^{-1} and tiller density within the center of a clone decreased as stands age, while tiller density increased toward the clone exterior (Matlaga et al., 2012). Therefore, enhanced N uptake, resulting from N-fertilization, may supply adequate amounts of various nutrients to individual tillers to ensure development and activation of the essential enzyme systems necessary for tiller survival and growth (Power and Alessi, 1978).

Pearson correlation coefficients revealed strong relationships between yield components and biomass yields (**Table 4**) and strong linear relationships occurred between biomass yields and total number of tillers, reproductive tillers, and tiller weights. Boe and Beck (2008) described that strong linear relationships have been observed between biomass yields and tiller density (tiller m^{-2}) and tiller weight (mass tiller^{-1}) in switchgrass. Das et al. (2004) suggested that tiller density per plant can be used as an indirect selection trait for increasing biomass yield, which can be applicable for *M.* × *giganteus*. Moreover, no relationship was found between biomass yields and the number of vegetative tillers, while the number of reproductive tillers was highly correlated with biomass yields, implying that as reproductive tiller increased, biomass yield also increased. With regard to reproductive tillers, Boe and Casler (2005) reported that biomass produced by high-yielding switchgrass cultivars contained predominately reproductive tillers with the maximum number of phytomers tiller^{-1}, and low-yielding types mostly made up of a large number of vegetative tillers having fewer phytomers and lower weight phytomer^{-1} than reproductive tillers. Boe and Casler (2005) also wrote that switchgrass biomass yields at Madison, WI, USA, were much higher than at Brookings, SD, USA, with the differences resulting from the number of reproductive tillers; the reproductive tillers were approximately three times heavier than the vegetative tillers for cultivars of switchgrass across several environments. In this experiment, the total number of tillers between fertilized and unfertilized plots was significantly different, whereas the number of vegetative tillers was not affected by N fertilization. In addition, adding N fertilization

led to an increased number of reproductive tillers, and a correlation between reproductive tiller numbers and biomass yield increased over years. Wilkins (1995) reported that the application of N resulted in the portion of reproductive tiller in perennial ryegrass. This indicates that the increased total tiller number resulted from an increase in reproductive tiller number over consecutive N applications, which ultimately increased the biomass yields.

There has been substantial interest in *M.* × *giganteus* as a bioenergy feedstock due to its high yield potential. Results from our 4-year field evaluation suggest that N fertilization might be necessary for sustainable biomass production with 60 kg N ha^{-1} being potentially adequate for maximum biomass yield. Nitrogen fertilization is necessary to maintain the tiller density and reproductive development, which are critical yield components for *M.* × *giganteus* biomass production. These findings indicate that determining optimal agronomic management could be a useful tool for improving *M.* × *giganteus* biomass yields.

AUTHOR CONTRIBUTIONS

M-SL, JG, and DL: Contributing substantial data analysis and interpretation for the work; revising the work for important intellectual content; approving final version to be published; and agreeing to be accountable. AW: Contributing substantial data acquisition, analysis, and interpretation for the work; drafting the work and revising the work critically for important intellectual content; approving final version to be published; and agreeing to be accountable. TV: Contributing substantial conception and design of the work; data analysis and interpretation for the work; revising the work for important intellectual content; approving final version to be published; and agreeing to be accountable.

FUNDING

ACKNOWLEDGMENTS

REFERENCES

Amaducci, S., Facciotto, G., Beirgante, S., Perego, A., Serra, P., Ferrarini, A., et al. (2017). Biomass production and energy balance of herbaceous and woody crops on marginal soils in the Po valley. *GCB Bioenergy* 9, 31–45. doi: 10.1111/gcbb.12341

Anderson, E., Arundale, R., Maughan, M., Oladeinde, A., Wycislo, A., and Voigt, T. (2011). Growth and agronomy of *Miscanthus* × *giganteus* for biomass production. *Biofuels* 2, 167–183. doi: 10.4155/bfs.10.80

Anderson, E. K., Lee, D., Allen, D. J., and Voigt, T. B. (2015). Agronomic factors in the establishment of tetraploid seeded *Miscanthus* × *giganteus*. *GCB Bioenergy* 7, 1075–1083. doi: 10.1111/gcbb.12192

Arundale, R. A., Dohleman, F. G., Heaton, E. A., McGrath, J. M., Voigt, T. B., and Long, S. P. (2014a). Yields of *Miscanthus × giganteus* and *Panicum virgatum* decline with stand age in the Midwestern USA. *GCB Bioenergy* 6, 1–13. doi: 10.1111/gcbb.12077

Arundale, R. A., Dohleman, F. G., Voigt, T. B., and Long, S. P. (2014b). Nitrogen fertilization does significantly increase yields of stands of *Miscanthus × giganteus* and *Panicum virgatum* in multiyear trials in Illinois. *Bioenergy Res.* 7, 408–416. doi: 10.1007/s12155-013-9385-5

Beale, C. V., and Long, S. P. (1997). Seasonal dynamics of nutrient accumulation and partitioning in the perennial C4-grasses *Miscanthus × giganteus* and *Spartina cynosuroides*. *Biomass Bioenergy* 12, 419–428. doi: 10.1016/S0961-9534(97)00016-0

Beard, J. B., and Beard, H. J. (2005). *Beard's Turfgrass Encyclopedia*. East Lansing, MI: Michigan State University Press.

Boe, A. (2007). Variation between two switchgrass cultivars for components of vegetative and seed biomass. *Crop Sci.* 47, 636–642. doi: 10.2135/cropsci2006.04.0260

Boe, A., and Beck, D. L. (2008). Yield components of biomass in switchgrass. *Crop Sci.* 48, 1306–1311. doi: 10.2135/cropsci2007.08.0482

Boe, A., and Casler, M. D. (2005). Hierarchical analysis of switchgrass morphology. *Crop Sci.* 45, 2465–2472. doi: 10.1007/s00122-010-1488-1

Canode, C. L., and Law, A. G. (1978). Influence of fertilizer and residue management on grass seed production. *Agron. J.* 70, 543–546. doi: 10.2134/agronj1978.00021962007000040006x

Carroll, A., and Somerville, C. (2009). Cellulosic biofuels. *Annu. Rev. Plant Biol.* 60, 165–182. doi: 10.1146/annurev.arplant.043008.092125

Chimento, C., and Amaducci, S. (2015). Characterization of fine root system and potential contribution to soil organic carbon of six perennial bioenergy crops. *Biomass Bioenergy* 83, 116–122. doi: 10.1016/j.biombioe.2015.09.008

Christian, D. G., Riche, A. B., and Yates, N. E. (2008). Growth, yield and mineral content of *Miscanthus × giganteus* grown as a biofuel for 14 successive harvests. *Ind. Crops Prod.* 28, 320–327. doi: 10.1016/j.indcrop.2008.02.009

Clifton-Brown, J. C., Breuer, J., and Jones, M. B. (2007). Carbon mitigation by the energy crop, *Miscanthus*. *Glob. Change Biol.* 13, 2296–2307. doi: 10.1111/j.1365-2486.2007.01438.x

Clothier, B. E., and Green, S. R. (1997). Roots: the big movers of water and chemicals in soil. *Soil Sci.* 162, 534–543. doi: 10.1097/00010694-199708000-00002

Das, M. K., Fuentes, R. G., and Taliaferro, C. M. (2004). Genetic variability and trait relationships in switchgrass. *Crop Sci.* 44, 443–448. doi: 10.2135/cropsci2004.4430

Delogu, G., Cattivelli, L., Pecchioni, N., De Falcis, D., Maggiore, T., and Stanca, A. M. (1998). Uptake and agronomic efficiency of nitrogen in winter barley and winter wheat. *Eur. J. Agron.* 9, 11–20. doi: 10.1016/S1161-0301(98)00019-7

Ercoli, L., Mariotti, M., Masoni, A., and Bonari, E. (1999). Effect of irrigation and nitrogen fertilization on biomass yield and efficiency of energy use in crop production of Miscanthus. *Field Crops Res.* 63, 3–11. doi: 10.1016/S0378-4290(99)00022-2

Farooq, M., Wahid, A., Kobayashi, N., Fujita, D., and Basra, S. M. A. (2009). Plant drought stress: effects, mechanisms and management. *Agron. Sustain. Dev.* 29, 185–212. doi: 10.1051/agro:2008021

Fife, D. N., and Nambiar, E. K. S. (1997). Changes in the canopy and growth of *Pinus radiata* in response to nitrogen supply. *For. Ecol. Manag.* 93, 137–152. doi: 10.1016/S0378-1127(96)03917-5

Guo, J., Thapa, S., Voigt, T., Rayburn, A. L., Boe, A., and Lee, D. K. (2015). Phenotypic and biomass yield variations in natural populations of prairie cordgrass (*Spartina pectinata* Link) in the USA. *Bioenergy Res.* 8, 1371–1383. doi: 10.1007/s12155-015-9604-3

Haferkamp, M. R., and Copeland, T. D. (1984). Shoot growth and development of Alamo switchgrass as influenced by mowing and fertilization. *J. Range Manag.* 37, 406–412. doi: 10.2307/3899625

Halvorson, A. D., and Reule, C. A. (1994). Nitrogen fertilizer requirements in an annual dryland cropping system. *Agron. J.* 86, 315–318. doi: 10.2134/agronj1994.00021962008600020020x

Heaton, E. A., Dohleman, F. G., and Long, S. P. (2008). Meeting US biofuel goals with less land: the potential of Miscanthus. *Glob. Change Biol.* 14, 2000–2014. doi: 10.1111/j.1365-2486.2008.01662.x

Heaton, E. A., Voigt, T., and Long, S. P. (2004). A quantitative review comparing the yields of two candidate C4 perennial biomass crops in relation to nitrogen, temperature and water. *Biomass Bioenergy* 27, 21–30. doi: 10.1016/j.biombioe.2003.10.005

Himken, M., Lammel, J., Neukirchen, D., Czypionka-Krause, U., and Olfs, H.-W. (1997). Cultivation of Miscanthus under West European conditions: seasonal changes in dry matter production, nutrient uptake and remobilization. *Plant Soil* 189, 117–126. doi: 10.1023/A:1004244614537

Hodkinson, T. R., Chase, M. W., Takahashi, C., Leitch, I. J., Bennett, M. D., and Renvoize, S. A. (2002). The use of DNA sequencing (ITS and TRNL-F), AFLP, and fluorescent in situ hybridization to study allopolyploid *Miscanthus* (Poaceae). *Am. J. Bot.* 89, 279–286. doi: 10.3732/ajb.89.2.279

Holland, E. A., Braswell, B. H., Sulzman, J., and Lamarque, J. F. (2005). Nitrogen deposition onto the United States and Western Europe: synthesis of observations and models. *Ecol. Appl.* 15, 38–57. doi: 10.1890/03-5162

Kardol, P., Campany, C. E., Souza, L., Norby, R. J., Weltzin, J. F., and Classen, A. T. (2010). Climate change effects on plant biomass alter dominance patterns and community evenness in an experimental old-field ecosystem. *Glob. Change Biol.* 16, 2676–2687. doi: 10.1111/j.1365-2486.2010.02162.x

Lambers, H., Chapin III, F. S., and Pons, T. L. (2008). *Plant Physiological Ecology*. 2nd Edn. New York, NY: Springer-Verlag.

Lee, D. K., and Boe, A. (2005). Biomass production of switchgrass in central South Dakota. *Crop Sci.* 45, 2583–2590. doi: 10.2135/cropsci2005.04-0003

Lewandowski, I. (1998). Propagation method as an important factor in the growth and development of *Miscanthus × giganteus*. *Ind. Crops Prod.* 8, 229–245. doi: 10.1016/S0926-6690(98)00007-7

Lewandowski, I., Clifton-Brown, J. C., Scurlock, J. M. O., and Huisman, W. (2000). Miscanthus: European experience with a novel energy crop. *Biomass Bioenergy* 19, 209–227. doi: 10.1016/S0961-9534(00)00032-5

Lewandowski, I., and Schmidt, U. (2006). Nitrogen, energy and land use efficiencies of miscanthus, reed canary grass and triticale as determined by the boundary line approach. *Agric. Ecosyst. Environ.* 112, 335–346. doi: 10.1016/j.agee.2005.08.003

Mann, J. J., Barney, J. N., Kyser, G. B., and DiTomaso, J. M. (2013). Root system dynamics of *Miscanthus × giganteus* and *Panicum virgatum* in response to rainfed and irrigated conditions in California. *BioEnergy Res.* 6, 678–687. doi: 10.1007/s12155-012-9287-y

Matlaga, D. P., Schutte, B. J., and Davis, A. S. (2012). Age-dependent demographic rates of the bioenergy crop *Miscanthus × giganteus* in Illinois. *Invasive Plant Sci. Manag.* 5, 238–248. doi: 10.1614/IPSM-D-11-00083.1

Maughan, M., Bollero, G., Lee, D. K., Darmody, R., Bonos, S., Cortese, L., et al. (2012). *Miscanthus × giganteus* productivity: the effects of management in different environments. *GCB Bioenergy* 4, 253–265. doi: 10.1111/j.1757-1707.2011.01144.x

Miguez, F. E., Villamil, M. B., Long, S. P., and Bollero, G. A. (2008). Meta-analysis of the effects of management factors on *Miscanthus × giganteus* growth and biomass production. *Agric. For. Meteorol.* 148, 1280–1292. doi: 10.1016/j.agrformet.2008.03.010

Monti, A., and Zatta, A. (2009). Root distribution and soil moisture retrieval in perennial and annual energy crops in Northern Italy. *Agric. Ecosyst. Environ.* 132, 252–259. doi: 10.1016/j.agee.2009.04.007

Muir, J. P., Sanderson, M. A., Ocumpaugh, W. R., Jones, R. M., and Reed, R. L. (2001). Biomass production of 'Alamo' switchgrass in response to nitrogen, phosphorus, and row spacing. *Agron. J.* 93, 896–901. doi: 10.2134/agronj2001.934896x

Neukirchen, D., Himken, M., Lammel, J., Czypionka-Krause, U., and Olfs, H. W. (1999). Spatial and temporal distribution of the root system and root nutrient content of an established *Miscanthus* crop. *Eur. J. Agron.* 11, 301–309. doi: 10.1016/S1161-0301(99)00031-3

Paruelo, J. M., Lauenroth, W. K., Burke, I. C., and Sala, O. E. (1999). Grassland precipitation-use efficiency varies across a resource gradient. *Ecosystems* 2, 64–68. doi: 10.1007/s100219900058

Power, J. F., and Alessi, J. (1978). Tiller development and yield of standard and semidwarf spring wheat varieties as affected by nitrogen fertilizer. *J. Agric. Sci.* 90, 97–108. doi: 10.1017/S0021859600048632

Richter, G. M., Riche, A. B., Dailey, A. G., Gezan, S. A., and Powlson, D. S. (2008). Is UK biofuel supply from *Miscanthus* water-limited? *Soil Use Manag.* 24, 235–245. doi: 10.1111/j.1475-2743.2008.00156.x

Sanderson, M. A., and Reed, R. L. (2000). Switchgrass growth and development: water, nitrogen, and plant density effects. *J. Range Manag.* 53, 221–227. doi: 10.2307/4003287

Saneoka, H., Moghaieb, R. E., Premachandra, G. S., and Fujita, K. (2004). Nitrogen nutrition and water stress effects on cell membrane stability and leaf water relations in *Agrostis palustris* Huds. *Environ. Exp. Bot.* 52, 131–138. doi: 10.1016/j.envexpbot.2004.01.011

Smika, D. E., Haas, H. J., Rogler, G. A., and Lorenz, R. J. (1961). Chemical properties and moisture extraction in rangeland soils as influenced by nitrogen fertilization. *J. Range Manag.* 14, 213–216. doi: 10.2307/3895152

Thompson, D. J., and Clark, K. W. (1989). Influence of nitrogen fertilization and mechanical stubble removal on seed production of Kentucky bluegrass in Manitoba. *Can. J. Plant Sci.* 69, 939–943. doi: 10.4141/cjps89-114

Thompson, D. J., and Clark, K. W. (1993). Effects of clipping and nitrogen fertilization on tiller development and flowering in Kentucky bluegrass. *Can. J. Plant Sci.* 73, 569–575. doi: 10.4141/cjps93-077

Van Schaik, A. H., Struik, P. C., and Damian, T. G. (1997). Effects of irrigation and N on the vegetative growth of *Aloe barbadensis* Mill. in Aruba. *Trop. Agric.* 74, 104–109.

Viets, F. G. (1962). Fertilizers and the efficient use of water. *Adv. Agron.* 14, 223–264. doi: 10.1016/S0065-2113(08)60439-3

Vogel, K. P., Brejda, J. J., Walters, D. T., and Buxton, D. R. (2002). Switchgrass biomass production in the Midwest USA. *Agron. J.* 94, 413–420. doi: 10.2134/agronj2002.0413

Wilkins, P. W. (1995). Independence of dry matter yield and leaf yield among perennial ryegrass varieties differing in seasonal yield distribution. *Grass Forage Sci.* 50, 155–161. doi: 10.1111/j.1365-2494.1995.tb02308.x

Xi, B., Wang, Y., Jia, L., Bloomberg, M., Li, G., and Di, N. (2013). Characteristics of fine root system and water uptake in a triploid *Populus tomentosa* plantation in the North China Plain: implications for irrigation water management. *Agric. Water Manag.* 117, 83–92. doi: 10.1016/j.agwat.2012.11.006

Nitrogen Reserve Pools in Two *Miscanthus × giganteus* Genotypes under Contrasting N Managements

Ryan M. Dierking[1], Damian J. Allen[2,3], Suzanne M. Cunningham[3], Sylvie M. Brouder[3] and Jeffrey J. Volenec[3]*

[1] Actagro, LLC, Fresno, CA, United States, [2] Mendel BioEnergy Seeds, Mendel Biotechnology Inc., Hayward, CA, United States, [3] Department of Agronomy, Purdue University, West Lafayette, IN, United States

Nitrogen (N) reserves in vegetative tissues contribute N to regrowth of *Miscanthus × giganteus* shoots in spring, but our understanding of how N fertilization and plant genotype affect this process is incomplete. Our specific objectives were to: (1) determine how N fertilizer management impacts accumulation of dry matter and N among aboveground and belowground tissues and organs; (2) understand how changes in N management and tissue N concentration influence seasonal fluctuations in concentrations of buffer-soluble proteins and amino acids in putative storage organs including rhizomes and roots; and (3) characterize genotypic variability and genotype × N interactions for N reserve accumulation and use among *Miscanthus × giganteus* genotypes. Established plots of the IL Clone and Nagara-sib population were fertilized with 0–0, 0–150, 75–75, 150–0, and 150–150 kg N ha^{-1} where the first numeral denotes the N rate applied in 2011 (Year 1) and the second number denotes the N rate applied in 2012 (Year 2). Rhizomes, roots, stembases, and shoots were sampled at 6-week intervals between March and August and then in November at dormancy. Concentrations of N, soluble protein and amino-N increased in all tissues with fertilizer N application. With the exception of rhizome amino-N, concentrations of these N pools in roots and rhizomes declined as plants resumed growth in spring and increased sharply between August and November as growth slowed. Losses in shoot and stembase N mass between August and November were similar to total N accumulation in roots and rhizomes during this interval. Compared to the unfertilized control, specific N managements enhanced growth of above- and belowground tissues. The IL Clone generally had greater biomass yield of all organs than the Nagara-sib; the exception being shoot biomass in November when extensive leaf senescence reduce yield of the IL Clone. High biomass yields were obtained with 75 kg N ha^{-1} applied annually rather than semi-annual N applications of 150 kg N^{-1} ha that depended on N recycling from roots/rhizomes as a supplemental N source.

Keywords: *Miscanthus*, nitrogen, reserves, genotype, rhizome, growth

INTRODUCTION

Second generation lignocellulosic biofuels are expected to include plant species that produce large amounts of high-fiber biomass with a reduction in fertilizer input, especially nitrogen (N) (Heaton E. et al., 2004; Wang et al., 2012). This reduction in N input is critical to system net energy balance as the synthesis of inorganic N fertilizer consumes vast amounts of natural gas

(Erisman et al., 2008). Lower N fertilizer input for perennial bioenergy crops may be plausible, in part, due to their ability to accumulate N reserves in storage organs that supplement soil N pools in providing N to shoots when growth is initiated in spring and resumes after biomass harvest in summer (Volenec et al., 1996). However, our understanding of N reserves in the context of N use efficiency (NUE) of *Miscanthus* × *giganteus* is fragmented and incomplete.

The NUE of *Miscanthus* has been examined from several perspectives. Beale and Long (1997) reported high biomass production per unit N based upon the low N removal in harvested aboveground biomass. They reported late-season translocation of N from biomass to rhizomes as one factor contributing to this high NUE. These results were later confirmed by Heaton et al. (2009) who showed large late-season declines in aboveground biomass N concentrations. Using ^{15}N Christian et al. (2006) verified intra-plant N cycling from shoots to other tissues with rhizomes being a large late-season N sink. Significant amounts of rhizome N were transferred to shoots in subsequent growing seasons suggesting that this N was serving as a reserve pool. However, large amounts of ^{15}N remained in rhizomes through Year 3 indicating that some rhizome N pools may not be readily mobilized.

Previous work with perennial plants used for forage and pasture can inform hypotheses regarding N storage in *Miscanthus* and other perennial biomass crops. For example, several forage legumes accumulate vast quantities of N in taproots during autumn that are subsequently used for shoot growth initiation in spring and shoot regrowth after defoliation in summer (Hendershot and Volenec, 1993a,b; Barber et al., 1996; Li et al., 1996); times when N from N_2 fixation is inadequate to meet plant N needs (Vance et al., 1979). In alfalfa (*Medicago sativa* L.) this N accumulates primarily as vegetative storage proteins (VSPs, Cunningham and Volenec, 1996) that, like seed storage proteins, are rapidly degraded and translocated to regrowing shoots to meet their N needs. Like alfalfa, white clover (*Trifolium repens* L.) also appears to accumulate species-specific VSPs during autumn that are mobilized when growth resumes in spring (Corre et al., 1996). However, not all perennial legumes used for forage accumulate VSPs as a storage N form. While taproots of red clover (*T. pratense* L.), sweetclover [*Melilotus officinalis* (L.) Lam.] and birdsfoot trefoil (*Lotus corniculatus* L.) accumulate N in autumn that is depleted when shoot growth resumes in spring, these species do not appear to accumulate taproot VSPs (Li et al., 1996). Reserve N accumulation is not limited to perennial legumes. Uptake of nitrate and ammonium from the soil by forage grasses is severely reduced by defoliation in summer (Bakken et al., 1998; Louahlia et al., 1999). These plants mobilize leaf sheath and root N pools to regrowing leaf blades (Ourry et al., 1989, 1990). Furthermore, when soil N supply is adequate, VSPs accumulate in sheath tissues of ryegrass (*Lolium perenne* L.) and these are subsequently mobilized to new leaves during post-defoliation regrowth in summer (Louahlia et al., 1999). Like perennial legumes, however, not all perennial grasses accumulate VSPs as the primary N reserve in vegetative tissues. For example,

Calamagrostis epigejos utilizes both free amino acids and soluble proteins in roots and stubble soluble proteins as the principle N sources during regrowth after defoliation (Kavanova and Gloser, 2005).

Potential contribution of both reserve N and mineralized soil N pools to shoot N of regrowing *Miscanthus* increases uncertainty regarding N fertilizer requirements when compared to conventional annual row crops like maize. Depending on soil characteristics, prevailing environment, and stand age, yield responses of *Miscanthus* to N fertilizer in research plots vary widely from unresponsive to N fertilizer (Lewandowski et al., 2000; Christian et al., 2008; Arundale et al., 2014; Larsen et al., 2014; Finnan and Burke, 2016) to requiring >100 kg N ha^{-1} annually (Lewandowski et al., 2000; Khanna et al., 2008; Pedroso et al., 2014; Dierking et al., 2016). A recent Extension guide for growing *Miscanthus* biomass in the central United States suggests applying 80 to 130 kg N ha^{-1} to replace the N removed in a 30 t ha^{-1} biomass yield (Heaton et al., 2016). Improving our understanding the nature and extent of N cycling in *Miscanthus* should inform future N recommendations and improve both NUE and ultimately system net energy balance.

Finally, virtually all of the published research has focused on N responses of the "IL Clone" of *Miscanthus* × *giganteus*. However, there are substantial differences among other *Miscanthus* × *giganteus* ecotypes and populations for most phenotypic traits including cell wall structure and biomass combustion efficiencies, flowering, leaf senescence, mineral concentrations/contents, and yield differences (Jørgensen, 1997; Clifton-Brown and Lewandowski, 2002; Hodgson et al., 2010; Allison et al., 2011; da Costa et al., 2014; Iqbal and Lewandowski, 2014). The progenitor species to *Miscanthus* × *giganteus* are known outcrossing species and possess high levels of heterozygosity and vary phenotypically (Zhao et al., 2013). For example, Aurangzeb (2012) evaluated nine distinct *Miscanthus* × *giganteus* genotypes derived from novel crosses among progenitor lines and observed significant morphological differences in crown size and leaf structure. Jeżowski (2008) working with novel *Miscanthus* genotypes during establishment also observed differences in crown and tiller morphology. Less is known regarding genotypic differences in mineral nutrition including N storage and its impact on NUE. Here we report how N management strategies alter N storage patterns and pools, and subsequent N mobilization to regrowing shoots of two *Miscanthus* × *giganteus* lines previously shown to differ in biomass, NUE, and late-season leaf retention (Dierking et al., 2016). Our specific objectives were to: (1) determine how N fertilizer management impacts accumulation of dry matter (DM) and N among aboveground and belowground tissues and organs; (2) understand how changes in N management and tissue N concentration influence seasonal fluctuations in concentrations of buffer-soluble proteins and amino acids in putative storage organs including rhizomes and roots; and 3) characterize genotypic variability and genotype × N interactions for N reserve accumulation and use among *Miscanthus* × *giganteus* genotypes.

MATERIALS AND METHODS

Location, Fertilization, and Genetic Materials

For a full description of the site, N management strategies, and plant material see Dierking et al. (2016). The scope of that original experiment was reduced in magnitude as described below in order to facilitate the intensive sampling associated with this study. Briefly, the experiment was planted at Lafayette, IN (40.484096, −86.815827) on a Billett loam in 2010 at a population density of 19,760 plants ha^{-1}. Two of four contrasting *Miscanthus* × *giganteus* genotypes (IL Clone; open pollinated (OP) Nagara-sib) were selected for study based on pronounced variation in aboveground morphology and previous differences in NUE (Dierking et al., 2016). A subset of the most extreme five of seven N management treatments was selected for this study including 0–0, 0–150, 75–75, 150–0, and 150–150 kg N ha^{-1} where the first numeral denotes the N rate applied in 2011 (Year 1) and the second number denotes the N rate applied in 2012 (Year 2). Nitrogen was hand-applied as Agrotain^{TM}-coated urea on June 1 and May 2 of Years 1 and 2, respectively. Each genotype-N management combination was replicated three times. Mean monthly temperatures and precipitation were recorded at a weather station on the experimental site (**Table 1**). The 50-year weather data record was obtained from the Purdue University Airport located 15 km southwest of the study site.

Above and Belowground Sampling

A single plant from the outer two rows of four row plots was collected from each plot every 6 weeks starting in March and ending in August of 2012. A final sample was collect just prior to machine harvest in November 2012. Border effects were minimized by surrounding each plot with other

TABLE 1 | Monthly average temperatures and precipitation for the duration of the study.

Month	Temperature, °C			Precipitation, mm		
	2011	2012	Average	2011	2012	Average
January	−5	0	−3.9	18.5	58.7	48.7
February	0	1.7	−1.7	67.6	31.5	41.9
March	5.6	13.9	4.6	54.6	48.5	65.3
April	12.8	12.2	11	200.4	58.2	94.5
May	17.8	19.4	16.6	30.7	76	99.6
June	22.8	22.2	21.8	164.9	28.5	107.7
July	26.7	27.2	23.8	85.6	23.1	95.8
August	23.9	22.2	22.8	124.5	125.5	92
September	18.3	17.2	18.9	95.8	99.8	73.4
October	12.8	10.6	12.3	63.3	141.2	65.8
November	8.9	4.4	5.7	142.5	20.3	74.2
December	2.8	2.8	−0.5	84.1	64.5	66.3

Also included are the 50-year average temperatures and precipitation for this location.

Miscanthus × *giganteus* plants established at the same population and planted on the same day. During sampling, aboveground shoot biomass was removed approximately 15 cm above the soil surface. Biomass was weighed immediately, coarsely chopped and a subsample (about 500 g fresh weight) collected. This subsample was weighed, dried in a forced-air oven at 60°C until constant weight was attained and the percent moisture used to calculate plant biomass yield. After the aboveground shoot tissues were collected, all rhizomes and associated roots for the plant were excavated with shovels (dimension means ± standard errors: surface area, 2028 ± 62 cm^2; depth: 15 ± 0.3 cm; volume: 31,262 cm^3 ± 1383 cm^3). These tissues were cleaned under a stream of cold tap water and separated into roots, rhizomes, and stem bases (shoot tissue between the soil surface and where shoot removal occurred). Tissues were blotted dry, weighed immediately to determine fresh weights, and a representative subsample transferred to paper bags. These samples were placed in −80°C freezer for at least 24 h before being transferred to −4°C. Tissues were held at −4°C until lyophilized (FreeZone 12 freeze dryer, Labconco Corporation, Kansas City, MO, United States). Freeze-dried tissues were weighed and percent moisture used to calculate DM yields of below-ground tissues and stembases. Tissues were initially ground to pass a 6-mm screen (Wiley mill, Thomas Scientific, Swedesboro, NJ, United States), then re-ground to pass a 1-mm screen using a cyclone sample mill (Udy Corp., Fort Collins, CO, United States) for laboratory analysis. Lyophilized tissues were stored at −4°C.

Nitrogen, Buffer-Soluble Protein, and Amino Acid-N Analysis

Tissues were analyzed for total N concentration using a flash combustion elemental analyzer (Flash EA 1112 Series, Thermo Fisher Scientific, Netherlands). Procedures to determine buffer-soluble protein and amino acid-N concentrations in rhizome, root, and stem base tissues were conducted at temperatures between 0 and 4°C unless otherwise stated. Proteins were extracted by suspending 30 mg of tissue and equal masses of insoluble polyvinylpolypyrrolidone (Sigma Chemical Co., St. Louis; product P6755) in 1 mL of 100 mM $NaPO_4$ buffer (pH 6.8) containing 10 mM 2-mercaptoethanol and 1 mM phenylmethylsulfonyl fluoride. Tubes were kept on ice while being vortexed four times at 5-min intervals. Samples were centrifuged at 14,000 × *g* for 10 min. Soluble protein in the supernatant was estimated using the protein dye-binding method of Bradford (1976). Bovine serum albumin was used as a standard. Concentration of buffer-soluble amino acids in the supernatant was determined using ninhydrin with glycine as the standard (Rosen, 1957).

Yield and N Content Calculations

Total aboveground mass was estimated by adding stembase dry mass to the dry mass of the shoots, while the total belowground biomass was estimated as the sum of the dry masses of the roots and rhizomes. The N content was calculated as the

product of N concentration and dry mass of each tissue. These values were summed to determine the total belowground and aboveground N mass per plant. Total DM and N content per hectare in November at harvest was determined as the product of the soil surface area occupied per plant and plant population.

Statistical Analysis

The experimental design was a randomized complete-block design with a factorial arrangement of five N managements and two genotypes replicated three times. Plots were sampled repeatedly up to six times (tissue dependent). A split-plot-in-time analysis of variance analysis was used to partition variation into genotype, N management, replicate, and month effects and interactions using Minitab (17.3.1). Genotype and N management main effects were tested using the genotype × replicate and N management × replicate interaction terms, respectively. Harvest effects and interactions were tested with the mean square error term (Cochran and Cox, 1957). Where the *F*-test was significant ($P < 0.05$) the least significant difference (LSD) was calculated unless otherwise indicated (**Table 2**).

RESULTS

Weather

Temperatures during the experiment were similar to the long-term average with the exception of warmer than normal temperatures in March in 2012 and July of both years (**Table 1**). Precipitation in 2011 was greater than normal in April, June, and November, while January and May of 2011 were dry. In 2012 June, July, and November were drier than normal and October wetter than the 50-year average.

Effects of Genotype and N Management on Tissue Dry Matter Yields

A significant genotype × harvest interaction was observed. Shoot mass per plant increased in both genotypes, but mass was greater in the IL Clone in July and August, whereas the Nagara-sib had greater shoot mass in November (**Figure 1A**). The N treatment main effect for shoot yield was tested with less precision in the split-plot analysis and was not statistically significant ($P > 0.05$). Trends in shoot mass averaged across genotypes and harvests varied with N management ranging from 504 and 549 g/plant, respectively, for the 0–0 and 150–0 treatments not receiving N in Year 2 to over 600 g/plant for treatments receiving N in Year 2 (**Figure 1A**).

The N treatment x harvest and genotype x harvest interactions were significant for stembase mass per plant (**Table 2**). Stembases of the IL Clone were larger from June through August when compared to the Nagara-sib, but the IL Clone had lower stembase mass in November (**Figure 1B**). Stembases were not present at the March harvest, but increased rapidly during April and July. Stembase mass of the 0–0 N treatment was lower than that of the 0–150 N treatment from July to November, and the 150–0 and 75–75 treatments in July. By November stembase mass of the 0–0 and 75–75 N treatments declined markedly and were lower than the other N treatments. Averaged over genotypes and harvests stembase mass of the 0–0 N treatment was lower than that of all other N treatments (data not shown).

Nitrogen management did not impact root and rhizome mass significantly (**Table 2**). Significant genotype and harvest main effects were observed for both the root and rhizome mass per plant. Averaged across N treatments and harvests, the IL Clone had greater root and rhizome mass than the Nagara-sib (**Figures 1C,D**). Root mass initially increased from March to April followed by large increases between July and November.

TABLE 2 | Summary of analysis of variance results showing the effects of nitrogen management (N), genotype (G), month of harvest (Harv.) and corresponding interactions on dry wt., and concentrations of N, protein, and amino-N in shoot, stem base, root and rhizome tissues of *Miscanthus × giganteus*.

		Main effect or interaction						
Tissue	Trait	N	G	Harv.	N × G	N × Harv.	G × Harv.	N × G × Harv.
Shoot	Dry weight	ns	ns	**	ns	ns	**	ns
	N	**	ns	**	ns	*	ns	ns
Stem base	Dry weight	*	ns	**	ns	†	**	ns
	N	**	ns	**	ns	†	ns	ns
	Protein	*	ns	**	ns	ns	**	ns
	Amino-N	**	ns	**	ns	**	ns	ns
Root	Dry weight	ns	*	**	ns	ns	ns	ns
	N	**	*	**	**	*	ns	ns
	Protein	**	ns	**	†	**	ns	†
	Amino-N	**	*	**	**	**	ns	ns
Rhizome	Dry weight	ns	**	**	ns	ns	ns	ns
	N	**	*	**	*	**	ns	ns
	Protein	**	ns	**	**	**	ns	†
	Amino-N	**	ns	**	*	**	ns	ns

*Significance levels (†, *, **) denoted significant differences at P < 0.10, 0.05, and 0.01 levels of probability, respectively.*
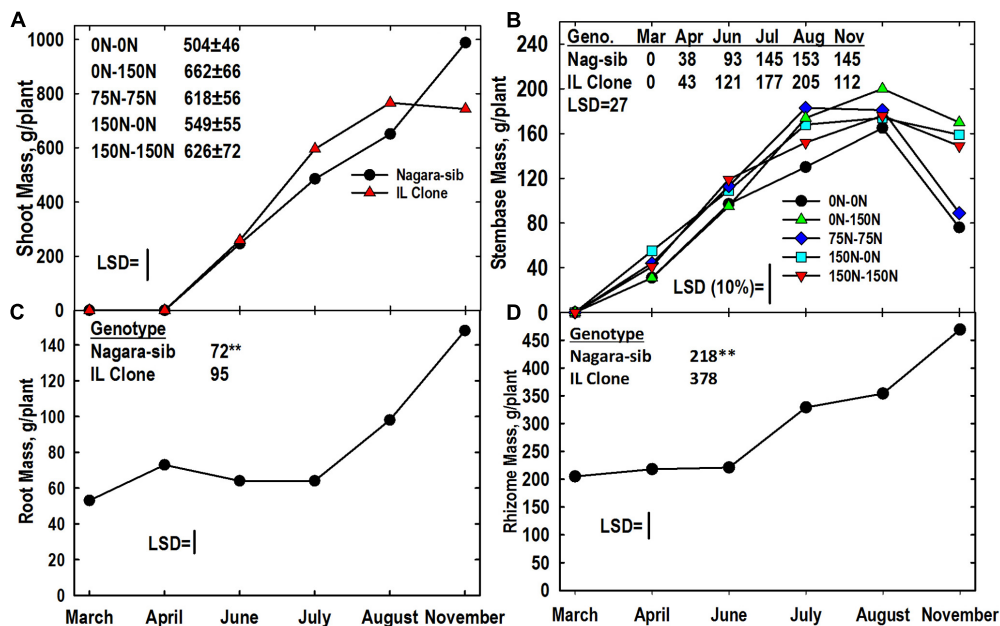
FIGURE 1 | Tissue dry matter yields of two *Miscanthus* genotypes (Nagara-sib, IL Clone) as influenced by nitrogen (N) management. **(A)** Means and least significant difference (LSD) for the genotype × harvest interaction on shoot biomass yield and the main effect means ± standard error of N management on shoot mass (tabulated). **(B)** Stembase means and LSDs for the N management × harvest interaction (plotted) and genotype × harvest interaction (tabulated) effects. The N treatments (all in kg N ha^{-1}) included: no N application either year (0N–0N), N application only in Year 1 (150N–0N) or Year 2 (0N–150N), or N application both years of the study (75N–75N; 150N–150N). **(C)** Means and LSDs for the main effects of harvest (plotted) and genotype (tabulated) on root mass. **(D)** Means and LSDs for the main effects of harvest (plotted) and genotype (tabulated) on rhizome mass. Tissue sampling commenced in March of Year 2. The LSDs are provided at $P < 0.05$. In **(C,D)** genotypic differences designated with **$P < 0.01$.

Rhizome mass also exhibited a large increase from June to November.

Tissue Nitrogen

The main effect of genotype was significant for root, and rhizome N concentrations (**Figures 2C,D**). The magnitude of these differences was relatively small, but consistent, with the Nagara-sib having higher N concentrations than the IL Clone. All tissues had a significant N management × harvest interaction, however, the significance level was at the 10% level of probability for shoot and stembase tissues. As expected shoot N concentrations in June were greatest in the 150–150 and 0–150 N treatments that received the highest N fertilization rates in Year 2 and lowest in plants from the 0–0 N control plots. Shoot N concentrations declined by nearly 50% in July but the relative rankings of the N treatments remained similar through June. Shoot N concentrations in August were similar to July values, but by November shoot N declined and only plots receiving 150 kg N ha^{-1} in Year 2 had higher concentrations than the 0–0 control plots.

Stembase N concentrations declined rapidly between April and July as new shoots initially emerged, but eventually extended past this lower portion of the canopy (**Figure 2B**). Stembase N concentrations of the 0–0 plots in April were lower than all treatments that had received N the previous year (**Figure 2B**). While N concentrations in stembases of the 0–0 plots remained lower than other treatments throughout the growing season,

stembase N concentrations of the 0–150 N treatment increased relative to other treatments and were similar to the 150–150 N treatment in June. By November stembase concentrations of the 150–0 N treatment declined to values similar to the 0–0 control, and both of these were lower than the 150–150 N treatment

As anticipated root N concentrations in March and April were highest in plots fertilized with high N in Year 1 (150–0, 150–150) and lowest in plots not receiving N in Year 1 (0–0, 0–150) (**Figure 2C**). Application of N in Year 2 increased N concentrations in roots of the 0–150 treatment in June when compared to the 0–0 control, while root N concentration of the unfertilized 150–0 N treatment declined. The 0–0 treatment had lower root N than the other treatments in July. In August and November the 0–0 and 150–150 N treatment had the lowest and highest root N concentrations, respectively, with the other N treatments intermediate. Irrespective of N application, all treatments exhibited a general increase in root N concentration between August and November. The genotype × N treatment interaction was significant for root N concentration (**Table 3**). Root N concentration of the IL Clone was greater than the Nagara-sib in the 0–150 N treatment, whereas the reverse was true at the 150–150 N treatment.

Like roots, rhizome N concentrations in March and April reflected Year 1 N management with higher concentrations in the 150–150 and 150–0 N treatments (**Figure 2D**). Rhizome
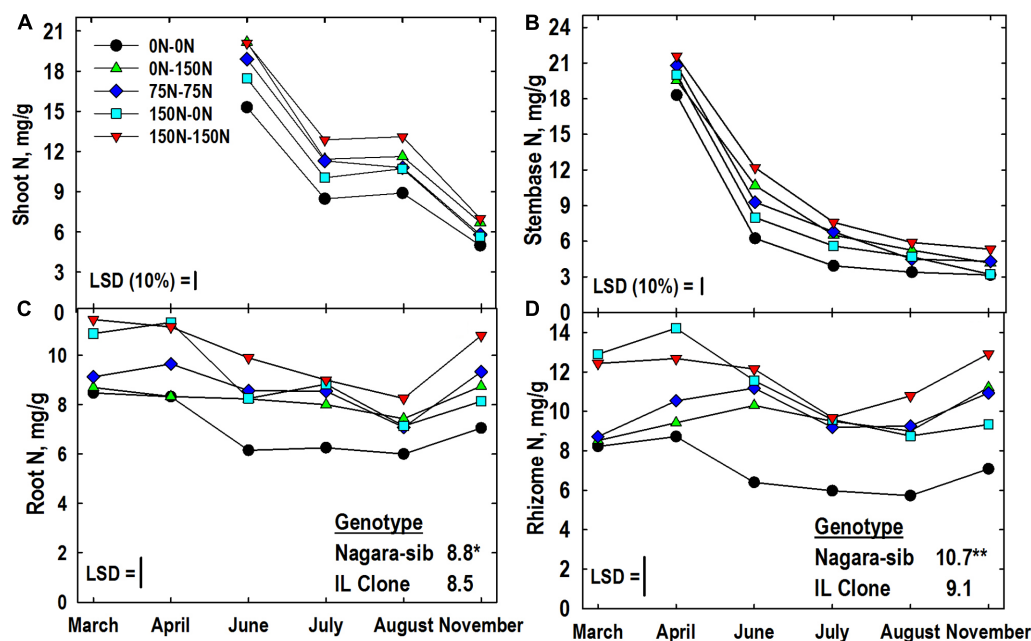
FIGURE 2 | Tissue N concentrations of two *Miscanthus* genotypes (Nagara-sib, IL Clone) as influenced by N management. **(A)** Shoot N means and least significant differences (LSDs) for the N management × harvest interaction effect. **(B)** N management × harvest interaction means for stembase N concentrations. **(C)** Root N means and LSDs for the N management × harvest interaction effect (plotted) and genotype main effect (tabulated). **(D)** Rhizome N means and LSDs for the N management × harvest interaction effect (plotted) and genotype main effect (tabulated). The N treatments (all in kg N ha^{-1}) included: no N application either year (0N–0N), N application only in Year 1 (150N–0N) or Year 2 (0N–150N), or N application both years of the study (75N–75N; 150N–150N). Tissue sampling commenced in March of Year 2. The LSDs are provided at $P < 0.05$ unless otherwise noted. Genotypic differences designated with *$P < 0.05$, **$P < 0.01$, respectively.

N concentrations from June to August were lower in the 0–0 N treatment when compared to the other treatments. Between August and November rhizome N concentrations increased in treatments that receive N in Year 2. By comparison, the 0–0 and 150–0 N treatments exhibited only a slight increase in rhizome N between August and November. In general rhizome N concentrations were depleted between April and July, and N subsequently re-accumulated by November. Rhizome N concentration also exhibited a

significant genotype × N treatment interaction (**Table 3**). Averaged across harvests, rhizome N concentrations of the Nagara-sib generally increased with increasing N fertilization (e.g., 0–0 to 75–75 to 150–150), while concentration of N in rhizomes of the IL Clone were higher than the 0–0 control plots when N was applied, but similar among the N treatments themselves. In general, the Nagara-sib had higher rhizome N concentrations than the IL Clone with the exception of the 0–150 N treatment.

TABLE 3 | Influence of nitrogen (N) management on concentrations of N, buffer-soluble protein, and amino acid-N in roots and rhizomes of two *Miscanthus* genotypes (Nag., Nagara-sib; IL, IL Clone).

	Root						Rhizome					
	N mg/g DW		Protein mg/g DW		Amino-N μM/g DW		N mg/g DW		Protein mg/g DW		Amino-N μM/g DW	
N Mgmt	Nag.	IL	Nag.	IL	Nag.	IL	Nag.	IL	Nag.	IL	Nag.	IL
0N–0N	7.2	6.8	2.4	2.4	50	42	7.7	6.3	3.5	3.6	103	81
0N–150N	7.9	8.6	2.7	3.0	65	79	9.7	9.5	4.0	5.0	164	186
75N–75N	8.9	8.6	2.9	3.1	85	76	10.8	9.2	4.9	5.0	199	163
150N–0N	9.4	8.8	3.2	3.1	98	76	11.8	10.2	5.4	4.9	204	187
150N–150N	10.7	9.5	3.8	3.4	134	91	13.6	10.3	5.9	5.2	275	217
LSD	0.7		0.3†		14		1.1		0.5		32	

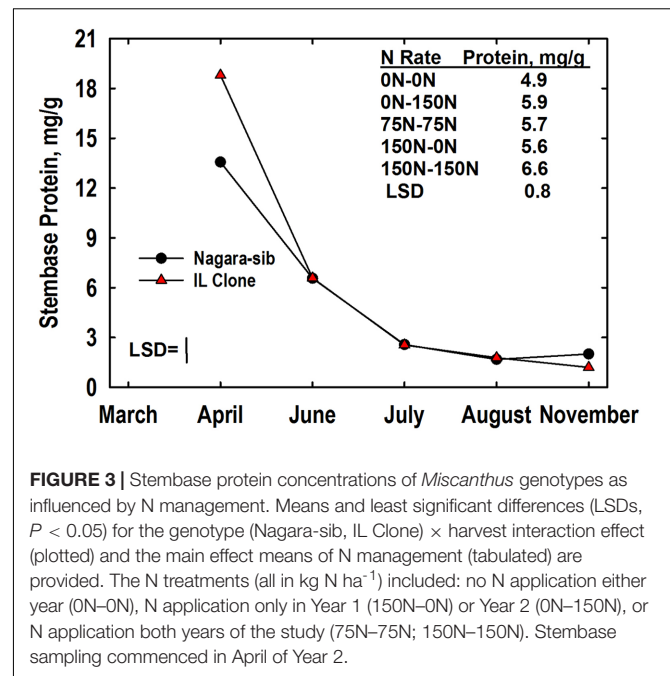†LSD at the 10% level of probability. Data were averaged harvests in Year 2. Nitrogen treatments (all in kg N ha^{-1}) included: no N application either year (0N–0N), N application only in Year 1 (150N–0N) or Year 2 (0N–150N), or N application both years of the study (75N–75N; 150N–150N). The least significant difference (LSD) at $P \leq 0.05$ level of probability is provided unless indicated otherwise.

Buffer-Soluble Protein and Amino Acid-N Pools

Total buffer-soluble proteins were analyzed in this study as a surrogate for yet uncharacterized VSPs in storage organs of this species. Like N, stembase protein concentrations declined markedly between April and July harvests (**Figure 3**). There was a significant genotype × harvest interaction for stembase protein. Concentrations of protein in stembases of the IL Clone were higher than those of the Nagara-sib in April but stembase protein levels of genotypes were similar at all subsequent harvests. Averaged over genotypes and harvests, the main effect of N management on stembase protein concentration also was significant. Stembase protein concentrations of plants fertilized with N in Year 2 (75–75, 0–150, 150–150) were higher than the 0–0 control N treatment. In addition, the stembase protein concentrations of the 150–150 N treatment were higher than those of the 75–75 and 150–0 N treatments. Shoot tissues were not analyzed for concentrations of buffer-soluble protein and amino acid N.

A significant harvest × N treatment interaction was observed for root protein concentration. Like root N, protein concentrations were highest in roots of plants fertilized with 150 kg N ha^{-1} in Year 1 (**Figure 4A**). Root protein concentrations declined in all N treatments in April, with continued rapid decline in the 0–0, 150–0, and 150–150 N treatments until June at which time the 0–0 N treatment had a lower root protein concentration than the other N treatments. Low root protein concentrations were observed in August, and there was no difference associated with N treatment. However, protein concentrations increased markedly between August and November with the highest concentrations observed in roots of plants fertilized with N in Year 2. Root protein levels in November were equal to or higher than those observed the previous March for all treatments where N was provided in Year 2. In contrast, root protein levels in November were lower than March concentrations for the 0–0 and 150–0 N treatments. Root protein concentration also exhibited a significant genotype × N treatment interaction (**Table 3**). The IL Clone had greater protein concentrations in roots of plants in the 0–150 N treatment whereas the Nagara-sib had higher root protein than the IL Clone for plants in the 150–150 N treatment.

The harvest × N treatment interaction also was significant for rhizome protein concentration. March protein concentrations were higher in rhizomes of the 150–0 and 150–150 N treatments when compared to the other N treatments (**Figure 4B**). Rhizome protein concentrations declined in all treatments until June, but the extent of decline was altered by N fertilizer application. For example, rhizome protein concentrations of the 0–0 and 0–150 N treatments were similar to each other at March and April harvests, but N application in early May slowed the decline in rhizome protein levels of the 0–150 N treatment when plots were sampled in June. Likewise, the protein concentrations for the 150–0 and 150–150 N treatments were similar in March, but by the June harvest protein concentrations in rhizomes of the 150–0 N treatment were more extensively depleted than the 150–150 N treatment that received N fertilizer in May. Rhizome
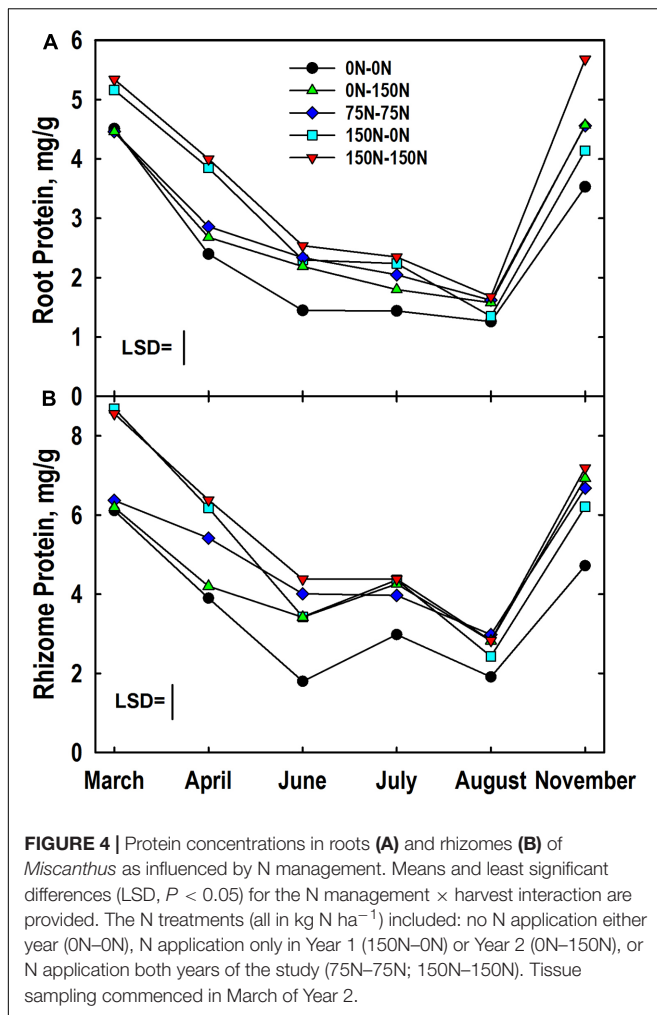
FIGURE 3 | Stembase protein concentrations of *Miscanthus* genotypes as influenced by N management. Means and least significant differences (LSDs, *P* < 0.05) for the genotype (Nagara-sib, IL Clone) × harvest interaction effect (plotted) and the main effect means of N management (tabulated) are provided. The N treatments (all in kg N ha^{-1}) included: no N application either year (0N–0N), N application only in Year 1 (150N–0N) or Year 2 (0N–150N), or N application both years of the study (75N–75N; 150N–150N). Stembase sampling commenced in April of Year 2.

protein concentrations remained low in the 0–0 N treatment from June to August. Large increases in rhizome protein concentration occurred for all N treatments between August and November, and for the 75–75 and 0–150 treatments protein concentrations returned to levels observed the previous March. The genotype × N treatment interaction also was significant for rhizome protein concentration (**Table 3**). Protein concentrations in rhizomes of the Nagara-sib increased incrementally as N treatment increased from 0–0 to 150–150. In contrast, protein concentrations in rhizomes of the IL Clone were elevated to a similar level over the 0–0 N treatment irrespective of the N fertilizer application rate or timing.

The harvest × N treatment interaction was significant for amino-N concentrations of stembases (**Figure 5A**). Stembase amino-N concentrations in April of the 0–0 and 0–150 N treatments were lower than treatments that had received N in Year 1. Stembase amino-N declined by June, especially in the 0–0 and 150–0 N treatments. Application of N in Year 2 slowed the decline in amino-N concentrations in the 75–75, and 150–150 N treatments resulting in large differences among treatments in June and July. By the November sampling concentrations of amino-N in the 0–0 and 150–0 N treatments were similar and lower than the 150–150 N treatment.

The harvest × N treatment interaction also was significant for root amino-N concentrations (**Figure 5B**). Large differences in root amino-N were observed in March and April, with the 0–0 and 0–150 N treatments being lower than plants fertilized with 150 kg N ha^{-1} the previous year. Root amino-N declined in all treatments by June and remained low through August when only the 0–0 and 150–150 N treatments differed. Root amino-N accumulated between August and November, especially in plots fertilized with N in Year 2. The genotype × N treatment interaction also was significant for root amino-N concentration

FIGURE 4 | Protein concentrations in roots **(A)** and rhizomes **(B)** of *Miscanthus* as influenced by N management. Means and least significant differences (LSD, $P < 0.05$) for the N management × harvest interaction are provided. The N treatments (all in kg N ha^{-1}) included: no N application either year (0N–0N), N application only in Year 1 (150N–0N) or Year 2 (0N–150N), or N application both years of the study (75N–75N; 150N–150N). Tissue sampling commenced in March of Year 2.

FIGURE 5 | Amino-N concentrations in stembase **(A)**, root **(B)**, and rhizome **(C)** tissues of *Miscanthus* as influenced by N management. Means and least significant differences (LSD, $P < 0.05$) for the N management × harvest interaction are provided. Nitrogen treatments (all in kg N ha^{-1}) included: no N application either year (0N–0N), N application only in Year 1 (150N–0N) or Year 2 (0N–150N), or N application both years of the study (75N–75N; 150N–150N). Tissue sampling commenced in March (roots, rhizomes) or April (stembases) of Year 2.

(**Table 3**). Root amino-N of the Nagara-sib generally increased incrementally as N treatment increased from 0–0 to 150–150 N. Amino-N in roots of the IL Clone increased from 42 μM/g for the 0–0 N treatment to 76 to 79 μM/g for 0–150, 75–75, and 150–0 N treatments. Roots of the IL Clone in the 150–150 N treatment contained the highest amino-N concentrations (91 μM/g), but this was less than that observed for the Nagara-sib provided this N regime.
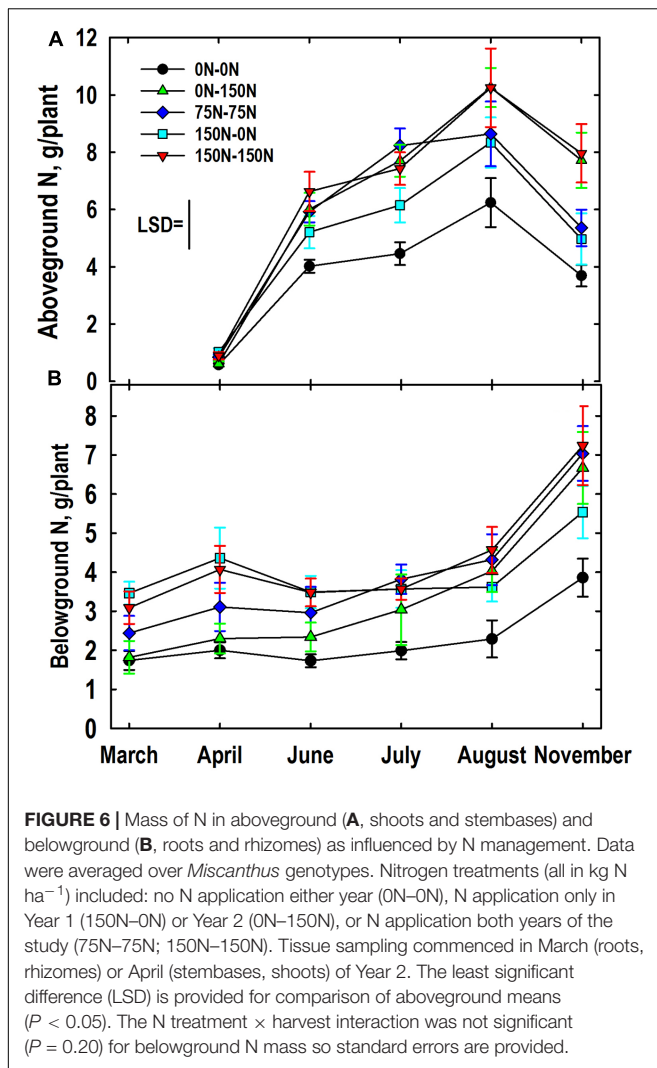
Concentration of amino-N in rhizomes of the 150–0 and 150–150 N treatments were greater in March and April when compared to the other treatments (**Figure 5C**). Between April and June large reductions in rhizome amino-N concentrations were observed for the 0–0 and 150–0 N treatments, while amino N concentrations in rhizomes of the other treatments remained unchanged. By comparison, amino-N concentrations in rhizomes of the 0–150 N treatment that was similar to the 0–0 N treatment in March and April were higher than these plots in June and at subsequent samplings. Amino-N accumulated in rhizomes between August and November in all but the 150–0 N treatment with final concentrations reflecting N fertilizer applications in Year 2. The genotype × N treatment interaction also was significant for rhizome amino-N (**Table 3**). Averaged across
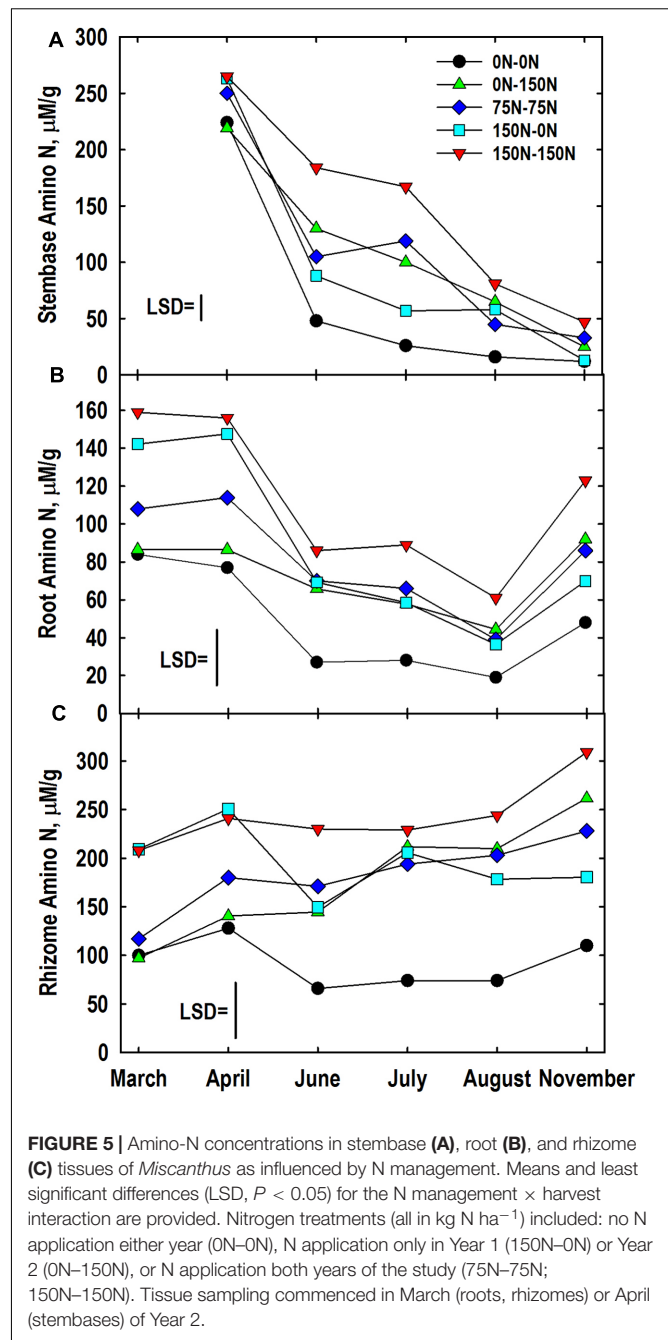
harvests, rhizome amino-N concentrations generally increased in both genotypes with N fertilization. Amino-N concentrations of the Nagara-sib were greater than the IL Clone when fertilized with N both years (75–75 and 150–150 N treatments).

Nitrogen Contents in above- and belowground Tissues

The genotype main effect on aboveground N mass (N concentration × tissue mass; summed for shoots and stembases) was not significant. The harvest × N treatment interaction for aboveground N mass was significant. Averaged

FIGURE 6 | Mass of N in aboveground (**A**, shoots and stembases) and belowground (**B**, roots and rhizomes) as influenced by N management. Data were averaged over *Miscanthus* genotypes. Nitrogen treatments (all in kg N ha^{-1}) included: no N application either year (0N–0N), N application only in Year 1 (150N–0N) or Year 2 (0N–150N), or N application both years of the study (75N–75N; 150N–150N). Tissue sampling commenced in March (roots, rhizomes) or April (stembases, shoots) of Year 2. The least significant difference (LSD) is provided for comparison of aboveground means ($P < 0.05$). The N treatment × harvest interaction was not significant ($P = 0.20$) for belowground N mass so standard errors are provided.

over genotypes aboveground N mass was similar for all N treatments in April (**Figure 6A**). As expected aboveground N mass increased markedly from April to July at which time the 0–0 N treatment had less accumulated N than all other treatments, and the 150–0 N treatment had less than the 75–75 N treatment. Aboveground N mass increased in all plots between July and August except the 75–75 N treatment where the aboveground N mass was similar to the 150–0 N treatment. From August and November aboveground N mass declined and treatment differences established in August were largely maintained.

The main effect of genotype on belowground N mass (N concentration × tissue mass; summed for rhizomes and roots) was significant with the IL Clone averaging more N mass belowground than the Nagara-sib (4.24 vs. 2.99 g/plant, respectively). The main effects of N treatment and harvest on belowground N mass were also highly significant. Averaged over N treatments and genotypes, belowground N mass was lowest in March (2.5 g/plant); an amount similar to values observed in April (3.2 g/plant) and June (2.8 g/plant). However, belowground N masses in July (3.4 g/plant) were higher than those observed

in March, and those observed in August (3.8 g/plant) exceeded belowground N masses observed in both March and June. Belowground N mass in November (6.0 g/plant) was higher than all other observed values. The harvest × N treatment interaction was not significant ($P = 0.20$) because trends over harvests were generally similar among N treatments. Nevertheless, the harvest × N treatment means with their standard errors are provided (**Figure 6B**) in order to be consistent with presentation of other N and tissue mass data (**Figures 1–5, 6A**). Means differing by twice the standard error or more are considered significantly different. Belowground N mass in March and April of the 0–0 and 0–150 N treatments were lower than the 150–0 and 150–150 N treatments, with the 75–75 N treatment intermediate. Belowground N mass of the 0–150 N treatment was greater than the 0–0 N treatment in June and subsequent harvest reflecting the large N fertilizer application this treatment received in Year 2. Likewise, belowground N mass of the 150–0 N treatment that was initially high in March did not increase between June and August ultimately placing this N treatment intermediate between the 0–0 N control and the other N treatments all of which received N in Year 2. All plants accumulated N belowground between August and November irrespective of N treatment, however, the trajectory of N accumulation was greater in plots fertilized with N in Year 2.

DISCUSSION

Yield and Tissue N

This experiment varied N management over two growing seasons to alter N concentrations and N pools in putative storage organs in order to inform the relationships between uptake, accumulation, and remobilization of N, and plant growth/biomass yield. To broaden the inference space we used the commonly grown IL Clone of *Miscanthus* and the lesser studied Nagara-sib germplasm that have previously been shown to differ in yield, N use efficiency, and late-season leaf senescence (Dierking et al., 2016). Application of N fertilizer increased tissue N concentrations of all organs, and when compared to the unfertilized 0–0 N control plants, and there was a trend to enhance biomass yield (**Figures 1, 2**). Several reports also have indicated greater biomass yield of *Miscanthus* in response to N fertilization (Himken et al., 1997; Heaton E.A. et al., 2004; Christian et al., 2008; Miguez et al., 2008; Maughan et al., 2012). However, others have found no response of *Miscanthus* to N fertilizer (Lewandowski et al., 2000; Christian et al., 2008; Arundale et al., 2014; Larsen et al., 2014; Finnan and Burke, 2016).

Although root and rhizome N concentrations of the 0–150 N treatment increased significantly after N fertilizer application at the beginning of Year 2 (**Figures 2C,D**) season-average dry weights of these tissues did not increase in response to this N (**Table 2**). Wiesler et al. (1997) did observe that shoot growth of *Miscanthus sinensis* was enhanced immediately after N application whereas root and rhizome growth were less responsive to N fertilization. Amougou et al. (2011) also observed no increase in root and rhizome mass when *Miscanthus* was fertilized with 120 kg N ha^{-1}despite a large increase in

tissue N concentrations. These authors reported total N mass accumulation in belowground organs that ranged from 94 to nearly 300 kg N ha^{-1} depending on management and time of sampling. Similar variation and absolute levels of belowground N mass accumulation have been reported in other studies (Neukirchen et al., 1999; Christian et al., 2006; Dohleman et al., 2012; Dufossé et al., 2014). By comparison, when N mass per plant data (**Figure 6B**) are scaled to the 19760 plant ha^{-1} plant populations, we estimated that belowground tissues contained between 34 (0–0 treatment) and 71 (150–0 treatment) kg N ha^{-1} in March. Belowground N mass increased to 77 and 142 kg N ha^{-1} by November for the 0–0 and 150–150 N treatments, respectively. Part of this November increase in belowground N is presumed to originate from N translocated from senescing aboveground tissues (Beale and Long, 1997; Heaton et al., 2009; Cadoux et al., 2012). Based on plant populations and N mass plant^{-1}, N content of the aboveground tissues declined on average 56 kg N ha^{-1} (range 46 to 67 kg N ha^{-1}) between August and November (**Figure 6A**). During this time interval, belowground biomass accumulated an average of 46 kg N ha^{-1} (range 31 to 57 kg N ha^{-1}). Assuming no N leached from tissues and minimal additional N uptake from August to November as reported by Burks (2013), these changes represent an 82% recovery of N lost by aboveground tissues in belowground storage organs. Our predicted N transfer values are similar to those reported by Christian et al. (2006) who calculated that 60 and 74 kg N ha^{-1} moved from aboveground to belowground organs of 2- and 3-year-old plants, respectively. Strullu et al. (2011) reported slightly higher estimates of N transfer from aboveground to belowground tissues (up to 145 kg N ha^{-1}). The higher values were for late-season harvests that had higher biomass yields than observed in our study.

The traditional fertilization strategy of annual application of N (75–75, 150–150 N treatments) along with the 0–0 control treatment provided useful context for understanding the effectiveness of alternate-year N fertilizer applications (150–0, 0–150). In general, tissue N concentrations were lowest for the 0–0 N treatment, highest for the 150–150 N treatment, and intermediate for the 75–75 N treatment (**Figure 2**). Plants provided high N only in Year 1 (150–0 N treatment) had high N concentrations and masses in roots and rhizomes initially that were depleted during the following growing season (**Figure 6**). In contrast, plants provided high N only in Year 2 began with low N concentrations and masses in roots and rhizomes, but these increased quickly following N application; a response previously reported by others (Amougou et al., 2011; Strullu et al., 2011). Biomass yield of plants receiving N only in Year 1 (150–0 N treatment) was similar to the 0–0 N treatment (**Figure 1A**) suggesting that previously accumulated N in belowground organs in Year 1 was not sufficient to meet the shoot N needs of plants in Year 2. This conclusion is also supported by the reduced aboveground N mass of the 150–0 N treatment in June and July when compared to the N-fertilized treatments even though belowground biomass of the 150–0 N treatments contains large amounts of N (**Figure 6**). Annual application of 75 kg N ha^{-1} in this study resulted in both high yield and well-developed roots and rhizomes compared to alternate-year N application at double

the rate that rely on N recycling/remobilization in the unfertilized year. Himken et al. (1997) also recommended annual applications of 50 to 70 kg N ha^{-1} for high yields of well-established stands of *Miscanthus* in Europe; a fertilizer management strategy endorsed by others, especially when large amounts of biomass are removed from the field (Heaton et al., 2009; Strullu et al., 2011; Dohleman et al., 2012; Ferchaud et al., 2016).

Protein and Amino N Fluxes and N Management Strategies

Although root and rhizome N concentrations were generally similar (**Figures 2C,D**), rhizomes tended to have greater concentrations of amino-N and buffer-soluble protein when compared to roots (**Figures 4**, **5**). This, along with their three-fold greater mass when compared to roots (**Figures 1C,D**) indicates that fluxes in N reserve pools to/from rhizomes represent a greater N mass flow and likely contribute more N to shoot growth in spring than N reserve pools in roots. Root and rhizome protein concentrations both declined in spring when growth resumed and accumulated in autumn as growth subsided and plants acclimated for winter (**Figure 4**). This general pattern agrees with previous research on vegetative storage proteins in perennials (Hendershot and Volenec, 1993b; Avice et al., 2003). As expected, protein concentrations of both tissues in March of Year 2 generally reflected Year 1 N management whereas protein concentrations in November of Year 2 responded to that season's N management. Addition of N fertilizer has previously been shown to increase protein accumulation in storage organs of perennials and enhanced subsequent shoot growth rates after defoliation (Volenec et al., 1996; Avice et al., 2003). Likewise, preloading N in belowground storage organs of *Miscanthus* with N in Year 1 (150–0 N treatment; **Figure 6B**) also enhanced initial aboveground growth in Year 2 (**Figure 6A**) when compared to the 0–0 N treatment control plants; however, the enhanced initial growth was not sustained and season-average shoot mass of the 150–0 N treatment (549 g/plant) was similar to the 0–0 N treatment (504 g/plant) (**Figure 1A**).

Amino-N concentrations in March and November in both roots and rhizomes were closely associated with N management imposed over the 2-year period (**Figure 5**). Reduction in amino-N concentrations of roots and rhizomes of N-deprived (0–0 and 150–0 N treatments) plants suggest this pool is an important contributor of N to shoot growth in spring. Gloser (2002, 2005) also reported extensive loss of amino acids from rhizomes of *C. epigejos* in spring followed by a gradual increase in this N pool from July through November. He concluded that amino acids in rhizomes, roots and stem bases have a central role in N storage, winter survival, and spring growth of this species. While root amino N concentrations underwent a depletion-accumulation cycle similar to root and rhizome protein (**Figure 4**), amino-N concentrations of rhizomes of plants receiving N in Year 2 gradually increased from March to November. This contrasting trend in the amino-N pool, when compared to the rhizome protein pool, may be misleading as it does not capture potential rapid turnover of and flux through the amino-N pool. This is similar to reserve carbon pools in summer

in perennial plants where starch reserves vary markedly following defoliation but only modest changes in sugar concentrations are observed (Gallagher et al., 1997; Teixeira et al., 2007). Labeling studies are necessary to inform the rate and extent of turnover of the amino-N pool in roots, but especially rhizomes of *Miscanthus*. Frak et al. (2002) used ^{15}N labeling to understand the dynamics and temporal succession of individual amino acids involved in N remobilization in walnut (*Juglans nigra* × *regia*) trees. Others have used dual-labeling with both ^{15}N and ^{13}C to understand the magnitude of contribution of taproot C and N reserves, including amino acids, to shoot C and N nutrition and ultimately biomass growth (Avice et al., 1996).

Genotypic Effects

Previous work (Dierking et al., 2016) revealed significant differences in growth and N use efficiency among these *Miscanthus* genotypes. Genotypes differed in all biomass traits (**Figure 1**) including a significant reduction in shoot biomass between August and November for the IL Clone as leaves senesced, while leaves of the Nagara-sib remained largely intact (Dierking et al., 2016). Mass of roots and rhizomes were generally greater for the IL Clone (**Figures 1C,D**) and this greater mass may have diluted root and rhizome N pools and contributed to the lower N concentrations of these tissues (**Figures 2C,D**).

Genotypes differed in concentrations of N, protein, and amino-N in rhizomes and these differences occasionally interacted with N management (**Tables 2, 3**). For example, when compared to the IL Clone, N pools in roots and rhizomes of Nagara-sib were greater in the 150–150 N treatment, whereas the reverse was generally observed for the 0–150 N treatment (**Table 3**). Both genotype- and fertilizer-induced differences in accumulation of protein and amino-N in storage organs has been previously reported for several perennial species (Haagenson et al., 2003; Gloser, 2005; Patton et al., 2007; Berg et al., 2009; Lissbrant et al., 2010). Initial shoot growth in spring and shoot regrowth after defoliation were generally positively associated with accumulation of protein and/or amino-N in storage organs in these studies. In this study shoot mass of the IL Clone tended to be greater than that of the Nagara-sib in July and August (**Figure 1A**) indicating that, despite lower N pool concentrations in roots and rhizomes (**Figures 2C,D** and **Table 3**), the nearly two-fold greater mass of rhizomes (**Figure 1D**) could have contributed more N mass from reserves to initial shoot growth.

Additional work with a larger array of *Miscanthus* genotypes may inform the relationships among N reserve pools and genotypic differences in growth and stress tolerance.

CONCLUSION

As expected, both N concentration and content of above- and belowground plant tissues were greatly influenced by N management. The N accumulated as amino-N and protein in roots and rhizomes, with the latter organ accumulating the most reserve N mass. Belowground N pools accumulated the previous year were depleted when shoot growth resumed in spring, but alone, were insufficient to maintain rapid shoot growth into summer. Highest biomass yields were associated with moderate amounts of N (e.g., 75 kg N ha^{-1}) applied annually. Finally, application of N fertilizer to unfertilized *Miscanthus* (e.g., 0–150 treatment) results in rapid recovery of both tissue N concentrations levels and biomass accumulation rate.

REFERENCES

Allison, G. G., Morris, C., Clifton-Brown, J., Lister, S. J., and Donnison, I. S. (2011). Genotypic variation in cell wall composition in a diverse set of 244 accessions of *Miscanthus*. *Biomass Bioenergy* 35, 4740–4747. doi: 10.1016/j.biombioe.2011.10.008

Amougou, N., Bertrand, I., Machet, J. M., and Recous, S. (2011). Quality and decomposition in soil of rhizome, root and senescent leaf from *Miscanthus x giganteus*, as affected by harvest date and N fertilization. *Plant Soil* 338, 83–97. doi: 10.1007/s11104-010-0443-x

Arundale, R. A., Dohleman, F. G., Voigt, T. B., and Long, S. P. (2014). Nitrogen fertilization does significantly increase yields of stands of *Miscanthus × giganteus* and *Panicum virgatum* in multiyear trials in Illinois. *BioEnergy Res.* 7, 408–416. doi: 10.1007/s12155-013-9385-5

Aurangzeb, M. (2012). *Performance Evaluation of Nine Varieties of Miscanthus in Iowa*. Master's thesis, Iowa State University, Ames, IA.

Avice, J. C., Dily, F. L., Goulas, E., Noquet, C., Meuriot, F., Volenec, J. J., et al. (2003). Vegetative storage proteins in overwintering storage organs of forage legumes: roles and regulation. *Can. J. Bot.* 81, 1198–1212. doi: 10.1139/b03-122

Avice, J. C., Ourry, A., Lemaire, G., and Boucaud, J. (1996). Nitrogen and carbon flows estimated by 15N and 13C pulse-chase labeling during regrowth of alfalfa. *Plant Physiol.* 112, 281–290.

Bakken, A. K., Macduff, J. H., and Collison, M. (1998). Dynamics of nitrogen remobilization in defoliated *Phleum pratense* and *Festuca pratensis* under short and long photoperiods. *Physiol. Plant.* 103, 426–436. doi: 10.1034/j.1399-3054.1998.1030316.x

Barber, L. D., Joern, B. C., Volenec, J. J., and Cunningham, S. M. (1996). Supplemental nitrogen effects on alfalfa regrowth and nitrogen

mobilization from roots. *Crop Sci.* 36, 1217–1223. doi: 10.2135/cropsci1996. 0011183X003600050025x

Beale, C. V., and Long, S. P. (1997). Seasonal dynamics of nutrient accumulation and partitioning in the perennial C₄-grasses *Miscanthus × giganteus* and *Spartina cynosuroides*. *Biomass Bioenergy* 12, 419–428. doi: 10.1016/S0961-9534(97)00016-0

Berg, W. K., Cunningham, S. M., Brouder, S. M., Joern, B. C., Johnson, K. D., and Volenec, J. J. (2009). Influence of phosphorus and potassium on alfalfa yield, taproot C and N pools, and transcript levels of key genes after defoliation. *Crop Sci.* 49, 974–982. doi: 10.2135/cropsci2008.07.0395

Bradford, M. M. (1976). A rapid and sensitive method for the quantitation of microgram quantities of protein utilizing the principle of protein-dye binding. *Anal. Biochem.* 72, 248–254. doi: 10.1016/0003-2697(76)90527-3

Burks, J. L. (2013). *Eco-physiology of Three Perennial Bioenergy Systems*. Ph.D. dissertation, Purdue University, West Lafayette, IN.

Cadoux, S., Riche, A. B., Yates, N. E., and Machet, J. M. (2012). Nutrient requirements of *Miscanthus x giganteus*: conclusions from a review of published studies. *Biomass Bioenergy* 38, 14–22. doi: 10.1016/j.biombioe.2011. 01.015

Christian, D. G., Poulton, P. R., Riche, A. B., Yates, N. E., and Todd, A. D. (2006). The recovery over several seasons of 15 N-labelled fertilizer applied to *Miscanthus × giganteus* ranging from 1 to 3 years old. *Biomass Bioenergy* 30, 125–133. doi: 10.1016/j.biombioe.2005.11.002

Christian, D. G., Riche, A. B., and Yates, N. E. (2008). Growth, yield and mineral content of *Miscanthus x giganteus* grown as a biofuel for 14 successive harvests. *Ind. Crops Prod.* 28, 320–327. doi: 10.1016/j.indcrop.2008.02.009

Clifton-Brown, J. C., and Lewandowski, I. (2002). Screening *Miscanthus* genotypes in field trials to optimise biomass yield and quality in Southern Germany. *Eur. J. Agron.* 16, 97–110. doi: 10.1016/S1161-0301(01)00120-4

Cochran, W. G., and Cox, G. M. (1957). "Factorial experiments with main effects confounded: split-plot designs," in *Experimental Designs*, 2nd Edn (New York, NY: John Wiley & Sons), 293–316.

Corre, N., Bouchart, V., Ourry, A., and Boucaud, J. (1996). Mobilization of nitrogen reserves during regrowth of defoliated *Trifolium repens* L., and identification of potential vegetative storage proteins. *J. Exp. Bot.* 301, 1111–1118. doi: 10.1093/ jxb/47.8.1111

Cunningham, S. M., and Volenec, J. J. (1996). Purification and characterization of vegetative storage proteins from alfalfa (*Medicago sativa* L.) taproots. *J. Plant Physiol.* 147, 625–632. doi: 10.1016/S0176-1617(11)81469-0

da Costa, R. M., Lee, S. J., Allison, G. G., Hazen, S. P., Winters, A., and Bosch, M. (2014). Genotype, development and tissue-derived variation of cell-wall properties in the lignocellulosic energy crop *Miscanthus*. *Ann. Bot.* 114, 1265–1277. doi: 10.1093/aob/mcu054

Dierking, R. M., Allen, D. J., Brouder, S. M., and Volenec, J. J. (2016). Yield, biomass composition, and N use efficiency during establishment of four *Miscanthus × giganteus* genotypes as influenced by N management. *Biomass Bioenergy* 91, 98–107. doi: 10.1016/j.biombioe.2016.05.005

Dohleman, F. G., Heaton, E. A., Arundale, R. A., and Long, S. P. (2012). Seasonal dynamics of above-and below-ground biomass and nitrogen partitioning in *Miscanthus × giganteus* and *Panicum virgatum* across three growing seasons. *GCB Bioenergy* 4, 534–544. doi: 10.1111/j.1757-1707.2011.01153.x

Dufossé, K., Drewer, J., Gabrielle, B., and Drouet, J. L. (2014). Effects of a 20-year old *Miscanthus × giganteus* stand and its removal on soil characteristics and greenhouse gas emissions. *Biomass Bioenergy* 69, 198–210. doi: 10.1016/j. biombioe.2014.07.003

Erisman, J. W., Sutton, M. A., Galloway, J., Klimont, Z., and Winiwarter, W. (2008). How a century of ammonia synthesis changed the world. *Nat. Geosci.* 1, 636–639. doi: 10.1038/ngeo325

Ferchaud, F., Vitte, G., Machet, J. M., Beaudoin, N., Catterou, M., and Mary, B. (2016). The fate of cumulative applications of 15 N-labelled fertiliser in perennial and annual bioenergy crops. *Agric. Ecosyst. Environ.* 223, 76–86. doi: 10.1016/j.agee.2016.02.030

Finnan, J., and Burke, B. (2016). Nitrogen fertilization of *Miscanthus x giganteus*: effects on nitrogen uptake, growth, yield and emissions from biomass combustion. *Nutr. Cycling Agroecosyst.* 106, 249–256. doi: 10.1007/s10705-016-9793-y

Frak, E., Millard, P., Le Roux, X., Guillaumie, S., and Wendler, R. (2002). Coupling sap flow velocity and amino acid concentrations as an alternative method to

15N labeling for quantifying nitrogen remobilization by walnut trees. *Plant Physiol.* 130, 1043–1053.

Gallagher, J. A., Volenec, J. J., Turner, L. B., and Pollock, C. J. (1997). Starch hydrolytic enzyme activities following defoliation of white clover. *Crop Sci.* 37, 1812–1818. doi: 10.2135/cropsci1997.0011183X003700060025x

Gloser, V. (2002). Seasonal changes of nitrogen storage compounds in a rhizomatous grass *Calamagrostis epigejos*. *Biol. Plant.* 45, 563–568.

Gloser, V. (2005). The consequences of lower nitrogen availability in autumn for internal nitrogen reserves and spring growth of *Calamagrostis epigejos*. *Plant Ecol.* 179, 119–126. doi: 10.1007/s11258-004-6736-5

Haagenson, D. M., Cunningham, S. M., and Volenec, J. J. (2003). Autumn defoliation effects on alfalfa winter survival, root physiology, and gene expression. *Crop Sci.* 43, 1340–1348. doi: 10.2135/cropsci2003.1340

Heaton, E. A., Boersma, N., Caveny, J. D., Voigt, T. B., and Dohleman, F. G. (2016). *Miscanthus (Miscanthus x giganteus) for Biofuel Production*. Available at: http://articles.extension.org/pages/26625/miscanthus-miscanthus-x-giganteus-for-biofuel-production [accessed May 17, 2017].

Heaton, E. A., Dohleman, F. G., and Long, S. P. (2009). Seasonal nitrogen dynamics of *Miscanthus × giganteus* and *Panicum virgatum*. *GCB Bioenergy* 1, 297–307. doi: 10.1111/j.1757-1707.2009.01022.x

Heaton, E. A., Long, S. P., Voigt, T. B., Jones, M. B., and Clifton-Brown, J. (2004). *Miscanthus* for renewable energy generation: European Union experience and projections for Illinois. *Mitig. Adapt. Strat. Glob. Change* 9, 433–451. doi: 10.1023/B:MITI.0000038848.94134.be

Heaton, E., Voigt, T., and Long, S. P. (2004). A quantitative review comparing the yields of two candidate C4 perennial biomass crops in relation to nitrogen, temperature and water. *Biomass Bioenergy* 27, 21–30. doi: 10.1016/j.biombioe. 2003.10.005

Hendershot, K. L., and Volenec, J. J. (1993a). Nitrogen pools in taproots of *Medicago sativa* L. after defoliation. *J. Plant Physiol.* 141, 129–135. doi: 10.1016/ S0176-1617(11)80748-0

Hendershot, K. L., and Volenec, J. J. (1993b). Taproot nitrogen accumulation and use in overwintering alfalfa (*Medicago sativa* L.). *J. Plant Physiol.* 141, 68–74. doi: 10.1016/S0176-1617(11)80853-9

Himken, M., Lammel, J., Neukirchen, D., Czypionka-Krause, U., and Olfs, H. W. (1997). Cultivation of *Miscanthus* under West European conditions: seasonal changes in dry matter production, nutrient uptake and remobilization. *Plant Soil* 189, 117–126. doi: 10.1023/A:1004244614537

Hodgson, E. M., Lister, S. J., Bridgwater, A. V., Clifton-Brown, J., and Donnison, I. S. (2010). Genotypic and environmentally derived variation in the cell wall composition of *Miscanthus* in relation to its use as a biomass feedstock. *Biomass Bioenergy* 34, 652–660. doi: 10.1016/j.biombioe.2010.01.008

Iqbal, Y., and Lewandowski, I. (2014). Inter-annual variation in biomass combustion quality traits over five years in fifteen *Miscanthus* genotypes in south Germany. *Fuel Process. Technol.* 121, 47–55. doi: 10.1016/j.fuproc.2014. 01.003

Jeżowski, S. (2008). Yield traits of six clones of *Miscanthus* in the first 3 years following planting in Poland. *Ind. Crops Prod.* 27, 65–68. doi: 10.1016/j.indcrop. 2007.07.013

Jørgensen, U. (1997). Genotypic variation in dry matter accumulation and content of N, K and Cl in *Miscanthus* in Denmark. *Biomass Bioenergy* 12, 155–169. doi: 10.1016/S0961-9534(97)00002-0

Kavanova, M., and Gloser, V. (2005). The use of internal nitrogen stores in the rhizomatous grass *Calamagrostis epigejos* during regrowth after defoliation. *Ann. Bot.* 95, 457–463. doi: 10.1093/aob/mci054

Khanna, M., Dhungana, B., and Clifton-Brown, J. (2008). Costs of producing *Miscanthus* and switchgrass for bioenergy in Illinois. *Biomass Bioenergy* 32, 482–493. doi: 10.1016/j.biombioe.2007.11.003

Larsen, S. U., Jørgensen, U., Kjeldsen, J. B., and Lærke, P. E. (2014). Long-term *Miscanthus* yields influenced by location, genotype, row distance, fertilization and harvest season. *Bioenergy Res.* 7, 620–635. doi: 10.1007/s12155-013-9389-1

Lewandowski, I., Clifton-Brown, J. C., Scurlock, J. M., and Huisman, W. (2000). *Miscanthus*: European experience with a novel energy crop. *Biomass Bioenergy* 19, 209–227. doi: 10.1016/S0961-9534(00)00032-5

Li, R., Volenec, J. J., Joern, B. C., and Cunningham, S. M. (1996). Seasonal changes in nonstructural carbohydrates, protein, and macronutrients in roots of alfalfa, red clover, sweetclover, and birdsfoot trefoil. *Crop Sci.* 36, 617–623. doi: 10.2135/ cropsci1996.0011183X003600030016x

Lissbrant, S., Brouder, S. M., Cunningham, S. M., and Volenec, J. J. (2010). Identification of fertility regimes that enhance long-term productivity of alfalfa using cluster analysis. *Agron. J.* 102, 580–591. doi: 10.2134/agronj2009. 0300

Louahlia, S., Macduff, J. H., Ourry, A., Humphreys, M., and Boucaud, J. (1999). Nitrogen reserve status affects the dynamics of nitrogen remobilization and mineral nitrogen uptake during recovery of contrasting cultivars of *Lolium perenne* from defoliation. *New Phytol.* 142, 451–462. doi: 10.1046/j.1469-8137. 1999.00419.x

Maughan, M., Bollero, G., Lee, D. K., Darmody, R., Bonos, S., Cortese, L., et al. (2012). *Miscanthus* × *giganteus* productivity: the effects of management in different environments. *GCB Bioenergy* 4, 253–265. doi: 10.1111/j.1757-1707. 2011.01144.x

Miguez, F. E., Villamil, M. B., Long, S. P., and Bollero, G. A. (2008). Meta-analysis of the effects of management factors on *Miscanthus* × *giganteus* growth and biomass production. *Agric. For. Meteorol.* 148, 1280–1292. doi: 10.1016/j. agrformet.2008.03.010

Neukirchen, D., Himken, M., Lammel, J., Czypionka-Krause, U., and Olfs, H. W. (1999). Spatial and temporal distribution of the root system and root nutrient content of an established *Miscanthus* crop. *Eur. J. Agron.* 11, 301–309. doi: 10.1016/S1161-0301(99)00031-3

Ourry, A., Bigot, J., and Boucaud, J. (1989). Protein mobilization from stubble and roots, and proteolytic activities during post-clipping regrowth of perennial ryegrass. *J. Plant Physiol.* 134, 298–303. doi: 10.1016/S0176-1617(89)80246-9

Ourry, A., Boucaud, J., and Salette, J. (1990). Partitioning and remobilization of nitrogen during regrowth in nitrogen-deficient ryegrass. *Crop Sci.* 30, 1251–1254. doi: 10.2135/cropsci1990.0011183X003000060019x

Patton, A. J., Cunningham, S. M., Volenec, J. J., and Reicher, Z. J. (2007). Differences in freeze tolerance of zoysiagrasses: I. Role of proteins. *Crop Sci.* 47, 2162–2169. doi: 10.2135/cropsci2006.11.0739

Pedroso, G. M., Hutmacher, R. B., Putnam, D., Six, J., van Kessel, C., and Linquist, B. A. (2014). Biomass yield and nitrogen use of potential C4 and C3 dedicated energy crops in a Mediterranean climate. *Field Crops Res.* 161, 149–157. doi: 10.1016/j.fcr.2014.02.003

Rosen, H. (1957). A modified ninhydrin colorimetric analysis for amino acids. *Arch. Biochem. Biophys.* 67, 10–15. doi: 10.1016/0003-9861(57)90241-2

Strullu, L., Cadoux, S., Preudhomme, M., Jeuffroy, M.-H., and Beaudoin, N. (2011). Biomass production and nitrogen accumulation and remobilization by *Miscanthus* × *giganteus* as influenced by nitrogen stocks in belowground organs. *Field Crops Res.* 121, 381–391. doi: 10.1016/j.fcr.2011.01.005

Teixeira, E. I., Moot, D. J., and Mickelbart, M. V. (2007). Seasonal patterns of root C and N reserves of Lucerne crops (*Medicago sativa* L.) grown in a temperate climate were affected by defoliation regime. *Eur. J. Agron.* 26, 10–20.

Vance, C. P., Heichel, G. H., Barnes, D. K., Bryan, J. W., and Johnson, L. E. (1979). Nitrogen fixation, nodule development, and vegetative regrowth of alfalfa (*Medicago sativa* L.) following harvest. *Plant Physiol.* 64, 1–8. doi: 10.1104/pp.64.1.1

Volenec, J. J., Ourry, A., and Joern, B. C. (1996). A role for nitrogen reserves in forage regrowth and stress tolerance. *Physiol. Plant.* 97, 185–193. doi: 10.1111/ j.1399-3054.1996.tb00496.x

Wang, M., Han, J., Dunn, J. B., Cai, H., and Elgowainy, A. (2012). Well-to-wheels energy use and greenhouse gas emissions of ethanol from corn, sugarcane and cellulosic biomass for US use. *Environ. Res. Lett.* 7:045905. doi: 10.1088/1748-9326/7/4/045905

Wiesler, F., Dickmann, J., and Horst, W. J. (1997). Effects of nitrogen supply on growth and nitrogen uptake by *Miscanthus sinensis* during establishment. *J. Plant Nutr. Soil Sci.* 160, 25–31. doi: 10.1002/jpln.19971600107

Zhao, H., Wang, B., He, J., Yang, J., Pan, L., Sun, D., et al. (2013). Genetic diversity and population structure of *Miscanthus sinensis* germplasm in China. *PLOS ONE* 8:e75672. doi: 10.1371/journal.pone.0075672

Establishment, Growth, and Yield Potential of the Perennial Grass *Miscanthus × Giganteus* on Degraded Coal Mine Soils

Stanisław Jeżowski[1†], Michal Mos[2,3†], Sam Buckby[3], Joanna Cerazy-Waliszewska[1], Wojciech Owczarzak[4], Andrzej Mocek[2], Zygmunt Kaczmarek[1] and Jon P. McCalmont[5]*

[1] Institute of Plant Genetics, Polish Academy of Sciences, Poznań, Poland, [2] Energene Sp. z o.o., Łódź, Poland, [3] Terravesta Ltd, Cedar Farm, Lincoln, United Kingdom, [4] Department of Soil Sciences and Land Protection, Poznan University of Life Sciences, Poznań, Poland, [5] Institute of Biological, Environmental and Rural Sciences, Aberystwyth University, Aberystwyth, United Kingdom

Miscanthus × giganteus is a giant C4 grass native to Asia. Unlike most C4 species, it is relatively cold tolerant due to adaptations across a wide range of altitudes. These grasses are characterized by high productivity and low input requirements, making them excellent candidates for bioenergy feedstock production. The aim of this study was to investigate the potential for growing *Miscanthus* on extremely marginal soils, degraded by open lignite (brown coal) mining. Field experiments were established within three blocks situated on waste heaps originating from the lignite mine. Analyses were conducted over the first 3 years following *Miscanthus* cultivation, focusing on the effect of organic and mineral fertilization on crop growth, development and yield in this extreme environment. The following levels of fertilization were implemented between the blocks: the control plot with no fertilization (D0), a plot with sewage sludge (D1), a plot with an identical amount of sewage sludge plus one dose of mineral fertilizer (D2) and a plot with an identical amount of sewage sludge plus a double dose of mineral fertilizer (D3). Crop development and characteristics (plant height, tillering, and biomass yield [dry matter]) were measured throughout the study period and analyzed using Analysis of Variance (ANOVA). Significant differences were apparent between plant development and 3rd year biomass production over the course of the study (0.964 kg plant^{-1} for DO compared to 1.503 kg plant^{-1} for D1). Soil analyses conducted over the course of the experiment showed that organic carbon levels within the soil increased significantly following the cultivation of *Miscanthus*, and overall, pH decreased. With the exception of iron, macronutrient concentrations remained stable throughout. The promising yields and positive effects of *Miscanthus* on the degraded soil suggests that long term plantations on land otherwise unsuitable for agriculture may prove to be of great environmental and economic significance.

Keywords: *Miscanthus*, biomass, phyto-remediation, soil reclamation, brown fields

INTRODUCTION

There is growing European and global interest in the share of green energy within the overall energy budget of member states. In accordance with the recommendations of the European Commission, the European Union agreed to an increased contribution to total energy from renewables to on average of 20% by 2020 (The European Parliament, and the council of the European Union, 2009). Of this 20%, 60% is to be sourced from perennial energy crops (e.g., *Miscanthus*, willow, poplar, etc.), without impacting on food production. This implies that such energy crops are to be grown on more marginal agricultural land (FAO, 1999; Hastings et al., 2009; Communication from the Commission to the European Parliament, 2014), typically of poor quality and unsuitable for conventional crop cultivation. Such land is often a result of contamination through industrial activity, e.g., heavy metal burdens or general degradation by mining. In Poland, primary areas of concern are waste heaps left after opencast lignite mining. The reclamation process for such areas can be extremely challenging and prolonged since soils in those heaps are mineral, sterile rocks lacking the organic layer required to provide an optimal environment for plant growth and development.

In response to these challenges, this study tests the growth potential of *M. × giganteus (M×g)* as an aid to reclamation of open cast lignite mining areas. *M×g* is a high yielding, low input, perennial, giant grass, belonging to the group of C4 carbon pathway plants (Jeżowski, 1994, 2001; Deuter and Jeżowski, 2000; Heaton et al., 2004; Sacks et al., 2013). The potential of the crop for biomass, bioenergy and biofuel production is widely recognized (El Bassam, 1997; Deuter and Jeżowski, 1998; Lewandowski, 2006; Hastings et al., 2008; Faber and Kuś, 2009; Chung and Kim, 2012; Clifton-Brown et al., 2013). Moreover, *Miscanthus* can play a useful role in improving soil structure and levels of organic matter (Jeżowski, 1994; Majtkowski, 1998; Faber et al., 2007). The crop is characterized by extensive root/rhizome networks, that can reduce soil compaction and allow a greater water buffering capacity (Wanat et al., 2013). In addition, the plants can input relatively high levels of organic material into the soil each year (Faber et al., 2007). Approximately 30% of the total annual biomass production (leaf litter drop) will fall to the ground over winter (Lewandowski et al., 2000; Clifton-Brown et al., 2001); a significant proportion of this is re-cycled into the soil as organic matter (Hansen et al., 2004; McCalmont et al., 2017).

The primary aim of this study was to investigate the potential for growth, development and yield of *M×g* in the first 3 years following cultivation in the poor soil conditions of post mining waste heaps. The following hypotheses were tested:

H_1: *M×g* can be successfully established and produce viable yields on post mining soils after the third year of growth following preliminary reclamation measures prior to planting. H_0: Post mining land in the first few years of reclamation is not suitable for the successful establishment of *M×g*.

Additionally, it was intended to determine if the plantation of the grasses on such soils could play a useful, or even profitable role, in the reclamation of these soils following appropriate cultivation and fertilization procedures.

MATERIALS AND METHODS

Plant Material

The planted material was the clonal, *Miscanthus × giganteus* (*M×g*); a naturally occurring sterile hybrid formed through the crossing of *M. × sinensis* and *M. × sacchariflorus* (Greef and Deuter, 1993). The initial material for selection was a clone of *M×g* imported to Poznań in 1998 by the Institute of Plant Genetics, the Polish Academy of Sciences (IPG PAS) from TINPLANT GmbH in Klein Wanzleben (Germany). The best plants, selected by their yields of biomass and reproduced using rhizomes, are still growing today in the collection plot of IPG PAS.

Field Trials

Growth and yield potential of the *M×g* plants was assessed during the period from May 2012 to February 2015 at field trials established in reclaimed areas of waste heaps at the Adamów open lignite mine near Turek. This site is located at the eastern side of the Wielkopolska region (53° 43′ N, 18° 41′ E), consisting largely of mine spoil arranged in biologically inactive heaps containing few plant available nutrients. There is a distinct contrast between these sites and natural soils, which have organic, biologically active upper layers; post-mining soils, at least in the first few years, contain no organic compounds. As such, preliminary reclamation measures were applied 3 years prior to establishment. In spring of 2009, a legume mix (*Medicago sativa* ssp. *sativa*, *Medicago sativa* ssp. *media (M × varia)* Martyn) was planted at the site in an attempt to establish a suitable soil for the cultivation of *M×g*.

The *M×g* field trial was then established in early May 2012, and planted in 3 blocks, with each block divided into 4 m × 25 m (5 m × 5 m) plots planted at a density of 1 plant m^{-2} (equivalent to 10,000 plants ha^{-1}). The plots were randomized within each block to ensure the results were not skewed by environmental conditions (**Supplementary Figure S1**). One of the following four fertilization treatments, consisting of organic and supplementary mineral matter, were added to each plot prior to planting only in year 1:

D0: Control plot with no fertilization and no sewage sludge
D1: Sewage sludge only
D2: Sewage sludge + a single dose of mineral fertilizer (0.5 kg plot^{-1})
D3: Sewage sludge + a doubled dose of mineral fertilizer (1 kg plot^{-1})

In October 2011, sewage sludge, defined here as processed human waste, sourced from a municipal sewage treatment plant was applied to each experimental plot at a weight of 1 Mg; this would equate to an addition of organic matter (O.M.) at 400 Mg ha^{-1}. Polish legislation states that on agricultural land, sewage sludge is normally applied at a rate of 80–100 Mg ha^{-1}. The lack

of biologically active layer upon the mine spoil suggested that the normal rates would not be sufficient. The soil was ploghed to a depth of 30 cm and wet sewage sludge was applied by hand as an even spread and mixed with the mine spoil using a tractor and powered cultivator.

The sewage sludge met all guidelines laid out by the Polish legislation in terms of mineral and organic xenobiotics and in terms of sanitary and hygiene standards. The chemical parameters of the sewage sludge were as follows: pH 7.92, dry matter (D.M.) 19.97%, organic carbon (C org.) 336.2 g kg D.M.$^{-1}$, total nitrogen 43.36 g kg D.M.$^{-1}$, C: N ratio of 8:1 and organic matter (O.M.) 600 g kg D.M.$^{-1}$ consisting of 56% C org. Following the mixing of the sewage sludge into the soil, the chemical composition of the soil was as follows: pH 7.42, Corg 4.75 mg kg^{-1}, Norg 0.91 mg kg^{-1}, and a C:N ratio of 5:1. The additional mineral fertilization was used to test whether the addition of sewage sludge alone is sufficient for the growth and development of $M \times g$ on such poor soil. For the mineral fertilization, a mix of the Azofoska fertilizer (Azofoska Granules, GRUPA INCO S.A., Poland) was used with the following chemical composition: 13% nitrogen, 19% phosphorus, 16% potassium, 0.18% copper, 0.045% zinc, 0.27% manganese, and 0.09% boron. Fertilization was applied under deep ploghing preceding the field trial.

Over the course of the 3-year period of the study, parameters were evaluated annually. From the center of each plot, six randomly selected plants were collected for analyses: biomass yield (dry matter), plant height and tillering (stem density) were assessed for each plant. The replication of each fertilization mixture treatment gave total of 18 plants for each fertilization treatment. Plant height was measured to the top ligule (excluding the flag leaf) on the tallest stem for each plant; this is very similar to canopy height in $M \times giganteus$. For tillering measurements, only stems above 10cm were counted and stems were differentiated from a newly emerged bud by the presence of a ligule leaf. Biomass was harvested during February to March from three successive vegetated periods: 2012–2013, 2013–2014, and 2014–2015.

Soil Analyses – Analytical Methods

Soil samples were collected by 30 cm corers with a 2 cm diameter. For each plot, a total of five samples were collected; these were then mixed to form one sample before analysis was conducted. Dry mass was assessed in the organic materials (sewage sludge, compost) and in the plant material after drying in a dryer

with hot air flow (at 70°C) to constant weight. Total nitrogen was determined after sample mineralization in concentrated sulphuric acid in an open system by Kjeldahl's (e.g., Bremner, 1960) method using automatic Kjeltec II Plus set (Tecator). Organic carbon content was determined after the sample mineralization in potassium dichromate by Tiurin's method (Mebius, 1960). Ash component contents in the organic materials and plant samples were assessed after the sample mineralization in a muffle furnace (at 450°C for 5 h) and the ash dissolution in nitric acid. Phosphorus content was determined by vanadium and molybdenum method in Backman DU 640 spectrometer at wavelength 436 nm. Potassium, sodium and calcium were assessed by flame photometry (FES) and magnesium, chromium, and the other heavy metals (only in the organic materials) were determined by atomic absorption spectrometry (AAS) in PU 9100X Phillips apparatus (Ostrowska et al., 1991).

Statistical Analyses

The data were analyzed by various uni- and multivariate statistical methods (Caliński and Kaczmarek, 1973; Morrison, 1976) in two stages. In stage one a two-factor (three years and four treatments) analysis of variance (ANOVA) was used to test the null hypotheses of no differences between years or between treatments, and, the null hypothesis of no year and treatment interaction.

In stage two, a multivariate analysis of variance was used and a canonical analysis was performed to provide a graphical presentation of treatments with regards to three morphological traits (plant height, tillering and plant biomass yield). The configuration of treatments in the space of the first two canonical variables with the shortest dendrite connecting the points representing those treatments was made. The differences in plant morphology with regards to the differing treatment methods between the first and second years, and, the second and third years were also tested using Duncan's multiple range test (DMRT) (Gomez and Gomez, 1984). However, configurations of treatments in the space of the first two canonical variables (V_1 and V_2) were also performed with regards to increments in the analyzed characteristics of yield for the first year (Y1) and between successive years (Y2–Y1 and Y3–Y2) of the cultivation.

RESULTS

The $M \times g$ plants survived the first winter of 2012/2013 with 99% over wintering survival rate. Winter temperatures were not

TABLE 1 | Results of the two-way analysis of variance for structural traits of *Miscanthus*; plant height, tillering, and plant dry matter yield (*significant at $P \leq 0.05$).

Source of variation	Df (degrees of freedom)	Mean square		
		Plant height	**Tillering**	**Plant biomass yield**
Doses (D)	3	8952.64*	311.92*	10.86*
Year (Y)	2	13322.17*	6249.35*	678.17*
Interaction D × Y	6	317.68	98.44*	3.28
Error	60	324.04	35.58	4.16

low enough to seriously impact the survival rate; the November to March average temperature at the site was −4°C. Sufficient snowfall provided an insulating layer that helped to protect the vulnerable, first year plants from frost damage. Precipitation total in the growing season (from the beginning of April to the end of October) in the successive years (2012, 2013, and 2014) for the town of Turek was 405, 435, and 460 mm, respectively. Mean temperatures for each growing seasons were 15.4°C, 15.0°C, and 14.9°C.
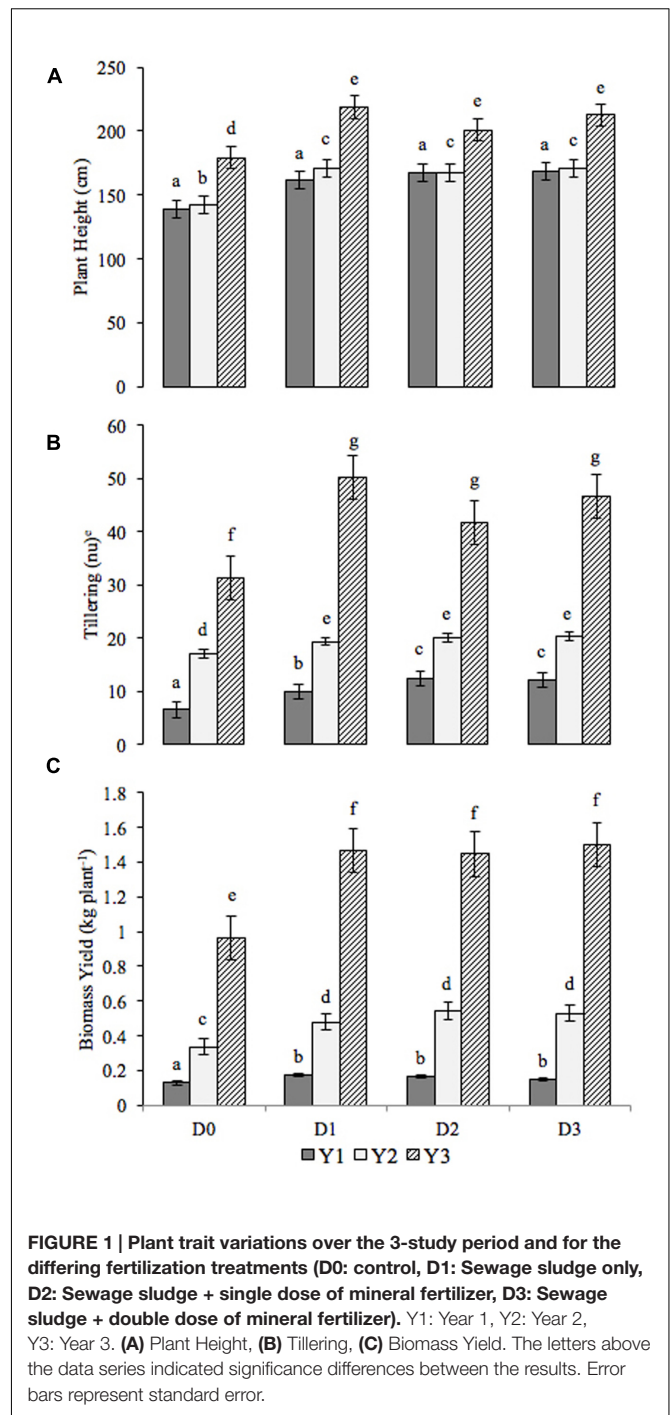
Results showed that a significant ($P<0.05$) variation in plant traits occurred with regard to the fertilization method (D) as well as the year of analyses (Y). In turn, the interaction between years of analyses and doses of fertilization (Y × D) proved significant only for plant tillering (**Table 1**).

The variation in plant traits and biomass yield for each year, and, for each fertilization method are displayed in **Figure 1**. Over the 3-year study period, the mean values (derived from the three replications) of plant traits (plant height, tillering and biomass yield) were generally significantly greater ($P < 0.05$) for the fertilized plots (D1, D2, and D3) than the control plot (D0). There are no significant differences between the individual fertilization treatments (D1, D2 and D3) across the individual years other than with regard to tillering. In year one, plots treated with municipal sewage sludge and mineral fertilizer (D2 and D3) yielded a greater number of tillers than those treated only with organic fertilization. There was however, no significant difference in tiller number between the doses (D2 and D3) of mineral fertilizer. By year three, mean plant height in the fertilized plots was 210.61 ± 9.14 cm compared to 179.33 cm in the control, tillering was 46.16 ± 4.27 stems plant^{-1} compared to 31.33 and biomass yield was 1.473 ± 0.28 kg plant^{-1} compared to 0.964 kg plant^{-1} in the fertilized and control plots, respectively.

Since the analyses were conducted across the first 3 years of plant growth and development, and covered the third year where plants might be expected to approach their full yield potential (Greef, 1996; El Bassam, 1997; Deuter and Abraham, 2000; Pude and Jeżowski, 2003; Jeżowski, 2008; Jeżowski et al., 2011); increments of increase in the investigated traits were also analyzed with regards to the fertilization levels.

Between the first and second year of cultivation (Y2–Y1), the greatest increase in plants heights were evident in the plots fertilized with only municipal sewage sludge (D1); the same remains true for the second and third years. Between year two and year three, all fertilized plots showed greater increases in plant height than the control plants. There were no significant differences in plant height relating to the method of fertilization (D1, D2 and D3).

Between year one and year two, the tillering results show that the plants in the control plot grew significantly more stems than those in fertilized plots. The opposite was seen between years two and three, whereby plants treated with fertilizer added significantly more stems than those which had not been treated (mean of 26.33 ± 4.58 stems plant^{-1} compared to the control 14.33 stems plant^{-1}). As is the case with plant height, there was no significant difference in tillering between fertilization techniques (D1, D2, and D3). Biomass yield increases were significantly lower between all years in the control plots

FIGURE 1 | Plant trait variations over the 3-study period and for the differing fertilization treatments (D0: control, D1: Sewage sludge only, D2: Sewage sludge + single dose of mineral fertilizer, D3: Sewage sludge + double dose of mineral fertilizer). Y1: Year 1, Y2: Year 2, Y3: Year 3. **(A)** Plant Height, **(B)** Tillering, **(C)** Biomass Yield. The letters above the data series indicated significance differences between the results. Error bars represent standard error.

compared to the fertilized plots. Between years one and two biomass yields were, on average 3.54 ± 0.44 kg plant^{-1} in the fertilized plots compared to 2.08 kg plant^{-1} in the control plots. These figures increased between year two and year three; fertilized plants gained an average of 9.55 ± 044 kg plant^{-1} compared to 6.27 kg plant^{-1} in the unfertilized control plots. Again, no significant differences were evident in the biomass yield between fertilization methods (D1, D2, and D3; **Table 2**).

TABLE 2 | Increases in the mean values of plant traits related to different fertilizer doses (D0: control, D1: Sewage sludge only, D2: Sewage sludge + single dose of mineral fertilizer, D3: Sewage sludge + double dose of mineral fertilizer) between the first and second (Y_1–Y_2) and second and third (Y_3–Y_2) years of the experiment.

Method of fertilization	Year	Plant Trait		
		Plant height (cm)	Tillering (stems number)	Plant biomass yield (kg)
D0	Y_2–Y_1	3.33a	10.50b	2.08b
D1		9.35a	9.33a	3.03a
D2		5.00a	7.50a	3.79a
D3		2.62a	8.16a	3.80a
D0	Y_3–Y_2	37.17a	14.33b	6.27b
D1		47.98a	30.83a	9.88a
D2		38.34a	21.66a	9.04a
D3		41.49a	26.33a	9.73a

Superscripts denote significant differences between results (P < 0.05).

A more in-depth interpretation of the recorded results was provided by the application of the analysis of canonical variables V1 and V2. This facilitated a graphic presentation of the results with regards to the effect of individual fertilization methods (D0, D1, D2, and D3) on plant physiology (see Supplementary Data Sheet). This analysis also made it possible to plot a dendrite for the shortest linkages between these doses for the 3-year study period; graphical representations of these results can be found in the Supplementary Information presented with this study. Results of this analysis largely agreed with the ANOVA results previously presented (significant differences in the mean values of morphological and yield traits existed only between control [no fertilizer] and fertilized treatments, and, that there were generally no significant differences between fertilization methods). The only exception to this was observed for the increment of increase in plant tillering between years one and two. The analysis suggested that the application of fertilization treatment D1 (organic fertilization) gave the greatest increase in number of stems in the earlier years when compared to D2 and D3 (organic fertilization supplemented with mineral fertilization). This may also indicate that when $M{\times}g$ was approaching its full yielding potential on degraded soils (between years two and three), organic fertilization applied at an adequately high dose is the most effective treatment with regards to tillering. Supplementary mineral fertilization in this later period may have had a lesser effect due to the abundance of essential nutrients (N, P, K, C, and Mg etc.) contained within the organic fertilizer. This implies that additional mineral fertilization had only a slight effect on variation in growth, development and yield (**Figure 2**).

Throughout the study period, soil analysis was conducted to monitor the pH, organic carbon (C org), organic nitrogen (N org) and nutrient content. The pH remained relatively stable in the first 2 years, before decreasing in year three. Perhaps one of the most notable changes was the increasing C org content within the soil across all plots and fertilization doses. The results show that on the control plots (D0), where no fertilization was added, concentrations of C org increased significantly between year one and year three. This indicates that the cultivation of $M{\times}g$ naturally supplies carbon to land where organic matter may otherwise be lacking. The concentration of macronutrients

within the soil all increased significantly in the fertilized plots, but remained to most extent, at constant pre-experiment levels in unfertilized plots. The most evident exception to this was the levels of Fe; these significantly decreased between years one and three (**Figure 2**).

DISCUSSION

This current study presents the results of a simple yield and trait development trial investigating the impact of fertilizer treatment on the performance of $M{\times}g$ cultivated on reclaimed brown coal mining sites. Whilst many studies report the effect of fertilization of $M{\times}g$ on growth, development and yield when cultivated on soils classified as suitable quality for agricultural use (e.g., Greef, 1996; El Bassam, 1997; Munzer, 2000; Pude, 2000), few studies consider the growth on extremely marginal soils. Several studies (e.g., Pogrzeba et al., 2013; Nsanganwimana et al., 2016) assess the cultivation and growth of various species of miscanthus on heavy metal contaminated land, however, little attention is given with regards to degraded (biologically inactive) mine soils, or, plant growth and trait development. In Europe alone, it is estimated that mine spoil and degraded soils cover thousands of hectares (Brown et al., 2003; Augustsson et al., 2015). For this reason, the study presented here may be considered, to a certain degree, pioneering research as it opens new opportunities for the cultivation of energy grasses on extremely marginal soils, otherwise unsuitable for agricultural use (Communication from the Commission to the European Parliament, 2014). If carried out on a large scale, the growth of $M{\times}g$ on poor quality land could, in part, satisfy the demands laid out by the European Commission communication (OJ C 163 of 28 May 2014). Growing on such land presents no implications to other arable agriculture and could increase the proportion of perennial crops being utilized within the energy sector. Beyond the production of biomass, the long-term cultivation of $M{\times}g$ may also have an advantageous effect on remediation of the degraded soils on which they are grown, restoring their physico–chemical and biological equilibrium. These plants, during both the growing season and harvest, naturally condition the upper layers of degraded soil by
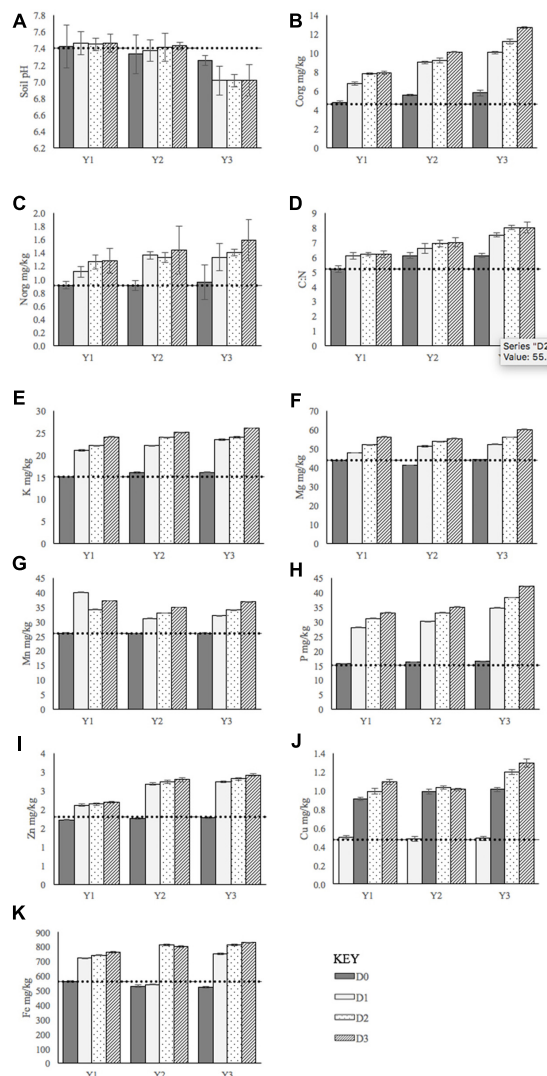
FIGURE 2 | Soil pH and concentrations of macronutrients throughout the 3-year study period. Y1: Year 1, Y2: Year 2, Y3: Year 3. **(A)** Soil pH. **(B)** Organic carbon concentration, **(C)** Organic nitrogen concentration, **(D)** Carbon to nitrogen ration, **(E)** Potassium concentration, **(F)** Magnesium concentration, **(G)** Manganese concentration, **(H)** Phosphorus concentration, **(I)** Zinc concentration, **(J)** Copper concentration, **(K)** Iron concentration. In all cases, the dashed line represents soil conditions prior to the study. Error bars represent standard error. Doses of fertilization defined as: D0: control, D1: Sewage sludge only, D2: Sewage sludge + single dose of mineral fertilizer, D3: Sewage sludge + double dose of mineral fertilizer.

supplying organic carbon through leaf drop, biomass residues and root exudates. Additionally, they aid the cycling of many other essential nutrients, e.g., N, P, K, Ca, Na, Mg, Fe, and Si (e.g., El Bassam, 1997; Himken et al., 1997; Majtkowski, 1998; Ercoli et al., 1999; Kahle et al., 2001; Kozak et al., 2006; Danalatos et al., 2007; Kalembasa and Malinowska, 2007; Borzącka-Walker, 2008; Christian et al., 2008; Curley et al., 2009). The ability of $M\times g$ to supply carbon to the soil is demonstrated within this study; organic carbon levels significantly increased in the soil

following the cultivation of the plants even without fertilization. The concentrations of most macronutrients remained relatively stable in plots where no fertilizer was added, suggesting that whilst the crop may aid in the cycling of nutrients, in most cases, it does not significantly affect the concentrations.

The results indicate that crop performance on brown coal mining sites was significantly enhanced by the application of fertilizer. The best growth, development and yields of $M\times g$ over a period of 3 years (from planting to reaching full yield by plants in the third year) were achieved by a very high dose of organic fertilization (approximately 400 Mg fresh matter ha^{-1}) contained, for example, in municipal sewage sludge. Supplemental mineral fertilization in this, case showed no significant effect. These analyses also showed that by the third year of establishment, the plants yielded around 1.5 kg D.M. $plant^{-1}$ ($\sim$15 Mg D.M. ha^{-1} at a density of 10,000 plants ha^{-1}). The results suggest that the nutrient content in the sewage sludge alone was sufficient to fulfill the requirements of $M\times g$. $M\times g$ is highly efficient with regards to nitrogen use, and as such, is typically unresponsive (in terms of harvestable yield at least) to concentrations of mineralized N above 50 kg ha^{-1} (McCalmont et al., 2017). There were no significant differences in yield ha^{-1} between the mineral fertilization doses (D1, D2, and D3). This would suggest that demand for N had been satisfied by existing mineral levels in the soil along with the nitrification of organic N added in the sewage sludge.

Contempory studies (Hastings et al., unpublished) discuss the economic viability of growing $M\times g$. Current harvest prices in the United Kingdom equate to $\sim$ €89 [exchange rate correct at time of writing] Mg^{-1} for bales with <14% moisture content. Based on this price, and the yields achieved within this study, biomass from 1 ha of $M\times g$ grown on post mining land would have a value of €1330. The cost typical of rhizome propagation in the United Kingdom is €2364–2956 ha^{-1} (Terravesta, personal communication), however, on marginal post mining soils this cost will be higher due to the preliminary work needed to establish a suitable organic soil. Harvesting costs also need to be considered; Hastings et al. (unpublished) suggest these to be €48.09 Mg^{-1} for a $\sim$13 ha field used within their study. Commercial prices are considerably cheaper; $\sim$ €29.70 Mg^{-1} (Terravesta, personal communication). Using the yields (15 Mg ha^{-1}) of this study, this would equate to harvesting costs of €436 - €721 ha^{-1} for the commercial and experimental estimates, respectively. Assuming that harvest starts in year 3, and using the more expensive experimental costing, after year 3 the overall cost incurred (propagation cost [€2956] + harvest cost [€721] – biomass value [€1330]) would be $\sim$ €2347 ha^{-1}. After initial planting there are no further establishment costs and the crop requires few inputs. Thus, if the biomass value and harvest costs remain constant, this figure decreases by €609 (biomass value – harvesting costs) each year. Therefore, using the figures provided, a plantation on reclaimed soil could be profitable after the seventh year of establishment. However, due to the nature of the land (unstable and undulating terrain), conventional forage harvest methods may have to be adapted to cut the crop at a greater height (15–20 cm rather than 10 cm). This would result in a biomass yield decrease of $\sim$0.5 Mg ha^{-1}. As such, it is

more plausible to suggest that such a plantation would become profitable after year 10. It should be stressed here, that whilst the establishment of $M \times g$ on post mining land could be profitable, its role in the reclamation of land is of great significance. This study shows that following establishment, organic content in the soil increases. Therefore, a long-term plantation (15 to 20 years) could significantly contribute to the reclamation of extremely degraded soils, on which other economically important plant species maybe grown in the future (Ussiri and Lal, 2014; Lord, 2015). Although the process of reclamation by the growth of $M \times g$ may take longer than other conventional methods, the costs associated with the process maybe greatly reduced. Estimates suggest remediation can range from €147,774–€472,876 ha^{-1} for post mining waste (English Partnerships, 2008).

The results of this study indicate that $M \times g$ shows great growth potential on land that is unsuitable for other agricultural uses. However, there are a number of factors to be considered. The dose of organic matter in the form of sewage sludge was four times that of normal agricultural application, due to the poor nature of the soil. Given the yields of the control plots ($\sim$0.9 kg plant^{-1} which equates to $\sim$9 Mg ha^{-1}), it is possible that viable yields could be achieved with much lower doses of organic fertilizer. Increasing plant density may also increase the yields of biomass per hectare. These factors are potential avenues for future work. Furthermore, the quality of the biomass produced by plants cultivated on degraded land would need to be assessed prior to commercial and economic use. If the harvested biomass was to contain elevated levels of heavy metals, it would be unsuitable for combustion as this would result in the slagging and corrosion of biomass boilers (Obernberger, 1998). However, should this be the case, there are other possible feedstock applications, such as anaerobic digestion (a process where the digestate encompassing the contaminants can be contained), that could be considered (e.g., Kiesel and Lewandowski, 2015).

AUTHOR CONTRIBUTIONS

MM and SJ contributed equally to this work as the first authors (60% contributions in experimental design, data collections, and manuscript writing). MM work leader. JC-W, SB, and SO – 5% each contribution in data analyses and manuscript writing. ZK, WO, and AM – 5% each contribution in data analyses, experimental design, data collections, and manuscript writing. JM – 10% contribution in data analyses and manuscript writing.

ACKNOWLEDGMENTS

SUPPLEMENTARY MATERIAL

The Supplementary Material for this article can be found online at: http://journal.frontiersin.org/article/10.3389/fpls.2017.00726/full#supplementary-material

FIGURE S1 | The randomised experimental field trial design.

REFERENCES

Augustsson, A. L. M., Uddh-Söderberga, T. E., Hogmalmb, K. J., and Filipssona, M. E. M. (2015). Metal uptake by homegrown vegetables – The relative importance in human health risk assessments at contaminated sites. *Environ. Res* 138, 181–190. doi: 10.1016/j.envres.2015.01.020

Borzącka-Walker, M. (2008). *Produkcyjnośæ Miskanta (Miscanthus ssp.) w Różnych Warunkach Siedliskowych i Pogodowych [Productivity of Miscanthus ssp. under Different Habitat and Weather Conditions].* Doctoral dissertation, Institute of Soil Science and Plant Cultivation, SRI, Puławy, 1–105.

Bremner, J. M. (1960). Determination of nitrogen in soil by the Kjeldahl method. *J. Agric. Sci.* 55, 11–33. doi: 10.1017/S0021859600021572

Brown, S. L., Henry, C. L., Chaney, R. L., Compton, H., and DeVolder, P. (2003). Using municipal biosolids in combination with other residuals to restore metal-contaminated mining areas. *Plant Soil* 249, 203–215. doi: 10.1023/A:1022558013310

Caliński, T., and Kaczmarek, Z. (1973). "Metody kompleksowej analizy doświadczenia wielocechowego [Methods of comprehensive analysis of multivariate experiment],"in *Proceedings of the Third Colloquium on Methodology in Agrobiometry, PAN i PTB,* Warszawa, 258–320.

Christian, D. C., Riohe, A. B., and Yates, N. E. (2008). Growth, yield and mineral content of *Miscanthus × giganteus* grown as a biofuel for 14 successive harvest. *Ind. Crops Prod.* 28, 320–327. doi: 10.1016/j.indcrop.2008.02.009

Chung, J. H., and Kim, D. S. (2012). *Miscanthus* as a potential bioenergy crop in East Asia. *J. Crop Sci. Biotechnol.* 15, 65–77. doi: 10.1007/s12892-012-0023-0

Clifton-Brown, J., Robson, P., Davey, C., Farrar, K., Hayes, C., Huang, L., et al. (2013). "Breeding Miscanthus for bioenergy," in *Bioenergy Feedstocks: Breeding and Genetics*, eds M. Saha, H. S. Bhandari, and J. H. Bouton (Hoboken, NJ: John Wiley & Sons, Inc), 67–81. doi: 10.1002/9781118609477.ch5

Clifton-Brown, J. C., Lewandowski, I., Andersson, B., Basch, G., Christian, D. G., Kjeldsen, J. B., et al. (2001). Performance of 15 *Miscanthus* genotypes at five sites in Europe. *Agron. J.* 93, 1013–1019. doi: 10.2134/agronj2001.9351013x

Communication from the Commission to the European Parliament (2014). A policy framework for climate and energy for the period from 2020 to 2030. Brussels: European Commission, 1–27.

Curley, E. M., O' Flynn, M. G., and McDonell, K. P. (2009). Nitrate leaching losses from *Miscanthus × giganteus* impact on groundwater quality. *J. Agron.* 8, 107–112. doi: 10.3923/ja.2009.107.112

Danalatos, N. G., Archontoulis, S. V., and Mitsios, I. (2007). Potential growth and biomass productivity of *Miscanthus × giganteus* as affected by plant density and N-fertilization in central Greece. *Biomass Bioenergy* 31, 145–152. doi: 10.1016/j.biombioe.2006.07.004

Deuter, M., and Abraham, J. (2000). *Wiessenstand in der Miscanthus*. Universtat in Bonn. Beitrage zu agrarwissenschaften. *Band* 19, 8–14.

Deuter, M., and Jeżowski, S. (1998). Szanse i problem hodowli traw z rodzaju *Miscanthus* jako roślin alternatywnych [Chances and problems for growing grasses from the genus Miscanthus as alternative plants]. *Hodowla Nasiennictwo* 4, 45–48.

Deuter, M., and Jeżowski, S. (2000). Breeding conditions of the giant grasses Miscanthus genus Post. *Nauk Rol.* 2, 59–67.

El Bassam, N. (1997). Renewable energy. *REU Tech. Ser.* 46, 4–196.

English Partnerships (2008). *Contamination and Dereliction Remediation Costs*. Available at: http://www.regenerate.co.uk/EP_Contamination%20&%20 Remediation%20costs.pdf [accessed February 23, 2017].

Ercoli, L., Mariotti, A., Masoni, A., and Bonari, E. (1999). Effect of Irrigation and Nitrogen Fertilization on Biomass Field and Efficiency of Energy Use in Crop Production of *Miscanthus*. *Field Crops Res.* 63, 3–11. doi: 10.1016/S0378-4290(99)00022-2

Faber, A., Borek, R., and Borzęcka–Walker, M. (2007). Szacunek sekwestracji węgla w uprawach roślin energetycznych miskanta i wierzby [Estimated carbon sequestration in cultures of energy crops Miscanthus and willow]. *Acta Agrophys.* 4, 84–89.

Faber, A., and Kuś, J. (2009). *Produkcja roślinna na cele energetyczne a racjonalne wykorzystanie rolniczej przestrzeni produkcyjnej Polski [Plant production for energy purposes and rational use of agricultural production space in Poland]*. Puławy: Wyd. IUNG-PIB, 63–75.

FAO (1999). *CGIAR Research Priorities for Marginal Lands. Consultative Group on International Agricultural Research (CGIAR)*. Available at: http://www.fao.org/Wairdocs/TAC/X5784E/x5784e00.htm#Contents [accessed January 17, 2013].

Gomez, K. A., and Gomez, A. A. (1984). *Statistical Procedures for Agricultural Research*. New York, NY: Wiley, 1–100.

Greef, J. M. (1996). Etablirung und Biomassebildung von *Miscanthus × giganteus*. Gotingen: Cuvillier Verlag, 1–162.

Greef, J. M., and Deuter, M. (1993). Syntaxonomy of *Miscanthus × giganteus* GREEF et DEU. *Angewandte Botanik* 67, 87–90.

Hansen, E. M., Christensen, B. T., Jensen, L. S., and Kristensen, K. (2004). Carbon sequestration in soil beneath long-term Miscanthus plantations as determined by 13C abundance. *Biomass Bioenergy* 26, 97–105. doi: 10.1016/S0961-9534(03)00102-8

Hastings, A., Clifton-Brown, J., Wattenbach, M., Mitchell, P., Stampfl, P., and Smith, P. (2009). Future energy potential of *Miscanthus* in Europe. *Glob. Change Biol. Bioenergy* 1, 180–196. doi: 10.1111/j.1757-1707.2009.01012.x

Hastings, A., Clifton-Brown, J., Wattenbach, M., Stampfel, P., Mitchell, P., and Smith, P. (2008). Potential of Miscanthus grasses to provide energy and hence reduce greenhouse gas emissions. *Agron. Sustain. Dev.* 28, 465–472. doi: 10.1051/agro:2008030

Heaton, E. A., Clifton-Brown, J., Voigt, T. B., Jones, M. B., and Long, S. P. (2004). Miscanthus for renewable energy generation: European Union experience and projections for Illinois. *Mitig. Adapt. Strategies Glob. Change* 9, 433–451. doi: 10.1023/B:MITI.0000038848.94134.be

Himken, M., Lammel, J., Neukirchen, D., Czypionka–Krause, U., and Olfs, H. (1997). Cultivation of *Miscanthus* under West European conditions: seasonal changes in dry matter production, nutrient uptake and remobilization. *Plant Soil* 189, 117–126. doi: 10.1023/A:1004244614537

Jeżowski, S. (1994). *Miscanthus sinensis* 'Giganteus'- a grass for industrial and energetic purpose. *Genet. Pol.* 35A, 372–337.

Jeżowski, S. (2001). Rośliny energetyczne - ogólna charakterystyka, uwarunkowania fizjologiczne i znaczenie w produkcji ekopaliwa [Energy crops – general characteristics, physiological condiitons and role in ecofuel production]. *Post. Nauk. Roln.* 2, 19–27.

Jeżowski, S. (2008). Yield traits of six clones of Miscanthus in the 3 years following planting in Poland. *Ind. Crop. Prod.* 27, 65–68. doi: 10.1016/j.indcrop.2007.07.013

Jeżowski, S., Głowacka, K., and Kaczmarek, Z. (2011). Variation in biomass yield and morphological traits of energy grasses from the genus *Miscanthus* during the first years of crop establishment. *Biomass Bioenergy* 35, 814–821. doi: 10.1016/j.biombioe.2010.11.013

Kahle, P., Beuch, S., Boelcke, B., Leinweber, P., and Schulten, H. (2001). Cropping Miscanthus in central Europe: biomass production and influence on nutrients and soil organic matter. *Eur. J. Agron.* 15, 171–184. doi: 10.1016/S1161-0301(01)00102-2

Kalembasa, D., and Malinowska, E. (2007). Wpływ dawek osadu ściekowego na plon i skład chemiczny trawy *Miscanthus sacchariflorus* [The effect of sewage sludge doses on yield and chemical composition of grass *Miscanthus sacchariflorus*]. *Fragm. Agron.* 1, 113–117.

Kiesel, A., and Lewandowski, I. (2015). Miscanthus as biogas substrate-Cutting tolerance and potential for anaerobic digestion. *GCB Bioenergy* 9, 153–167. doi: 10.1111/gcbb.12330

Kozak, K., Kotecki, A., and Dobrzański, Z. (2006). The effect of nitrogen fertilisation on growth and yield of *Miscanthus giganteus*. *Chem. Agric.* 7, 209–227.

Lewandowski, I. (2006). "Miscanthus - a multifunctional biomass crop for the future," in *Alternative Plants for Sustainable Agriculture*, eds S. Jeżowski, K. M. Wojciechowicz, and E. Zenkteler (Poznań: Institute of Plant Genetics PAS), 83–90.

Lewandowski, I., Clifton-Brown, J. C., Scurlock, J. M. O., and Huisman, W. (2000). Miscanthus: European experience with a novel energy crop. *Biomass Bioenergy* 19, 209–227. doi: 10.1016/S0961-9534(00)00032-5

Lord, R. A. (2015). Reed canarygrass (*Phalaris arundinacea*) outperforms Miscanthus or willow on marginal soils, brownfield and non-agricultural sites for local, sustainable energy crop production. *Biomass Bioenergy* 78, 110–125. doi: 10.1016/j.biombioe.2015.04.015

Majtkowski, W. (1998). Przydatnośæ wybranych gatunków traw typu C4 do upraw alternatywnych w Polsce [Suitability of selected C4 grasses for alternative cultures in Poland]. *Hod. Ros. Nas.* 2, 41–48.

McCalmont, J. P., Hastings, A., McNamara, N. P., Richter, G. M., Robson, P., Donnison, I. S., et al. (2017). Environmental costs and benefits of growing Miscanthus for bioenergy in the UK. *GCB Bioenergy.* 9, 489–507. doi: 10.1111/gcbb.12294

Mebius, L. (1960). A rapid method for the determination of organic carbon in soil. *Anal. Chim. Acta* 22, 120–124. doi: 10.1016/S0003-2670(00)88254-9

Morrison, D. F. (1976). *Multivariate Statistical Methods,* 2nd Edn. Tokyo: McGraw-Hill, 1–56.

Munzer, W. (2000). Rhizompflanzen, Alternative? Beitrage zu Agrarwissenschaften. *Unvarstat Bonn* 19, 15–20.

Nsanganwimana, F., Waterlot, C., Louvel, B., Pourrut, B., and Douay, F. (2016). Metal, nutrient and biomass accumulation during the growing cycle of Miscanthus established on metal-contaminated soils. *J. Plant Nutr. Soil Sci.* 179, 257–269. doi: 10.1002/jpln.201500163

Obernberger, I. (1998). Decentralized biomass combustion: state of the art and future development. *Biomass Bioenergy* 14, 33–56. doi: 10.1016/S0961-9534(97)00034-2

Ostrowska, A., Gawliński, S., and Szczubialka, Z. (1991). *Metody analizy i oceny właściwości gleb i roślin-katalog*. Warszawa: Wydawnictwo IOŚ.

Pogrzeba, M., Krzyżak, J., and Sas-Nowosielska, A. (2013). *Environmental Hazards Related to Miscanthus × giganteus Cultivation on Heavy Metal Contaminated Soil*. E3S Web Conf. 1:29006. doi: 10.1051/e3sconf/20130120006

Pude, R. (2000). "Anbau und rttrage von Miscanthus in Europa. Materiały konferencyjne," in Proceedings of the Polsko-niemiecka Konferencja na Temat Wykorzystania Trzciny Chińskiej, Połczyn-Zdrój, 91–95.

Pude, R., and Jeżowski, S. (2003). Effect of selected morphogenetic traits on growth and development of *Miscanthus* ssp. *Biuletyn IHAR* 227, 573–583.

Sacks, E. J., Juvik, J. A., Lin, Q., Stewart, R., and Yamada, T. (2013). "The gene pool of *Miscanthus* species and its improvement," in *Genomics of the Saccharinae*, ed. A. H. Paterson (New York, NY: Springer), 73–101.

The European Parliament, and the council of the European Union (2009). Directive 2009/28/EC of the European Parliament and of the council. *Offic. J. Euro. Union* L140, 16–62.

Ussiri, D. A., and Lal, R. (2014). Miscanthus agronomy and bioenergy feedstock potential on minesoils. *Biofuels* 5, 741–770. doi: 10.1080/17597269.2015.1024388

Wanat, N., Austruy, A., Joussein, E., et al. (2013). Potentials of *Miscanthus × giganteus* grown on highly contaminated Technosols. *J .Geochem. Explor.* 126–127, 78–84. doi: 10.1016/j.gexplo.2013.01.001

Genetic Diversity of Salt Tolerance in *Miscanthus*

Chang-Lin Chen[1,2], Hanneke van der Schoot[1], Shiva Dehghan[1], Claire L. Alvim Kamei[1,3], Kai-Uwe Schwarz[4], Heike Meyer[4], Richard G. F. Visser[1] and C. Gerard van der Linden[1]*

[1] Plant Breeding, Wageningen University and Research, Wageningen, Netherlands, [2] Graduate School Experimental Plant Science, Wageningen University and Research, Wageningen, Netherlands, [3] Department of Comparative Development and Genetics, Max Planck Institute for Plant Breeding Research, Cologne, Germany, [4] Julius Kühn-Institute, Institute for Crop and Soil Science, Braunschweig, Germany

Miscanthus is a woody rhizomatous C4 grass that can be used as a CO_2 neutral biofuel resource. It has potential to grow in marginal areas such as saline soils, avoiding competition for arable lands with food crops. This study explored genetic diversity for salt tolerance in *Miscanthus* and discovered mechanisms and traits that can be used to improve the yield under salt stress. Seventy genotypes of *Miscanthus* (including 57 *M. sinensis,* 5 *M. sacchariflorus,* and 8 hybrids) were evaluated for salt tolerance under saline (150 mM NaCl) and normal growing conditions using a hydroponic system. Analyses of shoot growth traits and ion concentrations revealed the existence of large variation for salt tolerance in the genotypes. We identified genotypes with potential for high biomass production both under control and saline conditions that may be utilized for growth under marginal, saline conditions. Several relatively salt tolerant genotypes had clearly lower Na^+ concentrations and showed relatively high K^+/Na^+ ratios in the shoots under salt stress, indicating that a Na^+ exclusion mechanism was utilized to prevent Na^+ accumulation in the leaves. Other genotypes showed limited reduction in leaf expansion and growth rate under saline conditions, which may be indicative of osmotic stress tolerance. The genotypes demonstrating potentially different salt tolerance mechanisms can serve as starting material for breeding programs aimed at improving salinity tolerance of *Miscanthus*.

Keywords: *Miscanthus*, salt tolerance, osmotic stress, ionic stress, ion homeostasis

INTRODUCTION

Miscanthus is a C4 perennial grass originating from Southeast Asia, the Pacific islands, and tropical Africa. The genus *Miscanthus* has a basic chromosome number of 19, and includes the nominally diploid species *Miscanthus sinensis* ($2N = 2x = 38$) and tetraploid species *Miscanthus sacchariflorus* ($2N = 4x = 76$) plus a triploid interspecific hybrid, *Miscanthus × giganteus* ($3n = 3x = 57$). This hybrid was identified as a good candidate for energy production by direct combustion (Zub and Brancourt-Hulmel, 2010). However, *Miscanthus × giganteus* has several disadvantages. Since *Miscanthus × giganteus* is a sterile triploid, it is difficult to improve its genetics by crossing. In addition, its sterility requires propagation from rhizomes or tissue culture, which is relatively more expensive than from seeds (Greef and Deuter, 1993). To screen and explore natural genetic diversity from other sources is therefore important for genetic improvement of the crop. A good alternative for breeding purposes is the diploid species *M. sinensis*. An important breeding goal for

any bioenergy crop and also *Miscanthus* is to achieve economically viable yields in marginal lands, thus avoiding competition with food crops and interfering with food security (Somerville et al., 2010).

High soil salinity is one of the major constraints of crop growth because it decreases crop yield and quality. Almost 20% of the world's irrigated land is adversely influenced by salinity (Flowers and Yeo, 1995; Munns and Tester, 2008; Rengasamy, 2010b; Qadir et al., 2014), and the problem of soil salinity is further increasing because of poor drainage and climatic change (Bennett and Khush, 2003). Salinity affects plant growth because of osmotic stress, ionic stress, and nutritional imbalance (Ashraf and Harris, 2004; Munns and Tester, 2008). Osmotic stress affects growth immediately and is in saline soils caused by limitation of water uptake resulting from the high salt concentration in the soil. Ionic stress develops over time and is due to ion accumulation within the shoots. Osmotic stress accounts for roughly 75% of the biomass decrease under salt stress, and ionic stress reduces it by another 20% (Munns and Tester, 2008). The strong effect of salinity on crop yield makes salinity tolerance in crops an important target for breeding. However, breeding for salt tolerance is not straightforward due to its genetic complexity.

Salt stress affects all the major processes underlying plant growth, including lipid and energy metabolism, photosynthesis, and protein synthesis (Parida and Das, 2005). This leads to reduction in transpiration, chlorophyll content, tiller number, and biomass (Hassanein, 1999; Chartzoulakis and Klapaki, 2000). The altered water status and unbalanced ion homeostasis resulting from saline conditions induce several mechanisms to reduce damage in the plant. Osmotic tolerance can be achieved by adapting water uptake properties of the roots, plant hydraulics, and by adjusting the plant's osmotic potential. Production of compatible solutes like proline (Khatkar and Kuhad, 2000), glycine betaine (Khan et al., 2000; Wang and Nii, 2000), sugars (Kerepesi and Galiba, 2000), and polyols (Bohnert et al., 1995; Zhifang and Loescher, 2003) facilitates osmotic adjustment or osmotic protection. To avoid toxic ion concentrations in shoots, plants exclude access sodium and chloride ions from the shoot. Bread wheat for instance has a low rate of Na^+ transport to the shoot and maintains a high ratio of K^+/Na^+ in the leaves, which contributes to salt tolerance, while surum wheat is more salt-sensitive due to its poor ability to exclude Na^+ from the shoot (Gorham et al., 1990). Shoot exclusion was shown to be facilitated by a members of the high-affinity K^+ transporter (HKT) family (HKT1;5) that can take Na^+ from the xylem into the parenchyma cells to minimize the accumulation of Na^+ in the shoot (Conde et al., 2011). Tissue tolerance to high salt concentrations is a mechanis often utilized by halophytes, and it can be achieved by compartmentalization of Na^+ and Cl^- in cellular organelles like the vacuoles (Adams et al., 1992) and involves tonoplast Na^+/H^+ antiporters (NHX) that regulate cytosolic Na^+ concentration and pH (Bassil et al., 2012). In mature leaves, senescence may reflect the toxic effect of high levels of Na^+ concentration and low tissue tolerance to Na^+ (Munns and James, 2003). The combination of accumulation of Na^+ in leaves, lack of necrosis, and relatively little reduction of biomass can be indicative of tissue tolerance (Munns and James, 2003; Rajendran et al., 2009).

Salt stress not only affects the quantity but also the quality of *Miscanthus* biomass. *Miscanthus* genotypes with less ions in the harvestable biomass are particularly important because high concentrations of minerals can be corrosive to combustion equipment (Jorgensen, 1997). Thus, it is essential for *Miscanthus* to produce stable biomass with low ion concentrations under salt stress. Only few studies have been done in relation to salt tolerance of *Miscanthus* (Li et al., 2014; Plazek et al., 2014; Sun et al., 2014; Stavridou et al., 2016), and *Miscanthus* may be considered a moderately salt tolerant crop with salt concentrations higher than 100 mM NaCl (approximately 10 dS/m) reducing crop yields considerably. Until now the genetic diversity of salt tolerance in *Miscanthus* germplasm has not been investigated, although Sun et al. (2014) indicate that *M. sinensis* may harbor significant genetic variation for salt tolerance. The current study aims to explore genetic diversity of *Miscanthus* breeding material to identify genotypes for cultivation in saline soils, and genotypes that harbor salt tolerance traits and can serve as material for improvement of *Miscanthus* salt tolerance. The results showed that several genotypes with relatively high salt tolerance appeared to rely on different mechanisms, offering opportunities for breeding programs aimed at improved tolerance of *Miscanthus*.

MATERIALS AND METHODS

Plant Materials

Seventy genotypes of *Miscanthus* were evaluated for salt tolerance (**Table 1**). The set included 57 *M. sinensis*, 5 *M. sacchariflorus* and eight hybrids (OPM-9 is *Miscanthus* × *giganteus*) and each genotype was cloned and propagated by tissue culture. The genotypes were supplied by different sources (Aberystwyth University, Institute for Agricultural and Fisheries Research ILVO, and Wageningen University & Research). Two genotypes were tested in a pilot experiment to establish optimal experimental conditions.

Pilot Experiment

Two genotypes (OPM-13 and OPM-38) were grown under different levels of salinity (0 mM, 125 mM, and 250 mM NaCl). The seedlings were propagated *in vitro*, transferred to the hydroponics system and allowed to acclimate for 1 week. The hydroponics system consisted of containers (22 L, 40 cm length, 30 cm width and 20 cm height) that can hold up to 12 *Miscanthus* plants. A maximum of 16 containers can be connected as a unit to a single reservoir, with capacity of 500l nutrient solution. For the pilot experiment, three units were used for the three different salt levels, each with two connected containers. The nutrient solution was half-strength modified Hoagland's solution (Supplemental Table 1), maintained at pH 5.8 and refreshed weekly. Seedlings with four leaves were selected and transferred to the hydroponics containers. Each container had two genotypes in four replications (8 plants). After 1 week of acclimation, NaCl was added to the nutrient solutions of two of the units with a 25 mM daily increment until a concentration of 125 mM NaCl. Only one of those units received two more additions of 62.5 mM NaCl to reach 250 mM NaCl. The average day/night temperatures were

TABLE 1 | *Miscanthus* genotypes screened for salt tolerance.

No.	Supplier	Genotype
OPM-4	IBERS	*M. sacchariflorus*
OPM-5	IBERS	Hybrid (*M. sinensis* × *M. sacchariflorus*)
OPM-6	IBERS	Hybrid (*M. sacchariflorus* × *M. sinensis*)
OPM-7	IBERS	Hybrid (*M. sacchariflorus* × *M. sinensis*)
OPM-8	IBERS	Hybrid (*M. sacchariflorus* × *M. sinensis*)
OPM-9	IBERS	Hybrid (*Miscanthus* × *giganteus*)
OPM-10	IBERS	Hybrid (*M. sacchariflorus* × *M. sinensis*)
OPM-11	IBERS	*M. sinensis*
OPM-13[*]	WUR	*M. sinensis*
OPM-16	IBERS	Hybrid (*M. sacchariflorus* × *M. sinensis*)
OPM-19	IBERS	*M. sacchariflorus*
OPM-20	IBERS	Hybrid (*M. sacchariflorus* × *M. sinensis*)
OPM-24	IBERS	*M. sacchariflorus*
OPM-26	IBERS	*M. sacchariflorus*
OPM-30	IBERS	*M. sinensis*
OPM-31	IBERS	*M. sinensis*
OPM-32	IBERS	*M. sinensis*
OPM-33	IBERS	*M. sinensis*
OPM-34	IBERS	*M. sacchariflorus*
OPM-37	WUR	*M. sinensis*
OPM-38[*]	WUR	*M. sinensis*
OPM-41	WUR	*M. sinensis*
OPM-42	WUR	*M. sinensis*
OPM-44	WUR	*M. sinensis*
OPM-45	WUR	*M. sinensis*
OPM-47	WUR	*M. sinensis*
OPM-48	WUR	*M. sinensis*
OPM-49	WUR	*M. sinensis*
OPM-50	WUR	*M. sinensis*
OPM-56	WUR	*M. sinensis*
OPM-57	WUR	*M. sinensis*
OPM-58	WUR	*M. sinensis*
OPM-59	WUR	*M. sinensis*
OPM-62	WUR	*M. sinensis*
OPM-64	WUR	*M. sinensis*
OPM-65	WUR	*M. sinensis*
OPM-66	WUR	*M. sinensis*
OPM-67	WUR	*M. sinensis*
OPM-68	WUR	*M. sinensis*
OPM-69	WUR	*M. sinensis*
OPM-71	WUR	*M. sinensis*
OPM-72	WUR	*M. sinensis*
OPM-73	WUR	*M. sinensis*
OPM-74	WUR	*M. sinensis*
OPM-75	WUR	*M. sinensis*
OPM-76	WUR	*M. sinensis*
OPM-77	WUR	*M. sinensis*
OPM-78	WUR	*M. sinensis*
OPM-79	WUR	*M. sinensis*
OPM-81	IBERS	*M. sinensis*
OPM-82	WUR	*M. sinensis*

(Continued)

TABLE 1 | Continued

No.	Supplier	Genotype
OPM-83	WUR	*M. sinensis*
OPM-84	WUR	*M. sinensis*
OPM-86	WUR	*M. sinensis*
OPM-87	WUR	*M. sinensis*
OPM-88	WUR	*M. sinensis*
OPM-89	WUR	*M. sinensis*
OPM-90	WUR	*M. sinensis*
OPM-91	WUR	*M. sinensis*
OPM-92	WUR	*M. sinensis*
OPM-94	WUR	*M. sinensis*
OPM-96	IBERS	*M. sinensis*
OPM-97	IBERS	*M. sinensis*
OPM-98	WUR	*M. sinensis*
OPM-99	WUR	*M. sinensis*
OPM-100	ILVO	*M. sinensis*
OPM-101	WUR	*M. sinensis*
OPM-103	WUR	*M. sinensis*
OPM-104	WUR	*M. sinensis*
OPM-107	WUR	*M. sinensis*
OPM-108	WUR	*M. sinensis*
OPM-109	IBERS	*M. sinensis*

The OPM code for the genotypes was used within the EU project OPTIMISC.
IBERS, Institute of Biological, Environmental, and Rural Sciences; Aberystwyth University, UK; ILVO, The Institute for Agricultural and Fisheries Research, Belgium; WUR, Wageningen University & Research; The Netherlands.
in pilot experiment.

set at 25/18°C, and the photoperiod regime was 16 h light and 8 h dark. Greenhouse environmental humidity was controlled at 70%. Additional lighting (100 Wm^{-2}) was used when the incoming shortwave radiation was below 200 Wm^{-2}. After 2 weeks of salt treatment the shoot dry weight and Na$^+$ and Cl$^-$ concentrations of the shoots were measured and evaluated.

Main Experiment Design

Seedlings from the 70 genotypes were propagated *in vitro* for 6 weeks, and allowed to form roots. Then they were transferred to the greenhouse and allowed to acclimate for 2 weeks on hydroponic containers in the greenhouse (Unifarm, Wageningen University & Research). Uniform seedlings with four leaves were selected and transferred to the hydroponics system for evaluation. Four independently controlled hydroponics units were used; two units for control and the other two for the salt treatment (Supplemental Figure 1), and each unit consisted of 12 connected containers that could hold 12 plants. The hydroponics system was filled with half-strength modified Hoagland's solution. After 1 week in the hydroponics system, NaCl was added to two of the four units with a 50 mM daily increment to bring the final concentration to 150 mM NaCl. The experiment had a split plot design with four replicate plants per genotype per treatment. For this, the 70 genotypes and two dummy plants were randomly assigned to the plant positions in six containers as one replication. Two replications of 70

genotypes were grown in 12 containers on each unit, to a total of four replications on two units per treatment. The nutrient solution was refreshed weekly and maintained at pH 5.8. The greenhouse conditions were similar to the pilot experiment.

Assessment of Growth Traits

During the experiment, data was collected for plant height, leaf expansion, and tiller number for all plants grown under control and saline conditions. Plant height was measured from the base of the plant to the tip of the highest leaf with a ruler at day 1, day 10 and day 17 after starting the stress treatment. Growth rate was taken as the growth in height per day, expressed as cm/day. This was calculated as the difference in plant height between two timepoints, divided by the number of days between the timepoints. To measure leaf expansion, the youngest leaf of each plant was marked at the beginning of salt treatment and the length of this leaf was measured three times, 1, 3, 5, and 7 days after starting the stress treatment. Leaf expansion rate was expressed as the average leaf length increase per day and calculated as the difference of the leaf lengths at day 7 and day 1 divided by the number of days between these measurements (expressed as cm/day). Leaf senescence was measured by visual scoring of all leaves of each plant 17 days after starting the salt treatment. Leaf senescence scale is from 1 to 9 according the percentage of senescence area (1 = no senescence, 3 = senesced area 1–30%, 5 = senesced area 30–60%, 7 = senesced areas 60–90%, 9 = senesced area >90%). At harvest, 17 days after starting the stress treatment, all seedlings from the control and salt treatments were separated into shoots and roots. Plant shoot fresh weight was measured immediately at harvest. Both plant parts were dried separately in a forced-air oven at 70°C for 2 days, and the dry weight was measured.

Ion Chromatography

For determination of the ion concentrations in the shoots and roots of each genotype, four replicated samples per genotype were ground to fine powder using a hammer mill with 1 mm sieve following the protocol described by Nguyen et al. (2013). Dry leaf and root powders (25 ± 1 mg) were ashed at 575°C for 5 h. Ashed samples were dissolved by shaking for 30 min in 1 ml 3 M formic acid at 99°C and then diluted with 9 ml MiliQ water. The samples were shaken again at 80°C for another 30 min. A final 500x dilution was subsequently prepared by mixing 0.2 ml sample solution with 9.8 ml MiliQ to assess the Na^+, K^+, Cl^-, and Ca^{2+} content of each root and leaf sample using Ion Chromatography (IC) system 850 Professional, Metrohm (Switzerland).

Statistical Analysis of Phenotypic Data

Analysis of variance (ANOVA) was done in a split plot design using Genstat 15th version. The four hydroponics units contained four replicated whole plots (schematically represented in supplementary Figure 1). The whole plots were divided in two split plots of two adjacent units. The two treatments were assigned to one of the two units in a split plot. Each split plot contained six adjacent containers as a block (2 blocks per unit, and four blocks per treatment). Within each block, genotypes were randomly distributed. The growth rate and leaf expansion of each genotype in control and saline conditions were compared by student's T-test. Correlation coefficients (r) among all the parameters were calculated. All statistical analyses were performed using the statistical software package Genstat 15th edition (VSN International Hemel Hempstead, UK).

RESULTS

Growth Responses to Salinity Stress

In a pilot experiment, two genotypes (OPM-13 and OPM-38) were grown on hydroponics at three different salt conditions (0, 125, and 250 mM NaCl). Growth of these *Miscanthus* genotypes was already affected at 125 mM (Shoot Dry Weight was reduced by 24 and 68% for OPM-38 and OPM-13, respectively, and 36 and 63% at 250 mM NaCl). At both salinity levels, Na^+ and Cl^- concentrations of the shoots were significantly increased (Supplementary Table 2). The high salt concentration of 250 mM seriously damaged the seedlings, which may confound the physiological interpretation of ion concentration data in relation to ion homeostasis. We concluded that a salt stress of 150 mM NaCl of the plants would affect growth of the plants considerably but inflict only limited damage. Therefore, we chose a salt stress level of 150 mM NaCl for identifying salt tolerant genotypes and traits contributing to salt tolerance.
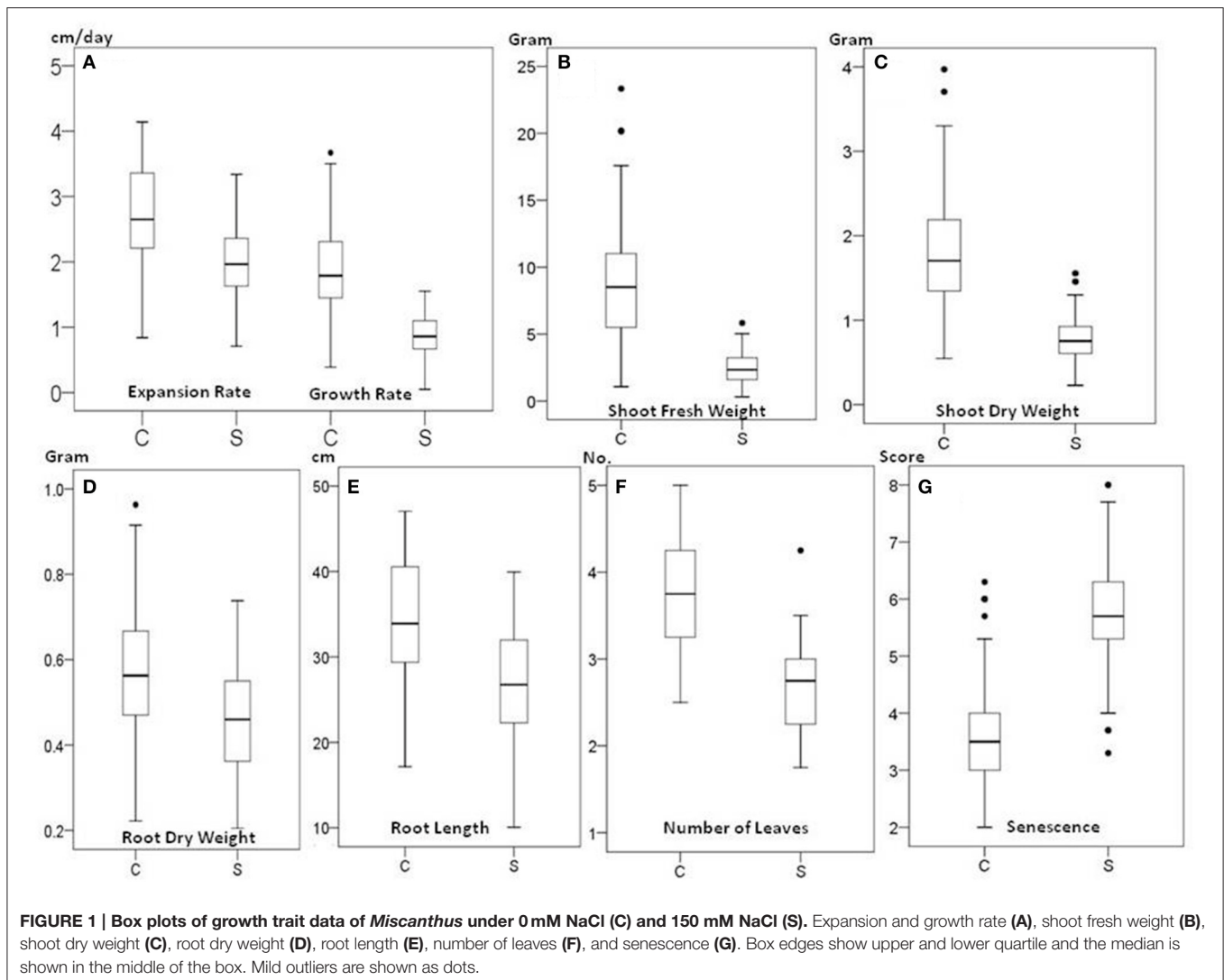
The 70 genotypes showed a wide variation in response to 150 mM NaCl salt treatment. There were significant differences in leaf expansion, growth rate, shoot fresh weight, shoot dry weight, root dry weight, root length, the number of leaves, and senescence score between the 70 genotypes ($P < 0.001$) and between control and salt treatment ($P < 0.001$) (**Figures 1A–G**). The reduction under saline conditions compared to control conditions for expansion of young leaves and growth rate in plant height was 27 and 54%, respectively. The average shoot dry weight decreased by 58% from 1.83 g under control conditions to 0.77 g under salt stress conditions. The average root dry weight was also decreased but to a lesser extent, from 0.57 g in control conditions to 0.45 g under salt stress. The average number of leaves was reduced from 3.8 to 2.6 as a result of salt stress, and senescence was increased around 1.5-fold at harvest in salt-stressed plants.

Growth Rates

The height of the salt treated plants was reduced 14–88% while the growth rate was decreased from 41 to 86% in the 70 genotypes. The growth rate of the seedlings was highly correlated to height both under salt ($r = 0.81$) and control conditions ($r = 0.94$). This trait also showed significant correlation with shoot dry weight under salinity ($r = 0.68$) and control conditions ($r = 0.76$). The growth rate of 22 genotypes was not significantly different at early stages between control and salt conditions (**Table 2**).

Leaf Expansion Rates

The leaf expansion rate of the 70 genotypes was on average reduced by 27% from 2.67 cm/day under control conditions to 1.96 cm/day under saline conditions. Expansion rate of the second young leaf showed a more marked difference between the salt-treated and control seedlings than the flag leaf. There were significant effects for genotype ($p < 0.001$), treatment

FIGURE 1 | Box plots of growth trait data of *Miscanthus* under 0 mM NaCl (C) and 150 mM NaCl (S). Expansion and growth rate **(A)**, shoot fresh weight **(B)**, shoot dry weight **(C)**, root dry weight **(D)**, root length **(E)**, number of leaves **(F)**, and senescence **(G)**. Box edges show upper and lower quartile and the median is shown in the middle of the box. Mild outliers are shown as dots.

($p < 0.001$) and genotype by treatment interaction ($p = 0.004$) for leaf expansion rate (**Table 2**). Expansion rate differences between control and salt-treated genotypes ranged from 3 to 48%. In 46 genotypes, the leaf expansion under salt stress was not significantly different from control. Leaf expansion rate significantly correlated with shoot dry weight under salinity ($r = 0.86$) and control conditions ($r = 0.82$).

Na$^+$ Accumulation in Leaves

The 70 genotypes showed large differences in leaf Na$^+$ concentration of salt-stressed plants, from 4.25 mg/g in OPM-59 to 47.22 mg/g in OPM-47, and the K$^+$/Na$^+$ ratio ranged from 5.39 in OPM-59 to 0.49 in OPM-47 (**Figure 2**, Supplementary Figure 2). Of the six genotypes with the highest Na$^+$ concentrations in the leaves (OPM-47, 49, 57, 66, 67, and 94), OPM-49 and 57 had a relatively high tiller number and low percentage of dead leaves and OPM-57 had slightly higher than average biomass (**Table 3**). This indicates that these genotypes may utilize a tissue tolerance mechanism, possibly

by accumulation of Na$^+$ in vacuoles. On the other hand, some genotypes showed low shoot sodium concentrations under salt stress. Six genotypes (OPM-4, 32, 37, 59, 69, and 71) not only showed the lowest Na$^+$ concentration but also had the highest K$^+$/Na$^+$ ratio in leaves. Additionally, these genotypes demonstrated less senescence on leaves compared with the high-Na$^+$ genotypes, relatively high biomass, and low leaf Na$^+$ /root Na$^+$ ratio. This indicates that these genotypes may utilize a shoot exclusion mechanism under saline conditions. Among these, OPM-37 was relatively tolerant and it also had the highest biomass of all genotypes under saline conditions (**Table 4**).

Ion Homeostasis Change to Salinity Stress

The boxplots in **Figures 3A,B** show the genotypic variation of the ion contents in both shoots and roots under control and salt conditions. There were significant differences in the ion concentrations ($P < 0.001$) in shoots and roots of 70 genotypes under control and salt treatment ($P < 0.001$). The interaction between genotypes and treatments was significant

TABLE 2 | Plant growth rate (plant height increase) and leaf expansion rate of leaves of miscanthus genotypes grown on hydroponics at 0 mM NaCl and 150 mM NaCl.

Genotype	Growth rate (cm/day)				Sig.	Expansion rate (cm/day)				Sig.
	0 mM		150 mM			0 mM		150 mM		
	Mean	S.D.	Mean	S.D.		Mean	S.D.	Mean(cm)	S.D.	
OPM-4	2.31	1.08	0.56	0.38	*	3.39	0.62	2.38	0.71	
OPM-5	2.98	0.36	1.38	0.31	***	3.66	0.69	2.92	0.76	
OPM-6	2.56	0.43	0.68	0.26	***	3.91	1.34	2.06	0.15	*
OPM-7	2.00	0.57	1.43	0.22		2.05	0.76	2.47	0.23	
OPM-8	2.29	0.45	0.53	0.25	***	2.46	0.95	1.54	0.24	
OPM-9	1.77	0.80	0.57	0.39	*	1.87	0.80	1.64	0.57	
OPM-10	1.51	1.13	0.71	0.50		3.28	1.29	2.36	0.95	
OPM-11	2.52	0.36	1.55	0.34	**	3.95	0.54	3.13	0.52	
OPM-16	1.99	0.89	0.90	0.43		3.62	0.93	2.23	0.40	*
OPM-19	3.50	0.78	1.36	0.25	**	4.14	0.19	2.59	0.24	***
OPM-20	2.67	0.72	1.06	0.95	*	3.89	0.61	2.67	0.61	*
OPM-24	3.10	1.27	0.78	0.47	*	3.36	1.01	2.00	1.07	
OPM-26	1.40	0.80	0.38	0.39		1.52	0.35	1.93	0.64	
OPM-30	1.81	0.52	0.86	0.47	*	2.65	0.58	1.76	0.15	*
OPM-31	1.14	0.32	0.60	0.18	*	1.94	0.71	1.67	0.44	
OPM-32	3.67	0.41	1.28	0.48	***	3.68	0.97	2.78	1.00	
OPM-33	1.11	0.31	0.42	0.12	**	1.53	0.69	0.99	0.27	
OPM-34	1.28	0.55	0.75	0.12		1.34	0.39	1.20	0.30	
OPM-37	2.27	1.00	0.95	0.52		2.82	1.28	2.37	0.70	
OPM-41	1.47	0.28	0.71	0.33	*	2.44	0.11	1.51	0.44	**
OPM-42	1.49	0.50	0.91	0.17		2.35	0.65	2.01	0.33	
OPM-44	0.81	0.68	0.40	0.30		1.81	0.49	1.65	0.31	
OPM-45	1.47	0.57	0.38	0.34	*	1.30	0.71	0.95	0.28	
OPM-47	0.39	0.16	0.05	0.03	**	0.84	0.28	0.71	0.08	
OPM-48	1.78	0.12	1.08	0.26	**	2.35	0.23	2.40	0.34	
OPM-49	1.87	0.52	0.82	0.19	**	3.14	0.44	2.06	0.15	**
OPM-50	1.44	0.39	0.58	0.49	*	3.68	1.01	2.49	0.18	
OPM-56	2.24	0.30	0.89	0.84	*	3.45	0.67	2.46	0.74	
OPM-57	3.02	0.91	0.88	0.18	**	4.10	0.51	2.39	0.27	***
OPM-58	1.57	0.52	0.61	0.46	*	2.66	0.50	1.41	0.54	*
OPM-59	2.50	0.05	1.17	0.14	***	3.56	0.25	2.41	0.20	***
OPM-62	1.54	0.42	0.46	0.34	**	2.75	0.59	1.49	0.37	*
OPM-64	1.61	0.30	1.07	0.34		2.66	0.24	1.97	0.41	*
OPM-65	2.35	0.36	1.22	0.27	**	3.13	0.37	2.10	0.18	**
OPM-66	0.96	0.12	0.82	0.14		1.54	0.08	1.49	0.27	
OPM-67	1.23	0.63	0.47	0.38		2.67	0.86	1.89	0.19	
OPM-68	0.84	0.62	0.59	0.13		1.49	0.44	1.31	0.25	
OPM-69	2.76	0.68	1.28	0.50	*	2.31	0.94	2.12	0.50	
OPM-71	2.00	0.84	1.31	0.20		3.00	0.72	2.46	0.15	
OPM-72	1.45	0.62	1.01	0.35		2.42	0.67	1.84	0.09	
OPM-73	1.61	0.92	0.90	0.41		2.22	1.38	2.54	0.65	
OPM-74	2.24	0.26	0.86	0.46	**	2.58	0.70	1.81	0.69	
OPM-75	1.65	0.17	1.11	0.24	**	2.32	0.36	1.93	0.25	
OPM-76	1.24	0.87	0.72	0.26		2.23	0.41	2.08	0.36	
OPM-77	1.83	0.45	1.00	0.49	*	2.21	0.39	1.50	0.32	*
OPM-78	2.25	0.33	1.27	0.33	**	2.70	0.93	2.13	0.81	
OPM-79	3.39	0.51	1.21	0.84	**	4.00	1.01	3.34	0.83	
OPM-81	1.42	0.39	0.68	0.20	*	2.22	0.71	1.43	0.35	

(Continued)

TABLE 2 | Continued

Genotype	Growth rate (cm/day)				Sig.	Expansion rate (cm/day)				Sig.
	0 mM		150 mM			0 mM		150 mM		
	Mean	S.D.	Mean	S.D.		Mean	S.D.	Mean(cm)	S.D.	
OPM-82	1.58	0.53	1.10	0.11		2.65	0.22	2.09	0.26	*
OPM-83	1.35	0.48	0.88	0.16		1.89	0.56	1.63	0.16	
OPM-84	1.96	0.36	1.07	0.20	**	2.85	0.41	2.31	0.12	*
OPM-86	1.80	0.20	0.83	0.28	***	2.39	0.61	1.81	0.39	
OPM-87	2.50	0.20	0.83	0.44	***	3.26	0.27	1.96	0.50	**
OPM-88	2.10	0.86	0.89	0.34	*	2.63	1.21	1.91	0.53	
OPM-89	2.48	0.14	1.15	0.08	***	3.65	0.24	2.07	0.39	***
OPM-90	1.80	0.22	0.78	0.05	***	2.88	0.38	1.96	0.10	**
OPM-91	1.78	0.45	0.74	0.38	*	2.82	0.57	1.69	0.48	*
OPM-92	2.70	0.29	1.46	0.34	***	3.74	0.38	2.35	0.16	***
OPM-94	0.88	0.42	0.50	0.38		0.94	0.58	0.87	0.30	
OPM-96	2.08	0.32	0.76	0.41	**	3.29	0.27	1.72	0.52	**
OPM-97	1.96	0.40	1.22	0.16	*	3.34	0.24	2.17	0.30	***
OPM-98	1.61	0.48	1.06	0.47		2.24	0.82	1.84	0.25	
OPM-99	1.58	0.21	0.89	0.10	***	2.65	0.39	2.25	0.75	
OPM-100	1.76	0.40	0.78	0.49	*	1.61	0.56	1.37	0.41	
OPM-13	1.17	0.64	0.61	0.44		2.18	0.32	1.62	0.39	
OPM-103	1.11	0.35	0.53	0.46		1.56	0.43	1.20	0.24	
OPM-104	1.45	0.38	0.67	0.30	*	2.21	0.46	1.70	0.49	
OPM-107	3.00	0.27	1.14	0.36	***	3.78	0.36	2.24	0.32	***
OPM-108	1.42	0.28	0.85	0.25	*	1.80	0.32	1.39	0.14	
OPM-109	2.90	0.59	1.54	0.47	*	3.51	0.95	2.41	0.59	

*, **, ***, significant at P < 0.05; 0.01; 0.001 respectively.

($P < 0.001$) for both Na^+ and Cl^- concentration under salt stress. In both shoots and roots, the Na^+ and Cl^- concentrations increased significantly under salt stress ($P < 0.001$), while $[K^+]$ and $[Ca^{2+}]$ decreased at 150 mM NaCl. In the leaves, Na^+ and Cl^- concentrations increased 4.6- and 3.1-fold under salt treatment, accumulating to 12.55 mg/g for Na^+ and 18.07 mg/g for Cl^- (**Figure 3A**) but K^+ and Ca^{2+} concentrations in the shoots under saline conditions were 0.5- and 0.6 -fold lower than those under control conditions. In the roots, Na^+ and Cl^- concentrations showed 13- and 5-fold increases under salt treatment, respectively accumulating to 37.23 mg/g for Na^+ and 19.66 mg/g for Cl^- (**Figure 3B**) while both K^+ and Ca^{2+} concentrations decreased by 50% compared with those under control conditions. Under salt stress, Na^+ concentration in the roots was much higher than in shoots (3.6-fold), while Cl^- concentration in roots was slightly higher than in shoots (1.23-fold). This indicates that these genotypes may have an active mechanism to keep the Na^+ concentration low in the shoots.

Salt Tolerant Genotypes

Salt tolerance was assessed as the percentage of shoot dry weight under saline relative to control conditions. The set of 70 genotypes grown at 150 mM NaCl in the hydroponic system showed large variation for salt tolerance, from 26% for OPM-24 to 69% for OPM-31 (**Figure 4**, Supplementary Figure 3). Salt tolerance of the commercial genotype OPM-9 (*Miscanthus* ×

giganteus) was 42%. The shoot dry weight in salt stress varied from 0.23 to 1.56 g, and from 0.55 to 3.97 g under control conditions. The reduction in shoot dry weight ranged from 30 to 73%. It is interesting to note that the genotypes with high salt tolerance (over 50%, <50% reduction in biomass) generally had relatively low biomass under control conditions. The top 10 genotypes for salt tolerance had less biomass (1.48 g) compared to overall average (1.83 g) under control conditions but the biomass was slightly higher than average (0.84 vs. 0.77 g) under salt stress (Supplementary Table 3). Those genotypes therefore were the most tolerant, but typically not the most productive under control conditions. The top 10 genotypes with high yield had on average more biomass under control conditions (2.99 vs. 1.83 g) and more biomass compared to the overall average under salt stress (1.23 vs. 0.77 g). These genotypes were still more productive under saline conditions, even if they were less tolerant to salinity (Supplementary Table 3). The genotype OPM-37 seemed to be interesting because it has the highest yield (1.56 g) under salt stress, is among the higher producers (3.16 g) under control conditions, and is relatively salt tolerant (49%).

Associations between Growth Traits and Salt

Correlations between the different physiological traits and ion concentrations are given in **Table 5**. A highly significant negative
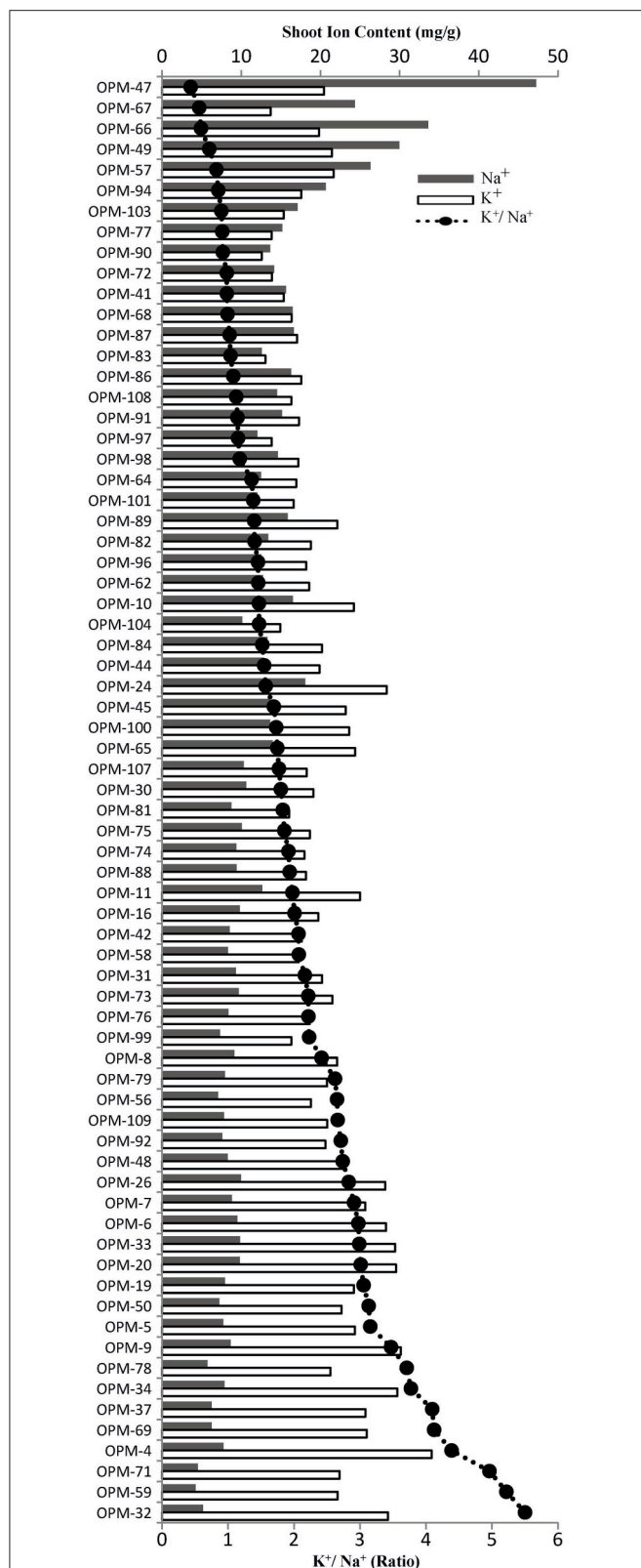
FIGURE 2 | Shoot Na$^+$ and K$^+$ concentration (gray and white bars, respectively) and shoot K$^+$/Na$^+$ ratio (line-scatter plot) in leaves of 70 Miscanthus genotypes grown under saline conditions (150 mM NaCl).

correlation of Cl$^-$ and Na$^+$ concentrations in shoots was found with growth traits (shoot dry weight, shoot fresh weight, root dry weight, and root length) under salt stress. Leaf Cl$^-$ and Na$^+$ concentrations were negatively correlated ($P < 0.001$) to the shoot biomass ($r = -0.43$ and -0.53, respectively) at 150 mM NaCl. Under salt treatment, there was a high correlation between Cl$^-$ and Na$^+$ concentrations in both leaves ($r = 0.94$) and roots ($r = 0.66$) but under control conditions there was only a weak correlation in leaves ($r = 0.26$) and no significant correlation in roots. The shoot dry weight was positively correlated with leaf expansion rate, root dry weight, growth rate, and root length under salt stress ($r = 0.86, 0.85, 0.68,$ and $0.62,$ respectively). The correlation between K$^+$ and Na$^+$ concentrations in leaves and roots were not significant under salt stress while there was weak correlation for these traits in both leaves ($r = 0.48$) and roots ($r = 0.44$) under control conditions. However, the K$^+$ concentration in leaves was positively correlated with shoot fresh weight ($r = 0.41$) and weakly correlated with shoot dry weight ($r = 0.30$) at 150 mM NaCl, similar to the correlations at 0 mM NaCl ($r = 0.4$ and 0.28, respectively). The ratio of K$^+$/Na$^+$ was positively ($P < 0.001$) related to the shoot biomass ($r = 0.56$) in all genotypes under salt treatments but it was weak ($r = 0.31$) under control conditions.

DISCUSSION

Bioenergy crops are an important alternative to fossil fuel, and a valuable addition to other alternative forms of energy (Brosse et al., 2012). Growing these crops on underutilized, marginal soils like saline soils would avoid competition with food crops for agricultural land. The potential for improvement of *Miscanthus* for salinity tolerance still remains to be established, as most research has focused only on *Miscanthus × giganteus* (Plazek et al., 2014; Stavridou et al., 2016) and genetic diversity for salinity tolerance of *Miscanthus* germplasm is largely unknown. The current study evaluated seventy *Miscanthus* genotypes under salt stress and showed that broad diversity for salt tolerance and salt tolerance traits is present in *Miscanthus*. Several highly salt tolerant genotypes utilizing different mechanisms can be considered as valuable breeding material.
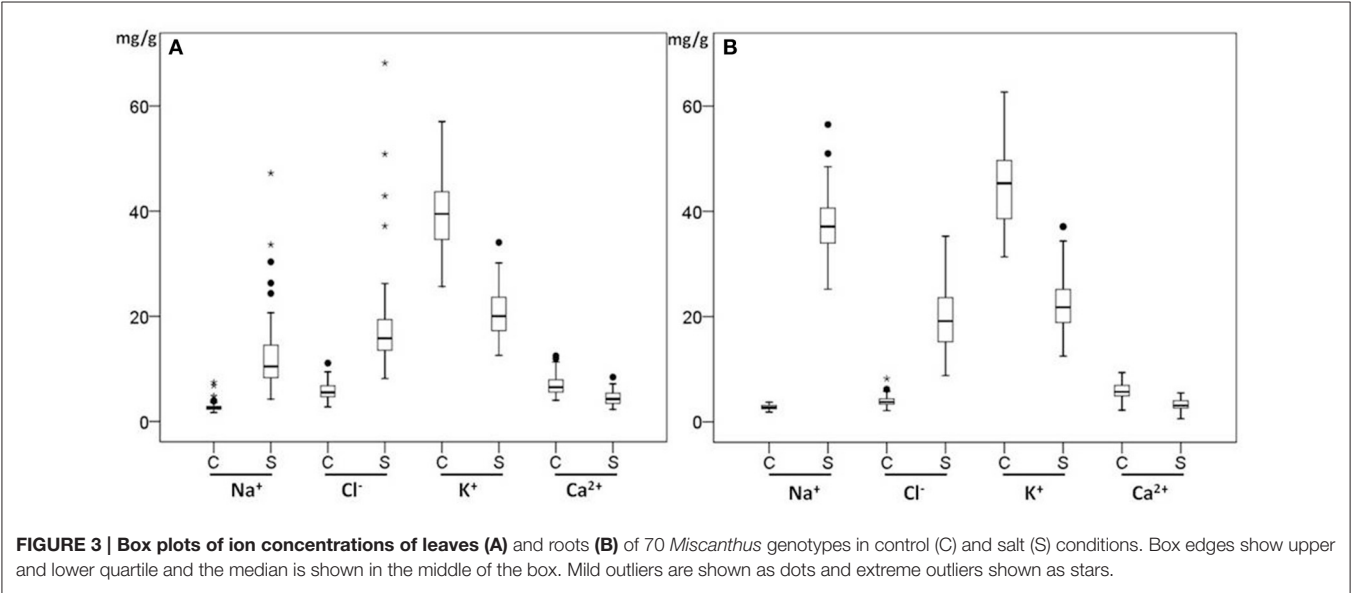
Screening System

A reliable screening system for salt tolerance traits is essential, as uniform exposure of plants to salt stress is hard to establish and control in field experiments (Munns and James, 2003; Almeida et al., 2016). Hydroponic systems supply uniform conditions for the root environment, and have a high capacity of genotypes at the same time (Nguyen et al., 2013; Chan-Navarrete et al., 2014). Using such a system, traits, and QTLs contributing to variation in salt tolerance in barley were already successfully identified (Long et al., 2013; Nguyen et al., 2013), and to variation in nitrogen use efficiency in spinach (Chan-Navarrete et al., 2016). It is important to keep in mind however that factors like soil texture and composition that in the field also may influence salinity tolerance do not play a role in this type of system. Also, root properties related to soil traits and exploration

TABLE 3 | Trait comparisons of 6 *Miscanthus* genotypes with high leaf Na$^+$ ion concentrations under salt stress, grown at 150 mM NaCl on hydroponics.

Genotype	OPM-47	OPM-49	OPM-57	OPM-66	OPM-67	OPM-94	Average of 70 genotypes
Tiller number	0	2.25	2	1.25	2.25	0	1.73
Dead leaves (%)	50	32	35	40	40	56	28
Leaf Na$^+$ (mg/g)	47.22	30.36	26.32	33.62	24.35	20.66	12.55
Root Na$^+$ (mg/g)	56.5	32.85	33.33	50.99	34.58	29.81	37.23
Leaf K$^+$ (mg/g)	20.45	21.44	21.66	19.81	13.69	17.58	20.67
Biomass (g)	0.23	0.63	0.82	0.35	0.64	0.31	0.77
Salt tolerance (%)	41	44	29	41	54	50	43
K$^+$/Na$^+$ in leaf	0.43	0.71	0.82	0.59	0.56	0.85	2.08
Leaf Na$^+$/Root Na$^+$	0.84	0.92	0.79	0.66	0.70	0.69	0.34

TABLE 4 | Trait comparisons of 6 *Miscanthus* genotypes with low leaf Na$^+$ concentrations under salt stress, grown at 150mM NaCl on hydroponics.

Genotype	OPM-4	OPM-32	OPM-37	OPM-59	OPM-69	OPM-71	Average of 70 genotypes
Tiller number	2.8	1	3	1.3	1.8	0	1.7
Dead leaves (%)	29	20	23	22	20	24	28
Leaf Na$^+$ (mg/g)	7.76	5.19	6.27	4.25	6.27	4.52	12.55
Root Na$^+$ (mg/g)	40.4	37.64	30.04	39	43	42.45	37.23
Leaf K$^+$ (mg/g)	34.05	28.53	25.68	22.17	25.85	22.41	20.67
Biomass (g)	0.79	1.13	1.56	0.96	0.88	1.05	0.77
Salt tolerance (%)	33	34	49	46	47	46	43
K$^+$/Na$^+$ in leaf	4.39	5.50	4.01	5.22	4.12	4.96	2.08
Leaf Na$^+$/Root Na$^+$	0.19	0.14	0.21	0.11	0.15	0.11	0.34

FIGURE 3 | Box plots of ion concentrations of leaves (A) and roots (B) of 70 *Miscanthus* genotypes in control (C) and salt (S) conditions. Box edges show upper and lower quartile and the median is shown in the middle of the box. Mild outliers are shown as dots and extreme outliers shown as stars.

of the soil will have a different impact on growth and yield. Another limitation of hydroponics evaluation is that it only allows screening of relatively young plants. Nevertheless, given the difficulty to maintain uniform screening conditions in a large population in the field (Tavakkoli et al., 2012), hydroponics provides a highly useful alternative. It is a fast and uniform way to identify high potential genotypes with interesting salt tolerance traits that particularly relate to ion homeostasis and other cellular

tolerance mechanisms, like osmotic adjustment and scavenging of reactive oxygen species (ROS). Indeed, several studies on salt tolerance using hydroponics systems found correlations between salt tolerance and Na$^+$ and K$^+$ concentrations in shoot (Munns and James, 2003; Jaarsma et al., 2013; Platten et al., 2013). Similarly, we identified several salt tolerant genotypes in our hydroponics-based screening with low Na$^+$ concentrations in the leaves (**Table 4**). These are likely to utilize Na$^+$ exclusion

TABLE 5 | Pearson correlations between the traits under salt stress (left lower triangle) and control (right upper triangle).

	Cl⁻ leaf	Na⁺ leaf	K⁺ leaf	Cl⁻ root	Na⁺ root	K⁺ root	K⁺/Na⁺ leaf	K⁺/Na⁺ root	Exp	GR	Height	SFW	SDW	RDW	RL	Tiller No.	Leaf No.	Sen	DL
Cl⁻ leaf	0.09	0.26	0.76	-0.09	0.31	0.00	0.26	-0.24	0.20	0.52	0.44	0.45	0.35	0.09	0.28	0.13	0.63	0.01	0.21
Na⁺ leaf	0.94	0.01	0.48	-0.21	0.20	0.17	-0.47	-0.08	-0.07	0.03	0.00	-0.02	-0.09	-0.09	0.04	-0.12	0.22	-0.04	0.05
K⁺ leaf	0.00	-0.23	0.69	-0.26	0.31	0.20	0.18	-0.12	0.18	0.44	0.34	0.40	0.28	0.07	0.20	0.19	0.56	0.08	0.23
Cl⁻ root	0.25	0.11	0.31	0.14	0.11	0.05	-0.15	-0.09	-0.13	-0.24	-0.26	-0.22	-0.19	-0.04	-0.10	-0.22	-0.25	0.18	0.21
Na⁺ root	0.37	0.26	0.13	0.66	0.23	0.44	-0.04	-0.55	0.09	0.26	0.20	0.17	0.11	0.01	0.04	0.02	0.12	0.00	0.10
K⁺ root	-0.13	-0.16	0.28	0.37	0.07	0.29	-0.05	0.44	-0.17	-0.04	-0.11	-0.09	-0.10	-0.04	-0.14	0.06	-0.07	0.17	0.14
K⁺/Na⁺ leaf	-0.43	-0.65	0.67	0.20	0.02	0.24	0.14	0.13	0.21	0.39	0.33	0.35	0.31	0.12	0.06	0.28	0.23	-0.03	-0.04
K⁺/Na⁺ root	-0.24	-0.20	0.15	-0.03	-0.48	0.82	0.16	-0.01	-0.19	-0.21	-0.21	-0.16	-0.12	-0.05	-0.17	0.11	-0.06	0.11	0.02
Exp	-0.35	-0.43	0.28	-0.21	-0.20	0.01	0.48	0.06	0.80	0.74	0.85	0.81	0.82	0.81	0.60	0.49	0.35	0.03	-0.05
GR	-0.48	-0.51	0.16	-0.09	-0.19	0.19	0.44	0.22	0.74	0.73	0.94	0.83	0.76	0.53	0.47	0.34	0.61	-0.04	-0.01
Height	-0.45	-0.52	0.25	-0.21	-0.22	0.01	0.49	0.06	0.95	0.81	0.87	0.90	0.86	0.66	0.55	0.42	0.61	-0.03	-0.04
SFW	-0.37	-0.48	0.41	-0.08	-0.12	0.14	0.57	0.13	0.84	0.73	0.88	0.88	0.98	0.74	0.56	0.52	0.66	-0.02	-0.03
SDW	-0.43	-0.53	0.30	-0.17	-0.18	0.01	0.56	0.05	0.86	0.68	0.90	0.92	0.85	0.80	0.59	0.53	0.61	-0.02	-0.06
RDW	-0.42	-0.47	0.09	-0.20	-0.19	0.04	0.40	0.08	0.81	0.65	0.83	0.80	0.85	0.81	0.73	0.38	0.27	0.00	-0.11
RL	-0.34	-0.34	-0.03	-0.18	-0.18	-0.16	0.23	-0.11	0.61	0.60	0.70	0.59	0.62	0.72	0.72	0.21	0.36	-0.01	-0.03
Tiller No.	-0.18	-0.20	0.16	-0.44	-0.35	-0.29	0.11	-0.09	0.46	0.19	0.44	0.39	0.44	0.37	0.40	0.45	0.31	0.12	0.07
Leaf No.	-0.18	-0.32	0.48	0.07	0.13	0.10	0.42	0.00	0.29	0.29	0.32	0.47	0.35	0.22	0.28	0.25	0.68	-0.01	0.09
Sen	0.41	0.54	-0.33	-0.16	0.15	-0.27	-0.59	-0.27	-0.25	-0.33	-0.30	-0.33	-0.29	-0.27	-0.22	-0.06	-0.13	0.12	0.89
DL	0.55	0.69	-0.32	0.08	0.15	-0.12	-0.61	-0.11	-0.49	-0.49	-0.55	-0.57	-0.56	-0.52	-0.41	-0.32	-0.47	0.78	0.19

The left upper to right lower corner diagonal indicates the correlation between trait values for control and saline conditions.
Sen, Senescence; DL, Dead leaves; Exp, Expansion rate; GR, Growth rate; SFW, Shoot Fresh Weight; SDW, shoot dry weight; RDW, Root dry weight; RL, Root length.
From light red to dark red, increasingly more positive correlation. From light blue to dark blue, increasingly more negative correlation.

mechanisms and may be useful genitors for salinity tolerance breeding programs. OPM-37 was even among the highest biomass producers both under control and salt conditions, and should be evaluated under field conditions as a potential high producing genotype on saline soils.

Mechanisms and Useful Traits

When grown in saline soils, plants are exposed to osmotic stress and ionic stress (Ashraf and Harris, 2004; Munns and Tester, 2008). Since osmotic and ionic stress both decrease yield and growth rate, improving salt tolerance in crops needs to take into account both osmotic tolerance and ion exclusion (Genc et al., 2010). Osmotic tolerance appears to contribute more to salt

tolerance than avoiding ion toxicity in cultivated wheat and in barley (Rengasamy, 2010a). Leaf expansion is considered a good indicator for osmotic tolerance (Rajendran et al., 2009; Farouk, 2011). In our tested *Miscanthus* genotypes, leaf expansion showed highly significant correlation with shoot dry weight ($r = 0.86$) under salinity. The relatively high variation in the leaf expansion measurements may be caused by the relatively high variation in youngest leaf length between replicates of a genotype at the start of the measurements. This may be avoided by using more replicate plants and selecting only the plants with youngest leaves of comparable lengths, but that would require either a higher capacity (number of plants) of plants, or a reduction in the number of genotypes.
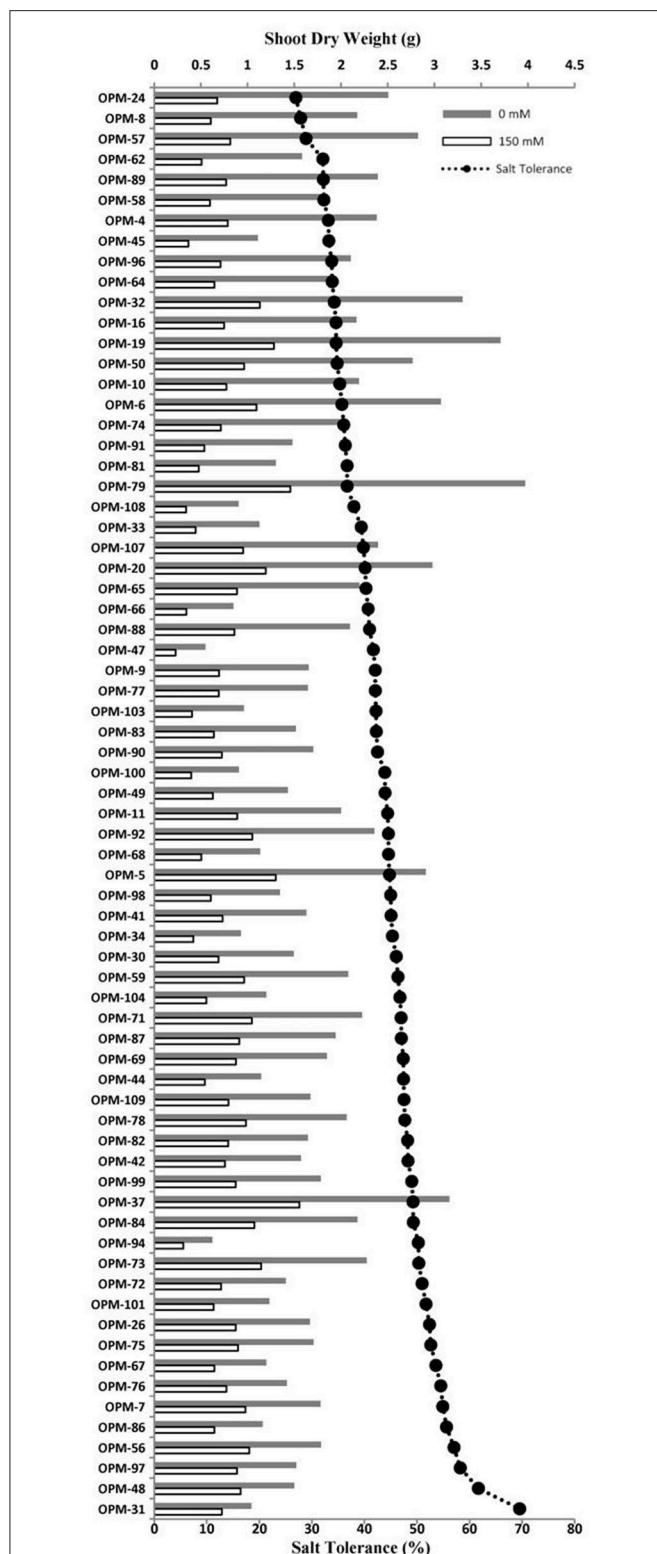
FIGURE 4 | Shoot dry weight (bars) and salt tolerance (line-scatter plot, calculated as the ratio of shoot dry weight under salt stress and shoot dry weight under control conditions) of 70 genotypes of *Miscanthus* grown in a hydroponics system at 0 mM NaCl (gray bars) and 150 mM NaCl (white bars).

The most likely candidate genotypes to have osmotic tolerance may be the ones that have both limited reduction in both leaf expansion rate and in growth rate at early stages of the stress. Forty-six of the *Miscanthus* genotypes evaluated in this study showed no significant difference in expansion rate and 22 genotypes had no significant difference in growth rate as a result of salt stress (**Table 2**). Nineteen genotypes (OPM-7, 10, 26, 34, 37, 42, 44, 66, 67, 68, 71, 72, 73, 76, 83, 94, 98, 13, and 103) had both little reduction of leaf expansion and height, which would imply that more than 25% of the tested genotypes may have some level of osmotic tolerance that minimizes the early effects of salinity.

Ion toxicity is induced by prolonged salinity due to the accumulation of ions in plant tissues, especially in the leaves (Munns and James, 2003). The leaf blades are more sensitive to ion toxicity than the roots, so adapting ion homeostasis to keep a relatively low Na^+ concentration in the leaf is important (Munns and Tester, 2008). Under salt stress, high Na^+ concentrations interfere with K^+ uptake and K^+ function (Shabala and Cuin, 2008). Maintaining a high K^+ concentration at relatively high Na^+ levels is therefore another important mechanism under salt stress, and the K^+/Na^+ ratio is considered an indicator of salt tolerance (Munns and James, 2003; Krishnamurthy et al., 2007). In a large-scale screen of 69 barley cultivars, 90% of the genotypes used an active K^+ maintenance mechanism to retain cytosolic K^+ concentrations, while 10% achieved this indirectly by efficiently excluding Na^+ from shoot (Chen et al., 2007; Schmer et al., 2008). In our evaluation, the K^+/Na^+ ratio was not only positively correlated ($r = 0.56$) to shoot dry weight in the 70 tested genotypes, but also negatively correlated ($r = -0.59$) to senescence under salt stress. Only 12 of the 70 genotypes had a K^+/Na^+ ratio of <1 (**Figure 2**), indicating that most *Miscanthus* genotypes were able to maintain a relatively high K^+ concentration compared to the Na^+ concentration.

Six genotypes with a high K^+/Na^+ ratio (more than twice the average value) had low Na^+ concentrations in the leaves (**Table 4**). Low Na^+ concentration in the shoots was successfully used as selection criteria to breed for salt tolerant cultivars in wheat, barley and rice (Lin et al., 2004; Lindsay et al., 2004; Xue et al., 2009; Genc et al., 2010; Thomson et al., 2010; Munns et al., 2012). We identified a number of genotypes with low Na^+ concentrations in the shoot and high salt tolerance, suggesting that these utilize Na^+ exclusion mechanisms similar to those used for improving salt tolerance in cereals. The genotypes with the lowest Na^+ concentrations in leaves also showed the lowest Na^+ shoot/ Na^+ root ratio (**Table 4**) implying that Na^+ is actively excluded from the shoots. The gene underlying the Na^+ exclusion introduced from wild relatives in both rice and wheat was shown to be a member of the Na^+-selective transporter HKT gene family. This HKT1;5 gene is expressed in parenchyma cells aligning the xylem in roots, and the HKT1;5 transporter was shown to filter Na^+ out of the xylem, thus preventing transport Na^+ from the roots to the shoots (Maser et al., 2002; Husain et al., 2003). Seven major and three minor alleles of OsHKT1;5 were identified in rice and the leaf Na^+ concentration was highly associated with *HKT1;5* allelic variation across diverse accessions (Platten et al., 2013). It is not unlikely that a *Miscanthus*

HKT1;5 ortholog is responsible for the variation in Na^+ shoot concentration in *Miscanthus*. It would therefore be worthwhile to study allelic variation and activity of this *Miscanthus* HKT1;5 ortholog under saline conditions in *Miscanthus* genotypes.

Because electrochemical balance is vital under stress, Cl^- and Na^+ uptake are often linked (Teakle and Tyerman, 2010). However, the Na^+ and Cl^- exclusion mechanisms are independent, with different genotypes having different mechanisms to regulate Na^+ or Cl^- transport (Teakle and Tyerman, 2010). For example, genotypes of *Glycine max* were more sensitive to Cl^- ion accumulation, but *G. soja* genotypes were more sensitive to high levels of Na^+ ions (Luo et al., 2005). In our *Miscanthus* genotypes, the average Cl^- root/shoot ratio was 1.23 but the Na^+ root/shoot ratio was 3.6 under salt treatment over 70 genotypes (**Figure 3**). This indicates that an active mechanism to avoid accumulation of Na^+ in the leaves is relatively abundant in *Miscanthus*, and a similar mechanism for Cl^- ion accumulation in the shoots is much less prevalent. Nevertheless, there was a high correlation ($r = 0.94$) between Cl^- and Na^+ concentrations in leaves and both Cl^- and Na^+ had negative correlations with shoot dry weight stress, $r = -0.43$ and $r = -0.53$ respectively (**Table 5**). It is interesting that four genotypes (OPM-59, 71, 78, and 109) showed low Cl^- concentrations (8.14–10.09 mg/g) compared with the average (18.06 mg/g) in leaves as well as a relatively high Cl^- root/shoot ratio (0.41–0.49) compared with the average (0.98). Those genotypes may have Cl^- exclusion mechanisms (Supplementary Table 4).

In the present study, two genotypes (OPM-49 and 57) also showed more tillers and less senescence even with having high shoot concentrations of Na^+ and Cl^-. This may be indicative for a tissue tolerance mechanism, with Na^+ and Cl^- compartmentalized into the vacuoles to avoid toxic concentrations within the cytoplasm (Munns and James, 2003).

Rhizome

Root traits studied in a hydroponic system may not be representative for root characteristics in the soil and the effect these have on yield (Tavakkoli et al., 2012). For a perennial with a rhizome, like *Miscanthus*, this may be even more true. Chinese ryegrass *Leymus chinensis* can adapt to salt stress by accumulating Na^+ in the rhizome (Mann et al., 2013; Li et al., 2014). A similar result was found for *Miscanthus × giganteus* in a pot experiment; the Na^+ concentration in rhizomes was 3-fold higher in the rhizome than that in shoot under 150 mM NaCl, and plants with larger rhizomes were more tolerant than plants with small rhizomes, with lower decreases in shoot dry weight under salinity (Plazek et al., 2014). This indicates that rhizomes may play an important role in salt tolerance of perennial grasses, and obviously this component of salt tolerance cannot be tested on a hydroponics system. However, keeping the limitations of the hydroponics system in mind, the advantages in terms of uniformity of plants and environmental conditions, as discussed before, can be exploited. We have shown here that identification of genetic variation for salt tolerance traits, and of mechanisms utilized by *Miscanthus* to counteract the effect of salinity can be done effectively on a hydroponics system. A selection of

genotypes with varying salt tolerance properties could thus be made, and these can be used to study salt tolerance mechanisms in more detail in soil-grown plants in pots or in the field.

Preferred Genotypes

Although *Miscanthus × giganteus* with its high yield is the most popular commercial genotype, it has several disadvantages. Firstly, its tolerance to abiotic stress is not as high as *M. sinensis* (Clifton-Brown et al., 2001). With respect to chilling tolerance, the rhizomes of *Miscanthus × giganteus* cannot survive below approximately −3°C but the hybrids of *M. sinensis* still live below −4.5°C (Clifton-Brown and Lewandowski, 2000). Shoot dry weight of *Miscanthus × giganteus* in pots was reduced by 50% after 64 days at 120 mM NaCl (Stavridou et al., 2016), while *M. sinensis* accessions exhibited <40% reduction under the same levels of salt stress (Sun et al., 2014). In our experiment, the reduction of *Miscanthus × giganteus* (OPM-9) at 150 mM NaCl for 2 weeks was 57%, which was identical to the average salt tolerance in 70 genotypes. This offers opportunities for selecting and breeding genotypes that surpass *Miscanthus × giganteus* in salt tolerance and growth on marginal, saline soils. OPM-37 for instance had the highest yield under salt stress, and OPM-31 the lowest reduction compared to yield under control conditions. The hybrids OPM-5 (*M. sinensis × M. sacchariflorus*), and OPM-7 (*M. sacchariflorus × M. sinensis*) used in our study had higher yield than *Miscanthus × giganteus* under control and salt stress as well as higher salt tolerance. These genotypes may be favorable choices for producing biomass on saline lands, and also may indicate the potential of new hybrids that combine favorable traits identified in this study. Lewandowski et al. (2016) indicated that OPM-5 and OPM-7 in a multi-location trial were not among the highest biomass producers under non-saline conditions. Whether these genotypes will be relatively good performers on saline soils remains to be established. Several genotypes had relatively high yields under both control and saline conditions, and may be preferred in soils with varying levels of salinity. These include OPM-5, OPM-6, OPM-19, OPM-20, OPM-32, OPM-37, and OPM-79. Among these seven genotypes, OPM-37, and OPM-5 have salt tolerance of 49% and 44%, respectively, just above the average (43%). These two genotypes may show osmotic mechanisms with limited reduction of the expansion rate. OPM-37 and OPM-5 had a less than average reduction in tiller number due to salt stress, and above average tiller number (3 and 3.25 respectively, while average tiller number was 1.7) under salt stress. These two genotypes have relatively high potential to be cultivated on marginal lands.

It is important to take into account how *Miscanthus* quality is used for bioenergy when choosing optimal genotypes for growth under saline conditions, or genitors for breeding programs. A low ion content of harvested material is very important for combustion quality because the high mineral content can reduce the ash melting point and cause corrosion issues, especially K^+ and Cl^- (Brosse et al., 2012). Jorgensen (1997) showed that during harvest season (spring) the K^+ and Cl^- concentrations in *M. sinensis* were reduced by 85–95% in the normal field because of relocation of minerals to storage organs and leaching by rain. However, the potential impact on combustion properties

for material grown on saline lands is largely unknown. Whether the ions accumulate in the senesced stem that is harvested still needs to be established. If the Na^+ and Cl^- accumulate in the shed leaves but not in the stems, genotypes with salt inclusion could also be considered as good genitors for breeding. If the ions still accumulate in the stems, the genotypes with salt exclusion would be preferred as starting material for breeding; OPM-59 and OPM-71 would be good candidates, with lowest concentrations of Na^+ and Cl^- under salt stress in the shoots. Another quality aspect to consider is the cell wall; stress is known to cause changes in the cell wall composition (Le Gall et al., 2015). Drought stress reduced the cellulose content but increased the hemicellulosic polysaccharides so that available cell wall polysaccharides were more easily released as fermentable sugars during processing (van der Weijde et al., 2016). However, the interaction between cell wall composition and salt stress in *Miscanthus* is still unexplored.

AUTHOR CONTRIBUTIONS

CC performed most of the experiments and wrote the paper. HV assisted with design and execution of the trials and analyses, SD performed the pilot trial, CA, KS, and HM created and provided *in vitro* material. RV contributed to the supervision, experimental strategy and discussion of the outcomes and to correcting the final manuscript, and CV supervised the study and

contributed to design, analysis, discussions, and writing of the final manuscript.

SUPPLEMENTARY MATERIAL

The Supplementary Material for this article can be found online at: http://journal.frontiersin.org/article/10.3389/fpls.2017.00187/full#supplementary-material

REFERENCES

Adams, P., Thomas, J. C., Vernon, D. M., Bohnert, H. J., and Jensen, R. G. (1992). Distinct cellular and organismic responses to salt stress. *Plant Cell Physiol.* 33, 1215–1223.

Almeida, D. M., Almadanim, M. C., Lourenço, T., Abreu, I. A., Saibo, N. J. M., and Oliveira, M. M. (2016). "Screening for abiotic stress tolerance in rice: salt, cold, and drought," in *Environmental Responses in Plants: Methods and Protocols* ed P. Duque (New York, NY: Springer), 155–182.

Ashraf, M., and Harris, P. J. C. (2004). Potential biochemical indicators of salinity tolerance in plants. *Plant Sci.* 166, 3–16. doi: 10.1016/j.plantsci.2003.10.024

Bassil, E., Coku, A., and Blumwald, E. (2012). Cellular ion homeostasis: emerging roles of intracellular NHX Na/H antiporters in plant growth and development. *J. Exp. Bot.* 63, 5727–5740. doi: 10.1093/jxb/ers250

Bennett, J., and Khush, G. S. (2003). Enhancing salt tolerance in crops through molecular breeding: a new strategy. *J. Crop Prod.* 7, 11–65. doi: 10.1300/J144v07n01_02

Bohnert, H. J., Nelson, D. E., and Jensen, R. G. (1995). Adaptations to environmental stresses. *Plant Cell* 7, 1099–1111. doi: 10.1105/tpc.7.7.1099

Brosse, N., Dufour, A., Meng, X., Sun, Q., and Ragauskas, A. (2012). *Miscanthus*: a fast-growing crop for biofuels and chemicals production. *Biofuels Bioprod. Biorefining* 6, 580–598. doi: 10.1002/bbb.1353

Chan-Navarrete, R., Dolstra, O., van Kaauwen, M., Lammerts van Bueren, E. T., and van der Linden, C. G. (2016). Genetic map construction and QTL analysis of nitrogen use efficiency in spinach (*Spinacia oleracea* L.). *Euphytica* 208, 621–636. doi: 10.1007/s10681-015-1618-6

Chan-Navarrete, R., Kawai, A., Dolstra, O., Lammerts van Bueren, E. T., and van der Linden, C. G. (2014). Genetic diversity for nitrogen use efficiency in spinach (*Spinacia oleracea* L.) cultivars using the Ingestad model on hydroponics. *Euphytica* 199, 155–166. doi: 10.1007/s10681-014-1186-1

Chartzoulakis, K., and Klapaki, G. (2000). Response of two greenhouse pepper hybrids to NaCl salinity during different growth stages. *Sci. Hortic Amsterdam* 86, 247–260. doi: 10.1016/S0304-4238(00)00151-5

Chen, Z., Zhou, M., Newman, I. A., Mendham, N. J., Zhang, G., and Shabala, S. (2007). Potassium and sodium relations in salinised barley tissues as a

basis of differential salt tolerance. *Funct. Plant Biol.* 34, 150–162. doi: 10.1071/FP06237

Clifton-Brown, J. C., and Lewandowski, I. (2000). Overwintering problems of newly established *Miscanthus* plantations can be overcome by identifying genotypes with improved rhizome cold tolerance. *New Phytol.* 148, 287–294. doi: 10.1046/j.1469-8137.2000.00764.x

Clifton-Brown, J. C., Lewandowski, I., Andersson, B., Basch, G., Christian, D. G., Kjeldsen, J. B., et al. (2001). Performance of 15 *Miscanthus* genotypes at five sites in Europe. *Agron. J.* 93, 133–139. doi: 10.2134/agronj2001.9351013x

Conde, A., Chaves, M. M., and Geros, H. (2011). Membrane transport, sensing and signaling in plant adaptation to environmental stress. *Plant Cell Physiol.* 52, 1583–1602. doi: 10.1093/pcp/pcr107

Farouk, S. (2011). Osmotic adjustment in wheat flag leaf in relation to flag leaf area and grain yield per plant. *J. Stress Physiol. Biochem.* 7, 117–138.

Flowers, T. J., and Yeo, A. R. (1995). Breeding for salinity resistance in crop plants: where next? *Aust. J. Plant Physiol.* 22, 875–884.

Genc, Y., Oldach, K., Verbyla, A., Lott, G., Hassan, M., Tester, M., et al. (2010). Sodium exclusion QTL associated with improved seedling growth in bread wheat under salinity stress. *Theor. Appl. Genet.* 121, 877–894. doi: 10.1007/s00122-010-1357-y

Gorham, J., Jones, R. G. W., and Bristol, A. (1990). Partial characterization of the trait for enhanced K^+-Na^+ discrimination in the D-genome of wheat. *Planta* 180, 590–597. doi: 10.1007/BF02411458

Greef, J. M., and Deuter, M. (1993). Syntaxonomy of *Miscanthus* X giganteus Greef-Et-Deu. *Angew. Bot.* 67, 87–90.

Hassanein, A. M. (1999). Alterations in protein and esterase patterns of peanut in response to salinity stress. *Biol. Plantarum* 42, 241–248. doi: 10.1023/A:1002112702771

Husain, S., Munns, R., and Condon, A. G. (2003). Effect of sodium exclusion trait on chlorophyll retention and growth of durum wheat in saline soil. *Aust. J. Agr. Res.* 54, 589–597. doi: 10.1071/AR03032

Jaarsma, R., de Vries, R. S. M., and de Boer, A. H. (2013). Effect of salt stress on growth, Na^+ accumulation and proline metabolism in potato (Solanum tuberosum) Cultivars. *PLoS ONE* 8:e60183. doi: 10.1371/journal.pone.0060183

Jorgensen, U. (1997). Genotypic variation in dry matter accumulation and content of N, K and Cl in *Miscanthus* in Denmark. *Biomass Bioenerg.* 12, 155–169. doi: 10.1016/S0961-9534(97)00002-0

Kerepesi, I., and Galiba, G. (2000). Osmotic and salt stress-induced alteration in soluble carbohydrate content in wheat seedlings. *Crop Sci.* 40, 482–487. doi: 10.2135/cropsci2000.402482x

Khan, M. A., Ungar, I. A., and Showalter, A. M. (2000). Effects of sodium chloride treatments on growth and ion accumulation of the halophyte *Haloxylon recurvum*. *Commun. Soil Sci. Plant* 31, 2763–2774. doi: 10.1080/00103620009370625

Khatkar, D., and Kuhad, M. S. (2000). Short-term salinity induced changes in two wheat cultivars at different growth stages. *Biol. Plantarum* 43, 629–632. doi: 10.1023/A:1002868519779

Krishnamurthy, L., Serraj, R., Hash, C. T., Dakheel, A. J., and Reddy, B.V.S. (2007). Screening sorghum genotypes for salinity tolerant biomass production. *Euphytica* 156, 15–24. doi: 10.1007/s10681-006-9343-9

Le Gall, H., Philippe, F., Domon, J.-M., Gillet, F., Pelloux, J., and Rayon, C. (2015). Cell wall metabolism in response to abiotic stress. *Plants* 4, 112–166. doi: 10.3390/plants4010112

Lewandowski, I., Clifton-Brown, J., Trindade, L. M., van der Linden, C. G., Schwarz, K.-U., Müller-Sämann, K., et al. (2016). Progress on optimizing miscanthus biomass production for the european bioeconomy: results of the eu fp7 project optimisc. *Front. Plant Sci.* 7:1620. doi: 10.3389/fpls.2016.01620

Li, X. Y., Wang, J. F., Lin, J. X., Wang, Y., and Mu, C. S. (2014). Rhizomes help the forage grass leymus chinensis to adapt to the salt and alkali stresses. *Sci. World J.* 2014:213401. doi: 10.1155/2014/213401

Lin, H. X., Zhu, M. Z., Yano, M., Gao, J. P., Liang, Z. W., Su, W. A., et al. (2004). QTLs for Na$^+$ and K$^+$ uptake of the shoots and roots controlling rice salt tolerance. *Theor. Appl. Genet.* 108, 253–260. doi: 10.1007/s00122-003-1421-y

Lindsay, M. P., Lagudah, E. S., Hare, R. A., and Munns, R. (2004). A locus for sodium exclusion (Nax1), a trait for salt tolerance, mapped in durum wheat. *Funct. Plant Biol.* 31, 138–1114. doi: 10.1071/FP04111

Long, N. V., Dolstra, O., Malosetti, M., Kilian, B., Graner, A., Visser, R. G. F., et al. (2013). Association mapping of salt tolerance in barley (*Hordeum vulgare* L.). *Theor. Appl. Genet.* 126, 2335–2351. doi: 10.1007/s00122-013-2139-0

Luo, Q., Yu, B., and Liu, Y. (2005). Differential sensitivity to chloride and sodium ions in seedlings of Glycine max and G. soja under NaCl stress. *J. Plant Physiol.* 162, 1003–1132. doi: 10.1016/j.jplph.2004.11.008

Mann, J. J., Barney, J. N., Kyser, G. B., and DiTomaso, J. M. (2013). Root system dynamics of miscanthus x giganteus and *Panicum virgatum* in response to rainfed and irrigated conditions in california. *Bioenerg. Res.* 6, 678–687. doi: 10.1007/s12155-012-9287-y

Maser, P., Eckelman, B., Vaidyanathan, R., Horie, T., Fairbairn, D. J., Kubo, M., et al. (2002). Altered shoot/root Na$^+$ distribution and bifurcating salt sensitivity in Arabidopsis by genetic disruption of the Na$^+$ transporter AtHKTI1. *Febs Lett.* 531, 157–161. doi: 10.1016/S0014-5793(02)03488-9

Munns, R., and James, R. A. (2003). Screening methods for salinity tolerance: a case study with tetraploid wheat. *Plant Soil* 253, 201–218. doi: 10.1023/A:1024553303144

Munns, R., James, R. A., Xu, B., Athman, A., Conn, S. J., Jordans, C., et al. (2012). Wheat grain yield on saline soils is improved by an ancestral Na$^+$ transporter gene. *Nat. Biotechnol.* 30, 360–364. doi: 10.1038/nbt.2120

Munns, R., and Tester, M. (2008). Mechanisms of salinity tolerance. *Annu. Rev. Plant Biol.* 59, 651–681. doi: 10.1146/annurev.arplant.59.032607.092911

Nguyen, V. L., Ribot, S. A., Dolstra, O., Niks, R. E., Visser, R. G. F., and van der Linden, C. G. (2013). Identification of quantitative trait loci for ion homeostasis and salt tolerance in barley (*Hordeum vulgare* L.). *Mol. Breed.* 31, 137–152. doi: 10.1007/s11032-012-9777-9

Parida, A. K., and Das, A. B. (2005). Salt tolerance and salinity effects on plants: a review. *Ecotox Environ. Safe.* 60, 324–349. doi: 10.1016/j.ecoenv.2004.06.010

Platten, J. D., Egdane, J. A., and Ismail, A. M. (2013). Salinity tolerance, Na$^+$ exclusion and allele mining of HKT1;5 in *Oryza sativa* and *O. glaberrima*: many sources, many genes, one mechanism? *BMC Plant Biol.* 13:32. doi: 10.1186/1471-2229-13-32

Plazek, A., Dubert, F., Koscielniak, J., Tatrzanska, M., Maciejewski, M., Gondek, K., et al. (2014). Tolerance of *Miscanthus* x giganteus to salinity depends on initial

weight of rhizomes as well as high accumulation of potassium and proline in leaves. *Ind. Crop Prod.* 52, 278–285. doi: 10.1016/j.indcrop.2013.10.041

Qadir, M., Quillérou, E., Nangia, V., Murtaza, G., Singh, M., Thomas, R. J., et al. (2014). Economics of salt-induced land degradation and restoration. *Natl. Resour. Forum* 38, 282–295. doi: 10.1111/1477-8947.12054

Rajendran, K., Teater, M., and Roy, S. J. (2009). Quantifying the three main components of salinity tolerance in cereals. *Plant Cell Environ.* 32, 237–249. doi: 10.1111/j.1365-3040.2008.01916.x

Rengasamy, P. (2010a). Osmotic and ionic effects of various electrolytes on the growth of wheat. *Soil Res.* 48, 120–124. doi: 10.1071/SR09083

Rengasamy, P. (2010b). Soil processes affecting crop production in salt-affected soils. *Funct. Plant Biol.* 37, 613–620. doi: 10.1071/FP09249

Schmer, M. R., Vogel, K. P., Mitchell, R. B., and Perrin, R. K. (2008). Net energy of cellulosic ethanol from switchgrass. *Proc. Natl. Acad. Sci. U.S.A.* 38, 464–469. doi: 10.1073/pnas.0704767105

Shabala, S., and Cuin, T. A. (2008). Potassium transport and plant salt tolerance. *Physiol. Plantarum* 133, 651–669. doi: 10.1111/j.1399-3054.2007.01008.x

Somerville, C., Youngs, H., Taylor, C., Davis, S. C., and Long, S. P. (2010). Feedstocks for lignocellulosic biofuels. *Science* 329, 790–792. doi: 10.1126/science.1189268

Stavridou, E., Hastings, A., Webster, R. J., and Robson, P. R. H. (2016). The impact of soil salinity on the yield, composition and physiology of the bioenergy grass *Miscanthus × giganteus*. *GCB Bioenergy* 9, 92–104. doi: 10.1111/gcbb.12351

Sun, Q., Yamada, T., and Takano, T. (2014). Salinity effects on germination, growth, photosynthesis, and ion accumulation in wild *Miscanthus* sinensis anderss. *Popul. Crop Sci.* 54, 2760–2771. doi: 10.2135/cropsci2013.09.0636

Tavakkoli, E., Fatehi, F., Rengasamy, P., and McDonald, G. K. (2012). A comparison of hydroponic and soil-based screening methods to identify salt tolerance in the field in barley. *J. Exp. Bot.* 63, 3853–3867. doi: 10.1093/jxb/ers085

Teakle, N. L., and Tyerman, S. D. (2010). Mechanisms of Cl$^-$ transport contributing to salt tolerance. *Plant Cell Environ.* 33, 566–589. doi: 10.1111/j.1365-3040.2009.02060.x

Thomson, M. J., de Ocampo, M., Egdane, J., Rahman, M. A., Sajise, A. G., Adorada, D. L., et al. (2010). Characterizing the Saltol quantitative trait locus for salinity tolerance in rice. *Rice* 3, 148–160. doi: 10.1007/s12284-010-9053-8

van der Weijde, T., Huxley, L. M., Hawkins, S., Sembiring, E. H., Farrar, K., Dolstra, O., et al. (2016). Impact of drought stress on growth and quality of *Miscanthus* for biofuel production. *GCB Bioenergy.* doi: 10.1111/gcbb.12382. [Epub ahead of print].

Wang, Y., and Nii, N. (2000). Changes in chlorophyll, ribulose bisphosphate carboxylase-oxygenase, glycine betaine content, photosynthesis and transpiration in *Amaranthus tricolor* leaves during salt stress. *J. Hortic. Sci. Biotechnol.* 75, 623–627. doi: 10.1080/14620316.2000.11511297

Xue, D., Huang, Y., Zhang, X., Wei, K., Westcott, S., Li, C., et al. (2009). Identification of QTLs associated with salinity tolerance at late growth stage in barley. *Euphytica* 169, 187–196. doi: 10.1007/s10681-009-9919-2

Zhifang, G., and Loescher, W. H. (2003). Expression of a celery mannose 6-phosphate reductase in *Arabidopsis thaliana* enhances salt tolerance and induces biosynthesis of both mannitol and a glucosyl-mannitol dimer. *Plant Cell Environ.* 26, 275–283. doi: 10.1046/j.1365-3040.2003.00958.x

Zub, H. W., and Brancourt-Hulmel, M. (2010). Agronomic and physiological performances of different species of *Miscanthus*, a major energy crop. A Review. *Agron. Sustain. Dev.* 30, 201–214. doi: 10.1051/agro/2009034

Stability of Cell Wall Composition and Saccharification Efficiency in *Miscanthus* across Diverse Environments

Tim van der Weijde[1,2], Oene Dolstra[1], Richard G. F. Visser[1] and Luisa M. Trindade[1]*

[1] Wageningen UR Plant Breeding, Wageningen University and Research, Wageningen, Netherlands, [2] Graduate School Experimental Plant Sciences, Wageningen University, Wageningen, Netherlands

To investigate the potential effects of differences between growth locations on the cell wall composition and saccharification efficiency of the bioenergy crop miscanthus, a diverse set of 15 accessions were evaluated in six locations across Europe for the first 3 years following establishment. High-throughput quantification of cellulose, hemicellulose and lignin contents, as well as cellulose and hemicellulose conversion rates was achieved by combining near-infrared reflectance spectroscopy (NIRS) and biochemical analysis. Prediction models were developed and found to predict biomass quality characteristics with high accuracy. Location significantly affected biomass quality characteristics in all three cultivation years, but location-based differences decreased toward the third year as the plants reached maturity and the effect of location-dependent differences in the rate of establishment reduced. In all locations extensive variation in accession performance was observed for quality traits. The performance of the different accessions in the second and third cultivation year was strongly correlated, while accession performance in the first cultivation year did not correlate well with performance in later years. Significant genotype-by-environment (G × E) interactions were observed for most traits, revealing differences between accessions in environmental sensitivity. Stability analysis of accession performance for calculated ethanol yields suggested that selection for good and stable performance is a viable approach. Environmental influence on biomass quality is substantial and should be taken into account in order to match genotype, location and end-use of miscanthus as a lignocellulose feedstock.

Keywords: miscanthus, multi-location trial, genotype-by-environment interaction, stability, GGE biplot, biomass quality, ethanol, near-infrared spectroscopy (NIRS)

INTRODUCTION

To expedite the utilization of renewable plant biomass as an alternative to fossil fuel it is necessary to develop high yielding biomass crops producing biomass of high quality in different environments (van der Weijde et al., 2013). Several second-generation energy crops have potential as a lignocellulose feedstock for biofuel production, but one of the strongest contenders is miscanthus (Heaton et al., 2010). Miscanthus is a highly productive perennial grass with a high nutrient-use efficiency, owing to its highly efficient C4 photosynthesis system and ability to translocate minerals to underground rhizomes at the end of the cultivation year (Heaton et al., 2010). The genus

Miscanthus comprises approximately 15 different species of which *M. sinensis*, *M. sacchariflorus* and their interspecific hybrids are considered to have the highest potential for biomass production (Jones and Walsh, 2001). These miscanthus species harbor great genetic diversity and occur naturally over a large geographical range in East Asia (Clifton-Brown et al., 2008). As a result miscanthus displays a wide adaptation to different soils types and climates, which may allow its exploitation as a second generation biofuel feedstock across a broad range of environments.

However, the potential of a lignocellulose feedstock for the production of biofuel is also highly determined by the compositional quality of the biomass. Lignocellulosic biomass is mainly composed of cellulose, hemicellulosic polysaccharides and lignin (Doblin et al., 2010). The content of polysaccharides determines how much fermentable sugars are theoretically available at a maximum conversion rate of 100%. The content of lignin, on the other hand, is one of the main factors that limit the extraction of fermentable sugars from the cell wall (Chundawat et al., 2011). Lignin is a complex aromatic polymer that crosslinks to hemicellulosic polysaccharides, forming a highly impermeable matrix that imparts strength to the plant cell wall and shields cell wall polysaccharides against chemical and enzymatic hydrolysis (Himmel and Picataggio, 2008; Chundawat et al., 2011). Cell wall compositional characteristics are therefore considered important quality criteria for biofuel feedstocks and the development of improved varieties with increased polysaccharide, reduced lignin content and increased saccharification efficiency is seen as crucial to reduce the production costs of cellulosic biofuels (Wyman, 2007; Torres et al., 2016; van der Weijde et al., 2017).

There is ample scope for the development of such varieties through breeding as extensive genetic variation for cell wall composition is found in miscanthus, with contents of cellulose ranging from ∼26 to 51%, hemicellulosic polysaccharides from ∼25 to 43% and lignin from ∼5 to 15% of dry matter in senesced biomass (Allison et al., 2011; Qin et al., 2012; Zhao et al., 2014). Cell wall compositional characteristics, however, are complex polygenic traits and are commonly affected by environmental as well as genetic determinants. Cell wall biosynthesis, particularly lignin deposition, is spatially and temporally regulated during the development of the plant and like any other complex metabolic pathway it can be reprogrammed in response to environmental signals (Boerjan et al., 2003; Pauly and Keegstra, 2010). The effect of environment on miscanthus cell wall composition was first demonstrated by Hodgson and coworkers, who studied the extent of genotypic and environmentally derived variation in cell wall composition in a study at five field trial locations (Hodgson et al., 2010). They concluded that the degree of observed genotypic variation in cell wall composition indicated a high potential for breeding for biomass quality characteristics, but also stressed the significance of environmentally derived variation in cell wall composition. However, this study was only conducted for one growth year, while miscanthus is a perennial crop that exhibits considerable morphological and physiological changes following the first few years after establishment. The variation in miscanthus cell wall composition has never been examined across multiple locations and harvest years, nor is the

effect this may have on biomass quality for biofuel production. Such information may reveal important insights into the stage at which genotype performance may accurately be assessed in breeding programs, as well as into the accuracy of single location vs. multi-locational trialing of germplasm.

In this study we investigated in-depth how differences between growth locations affect biomass quality in miscanthus. To this end we studied the cell wall composition and saccharification efficiency of a set of 15 accessions across different locations and cultivation years. The test comprised 4 *M. sacchariflorus*, 5 *M. sinensis* and 6 hybrid accessions, which were evaluated for 3 years in six locations across Europe: Aberystwyth (United Kingdom, UK), Adana (Turkey, TR), Potash (Ukraine, UA), Moscow (Russia, RU), Stuttgart (Germany, DE) and Wageningen (Netherlands, NL). Our focus was on quality traits relevant to the production of bioethanol, but an increase in our understanding of cell wall composition in relation to genetic and environmental factors is relevant to many of the value-chains for which miscanthus biomass has potential. This is the first multi-year, multi-location study on biomass quality in miscanthus and these insights are highly relevant to the development of new varieties through breeding, as well as to the biorefinery industry, as we gain understanding of the compositional quality of miscanthus biomass grown across diverse environments.

MATERIALS AND METHODS

Plant Materials

Fifteen miscanthus accessions, belonging to three different miscanthus species, were used in this study; five accessions of *M. sinensis,* including the commercial cultivar "*Goliath,*" four of *M. sacchariflorus*, including the commercial cultivar "*Robustus,*" and six hybrid accessions derived from crosses between *M. sinensis* and *M. sacchariflorus*, including the commercially-used clone "*M. × giganteus*" (**Table 1**). The accessions were tested

TABLE 1 | Accession, species and propagation information of the 15 *miscanthus* accessions used in this study.

Accession	Species	Plants
OPM 1	*M. sacchariflorus*	*In vitro*
OPM 2	*M. sacchariflorus*	*In vitro*
OPM 3	*M. sacchariflorus*	*In vitro*
OPM 4	*M. sacchariflorus* "Robustus"	*In vitro*
OPM 5	Hybrid	*In vitro*
OPM 6	Hybrid	*In vitro*
OPM 7	Hybrid	*In vitro*
OPM 8	Hybrid	*In vitro*
OPM 9	Hybrid "*M. × giganteus*"	*In vitro*
OPM 10	*M. sinensis*	*In vitro*
OPM 11	*M. sinensis* "Goliath"	*In vitro*
OPM 12	*M. sinensis*	Seed
OPM 13	*M. sinensis*	Seed
OPM 14	*M. sinensis*	Seed
OPM 15	Hybrid	Seed

in a multi-location trial with six locations (**Table 2**): Aberystwyth (UK), Adana (TR), Potash (UA), Moscow (RU), Stuttgart (DE), and Wageningen (NL). For a more detailed description of the trial sites, the reader is referred to Lewandowski et al. (2016). The trials were established using a completely randomized block design with three replications per accession between April and May 2012. The planting materials used to establish the trials were clones produced by *in vitro* propagation (OPM 1-11) or seed-derived plantlets (OPM 12-15). For each of the 15 accessions 49 plantlets were planted per plot in a 7-by-7 grid (total amount of plantlets = 6 locations × 15 accessions × 3 replicated plots × 49 plantlets per plot = 13.230). The planting density was two plants per m^2, resulting in a plot size of 25 m^2. Field trials were managed without irrigation, except for the trial in Adana, in which minimal irrigation was applied in the summer of the first year to ensure plant survival. All trials were fertilized once, prior to establishment of the trials, with a single application of 44 kg P ha^{-1} and 110 kg K ha^{-1}. The trials were harvested between January and April for three consecutive years after establishment of the trials (first harvest 2013, second harvest 2014, third harvest 2015). To minimize potential border effects, for each plot only the inner nine plants (3-by-3 grid) were harvested (the two outer rows of plants of every plot being regarded as border plants), bundled and processed further. Each bundle of biomass was weighed and subsequently a ~400 gram subsample from every bundle was drawn randomly for determination of moisture content. Moisture content was determined after chopping and drying of the subsample in a forced-air oven at 60°C for 72 h and used for the calculation of dry matter yields per plot. A second ~400 gram subsample of shoots was randomly drawn from each bundle and stripped from leaves. The remaining stem material was chopped and dried in a forced-air oven at 60°C for 72 h and used for the calculation of stem dry matter yields per plot. Subsequently, the dried stem material was ground using a hammer mill with a 1-mm screen and used for biomass quality analyses [n = 810 (3 years × 6 locations × 15 accessions × 3 blocks)].

Fiber Analyses

Neutral detergent fiber (NDF), acid detergent fiber (ADF) and acid-detergent lignin contents (ADL) of stem dry matter were determined according to protocols developed by Ankom Technology (ANKOM Technology Corporation, Fairpoint, NY), which are essentially based on the work of Goering and Van Soest (Van Soest, 1967; Goering and Van Soest, 1970). NDF and ADF fractions are the residues remaining after refluxing the samples in neutral or acid detergent solutions, respectively, using an ANKOM 2000 Fiber Analyzer (ANKOM Technology Corporation, Fairpoint, NY). Acid detergent lignin was determined after 3-h hydrolysis of the ADF residue in 72% H_2SO_4 with continuous shaking. All analyses were performed in triplicate and fiber fractions were expressed in gram per kg dry matter.

Determination of Saccharification Efficiency

Saccharification efficiency of the samples was assessed by the conversion of cellulose into glucose and hemicelluloses into xylose using a mild alkaline pretreatment and enzymatic saccharification reaction, essentially as described by van der Weijde et al. (2016a). Reactions were carried out in triplicate using 500 mg subsamples per stem sample. All subsamples were incubated for 13 min with α-amylase (thermostable α-amylase, ANKOM Technology Corporation, Fairpoint, NY), followed by three 5 minincubations with warm deionized water (~60°C) in order to remove interfering soluble sugars. The remaining biomass was then subjected to a mild alkaline pretreatment, carried out in 50 ml plastic centrifuge tubes with 15 ml 2% NaOH at 50°C with constant shaking (160 RPM) for 2 h in an incubator shaker (Innova 42, New Brunswick Scientific, Enfield, CT). In this study the objective of the pretreatment was not to maximize cellulose conversion but to treat samples to better allow discrimination of genotypic differences in cellulose conversion efficiency. Pretreated samples were washed to neutral pH with deionized water (2 ×, 5 min, 50°C) and with 0.1 M sodium citrate buffer (pH 4.6, 5 min, 50°C).

Saccharification reactions were subsequently carried out according to the NREL Laboratory Analytical Procedure "Enzymatic saccharification of lignocellulosic biomass" (Selig et al., 1996). Pretreated samples were hydrolyzed for 48 h with 300 µl (25.80 mg of enzyme) of the commercial enzyme cocktail Accellerase 1500 (DuPont Industrial Biosciences,

TABLE 2 | Location characteristics and long term annual and growth season (approximated April–September) temperature and rainfall for the six trial locations.

Location name	Latitude	Longitude	Altitude (m)	Air Temperature*, °C		Rainfall*, mm	
				Annual	April to Sept	Annual	April to Sept
Aberystwyth (UK)	52.43	−4.01	39	9.7	13.8	1038	401
Adana (TR)	37	35	27	19.0	26.1	575	75
Moscow (RU)	55	37	140	4.1	14.8	644	347
Potash (UA)	48.89	30.44	237	8.9	18.5	537	300
Stuttgart (DE)	48.74	8.93	463	9.8	16.4	725	379
Wageningen (NL)	51.59	5.39	10	10.3	15.8	826	376

*Climate data for Adana, 2000–2011; for Stuttgart, 1988–1999; for Potash, 2003–2012; for Wageningen, 2002–2012; for Aberystwyth, 1954–2000, and for Moscow, 1881–1980.

Leiden, NL) supplemented with 15 μl (0.12 mg of enzyme) endo-1,4-β-xylanase M1 (EC 3.2.1.8, Megazyme International Ireland, Bray, IE) in an incubator shaker (Innova 42, New Brunswick Scientific, Enfield, CT) set at 50°C and constant shaking (160 RPM). This enzyme mixture has the following reported specific activities: endoglucanase 2200–2800 carboxymethylcellulose (CMC) Units per gram, beta-glucosidase 450–775 p-nitrophenol-beta-D-glucoside (pNPG) Units per gram and the xylanase has an endoxylanase activity of 230 Units per mg. Reactions were carried out in 44 ml 0.1 M sodium citrate buffer (pH 4.6), containing 1.3 ml of a 1% benzoate solution for the prevention of microbial contamination.

Glucose and xylose contents in the enzymatic saccharification liquors were determined using enzyme-linked D-glucose (R-Biopharm, Darmstadt, DE) and D-xylose (Megazyme International Ireland, Bray, IE) assay kits. These assays were adapted to a 96-well microplate format and the increases in sample absorption following enzyme-mediated conversion reactions were spectrophotometrically determined at 340 nm using a Bio-Rad Microplate Reader (Bio-Rad, Richmond, CA, USA). Spectrophotometric determination of each sample was done in duplicate and all absorbance measurements were corrected using blanks, containing demineralized water instead of sample solution. Glucose and xylose release was determined by calculating the glucose and xylose content, respectively, in the saccharification liquor from absorbance measurements using Equation (1).

$$Glucose/xylose\ release\ (mg) = \frac{V \times MW}{\varepsilon \times d \times v \times 1000} \times df \times \Delta Abs \quad (1)$$

where V = final well volume (3.02 ml for glucose and 2.97 ml for xylose measurement); MW = molecular weight of glucose (180.16 g/mol for glucose and 150.13 for xylose); ε = the molar extinction coefficient of NADPH or NADH for glucose and xylose measurements, respectively (6.3 L $\times$ mol^{-1} $\times$ cm^{-1}); d = light path-length (=1.016 cm); v = sample volume (0.1 ml); df = dilution factor (10 for glucose and 5 for xylose measurement); and ΔAbs = increase in sample absorbance, corrected for the increase in blank absorbance. Cellulose conversion (CelCon, %) and hemicellulose conversion (HemCon, %) rates were calculated from the release of glucose/xylose relative to the content of cellulose/hemicellulose, respectively, as detailed in Equations (2) and (3).

$$CelCon\ \% = \frac{Glucose\ release\ (mg)}{CEL \times 1.111 \times S} \times 100\% \quad (2)$$

$$HemCon\ \% = \frac{Xylose\ release\ (mg)}{HEM \times 1.136 \times S} \times 100\% \quad (3)$$

where CEL = cellulose content (in g / kg dm = mg / g dm) in the sample, calculated as described below; 1.111 = the mass conversion factor that converts cellulose to equivalent glucose (the molecular weight ratio of 180.16–162.16 g/mol for glucose and anhydro-glucose) (Dien, 2010); HEM = hemicellulose content (in g/kg dm = mg/g dm) in the sample, calculated

as described below; 1.136 = the mass conversion factor that converts xylan to equivalent xylose (the molecular weight ratio of 150.13–132.12 g/mol for xylose and anhydro-xylose) (Dien, 2010); and S = the amount of sample material in gram dry matter. Calculated ethanol yield (CEY, g / kg dm) was calculated by considering full conversion of all the released glucose and xylose into ethanol, as detailed in equation 4.

$$CEY\ (g\,/\,kg\ dm) = \frac{Glucose\ release\ (mg) \times 2 \times MwE}{S \times MwG}$$
$$+ \frac{Xylose\ release\ (mg) \times \frac{3}{5} \times MwE}{S \times MwX} \quad (4)$$

where MwE = molecular weight of ethanol (= 46.06844 g/mol); MwG = molecular weight of glucose (180.15588 g/mol); MwX = molecular weight of xylose (= 150.13 g/mol); S = the amount of sample material in gram dry matter; multiplication factors 2 and $\frac{3}{5}$ refer to the amount of ethanol molecules formed from one molecule of glucose and xylose, respectively.

Analysis of Miscanthus Biomass Using Near Infrared Spectroscopy (NIRS)

Multivariate prediction models based on near-infrared (NIR) spectral data were developed to allow high-throughput prediction of biomass quality traits. Near-infrared absorbance spectra of stem and leaf samples were obtained using a Foss DS2500 near-infrared spectrometer (Foss, Hillerød, Denmark). Averaged spectra were obtained consisting of 8 consecutive scans from 400 to 2500 nm using an interval of 2 nm using ISI-Scan software (Foss, Hillerød, Denmark). Obtained spectra were further processed by weighted multiplicative scatter correction and mathematical derivatization and smoothing treatments using WinISI 4.9 statistical software (Foss, Hillerød, Denmark). These statistical transformations of spectra help to minimize effects resulting from light scatter and differences in particle size. Parameters for derivatization and smoothing were set at 2-6-4-1, in which the first number of this mathematical procedure refers to order of derivatization, the second number to the gap in the data-points over which the derivation is applied and the third and fourth number refers to the number of data-points used in the smoothing of the first and second derivative.

For the creation of prediction models a calibration set of 250 samples was selected from the complete set of samples (n = 810): 110 samples of the first cultivation year, 80 samples of the second cultivation year and 60 samples of the third cultivation year, all selected at random or for being identified by the software as spectral outliers. The biochemical reference data and near-infrared spectra of the calibration samples were used for the development and cross-validation of prediction models using WinISI version 4.9 (Foss, Hillerød, Denmark). The prediction equations were generated using modified partial least squares regression analyses (Shenk and Westerhaus, 1991). The optimal number of principal components used for development of the prediction models was manually determined to be 8. Inclusion of more factors hardly improved the prediction models as

determined by validation and increases the risk of "over-fitting" of the data. The prediction models were validated using the squared Pearson coefficient of correlation (r^2) between predicted and biochemical data and by evaluating for these samples the standard error of cross-validation (SECV) for each of the traits (**Table 3**). As good correlations ($r > 0.82$) were found between predicted and biochemical data, and the results of cross-validation were satisfactory, the prediction models were subsequently used to determine NDF, ADF, ADL, cellulose conversion, and hemicellulose conversion for all 810 stem samples. The predicted fiber fractions were used to calculate the concentrations (in g/kg dm) of cell wall (NDF) cellulose (CEL, equals ADF - ADL), hemicellulosic polysaccharides (HEM, equals NDF - ADF) and acid-detergent lignin (LIG, equals ADL) in stem dry matter.

Statistical Analyses

General analyses of variance (ANOVA) were performed to determine the significance of accession differences, locations, cultivation years and their interactions ($p < 0.05$) on cell wall composition and saccharification efficiency. Variance analyses were performed following the standard procedure of a mixed effect model with a random genetic effect, a fixed location effect, a random year effect and a fixed block effect, following the model (5):

$$R_{ijkr} = \mu + G_i + L_j + Y_k + B_r\,(L_j Y_k) + GL_{ij} + GY_{ik}$$
$$+ LY_{jk} + GLY_{ijk} + e_{ijkr} \qquad (5)$$

where R_{ijkr} is the response variable, μ is the grand mean, G_i is the genotype effect, L_j is the location effect, Y_k is the year effect, $B_r\,(L_j\,Y_k)$ is the block effect, GL_{ij} is the genotype-by-location interaction, GY_{ik} is the genotype-by-year interaction, LY_{jk} is the location-by-year interaction, GLY_{ijk} is the genotype-by-location-by year interaction and e_{ijkr} is the residual error. To study the potential of early selection correlation analyses were performed on accession means to identify the significance ($p < 0.05$) of correlations between traits across cultivation years using Pearson's correlation coefficients. In addition a Finlay Wilkinson stability analysis was performed using the calculated ethanol yield data of the third cultivation

year (6) (Finlay and Wilkinson, 1963; Malosetti et al., 2013):

$$R_{ij} = \mu + G_i + \beta_i \times L_j + e_{ij} \qquad (6)$$

where R_{ij} is the response variable, μ is the grand mean, G_i is the genotype effect, β_i is the regression coefficient of accession i for environment j (environmental sensitivity), L_j is a measure of environmental quality determined by the mean performance of accessions for CEY in environment j and e_{ij} is the residual error. Accession means per location for the third cultivation year were also used to fit a GGE model by singular value decomposition of environment-centered genotype by location data (7) (Malosetti et al., 2013):

$$R_{ij} = \mu + L_j + \sum_{k=1}^{k} \beta_{ik} \times L_{jk} + e_{ij} \qquad (7)$$

where accession performance is explained by K multiplicative terms (k = 1...K), each formed by the product of environmental sensitivity (β_{ik}) of accession i and environmental score (L_{jk}). A GGE biplot was constructed in which accession performance (accounting for both genotype main effect and genotype-by-location interaction) across environments is visualized in a scatter plot of accession and location scores for the first two principal components (Yan and Kang, 2002; Malosetti et al., 2013). Correlation analyses were performed to identify the significance, strength and direction of interrelationships between morphological and quality traits using Pearson's correlation coefficients. All statistical analyses were performed using Genstat for Windows, 18th edition software package (VSN International, Hemel Hempstead, UK).

RESULTS AND DISCUSSION

Impact of Accession, Location, and Cultivation Year on Biomass Quality

Cell wall composition and saccharification efficiency of 15 miscanthus accessions were studied in a multi-year, multi-location field experiment. Analyses of variance revealed that cell wall composition and saccharification efficiency differed significantly between accessions and that these traits were strongly affected by both trial location and cultivation year (**Tables 4, 5**). Miscanthus is a perennial crop that typically

TABLE 3 | Summary of cross-validation statistics of mPLS models used for the prediction of biomass quality traits from NIRS spectral data.

Constituent	Samples*	Chemical analysis			NIRS prediction			$r^{2¥}$	SECV§
		Mean	Min	Max	Mean	Min	Max		
NDF (g/kg dm)	246	85.04	71.55	92.69	85.04	71.28	92.35	0.99	0.88
ADF (g/kg dm)	243	54.96	38.43	68.55	54.97	39.40	68.47	0.99	1.13
ADL (g/kg dm)	239	9.22	4.88	14.45	9.20	5.26	14.42	0.88	0.79
Cellulose conversion (%)	237	29.89	8.17	52.10	30.21	13.14	46.81	0.92	3.22
Hemicellulose conversion (%)	243	12.43	5.84	22.20	12.34	6.70	20.27	0.82	2.06

*, Sample number varies as for every trait different samples may be removed by the software as outliers; depending on the model $^{¥}r^2$, coefficient of determination; §SECV, Standard error of cross-validation.

matures in 2–5 years, depending on the environmental conditions. During this process of maturation, miscanthus shows a pattern of increasing yields during the establishment phase, until at full maturity a plateau phase is reached, with relatively stable yields (Christian and Haase, 2001; Christian et al., 2008; Gauder et al., 2012; Hulle et al., 2012; Arnoult et al., 2015). Here we show that during this establishment phase, cell wall composition is changing as the crop matures.

Boxplots of biomass quality traits are provided in **Figures 1**, **2**, that depict the average and range in the performance of 15 accessions for each of the locations and cultivation years. Biomass composition in the first cultivation year differed considerably from that in the second and third, with substantially lower overall cell wall (NDF), cellulose (CEL) and to some extend lignin (LIG) contents and substantially higher contents of hemicellulosic polysaccharides (HEM) in the first year. For cultivation years 1, 2, and 3 mean NDF contents were ∼829, ∼860, and ∼876 g/kg dm, respectively. Similarly, mean CEL contents were ∼422, ∼474,

and ∼485 g/kg dm and LIG contents were ∼85, ∼93, and ∼99 g/kg dm, respectively. Mean HEM contents decreased from ∼322 in the first, to ∼293 in the second and ∼291 g/kg dm in the third year (**Figure 1**). Saccharification efficiency also differed substantially between cultivation years (**Table 5**) and was much higher in the first year than in the second or third year (**Figure 2**). Mean cellulose conversion (CelCon) reduced from ∼38% in the first year to ∼27% in the second and ∼22% in the third year. Similarly, mean hemicellulose conversion (HemCon) reduced from ∼14% in the first, to ∼11 in the second and ∼10% in the third year. These changes in biomass composition and quality culminated in substantial reductions in mean calculated ethanol yields (CEY) from ∼117 in the first, to 91 in the second and 77 g/kg dm in the third cultivation year (**Figure 2**). The ethanol yields reported in this study are relatively low compared to industrial standards, because very mild pretreatment conditions were chosen in this study as these are better suited to expose genotypic differences in saccharification efficiency (Torres et al., 2013; van der Weijde et al., 2017).

TABLE 4 | Analyses of variance for cell wall composition of 15 miscanthus accessions grown in six locations and evaluated for three successive cultivation years (2012–2013, 2013–2014 and 2014–2015).

| Source of variation[*]	Degrees of freedom	NDF (g/kg dm)		CEL (g/kg dm)		HEM (g/kg dm)		LIG (g/kg dm)	
		Mean squares	F prob.	Mean squares	F prob.	Mean squares	F prob.	Mean squares	F prob.
L	5	104619.6	<0.0001	145509.5	<0.0001	22834.8	<0.0001	8375.0	<0.0001
Residual[a]	12	489.8		835.1		992.9		196.1	
G	14	9644.3	<0.0001	18230.8	<0.0001	28602.2	<0.0001	5027.7	<0.0001
Y	2	150768.8	<0.0001	309417.8	<0.0001	84714	<0.0001	13962.3	<0.0001
GL	70	1308.7	0.0002	1312.6	<0.0001	697.5	<0.0001	143.1	0.0904
GY	28	960.2	0.0632	1139.5	0.0059	1548.2	<0.0001	465.4	<0.0001
LY	10	37187.4	<0.0001	31550	<0.0001	6469.7	<0.0001	2283.3	<0.0001
GLY	138	637.2	<0.0001	579.9	<0.0001	297.5	0.000	109.2	<0.0001
Residual[b]	500	242.8		308		184.6		50.3	

[*]G, Genotype; L, Location; Y, Year; GL, Genotype-by-location interaction; GY, Genotype-by-year interaction; LY, Location-by-year interaction; GLY, Genotype-by-location-by-year interaction. [a]Residual, Residual block stratum; [b]Residual, Residual block*units stratum.

TABLE 5 | Analyses of variance for conversion efficiency and calculated ethanol yield (CEY) of 15 miscanthus accessions grown in six locations and evaluated for three successive cultivation years (2012–2013, 2013–2014, and 2014–2015).

Source of variation[*]	Degrees of freedom	CelCon (%)		HemCon (%)		CEY (g/kg dm)	
		Mean squares	F prob.	Mean squares	F prob.	Mean squares	F prob.
L	5	2071.2	<0.0001	184.6	<0.0001	3171.3	<0.0001
Residual[a]	12	23.8		2.5		84.2	
G	14	283.2	<0.0001	51.1	<0.0001	3171.3	<0.0001
Y	2	18801.3	<0.0001	1151.8	<0.0001	84.2	<0.0001
GL	70	21.1	0.0003	3.1	0.0639	141.1	0.0099
GY	28	26.2	0.0002	2.5	0.3834	205.2	0.0007
LY	10	508.0	<0.0001	46.1	<0.0001	2836.9	<0.0001
GLY	138	10.7	<0.0001	2.3	<0.0001	88.4	<0.0001
Residual[b]	500	4.8		1.1		25.1	

[*]G, Genotype, L, Location, Y, Year; GL, Genotype-by-location interaction; GY, Genotype-by-year interaction; LY, Location-by-year interaction; GLY, Genotype-by-location-by-year interaction. [a]Residual, Residual block stratum; [b]Residual, Residual block*units stratum.
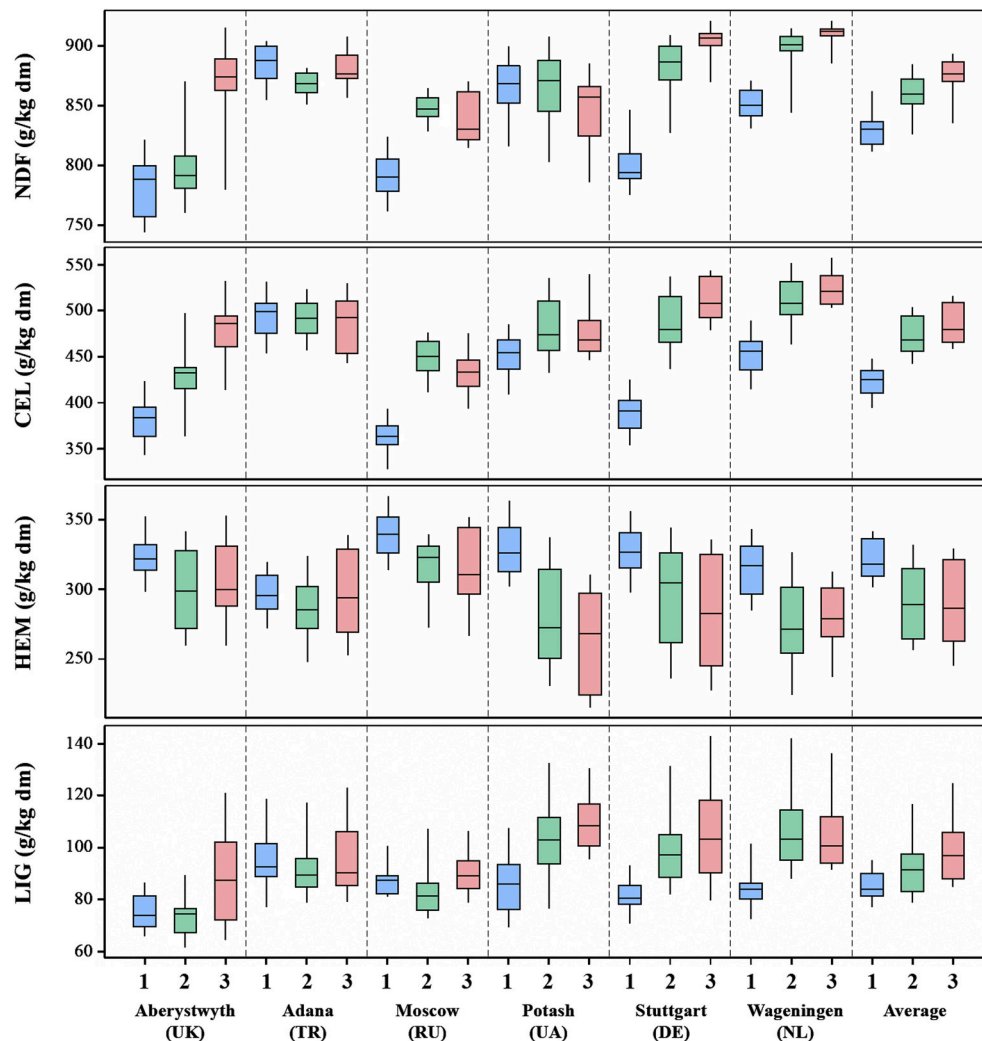
FIGURE 1 | Variation in accession means of 15 miscanthus accessions for cell wall composition characteristics in six growth locations and three cultivation years (1 = 2012–2013, 2= 2013–2014, and 3= 2014–2015).

Biomass quality traits were also highly influenced by the different environments in the trial location (**Tables 4**, **5**). Extreme differences came to light between Adana and the other locations for NDF, CEL, CelCon, and CEY. These differences were particularly evident in the first harvest year (**Figures 1**, **2**), which may be attributed to location-dependent differences in the rate of establishment, although inter-annual variation in weather conditions may also have contributed. Miscanthus has a tendency to mature more slowly at northern latitudes than at latitudes closer to the equator (Lewandowski et al., 2000; Clifton-Brown et al., 2001). After the first growth season miscanthus stands in Adana already reached near plateau yields (on average 8 t dm ha^{-1}), while yields in the other locations did not reach above 2 t dm ha^{-1} (Kalinina et al., unpublished data). However, these differences will become less pronounced toward the third harvest year, as stands in all locations start to reach full maturity.

For more in-depth evaluation of location differences in biomass quality, the material from the third cultivation year - assumed to represent mature, well-established miscanthus stands in all locations - was further examined (**Table 6**). Biomass composition varied extensively across locations, with mean NDF content ranging from 840 to 910 g/kg dm, CEL content from 434 to 524 g/kg dm, HEM content from 262 to 316 g/kg dm and LIG content from 89 to 109 g/kg dm (**Table 6**). The highest NDF and CEL contents were observed in Wageningen, while the lowest were observed in Moscow. These two locations were found to be the most contrasting of the evaluated locations regarding cell wall composition. Locations also differed extensively in saccharification efficiency. Mean cellulose conversion ranged from 17.3 to 26.4% across locations, with the lowest rate observed in Wageningen and the highest in Moscow. Likewise, mean hemicellulose conversion ranged from 8.7 to 12.3%, with the lowest rate observed in Wageningen and the highest in Potash.
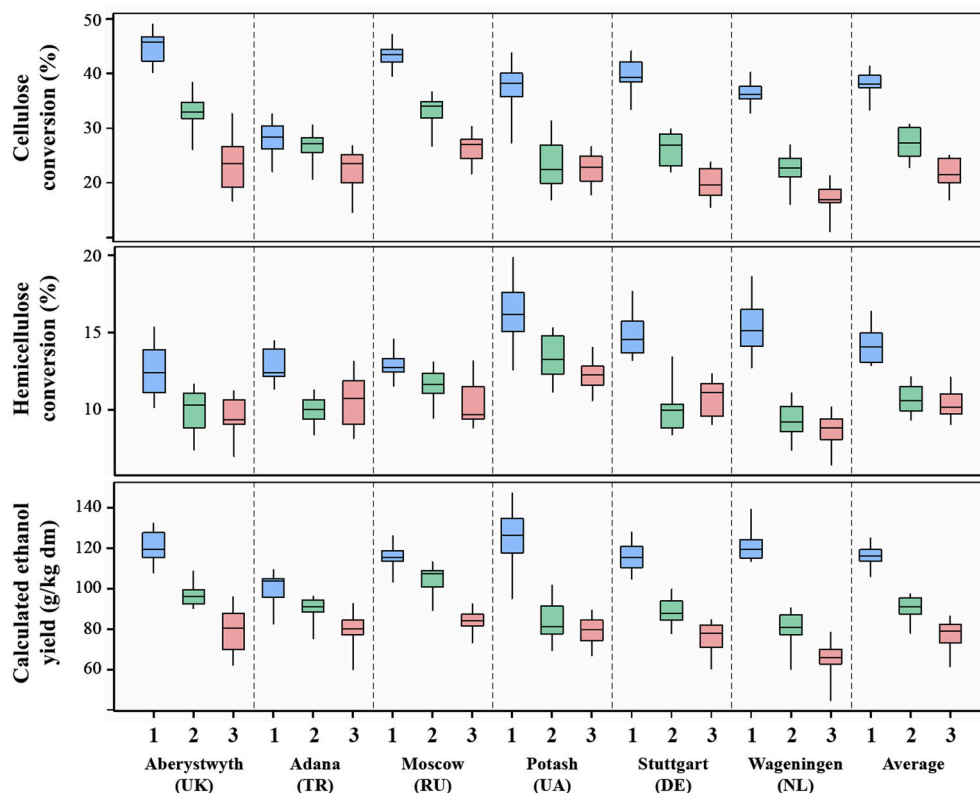
FIGURE 2 | Variation in accession means of 15 miscanthus accessions for conversion efficiency characteristics in six growth locations and three cultivation years (1 = 2012–2013, 2 = 2013–2014, and 3 = 2014–2015).

Calculated ethanol yields ranged from 65.6 to 83.5 g/kg dm across locations, with the highest yields for Moscow and the lowest for Wageningen. Which environmental parameters underlie such location-based differences in cell wall composition needs to be further investigated using a wider range of environments. However, variations in cell wall composition and cellulose degradation efficiency of natural miscanthus ecotypes in China were associated to latitude and total annual sunshine hours of the original habitat (Zhao et al., 2014). Furthermore, drought stress was recently identified as an environmental factor with implications for cell wall composition, increasing both cellulose content and saccharification efficiency of miscanthus (van der Weijde et al., 2016b).

Despite the large effects of location and cultivation year, significant variation in genotype performance was also evident (**Tables 4**, **5**). As can be seen in **Table 6**, the range of variation among accession within each location was extensive. Mean CEY over all locations was 77.2 g/kg dm with a mean range in variation among accessions of 27.9 g/kg dm (**Table 6**). To exemplify the extent of variation in accession performance we zoom in on the performance of accessions OPM-9 and OPM-13 in the third harvest year. Averaged across all locations, OPM-9 was shown to have a much higher mean lignin content (125 g/kg dm) then OPM-13 (85 g/kg dm, **Table 7**). This difference in lignin content and other cell wall characteristics contributed to the much higher CEY for OPM-13 (83 g/kg dm) compared to

OPM-9 (61 g/kg dm). It was previously shown that OPM-9 (*M. × giganteus*), the most widely exploited miscanthus variety, has a considerably lower quality for biofuel production compared to many other accessions (van der Weijde et al., 2016a), which is shown here to be the case across diverse environments.

The extent of variation amongst accessions in cell wall composition and conversion efficiency was not equal across locations (**Table 6**). In the third harvest year, the coefficient of trait variation (CV_t) across locations ranged from 0.9 to 3.7% for NDF, 3.4–6.4% for cellulose, 8.7–13.5% for hemicellulosic polysaccharides and 9.2–18.4% for lignin (**Table 6**). This showed that across locations particularly large variation in accession performance was observed for hemicelluloses and lignin. Variation in accession performance for conversion rates was also unequal across locations, with CV_t ranging from 10.1 to 18.3% for cellulose conversion and 8.0–14.8% for hemicellulose conversion. For four out of seven evaluated traits the largest variation in accession performance in the third year was observed in Aberystwyth.

Stability of Accession Performance

We observed that miscanthus cell wall composition is not stable during the establishment phase of miscanthus. Moreover, variation in accession performance differed across cultivation year, as indicated by the significance of genotype-by-year interaction effects (**Tables 4**, **5**). Therefore, early prediction of

TABLE 6 | Summary table of average, range and least significant differences for biomass quality traits of 15 accessions evaluated in six locations (cultivation year 3, 2014–2015).

Trait	Statistic	Aberystwyth (UK)	Adana (TR)	Moscow (RU)	Potash (UA)	Stuttgart (DE)	Wageningen (NL)	Mean	Range	LSD
LOCATION										
NDF	**Average**	**871.8**	**881.0**	**839.5**	**847.1**	**904.3**	**909.9**	875.6	70.4	6.5
(g/kg dm)	Range	135.1	49.9	54.8	98.8	50.7	34.9	70.7		
	CV_t (%)[§]	3.7	1.5	2.5	3.6	1.3	0.9	2.3		
	LSD[¥]	40.9	32.8	18.0	24.8	10.9	9.0			
Cellulose	**Average**	**478.1**	**487.3**	**433.7**	**476.1**	**513.2**	**524.4**	485.5	90.7	7.3
(g/kg dm)	Range	117.4	86.7	81.5	92.4	64.3	53.4	82.6		
	CV_t (%)	6.4	6.3	6.0	5.8	4.5	3.4	5.4		
	LSD	43.7	34.7	19.2	24.9	16.3	19.4			
Hemicellulose	**Average**	**305.3**	**298.6**	**315.6**	**262.3**	**284.1**	**280.7**	291.1	53.3	5.5
(g/kg dm)	Range	93.0	85.3	84.0	94.7	107.7	74.9	89.9		
	CV_t (%)	8.8	10.5	8.8	13.5	13.8	8.7	10.7		
	LSD	27.4	19.9	18.0	15.0	17.3	21.9			
Lignin	**Average**	**88.5**	**95.0**	**90.2**	**108.8**	**107.0**	**104.8**	99.0	20.3	3.1
(g/kg dm)	Range	56.0	43.4	27.3	34.7	63.1	44.6	44.9		
	CV_t (%)	18.3	13.2	9.2	9.7	18.4	12.2	13.5		
	LSD	19.8	9.7	6.8	7.2	11.6	11.4			
Cellulose	**Average**	**23.3**	**22.5**	**26.4**	**22.7**	**20.0**	**17.3**	22.0	9.0	0.9
conversion	Range	16.2	12.3	8.7	8.9	8.3	10.4	10.8		
(%)	CV_t (%)	18.3	15.0	10.1	12.3	14.0	14.1	14.2		
	LSD	19.8	3.6	2.0	3.0	2.0	2.2			
Hemicellulose	**Average**	**9.6**	**10.5**	**10.4**	**12.3**	**10.8**	**8.7**	10.4	3.6	0.4
conversion	Range	4.3	5.0	4.3	3.5	3.3	3.8	4.0		
(%)	CV_t (%)	11.9	14.8	12.7	8.0	10.3	11.0	11.5		
	LSD	2.2	1.7	1.6	1.6	2.0	1.4			
CEY[*]	**Average**	**79.3**	**79.8**	**83.5**	**79.5**	**75.5**	**65.6**	77.2	17.9	2.0
(g/kg dm)	Range	34.0	32.5	19.3	22.5	24.7	34.2	27.9		
	CV_t (%)	12.5	9.8	6.3	8.7	9.7	12.3	9.9		
	LSD	13.4	8.3	4.9	7.7	6.5	6.1			

[*]CEY, Calculated ethanol yield; [§]CV_t, Coefficient of trait variation (standard deviation over genotype means/location mean × 100%); [¥] LSD, least-significant difference (0.05).

genotype performance may not be reliable. For each location, correlations of accession performance for calculated ethanol yield across the different harvest years are depicted in **Figure 3**. A low similarity ($r^2 < 0.32$) in accession performance between the first and the third cultivation year was observed for all locations except for Adana ($r^2 = 0.45$). However, for all locations accession performance in CEY in the second cultivation year correlated reasonably well with that in the third cultivation year ($r^2 = 0.42$–0.83). Previously, Arnoult et al. (2015), already indicated that biomass quality in miscanthus harvested in the third cultivation year was reliably representative of that in the fourth and the fifth year in a single location. Here we validate that conclusion using data from multiple environments and even support that performance at full maturity can be estimated with reasonable accuracy from accession performance after two cultivation years. In contrast, selection for CEY based on CEY values obtained

after 1 year of cultivation is not recommended, due to its low predictive value of performance at full maturity.

The results also showed that some accessions performed more stable across the different environments than others and that ranking of accessions differs across locations. Such differential ranking was observed for all evaluated traits, except for lignin and hemicellulose conversion efficiency, as indicated by the statistical significance of genotype-by-environment interactions (**Tables 4**, **5**). When variance was analyzed on data of the third cultivation year only, statistically significant genotype-by-environment interactions were observed for all traits (Supplementary Tables S1, S2). This is the first report on genotype-by-location interactions for cell wall components and saccharification efficiency in miscanthus. Such interactions may have important implications for the set-up of selection experiments, as they implicate that the relative ranking of

TABLE 7 | Mean and variation in accession performance of 15 *Miscanthus* accessions over six trial locations (cultivation year 3, 2014–2015).

Accession	NDF (g/kg dm)		CEL (g/kg dm)		HEM (g/kg dm)		LIG (g/kg dm)		CelCon %		HemCon %		CEY (g/kg dm)	
	Mean	Range	Mean	Range	Mean	Range	Mean	Range	Mean	Range	Mean	Range	Mean	Range
OPM-1	893.0	47.0	516.1	63.5	259.2	75.1	117.7	30.7	19.6	6.0	10.7	3.5	73.0	15.0
OPM-2	835.6	106.0	470.2	96.1	269.4	83.6	96.1	51.8	25.1	12.1	11.5	2.6	84.1	19.9
OPM-3	878.5	103.3	511.1	109.5	252.3	60.9	115.1	38.1	19.3	8.7	11.1	5.3	71.5	19.0
OPM-4	876.7	92.4	509.9	87.4	260.5	81.2	106.4	32.2	21.5	9.6	11.9	4.3	79.5	24.0
OPM-5	892.7	67.2	512.0	66.1	282.5	48.0	98.1	23.1	19.9	6.4	10.8	3.7	75.2	16.7
OPM-6	859.8	80.9	478.9	81.0	286.6	37.3	94.3	12.8	24.6	6.5	12.1	4.4	86.6	13.9
OPM-7	888.9	46.2	479.6	67.4	311.3	65.0	98.0	19.1	20.2	8.4	9.2	5.2	71.1	21.7
OPM-8	876.9	89.5	480.8	100.5	291.7	32.2	104.4	20.2	20.8	10.4	10.1	2.8	73.1	18.7
OPM-9	869.3	120.3	499.1	91.4	245.6	41.4	124.7	36.6	16.8	11.4	10.1	4.2	61.3	29.1
OPM-10	889.0	76.8	505.5	109.9	286.4	61.7	97.2	20.1	20.5	12.4	10.6	4.3	75.4	27.7
OPM-11	878.7	54.0	461.2	83.1	329.2	51.5	88.3	28.5	23.7	8.8	9.2	4.6	79.2	16.7
OPM-12	873.0	88.2	463.7	127.1	322.5	53.7	86.8	24.4	24.4	11.3	9.0	2.6	80.0	20.6
OPM-13	873.1	86.3	459.2	107.8	328.7	45.0	85.1	24.6	25.2	10.9	9.7	2.8	83.3	17.0
OPM-14	880.1	61.2	472.2	91.2	322.5	36.9	85.4	27.3	24.2	8.3	9.7	3.2	82.5	17.7
OPM-15	868.7	86.3	462.4	107.6	318.3	68.0	88.0	24.4	24.8	11.4	9.8	3.3	82.2	19.8
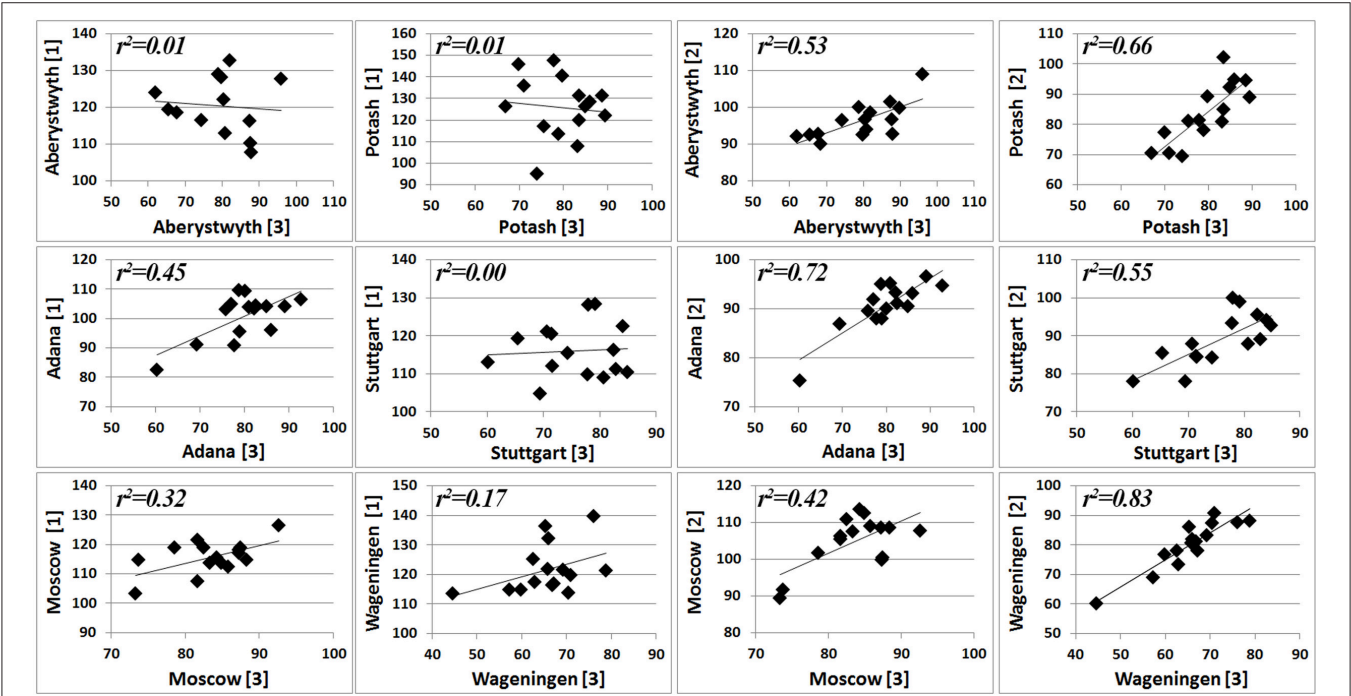
FIGURE 3 | Scatter plot matrix of calculated ethanol yields (g/kg dm) of the first [1] and the second [2] cultivation year of 15 miscanthus accessions in six locations compared to that of the third cultivation year [3].

accessions is dependent on the environment. Dealing with large genotype-by-environment interaction in breeding programs usually means that germplasm has to be trialed in multiple locations as selection based upon data from a single experiment might lead to wrong selection decisions. However, like for several forage crops such as silage maize (Dolstra et al., 1992; Cox et al., 1994; Argillier et al., 1997; Barrière et al., 2008; Torres et al., 2015), alfalfa (Sheaffer et al., 1998) and switchgrass (Hopkins et al., 1995), the variation attributed to

the genotype-by-environment interaction effect is considerably smaller than the variation attributed to the genotype and environment main effects (**Tables 4, 5**).

To further examine accession differences in environmental sensitivity, accession performance across locations was studied in more detail using the data from the third harvest year (**Table 7**). The largest variation in cellulose content across locations was observed for OPM 12, while the largest variation in contents of hemicellulosic polysaccharides and lignin was observed for OPM

TABLE 8 | Environmental sensitivity and genotype stability and superiority scores for calculated ethanol yield (g/kg dm) of 15 miscanthus accessions evaluated across six locations (cultivation year 3, 2014–2015).

Accession	Mean CEY	Environmental sensitivity[*]	Static stability[¥]	Superiority coefficient[§]	Superiority rank[‡]
OPM 1	73.05	0.54	29.65	132.10	11
OPM 2	84.05	0.66	52.48	17.40	2
OPM 3	71.51	0.93	55.73	161.90	13
OPM 4	79.53	1.13	76.25	54.10	7
OPM 5	75.23	0.93	43.31	103.70	9
OPM 6	86.64	0.78	34.05	16.30	1
OPM 7	71.13	1.21	65.50	174.00	14
OPM 8	73.13	0.99	49.76	145.50	12
OPM 9	61.29	1.50	93.61	405.00	15
OPM 10	75.43	1.48	118.93	131.50	10
OPM 11	79.25	0.94	38.76	56.00	8
OPM 12	80.03	1.03	53.48	45.10	6
OPM 13	83.25	0.92	40.40	22.00	3
OPM 14	82.52	0.85	40.66	28.70	4
OPM 15	82.24	1.04	50.60	34.80	5

[*]Environmental sensitivity, the slope of the regression line of the fitted Finlay Wilkinson (FW) model; [¥]Static stability, the variance around the accession mean across environments; [§]Superiority coefficient, the mean square distance between accession performance and maximum observed performance in each environment; [‡]Superiority rank, Accession ranking based on superiority coefficient.

FIGURE 4 | GGL biplot of variation in accession performance in calculated ethanol yield (g/kg dm) across six locations in the third cultivation year (2014–2015). Numbers represent accession OPM codes.

2. Similarly, OPM 9 displayed the largest variation for NDF and CEY, while OPM 10 and OPM 3, respectively displayed the largest variation in CelCon and HemCon.

To study such differences in the stability of accession performance, a Finlay Wilkinson stability analysis (Finlay and Wilkinson, 1963) was performed on CEY data of the third cultivation year, to estimate the environmental sensitivity of accessions for this trait (**Table 8**). The higher the sensitivity estimate, the more sensitive an accession is to the "quality" of the growth location for the evaluated trait. The environmental quality in this analysis refers to deviation of mean accession performance in that location from the mean accession performance over all evaluated locations. Accession performance of OPM 1 was found to be the least sensitive (sensitivity 0.54) and OPM 9 the most sensitive (sensitivity 1.50) to environmental quality (**Table 8**). The static stability parameter of each accession was also calculated, which is a measure of the variance in accession performance across locations (Becker and Leon, 1988). A smaller static stability means smaller variation in accession performance across locations. Accession performance of OPM 1 was the most stable (static stability 30) and OPM 10 the least stable (static stability 119) across environments (**Table 8**). The superiority coefficient is used to identify accessions that perform relatively well in all test locations and accounts for both mean performance and stability (Lin and Binns, 1988). OPM 6 ranked first in overall performance across environments (lowest superiority coefficient), while OPM 9 ranked last (**Table 8**).

A useful tool to visualize the variation in accession performance across locations is the GGE biplot (**Figure 4**) (Yan et al., 2000; Yan and Kang, 2002; Malosetti et al., 2013). The origin
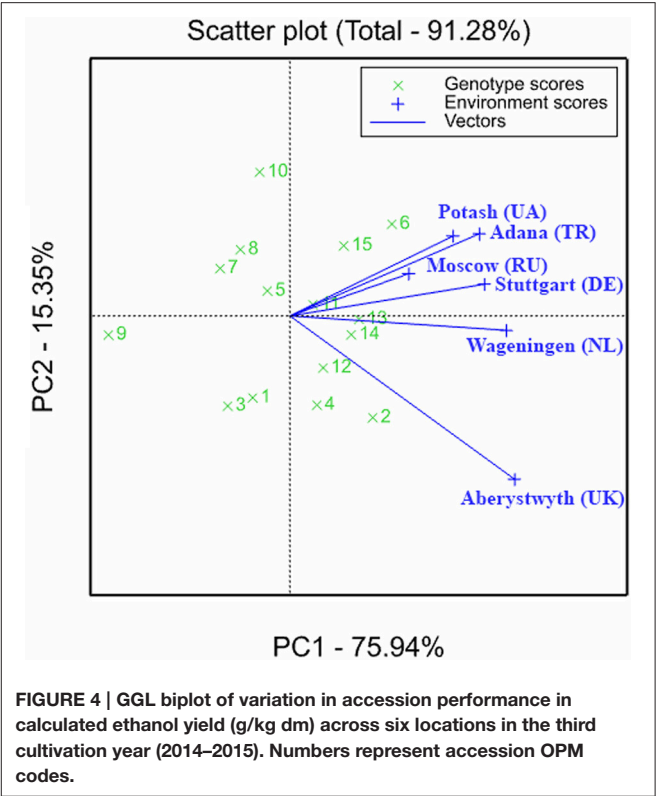
of the plot represents the average performance of accessions across the environments, the length of environment vectors is proportional to the genetic variance within environments (the extent of variation among accessions within one environment) and the angle between vectors is proportional to the correlation between environments (Yan and Kang, 2002; Malosetti et al., 2013). The first two principal components visualized in the biplot explained 91.28% of the variation (**Figure 3**). The angle between the vector for Potash and the vector for Aberystwyth is almost 90 degrees, indicating that there is virtually no correlation in accession performance between these two locations. The perpendicular projection of accessions on the environment vectors approximates accession performance per environment, showing that OPM 2 performed the best in Aberystwyth, while OPM 6 performed the best in all other trial locations. OPM 9 performed the worst in all locations. Along with the previous observation that OPM-6 had the lowest superiority coefficient and the highest mean performance in terms of CEY across locations (**Table 8**), this shows that the calculated ethanol yield of OPM-6 was relatively insensitive to differences between locations and was superior to the other accessions in 5 out of 6 trial locations. The selection of stable accessions to counter the effects of genotype-by-location interactions is a viable approach if, like is the case here, the performance of the stable accession is not much lower compared to adapted accessions. However, the stable and superior accession OPM-6 did perform relatively poor in Aberystwyth compared to OPM-2, but still had average performance among all accessions.

Implications for the Use of Miscanthus As a Lignocellulose Feedstock

There is a need for the development of novel miscanthus varieties with improved biomass quality for processing into cellulosic ethanol and other bioproducts. The large extent of observed genotypic variation in cell wall composition and saccharification efficiency observed in this study indicates potential for the selection of miscanthus accessions with favorable biomass quality characteristics. However, in addition to genetic factors also environmental factors substantially affect cell wall composition and conversion efficiency. This can be highly problematic, as a consistent supply of biomass of predictable composition and high quality is a crucial factor for the success of lignocellulose biorefineries (Perlack et al., 2005). Also from a breeding perspective a large environmental influence on the trait of interest is undesirable, as the environmentally derived part of the phenotypic variation is hard to control. This is especially problematic if the effect is unpredictable due to unknown and/or fluctuating environmental stimuli.

To combat this, genotypes with a stable and good performance across diverse locations are ideal. Differences in environmental sensitivity among the tested accessions were evident. However, accession ranking also varied across locations, which implicates that an accession that performs well in one location may not perform well in another. Stability analysis of accession performance for CEY in the third cultivation year, identified OPM-6 as a stable and superior accession, which had the best performance in 5 out of 6 locations and average performance in the remaining trial location. The selection of genotypes with a stable and superior performance across environments may thus be a viable approach, but it requires that breeding germplasm is evaluated in multiple and diverse locations.

Trials also need to be conducted over multiple years, before selections can be made reliably. Miscanthus is a perennial crop that matures in approximately 3 years and accession performance differed substantially between cultivation years. It was observed that establishment rates of miscanthus varied between the locations, with faster establishment of miscanthus in Adana than in the other locations. However, in all evaluated locations, accession performance for CEY in the second cultivation year was predictive of that at full maturity with reasonable accuracy, indicating that selections can be reliably made from the second cultivation year onwards.

The obtained results highlight the potential impact of environmental conditions and cultivation year on the quality of miscanthus biomass for biofuel production, but - in a wider perspective - are also relevant to many other potential biomass value-chains. Especially processes that rely on biomass fractionation, such as refinery processes, whose techno-economic efficiency may be considerably affected by such variation in cell wall. To increase our understanding of which environmental stimuli are the cause of the observed environmentally derived variation cell wall composition and conversion efficiency, further research is needed in which a broader range of environments is evaluated. In this way the most suitable production environment can be identified given certain biomass quality criteria posed by the end-user. Simultaneously, selection for biomass quality in miscanthus through breeding should take into account these effects of environmental factors and cultivation year on accession performance in order to identify stable and superior genotypes that consistently yield high quality biomass across diverse production environments. The influence of environmental conditions on biomass quality is substantial and should be taken into account in order to match genotype, location and end-use of miscanthus as a lignocellulose feedstock.

SUPPLEMENTARY MATERIAL

The Supplementary Material for this article can be found online at: http://journal.frontiersin.org/article/10.3389/fpls.2016.02004/full#supplementary-material

REFERENCES

Allison, G. G., Morris, C., Clifton-Brown, J., Lister, S. J., and Donnison, I. S. (2011). Genotypic variation in cell wall composition in a diverse set of 244 accessions of *Miscanthus*. *Biomass Bioenergy* 35, 4740–4747. doi: 10.1016/j.biombioe.2011.10.008

Argillier, O., Barrière, Y., Traineau, R., Emile, J. C., and Hebert, Y. (1997). Genotype × environment interactions for digestibility traits in silage maize estimated from *in vivo* measurements with standard sheep. *Plant Breeding* 116, 423–427. doi: 10.1111/j.1439-0523.1997.tb01025.x

Arnoult, S., Mansard, M.-C., and Brancourt-Hulmel, M. (2015). Early prediction of biomass production and composition based on the first six

years of cultivation. *Crop Sci.* 55, 1104–1116. doi: 10.2135/cropsci2014. 07.0493

Barrière, Y., Thomas, J., and Denoue, D. (2008). QTL mapping for lignin content, lignin monomeric composition, p-hydroxycinnamate content, and cell wall digestibility in the maize recombinant inbred line progeny F838 × F286. *Plant Sci.* 175, 585–595. doi: 10.1016/j.plantsci.2008.06.009

Becker, H., and Leon, J. (1988). Stability analysis in plant breeding. *Plant Breed.* 101, 1–23. doi: 10.1111/j.1439-0523.1988.tb00261.x

Boerjan, W., Ralph, J., and Baucher, M. (2003). Lignin biosynthesis. *Annu. Rev. Plant Biol.* 54, 519–546. doi: 10.1146/annurev.arplant.54.031902.134938

Christian, D. G., and Haase, E. (2001). "Agronomy of miscanthus," in *Miscanthus for energy and fibre*, eds B. Jones and M. Walsh (London: James and James (Science Publishers) Ltd.), 21–45.

Christian, D. G., Riche, A. B., and Yates, N. E. (2008). Growth, yield and mineral content of Miscanthus x giganteus grown as a biofuel for 14 successive harvests. *Ind. Crops Prod.* 28, 320–327. doi: 10.1016/j.indcrop.2008.02.009

Chundawat, S. P. S., Beckham, G. T., Himmel, M. E., and Dale, B. E. (2011). Deconstruction of lignocellulosic biomass to fuels and chemicals. *Annu. Rev. Chem. Biomol. Eng.* 2, 121–145. doi: 10.1146/annurev-chembioeng-061010-1 14205

Clifton-Brown, J. C., Chiang, Y. C., and Hodkinson, T. R. (2008). "Miscanthus: genetic resources and breeding potential to enhance bioenergy production," in *Genetic Improvement of Bioenergy Crops*, ed W. Vermerris (New York, NY: Springer Science+Business Media, LLC), 295–308.

Clifton-Brown, J. C., Lewandowski, I., Andersson, B., Basch, G., Christian, D. G., Kjeldsen, J. B., et al. (2001). Performance of 15 genotypes at five sites in Europe. *Agron. J.* 93, 1013–1019. doi: 10.2134/agronj2001.9351013x

Cox, W. J., Cherney, J. H., Pardee, W. D., and Cherney, D. J. R. (1994). Forage quality and harvest index of corn hybrids under different growing conditions. *Agron. J.* 86, 277–282. doi: 10.2134/agronj1994.00021962008600020013x

Dien, B. S. (2010). "Mass balances and analytical methods for biomass pretreatment experiments," in *Biomass to Biofuels: Strategies for Global Industries*, eds A. A. Vertès, N. Qureshi, H. P. Blaschek, and H. Yukawa. (Oxford: Blackwell), 213–232.

Doblin, M. S., Pettolino, F., and Bacic, A. (2010). Plant cell walls: the skeleton of the plant world. *Funct. Plant Biol.* 37, 357–381. doi: 10.1071/FP09279

Dolstra, O., Medema, J., and De Jong, A. (1992). Genetic improvement of cell-wall digestibility in forage maize (*Zea mays* L.). I. Performance of inbred lines and related hybrids. *Euphytica* 65, 187–194. doi: 10.1007/BF00023082

Finlay, K., and Wilkinson, G. (1963). The analysis of adaptation in a plant-breeding programme. *Crop Pasture Sci.* 14, 742–754. doi: 10.1071/AR9630742

Gauder, M., Graeff-Hönninger, S., Lewandowski, I., and Claupein, W. (2012). Long-term yield and performance of 15 different *Miscanthus* genotypes in southwest Germany. *Ann. Appl. Biol.* 160, 126–136. doi: 10.1111/j.1744-7348.2011.00526.x

Goering, H. K., and Van Soest, P. J. (1970). *Forage Fiber Analyses (Apparatus, Reagents, Procedures, and Some Applications)*. Washington, DC: U.S. Agricultural Research Service.

Heaton, E. A., Dohleman, F. G., Miguez, A. F., Juvik, J. A., Lozovaya, V., Widholm, J., et al. (2010). Miscanthus. A promising biomass crop. *Adv. Bot. Res.* 56, 76–137. doi: 10.1016/S0065-2296(10)56003-8

Himmel, M. E., and Picataggio, S. K. (2008). "Our challenge is to acquire deeper understanding of biomass recalcitrance and conversion," in *Biomass Recalcitrance*, ed M. E. Himmel (Oxford: Blackwell Publishing Ltd.), 1–6.

Hodgson, E. M., Lister, S. J., Bridgwater, A. V., Clifton-Brown, J., and Donnison, I. S. (2010). Genotypic and environmentally derived variation in the cell wall composition of *Miscanthus* in relation to its use as a biomass feedstock. *Biomass Bioenerg.* 34, 652–660. doi: 10.1016/j.biombioe.2010.01.008

Hopkins, A. A., Vogel, K. P., Moore, K. J., Johnson, K. D., and Carlson, I. T. (1995). Genotypic variability and genotype × environment interactions among switchgrass accessions from the Midwestern USA. *Crop Sci.* 35, 565–571. doi: 10.2135/cropsci1995.0011183X003500020047x

Hulle, S. V., Waes, C. V., Vliegher, A. D., Baert, J., and Muylle, H. (2012). "Comparison of dry matter yield of lignocellulosic perennial energy crops in a long-term Belgian field experiment," in *Grassland - a European resource? Proceedings of the 24th General Meeting of the European Grassland Federation, Lublin, Poland*, eds P. Goliński, M. Warda, and P. Stypiński (Poznań: Polskie Towarzystwo Łakarskie—Polish Grassland Society), 499–501.

Jones, M. B., and Walsh, M. (2001). *Miscanthus for Energy and Fibre*. London: James & James Ltd.

Lewandowski, I., Clifton-Brown, J. C., Scurlock, J. M. O., and Huisman, W. (2000). Miscanthus: European experience with a novel energy crop. *Biomass Bioenerg.* 19, 209–227. doi: 10.1016/S0961-9534(00)00032-5

Lewandowski, I., Clifton-Brown, J., Trindade, L. M., Van Der Linden, G. C., Schwarz, K.-U., Müller-Sämann, K., et al. (2016). Progress on optimizing Miscanthus biomass production for the European bioeconomy: results of the EU FP7 Project OPTIMISC. *Front. Plant Sci.* 7:1620. doi: 10.3389/fpls.2016.01620

Lin, C.-S., and Binns, M. R. (1988). A superiority measure of cultivar performance for cultivar × location data. *Can. J. Plant Sci.* 68, 193–198. doi: 10.4141/cjps88-018

Malosetti, M., Ribaut, J.-M., and Van Eeuwijk, F. A. (2013). The statistical analysis of multi-environment data: modeling genotype-by-environment interaction and its genetic basis. *Front. Physiol.* 4:44. doi: 10.3389/fphys.2013. 00044

Pauly, M., and Keegstra, K. (2010). Plant cell wall polymers as precursors for biofuels. *Curr. Opin. Plant Biol.* 13, 304–311. doi: 10.1016/j.pbi.2009. 12.009

Perlack, R. D., Wright, L. L., Turhollow, A. F., Graham, R. L., Stokes, B. J., and Erbach, D. C. (2005). *Biomass as Feedstock for a Bioenergy and Bioproducts industry: The Technical Feasibility of a Billion-ton Annual Supply*. (Oak Ridge, TN: Oak Ridge National Laboratory).

Qin, J., Yang, Y., Jiang, J., Yi, Z., Xiao, L., Ai, X., et al. (2012). Comparison of lignocellulose composition in four major species of Miscanthus. *Afr. J. Biotechnol.* 11, 8. doi: 10.5897/AJB11.3248

Selig, M., Weiss, N., and Ji, Y. (1996). "Enzymatic saccharification of lignocellulosic biomass," in *LAP-009 NREL Analytical Procedure* (Golden, CO: National Renewable Energy Laboratory), 1–8.

Sheaffer, C. C., Cash, D., Ehlke, N. J., Henning, J. C., Jewett, J. G., Johnson, K. D., et al. (1998). Entry × environment interactions for Alfalfa Forage quality. *Agron. J.* 90, 774–780. doi: 10.2134/agronj1998.00021962009000060010x

Shenk, J. S., and Westerhaus, M. O. (1991). Populations structuring of near infrared spectra and modified partial least squares regression. *Crop Sci.* 31, 1548–1555. doi: 10.2135/cropsci1991.0011183X003100060034x

Torres, A. F., Noordam-Boot, C. M. M., Dolstra, O., Vlaswinkel, L., Visser, R. G. F., and Trindade, L. M. (2015). Extent of genotypic variation for maize cell wall bioconversion traits across environments and among hybrid combinations. *Euphytica* 206, 501–511. doi: 10.1007/s10681-015-1517-x

Torres, A. F., Slegers, P. M., Noordam-Boot, C. M. M., Dolstra, O., Vlaswinkel, L., Boxtel, A. J. B., et al. (2016). Maize feedstocks with improved digestibility reduce the costs and environmental impacts of biomass pretreatment and saccharification. *Biotechnol. Biofuels* 9, 1–15. doi: 10.1186/s13068-016-0479-0

Torres, A. F., van der Weijde, T., Dolstra, O., Visser, R. G. F., and Trindade, L. M. (2013). Effect of Maize biomass composition on the optimization of dilute-acid pretreatments and enzymatic saccharification. *Bioenergy Res.* 6, 1038–1051. doi: 10.1007/s12155-013-9337-0

van der Weijde, T., Alvim Kamei, C. L., Torres, A. F., Vermerris, W., Dolstra, O., Visser, R. G. F., et al. (2013). The potential of C4 grasses for cellulosic biofuel production. *Front. Plant Sci.* 4:107. doi: 10.3389/fpls.2013. 00107

van der Weijde, T., Huxley, L. M., Hawkins, S., Sembiring, E. H., Farrar, K., Dolstra, O., et al. (2016b). Impact of drought stress on growth and quality of miscanthus for biofuel production. *GCB Bioenergy* doi: 10.1111/gcbb.12382. [Epub ahead of print].

van der Weijde, T., Kiesel, A., Iqbal, Y., Muylle, H., Dolstra, O., Visser, R. G. F., et al. (2017). Evaluation of *Miscanthus sinensis* biomass quality as feedstock for conversion into different bioenergy products. *GCB Bioenergy* 9, 176–190. doi: 10.1111/gcbb.12355

van der Weijde, T., Torres, A. F., Dolstra, O., Dechesne, A., Visser, R. G., and Trindade, L. M. (2016a). Impact of different lignin fractions on saccharification efficiency in diverse species of the bioenergy crop Miscanthus. *Bioenergy Res.* 9, 146–156. doi: 10.1007/s12155-015-9669-z

Van Soest, P. J. (1967). Development of a comprehensive system of feed analyses and its application to forages. *J. Anim. Sci.* 26, 119–128. doi: 10.2527/jas1967.261119x

Wyman, C. E. (2007). What is (and is not) vital to advancing cellulosic ethanol. *Trends Biotechnol.* 25, 153–157. doi: 10.1016/j.tibtech.2007.02.009

Yan, W., Hunt, L. A., Sheng, Q., and Szlavnics, Z. (2000). Cultivar evaluation and mega-environment investigation based on the GGE Biplot. *Crop Sci.* 40, 597–605. doi: 10.2135/cropsci2000.403597x

Yan, W., and Kang, M. S. (2002). *Gge Biplot Analysis: A Graphical Tool for Breeders, Geneticists, and Agronomists.* Boca Raton, FL: CRC press.

Zhao, H., Li, Q., He, J., Yu, J., Yang, J., Liu, C., et al. (2014). Genotypic variation of cell wall composition and its conversion efficiency in Miscanthus sinensis, a potential biomass feedstock crop in China. *GCB Bioenergy* 6, 768–776. doi: 10.1111/gcbb.12115

Harvest Time Optimization for Combustion Quality of Different Miscanthus Genotypes across Europe

Yasir Iqbal[1]*, Andreas Kiesel[1], Moritz Wagner[1], Christopher Nunn[2], Olena Kalinina[1], Astley F. S. J. Hastings[3], John C. Clifton-Brown[2] and Iris Lewandowski[1]

[1] Biobased Products and Energy Crops (340b), University of Hohenheim, Stuttgart, Germany, [2] Institute of Biological, Environmental and Rural Sciences, Aberystwyth University, Wales, UK, [3] The School of Biological Sciences, University of Aberdeen, Aberdeen, UK

Delayed harvest can improve the quality of miscanthus biomass for combustion and enhance the long-term sustainability of the crop, despite accompanying yield losses. The aim of this study is to identify the optimal harvesting time, which can deliver improved biomass quality for combustion of novel miscanthus genotypes at various sites across Europe, without high yield losses and without compromising their environmental performance. The relevant field trials were established as part of the European project OPTIMISC with 15 genotypes at six sites across Europe. For this study, the five highest yielding genotypes from each germplasm group and three sites with contrasting climatic conditions (Stuttgart, Germany; Adana, Turkey; and Moscow, Russia) were selected for assessment. The biomass samples were collected between August and March (depending on site) and subjected to mineral and ash content analysis. At Stuttgart, the delay in harvesting time led to a significant variation in combustion quality characteristics, such as N content (0.64–0.21%), ash content (5.15–2.60%), and ash sintering index (1.30–0.20). At Adana, the delay in harvesting time decreased the N content from 0.62 to 0.23%, ash content from 10.63 to 3.84%, and sintering index from 0.54 to 0.07. At Moscow, the impact of delay in harvesting was not significant, except for N, Mg, and ash sintering index. Overall, a delay in harvesting time improved the combustion quality characteristics of each genotype, but at the expense of yield. Yield losses of up to 49% in Stuttgart and Adana and 21% for Moscow were recorded, with variations between genotypes and sites. The harvesting time also affected nutrient offtake, which in turn influences the long-term environmental performance of the crop. The highest N, P, and K offtakes were recorded at Stuttgart for each harvesting time except for final harvest (March), where Moscow had the highest N offtake. This study describes the three criteria (biomass quality, yield losses, nutrient offtake) for determining the ideal harvesting time, which gives the best compromise between dry matter yields and biomass quality characteristics without negatively affecting the environmental performance of the crop.

Keywords: miscanthus, harvesting time, genotype, combustion quality, yield loss, nutrient offtake

INTRODUCTION

The challenges of climate change and global warming, linked with the ongoing depletion of fossil fuels, have led researchers and policy makers to search for ways of replacing conventional fuels with renewable and sustainable low-emission fuels. A wide range of biomass resources, such as agricultural and forestry residues, herbaceous dedicated energy crops, woody biomass, and other biodegradable wastes, can be exploited for this purpose (Zabed et al., 2016). The use of lignocellulosic biomass, especially dedicated non-food crops such as miscanthus, switchgrass, and reed canary grass, offers an opportunity to deliver high biomass yields under low-input conditions, potentially also from less suitable agricultural land.

Miscanthus is a very resource-efficient C4 perennial energy grass (Clifton-Brown et al., 2015), which has the potential to grow under marginal conditions (Mi et al., 2014). In Europe, it is the leading perennial energy grass and its biomass is mainly used for combustion to produce heat and electricity. Biomass-based combustion is the preferred utilization option, because it is simple, well known and state-of-the-art technologies are already in place, from small- to large-scale applications (Obernberger and Thek, 2008). By 2020, it is expected that biomass-based energy production will reach 139.5 Mtoe, of which 110.4 Mtoe will be produced in the form of heat and electricity (SWD, 2014). Combustion offers an opportunity to exploit a wide range of biomass resources for this purpose (Arvelakis and Koukios, 2013). However, for an efficient combustion process, biomass quality of specific characteristics is required. The major challenge for the combustion of miscanthus biomass is the low ash melting temperature, which not only reduces the conversion efficiency but also leads to other technical problems such as damage to boiler surfaces (Aho and Silvennoinen, 2004). In addition, it increases the overall operational costs. Therefore, it is important to optimize the constituents of miscanthus biomass for an effective combustion process. For example, high potassium (K), chloride (Cl), and ash contents cause corrosion and fouling (Baxter et al., 2012, 2014; Iqbal and Lewandowski, 2016), and a high moisture content has a direct influence on the heating value (Meehan et al., 2014). For this reason, these biomass constituents need to be kept as low as possible to counter mechanical and technical limitations.

There are several possibilities for enhancing miscanthus biomass quality for combustion. These include technical improvements (Blomberg, 2012), adoption of efficient conversion processes (Wang et al., 2012) and optimization of biomass quality during its production (Iqbal and Lewandowski, 2014). At field level, biomass quality can be improved by adjusting the harvesting time, which can be an efficient and cost-effective measure. Any change in harvest date has a significant influence on both miscanthus biomass composition and yield. However, the response to delayed harvesting varies from genotype to genotype due to differences in phenology (time of flowering and senescence) and morphology (stem thickness, leaf-to-stem ratio). The phenological differences directly influence the nutrient translocation process (Purdy et al., 2015) and

the morphological differences affect the leaching of minerals through rainfall (Jørgensen, 1997). An optimal harvest date can improve combustion quality by allowing enough time for the translocation of nutrients back to rhizomes and the leaching of minerals and ash (Iqbal and Lewandowski, 2014). A quality improvement with delayed harvest has been described for the commercially grown standard clone, *Miscanthus × giganteus*. However, there is a trade-off between quality improvement and yield, because yield losses of up to 35% can occur between peak yield and a delayed harvest in early spring (Lewandowski and Heinz, 2003). Despite influencing the biomass quality and yield, harvesting time also affects the environmental performance of crop. For example, earlier harvest leads to high nutrient offtake (Smith and Slater, 2011) which subsequently increases the fertilizer input. Many studies have been carried out to evaluate the impact of delaying the harvest time on biomass quality for combustion (Hayes, 2013; Kludze et al., 2013; Bilandzija et al., 2016). However, the mechanisms behind the biomass quality improvement through delayed harvest and the trade-off between quality and yield for different genotypes has not yet been fully described. Therefore, the aim of this study is to identify the optimal harvesting time, which can deliver improved biomass quality of novel miscanthus genotypes at various sites across Europe, without high yield losses and compromising their environmental performance.

For this purpose, three of the six field-trial sites were selected from the European project "OPTIMISC": Adana (Turkey), Stuttgart (Germany), and Moscow (Russia). From the 15 miscanthus genotypes trialed in this project, three of the highest-yielding were chosen from the germplasm "groups" OPM-3 (*Miscanthus sacchariflorus*), OPM-6 (*M. sacchariflorus × Miscanthus sinensis* hybrid), OPM-14 (*M. sinensis*) to be compared with the "standard genotypes" *M. × giganteus* (OPM-9) and *M. sinensis* Goliath (OPM-11). The genotypes were harvested at various dates between late summer and early spring. For each harvest date, the quality parameters relevant for combustion (mineral, ash, moisture) were analyzed and the biomass yield assessed.

MATERIALS AND METHODS

Field Trial Description

The field trials were established in 2012 as a part of the EU-funded project OPTIMISC (FP7 No. 289159) with 15 miscanthus genotypes at six sites across Europe. Each genotype was established in a randomized block design with three replications. A full description of the field trials can be found in Lewandowski et al. (2016). From these trials, three sites (Stuttgart, Adana, and Moscow) were selected with the aim of covering a wide range of climatic diversity. From each site, the five most promising genotypes (in terms of dry matter yield) were selected and at least one genotype was also chosen from each species group in order to cover genetic diversity. The genotypes selected are presented in **Table 1**. This study was based on the data from the third growth year.

TABLE 1 | Description of miscanthus genotypes used in this study (Lewandowski et al., 2016).

Genotype name	Abbreviation	Provider
Miscanthus sacchariflorus	OPM-3	IBERS
Miscanthus sinensis × Miscanthus sacchariflorus hybrid	OPM-6	IBERS
Miscanthus × giganteus	OPM-9	IBERS
Miscanthus sinensis "Goliath"	OPM-11	IBERS
Miscanthus sinensis	OPM-14	WUR

Site Conditions and Management Practices

The soil texture at Adana and Moscow is silty clay loam to sandy clay loam and at Stuttgart clay loam. **Table 2** shows soil bulk density, stone fraction, and nutrient status [mineral nitrogen (Nmin), phosphorus (P), potassium (K), magnesium (Mg)] at different soil depths for each site.

Meteorological data (monthly rainfall and minimum air temperature from September to March) are shown in **Figure 1**.

Regarding management practices, all the selected sites received the same amount of nutrient application with 60 kg N/ha, 100 kg P/ha, and 140 kg K/ha. Adana also received sufficient irrigation each year to ensure growth was not inhibited of around 200 mm/year.

Sample Collection

The work was begun in August 2014 with sequential harvests of aboveground biomass, which we called "quality cuts," starting from August through to January or March, depending on the site. Quality cuts were performed to collect biomass specifically for quality analyses avoiding any damage to the middle 4 m^2 of each plot, which were used for yield estimations at final harvest. In Stuttgart, quality cuts were performed in August, September, October, November, January, and March. In Adana, they were performed in August, September, October, November, and January. In Moscow, they were performed in August, September, and March because heavy frost killed the aboveground biomass just before the September sampling date and no further quality cuts could be performed until the final harvest in March. Data on morphological characteristics such as leaf-to-stem ratio and stem thickness were collected. The data on leaf-to-stem ratio was collected for every harvesting time, whereas stem thickness was measured only at Stuttgart during final harvest. The same harvesting procedure was adopted at each site. Eight stems were collected randomly from the second-outer row of each plot using manual cutters and leaving stubble of about 5 cm at each harvest date. To ensure the collection was random, a marked pole was used. The quality cut samples were chopped and dried to constant weight (at 60°C for at least 48 h) in a cabinet dryer at each site. The dried biomass samples from Adana and Moscow were shipped to Stuttgart for analysis.

Chemical Analysis

The milling of all samples was performed in Stuttgart using a SM 200 (Retsch, Haan) cutting mill equipped with a 1-mm sieve and analyzed in the laboratory for nitrogen (N), phosphorus (P), potassium (K), sodium (Na), silicon (Si), calcium (Ca), magnesium (Mg), and ash content. N analysis was carried out by using Vario Macro cube, Elementar Analysensysteme (GmbH, Hanau, Germany) by following the Dumas principle (Naumann and Bassler, 1976/2012; VDLUFA Methods Book III). The extracts were prepared and P, K, Na, Ca, Si, and Mg contents were measured by using ICP-OES (Vista Pro, Varian Inc., Palo Alto, CA, USA). For determination of ash content, samples were kept in Muffle furnace at 550°C for 4 h (Naumann and Bassler, 1976/2012; VDLUFA Methods Book III). The laboratory methods adopted for mineral analysis and ash are described in detail by Iqbal and Lewandowski (2014) and Iqbal and Lewandowski (2016).

The ash-sintering index was developed by correlating biomass composition with ash melting behavior during combustion, based on previous knowledge (Iqbal and Lewandowski, 2016). This index helps to estimate ash melting behavior during the combustion process. An ash-sintering index value (Na + K/Ca + Si) between 0 and 0.20 predicts no to slight sintering risk, between 0.20 and 0.40 slight to strong sintering risk and values above 0.40 strong sintering risk to complete ash melting, depending on biomass composition.
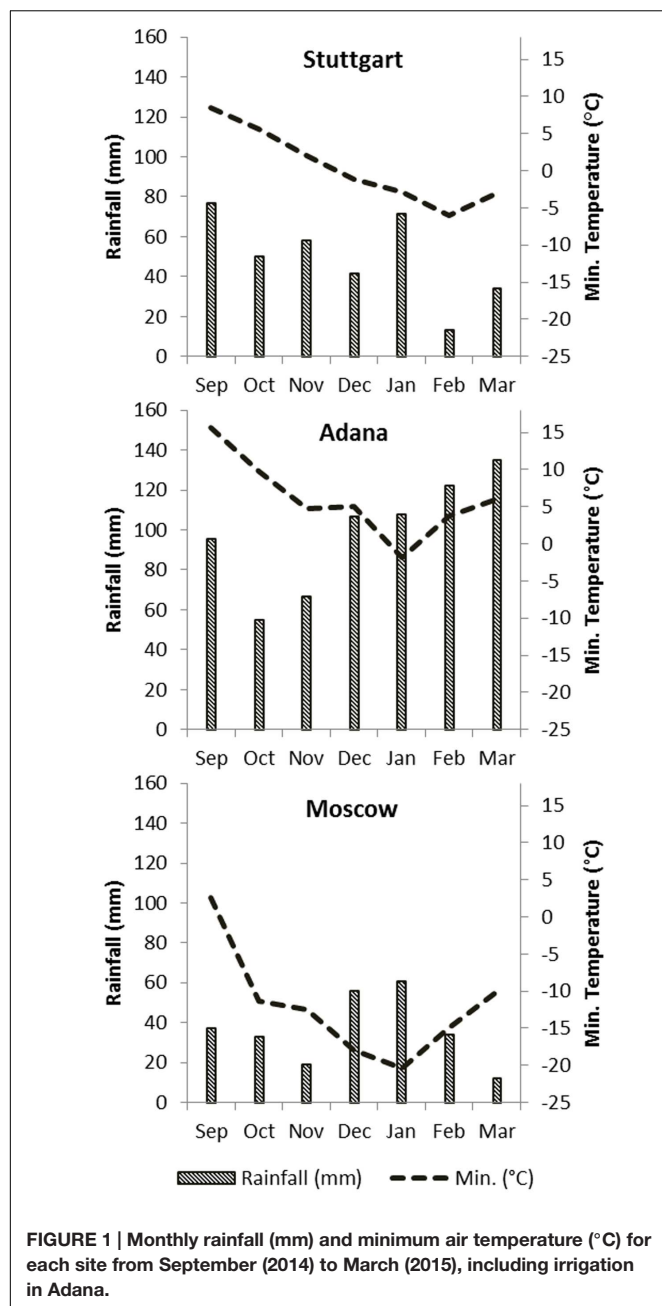
Statistical Analysis

The laboratory analysis data were used to quantify the impact of genotype, harvesting time, site effect, and the interaction between

TABLE 2 | Bulk density, stone fraction, and nutrient status for different soil depths for each site.

Site	Depth (cm)	Bulk density (g/cm^3)	Stone fraction (%)	K$_2$O (mg/100g)	P$_2$O$_5$ (mg/100g)	Mg (mg/100g)	Nmin (mg/kg soil)
Stuttgart	0–30	1.31	6.7	23.5	26.3	26.7	18.0
	30–60	1.66	9.9	8.4	3.6	23.5	3.2
	60–90	1.40	9.9	5.0	3.0	21.7	1.9
Adana	0–30	1.51	10.4	17.7	3.2	15.5	16.6
	30–60	1.64	9.7	12.8	2.0	17.7	14.1
	60–90	1.40	9.7	14.4	3.2	17.7	13.4
Moscow	0–30	1.57	1.8	2.5	11.1	10.8	26.2
	30–60	1.70	3.6	3.6	2.0	16.4	27.0
	60–90	1.40	3.6	3.5	2.3	14.0	na

na, not available.

FIGURE 1 | Monthly rainfall (mm) and minimum air temperature (°C) for each site from September (2014) to March (2015), including irrigation in Adana.

genotype and harvesting time on combustion-relevant quality parameters. Statistical analysis was performed in SAS version 9.4 (SAS Institute Inc., Cary, NC, USA) using the Proc mixed model with genotype, harvesting time and site effect as fixed and the interaction between genotype and harvesting time as random effects. All variables were tested at a P-value of 0.05. The notation of the model is:

$$y_{ijkl} = \mu + \alpha_i + \beta_j + \gamma_{jl} + (\alpha\beta)_{ij} + (\alpha\gamma)_{il} + e_{ijkl} \quad (1)$$

where y_{ijkl} represents the quality parameter for k-th replicate of genotype i; at site j and harvesting time l, μ is the general mean

of the model; α_i is the effect of genotype i; β_j is the effect of site j; γ_{jl} is the effect of harvesting time for site j for harvesting time j; $(\alpha\beta)_{ij}$ is the interaction between genotype i and site j; $(\alpha\gamma)_{il}$ is the interaction between genotype i and harvesting time l, e_{ijkl} is the error value for corresponding observation.

RESULTS

Biomass Composition Analysis Relevant for Combustion Quality

N, P, K Content in the Harvested Biomass

The statistical analysis evaluated the impacts of harvesting time, site, genotype, and genotype × harvesting time interaction on biomass composition. The statistical model showed that the impacts of harvesting time, site, and genotype were significant for all biomass quality parameters. The interaction between harvesting time and genotype was also significant for all quality parameters but the interaction between genotype and site was not significant (**Table 3**).

Overall, with the delay in harvesting time from August to January or March depending on site, the biomass quality characteristics improved significantly as N, P, and K declined with delay.

For low NO_x emissions during the combustion process, it is important to keep the N content in feedstock as low as possible. The N content of all genotypes was significantly higher at Moscow than at the other sites. The response to a delayed harvest also differed depending on site. For example, N content at Stuttgart decreased from 0.64 to 0.21% of dry matter (DM) with delay in harvesting time, which was more rapid than at the other sites. This decrease was significant with the delay until January, but no significant decrease was recorded from January to March. Overall, N, P, and K contents decreased significantly with delay in harvesting time at all sites except Moscow, where a significant decrease was only recorded for N. At final harvest, mean K content of all genotypes was lowest at Moscow (0.11 mg/g DM), followed by Adana (1.95 mg/g DM), and Stuttgart (3.38 mg/g DM). For N, the highest mean content at final harvest (0.61% DM) was recorded for Moscow, followed by Adana (0.28% DM) and Stuttgart (0.22% DM). The highest P content of all genotypes and sites was found in OPM-14 at Stuttgart in October (1.78 mg/g DM) (**Figure 2**).
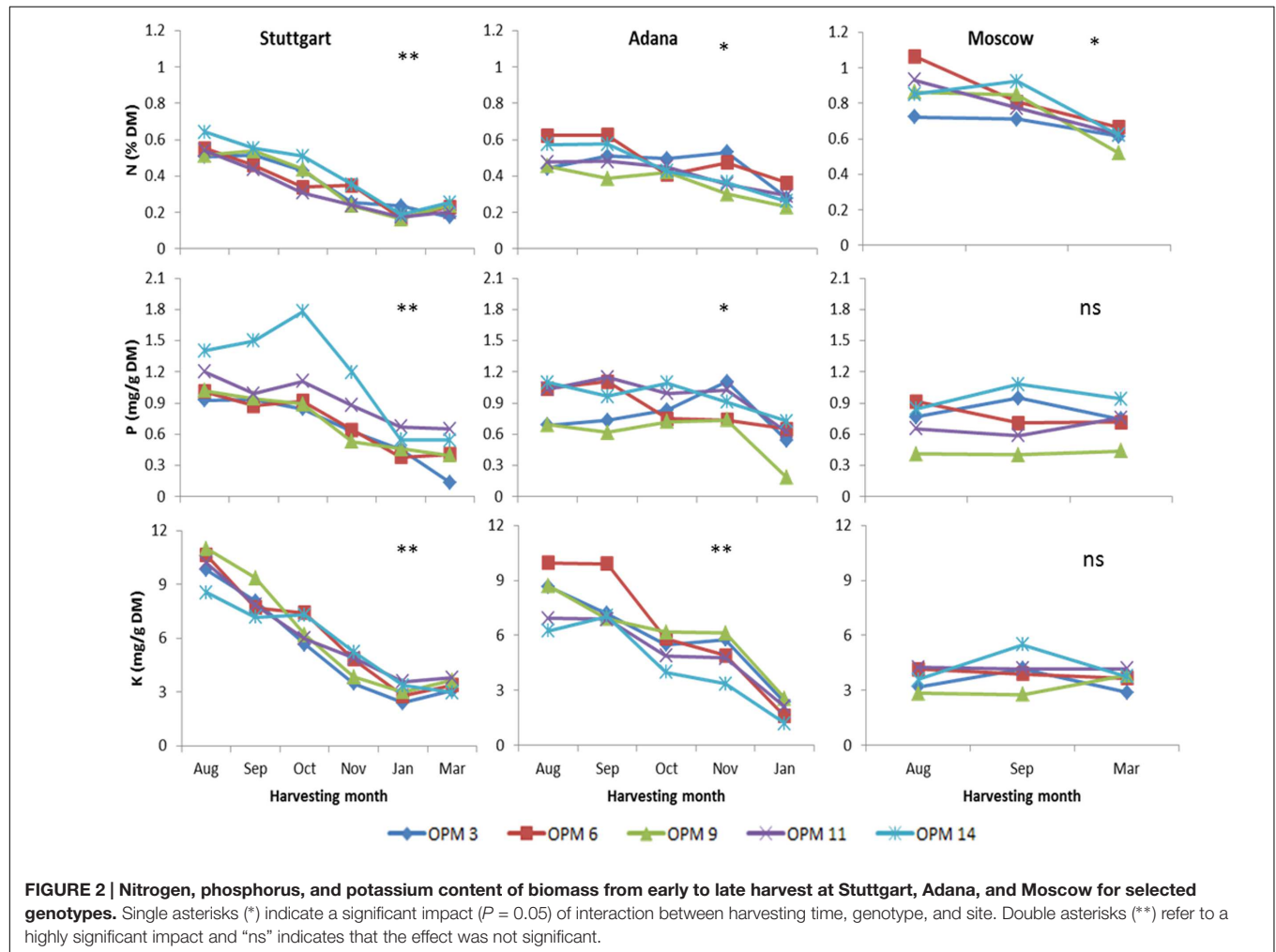
Ash Content and Ash-Forming Elements (Ca, Mg, Si)

The ash content was highest at Adana, varying from 10.63% for OPM-11 in September to 3.84% for OPM-9 in January. The impact of harvesting time on ash and ash-forming elements (Ca, Mg, Si) was only significant at Stuttgart and Adana. As the major ash-forming element, the Si content followed the same trend as for ash with the delay in harvesting time at each site. No significant difference in ash and Si content between genotypes was recorded at Stuttgart and Moscow, whereas at Adana the variation was significant. At Adana, ash, Si, Ca, and Mg contents were lowest for OPM-9 in comparison to the other genotypes. At Stuttgart, the lowest ash content was recorded in OPM-3 and OPM-6 (**Figure 3**).

TABLE 3 | P-values for various quality parameters.

Effect	N	P	K	Ca	Mg	Si	Ash	Sintering index
HT	<0.001	<0.001	<0.001	0.0569	0.0003	<0.001	<0.001	<0.001
Site	<0.001	<0.001	<0.001	<0.001	<0.001	<0.001	<0.001	<0.001
GN	0.006	0.001	0.0006	<0.001	<0.001	<0.001	<0.0001	<0.0001
HT × GN	<0.001	<0.001	<0.001	<0.001	<0.001	<0.001	<0.001	<0.001
Site × GN	ns	ns	ns	ns	ns	ns	ns	ns

HT, harvesting time; GN, genotype; ns, not significant.

FIGURE 2 | Nitrogen, phosphorus, and potassium content of biomass from early to late harvest at Stuttgart, Adana, and Moscow for selected genotypes. Single asterisks (*) indicate a significant impact ($P = 0.05$) of interaction between harvesting time, genotype, and site. Double asterisks (**) refer to a highly significant impact and "ns" indicates that the effect was not significant.

Optimization of Harvesting Time

The ideal harvesting time for combustion depends on the quality of harvested biomass, yield losses, and nutrient offtake. The biomass quality for combustion was evaluated through the development of an ash sintering index based on biomass composition.

Ash-Sintering Index

Despite high ash content at Adana, the value of the ash-sintering index was below 0.20 at final harvest for all genotypes. This indicates that there will be little to no sintering during combustion when biomass is harvested in January at this site. In

some cases, delayed harvest did not have a significant effect on ash sintering. For example, at Adana, no significant improvement in the ash-sintering index was recorded for OPM-11 and OPM-14 with the delay in harvesting time. At Stuttgart, for the January and March harvesting times, the value of the ash-sintering index was below 0.40 for all genotypes (except OPM-11 in January, where ash sintering index = 0.42) (**Figure 4**).

Yield Losses

The yield loss from peak yield was considered one of the criteria for identifying the ideal harvesting time at each site. The peak yield (t/ha) month was taken as the baseline value for the
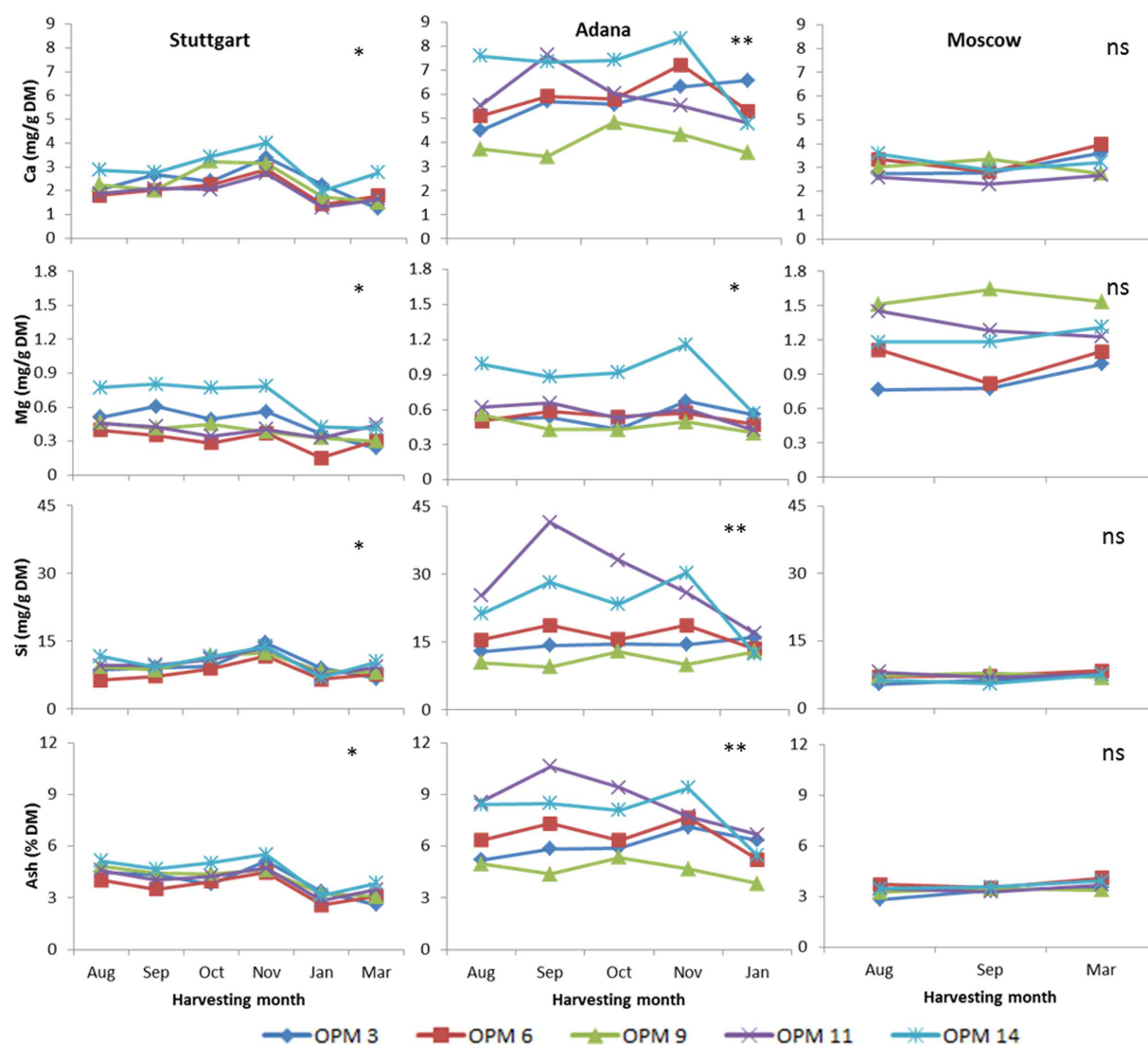
FIGURE 3 | Ash content and major ash-forming elements for each harvesting time, genotype, and site. Single asterisks (*) indicate a significant impact ($P = 0.05$) of interaction between harvesting time, genotype, and site. Double asterisks (**) refer to a highly significant impact and "ns" indicates that the effect was not significant.

calculation of percentage yield loss with the delay in harvesting time. For Stuttgart and Moscow, September harvest delivered the mean peak yield of all genotypes whereas for Adana, August was considered as peak yield month. At Stuttgart, the yield losses were below 40% when harvesting was delayed from September to January (**Figure 5**), whereas at Adana they reached 49% from peak yield (August) to final harvest in January. For Moscow, the yield loss from the peak-yield month (September) to final harvest (March) was 21%. As there were no yield data between September and March, Moscow is not presented in (**Figure 5**).

Nutrient Offtake (N, P, K)

Another important factor for the identification of optimal harvesting time is nutrient offtake, because it directly influences the long-term environmental performance of the crop. High

nutrient offtake at a specific harvesting time not only effects biomass quality but also leads to high fertilizer inputs. After the peak-yield month, nutrient offtake significantly decreased at each site with the delay in harvesting time. The highest N, P, and K offtakes were recorded at Stuttgart for each harvesting time, except for the final harvest (March) where Moscow had the highest N offtake (**Table 4**). In Stuttgart and Moscow, the highest N (101.2 and 72.9 kg/ha, respectively) and P offtakes (21.3 and 6.7 kg/ha, respectively) were recorded in September, whereas in Adana the highest offtakes were in August (N = 83.9 kg/ha, P = 15 kg/ha) (**Table 4**). The highest K offtake was recorded in August in Stuttgart (168.3 kg/ha) and Adana (131.4 kg/ha), but in September in Moscow (36.3 kg/ha) (**Table 4**). The high N, P, and K offtakes at Stuttgart can be explained by the high initial nutrient loading at this site.
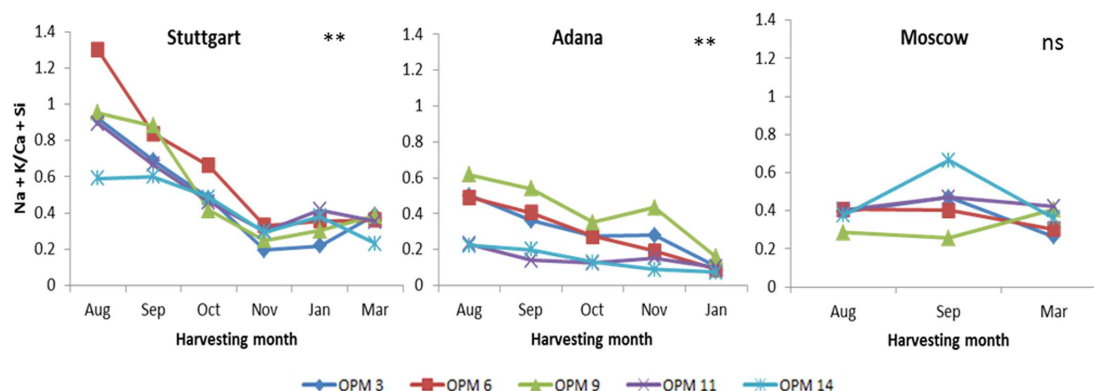
FIGURE 4 | Values of ash sintering index (Na + K/Ca + Si) for each genotype and harvesting time at Stuttgart, Adana and Moscow. Double asterisks (**) indicate a highly significant impact ($P = 0.05$) of interaction between harvesting time, genotype, and site whereas "ns" indicates that effect was not significant.
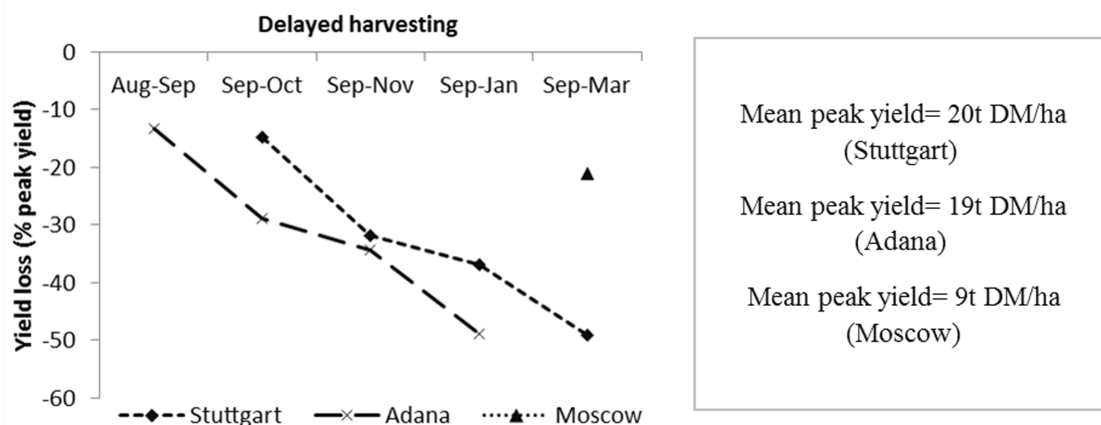
FIGURE 5 | Yield losses (%) with delay in harvesting time from peak yield for Stuttgart, Adana, and Moscow. The mean peak yield of all genotypes at each site is also shown.

DISCUSSION

This study assessed the variation in biomass quality characteristics between genotypes, mainly due to morphological and phenological differences such as stem diameter and time of flowering and senescence. For the morphological differences, stem thickness and leaf-to-stem ratio play a key role in determining biomass quality for combustion at a specific harvesting time. The genotypes assessed can be listed in the following order of stem thickness OPM-3 > OPM-9 > OPM-11 > OPM-14 > OPM-6. The thick-stemmed genotypes (*M. sacchariflorus* and *M. × giganteus*) showed a low leaf proportion (**Figure 6**).
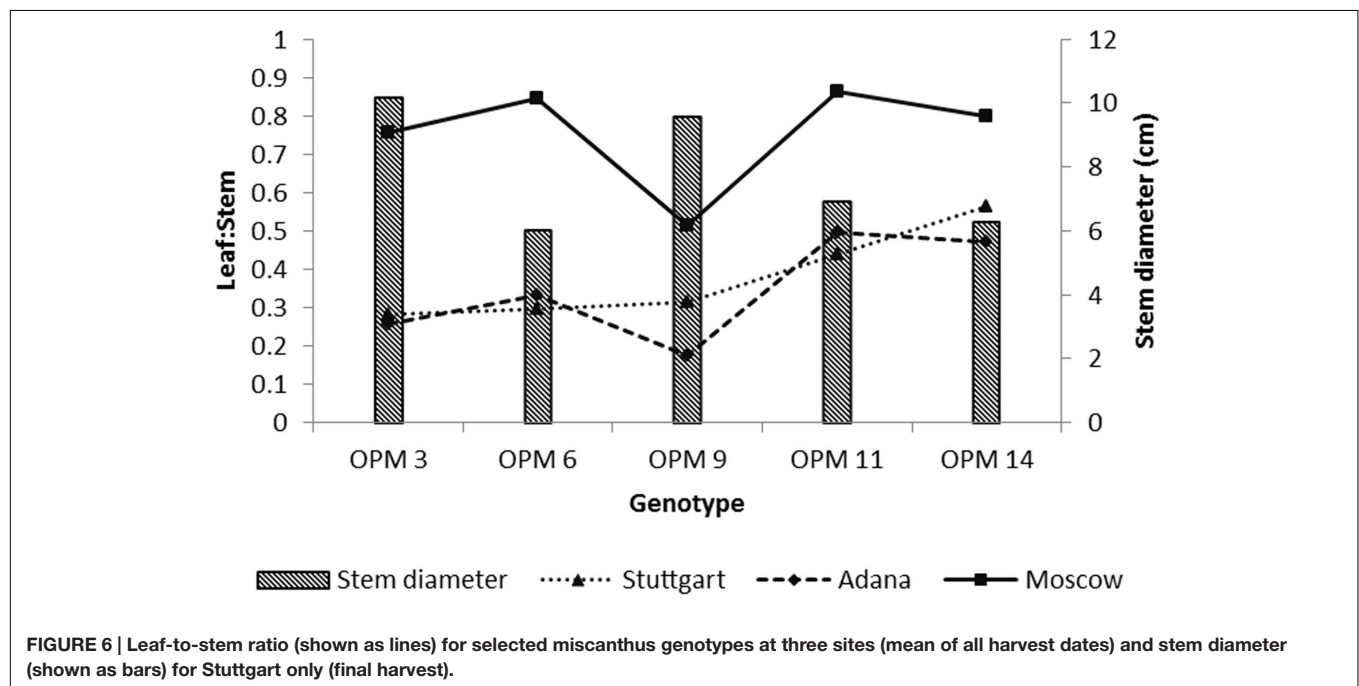
The leaves have high mineral and ash contents, therefore a low leaf proportion is favorable for combustion (Baxter et al., 2014). The low leaf proportion of *M. × giganteus* may explain why this genotype had the lowest ash content at final harvest in Adana and Moscow. At Stuttgart, it was only slightly

higher than the genotype with the lowest ash content. Stem diameter is an important morphological characteristic because it directly influences the rate of leaching. Other studies have found that thin-stemmed genotypes (*M. sinensis*) show more efficient leaching of minerals than thick-stemmed genotypes (*M. × giganteus*) (Jørgensen, 1997; Iqbal and Lewandowski, 2014). In our study, the thin-stemmed OPM-6 showed a rapid improvement in sintering index with delayed harvesting. It is assumed that it is the leaching of K which leads to this improved sintering index, because the same trend was found for K as for the sintering index with delay in harvesting time. From the literature, it is also evident that the rate of fouling and sintering during combustion is determined by the K content (Blomberg, 2007). In plants, K is present as a soluble ion (Jørgensen, 1997). Therefore the K content of biomass is largely influenced by stem thickness and rate of leaching. Kludze et al. (2013) recorded up to 31% reduction in K content of miscanthus through translocation and efficient leaching with winter precipitation with delayed

TABLE 4 | Mean nutrient offtake (N, P, K) at each site and harvesting month for all five genotypes.

Harvesting month	N (kg/ha)			P (kg/ha)			K (kg/ha)		
	Stuttgart	Adana	Moscow	Stuttgart	Adana	Moscow	Stuttgart	Adana	Moscow
August	91.4	83.9	39.0	18.3	15.0	3.2	168.3	131.4	15.6
September	101.2	71.9	72.9	21.3	13.0	6.7	162.0	107.3	36.3
October	77.2	45.1	na	20.3	9.3	na	124.8	54.0	na
January	49.0	27.8	na	12.3	5.2	na	74.8	19.1	na
March	27.9	na	42.5	5.2	na	4.9	43.9	na	25.7

na, not available.

FIGURE 6 | Leaf-to-stem ratio (shown as lines) for selected miscanthus genotypes at three sites (mean of all harvest dates) and stem diameter (shown as bars) for Stuttgart only (final harvest).

harvest. Based on our own results, we conclude that genotypes with low leaf share and thin stems would be most suitable for combustion purposes. However, for the genotypes tested here, low leaf share seems to be accompanied by thick stems. For example, *M. × giganteus* had low leaf to stem ratio but also develop thick stems. Therefore, future breeding program should focus on developing combustion specific genotypes with thin stems and low leaf share.

The variation in leaf-to-stem ratio between genotypes at the three sites shows that, in addition to genotypic variation, there is also a site affect. This site effect can be explained through differences in rainfall, because the timing and amount of rainfall affects the leaching rate of minerals (Iqbal and Lewandowski, 2014). For example, Adana had highest rainfall from October to January, which are the months most relevant for leaching because the biomass is senescent during this period. This led to a rapid improvement in sintering index before final harvest. The significantly highest ash content of all genotypes at Adana compared to the other sites is another indication of the site effect. This can be explained by differences in soil type. The soluble silica (Si) content varies with soil type. For example, clay soils have high

soluble Si content, which subsequently leads to high uptake of Si (Bakker and Elbersen, 2005). The high soluble Si content in soil at Adana may have caused the comparatively high ash content of the harvested biomass.

Phenology is another important factor that explains the genotypic variation between sites. In this study, the *M. sinensis* types flowered earliest, followed by the hybrids and then *M. × giganteus*. Genotypes with early flowering and senescence, such as *M. sinensis*, delivered higher biomass qualities than genotypes with late flowering and senescence, such as *M. × giganteus*, because the time of flowering directly influences the nutrient relocation process. Early flowering genotypes initiate the relocation of nutrients earlier and complete it before winter frost kills the stems (Jensen et al., 2016). The time of flowering and senescence for these genotypes is described by Nunn et al., unpublished.

In the results section, three criteria (biomass quality, yield losses, nutrient offtake) were described for determining ideal harvesting time, which gives the best compromise between dry matter yields and biomass quality characteristics without negatively affecting the environmental performance of the crop.

However, no hard criteria in terms of biomass quality, yield losses or nutrient offtake can be set for the identification of the ideal harvesting time, because threshold values have not yet been fully defined for miscanthus. From a biomass quality perspective, the N content of most of the genotypes at final harvest at Stuttgart and Adana falls within the defined threshold limits of the European pellet norms (ENplus A1). Therefore, N content could be used as one biomass quality parameter for identifying the ideal harvesting time. Delayed harvesting can lead to biomass yield losses and also reduce net energy yield ha-1. Early harvesting (November) of miscanthus biomass will lead to a higher net energy yield (GJ/ha) for combustion than delayed harvesting, as reported by Kiesel et al. (2017). However, it not only influences the thermal conversion of biomass but also compromises the nutrient balance of the crop by increasing nutrient offtake. In this study, nutrient offtake (N, P, K) was reduced by up to 70% at Stuttgart through delay in harvesting from August to March. In addition, it is practically not possible to fully close the nutrient cycle in the combustion chain, as can be done in the biogas chain through the recycling of biogas digestates as fertilizer. During combustion, N is lost and currently ash is not allowed as fertilizer as it is classified as waste. Results of this study indicate that delayed harvesting is accompanied by lower nutrient offtakes. In terms of nutrient use efficiency, it is preferable to harvest the biomass as late as possible.

Based on the results of this study, January harvesting can be recommended at Stuttgart for all genotypes, because there was no significant improvement in quality characteristics, especially N and K content, from January to March. However, a delay in harvest from January to March led to additional yield losses of about 12% and the nutrient offtake in January was already reduced by up to 46% compared to August. For some genotypes, such as OPM-3, OPM-9, and OPM-14, even a harvest in November is thinkable, since the N content and sintering index was low at this harvest dates and further improvements by delaying harvest might not be justified by the additional yield losses. However, earlier harvest will lead to higher moisture content (Kiesel et al., 2017) and requires adapted harvest procedure (e.g., windrowing and wilting on field). Biomass with high moisture content poses some additional challenges, such as increased logistics costs and a high risk of spoilage and self-heating during storage. In addition, in case of early harvest, nutrient offtake was also high which compromised the environmental performance of crop. For Adana, January (which was final harvest) can also be recommended for all genotypes, because the biomass quality not only met the threshold values for N content set by European pellet norms (ENplus A1), but also the sintering index was below 0.2. At this harvesting time, the N offtake was reduced by 67% compared to early harvest (August), but yield losses were comparatively high (49%). The results for Adana show that genotypes other than those investigated here would probably be more suitable for biomass production for combustion. Genotypes better adapted to drought conditions could make better use of the biomass production potential.

In Moscow, where no harvesting was possible between September and March due to heavy snowfall, the absence of significant compositional changes through leaf fall or relocation of nutrients can be explained by the short vegetative period. The harsh frost and the mean temperature well below 0 ($-12°C$) for most of this period (September to March) led to no further crop development and compositional changes. Purdy et al. (2015) found that long periods with temperatures below 0 kill the aboveground stems and negatively affect remobilization of nutrients back to rhizomes. Therefore, there was no significant biomass quality improvement through a delay in harvesting time. However, delaying the harvest until March improved the environmental performance of the crop by reducing N offtake up to 42% (compared to September) with yield losses of only 21%. This indicates that March could be more appropriate than an early harvest, but still the N content is very high compared to the other sites. From the results of this study, we conclude that genotypes which are adapted to short vegetation period and are early senescing need to be developed for sites like Moscow. This would allow the crop to complete the growth cycle more and actively relocate nutrients before first harsh frosts occur. This would help to improve the biomass quality for combustion.

At each location, the yield loss through delayed harvest is mainly due to leaf fall, stem breakage, and inefficient harvesting and collection especially caused by broken stems lying on the ground. However, no specific data on leaf fall and stem breakage were collected from early to late harvest.

From the above discussion, it can be concluded that harvesting time should be decided on and adjusted according to the prevailing weather conditions and thus may vary from one region to another. For example, in many miscanthus-growing regions in the northern hemisphere, frequent rainfall in March, in combination with the thawing effect, may cause soil softening and make the use of harvesting machinery difficult. Under such conditions, minor improvements in combustion quality at the expense of surface damage and soil compaction will not be worthwhile. Therefore, in such a scenario, an early harvest can be performed before the start of the wet season to avoid any soil damage.

AUTHOR CONTRIBUTIONS

YI was leading the writing process. MW, AH, JC-B, CN, and OK provided valuable input for improving the manuscript. Furthermore, AK provided support in discussion of the results. IL added valuable contribution to each chapter and in manifold discussions.

FUNDING

ACKNOWLEDGMENTS

REFERENCES

Aho, M., and Silvennoinen, J. (2004). Preventing chlorine deposition on heat transfer surfaces with aluminium–silicon rich biomass residue and additive. *Fuel* 83, 1299–1305. doi: 10.1016/j.fuel.2004.01.011

Arvelakis, S., and Koukios, E. G. (2013). Critical factors for high temperature processing of biomass from agriculture and energy crops to biofuels and bioenergy. *Wiley Interdiscip. Rev. Energy Environ.* 2, 441–455. doi: 10.1002/wene.28

Bakker, R. R., and Elbersen, H. W. (2005). "Managing ash content and quality in herbaceous biomass: an analysis from plant to product," in *Proceedings of the 14th European Biomass Conference*, Paris, 17–21.

Baxter, X. C., Darvell, L. I., Jones, J. M., Barraclough, T., Yates, N. E., Shield, I., et al. (2012). Study of *Miscanthus x giganteus* ash composition – Variation with agronomy and assessment method. *Fuel* 95, 50–62. doi: 10.1016/j.fuel.2011.12.025

Baxter, X. C., Darvell, L. I., Jones, J. M., Barraclough, T., Yates, N. E., Shield, I., et al. (2014). *Miscanthus* combustion properties and variations with *Miscanthus* agronomy. *Fuel* 117, 851–869. doi: 10.1016/j.fuel.2013.09.003

Bilandzija, N., Jurisic, V., Voca, N., Leto, J., Matin, A., Sito, S., et al. (2016). Combustion properties of *Miscanthus × giganteus* biomass – optimization of harvest time. *J. Energy Inst.* (in press). doi: 10.1016/j.joei.2016.05.009

Blomberg, T. (2007). "Free alkali-index for optimizing the fuel mixture in biomass co-firing," in *Proceedings of 7th International Conference on Heat Exchanger Fouling and Cleaning - Challenges and Opportunities*, eds H. Müller-Steinhagen, M. Reza Malayeri, and A. Paul Watkinson (Tomar: Engineering Conferences International).

Blomberg, T. (2012). Correlation of the corrosion rates of steels in a straw fired boiler with the thermodynamically predicted trend of KOH(g) in the flue gases. *Biomass Bioenergy* 39, 489–493. doi: 10.1016/j.biombioe.2012.01.016

Clifton-Brown, J., Schwarz, K., and Hastings, A. (2015). History of the development of *Miscanthus* as a bioenergy crop: from small beginnings to potential realisation. *Biol. Environ. Proc. R. Ir. Acad.* 115B, 45–57. doi: 10.3318/bioe.2015.05

Hayes, D. J. M. (2013). Mass and compositional changes, relevant to biorefining, in *Miscanthus x giganteus* plants over the harvest window. *Bioresour. Technol.* 142, 591–602.

Iqbal, Y., and Lewandowski, I. (2014). Inter-annual variation in biomass combustion quality traits over five years in fifteen *Miscanthus* genotypes in south Germany. *Fuel Process. Technol.* 121, 47–55. doi: 10.1016/j.fuproc.2014.01.003

Iqbal, Y., and Lewandowski, I. (2016). Biomass composition and ash melting behaviour of selected miscanthus genotypes in Southern Germany. *Fuel* 180, 606–612. doi: 10.1016/j.fuel.2016.04.073

Jensen, E., Robson, P., Farrar, K., Thomas Jones, S., Clifton-Brown, J., Payne, R., et al. (2016). Towards *Miscanthus* combustion quality improvement: the role of flowering and senescence. *GCB Bioenergy* 9, 891–908. doi: 10.1111/gcbb.12391

Jørgensen, U. (1997). Genotypic variation in dry matter accumulation and content of N, K and Cl in *Miscanthus* in Denmark. *Biomass Bioenergy* 12, 155–169.

Kiesel, A., Nunn, C., Iqbal, Y., Van der Weijde, T., Wagner, M., Özgüven, M., et al. (2017). Site-specific management of *Miscanthus* genotypes for combustion and anaerobic digestion: a comparison of energy yields. *Front. Plant Sci.* 8:347.

Kludze, H., Deen, B., and Dutta, A. (2013). Impact of agronomic treatments on fuel characteristics of herbaceous biomass for combustion. *Fuel Process. Technol.* 109, 96–102. doi: 10.1016/j.fuproc.2012.09.043

Lewandowski, I., Clifton-Brown, J., Trindade, L. M., van der Linden, G. C., Schwarz, K. U., Müller-Sämann, K., et al. (2016). Progress on optimizing miscanthus biomass production for the European bioeconomy: results of the EU FP7 project OPTIMISC. *Front. Plant Sci.* 7:1620. doi: 10.3389/fpls.2016.01620

Lewandowski, I., and Heinz, A. (2003). Delayed harvest of miscanthus—influences on biomass quantity and quality and environmental impacts of energy production. *Eur. J. Agron.* 19, 45–63. doi: 10.1016/S1161-0301(02)00018-7

Meehan, P., Mc Donnell, K., Grant, J., and Finnan, J. (2014). The effect of harvest time and pre harvest treatment on the moisture content of *Miscanthus × giganteus*. *Eur. J. Agron.* 56, 37–44. doi: 10.1016/j.eja.2014.03.003

Mi, J., Liu, W., Yang, W., Yan, J., Li, J., and Sang, T. (2014). Carbon sequestration by *Miscanthus* energy crops plantations in a broad range semi-arid marginal land in China. *Sci. Total Environ.* 496, 373–380.

Naumann, C., and Bassler, R., (1976/2012). *Die Chemische Untersuchung von Futtermitteln. Methodenbuch/Verband Deutscher Landwirtschaftlicher Untersuchungs-und Forschungsanstalten*, Bd. 3. Darmstadt: VDLUFA-Verl.

Obernberger, I., and Thek, G. (2008). Combustion and gasification of solid biomass for heat and power production in Europe-state-of-the-art and relevant future developments. *Paper Presented at the Proc. of the 8th European Conference on Industrial Furnaces and Boilers*, Vilamoura.

Purdy, S. J., Cunniff, J., Maddison, A. L., Jones, L. E., Barraclough, T., Castleet, M., et al. (2015). Seasonal carbohydrate dynamics and climatic regulation of senescence in the perennial grass. *Miscanthus. Bioenergy Res.* 8, 28–41. doi: 10.1007/s12155-014-9500-2

Smith, R., and Slater, F. M. (2011). Mobilization of minerals and moisture loss during senescence of the energy crops *Miscanthus×giganteus*, *Arundo donax* and *Phalaris arundinacea* in Wales, UK. *Glob. Change Biol. Bioenergy* 3, 148–157. doi: 10.1111/j.1757-1707.2010.01069.x

SWD (2014). *Communication from the Commission to the European Parliament and the Council: European Energy Security Strategy*. Brussels: European commission.

Wang, L., Hustad, J. E., Skreiberg, Ø, Skjevrak, G., and Gronli, M. (2012). A critical review on additives to reduce ash related operation problems in biomass combustion applications. *Energy Proc.* 20, 20–29. doi: 10.1016/j.egypro.2012.03.004

Zabed, H., Sahu, J. N., Boyce, A. N., and Faruq, G. (2016). Fuel ethanol production from lignocellulosic biomass: an overview on feedstocks and technological approaches. *Renew. Sustain. Energy Rev.* 66, 751–774. doi: 10.1016/j.rser.2016.08.038

Site-Specific Management of Miscanthus Genotypes for Combustion and Anaerobic Digestion: A Comparison of Energy Yields

Andreas Kiesel[1]*, Christopher Nunn[2], Yasir Iqbal[1], Tim Van der Weijde[3], Moritz Wagner[1], Mensure Özgüven[4], Ivan Tarakanov[5], Olena Kalinina[1], Luisa M. Trindade[3], John Clifton-Brown[2] and Iris Lewandowski[1]

[1] Department Biobased Products and Energy Crops, Institute of Crop Science, University of Hohenheim, Stuttgart, Germany, [2] Institute of Biological, Environmental and Rural Sciences, Aberystwyth University, Aberystwyth, UK, [3] Department of Plant Breeding, Wageningen University, Wageningen, Netherlands, [4] Faculty of Agriculture and Natural Sciences, Konya Food and Agriculture University, Konya, Turkey, [5] Russian State Agrarian University–Moscow Timiryazev Agricultural Academy, Moscow, Russia

In Europe, the perennial C_4 grass miscanthus is currently mainly cultivated for energy generation via combustion. In recent years, anaerobic digestion has been identified as a promising alternative utilization pathway. Anaerobic digestion produces a higher-value intermediate (biogas), which can be upgraded to biomethane, stored in the existing natural gas infrastructure and further utilized as a transport fuel or in combined heat and power plants. However, the upgrading of the solid biomass into gaseous fuel leads to conversion-related energy losses, the level of which depends on the cultivation parameters genotype, location, and harvest date. Thus, site-specific crop management needs to be adapted to the intended utilization pathway. The objectives of this paper are to quantify (i) the impact of genotype, location and harvest date on energy yields of anaerobic digestion and combustion and (ii) the conversion losses of upgrading solid biomass into biogas. For this purpose, five miscanthus genotypes (OPM 3, 6, 9, 11, 14), three cultivation locations (Adana, Moscow, Stuttgart), and up to six harvest dates (August–March) were assessed. Anaerobic digestion yielded, on average, 35% less energy than combustion. Genotype, location, and harvest date all had significant impacts on the energy yield. For both, this is determined by dry matter yield and ash content and additionally by substrate-specific methane yield for anaerobic digestion and moisture content for combustion. Averaged over all locations and genotypes, an early harvest in August led to 25% and a late harvest to 45% conversion losses. However, each utilization option has its own optimal harvest date, determined by biomass yield, biomass quality, and cutting tolerance. By applying an autumn green harvest for anaerobic digestion and a delayed harvest for combustion, the conversion-related energy loss was reduced to an average of 18%. This clearly shows that the delayed harvest required to maintain biomass

quality for combustion is accompanied by high energy losses through yield reduction over winter. The pre-winter harvest applied in the biogas utilization pathway avoids these yield losses and largely compensates for the conversion-related energy losses of anaerobic digestion.

INTRODUCTION

Miscanthus is a resource-use efficient, high-yielding perennial C4 grass species native to East Asia, including China, Korea, Taiwan, and Japan (Lewandowski and Schmidt, 2006; Clifton-Brown et al., 2015). The cultivation of miscanthus is characterized by its perennial nature and low nitrogen-fertilization demand, due to its effective nutrient recycling system (Christian et al., 2008; Strullu et al., 2011; Cadoux et al., 2012). This leads to a generally benign environmental profile, often associated with soil carbon sequestration (McCalmont et al., 2017). For these reasons, miscanthus biomass utilization generally shows a low global-warming and resource-depletion potential (Felten et al., 2013; Styles et al., 2015; Meyer et al., 2016). Despite these positive aspects, the miscanthus cultivation area is still rather small in Europe, mainly due to its high establishment costs and the current lack of valorisation options.

The only cultivar presently commercially available is *Miscanthus x giganteus* (Mxg), a natural, sterile hybrid of *Miscanthus sacchariflorus* and *Miscanthus sinensis*, which was introduced into Europe in 1935 (Greef et al., 1997; Clifton-Brown et al., 2015). As Mxg is sterile, only clonal propagation is possible. This is costly and does not allow for crop development by conventional breeding. Therefore, miscanthus breeding for European conditions is mainly focussing on the groups *M. sinensis*, *M. sacchariflorus,* and *Miscanthus floridulus*, which offer broad genetic variability and the possibility of reducing establishment costs through economical, seed-based propagation (van der Weijde et al., 2013; Clifton-Brown et al., 2017). In the EU project OPTIMISC (FP7 No. 289159), early stage crossings from the ongoing miscanthus breeding programmes of Aberystwyth (IBERS) and Wageningen University (WUR) were tested at several locations, under different stress conditions and for various utilization options (Lewandowski et al., 2016).

Combustion is one of the most common utilization options for miscanthus biomass, but production of cellulosic ethanol and anaerobic digestion were identified as promising alternatives (van der Weijde et al., 2013, 2017b; Mayer et al., 2014; Wahid et al., 2015; Kiesel and Lewandowski, 2017). For each utilization option, ideal harvest time is of crucial importance to maintain high quality and yield. For combustion, the harvest time is delayed to reduce the contents of moisture, ash, and critical elements (Iqbal and Lewandowski, 2014). However, there is a trade-off here between yield and quality, as leaf losses occur over winter and lead to a decrease in biomass yield (Iqbal et al., under review). For biogas, an early green harvest delivers a higher quality, since the substrate-specific methane yield decreases with ongoing lignification (Kiesel and Lewandowski, 2017). Here again there is a trade-off, as a very early green harvest delivers

a lower yield, due to insufficient utilization of the vegetation period, and also impairs the crop growth the next season due to insufficient relocation of carbohydrates (Purdy et al., 2015; Kiesel and Lewandowski, 2017). The latter is referred to as "cutting tolerance," which has been defined for miscanthus as the ability of the crop to recover from an early green harvest without yield reductions in the following year (Kiesel and Lewandowski, 2017). As the ideal harvest time is a compromise between yield, quality, and cutting tolerance in both utilization options, the development of the energy yield (which includes biomass yield and quality) needs to be quantified throughout the year. In addition, a comparison of energy yield between combustion and anaerobic digestion is required to establish the loss associated with the generation of the higher-value product. In this case, biomethane—which is upgraded solid biomass— is seen as a higher-value product. As a gaseous fuel, it has a broader range of applications, including transport fuel, and its application in combined heat and power generation is easier, including transport, storage, and utilization of biomethane in existing natural gas infrastructure.

In addition to harvest time, the genotype also affects biomass quality. For combustion, genotypes with low contents of moisture, ash and critical elements at harvest are optimal, while for anaerobic digestion a low degree of lignification and ease of digestibility is preferred. Iqbal and Lewandowski (2014) found notable genotypic differences in contents of ash and critical elements, which can be partly attributed to genotypic differences in nutrient relocation and leaching of soluble elements. For biogas and ethanol utilization, van der Weijde et al. (2017b) observed both a higher saccharification potential and substrate-specific methane yield in less lignified genotypes. Location may also play a crucial role. For example, drought conditions can increase the saccharification potential of miscanthus biomass (van der Weijde et al., 2017a).

The objective of this paper is (i) to identify the effect of genotype, environment and harvest time on yield and biomass quality for anaerobic digestion and combustion and (ii) to compare the energy yield of both pathways throughout the year. For this purpose, five miscanthus genotypes from the OPTIMISC multi-location field trials were sampled at monthly intervals throughout the end of the vegetation period until final harvest in spring at the locations in Adana (Turkey), Moscow (Russia), and Stuttgart (Germany). Energy yield, biomass yield, and a number of quality parameters (including substrate-specific methane yield) were assessed and compared for each sampling date. This allows identification of site-specific optimization potentials for each utilization option. This paper focuses on biomass quality for anaerobic digestion, but also includes some basic quality criteria relevant for the energy yield via combustion, such as

moisture and ash content. A detailed combustion quality analysis, including the content of critical elements, and a quantification of the trade-off between yield and biomass quality can be found in Iqbal et al. (under review). Further the net energy yield via anaerobic digestion and combustion, which considers moisture and ash content, was assessed and compared, to allow site-specific identification of the best suited harvest date for each utilization option.

MATERIALS AND METHODS

Field Trial

The field trial was established in 2012 as part of the EU-financed project OPTIMISC (FP7 No. 289159) to compare 15 miscanthus genotypes at 6 sites across Europe and Russia: at Aberystwyth (UK), Adana (Turkey), Moscow (Russia), Potash (Ukraine), Stuttgart (Germany), and Wageningen (Netherlands). It was set up in a randomized block design with three biological replications at each location. A detailed description of the field trial including genotypes used, soil and climatic conditions can be found in Kalinina et al. (under review) and Lewandowski et al. (2016). For this paper, five genotypes (best yields) and three locations (contrasting climates) were selected, where at least one representative from each miscanthus group (species) was included. The selected genotypes are shown in **Table 1** and the chosen locations were Adana, Moscow, and Stuttgart.

The genotypes were sampled at intervals of 1–2 months from the end of vegetation period until the final harvest in spring (**Table 2**). In Moscow and Stuttgart, the final harvest was performed in March. In Adana, it took place in January, because the plants had already started to regrow. In Moscow, sampling was interrupted after September to the final harvest, because the aboveground parts of the crop were completely killed by a harsh frost a few days before the sampling date in September.

Figure 1 depicts rainfall and temperature data for the three locations Adana, Moscow, and Stuttgart. In Adana, a seasonal drought period occurred in July and August. There was only little frost in January 2015 (**Figure 1A**). In Moscow, July was particularly dry and the plants faced a serious drought (**Figure 1B**). The winter started very abruptly at the end of September with harsh frosts and the crop was frozen most of the time until March. In Stuttgart, June was abnormally dry, but in the following 2 months the rainfall was higher than usual (**Figure 1C**). Overall, the winter 2014/2015 was mild, but there was a frost period in January and February 2015.

Biomass Yield Estimation

On each sampling date, eight tillers were collected randomly from each genotype. The samples were taken from the second outer row to avoid damaging the core plot, which was used for final harvest biomass yield estimation. To ensure the samples were taken randomly, a bar with marks every 60 cm was used. The tiller closest to each 60-cm mark was collected. The central four m^2 of each plot were used for biomass yield estimation at final harvest in January (Adana) or March (Moscow, Stuttgart) and harvested manually using a hedge trimmer or sickle bar mower. Before the final harvest, another eight tillers were collected randomly.

TABLE 1 | Miscanthus "genotypes" used in this investigation (Lewandowski et al., 2016).

Genotype ID	Provider	Species
OPM 3	IBERS	*Miscanthus sacchariflorus*
OPM 6	IBERS	*Miscanthus sinensis* x *Miscanthus sacchariflorus* hybrid
OPM 9	IBERS	*Miscanthus* x *giganteus*
OPM 11	IBERS	*Miscanthus sinensis* "Goliath"
OPM 14*	WUR	*Miscanthus sinensis*

strictly speaking, OPM 14 is a "within species" hybrid rather than a true genotype, but for convenience is referred to throughout as a "genotype."

All samples were dried to constant weight at 60°C in a cabinet dryer and fresh and dry weight was recorded. Dry matter content and reciprocal value moisture content were calculated according to weight loss. Based on the weight of the eight tillers at each sampling date and the biomass yield at final harvest, the dry and fresh matter yield at each sampling date was calculated (Equation 1). The dry matter yield at each sampling date was calculated using a ratio of the stem weights at the sampling date and the final harvest. The details of this calculation are described by Nunn et al. (under review).

$$Yield_n = \frac{Weight\ 8\ tillers_n}{Weight\ 8\ tillers_m} * Yield_m \tag{1}$$

where

Yield$_n$ = Biomass yield at sampling date n

Weight 8 tillers$_n$ = Weight of eight tillers at sampling date n

Weight 8 tillers$_m$ = Weight of eight tillers at final harvest in March (January at Adana)

Yield$_m$ = Biomass yield at final harvest in March (January at Adana), estimated at central 4 m^2.

Laboratory Analysis

All dried samples were send to University of Hohenheim, where all further analysis have been performed. The biomass samples were milled in a cutting mill SM 200 (Retsch, Haan) using a 1 mm sieve before further laboratory analysis. The ash content of all samples was assessed by incineration in a muffle kiln at 550°C for 4 h according to VDLUFA book III method 8.1 (Naumann and Bassler, 1976/2012).

Content of neutral detergent fiber (NDF), acid detergent fiber (ADF) and acid detergent lignin (ADL) was estimated by near infrared spectroscopy (NIRS). Calibration and validation samples were analyzed using an ANKOM^{2000} Fiber Analyzer and Daisy II Incubator (ANKOM Technology, Macedon, USA) according to VDLUFA book III method 6.5.1 (NDF), 6.5.2 (ADF), and 6.5.3 (ADL) (Naumann and Bassler, 1976/2012). The standard error of the NIRS calibration (SEC) and prediction (SEP) and the R^2 of the NIRS calibration and validation are shown in **Table 3**. The ADL content is considered lignin. Cellulose content was calculated by subtracting ADL from ADF, and hemicellulose by subtracting ADF from NDF.

The specific methane yield (SMY) was measured in a biogas batch test at 39°C according to VDI guideline 4630. The biogas

TABLE 2 | Sampling dates and location characteristics. na = not applicable/no sampling performed.

Location	Latitude Longitude Altitude (m)	Sampling date					
		1 August (A)	2 September (S)	3 October (O)	4 November (N)	5 January (J)	6 March (M)
Adana	37.00 35.00 27	20.8.14	20.9.14	20.10.14	20.11.14	20.01.15	na
Moscow	55.50 37.33 140	20.8.14	20.9.14	na	na	na	13.03.15
Stuttgart	48.74 8.93 463	28.8.14	25.9.14	23.10.14	27.11.14	22.01.15	18.03.15

batch method was certified by the KTBL and VDLUFA inter-laboratory comparison test in 2014 and 2015 and is described in detail in Kiesel and Lewandowski (2017). The SMY was analyzed by using 200 mg oDM of the dried and milled biomass samples and 30 g of inoculum, which contained various macro- and micronutrients according to Angelidaki et al. (2009). The fermentation was performed for 35 days in gastight fermentation flasks and the biogas production was measured by the pressure increase using a HND-P pressure meter (Kobold Messring GmbH, Hofheim). The methane content of the biogas was measured by using a GC 2014 gas chromatograph (Shimadzu, Kyoto). However, for capacity reasons it was not possible to analyse all samples. Therefore, a minimum of one field replication of each genotype from each sampling date and each location was selected randomly to be analyzed. All samples were analyzed in one run of the biogas batch test to assure statistical soundness. A randomized block design with four technical replicates was applied. For capacity reasons, the batch test had to be split into two water baths. Replicates 1 and 2 were analyzed in one and replicates 3 and 4 in the other.

The methane yield per hectare was calculated based on estimated dry matter yield (DMY), ash content and SMY. As the SMY was mostly analyzed for only one of the three field replications, this value (or the average of all field replications analyzed) was assumed for all three field replications.

The net energy yield of anaerobic digestion was calculated by multiplying the methane yield per hectare by the calorific value of methane (35.883 MJ m^{-3}) as shown in Equation (2). The net energy yield of combustion was calculated according to Equation (3), in which an average calorific value of 18 MJ kg^{-1} for dry miscanthus biomass (Kołodziej et al., 2016) and 2.443 MJ kg^{-1} enthalpy of water vaporization was assumed. The net energy yield is considering not only ash and moisture content of the biomass, but also the energy required to evaporate the incorporated water.

$$Net\ Energy\ Yield_{Anaerobic\ digestion} = CV_{Methane} * SMY \\ * DMY * (1-AC) \quad (2)$$

$$Net\ Energy\ Yield_{Combustion} = CV_{Miscanthus} * DMY * (1-AC) \\ - EE_{Water} * FMY * MC \quad (3)$$

where

$CV_{Methane}$ = calorific value of methane (35.883 MJ m^{-3})
SMY = substrate-specific methane yield
DMY = dry matter yield of miscanthus
AC = ash content of the miscanthus biomass
$CV_{Miscanthus}$ = calorific value of dry miscanthus biomass (18 MJ kg^{-1})
EE_{Water} = evaporation enthalpy water (2.443 MJ kg^{-1})
FMY = fresh matter yield of miscanthus
MC = moisture content of the miscanthus biomass.

Statistical Analysis

Statistical analysis was performed using the software SAS version 9.4 (SAS Institute Inc., Cary, North Carolina). The program "Procmixed" was used and a mixed model applied (Equation 4). A test on homogeneity of variance and normal probability of residues was performed. The effects were tested at a level of probability of $\alpha = 0.05$.

$$y = \mu + Loc + Geno + Loc * Geno + HD\,(Loc) \\ + Geno * HD(Loc) + e \quad (4)$$

where

μ = general mean effect
Loc = effect of location (Adana, Moscow, Stuttgart)
Geno = effect of genotype (OPM 3, 6, 9, 11, 14)
Loc∗Geno = effect of interaction of location and genotype
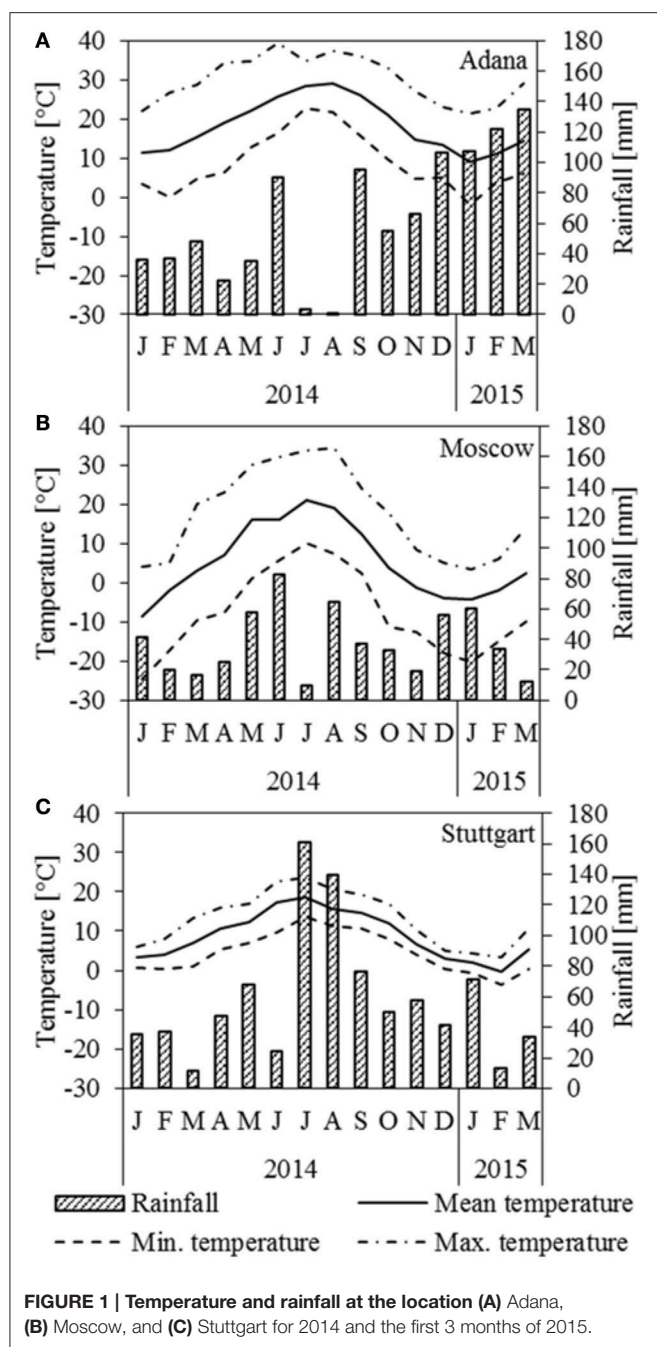HD(Loc) = effect of location specific sampling date
Geno ∗ HD(Loc) = effect of interaction of genotype and location specific sampling date
e = residual error.

RESULTS

In the following chapter, the results of each genotype at each harvest date and location are shown in figures, but for clarity

FIGURE 1 | Temperature and rainfall at the location (A) Adana, (B) Moscow, and (C) Stuttgart for 2014 and the first 3 months of 2015.

TABLE 3 | NIRS calibration and validation statistics.

	Calibration			Validation		
	Number of samples	Standard error of calibration	R^2	Number of samples	Standard error of prediction	R^2
NDF	160	1.2672	0.953	20	2.345	0.858
ADF	160	1.3331	0.959	20	2.699	0.834
ADL	160	0.6492	0.888	20	0.773	0.706

parameters, such as methane yield per hectare and net energy yield of biogas and combustion (**Table 4**). This may be influenced by the high variance in yield, caused by the fairly rough yield estimation using eight tillers. The interaction of genotype and sampling date per location [Geno∗HD(Loc)] showed a significant impact only on dry matter, hemicellulose and lignin content. Again, the variance due to the small sampling size of eight tillers may have been too high. However, larger sampling size was not feasible to avoid impact on the field trial.

Biomass Yield and Dry Matter Content

There was a large difference in biomass yield development throughout the year between the Adana location (the warmest in this study) and the other two locations (**Figure 2**).

In Adana, the biomass yield was significantly highest in August and then declined steadily until final harvest in March (**Figure 2A**). The highest biomass yields at each sampling date were found for OPM 9, which declined from 22.6 t DM ha^{-1} in August to 13.0 t DM ha^{-1} in March. Significantly lower biomass yields were found in OPM 3. The biomass yields of all the other genotypes showed no significant differences.

In Moscow, significantly higher biomass yields were found in September (**Figure 2B**) and OPM 3 (11.2 t DM ha^{-1}) was the highest-yielding genotype in this month (**Figure 2B**). At final harvest in March, OPM 6 and 9 had the highest DM yields (10.3 and 7.7 t DM ha^{-1}). These had stayed quite stable over winter, while the yield of OPM 3 had declined severely to 4.7 t DM ha^{-1}.

In Stuttgart, the biomass yield behavior was similar to that in Moscow. Significantly higher biomass yields were found in September and October and all genotypes showed significant yield losses over winter (**Figure 2C**). The highest DM yields were found for OPM 6, which increased to 25.0 t DM ha^{-1} in September and then decreased to 16.2 t DM ha^{-1} in March. However, the biomass yields of OPM 6 were only significantly different from OPM 14. Interestingly, OPM 9 (Mxg) showed comparatively low biomass yields in the course of the year but an increase from January to March (10.2–13.4 t DM ha^{-1}). Yield measurement in OPM 9 was difficult due to the shape of the crop (center of the plot was considerably higher than the border rows), which may have led to an underestimation of yield, especially in January. However, the final harvest in March was performed at the center of the plot and therefore delivered reasonable biomass yields.

The dry matter content (DMC) increased steadily at all locations throughout the year and the significantly highest DMC was recorded at final harvest in March/January (**Figure 2**). In

reasons letters are displayed only for the sampling dates per location [HD(Loc)]. Tables with means for genotype and location at each harvest date and the respective letter displays are given in the supplementary material.

Fixed Effects

Location (Loc) and sampling date per location [HD(Loc)] showed highly significant impacts on all traits analyzed (**Table 4**). Genotype (Geno) and interaction of location and genotype (Loc∗Geno) had a highly significant impact on quality parameters and a still significant impact on yield-related

TABLE 4 | *P*-values of fixed effects.

	Yield	Dry matter content	Ash content	Cellulose content	Hemicellulose content	Lignin content	SMY	Methane yield per hectare	Net energy yield biogas	Net energy yield combustion
Loc	<0.001	<0.001	<0.001	<0.001	<0.001	<0.001	<0.001	<0.001	<0.001	<0.001
Geno	0.010	<0.001	<0.001	<0.001	<0.001	<0.001	<0.001	0.037	0.039	0.006
Loc*Geno	0.006	0.001	<0.001	<0.001	<0.001	<0.001	0.015	0.029	0.030	0.036
HD(Loc)	<0.001	<0.001	<0.001	<0.001	0.007	<0.001	<0.001	<0.001	<0.001	<0.001
Geno* HD(Loc)	ns	<0.001	ns	ns	0.001	0.037	ns	ns	ns	ns

Adana, OPM 6 showed the highest DMC throughout the year and at final harvest in January (**Figure 2A**). It was also the only genotype in Adana that achieved a DMC of above 80% FM at final harvest, which is crucial for safe storage of the biomass. In Moscow, no significant differences in DMC were detected between the genotypes, but OPM 9 was the only genotype with a DMC of below 80% FM at final harvest (**Figure 2B**). In Stuttgart, OPM 6 showed the highest DMC from August to November, but further drying was hindered by lodging of the crop (**Figure 2C**). In January, OPM 11 and 14 showed the highest DMC. However, the differences in DMC at final harvest in March were very small, due to good weather conditions (frost in winter, dry before harvest).

Methane Yield and SMY

In Moscow, the substrate-specific methane yield (SMY) did not change significantly throughout the year (**Figure 3B**). In Adana and Stuttgart, it decreased significantly from August to final harvest in March (**Figures 3A,C**). However, the impact of the SMY on methane yield was only slight compared to that of biomass yield. It can be clearly seen that MY follows the same trend as dry matter yield and is therefore not described separately here.

The SMY of OPM 9 was the significantly lowest of all assessed genotypes at all locations. That of OPM 14 was very similar at all three locations, while that of OPM 9 and 11 was significantly higher in Stuttgart than in Adana and Moscow. The SMY of OPM 3 and OPM 6 was significantly lower in Adana than in Stuttgart, but there was no significant difference between Stuttgart and Moscow.

Fibre and Ash Contents

Ash content was strongly influenced by location and Adana showed the significantly highest ash contents at each sampling date (**Figure 4**). In Adana, the ash content only decreased significantly from November to January. In Stuttgart, a significant decrease was also observed from November to January and the biomass sampled in January and March had the significantly lowest ash content. In contrast, the ash content in Moscow increased slightly, but significantly, from August to March. Genotype OPM 11 showed the significantly highest ash content at Adana and OPM 14 at Stuttgart. In Moscow, no significant genotypic differences were recorded.

The cellulose content increased steadily at Adana and Stuttgart, where the significantly highest contents were recorded

for sampling dates January and March (**Figure 5**). All genotypes showed the significantly highest cellulose contents at Stuttgart, but those at Adana and Moscow were mostly not significantly different. Here, OPM 9 showed the significantly highest cellulose content of all genotypes (not significantly higher than OPM 11 in Adana). In Stuttgart, the significantly highest cellulose contents were found with OPM 6 and OPM 9. In Moscow, both cellulose and hemicellulose contents did not significantly change over the year; only a slight, but significant decrease in lignin was recorded.

In Adana, the hemicellulose content increased slightly with later sampling dates and the significantly highest hemicellulose content was found in January, but it was not significantly different from November and October (**Figure 5A**). In Stuttgart, the hemicellulose content increased slightly until November (significantly highest) and then decreased at the same rate (**Figure 5C**). At all locations, OPM 9 had the significantly lowest hemicellulose content, except OPM 3 at Stuttgart. The hemicellulose content of all genotypes was highest (mostly significantly) at the Moscow location.

The lignin content increased steadily with later sampling dates at the Adana and Stuttgart locations, where the significantly highest lignin contents were recorded in January and March (**Figure 5**). At all locations, OPM 9 showed the significantly highest lignin content, however it was not significantly higher than that of OPM 3 at Stuttgart.

Net Energy Yields

The net energy yield of anaerobic digestion is influenced by dry matter yield, SMY, and ash content, whereas the net energy yield of combustion is influenced by dry matter yield, moisture content and ash content. For both, dry matter yield has the largest impact. As the development of both net energy yields clearly follows that of dry matter yield, it is not described separately here (**Figure 6**). In Adana, the highest net energy yield of combustion and anaerobic digestion was recorded for OPM 9 in August at 344 and 203 GJ ha^{-1}, respectively. At this location, the net energy yield of both combustion and anaerobic digestion decreased steadily, by 37 and 49% respectively, until final harvest in January. In Moscow, the genotypes with the highest net energy yield of combustion and anaerobic digestion in September were OPM 3 at 168 and 113 GJ ha^{-1} and OPM 6 at 143 and 92 GJ ha^{-1}, respectively. While the net energy yield of OPM 3 decreased noticeably (−53% for combustion and −60% for anaerobic digestion), OPM 6 showed a net energy
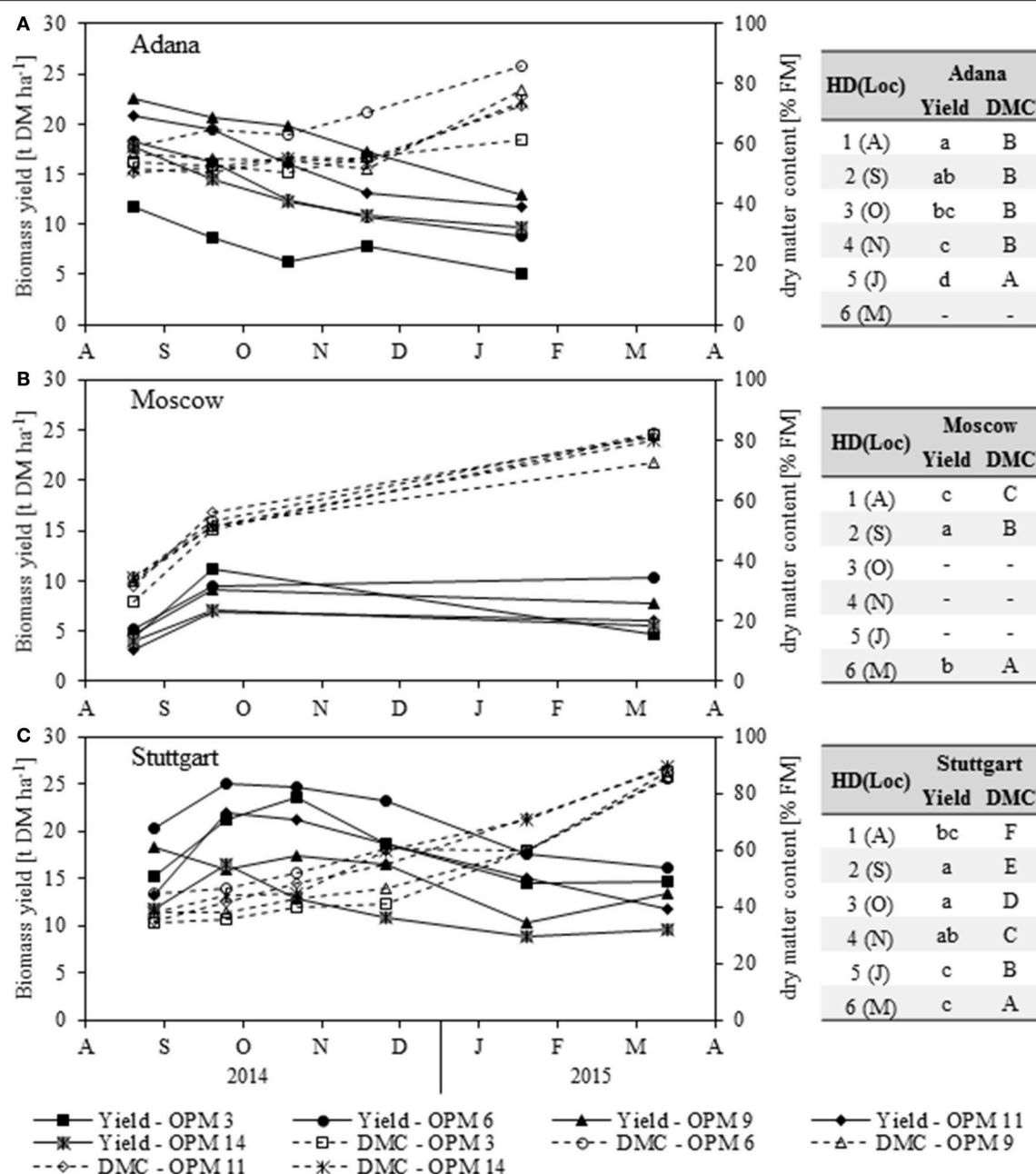
FIGURE 2 | Biomass dry matter yield (Yield) and dry matter content (DMC) of each genotype [OPM 3, 6, 9, 11, 14] for each sampling date (1 = August (A), 2 = September (S), 3 = October (O), 4 = November (N), 5 = January (J), 6 = March (M)] at the locations (A) Adana, **(B)** Moscow and **(C)** Stuttgart. Tables include the letter display for the sampling date per location [HD(Loc)] for the traits yield and DMC. Different lower- (Yield) and upper-case (DMC) letters indicate significant differences at a probability level of $\alpha = 0.05$ for sampling dates at a specific location.

yield of combustion and anaerobic digestion of 172 and 99 GJ ha^{-1}, respectively. In Stuttgart, the highest net energy yield of combustion was observed in October and of anaerobic digestion in September for OPM 6 at 370 and 259 GJ ha^{-1}, respectively. Here, at final harvest in March, the energy yield of combustion and anaerobic digestion of OPM 6 was 275 and 154 GJ ha^{-1}, respectively.

A comparison of the two energy yields shows that, on average over all locations, genotypes and sampling dates, anaerobic digestion delivers 65% of the energy yield of combustion. However, there are noteworthy differences between location, genotypes and harvest dates. Early sampling in August improves the net energy yield of anaerobic digestion through an increase in SMY, but impairs the net energy yield of combustion through a
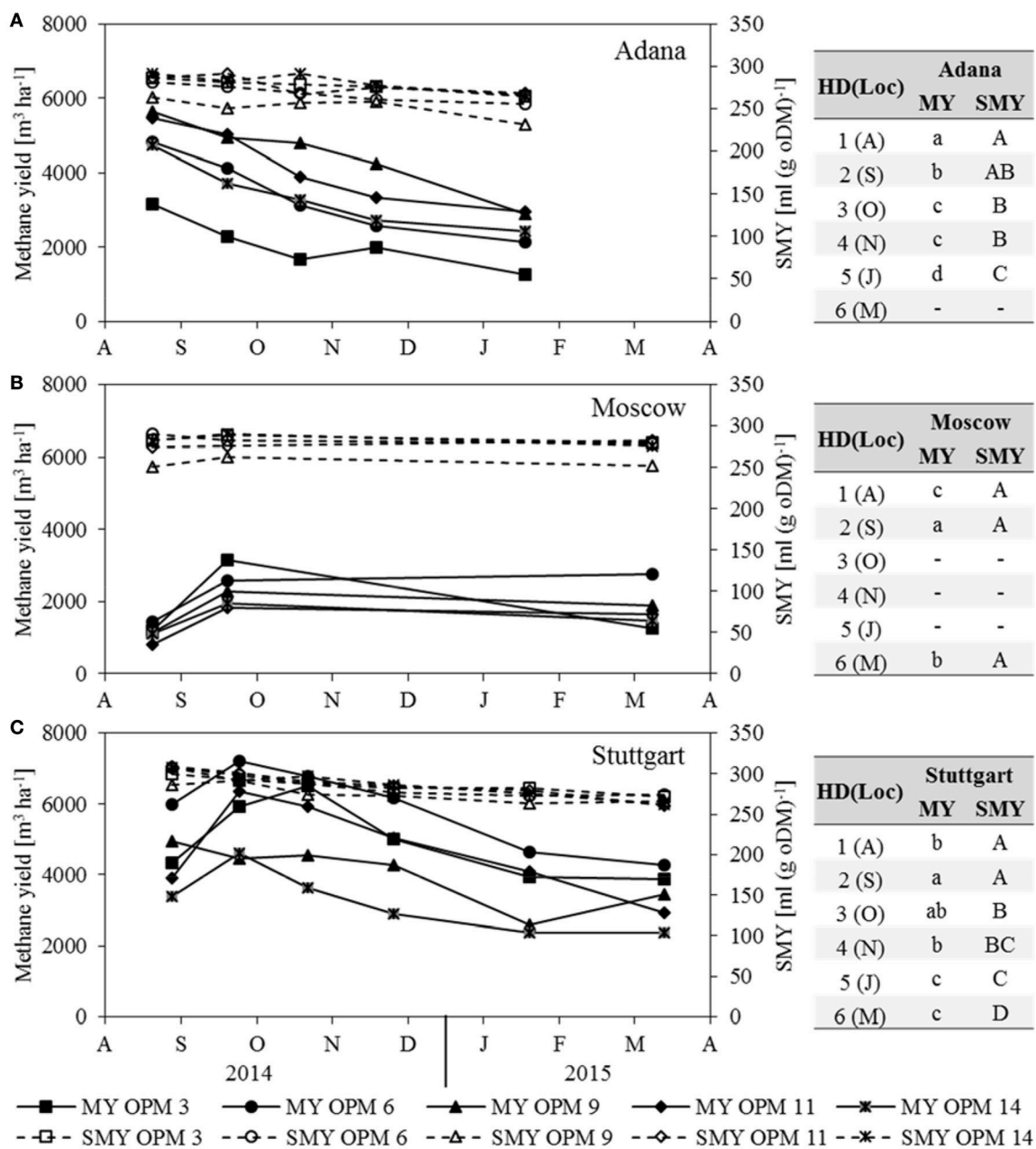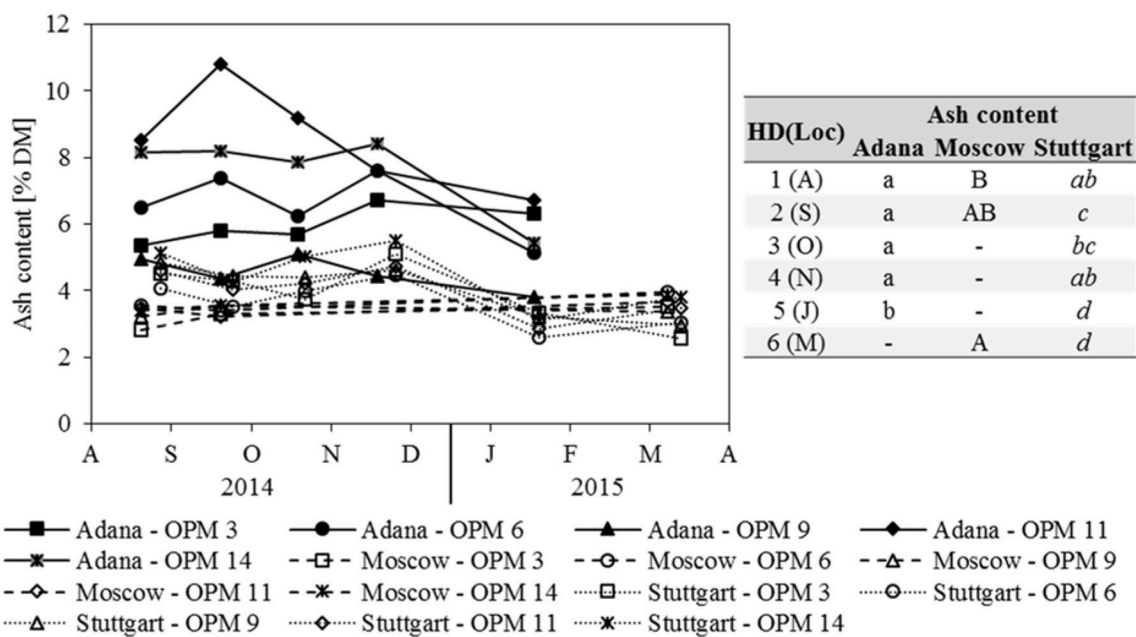
FIGURE 3 | Methane yield (MY) and substrate-specific methane yield (SMY) for each genotype [OPM 3, 6, 9, 11, 14) and sampling date (1 = August (A), 2 = September (S), 3 = October (O), 4 = November (N), 5 = January (J), 6 = March (M)] at the locations (A) Adana, **(B)** Moscow and **(C)** Stuttgart. Tables include the letter display for the sampling date per location [HD(Loc)] for the traits methane yield (MY) and substrate-specific methane yield (SMY). Different lower- (MY) and upper-case (SMY) letters indicate significant differences at a probability level of $\alpha = 0.05$ for sampling dates at a specific location.

higher moisture content. In August, the average net energy yield of anaerobic digestion for all locations and genotypes was 75% that of combustion; in Stuttgart and Moscow even 79 and 83%, respectively. Late harvest in January or March leads to a decrease in SMY and improved quality for combustion (lower moisture content). At final harvest, the net energy yield of anaerobic digestion, averaged over all locations and genotypes, was 55% of that of combustion; for OPM 9 even as low as 52%.

DISCUSSION

The energy yields (used here synonymously with "net energy yield") per hectare of combustion and anaerobic digestion are mainly influenced by the harvestable biomass yield per hectare, but are differentially sensitive to content of organic and inorganic compounds in the biomass. The different biomass fractions, e.g., moisture, ash, and lignin content, interact to

FIGURE 4 | Ash content for each genotype (OPM 3, 6, 9, 11, 14) and sampling date [1 = August (A), 2 = September (S), 3 = October (O), 4 = November (N), 5 = January (J), 6 = March (M)] at the three locations Adana, Moscow, and Stuttgart. Tables include the letter display for the sampling date per location [HD(Loc)] for the traits ash content. Different lower- (Adana) and upper-case (Moscow) and italic (Stuttgart) letters indicate significant differences at a probability level of α = 0.05 for sampling dates at a specific location.

produce a thermal calorific value (combustion) or substrate-specific methane yield (anaerobic digestion). In combustion, inorganics such as ash mainly reduce the combustible proportion of the yield, whereas vaporization of water consumes additional energy and reduces the calorific value. For this reason, moisture content has the strongest quality-related impact on the energy yield of combustion. Biomass quality for anaerobic digestion is mainly related to the organic composition, in particular the lignin content. Here the energy yield is directly measured by the substrate-specific methane yield (SMY) in a biogas batch test, which is therefore the sole determining quality factor. Other biomass quality characteristics, such as lignin content, are only used to explain differences in SMY. The moisture content is not relevant for the energy yield of anaerobic digestion, since it is already considered during estimation of dry matter yield. In both conversion pathways, ash content reduces the amount of combustible and digestible biomass to the same extent (SMY is also calculated on the basis of organic dry matter), therefore it is not discussed in the following section.

All these yield and quality traits are influenced by genotype, location, harvest date and interaction of genotype and location. The following sections first discuss the impacts of the above determinants on energy yields of combustion and anaerobic digestion and then the energy yields are compared.

Factors Influencing Energy Yield

In both utilization pathways, harvestable yield (standardized by calculating dry matter at the different harvest times) had the largest impact on energy yield. Since location, genotype, and harvest date all have an influence on harvestable dry matter yield, these also had a considerable impact on energy yield. In Adana, the maximum biomass yield was recorded before the first sampling date of this investigation (Nunn et al., under review), after which the yield declined steadily because drought in July and August ended the growth season. Interestingly, the standard genotype Mxg (OPM 9) performed best in terms of energy yield under the water-limited conditions in 2014 in Adana. The low irrigation levels applied to ensure survival of the crop will have influenced the performance of the genotypes. Indeed, Mxg is well known for sensitivity to drought (Clifton-Brown et al., 2002). However, from these observations, we conclude that while none of the genotypes tested here are optimally adapted to the climatic conditions of the Mediterranean area, *M. sinensis* coped better than the others.

In Moscow, the yield was comparatively low due to the short growing season determined by the more extreme continental climate (**Figure 1B**). This clearly shows that cold-tolerant genotypes, which start growing at lower temperatures, are required for such locations in order to make best use of the available vegetation period. However, Fonteyne et al. (2016) found that, for a C4 plant, miscanthus shows a comparatively high chilling tolerance. In Stuttgart, the mild continental climate with high water availability (**Figure 1C**) supported active growth for a longer period, resulting in higher autumn yields than in Moscow and Adana. Considerable genotypic differences were observed in Stuttgart, where the novel genotype OPM 6 performed best. This was mainly influenced by its high shoot density (Kalinina et al., under review). The effect of plant
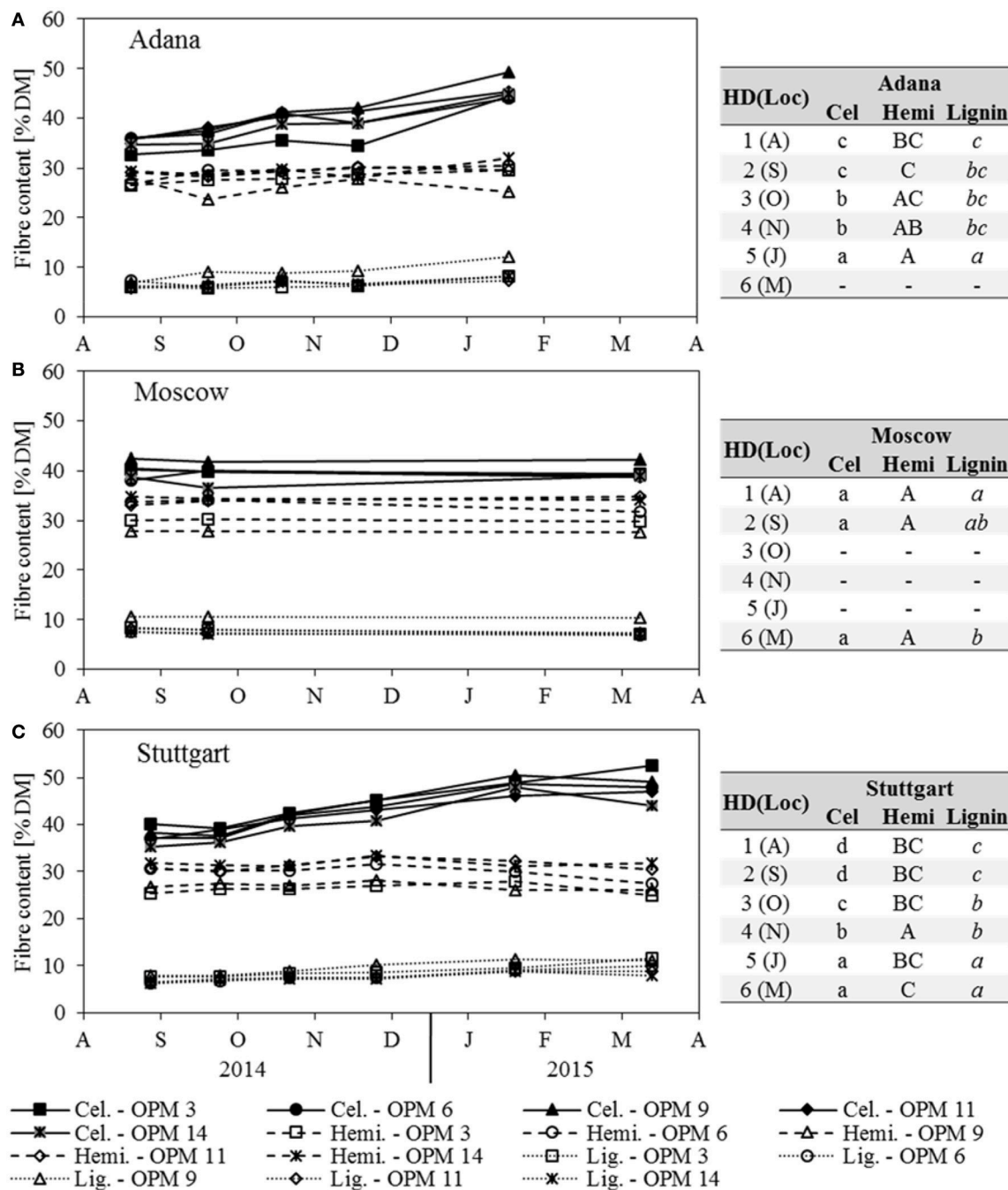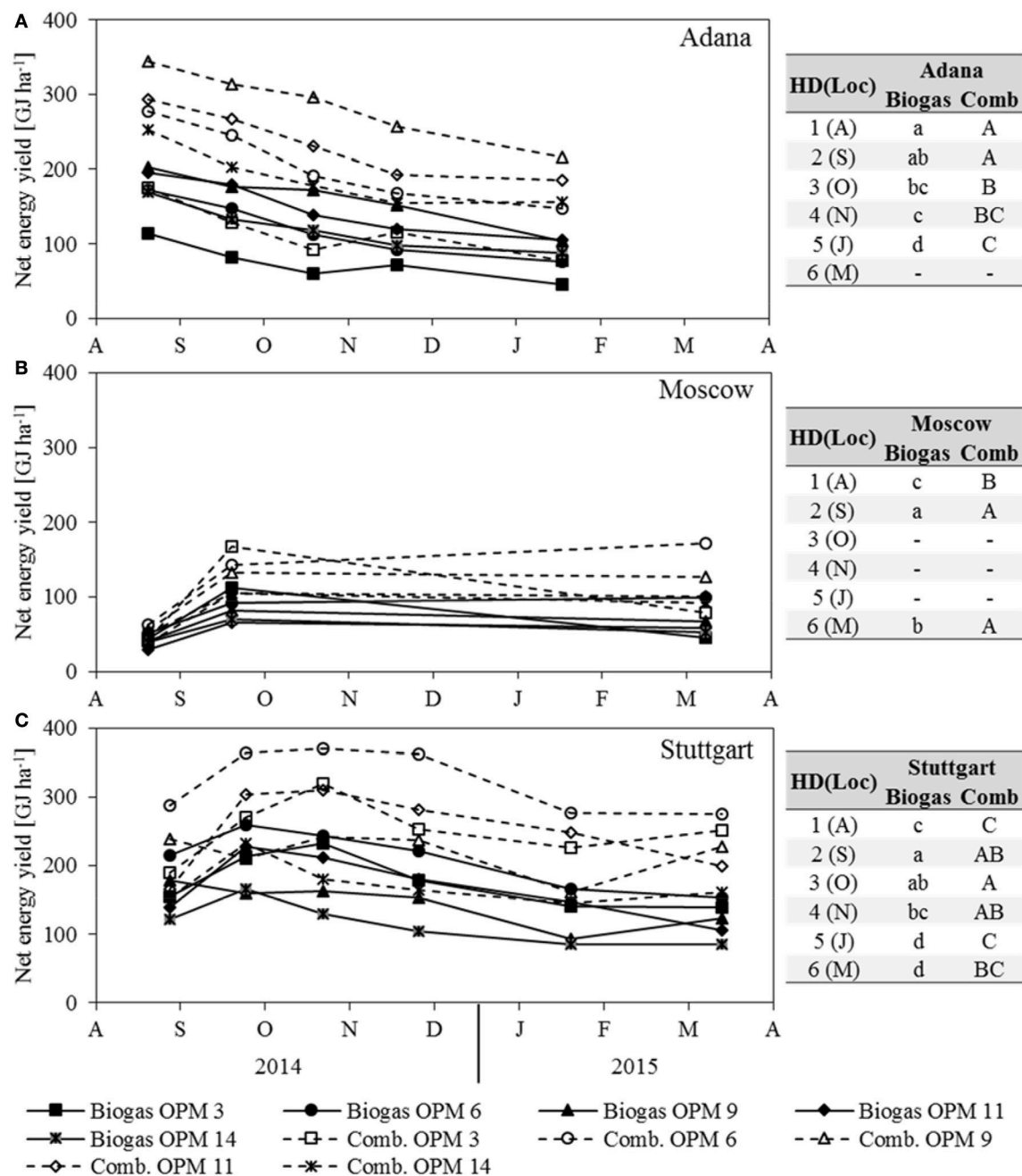
FIGURE 5 | Cellulose (Cel), hemicellulose (Hemi) and lignin content of each genotype (OPM 3, 6, 9, 11, 14) and sampling date [1 = August (A), 2 = September (S), 3 = October (O), 4 = November (N), 5 = January (J), 6 = March (M)] at the three locations (A) Adana, **(B)** Moscow, and **(C)** Stuttgart. Tables include the letter display for the sampling date per location [HD(Loc)] for the traits cellulose, hemicellulose and lignin content. Different lower- (Cel) and upper-case (Hemi) and italic (Lignin) letters indicate significant differences at a probability level of α = 0.05 for sampling dates at a specific location.

morphology on biomass yield demonstrates the opportunities of breeding high-yielding hybrids.

Earlier studies have found that moisture content is not only influenced by harvest date, but also determined by complex interactions between genotype and growth location environment

(Iqbal and Lewandowski, 2014). Obviously, moisture content impacts the energy yield of combustion, since it directly reduces the heating value. However, the moisture content at final harvest is not only crucial for combustion quality, but also for safe storage of the biomass.

FIGURE 6 | Net energy yield of anaerobic digestion (Biogas) and combustion (Comb) of each genotype (OPM 3, 6, 9, 11, 14) and each sampling date [1 = August (A), 2 = September (S), 3 = October (O), 4 = November (N), 5 = January (J), 6 = March (M)] at the three locations (A) Adana, **(B)** Moscow, and **(C)** Stuttgart. Tables include the letter display for the sampling date per location [HD(Loc)] for the net energy yield of anaerobic digestion (Biogas) and combustion (Comb). Different lower- (Biogas) and upper-case (Comb) letters indicate significant differences at a probability level of $\alpha = 0.05$ for sampling dates at a specific location.

Genotypes with active senescence could help maintain sufficiently low moisture content at final harvest (Nunn et al., under review). This is especially relevant for locations with mild winters, as frost kills the aboveground biomass, thus accelerating senescence, initiating ripening, and drying the biomass (Robson et al., 2012). The largest genotypic differences in moisture

content at final harvest were recorded in Adana, where almost no frost occurred over winter. At the other locations, only small differences in moisture content between genotypes were recorded, because there were sufficiently harsh frosts (below $-3°C$ daily mean temperature). In Adana, only OPM 6, a *M. sinensis* x *M. sacchariflorus* hybrid, showed a sufficiently low

moisture content of below 20% FM, while OPM 3, a pure *M. sacchariflorus* genotype, showed a particularly high moisture content. Genotypes with active senescence could also be useful at the Stuttgart location, because sufficient frosts to dry the crop below a moisture content of 20% do not occur every year. Iqbal and Lewandowski (2014) reported high differences in moisture content between single years at this location. Here, OPM 11 and 14 showed favorable development of moisture content until January, but after the February frost period, all genotypes had the same low moisture content at final harvest in March. In Adana, OPM 6 showed a gradual reduction in moisture content from autumn to spring. In Stuttgart, a similar decrease in moisture content from August until November was observed, but lodging hindered further drying. Genotypes with active senescence not only offer the potential to ensure sufficient drying even at locations with mild winters, but additionally allow optimization of harvest time for combustion (Iqbal et al., under review).

Moisture contents of above 60% have a greater impact on energy yield (Equation 3). Such high moisture contents were only recorded in August at Moscow and in August and September at Stuttgart. Drying over winter positively influenced the energy yield of combustion, but the improved biomass quality did not compensate for the yield losses e.g., due to leaf fall. This "trade-off" between biomass yield and quality is well known (Lewandowski et al., 2003; Cadoux et al., 2012) but has rarely been quantified due to the lack of serial harvests through the winter months. This paper quantifies the energy yield losses of delayed harvest in late winter compared to harvest at peak yield for the first time. Average energy yield losses were found to be 43% in Adana, 20% in Stuttgart and only 11% in Moscow. Some genotypes showed high energy yield losses over winter, such as OPM 3 in Adana (56%) and Moscow (53%), and OPM 11 in Stuttgart (36%). Genotype OPM 9 showed comparatively low losses at all locations (37% in Adana, 6% in Stuttgart and 4% in Moscow). However, as mentioned earlier, the biomass yield measurement of OPM 9 in Stuttgart was subject to technical variation, which could have negatively influenced these results from August to January. Other genotypes also showed contrasting results at the three locations, e.g., OPM 11 had high losses in Stuttgart (36%), but low losses in Moscow (4%) and Adana (36%). The yield losses could be associated with the leaf shares and OPM 9 showed the lowest leaf-to-stem ratio (Iqbal et al., under review). From an energy point of view, an earlier harvest would be theoretically advantageous for combustion, but is in conflict with biomass quality (see also Iqbal et al., under review).

The energy yield of anaerobic digestion is influenced more by DM yield than SMY, because SMY variations in the serial harvests were lower than initially expected. Similar findings have recently also been reported from other experiments (Wahid et al., 2015; Kiesel and Lewandowski, 2017). The biomass analyzed in the present study was milled (1 mm), which can affect the SMY. Frydendal-Nielsen et al. (2016) used a larger particle size than in our study and measured a lower SMY for miscanthus. In their study, pre-treatment increased the SMY of miscanthus significantly due to size reduction of the biomass particles. The SMY values in our paper show more the technical potential than the biogas yield, which would be obtained in full-scale biogas plants using chopped biomass. The current standard chip format for anaerobic digestion was developed for maize. Thus, presumably a pre-treatment would be required for miscanthus to achieve a similar SMY in full-scale biogas plants to that measured in our study. Various pre-treatment methods, including physical (e.g., milling, ultrasonic, steam-explosion), chemical (acid or alkaline), and biological methods (white and brown rot fungi, enzymes), to improve digestibility and methane yield of difficult and lignocellulosic substrates in anaerobic digestion are described in literature (Patinvoh et al., 2017). In recent years, suitable pre-treatment technology has become more available and is increasingly utilized in practice.

At the Adana and Stuttgart locations, the SMY decreased significantly with later harvest dates as the lignin content increased. Under anaerobic conditions, lignin is generally not digested and also inhibits the digestibility of other compounds (den Camp et al., 1988). Of all genotypes, OPM 9 had significantly lower SMY's, which correlates with the highest lignin content across all locations. Again, it is worth mentioning that the biomass was milled (1 mm) prior to the biogas batch test. This milling can be considered pre-treatment, which is known to increase digestibility of lignocellulosic biomass (Menardo et al., 2013; Frydendal-Nielsen et al., 2016). The SMY could have been positively affected by milling, especially for later harvest dates and genotypes with a higher degree of lignification. The effect of location on SMY is not clear. In the present study, Adana often had a significantly lower SMY, but also the lowest lignin content. Generally, drought conditions are expected to increase the lignin content (Le Gall et al., 2015). However, van der Weijde et al. (2017a) reported that drought conditions decreased lignin contents of miscanthus and increased the proportion of cellulose converted to ethanol. In our study, the drought conditions in Adana seemed to decrease the lignin content, but no positive effect on the SMY was observed.

Since biomass yield is more relevant than SMY for the energy yield of anaerobic digestion, the priority should be placed on harvesting at biomass peak yield. However, sufficient green-cutting tolerance is a prerequisite for this (Kiesel and Lewandowski, 2017). Green-cutting tolerance is assumed to be determined by relocation of carbohydrates from the aboveground biomass to the rhizome in late summer and early autumn (Purdy et al., 2015). By contrast, an increased nitrogen fertilizer application had almost no impact on the regrowth the following year of a 5-year-old Mxg crop in Stuttgart (Kiesel and Lewandowski, 2017). Green cuts also result in larger nutrient offtakes (Kiesel and Lewandowski, 2017), which need to be replaced, e.g., by digestate, to maintain long-term productivity of the crop.

Based on recent cutting trials with Mxg, a harvest in late October does not affect biomass yield the following year in Stuttgart, but earlier harvest can reduce DM yields by 40–60% (Kiesel and Lewandowski, 2017). Due to the harsh frost just before the sampling date in September in Moscow, it can be assumed that green harvest in late September or early October is feasible. In Adana, the season end was not defined by frost, but by drought in July and August. For this reason, it is questionable which harvest date would be tolerated by the crop here. Due to the favorable growing conditions before the drought period, the

plants flowered very early, which may have induced senescence and carbohydrate relocation (Jensen et al., 2016). However, Purdy et al. (2015) observed no influence of flowering on carbohydrate relocation, but the growing conditions at their locations in UK were completely different from Adana. The steady biomass yield decrease in Adana shows there was no biomass growth after the drought period. This can be seen as an indication that an August green harvest could be tolerated by the crop here. Should this be the case, biomass yield losses and the necessary irrigation for crop survival during the drought period could be avoided. Cutting tolerance presumably also depends on genotype and location but this needs to be assessed for further genotypes and locations. A more detailed assessment of possible harvest dates in autumn (from September to late October) would be required to identify the feasibility of a harvest at biomass peak yield. For this reason, multi-location cutting tolerance studies should be performed for new leading genotypes such as OPM-6.

Combustion vs. Anaerobic Digestion

Combustion has many advantages over anaerobic digestion. In this paper, the energy yield of anaerobic digestion, averaged over all harvest dates, was 35% lower than that of combustion. In addition, dry-harvested biomass can be stored easily for combustion, if the moisture is below 20%. Green-harvest could still be problematic for combustion due to content of critical elements and low ash melting temperature (Iqbal et al., under review). The identification of optimum harvest date requires a number of factors to be considered, including combustion technology applied, biomass yield, moisture content and various biomass quality aspects (Iqbal et al., under review). Therefore, it may not always be possible to harvest miscanthus at biomass peak yield for combustion and the state-of-the-art for most combustion applications is to delay harvest until March to improve biomass quality and moisture content. For this reason, it is perhaps less useful to compare energy yields for anaerobic digestion and combustion on the same harvest dates. If it is assumed that the crop tolerates green harvest in late August in Adana, anaerobic digestion delivers, on average, a 14% higher energy yield than combustion at final harvest in January. Harvest in late September for anaerobic digestion in Moscow and Stuttgart supplies only a 19 and 7% lower energy yield, respectively, than harvest for combustion in March. Even with delaying the harvest in Adana (September) and Stuttgart

(October) to improve the cutting tolerance, the energy yield of anaerobic digestion is, on average, only 18% lower than that of combustion at final harvest.

Recommendations for Site-Specific Genotype Choice

For both utilization options, genotypes with a high dry matter yield are required. Whereas, for anaerobic digestion the autumn biomass yield (often equal to peak yield) is crucial, for combustion a high biomass yield in late winter or spring is necessary. For this reason, genotypes such as OPM 9 with lower losses over winter (e.g., due to lower leaf share) are better suited for combustion. However, senescence of OPM 9 can be insufficient when winters are too mild, which leads to higher moisture content of the biomass accompanied by difficulties for harvest, storage and combustion. At such locations, high-yielding *M. sinensis* (e.g., OPM 11) or *M. sinensis* x *M. sacchariflorus* hybrids (such as OPM 6) could help ensure low moisture content at spring harvest. Since lodging occurred in OPM 6, this genotype cannot be recommended for combustion, because lodging makes the harvest more difficult and hinders drying of the biomass over winter. For anaerobic digestion, the impact of lodging is less critical, but still renders the harvest more difficult. Although OPM 6 lodged in Stuttgart, its utilization for anaerobic digestion still seems promising, because this genotype had a combination of high yield potential in autumn, high SMY and low lignin content. In Adana, OPM 11 appears promising due to its high yield in late summer and high SMY, but the cutting tolerance remains to be assessed. In Moscow, the *M. sacchariflorus* genotype OPM 3 performed best for anaerobic digestion, but cannot be recommended due to its creeping rhizome. For this reason, the second best-performing genotype OPM 6 is recommended for anaerobic digestion at this location.

Anaerobic digestion is a promising utilization option for miscanthus biomass, as the energy losses from conversion into gaseous fuel can be largely compensated for by avoiding biomass losses over winter. A short summary of the main findings is shown in **Box 1**. The storage of green miscanthus biomass via ensiling also appears feasible and can be further improved through the use of additives (Whittaker et al., 2016). To optimize the harvest date for anaerobic digestion, the cutting tolerance should be assessed at several locations and for multiple genotypes. Further, biogas plant technology needs

---

BOX 1 | Short Summary of the main outcomes:

- Anaerobic digestion is a promising novel utilization pathway for miscanthus biomass, which provides both a higher value product and a high productivity per hectare
- Higher biomass yields due to harvest in autumn/at peak yield compensates largely for the conversion losses of anaerobic digestion. However, cutting tolerance of such novel genotypes needs to be assessed for a broad spectrum of locations.
- Biomass and energy losses due to delayed harvest for combustion, are the costs of quality improvements to meet the quality and storage requirements. Pre-winter harvest could increase energy yield of combustion, because higher moisture content is overcompensated by higher biomass yields. However, adapted and suitable technology for storage and combustion of wet biomass are required.
- Environmental impacts (soil organic carbon, biodiversity) of pre-winter harvest needs to be assessed, since mulch layer is likely to decrease due to reduced leaf fall and reduced winter-cover.
- Combustion and anaerobic digestion both require genotypes with a high biomass production. However, for combustion low yield losses over winter and a high stability of the crop (no lodging) are of importance, while for anaerobic digestion cutting tolerance and easier digestibility (low lignin content) are important.

to be adapted to process lignocellulosic miscanthus biomass or extended by suitable pre-treatment facilities. Encouraging practical experience has been gained using a MeWa Bio-QZ (ANDRITZ MeWa GmbH,Gechingen) at the full-scale research biogas plant of the University of Hohenheim. Anaerobic digestion of miscanthus has the potential to produce biogas more cheaply than other feedstocks and offers the co-benefit of easier nutrient recycling via digestate than via ash from combustion.

AUTHOR CONTRIBUTIONS

AK and IL were leading the preparation and writing of this paper. JC, LT, and all other co-authors contributed to the writing of the manuscript and in discussing the results. CN collected and provided data of the multilocation trials relevant for the preparation of this paper. YI, MÖ, IT, and OK supported and conducted sampling of the field trials.

SUPPLEMENTARY MATERIAL

The Supplementary Material for this article can be found online at: http://journal.frontiersin.org/article/10.3389/fpls.2017.00347/full#supplementary-material

REFERENCES

Angelidaki, I., Alves, M., Bolzonella, D., Borzacconi, L., Campos, J. L., Guwy, A. J., et al. (2009). Defining the biomethane potential (BMP) of solid organic wastes and energy crops: a proposed protocol for batch assays. *Water Sci. Technol.* 59, 927–934. doi: 10.2166/wst.2009.040

Cadoux, S., Riche, A. B., Yates, N. E., and Machet, J.-M. (2012). Nutrient requirements of *Miscanthus x giganteus*: conclusions from a review of published studies. *Biomass Bioenergy* 38, 14–22. doi: 10.1016/j.biombioe.2011.01.015

Christian, D. G., Riche, A. B., and Yates, N. E. (2008). Growth, yield and mineral content of *Miscanthus × giganteus* grown as a biofuel for 14 successive harvests. *Ind. Crops Prod.* 28, 320–327. doi: 10.1016/j.indcrop.2008.02.009

Clifton-Brown, J. C., Lewandowski, I., Bangerth, F., and Jones, M. B. (2002). Comparative responses to water stress in stay-green, rapid- and slow senescing genotypes of the biomass crop, Miscanthus. *New Phytol.* 154, 335–345. doi: 10.1046/j.1469-8137.2002.00381.x

Clifton-Brown, J., Hastings, A., Mos, M., McCalmont, J. P., Ashman, C., Awty-Carroll, D., et al. (2017). Progress in upscaling Miscanthus biomass production for the European bio-economy with seed-based hybrids. *GCB Bioenergy* 9, 6–17. doi: 10.1111/gcbb.12357

Clifton-Brown, J., Schwarz, K.-U., and Hastings, A. (2015). History of the development of Miscanthus as a bioenergy crop: from small beginnings to potential realisation. *Biol. Environ. Proc. R. Ir. Acad.* 115B, 1–13. doi: 10.3318/bioe.2015.05

den Camp, H. J. M. O., Verhagen, F. J. M., Kivaisi, A. K., and de Windt, F. E. (1988). Effects of lignin on the anaerobic degradation of (ligno) cellulosic wastes by rumen microorganisms. *Appl. Microbiol. Biotechnol.* 29, 408–412. doi: 10.1007/BF00265827

Felten, D., Fröba, N., Fries, J., and Emmerling, C. (2013). Energy balances and greenhouse gas-mitigation potentials of bioenergy cropping systems (Miscanthus, rapeseed, and maize) based on farming conditions in Western Germany. *Renewable Energy* 55, 160–174. doi: 10.1016/j.renene.2012.12.004

Fonteyne, S., Lootens, P., Muylle, H., van den Ende, W., Swaef, T., de Reheul, D., et al. (2016). Chilling tolerance and early vigour-related characteristics evaluated in two Miscanthus genotypes. *Photosynthetica* 54, 295–306. doi: 10.1007/s11099-016-0193-y

Frydendal-Nielsen, S., Hjorth, M., Baby, S., Felby, C., Jørgensen, U., and Gislum, R. (2016). The effect of harvest time, dry matter content and mechanical pretreatments on anaerobic digestion and enzymatic hydrolysis of miscanthus. *Bioresour. Technol.* 218, 1008–1015. doi: 10.1016/j.biortech.2016.07.046

Greef, J. M., Deuter, M., Jung, C., and Schondelmaier, C. (1997). Genetic diversity of European Miscanthus species revealed by AFLP fingerprinting. *Genet. Resour. Crop. Evol.* 44, 185–195. doi: 10.1023/A:1008693214629

Iqbal, Y., and Lewandowski, I. (2014). Inter-annual variation in biomass combustion quality traits over five years in fifteen Miscanthus genotypes in south Germany. *Fuel Process. Technol.* 121, 47–55. doi: 10.1016/j.fuproc.2014.01.003

Jensen, E., Robson, P., Farrar, K., Thomas Jones, S., Clifton-Brown, J., Payne, R., et al. (2016). Towards Miscanthus combustion quality improvement: the role of flowering and senescence. *GCB Bioenergy.* doi: 10.1111/gcbb.12391

Kiesel, A., and Lewandowski, I. (2017). Miscanthus as biogas substrate – Cutting tolerance and potential for anaerobic digestion. *GCB Bioenergy* 9, 153–167. doi: 10.1111/gcbb.12330

Kołodziej, B., Antonkiewicz, J., and Sugier, D. (2016). Miscanthus×giganteus as a biomass feedstock grown on municipal sewage sludge. *Ind. Crops Prod.* 81, 72–82. doi: 10.1016/j.indcrop.2015.11.052

Le Gall, H., Philippe, F., Domon, J.-M., Gillet, F., Pelloux, J., and Rayon, C. (2015). Cell wall metabolism in response to abiotic stress. *Plants* 4, 112–166. doi: 10.3390/plants4010112

Lewandowski, I., Clifton-Brown, J. C., Andersson, B., Basch, G., Christian, D. G., Jørgensen, U., et al. (2003). Environment and harvest time affects the combustion qualities of genotypes. *Agron. J.* 95:1274. doi: 10.2134/agronj2003.1274

Lewandowski, I., Clifton-Brown, J., Trindade, L. M., van der Linden, G. C., Schwarz, K.-U., Müller-Sämann, K. et al. (2016). Progress on optimizing miscanthus biomass production for the European bioeconomy: results of the EU FP7 project OPTIMISC. *Front. Plant Sci.* 7:1620. doi: 10.3389/fpls.2016.01620

Lewandowski, I., and Schmidt, U. (2006). Nitrogen, energy and land use efficiencies of miscanthus, reed canary grass and triticale as determined by the boundary line approach. *Agric. Ecosyst. Environ.* 112, 335–346. doi: 10.1016/j.agee.2005.08.003

Mayer, F., Gerin, P. A., Noo, A., Lemaigre, S., Stilmant, D., Schmit, T., et al. (2014). Assessment of energy crops alternative to maize for biogas production in the greater region. *Bioresour. Technol.* 166, 358–367. doi: 10.1016/j.biortech.2014.05.054

McCalmont, J. P., Hastings, A., McNamara, N. P., Richter, G. M., Robson, P., Donnison, I. S. et al. (2017). Environmental costs and benefits of growing Miscanthus for bioenergy in the UK. *GCB Bioenergy* 9, 489–507. doi: 10.1111/gcbb.12294

Menardo, S., Bauer, A., Theuretzbacher, F., Piringer, G., Nilsen, P. J., Balsari, P., et al. (2013). Biogas production from steam-exploded Miscanthus and utilization of biogas energy and CO_2 in greenhouses. *Bioenergy Res.* 6, 620–630. doi: 10.1007/s12155-012-9280-5

Meyer, F., Wagner, M., and Lewandowski, I. (2016). Optimizing GHG emission and energy-saving performance of miscanthus-based value chains. *Biomass Conv. Bioref.* doi: 10.1007/s13399-016-0219-5

Naumann, C., and Bassler, R. (1976/2012). *Die chemische Untersuchung von Futtermitteln*. Darmstadt: VDLUFA-Verl.

Patinvoh, R. J., Osadolor, O. A., Chandolias, K., Sárvári Horváth, I., and Taherzadeh, M. J. (2017). Innovative pretreatment strategies for biogas production. *Bioresour. Technol.* 224, 13–24. doi: 10.1016/j.biortech.2016.11.083

Purdy, S. J., Cunniff, J., Maddison, A. L., Jones, L. E., Barraclough, T., Castle, M., et al. (2015). Seasonal carbohydrate dynamics and climatic regulation of senescence in the perennial grass, Miscanthus. *Bioenergy Res.* 8, 28–41. doi: 10.1007/s12155-014-9500-2

Robson, P., Mos, M., Clifton-Brown, J., and Donnison, I. (2012). Phenotypic variation in senescence in Miscanthus: towards optimising biomass quality and quantity. *Bioenergy Res.* 5, 95–105. doi: 10.1007/s12155-011-9118-6

Strullu, L., Cadoux, S., Preudhomme, M., Jeuffroy, M.-H., and Beaudoin, N. (2011). Biomass production and nitrogen accumulation and remobilisation by *Miscanthus×giganteus* as influenced by nitrogen stocks in belowground organs. *Field Crops Res.* 121, 381–391. doi: 10.1016/j.fcr.2011.01.005

Styles, D., Gibbons, J., Williams, A. P., Dauber, J., Stichnothe, H., Urban, B., et al. (2015). Consequential life cycle assessment of biogas, biofuel and biomass energy options within an arable crop rotation. *GCB Bioenergy* 7, 1305–1320. doi: 10.1111/gcbb.12246

van der Weijde, T., Alvim Kamei, C. L., Torres, A. F., Vermerris, W., Dolstra, O., Visser, R. G., et al. (2013). The potential of C4 grasses for cellulosic biofuel production. *Front. Plant Sci.* 4:107. doi: 10.3389/fpls.2013.00107

van der Weijde, T., Huxley, L. M., Hawkins, S., Sembiring, E. H., Farrar, K., Dolstra, O., et al. (2017a). Impact of drought stress on growth and quality of Miscanthus for biofuel production. *GCB Bioenergy* 9, 770–782. doi: 10.1111/gcbb.12382

van der Weijde, T., Kiesel, A., Iqbal, Y., Muylle, H., Dolstra, O., Visser, R. G. F., et al. (2017b). Evaluation of *Miscanthus sinensis* biomass quality as feedstock for conversion into different bioenergy products. *GCB Bioenergy* 9, 176–190. doi: 10.1111/gcbb.12355

Wahid, R., Nielsen, S. F., Hernandez, V. M., Ward, A. J., Gislum, R., Jørgensen, U., et al. (2015). Methane production potential from *Miscanthus* sp: Effect of harvesting time, genotypes and plant fractions. *Biosyst. Eng.* 133, 71–80. doi: 10.1016/j.biosystemseng.2015.03.005

Whittaker, C., Hunt, J., Misselbrook, T., and Shield, I. (2016). How well does Miscanthus ensile for use in an anaerobic digestion plant? *Biomass Bioenergy* 88, 24–34. doi: 10.1016/j.biombioe.2016.03.018

Conflict of Interest Statement: The authors declare that the research was conducted in the absence of any commercial or financial relationships that could be construed as a potential conflict of interest.

Saccharification Performances of Miscanthus at the Pilot and Miniaturized Assay Scales: Genotype and Year Variabilities According to the Biomass Composition

Nassim Belmokhtar[1]*, Stéphanie Arnoult[2], Brigitte Chabbert[3], Jean-Paul Charpentier[1] and Maryse Brancourt-Hulmel[4]

[1] AGPF, Institut National de la Recherche Agronomique, Orléans, France, [2] GCIE-Picardie, Institut National de la Recherche Agronomique, Estrées-Mons, France, [3] FARE Laboratory, Institut National de la Recherche Agronomique, Université de Reims Champagne-Ardenne, Reims, France, [4] AgroImpact Unit, Institut National de la Recherche Agronomique, Estrées-Mons, France

HIGHLIGHTS

- Biomass production and cell wall composition are differentially impacted by harvesting year and genotypes, influencing then cellulose conversion in miniaturized assay.
- Using a high-throughput miniaturized and semi-automated method for performing the pretreatment and saccharification steps at laboratory scale allows for the assessment of these factors on the biomass potential for producing bioethanol before moving to the industrial scale.

The large genetic diversity of the perennial grass miscanthus makes it suitable for producing cellulosic ethanol in biorefineries. The saccharification potential and year variability of five genotypes belonging to *Miscanthus* × *giganteus* and *Miscanthus sinensis* were explored using a miniaturized and semi-automated method, allowing the application of a hot water treatment followed by an enzymatic hydrolysis. The studied genotypes highlighted distinct cellulose conversion yields due to their distinct cell wall compositions. An inter-year comparison revealed significant variations in the biomass productivity and cell wall compositions. Compared to the recalcitrant genotypes, more digestible genotypes contained higher amounts of hemicellulosic carbohydrates and lower amounts of cellulose and lignin. In contrast to hemicellulosic carbohydrates, the relationships analysis between the biomass traits and cellulose conversion clearly showed the same negative effect of cellulose and lignin on cellulose digestion. The miniaturized and semi-automated method we developed was usable at the laboratory scale and was reliable for mimicking the saccharification at the pilot scale using a steam explosion pretreatment and enzymatic hydrolysis. Therefore, this miniaturized method will allow the reliable screening of many genotypes for saccharification potential. These findings provide valuable information and tools for breeders to create genotypes combining high yield, suitable biomass composition, and high saccharification yields.

Keywords: Miscanthus, high-throughput pretreatment and saccharification, pilot-scale pretreatment and saccharification, hemicelluloses, cellulose, lignin, genotypic diversity, harvesting year

INTRODUCTION

To meet targeted demands for alternative fuel sources with less environmental impact, a large set of lignocellulosic biomasses has been explored within the last two decades (Wyman, 1994; Rubin, 2008). One of the most promising feedstocks is the perennial grass miscanthus due to its high biomass production per hectare with a low environmental impact (Clifton-brown et al., 2004; Lewandowski and Schmidt, 2006; Hastings et al., 2008; Cadoux et al., 2014) and its minor impact on the food supply (Clifton-brown et al., 2004; Heaton et al., 2008; Brosse et al., 2012). The genus *Miscanthus* comprises 20 species (Hodkinson et al., 2002), including *Miscanthus × giganteus, Miscanthus sinensis, Miscanthus sacchariflorus* and *Miscanthus tinctorius,* which are characterized by a high yield and energy content (Cadoux et al., 2014; Lee and Kuan, 2015). The mostly studied genotype in Europe and North America is *M. × giganteus,* which is a sterile interspecific hybrid of *M. sacchariflorus* and *M. sinensis* (Brosse et al., 2012).

The efficient hydrolysis of cellulose into fermentable glucose using fungal cellulolytic enzymes is a key step in the biorefinery process (Himmel et al., 2007). However, to provide rigidity, structural support, and protection against pathogens in living plants, the cellulosic fraction is part of a cohesive network of phenolic, non-cellulosic polysaccharides, and protein polymers (Pauly and Keegstra, 2008; De Souza et al., 2015). The inhibitory effect of cellulose crystallinity on cellulases and the non-productive binding of enzymes to lignin have been demonstrated (Yang and Wyman, 2004; Berlin et al., 2006). Furthermore, monocots, such as miscanthus, are characterized by the presence of hydoxycinnamic acids such as *p*-coumaric acids and ferulic acids, which play a significant role in cross-linking arabinoxylans to lignin hindering then cellulose digestibility (Iiyama et al., 1990; Ralph, 2010). In addition, non-cellulosic components have been reported to differ in their distribution, structure, and extractability across different harvests, organs, and miscanthus genotypes (Le Ngoc Huyen et al., 2010; Xue et al., 2013; Costa et al., 2016). Variability in cellulose and lignin content has been highlighted between miscanthus harvests in stems while glycans matrix was more easily extractable in leaves using profiling of polysaccharides epitopes pattern. Total contribution of leaves to total biomass seems to be a determining factor for saccharification efficiency (Costa et al., 2016). Moreover, pectins and mannans impact was established when lignin did not impact saccharification (De Souza et al., 2015). All these findings confirmed how complex is the understanding of cell wall recalcitrance to deconstruction.

To overcome these structural limitations, the optimal digestion of a lignocellulosic network needs physical and/or chemical pretreatments (Yang and Wyman, 2008; Hendriks and Zeeman, 2009). Several pretreatment technologies have

been extensively explored during the last decades, and their effectiveness was demonstrated by disrupting the lignocellulose structure of different energy crops (Mosier et al., 2005; Wyman et al., 2005). Steam explosion is one of the most promising pretreatments and has been successfully applied to miscanthus by solubilizing hemicelluloses and disrupting cellulose fibers during rapid depressurization, thereby increasing cellulose digestibility (Sørensen et al., 2008; Yeh et al., 2016). Hot water treatment has also been shown to be very efficient in increasing cellulose conversion of miscanthus (Li H.-Q. et al., 2013). To realize a techno-economic evaluation of the bioethanol production process, acid hydrolysis, wet oxidation, and steam explosion have been extensively tested and validated at the pilot scale on different biomasses, such as wheat straw and corn stover (Schell et al., 2003, 2004; Thomsen et al., 2006; Jørgensen et al., 2007).

In addition to the achievement of efficient pretreatments for second-generation bioethanol, the comparison of the saccharification potentials of a large set of biomass requires efficient and rapid tests including physico-chemical pretreatments. Some miniaturized and automated methods have been developed to evaluate large biomass populations. These tools are based on performing pretreatment and saccharification assays in 96-well microplate systems (Gomez et al., 2010; Santoro et al., 2010; Selig et al., 2010; Studer et al., 2011). Methods developed by Gomez et al. (2010, 2011) are based on using 96-well PCR plates thus allowing only low or moderate heating during pretreatment step. Those described by Studer et al. (2011) and Selig et al. (2010) are characterized by using metallic reactors that allow high temperature and pressure pretreatments in addition to resistance to corrosion and catalysts, such as dilute sulfuric acid and sodium hydroxide. The same team reported improvements of NREL's method, notably the replacing of aluminum by Hastelloy for 96-well plate, the manufacturing and use of polytetrafluoroethylene film tape for plate sealing rather than aluminum foil tape (Biswal et al., 2015; Healey et al., 2016; Serba et al., 2016). These promising methods make breeding and the best selection of less recalcitrant feedstocks for cellulosic ethanol possible.

Biomass production and cell wall composition have been shown to be highly variable among *Miscanthus* genotypes (Allison et al., 2011; Arnoult and Brancourt-Hulmel, 2015; Arnoult et al., 2015a; Costa et al., 2016). Moreover, the miscanthus biomass production and composition may be impacted by the environment, particularly by climatic conditions that can differ with harvesting date and year (Le Ngoc Huyen et al., 2010; Arnoult et al., 2015a,b). This potentially allows breeding of miscanthus varieties that adapt to their environment, resulting in a high yield, a suitable biomass composition, a high saccharification potential, and bioethanol conversion (Hodgson et al., 2010, 2011; Lygin et al., 2011).

The main objective of our study, therefore, is to explore the saccharification potential of miscanthus genotypes and the year variability effect by assessing the saccharification performances.

Our first hypothesis was that the saccharification potential was variable according to genotypes and harvesting years due to variations in biomass production and biomass composition. Therefore, we developed a high-throughput miniaturized

---

Abbreviations: ADF, acid detergent fiber; ADL acid detergent lignin; CV, coefficient of variation; DM, dry matter; ha, hectare; HPAEC, high-performance anion-exchange chromatography; HWT, hot water pretreatment; LCI, lignocellulose index; NDF, neutral detergent fiber; NDS, neutral detergent soluble; t, ton; UT, untreated; PCR, polymerase chain reaction.

and semi-automated method to evaluate the saccharification potential, and (i) for several years, we used this method to determine the impact of the harvesting year on the enzymatic digestibility of 5 miscanthus genotypes belonging to the *M. × giganteus* and *M. sinensis* species. Additionally, we examined the effect of the harvesting year on the biomass production and composition of these 5 genotypes. (ii) In light of these results, we investigated the relationships between biomass production, cell wall composition, and cellulose conversion according to the harvesting year. We studied five miscanthus genotypes harvested at the end of the winter in the fourth, fifth, and seventh years of cultivation.

Our second hypothesis was that the use of a satisfactory and relevant method at the miniaturized scale using a minimum amount of matter was reliable enough to assess the performance at the pilot scale. To address this hypothesis, we explored, at the pilot scale, the saccharification of the previously harvested 5 genotypes at the end of the winter of year 7. Then, we correlated the results of the cellulose conversion yields obtained between the pilot scale and the high-throughput miniaturized and semi-automated method we developed.

This study will provide useful knowledge and tools to breed suitable *Miscanthus* genotypes for cellulosic ethanol production.

MATERIALS AND METHODS

Location of the Experimental Field

The experimental field is located in the Hauts-de-France region of Northern France (49°53 N, 3°00 E) at the INRA experimental unit in Estrées-Mons.

Management of the Trial

The trial was planted by hand in spring 2007 at a rhizome planting density of 2 plants per m^2. The plants were watered immediately after planting to ensure good root contact with the soil. No irrigation was applied during the following years of cultivation. No fertilizer was applied. The weeds were controlled each year by hand and machine hoeing.

Field Production of the *Miscanthus* Genotypes

Twenty-one *Miscanthus* genotypes were planted in 2007 in a randomized complete block experimental design with three blocks (for details, see Arnoult et al., 2015a). Among these 21 genotypes, the following five genotypes were studied: two genotypes were identified as *M. sinensis* (ROT and SIL), and three genotypes were identified as *M. × giganteus* (FLO, GIB, and H8). Among the three *M. × giganteus* genotypes, H8 was considered an *M. × giganteus* genotype as it was a hybrid between *M. sacchariflorus* and *M. sinensis*. Using Amplified Fragment Length Polymorphism (AFLP) markers, the genotype named "FLO" belonged to the *M. × giganteus* species (Rambaud, personal communication). These five genotypes were chosen among the 21 previously studied genotypes (Arnoult et al., 2015a) due to (i) their relatively high biomass production per hectare and (ii) their contrasted biomass composition, particularly for cellulose and lignin contents.

These five genotypes were harvested from the experimental field at the end of the winter of years 4, 5, and 7 (2011, 2012, and 2014, respectively). A surface of 16 m^2 was cut 5 cm above the ground using a reed harvester.

Two sets of samples were collected for each of the 5 genotypes as follows: (i) a sample of 70 kg of biomass harvested in the whole 3 blocks in year 7 was used for the pilot-scale assay, and (ii) a sample of ∼500 g of biomass randomly chosen from the biomass harvested on each of the 3 blocks of the trial in years 4, 5, and 7 was used for the high-throughput assays and cell wall components quantification. For the pilot-scale assay, (i) we harvested 7th year miscanthus in 2014, which corresponds to the first year when the pilot was operational, and (ii) we needed to pool the biomass from three blocks of the trial to provide enough biomass for the pilot assays (70 kg).

Pilot-Scale Assays
Biomass Preparation and Steam Explosion Pretreatment

For each of the five genotypes, the 70 kg of biomass harvested from the experimental field was carried on the pilot site (*Procethol 2G*, Pomacle, France) and stored until its treatment in a dedicated storage area sheltered from rain. Then, all the matter of each genotype was separately ground in the pilot and resulted in a biomass size between 20 and 100 mm.

Thereafter, the ground biomass was loaded in 1 m^3 containers in the presence of sulfuric acid. After pressing, the presoaked biomass was placed in a steam reactor and heated. Moving the biomass into an atmospheric chamber caused a quick depressurization, resulting in the explosion of the miscanthus fibers. Only one replicate of this step was performed due to the limitation in available biomass amounts in the field. Additional measures on 21 samples from the same plot of *M. × giganteus* showed a good accuracy of the results at pilot scale (coefficient of variation = 1.99%, confidential data, Procethol 2G).

Enzymatic Hydrolysis of Steam-Exploded Miscanthus and Quantification of Released Glucose

A standard test of enzymatic hydrolysis was performed on the pretreated biomass. The pretreated biomass was incubated for 72 h with an enzymatic solution containing 10 IU of enzymes.g^{-1} DM. The enzymatic solution contained Genencor GC220 cellulase and β-glucosidase (N188, Novozymes). This step was replicated twice.

Released glucose after the pretreatment and enzymatic hydrolysis was performed by a high-performance anion-exchange chromatography (HPAEC) as described previously (Le Ngoc Huyen et al., 2010). This quantification of glucose was replicated twice.

Cell Wall Components Quantification (LANO Laboratory)
Sample Preparation

For each of the 5 genotypes harvested from three individual blocks of the trial, the sample of ∼500 g of the biomass harvested was dried at 65°C for 4 days in a well-ventilated oven. These dried samples were ground with a crusher (Viking, model GE

220, France) to a coarse size and then ground with a hammer crusher (Gondard Productions model, France) to pass through a 1-mm screen, as recommended for subsequent fiber analysis by Van Soest and Wine (1967).

Determination of the Cellulose, Hemicellulosic Carbohydrates, and Lignin Contents

The previous samples were analyzed by the laboratory LANO (Saint-Lô, France) for neutral detergent fiber (NDF), acid detergent fiber (ADF), and acid detergent lignin (ADL), according to a protocol that was adapted from the Van Soest method (Van Soest and Wine, 1967). Briefly, the NDF fraction corresponded to the ash-corrected residue that remained after refluxing for 60 min in a neutral-buffered detergent solution. The ADF fraction corresponded to the ash-corrected residue remaining after refluxing the samples in a solution of hexadecyltrimethylammonium bromide in 0.5 mol/L sulfuric acid. The ADL fraction was obtained by treating ADF with 72% sulfuric acid.

The NDF is considered to represent cellulose, hemicellulosic carbohydrates, and lignin; the ADF consists of cellulose and lignin; and the ADL consists of lignin (Van Soest and Wine, 1967). The cellulose, hemicellulosic carbohydrates (hemicelluloses), and lignin contents of each sample were estimated by subtracting the corresponding values from the NDF, ADF, and ADL fractions as shown below in Equations (1–3):

$$\text{Cellulose content} = \text{ADF} - \text{ADL} \tag{1}$$

$$\text{Hemicellulosic carbohydrates content} = \text{NDF} - \text{ADF} \tag{2}$$

$$\text{Lignin content} = \text{ADL} \tag{3}$$

The analytical dry matter content of each sample was determined at 103°C to express all the previous values in percentage of dry matter (% DM).

The Neutral Detergent Soluble (NDS) corresponds to the extractives and was calculated as following:

$$\text{NDS} = 100 - \text{NDF}$$

We calculated several ratios, the lignocellulose index (LCI) among others, which corresponded to the ratio between lignin and (lignin + cellulose + hemicellulosic carbohydrates).

Performing the High-Throughput Assays
High-Throughput Pretreatment and Saccharification

All samples were dried overnight at 50°C prior to ball milling to 1 mm screen in a fully automated system designed and provided by *Labman*® to French National Institute for Agricultural Research, Orleans. Biomass was then dispensed into 96-well microplates using another automatic dispenser station *Labman*®. Each sample was dispensed into 4 individual wells as a technical repetition.

For the hot water pretreatment, we used Hastelloy 96-well SBS-type microplates manufactured by Aspen machining® (*Golden*, Co, USA) based on drawings generously provided by NREL (*Golden*, CO, USA). After dispensing precisely 5 mg of biomass per well, 300 μL of deionized water were added to each sample. Hastelloy microplates were then tightly sealed with an adhesive film (3M®, 5,490) and clamped in the loader to be introduced in a 2-gallon stainless *Parr* reactor (4,665). Hot water pretreatment was performed at 180°C for 40 min. Heating was carried out using wet steam generated by an E-3000 Steam Generator provided by *Cellkraft*® (Sweden). This steam was heated at 180°C and introduced in the top of the Parr reactor. Pretreatment was stopped by depressurizing *Parr* vessel and cooling by adding water through valves placed in the top of the reactor.

After centrifugation (5,800 g, 10 min, 4°C), the adhesive film was removed, and 40 μL of the enzymatic solution containing 91 IU of cellulases.g^{-1} of DM in sodium acetate buffer (1 M, pH 5) were added based on NREL assays (Selig et al., 2010). Microplates were then sealed again using an adhesive film and incubated at 50°C during 70 h without shaking. For each sample, a control well was carried out without enzymes in order to estimate released non-cellulosic carbohydrates.

Quantification of Released Glucose in Microplates

Released glucose, after the pretreatment and enzymatic hydrolysis, was collected after centrifuging the microplates and quantified using the GOPOD assay kit (*Megazyme*®, USA). Glucose released in control wells was subtracted to determine the cellulose conversion yields expressed as a percentage of the cellulose content.

Data Analysis

Using data from the high-throughput assays, we calculated the biomass composition from the mean of three technical replicates, while the saccharification results were obtained from the mean of four technical replicates for each genotype. All sample CVs were <10%. Samples with CVs >10% were removed.

RStudio (version 3.3.2) was also used to perform an analysis of variance (ANOVA) to assess the effect of the harvesting year and genotype on the biomass production, cell wall composition, and saccharification yields. We also used the Tukey–Kramer test to achieve multiple comparison tests.

For these analyses, two linear models were built;

(i) A first model taking into account the block factor to test its effect on the studied variables as following:

$$Y_{ijk} = \mu + \alpha_i + \beta_j + \gamma_k + (\alpha\beta)_{ij} + (\alpha\gamma)_{ik} + \varepsilon_{ijk}$$

where Y_{ijk} is the phenotypic value of clone i in block j during the harvesting year k; μ is the overall mean; α_i is the fixed effect of the clone i; β_j is the fixed effect of the block j; γ_k is the fixed effect of the harvesting year k; $(\alpha\beta)_{ij}$ is the fixed interaction between clone i and the block j; $(\alpha\gamma)_{ik}$ is the fixed interaction between clone i and the harvesting year k; and ε_{ijk} is the residual error for clone i for block j during the harvesting year k.

(ii) As the block effect was not significant for all the variables tested (data not shown), we used in the following (ii) a second model as follows:

$$Y_{ij} = \mu + \alpha_i + \gamma_j + (\alpha\gamma)_{ij} + \varepsilon_{ij}$$

where Y_{ij} is the phenotypic value of clone i during the harvesting year j; μ is the overall mean; α_i is the fixed effect of the clone i; γ_j is the fixed effect of the harvesting year j; $(\alpha\gamma)_{ij}$ is the fixed interaction between clone i and the harvesting year j; and ε_{ij} is the residual error for clone i during the harvesting year j.

RESULTS

Impact of Harvesting Year According to Genotype

Biomass Production

The results summarized in **Figure 1** and the analysis of variance (**Table 1**) clearly indicated that the biomass production is significantly impacted by the harvesting year ($F = 39.8$, $p < 0.001$) and genotype ($F = 32.5$, $p < 0.001$) with a significant interaction between both factors ($F = 2.6$, $p < 0.05$). Indeed, the biomass production reached the highest yields at year 4 for the FLO and GIB genotypes, which reached 45.43 and 43.54 tDM.ha^{-1}, respectively, while the lowest yields were obtained at year 7, when the genotype H8, ROT, and SIL yields ranged from 11 to 19 tDM.ha^{-1}. Furthermore, multiple Tukey–Kramer comparison highlighted that the miscanthus genotypes were divided into the following two sub-populations: GIB-FLO and H8-ROT-SIL (**Supplementary Image 1**).

Biomass Composition

The cell wall fraction as estimated by NDF ranged from 80 to 87% of the biomass dry matter; NDS referred hereinafter as extractives, ranged 12.9–19.0, 13.8–19.5, and 14.9–19.5% of the biomass dry matter at years 4, 5, and 7, respectively. The determination of the harvesting year and genotype effects on dry matter and cellulose content was performed using an ANOVA and showed significant effects and interaction between these two factors (**Table 1**). However, the NDF and cellulose content seemed less affected by the harvesting year ($F = 16.8$ and $p < 0.001$, $F = 6.4$ and $p < 0.01$, respectively) than the genotype ($F = 31.9$ and $p < 0.001$, $F = 263.6$ and $p < 0.001$, respectively). Multiple comparisons also highlighted the following two sub-populations: GIB-FLO and H8-ROT-SIL (**Supplementary Image 1**). The NDF and cellulose contents are summarized in **Figures 2A,B,E,F**.

TABLE 1 | Analysis of variance of traits related to biomass production and chemical composition of miscanthus genotypes.

		F-value	*p*-value
Biomass yield	Genotype	32.5	<0.001
	Harvesting year	39.8	<0.001
	Genotype: Year	2.6	<0.05
NDF	Genotype	31.9	<0.001
	Harvesting year	16.8	<0.001
	Genotype: Year	2.3	<0.05
Extractives	Genotype	35.5	<0.001
	Harvesting year	16.9	<0.001
	Genotype: Year	2.3	<0.05
Cellulose	Genotype	263.6	<0.001
	Harvesting year	6.4	<0.01
	Genotype: Year	3.3	<0.01
Hemicellulosic carbohydrates	Genotype	124.5	<0.001
	Harvesting year	77.0	<0.001
	Genotype: Year	3.8	<0.01
Lignin	Genotype	42.9	<0.001
	Harvesting year	40.4	<0.001
	Genotype: Year	1.2	>0.05
Hemicellulosic carbohydrates/Cellulose ratio	Genotype	214.5	<0.001
	Harvesting year	63.7	<0.001
	Genotype: Year	3.4	<0.01
Lignin/Cellulose ratio	Genotype	19.7	<0.001
	Harvesting year	39.0	<0.001
	Genotype: Year	0.9	>0.05
LCI	Genotype	36.7	<0.001
	Harvesting year	38.2	<0.001
	Genotype: Year	0.9	>0.05
Released glucose from untreated biomass	Genotype	19.0	<0.001
	Harvesting year	47.9	<0.001
	Genotype: Year	6.9	<0.001
Released glucose from hot water-treated biomass	Genotype	109.5	<0.001
	Harvesting year	50.1	<0.001
	Genotype: Year	2.2	<0.05

FIGURE 1 | Impact of harvesting year (A) and genotypes **(B)** on biomass production.
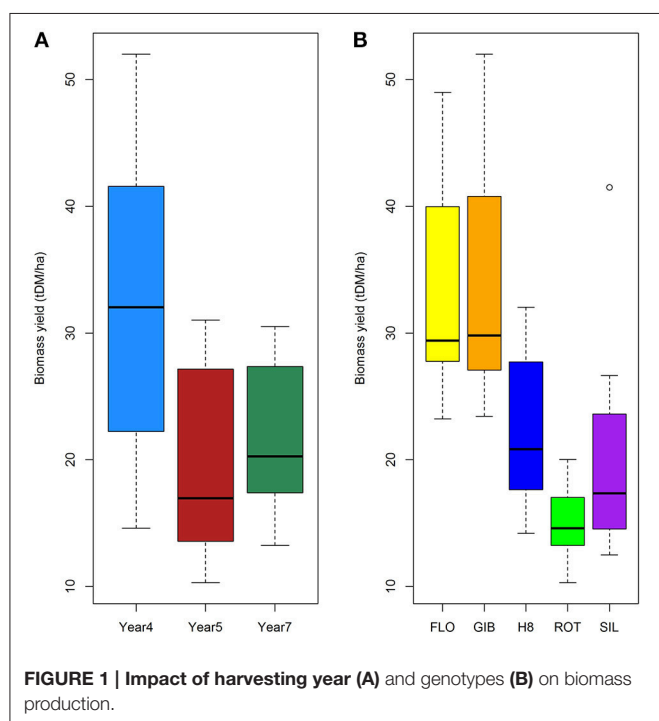
The same approach revealed that the content in hemicellulosic carbohydrates was also impacted by the harvesting year and genotype with a stronger effect of the latter ($F = 124.5$ and $p < 0.001$) compared to the former ($F = 77$ and $p < 0.001$). Our results also indicated a significant interaction between these two factors ($F = 3.8$ and $p < 0.01$). Overall, hemicellulosic carbohydrates content appeared to be higher in year 5 and lower in year 7 (**Figure 2C**). Additionally, Tukey–Kramer comparison confirmed that the two sub-populations of genotypes GIB-FLO contained less than 30% of hemicellulosic carbohydrates, while the second one, composed of H8, ROT, and SIL, reached more than 35% (**Figure 2G**).

Exploring the lignin content revealed significant and strong effects of harvesting year and genotype but no interaction between these two factors (**Table 1**). The results summarized in **Figure 2D** indicated that the lignin content was higher at year 4 and lower at year 5. Two sub-populations of genotypes were also found for this trait. In contrast to the H8, ROT, and SIL group, with <7% of DM (**Figure 2H**), the GIB-FLO group showed the highest lignin amounts (∼10% of DM).

Variance analysis was also applied to the Hemicellulosic carbohydrates/Cellulose ratio, Lignin/Cellulose ratio, and LCI. The results summarized in **Table 1** indicate that all these traits were significantly affected by harvesting year and genotype, but an interaction between these factors was only found for the Hemicellulosic carbohydrates/Cellulose ratio. Specifically, the Hemicellulosic carbohydrates/Cellulose ratio was highest at year 5, which is in contrast to the Lignin/Cellulose ratio and LCI, which were the lowest same year (**Figures 3A–C**). Based on the genotype, the group formed by H8, ROT, and SIL expressed the highest Hemicellulosic carbohydrates/Cellulose ratio, while the other group highlighted the highest Lignin/Cellulose ratio and LCI (**Figures 3D–F**).

Enzymatic Hydrolysis of Untreated and Hot Water-Treated Genotypes

Quantification of released glucose after enzymatic hydrolysis of untreated and hot water- treated miscanthus highlighted a very strong and significant effect of harvesting year and the genotypes according to analysis of variance (**Table 1**). Additionally, examination of the interaction between genotype and harvesting year indicated the significant interaction for the untreated samples ($F = 6.9$ and $p < 0.001$).

The ANOVA results clearly indicated that the harvesting-year effect on saccharification was more important without pretreatment, while genotype showed a much higher impact after the hot water treatment (**Table 1**). These findings can also be observed in **Figure 4** where, compared to year 4, the highest release of glucose was observed at years 5 and 7 (**Figures 4A,B**). After the hot water pretreatment, the impact of harvesting year was limited to year 5; while, compared to FLO and GIB, the genotype group composed of H8, ROT, and SIL appeared to be more digested, reaching more than 300 mg/g DM of released glucose (**Figures 4C,D**).

FIGURE 2 | Effect of harvesting year (A–D) and genotypes **(E–H)** on the biomass composition.
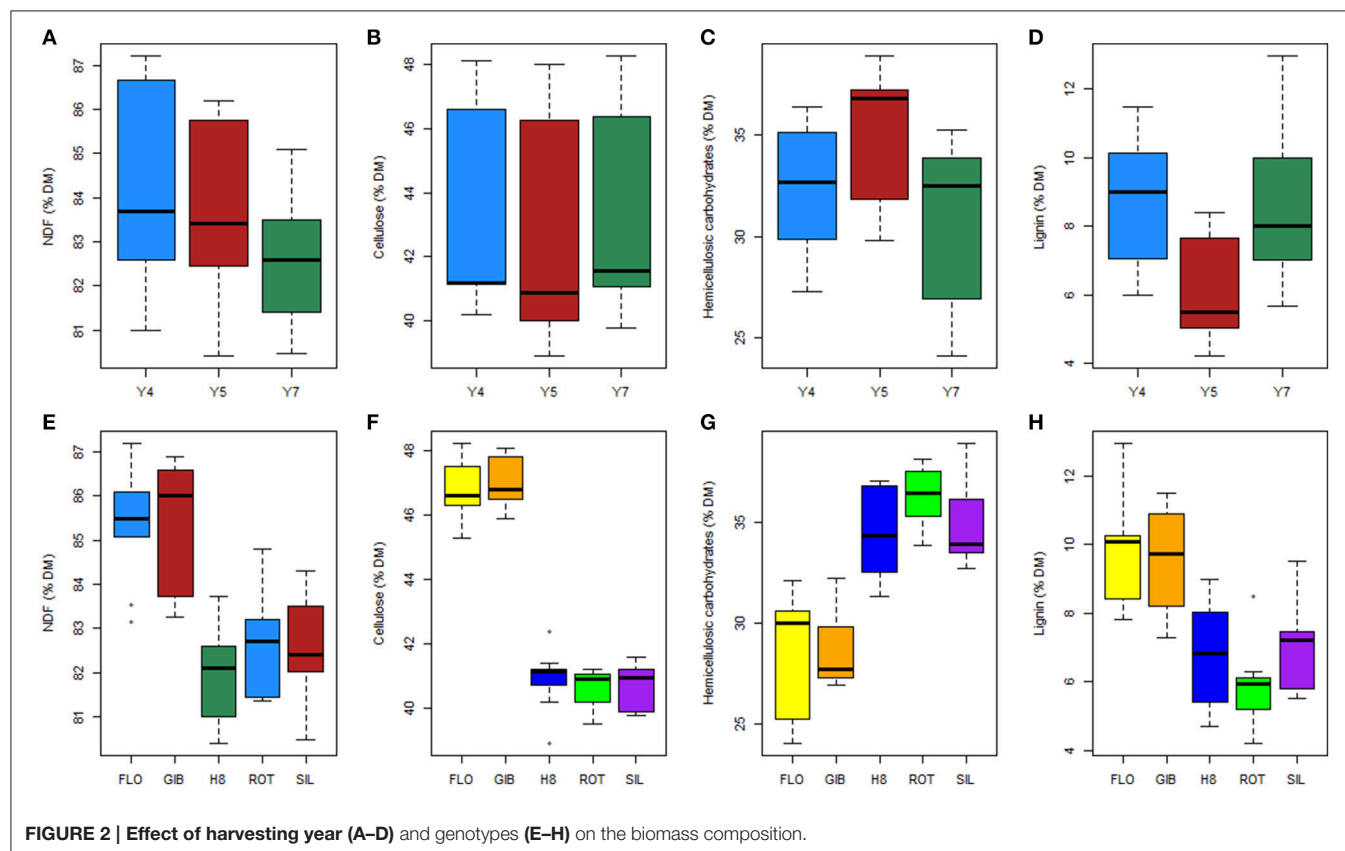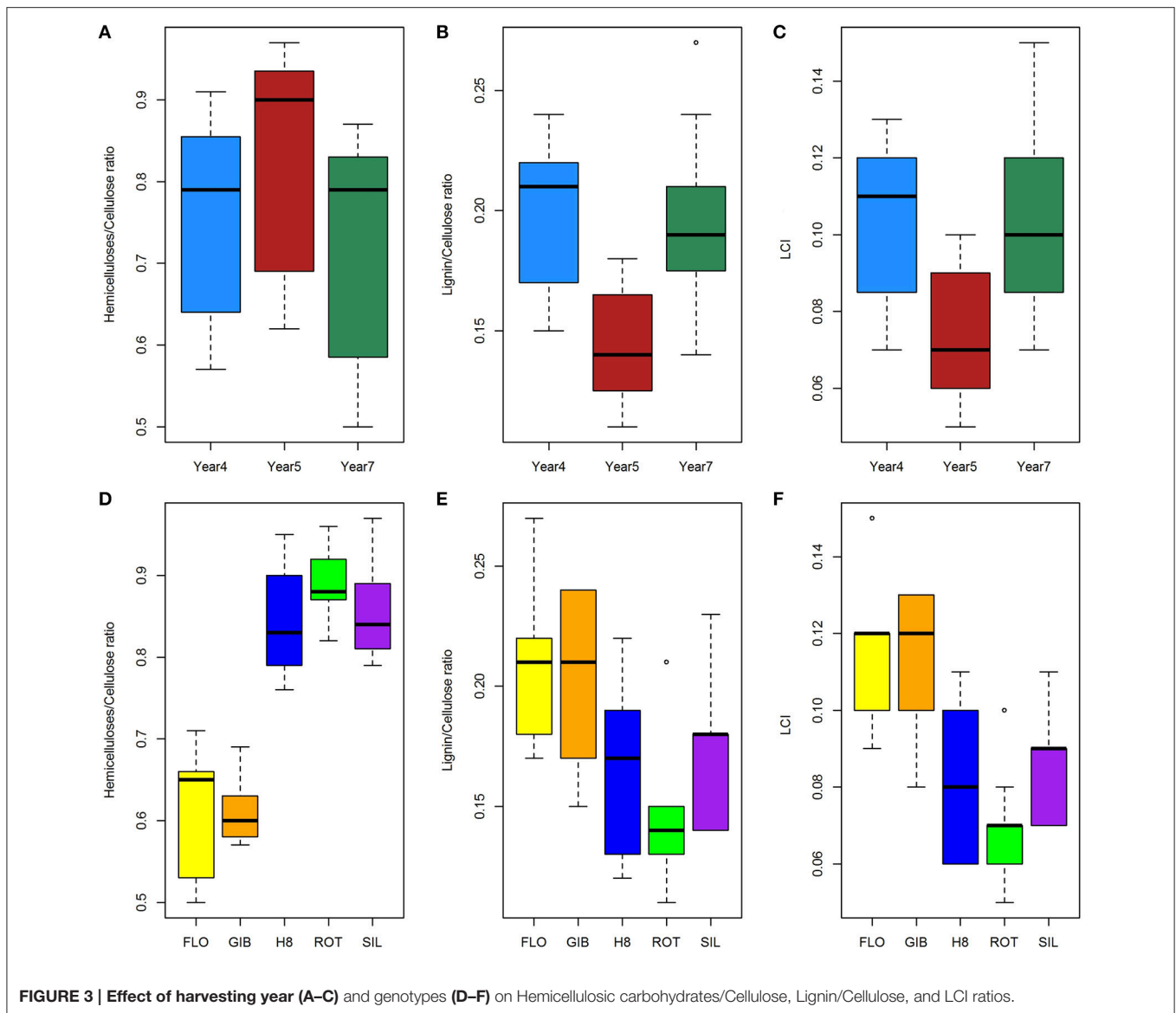
FIGURE 3 | Effect of harvesting year (A–C) and genotypes **(D–F)** on Hemicellulosic carbohydrates/Cellulose, Lignin/Cellulose, and LCI ratios.

Relationships between Biomass Production, Content of Main Cell-Wall Components, and Cellulose Conversion

Investigation of the relationships between miscanthus traits and released glucose after enzymatic hydrolysis of untreated and hot water-treated samples was conducted by focusing on the effects of genotype and harvesting year.

Correlation between enzymatic hydrolysis efficiency and cellulose, hemicellulosic carbohydrates, and lignin contents was significantly affected by the genotype. Indeed, the results detailed in **Table 2** indicate that saccharification of the untreated sample was slightly affected by extractives content ($r = 0.52$) and Biomass yield ($r = -0.47$) in FLO-GIB group while the group H8-ROT-SIL is mainly negatively impacted by lignin content ($r = -0.55$), Lignin/Cellulose ($r = -0.59$), and LCI ($r = -0.52$) ratios. Glucose release from hot water-treated

samples belonging to FLO and GIB genotypes was strongly impacted by hemicellulosic carbohydrates content ($r = 0.96$) and Hemicellulosic Carbohydrates/Cellulose ratio ($r = 0.95$). This group is also negatively impacted by extractives ($r = -0.53$), cellulose ($r = -0.52$), and lignin ($r = -0.78$) contents. However, glucose released from pretreated genotypes H8, ROT, and SIL was less impacted by the cell wall composition and biomass production (**Table 2**).

Correlation analysis, based on harvesting year, has also highlighted the differential impact of biomass traits on enzymatic hydrolysis of untreated and pretreated miscanthus genotypes. Those samples harvested at year 4 and hot water-treated were strongly affected by cellulose ($r = -0.88$) and hemicellulosic carbohydrates ($r = 0.82$) contents, followed by slight effect of lignin content ($r = -0.74$). In contrast, untreated samples were not impacted by cell wall composition. At year 5, a strong effect of lignin was highlighted ($r = -0.93$) followed
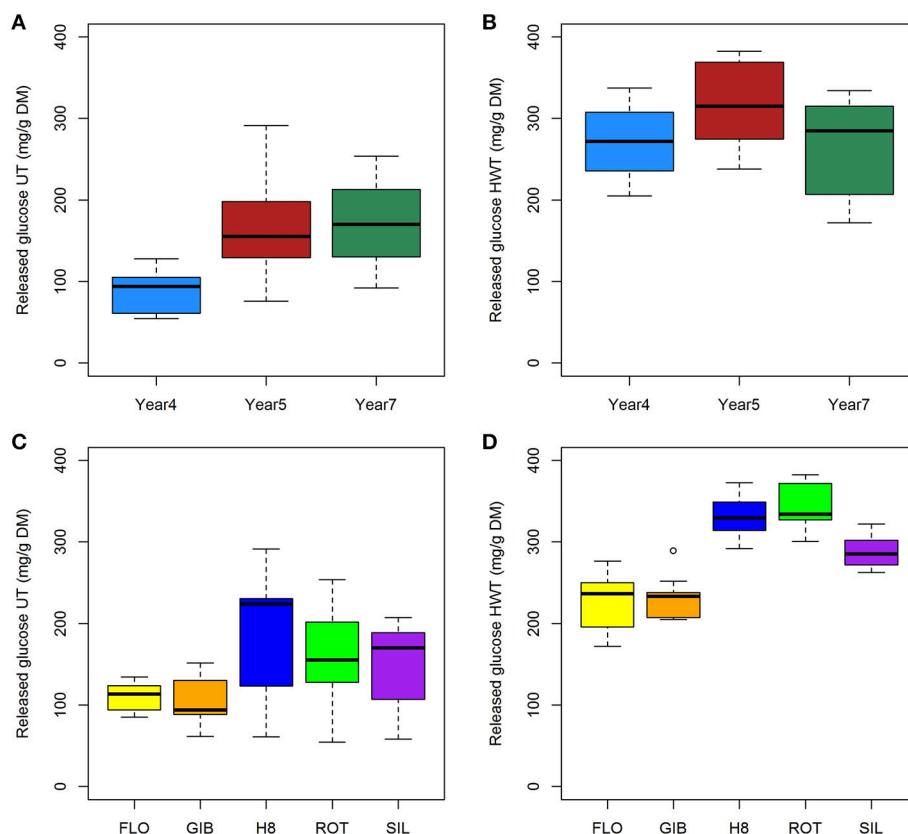
FIGURE 4 | Impact of harvesting year (A,B) and genotypes (C,D) on released glucose content from untreated (A,C) and hot water-treated (B,D) miscanthus.

TABLE 2 | Relationship analysis between biomass traits and enzymatic hydrolysis of cellulose based on correlation analysis (r-values).

		Genotype		Harvesting year		
		FLO, GIB	H8, ROT, and SIL	Year 4	Year 5	Year 7
Untreated biomass	Extractives	+0.52	+0.39	+0.05	+0.34	+0.57
	Cellulose	+0.03	−0.22	−0.03	−0.74	−0.78
	Hemicellulosic carbohydrates	−0.35	+0.23	+0.23	+0.63	+0.81
	Lignin	+0.08	−0.55	−0.41	−0.67	−0.83
	Biomass yield	−0.47	−0.35	+0.00	−0.53	−0.59
	Hemicellulosic carbohydrates/Cellulose ratio	−0.31	+0.25	+0.16	+0.69	+0.81
	Lignin/Cellulose ratio	+0.09	−0.59	−0.55	−0.63	−0.81
	LCI	+0.17	−0.52	−0.46	−0.61	−0.85
Hot water-treated biomass	Extractives	−0.53	−0.04	+0.74	+0.84	+0.73
	Cellulose	−0.52	−0.41	−0.88	−0.89	−0.92
	Hemicellulosic carbohydrates	+0.96	+0.59	+0.82	+0.89	+0.94
	Lignin	−0.78	−0.62	−0.74	−0.93	−0.91
	Biomass yield	+0.04	−0.51	−0.88	−0.77	−0.74
	Hemicellulosic carbohydrates/Cellulose ratio	+0.95	+0.60	+0.87	+0.89	+0.94
	Lignin/Cellulose ratio	−0.74	−0.61	−0.58	−0.91	−0.86
	LCI	−0.79	−0.64	−0.72	−0.92	−0.90

by cellulose ($r = -0.89$) and hemicellulosic carbohydrates ($r = 0.89$), which similarly affected digestion of pretreated miscanthus. Furthermore, compared to the year 4 samples, the three major cell wall polymers, especially cellulose ($r = -0.74$), displayed higher effect on digestion of 5th-year untreated miscanthus. Finally, strong correlations were established between hemicellulosic carbohydrates ($r = 0.81$), lignin ($r = -0.83$), LCI ($r = -0.85$), and enzymatic hydrolysis of untreated miscanthus at year 7. Glucose release from pretreated samples was also strongly impacted by hemicellulosic carbohydrates ($r = 0.94$), lignin ($r = -0.91$), and Hemicellulosic carbohydrates/Cellulose ($r = 0.94$), Lignin/Cellulose ($r = -0.86$), and LCI ($r = -0.90$) ratios. Cellulose conversion after hot water treatment was also positively affected by cell wall extractives on year 4 ($r = 0.74$), year 5 ($r = 0.84$), and year 7 ($r = 0.73$) while untreated genotypes were only slightly affected in year 5.

Cellulose Conversion of the Five Genotypes at the Pilot Scale

The enzymatic conversion yields of cellulose of steam exploded 7th-year miscanthus at the pilot-scale indicated that ROT genotype is the most digestible (68%), in contrast to H8 and SIL genotypes that express the same cellulose conversion yields (63%), and the less hydrolyzed ones, which are the FLO and GIB genotypes that reach only 52% (**Figure 5A**).

The comparison of these cellulose conversion yields, to those obtained using our miniaturized assay, revealed a very strong and positive correlation (**Figure 5B**). Indeed, compared to FLO and GIB, a coefficient of correlation $r = 0.98$ was obtained, confirming the better digestibility of the group formed by H8, ROT, and SIL genotypes.

DISCUSSION

This study explored the saccharification potential of miscanthus genotypes and year variability effect using pilot and miniaturized

assay scales and addressed our following hypothesis: (i) The saccharification potential varied according to the genotype and harvesting year due to variations in the biomass production and in content of the major cell wall components; particularly, cellulose and lignin displayed the same negative effect on cellulose conversion in contrast to hemicelluloses. (ii) The miniaturized assay we developed was reliable for mimicking the saccharification potential of various miscanthus genotypes at the pilot scale. We will, therefore, discuss hereafter the following two points: (i) The relationships between biomass production, content of the main cell wall components, and cellulose conversion according to harvesting year and genotype and (ii) in comparison to pilot scale, the reliability of mimicking the cellulose conversion of various genotypes in miniaturized assay.

Relationships between Biomass Production, Cell Wall Composition, and Cellulose Conversion, According to Harvesting Year and Genotype

Exploring biomass production and composition of the five miscanthus genotypes revealed a large genetic diversity. Based on variance analysis, this biomass quality diversity was found for the following three major cell wall polymers: cellulose, hemicellulosic carbohydrates, and lignin. The cell wall composition reported here is in agreement with previously reported *M. × giganteus* and *M. sinensis* data using Van Soest method (Arnoult et al., 2015a). This method allows sequential fractionation of the main cell wall polymers. However, non-cellulosic polysaccharides might be underestimated as neutral detergent solution can solubilize some pectins. In addition the fraction designated as hemicellulosic carbohydrates would thus mostly correspond to heteroxylans with few amounts of xyloglucan, mannan, and pectins (Le Ngoc Huyen et al., 2010; Costa et al., 2016). Furthermore, lignin concentrations as ADL residue were substantially lower than values obtained for miscanthus using Klason method (Le Ngoc
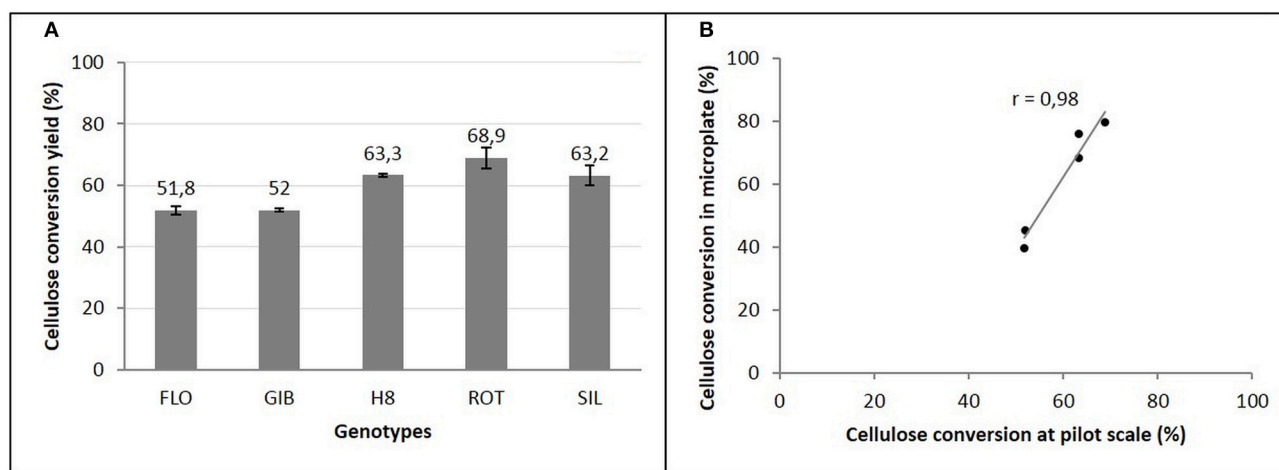

FIGURE 5 | Cellulose conversion yields of miscanthus genotypes at pilot scale (A) and its correlation with microplate saccharification **(B)**.

Huyen et al., 2010), as previously reported for other grass species (Hatfield et al., 1994; Bertrand et al., 2006). The acid detergent used in the Van Soest method can solubilize acid soluble lignin (Hatfield et al., 1994), giving a lignin-like fraction with a higher degree of recalcitrance as shown in forage digestibility studies (Van Soest, 1963).

Regarding the relationships between biomass production and composition, we highlighted that biomass production was positively correlated to cellulose and lignin, but negatively correlated to hemicellulosic carbohydrates, in agreement with the literature (Xu et al., 2012; Arnoult et al., 2015a). This suggests that miscanthus growth may be accompanied by higher contents in cellulose and lignin while other carbohydrates proportions decrease.

Comparison of released glucose from untreated and hot water-treated genotypes has also revealed that in both conditions, harvesting year and genotypes differentially affect cellulose digestion. Indeed, after pretreatment, harvesting year effect was limited to year 5 (**Figure 4**), while genotype impact became stronger. In contrast to pretreated genotypes, relationships analysis mainly indicated that cellulose conversion of untreated miscanthus was less impacted by cell wall traits quantified in this present study, suggesting an incomplete and inefficient enzymatic hydrolysis. In fact, biomass production negatively impacted cellulose conversion of hot water-treated samples, but the strength of this relationship was significantly impacted by the two genotype groups and three harvesting years. Similar findings have been recently reported by Domon et al. (2013) while exploring the impact of cold acclimation on miscanthus cell wall composition.

Variations in cellulose conversion yields, according to genotypes and harvesting years, is related to the cell wall and tissue architectures between the less recalcitrant ROT, H8, and SIL genotypes and the more recalcitrant FLO and GIB ones. Indeed, based on our results, the highest cellulose conversion yields displayed by ROT, H8, and SIL can be related to the highest Hemicellulosic carbohydrates/Cellulose ratio and lowest Lignin/Cellulose and LCI ratios, while more recalcitrant FLO and GIB displayed the lowest Hemicellulosic carbohydrates/Cellulose ratio and highest Lignin/Cellulose and LCI ratios. This lignocellulose index (LCI) is reported to be high when biomass is less digestible (Moorhead et al., 2013). Based on correlation analysis, extractives do not seem to explain observed differences on cellulose conversion between the three harvesting years. Hot water pretreatment applied to these genotypes may result in dissolving of hemicelluloses and slight increasing lignin content in the pretreated biomass as reported by Li H.-Q. et al. (2013).

To better understand results highlighted in this study, other cell wall traits must be addressed such as monosaccharide composition of hemicellulose fraction, glycome profile, and cellulose crystallinity index. Indeed, wet chemistry can allow us determining xylan chain substitution by arabinose and other components. For instance, a higher substitution degree of xylan chain by arabinose was reported to positively affect miscanthus saccharification and microbial decomposition (Li F. et al., 2013; Amin et al., 2014). Acetylation of xylan chains has also been reported to create steric hindrance for binding cellulolytic

enzymes (Selig et al., 2009; Gille and Pauly, 2012). Phenolic acids, *p*-coumaric and ferulic acid are also known to impact saccharification potential (Belmokhtar et al., 2013). Moreover, the role of minor cell wall components such as xyloglucans, rhamnogalacturonans, and homogalacturonans have been shown to be differentially distributed among different harvests, organs, and genotypes (Costa et al., 2016).

Variations in leaf/stem ratio can also explain differences in cellulose conversion between more and less recalcitrant genotypes as leaves have been reported to be more reactive to cellulases conversion as compared to stems (Le Ngoc Huyen et al., 2010; Costa et al., 2016). From the study of Arnoult et al. (2015a), ROT, H8, and SIL, displaying the highest cellulose conversion yields, show higher leaf/stem ratios (varied from 0.11 to 0.33 for the harvest in February of years 4 and 5) than FLO and GIB, displaying the lowest cellulose conversion yields (leaf stem ratios varied from 0.01 to 0.08 for the harvest in February of years 4 and 5). Indeed, ROT, H8, and SIL genotypes displayed more leaves at the February harvest than FLO and GIB, for which, the major part of the leaves fell to the ground before the harvest. As leaves contain less lignin than stems (Arnoult et al., 2015a), the higher quantity of leaves at harvest can be explained, in that ROT, H8, and SIL genotypes were less recalcitrant and then gave higher cellulose conversion yields. Indeed, the released glucose after enzymatic hydrolysis of hot water-treated miscanthus genotypes was positively correlated to the leaf/stem ratio (r-values of 0.57 and 0.79, respectively for the years 4 and 5). The correlation was also positive for the untreated miscanthus genotypes, even if this correlation was lower than for hot water-treated genotypes (r-values of 0.03 and 0.66, respectively for the years 4 and 5). The differences in cell wall and tissue architectures, between more and less recalcitrant genotypes, confirmed how hemicelluloses' interaction with cellulose and reduced lignin content was important for achieving higher cellulose conversion yields.

Cellulose conversion inhibition by high lignin and cellulose contents has been reported to be due to unproductive fixation of cellulolytic enzymes on lignin, while hemicelluloses are reported to deposit into cell walls via crosslink to cellulose by hydrogen bonds; thus, reducing cellulose crystallization (Xu et al., 2012; De Souza et al., 2015; van der Weijde et al., 2016). Indeed, reduction in cellulose crystallinity may result in efficient cellulase access to cellulose substrate (Yoshida et al., 2008). Lignin is also assumed to interact with hemicelluloses rather than with cellulose, which can reduce interactions between hemicelluloses and cellulose, thus increasing cellulose crystallinity.

To conclude, the genetic diversity on biomass production and cell wall composition can be used in breeding programs to improve the saccharification potential of genotypes for the objective of bioethanol production.

Reliability of Mimicking the Cellulose Conversion of Various Miscanthus Genotypes in the Miniaturized Assay in Comparison to the Pilot Scale

We investigated, for the first time at the pilot scale, the performance of five miscanthus genotypes contrasted for their

biomass composition belonging to the species *M. × giganteus* (FLO, GIB, and H8) and *M. sinensis* (ROT and SIL). Steam explosion and enzymatic hydrolysis were carried out at the pilot scale in close agreement to previously reported data of other feedstocks (Schell et al., 2003; Thomsen et al., 2006; Rocha et al., 2012). Our results highlighted significant differences between the explored genotypes exhibiting distinct recalcitrance. Compared to the results shown by Schell et al. on corn stover, these results seem to be much lower, probably due to the intrinsic properties of miscanthus (Schell et al., 2003).

Furthermore, we performed hot water pretreatment and enzymatic hydrolysis with saturating amounts of cellulolytic enzymes to screen more samples for their digestibility based on the method recently described by Selig et al. (2010). A high-throughput screening method was initially developed at NREL (Golden, CO, USA) where the pretreatment step used a strong pilot-scale boiler to produce steam heated to 180°C. Here, we adapted this pretreatment step to a laboratory scale using a small steam generator provided from CellKraft® (Sweden). This resulted in a little more time for reaching target temperature but was able to maintain it during 40 min. Results accuracy and reliability have been assessed using 5 normalization controls for inter-plate and inter-assay comparisons. It consists on running a standard biomass in 4 wells in addition to a biomass control well not containing cellulolytic enzymes. During the current study, CV corresponding for these normalization controls was lesser than 1.5% (**Supplementary Image 2**). The advantage of our high-throughput method therefore, relies in its laboratory scale and reliability.

We highlighted a strong correlation between the pilot and miniaturized assay for cellulose conversion, displaying different patterns between the digestible H8, ROT, and SIL group and the more recalcitrant FLO and GIB group. However, cellulose conversion yields were relatively high according to the miscanthus genotype. This difference between the pilot and miniaturized assays can be explained by the different experimental conditions between the pilot and miniaturized assay, such as pretreatment technology and enzyme loading. Indeed, the better digestibility observed at the pilot scale for the FLO and GIB genotypes may be explained by the presence of sulfuric acid and fiber explosion during the pretreatment carried out at the pilot-scale; while the hot water treatment used in the miniaturized assay seemed less efficient in these recalcitrant biomasses. In contrast, the more digestible genotypes ROT, H8, and SIL responded better to the hot water treatment used in the miniaturized assay. Furthermore, this original approach allowed us to highlight the same trend in the cellulose conversion potential of the five genotypes regardless of the harvesting year. Moreover, the inter-year comparison revealed distinct digestibility, which confirms the importance of our approach based on using sub-optimal pretreatments, while giving high cellulose conversion yields.

Therefore, this high-throughput miniaturized and automated method accurately mimics the performance at the pilot scale and will be reliable for assessing the performance of miscanthus tested in small field plot trials.

CONCLUSIONS

The miniaturized and automated pretreatment and saccharification method we developed allowed us to highlight the variability in saccharification potential according to miscanthus genotypes belonging to the most-studied species *M. × giganteus* and *M. sinensis* and harvesting year. This variability in saccharification potential was explained by variations in biomass production and cell wall composition. Indeed, we revealed that changes in the biomass production were positively correlated to cellulose and lignin content and negatively correlated to hemicellulosic carbohydrates polymers. Moreover, the relationship analysis between released glucose after pretreatment and saccharification and biomass quality traits indicated the same strong negative effect of lignin and cellulose, while hemicellulosic carbohydrates significantly increased miscanthus digestibility. For future investigations, it would be interesting to more deeply explore the involvement of esterified and etherified phenolic acids and the arabinose ramification of xylan chains in cell wall cross-linking, to better understand the observed genetic diversity highlighted in this study, especially the positive effect of hemicellulosic carbohydrates.

The results obtained in this study have also shown that our lignocellulosic biomass assessment system, which was developed based on very small quantities of matter in the image of the NREL system (USA), allows a fair and efficient evaluation of the saccharification potential, which has proven to be well correlated with the results obtained at the pilot scale close to industrial reality.

These findings could be used in breeding programs to develop less recalcitrant genotypes for cellulosic ethanol production at the industrial scale since our results at the miniaturized and pilot scales are well-correlated.

AUTHOR CONTRIBUTIONS

NB developed the miniaturized test and performed the corresponding analyses. SA analyzed the data from the pilot tests. BC contributed to the development of the initial miniaturized test and to the analysis of the enzymatic hydrolysis of cellulose. JPC coordinated the corresponding project and he supervised the development of the miniaturized tests. MB contributed to the development of the initial project. NB and SA wrote the first draft of the manuscript and all authors contributed to the final version.

ACKNOWLEDGMENTS

contribution of the GenoBois technological platform of INRA Val de Loire for allowing us to use the fully automated grinding and biomass dispensing station provided by the XyloForest French national project. We also thank Nathalie Boizot and Vincent Segura from INRA Val de Loire and Steve Decker from NREL (Golden, CO, USA) for assistance in high-throughput pretreatment and saccharification method development and for help in statistical analysis. We are also grateful for Guillaume Barbedette for initial studies at INRA Reims on miniaturized pretreatment and saccharification assay.

SUPPLEMENTARY MATERIAL

The Supplementary Material for this article can be found online at: http://journal.frontiersin.org/article/10.3389/fpls.2017.00740/full#supplementary-material

Supplementary Image 1 | Subdivision of genotypes into two distinct groups based on biomass traits. Biomass yield **(A)**, Cellulose **(B)**, Hemicellulosic carbohydrates **(C)**, Lignin **(D)**, Hemicellulosic carbohydrates/Cellulose **(E)**, Lignin/Cellulose **(F)**, LCI **(G)**.

Supplementary Image 2 | Repeatability of the saccharification assay.

REFERENCES

Allison, G. G., Morris, C., Clifton-Brown, J., Lister, S. J., and Donnison, I. S. (2011). Genotypic variation in cell wall composition in a diverse set of 244 accessions of Miscanthus. *Biomass Bioenerg.* 35, 4740–4747. doi: 10.1016/j.biombioe.2011.10.008

Amin, B. A. Z., Chabbert, B., Moorhead, D., and Bertrand, I. (2014). Impact of fine litter chemistry on lignocellulolytic enzyme efficiency during decomposition of maize leaf and root in soil. *Biogeochemistry* 117, 169–183. doi: 10.1007/s10533-013-9856-y

Arnoult, S., and Brancourt-Hulmel, M. (2015). A review on miscanthus biomass production and composition for bioenergy use: genotypic and environmental variability and implications for breeding. *Bioenergy Res.* 8, 502–526. doi: 10.1007/s12155-014-9524-7

Arnoult, S., Mansard, M. C., and Brancourt-Hulmel, M. (2015b). Early prediction of miscanthus biomass production and composition based on the first six years of cultivation. *Crop Sci.* 55, 1104–1116. doi: 10.2135/cropsci2014.07.0493

Arnoult, S., Obeuf, A., Béthencourt, L., Mansard, M.-C., and Brancourt-Hulmel, M. (2015a). Miscanthus clones for cellulosic bioethanol production: relationships between biomass production, biomass production components, and biomass chemical composition. *Ind. Crops Prod.* 63, 316–328. doi: 10.1016/j.indcrop.2014.10.011

Belmokhtar, N., Habrant, A., Ferreira, N. L., and Chabbert, B. (2013). Changes in phenolics distribution after chemical pretreatment and enzymatic conversion of *Miscanthus x giganteus* internode. *Bioenergy Res.* 6, 506–518. doi: 10.1007/s12155-012-9275-2

Berlin, A., Balakshin, M., Gilkes, N., Kadla, J., Maximenko, V., Kubo, S., et al. (2006). Inhibition of cellulase, xylanase and β-glucosidase activities by softwood lignin preparations. *J. Biotechnol.* 125, 198–209. doi: 10.1016/j.jbiotec.2006.02.021

Bertrand, I., Chabbert, B., Kurek, B., and Recous, S. (2006). Can the biochemical features and histology of wheat residues explain their decomposition in soil? *Plant Soil* 281, 291–307. doi: 10.1007/s11104-005-4628-7

Biswal, A. K., Hao, Z., Pattathil, S., Yang, X., Winkeler, K., Collins, C., et al. (2015). Downregulation of GAUT12 in *Populus deltoides* by RNA silencing results in reduced recalcitrance, increased growth and reduced xylan and pectin in a woody biofuel feedstock. *Biotechnol. Biofuels* 8:41. doi: 10.1186/s13068-015-0218-y

Brosse, N., Dufour, A., Meng, X., Sun, Q., and Ragauskas, A. (2012). Miscanthus: a fast-growing crop for biofuels and chemicals production. *Biofuels Bioprod. Biorefin.* 6, 580–598. doi: 10.1002/bbb.1353

Cadoux, S., Ferchaud, F., Demay, C., Boizard, H., Machet, J.-M., Fourdinier, E., et al. (2014). Implications of productivity and nutrient requirements on greenhouse gas balance of annual and perennial bioenergy crops. *GCB Bioenergy* 6, 425–438. doi: 10.1111/gcbb.12065

Clifton-brown, J. C., Stampfl, P. F., and Jones, M. B. (2004). Miscanthus biomass production for energy in Europe and its potential contribution to decreasing fossil fuel carbon emissions. *Global Change Biol.* 10, 509–518. doi: 10.1111/j.1529-8817.2003.00749.x

Costa, R. M., Pattathil, S., Avci, U., Lee, S. J., Hazen, S. P., Winters, A., et al. (2016). A cell wall reference profile for Miscanthus bioenergy crops highlights compositional and structural variations associated with development and organ origin. *New Phytol.* 213, 1710–1725. doi: 10.1111/nph.14306

De Souza, A. P., Alvim Kamei, C. L., Torres, A. F., Pattathil, S., Hahn, M. G., Trindade, L. M., et al. (2015). How cell wall complexity influences saccharification efficiency in *Miscanthus sinensis*. *J. Exp. Bot.* 66, 4351–4365. doi: 10.1093/jxb/erv183

Domon, J. M., Baldwin, L., Acket, S., Caudeville, E., Arnoult, S., Zub, H., et al. (2013). Cell wall compositional modifications of Miscanthus ecotypes in response to cold acclimation. *Phytochemistry* 85, 51–61. doi: 10.1016/j.phytochem.2012.09.001

Gille, S., and Pauly, M. (2012). O-acetylation of plant cell wall polysaccharides. *Front. Plant Sci.* 3:12. doi: 10.3389/fpls.2012.00012

Gomez, L. D., Whitehead, C., Barakate, A., Halpin, C., and McQueen-Mason, S. J. (2010). Automated saccharification assay for determination of digestibility in plant materials. *Biotechnol. Biofuels* 3:23. doi: 10.1186/1754-6834-3-23

Gomez, L. D., Whitehead, C., Roberts, P., and McQueen-Mason, S. J. (2011). High-throughput Saccharification assay for lignocellulosic materials. *J. Visual. Exp.* 53:e3240. doi: 10.3791/3240

Hastings, A., Clifton-Brown, J., Wattenbach, M., Stampfl, P., Mitchell, C. P., and Smith, P. (2008). Potential of Miscanthus grasses to provide energy and hence reduce greenhouse gas emissions. *Agron. Sustain. Dev.* 28, 465–472. doi: 10.1051/agro:2008030

Hatfield, R. D., Jung, H.-J. G., Ralph, J., Buxton, D. R., and Weimer, P. J. (1994). A comparison of the insoluble residues produced by the Klason lignin and acid detergent lignin procedures. *J. Sci. Food Agric.* 65, 51–58. doi: 10.1002/jsfa.2740650109

Healey, A. L., Lupoi, J. S., Lee, D. J., Sykes, R. W., Guenther, J. M., Tran, K., et al. (2016). Effect of aging on lignin content, composition and enzymatic saccharification in Corymbia hybrids and parental taxa between years 9 and 12. *Biomass Bioenerg.* 93, 50–59. doi: 10.1016/j.biombioe.2016.06.016

Heaton, E. A., Dohleman, F. G., and Long, S. P. (2008). Meeting US biofuel goals with less land: the potential of Miscanthus. *Global Change Biol.* 14, 2000–2014. doi: 10.1111/j.1365-2486.2008.01662.x

Hendriks, A. T., and Zeeman, G. (2009). Pretreatments to enhance the digestibility of lignocellulosic biomass. *Bioresour. Technol.* 100, 10–18. doi: 10.1016/j.biortech.2008.05.027

Himmel, M. E., Ding, S. Y., Johnson, D. K., Adney, W. S., Nimlos, M. R., Brady, J. W., et al. (2007). Biomass recalcitrance: engineering plants and enzymes for biofuels production. *Science* 315, 804–807. doi: 10.1126/science.1137016

Hodgson, E. M., Lister, S. J., Bridgwater, A. V., Clifton-Brown, J., and Donnison, I. S. (2010). Genotypic and environmentally derived variation in the cell wall composition of Miscanthus in relation to its use as a biomass feedstock. *Biomass Bioenerg.* 34, 652–660. doi: 10.1016/j.biombioe.2010.01.008

Hodgson, E. M., Nowakowski, D. J., Shield, I., Riche, A., Bridgwater, A. V., Clifton-Brown, J. C., et al. (2011). Variation in Miscanthus chemical composition and implications for conversion by pyrolysis and thermo-chemical bio-refining for fuels and chemicals. *Bioresour. Technol.* 102, 3411–3418. doi: 10.1016/j.biortech.2010.10.017

Hodkinson, T. R., Chase, M. W., Lledó, D. M., Salamin, N., and Renvoize, S. A. (2002). Phylogenetics of Miscanthus, Saccharum and related genera (Saccharinae, Andropogoneae, Poaceae) based on DNA sequences from ITS

nuclear ribosomal DNA and plastid trnL intron and trnL-F intergenic spacers. *J. Plant Res.* 115, 381–392. doi: 10.1007/s10265-002-0049-3

Iiyama, K., Lam, T. B. T., and Stone, B. A. (1990). Phenolic acid bridges between polysaccharides and lignin in wheat internodes. *Phytochemistry* 29, 733–737. doi: 10.1016/0031-9422(90)80009-6

Jørgensen, H., Kristensen, J. B., and Felby, C. (2007). Enzymatic conversion of lignocellulose into fermentable sugars: challenges and opportunities. *Biofuels Bioprod. Biorefin.* 1, 119–134. doi: 10.1002/bbb.4

Lee, W. C., and Kuan, W. C. (2015). Miscanthus as cellulosic biomass for bioethanol production. *Biotechnol. J.* 10, 840–854. doi: 10.1002/biot.201400704

Le Ngoc Huyen, T., Rémond, C., Dheilly, R. M., and Chabbert, B. (2010). Effect of harvesting date on the composition and saccharification of *Miscanthus x giganteus*. *Bioresour. Technol.* 101, 8224–8231. doi: 10.1016/j.biortech.2010.05.087

Lewandowski, I., and Schmidt, U. (2006). Nitrogen, energy and land use efficiencies of miscanthus, reed canary grass and triticale as determined by the boundary line approach. *Agric. Ecosyst. Environ.* 112, 335–346. doi: 10.1016/j.agee.2005.08.003

Li, F., Ren, S., Zhang, W., Xu, Z., Xie, G., Chen, Y., et al. (2013). Arabinose substitution degree in xylan positively affects lignocellulose enzymatic digestibility after various NaOH/H2SO4 pretreatments in Miscanthus. *Bioresour. Technol.* 130, 629–637. doi: 10.1016/j.biortech.2012.12.107

Li, H.-Q., Li, C.-L., Sang, T., and Xu, J. (2013). Pretreatment on Miscanthus lutarioriparious by liquid hot water for efficient ethanol production. *Biotechnol. Biofuels* 6:76. doi: 10.1186/1754-6834-6-76

Lygin, A. V., Upton, J., Dohleman, F. G., Juvik, J., Zabotina, O. A., Widholm, J. M., et al. (2011). Composition of cell wall phenolics and polysaccharides of the potential bioenergy crop –Miscanthus. *GCB Bioenergy* 3, 333–345. doi: 10.1111/j.1757-1707.2011.01091.x

Moorhead, D. L., Lashermes, G., Sinsabaugh, R. L., and Weintraub, M. N. (2013). Calculating co-metabolic costs of lignin decay and their impacts on carbon use efficiency. *Soil Biol. Biochem.* 66, 17–19. doi: 10.1016/j.soilbio.2013.06.016

Mosier, N., Wyman, C., Dale, B., Elander, R., Lee, Y. Y., Holtzapple, M., et al. (2005). Features of promising technologies for pretreatment of lignocellulosic biomass. *Bioresour. Technol.* 96, 673–686. doi: 10.1016/j.biortech.2004.06.025

Pauly, M., and Keegstra, K. (2008). Cell-wall carbohydrates and their modification as a resource for biofuels. *Plant J.* 54, 559–568. doi: 10.1111/j.1365-313X.2008.03463.x

Ralph, J. (2010). Hydroxycinnamates in lignification. *Phytochem. Rev.* 9, 65–83. doi: 10.1007/s11101-009-9141-9

Rocha, G. J. M., Gonçalves, A. R., Oliveira, B. R., Olivares, E. G., and Rossell, C. E. V. (2012). Steam explosion pretreatment reproduction and alkaline delignification reactions performed on a pilot scale with sugarcane bagasse for bioethanol production. *Ind. Crops Prod.* 35, 274–279. doi: 10.1016/j.indcrop.2011.07.010

Rubin, E. M. (2008). Genomics of cellulosic biofuels. *Nature* 454, 841–845. doi: 10.1038/nature07190

Santoro, N., Cantu, S. L., Tornqvist, C.-E., Falbel, T. G., Bolivar, J. L., Patterson, S. E., et al. (2010). A high-throughput platform for screening milligram quantities of plant biomass for lignocellulose digestibility. *Bioenergy Res.* 3, 93–102. doi: 10.1007/s12155-009-9074-6

Schell, D. J., Farmer, J., Newman, M., and McMillan, J. D. (2003). "Dilute-sulfuric acid pretreatment of corn stover in pilot-scale reactor," in *Biotechnology for Fuels and Chemicals: The Twenty-Fourth Symposium,* eds B. H. Davison, J. W. Lee, M. Finkelstein, and J. D. McMillan (Totowa, NJ: Humana Press), 69–85.

Schell, D. J., Riley, C. J., Dowe, N., Farmer, J., Ibsen, K. N., Ruth, M. F., et al. (2004). A bioethanol process development unit: initial operating experiences and results with a corn fiber feedstock. *Bioresour. Technol.* 91, 179–188. doi: 10.1016/S0960-8524(03)00167-6

Selig, M. J., Adney, W. S., Himmel, M. E., and Decker, S. R. (2009). The impact of cell wall acetylation on corn stover hydrolysis by cellulolytic and xylanolytic enzymes. *Cellulose* 16, 711–722. doi: 10.1007/s10570-009-9322-0

Selig, M. J., Tucker, M. P., Sykes, R. W., Reichel, K. L., Brunecky, R., Himmel, M. E., et al. (2010). Original research: Lignocellulose recalcitrance screening by integrated high-throughput hydrothermal pretreatment and enzymatic saccharification. *Ind. Biotechnol.* 6, 104–111. doi: 10.1089/ind.2010.0009

Serba, D. D., Sykes, R. W., Gjersing, E. L., Decker, S. R., Daverdin, G., Devos, K. M., et al. (2016). Cell wall composition and underlying QTL in an F1 pseudo-testcross population of switchgrass. *Bioenergy Res.* 9, 836–850. doi: 10.1007/s12155-016-9733-3

Sørensen, A., Teller, P. J., Hilstrøm, T., and Ahring, B. K. (2008). Hydrolysis of Miscanthus for bioethanol production using dilute acid presoaking combined with wet explosion pre-treatment and enzymatic treatment. *Bioresour. Technol.* 99, 6602–6607. doi: 10.1016/j.biortech.2007.09.091

Studer, M. H., Brethauer, S., DeMartini, J. D., McKenzie, H. L., and Wyman, C. E. (2011). Co-hydrolysis of hydrothermal and dilute acid pretreated Populus slurries to support development of a high-throughput pretreatment system. *Biotechnol. Biofuels* 4:19. doi: 10.1186/1754-6834-4-19

Thomsen, M. H., Thygesen, A., Jørgensen, H., Larsen, J., Christensen, B. H., and Thomsen, A. B. (2006). "Preliminary results on optimization of pilot scale pretreatment of wheat straw used in coproduction of bioethanol and electricity," in *Twenty-Seventh Symposium on Biotechnology for Fuels and Chemicals,* eds J. D. McMillan, W. S. Adney, J. R. Mielenz, and K. T. Klasson (Totowa, NJ: Humana Press), 448–460.

van der Weijde, T., Kiesel, A., Iqbal, Y., Muylle, H., Dolstra, O., Visser, R. G. F., et al. (2016). Evaluation of *Miscanthus sinensis* biomass quality as feedstock for conversion into different bioenergy products. *GCB Bioenergy* 9, 176–190. doi: 10.1111/gcbb.12355

Van Soest, P. (1963). Use of detergents in the analysis of fibrous feeds. 1. Preparation of fiber residues of low nitrogen content. *J. Assoc. Off. Agric. Chem.* 46, 825–829.

Van Soest, P. J., and Wine, R. H. (1967). Use of detergents in the analysis of fibrous feeds. IV. Determination of plant cell-wall constituents. *J. Assoc. Off. Anal. Chem.* 50, 50–55.

Wyman, C. E. (1994). Alternative fuels from biomass and their impact on carbon dioxide accumulation. *Appl. Biochem. Biotechnol.* 45, 897–915. doi: 10.1007/BF02941858

Wyman, C. E., Dale, B. E., Elander, R. T., Holtzapple, M., Ladisch, M. R., and Lee, Y. Y. (2005). Comparative sugar recovery data from laboratory scale application of leading pretreatment technologies to corn stover. *Bioresour. Technol.* 96, 2026–2032. doi: 10.1016/j.biortech.2005.01.018

Xu, N., Zhang, W., Ren, S., Liu, F., Zhao, C., Liao, H., et al. (2012). Hemicelluloses negatively affect lignocellulose crystallinity for high biomass digestibility under NaOH and H2SO4 pretreatments in Miscanthus. *Biotechnol. Biofuels* 5:58. doi: 10.1186/1754-6834-5-58

Xue, J., Bosch, M., and Knox, J. P. (2013). Heterogeneity and glycan masking of cell wall microstructures in the stems of *Miscanthus x giganteus*, and its parents *M. sinensis* and *M. sacchariflorus*. *PLoS ONE* 8:e82114. doi: 10.1371/journal.pone.0082114

Yang, B., and Wyman, C. E. (2004). Effect of xylan and lignin removal by batch and flowthrough pretreatment on the enzymatic digestibility of corn stover cellulose. *Biotechnol. Bioeng.* 86, 88–98. doi: 10.1002/bit.20043

Yang, B., and Wyman, C. E. (2008). Pretreatment: the key to unlocking low-cost cellulosic ethanol. *Biofuels Bioprod. Biorefin.* 2, 26–40. doi: 10.1002/bbb.49

Yeh, R.-H., Lin, Y.-S., Wang, T.-H., Kuan, W.-C., and Lee, W.-C. (2016). Bioethanol production from pretreated *Miscanthus floridulus* biomass by simultaneous saccharification and fermentation. *Biomass Bioenerg.* 94, 110–116. doi: 10.1016/j.biombioe.2016.08.009

Yoshida, M., Liu, Y., Uchida, S., Kawarada, K., Ukagami, Y., Ichinose, H., et al. (2008). Effects of cellulose crystallinity, hemicellulose, and lignin on the enzymatic hydrolysis of *Miscanthus sinensis* to monosaccharides. *Biosci. Biotechnol. Biochem.* 72, 805–810. doi: 10.1271/bbb.70689

Economic and Environmental Assessment of Seed and Rhizome Propagated *Miscanthus* in the UK

Astley Hastings[1]*, Michal Mos[2], Jalil A. Yesufu[3], Jon McCalmont[4], Kai Schwarz[5], Reza Shafei[4], Chris Ashman[4], Chris Nunn[4], Heinrich Schuele[6], Salvatore Cosentino[7], Giovanni Scalici[7], Danilo Scordia[7], Moritz Wagner[8] and John Clifton-Brown[4]

[1] Institute of Biological and Environmental Sciences, University of Aberdeen, Aberdeen, United Kingdom, [2] Blankney Estates Ltd., Lincolnshire, United Kingdom, [3] Bangor University, Bangor, United Kingdom, [4] Institute of Biological, Environmental and Rural Sciences, Aberystwyth University, Aberystwyth, United Kingdom, [5] Julius Kühn-Institut - Bundesforschungsinstitut für Kulturpflanzen, Braunschweig, Germany, [6] Das Deutsche Agrarzentrum, Potash, Ukraine, [7] Dipartimento di Agricoltura, Alimentazione e Ambiente (Di3A), Università degli Studi di Catania, Catania, Italy, [8] Institute of Crop Science, University of Hohenheim, Stuttgart, Germany

Growth in planted areas of *Miscanthus* for biomass in Europe has stagnated since 2010 due to technical challenges, economic barriers and environmental concerns. These limitations need to be overcome before biomass production from *Miscanthus* can expand to several million hectares. In this paper, we consider the economic and environmental effects of introducing seed based hybrids as an alternative to clonal *M. x giganteus* (*Mxg*). The impact of seed based propagation and novel agronomy was compared with current *Mxg* cultivation and used in 10 commercially relevant, field scale experiments planted between 2012 and 2014 in the United Kingdom, Germany, and Ukraine. Economic and greenhouse gas (GHG) emissions costs were quantified for the following production chain: propagation, establishment, harvest, transportation, storage, and fuel preparation (excluding soil carbon changes). The production and utilization efficiency of seed and rhizome propagation were compared. Results show that new hybrid seed propagation significantly reduces establishment cost to below £900 ha^{-1}. Calculated GHG emission costs for the seeds established via plugs, though relatively small, was higher than rhizomes because fossil fuels were assumed to heat glasshouses for raising seedling plugs (5.3 and 1.5 kg CO_2 eq. C Mg [dry matter (DM)]$^{-1}$), respectively. Plastic mulch film reduced establishment time, improving crop economics. The breakeven yield was calculated to be 6 Mg DM ha^{-1} y^{-1}, which is about half average United Kingdom yield for *Mxg*; with newer seeded hybrids reaching 16 Mg DM ha^{-1} in second year United Kingdom trials. These combined improvements will significantly increase crop profitability. The trade-offs between costs of production for the preparation of different feedstock formats show that bales are the best option for direct firing with the lowest transport costs (£0.04 Mg^{-1} km^{-1}) and easy on-farm storage. However, if pelleted fuel is required then chip harvesting is more economic. We show how current seed based propagation methods can increase the rate at which *Miscanthus* can be scaled up; ∼×100 those of current rhizome propagation.

These rapid ramp rates for biomass production are required to deliver a scalable and economic *Miscanthus* biomass fuel whose GHG emissions are ~1/20th those of natural gas per unit of heat.

INTRODUCTION

Greenhouse gas (GHG) emissions to the atmosphere have to be curtailed so that global warming is limited to between 1.5 to 2°C as agreed in the 2015 Paris Agreement on climate change, signed by 197 countries and currently ratified by 142 countries including the largest GHG emitters, the United States and China. An important action to achieve this GHG emissions goal is to decarbonize the energy supply (Intergovernmental Panel on Climate Change [IPCC], 2014a,b). The key challenge is to achieve this equitably, without harming the economy or the environment. Nuclear and renewable energy systems powered by wind, solar, hydro, tidal, and biomass have low, but not zero GHG emissions per GJ of energy produced. They all require infrastructure to be built with energy intensive materials and have operating GHG costs, particularly where the production and distribution of energy vectors still rely on a fossil fuel based supply chains. There are also emissions associated with land use change, with indirect consequences that are difficult to quantify in many cases, although a methodology for annualized GHG emissions from carbon stock change due to land-use change has been developed by the Directive 2009/28/CE, and recently amended in the EU 2015/1513.

At present the economic cost per unit of renewable energy generated is more than that produced by systems powered by fossil fuels, though it should be noted that the lower price of fossil fuel is largely determined by huge, and largely hidden, national and global subsidies for production and use, totalling between 0.5 to 2 trillion US dollars per year (World Bank, 2015). Renewable energy systems also currently rely on subsidies in various forms to support their production costs. Historically in the United Kingdom, these take the form of the United Kingdom's Renewable Obligation Certificates (ROCs), Feed in Tariffs (FIT), and Renewable Heat Incentives (RHI) (Department of Energy and Climate Change [DECC], 2013). The most recent for electricity generation is the Contracts for Difference (CfD) whereby the generator is guaranteed a wholesale price per MWh of electricity generated, called a Strike Price (Ofgem, 2016). The current strike price levels vary with technology and are significantly above the current range of wholesale prices per MWh for fossil and old nuclear electricity (Ofgem, 2016), which averages around £40 MWh. As examples, strike prices for the period 2016/17 are: anaerobic digestion – £150, dedicated biomass with combined heat and power (CHP) – £125, hydro – £100, onshore wind – £95, offshore wind – £155, large scale solar – £115 and tidal stream – £305. For comparison new nuclear has a strike price of £93 MWh for the first facility.

The current wholesale price for electricity includes carbon tax and the cost of fuel and so subtracting these the generators

get around £20 MWh to cover operating costs (OPEX) and the amortization of capital expenditure (CAPEX). It is therefore clear that without taxes on carbon and generation subsidies, renewables are not currently economically competitive. In order for these renewable energy systems to be used to reduce GHG emissions in an economically viable way, it is important to quantify the economic and environmental costs of energy production for a range of technological options.

Bioenergy systems are one form of renewable energy. After centuries of burning wood for energy or processing forage into horse power, the first generation of bioenergy feedstocks were food crops, such as maize, oil seed rape, sugar cane, and oil palm, used to produce bioethanol and biodiesel. These required a high input in terms of fertilizer and energy, which increased their carbon footprint (St. Clair et al., 2008). In addition, the carbon cost of converting the food crop feedstock to bioethanol or biodiesel was significant with a low ratio of energy produced to energy input, high GHG cost and a low productivity in terms of GJ of energy per hectare of land (Hastings et al., 2012). Another drawback of using food crops for energy production is the pressure put on the balance of supply and demand for these feedstocks which can impact the cost of food (Valentine et al., 2011) and the increase of indirect land use change (ILUC) to increase the arable cropped area (Searchinger et al., 2008) which consequentially increases their environmental footprint.

The second generation bioenergy crop *Miscanthus* almost always has a smaller environmental footprint than first generation annual bioenergy ones (Heaton et al., 2004, 2008; Clifton-Brown et al., 2008; Gelfand et al., 2013; McCalmont et al., 2015a; Milner et al., 2015). This is due to its perennial nature, nutrient recycling efficiency and need for less chemical input and soil tillage over its 20-year life-cycle than annual crops (St. Clair et al., 2008; Hastings et al., 2012). *Miscanthus* can be grown on agricultural land that is economically marginal for food crop production (Clifton-Brown et al., 2015). However, the planted area of *Miscanthus* for biomass in Europe has stagnated since 2010 for a range of reasons including technical challenges, economic barriers, and environmental concerns. *Miscanthus* is in the early stages of domestication (Clifton-Brown et al., 2015) and poor agronomy of many of the first crops planted by rhizome propagation resulted in patchy establishment and consequent yield losses (Zimmerman et al., 2013). This was further compounded by the ending of incentive schemes such as the United Kingdom Energy Crops Scheme (which closed in 2013 for new applications) and uncertain markets (e.g., Drax power station withdrew from burning *Miscanthus* in 2016 on the announcement of significant reductions in government support (Farmers weekly, 2016)). There are some signs of recovery in the United Kingdom biomass market with new dedicated

straw burning power stations, such as Brigg in Lincolnshire (taking some 25,000 tons of *Miscanthus* per annum), coming online and providing some market pull. However, significant uncertainty remains in the market place making the decision by farmers and land owners to grow *Miscanthus* difficult, as the land must be committed to the perennial crop for its 10- to 20-year economic lifetime. Unlike annual arable crops, farmers cannot maximize farm profitability by changing crop species each year to follow market prices; highly front loaded perennial crop establishment costs require a long-term market to return the investment.

Certainty in crop establishment is important to avoid unwanted planting gaps, patchiness and the resultant yield losses which persist for the lifetime of the crop. There is a need to accelerate stand establishment in cool temperate climates to minimize the time to achieve maximum economic harvest, which in the historical plantings was about 3–5 years (Lesur et al., 2013; Clifton-Brown et al., 2015) depending on the local environmental conditions. As the crop is established once in its lifetime of up to 20 years, the cost of establishment has to be amortized over its entire lifetime. This means that the actual cost of production per ton, in terms of its GHG, energy-use or monetary cost, is increased if the crop fails or is slow to reach full productive potential due to poor establishment.

Current development of techniques to introduce new and seed propagated hybrids of *Miscanthus* with the associated novel agronomies and developments in harvesting (Clifton-Brown et al., 2016) have been projected to make significant reductions in the cost of producing and processing the biomass for end uses. Here, we make an experimental and modeling assessment to quantify how technical developments impact the economic and environmental performance of the crop using several trials, including those from the OPTIMISC (Lewandowski et al., 2016) and GIANT-LINK projects (Clifton-Brown et al., 2016), of which the 'Blankney large scale seed trial' (5 ha, planted in 2012) was a part and is a back bone of this study. This was the first trial of its kind, creating essential knowledge critical to move *Miscanthus* from a clone based crop to one based on seed. Other field scale experiments, such as the 6 ha trial planted in Penglais (Aberystwyth) in 2012 for the Carbo-biocrop/ELUM projects[1,2] were also used (McCalmont et al., 2015b; Dondini et al., 2016). Subsequently, field trials, sized to be commercially relevant, were planted with improved hybrids and agronomies in 2013 near Stuttgart (Germany), Potash (Ukraine) and the United Kingdom (three sites) (unpublished data). Data from a further four sites planted in 2014 in the United Kingdom with newer hybrids produced during GIANT-LINK show that seeded genotypes are matching yields of *Mxg* (unpublished data). The trials used in this study and their relevant details are shown in **Table 1**. The setups for these trials are described in Clifton-Brown et al. (2016), Lewandowski et al. (2016), and Kalinina et al. (2017).

We report on measurements of the energy, carbon intensity and economic cost of each phase of *Miscanthus* production, from propagation to final biomass fuel preparation, made on field scale experiments in the United Kingdom and Europe. We have used a sensitivity analysis to identify critical foci for further research efforts to make biomass systems an economic and environmental alternative to fossil fuel energy systems.

---

[1] http://www.carbo-biocrop.ac.uk/

[2] http://www.elum.ac.uk/

TABLE 1 | Field trials used in this study with details of the propagation and harvesting methods used.

Name	Planting year	Propagation methods				Harvesting methods						Reference
		Rhizome	*In vitro* plugs	Seed plugs	Film	Hand	Direct chip	Mow	Swath drying	Bale	Pellet	
Blankney large scale (5 ha), United Kingdom	2012	√		√			√	√	√		√	Lewandowski et al., 2016
Penglais (6 ha), United Kingdom	2012	√					√					McCalmont et al., 2015b
Multi-location GXE trial OPTIMISC	2012		√	√		√						Kalinina et al., 2017
Lincoln commercial planting, United Kingdom	2012–present	√						√	√	√	√	Unpublished M. Mos
Ihinger Hof large scale (0.6 ha), DE	2013			√			√					Unpublished T. Truckses
DAZ large scale (2 ha), UA	2013			√			√					Unpublished H. Schuele
Multi-location GIANT LINK hybrid trial, United Kingdom	2014	√		√	√	√						Unpublished J. Clifton-Brown
Film effects plot trial, United Kingdom	2014	√		√	√	√						Unpublished C. Ashman
GIANT Elite seed trial, United Kingdom	2015	√		√	√	√						Unpublished R. Shafiei
Unterer Lindenhof large scale GNT	2015	√		√	√			√				Unpublished A. Kiesel

MATERIALS AND METHODS

This study used data from the *Miscanthus* crop trials detailed in **Table 1** as well as measurements made on commercial *Mxg* plots in the United Kingdom to examine the economic cost and GHG emissions of each component of the processes used to produce *Miscanthus* biomass fuel. The use of many experiments was necessary as individual agronomy tests require up to 4 years to produce results and many of the experiments were conducted in parallel, in multiple locations. For each production process the trial used is identified and the evaluation methodology described. Additional information from the literature was used for aspects of production not tested.

Units, Parameters, and Criteria Used

The actual costs in pounds sterling (GBP) at the time of the experiment in 2015 is used, references to cost in other studies are referred to in their quoted currency and converted to pounds sterling at an exchange rate of £1 = 1.2 and £1 = $1.26. Economic costs involving the use of machinery are based on 2015 market equipment rental rates in the United Kingdom and 2015 fuel prices, based on $50 per barrel of oil with United Kingdom retail prices of £0.80 l^{-1} for diesel and £0.13 kWh for electricity. Transport distances are in United Kingdom miles (eq. to 1.61 km). Harvests are reported in Mg (metric ton) and commercial harvest yields are derived from counting bales and multiplying by the average bale weight for the genotype and correcting for moisture content using measurements from on-farm moisture gauges used for straw and grain. Only the operational costs of producing *Miscanthus* were quantified in this study as these can be related to the operational costs for producing other crops, this means the overhead cost of land and buildings, which vary by county, were not considered.

The higher heating value of *Miscanthus* was taken as 18 GJ Mg^{-1} harvested dry matter (DM; Sims et al., 2006). GHG emissions are expressed as the amount of CO_2, N_2O, and CH_4 converted to their global warming potential (GWP) over 100 years as "equivalent CO_2," using $CH_4 = 34\ CO_2$ and $N_2O = 298\ CO_2$ (Intergovernmental Panel on Climate Change [IPCC], 2014a). GHG quantity is expressed as kg of C in the equivalent CO_2 (CO_2 eq. C). This is used to define the GHG emitted per MJ of energy (g CO_2 eq. C MJ^{-1}) in the crops energy or mass of crop (g CO_2 eq. C Mg^{-1}). A similar unit is used to define the embedded GHG's in machinery and fuel used per Mg of biomass harvested or ha of land worked upon. Machinery GHG cost is calculated from the United Kingdom average of 55 kg of machinery ha^{-1} and based upon a 10 year service life, this is 13 kg CO_2 eq. C ha^{-1} y^{-1}. Electricity emissions are United Kingdom national grid average 31.9 g CO_2 eq. C MJ^{-1} based on the 2015 generation mix (Digest of UK Energy Statistics, and Electricity Statistics [DUKES], 2016). GHG emissions from diesel fuel is 0.86 kg C kg^{-1} diesel.

Soil organic carbon changes (SOC) were not measured or considered in this study as the time period to observe change (1–3 years) was too short in the trials used. Although SOC changes under *Miscanthus* have been measured for rhizome propagation (Dondini et al., 2009; McCalmont et al., 2015a,b;

Dondini et al., 2016) and the impact modeled spatially (Milner et al., 2015; Pogson et al., 2016; Richards et al., 2016), the impact of seed propagation on SOC has not yet been evaluated.

The use of fertilizers is not considered in this study as they have not been used on the commercial plots in the trial, nor currently in commercial plantings in the United Kingdom which rely on the initial nitrogen, phosphorous, and potassium (NPK) load of arable or rotational pasture field, which is normally sufficient for successful *Miscanthus* crop establishment (Michal Mos, private communication). In addition previous experiments indicate that for the management considered in this study, spring harvests after plant senescence, N fertilization has little impact on yield due to the low take off at harvest (Clifton-Brown et al., 2007; Davis et al., 2010).

The yields used in the calculation of GHG emissions and crop economics this study used mean yields of 12–14 Mg ha^{-1} y^{-1} that have been observed from *Mxg* from current commercial plantings observed in the United Kingdom (private communication, M. Mos). We have assumed a logistic yield increase for establishment year yields and a linear decline in yield after 15 years Lesur et al. (2013). Inter-annual yield variation, due to weather conditions, as observed in long term trials (Clifton-Brown et al., 2007) and modeled *Miscanthus* yields for the United Kingdom, using weather data from 2000 to 2009 (Harris et al., 2014) using the MiscanFor model (Hastings et al., 2009, 2013) indicates that the weather related standard deviation of inter-annual yield variation in the United Kingdom is of the order 2.1 Mg ha^{-1} y^{-1} for a mean yield of 10.5 Mg ha^{-1} y^{-1} for the whole of the United Kingdom. The modeled yields are generally pessimistic as they calculate rain-fed yields and do not account for ground water support that is available in many United Kingdom arable farms.

Statistical Tests

Minitab 17 software (Minitab, Inc., State College, PA, United States) was used to conduct the data exploration, data conditioning and analyses. Descriptive statistics were used to calculate means and standard deviations of the tests and comparisons between treatments were made by one way ANOVA using the Tukey HSD test ($P < 0.05$).

Field Trials Used

The Blankney Trial was the first large commercially relevant scale *Miscanthus* trial in the United Kingdom using seeds. It was part of the proposal of both the United Kingdom and EU funded projects, GIANT-LINK[3] and OPTIMISC[4], respectively. The trial was located at Blankney, Lincolnshire. The objective was to raise sufficient seed to plant 4 hectares (at 20,000 plants ha^{-1}) to compare with *Mxg* planted from rhizomes (at 16,000 plants ha^{-1}). The trial is described as WP 5 in Lewandowski et al. (2016). This trial was used for the plug production, weed control and harvesting experiments and provided material for the pelleting trials. It should be noted that the seed propagated clones were not chosen for their high yield but the ability of the parents

---

[3]http://www.miscanthusbreeding.org/
[4]https://optimisc.uni-hohenheim.de/

to produce a sufficient quantity of seed to make the required agronomy tests.

The Penglais commercial-scale trial of *Mxg,* described by McCalmont et al. (2015b), was used to test yields in the Atlantic seaboard maritime climate, direct chipping and provided material for animal bedding trials.

The OPTIMISC multi-location, multi-hybrid trials described in Lewandowski et al. (2016), Kalinina et al. (2017), and Nunn et al. (in press) were used to determine yields of 15 germplasm types (of which 11 were clonal genotypes, and 4 from seed) in six contrasting soil and climatic conditions distributed in western Eurasia. The propagation of the clonal types was used to estimate the cost of *in vitro* plug production.

The commercial plantings managed by Terravesta Ltd. in Lincoln, United Kingdom were used to estimate the cost of preparing the soil for planting, production, storage, and planting of rhizomes and cutting and baling techniques to optimize *Miscanthus* fuel quality (M. Mos private communication).

Two large scale trials set up in OPTIMISC program in Stuttgart and Ukraine were used to trial establishment of seeded hybrids, weed control and commercial yields (Lewandowski et al., 2016) (private communication A. Kiesel).

The GIANT-LINK program multi-genotype replicated trials were used to test the yield of many novel seed based and clonal hybrids in contrasting locations (United Kingdom, Poland, Ukraine, and Germany), using *Mxg* as a comparison. These identified several new hybrids that had yields greater than or equal to *Mxg.* In addition different agronomies for direct seeding, plug planting and the use of mulch film were trialed and the processing of seed tested (private communication, J. Clifton-Brown).

The film effects trials in Aberystwyth and Hackthorn (United Kingdom) were used to measure the effect on crop establishment for direct seed, seed and plug and rhizome propagated plants. The trials were replicated with each of the different propagated methods being trialed with and without mulch film. The yields were measured for 2 years, here the comparison of *Mxg* and seed plug establishment is reported (paper in preparation, C. Ashman and D. Awty-Carroll).

The GIANT Elite seed trial, was similar to the GIANT-LINK and OPTIMISC multi-hybrid trial but tested new hybrid material that was bred during the GIANT-LINK project. Its primary purpose was to test yield performance and establishment rate in two contrasting locations. Twelve inter-species hybrids (designated GNTxx) were seed plug propagated and planted in triple replicated trials under mulch film in Oxford, United Kingdom and the Julius-Kuehn Institute (JKI) in Braunschweig in Germany. The plot sizes were 50 plants at a commercial size spacing. The trial is ongoing and the results presented here relate to the second year harvest (Private communication GIANT-LINK team).

Crop Establishment: Soil Preparation, Weed Control, and Mulch Film

Crop establishment has four cost components: creation of the plant material, soil preparation, planting, and weed control. The economic and GHG costs of each component were determined using measurements from the Blankney trials and commercial planting experience by Terravesta Ltd. The machinery used, the time and fuel consumption for each operation per hectare were measured or estimated. From this information the GHG emissions were calculated.

Soil preparation and weed control are site specific and depend on the initial land use and vegetation, ecology, soil texture and drainage and climatic conditions, which will govern the machinery, fuel and products used. It is important to reduce C_3 weeds as these emerge early and can out compete young *Miscanthus* plants. To date, it is normal to use Glyphosate [N-(phosphonomethyl)glycine] several weeks before plowing to remove the previous crop and or weeds. The soil is normally inversion plowed, though low-till methods are also possible. Just before planting, the soil is worked to a fine tilth with a tine or power harrow. For heavier and or marginal soils, two or more passes of a power harrow may be needed to prepare a fine tilth. The soil preparation input requirements depend on site/soil conditions and are the same whichever method of planting is used (rhizomes or plugs). During the first growing season, weeds were controlled to ensure minimal competition using a Jubilee (200 g/kg metsulfuron-methyl) + Starane (100 g/l fluroxypyr + 2.5 g/l florasulam) mix. Only one application is usually required with a GHG cost of 7 kg CO_2 eq. C ha^{-1}. This would be multiplied by the number of applications in the case of severe weed infestation. The base case ground preparation considered here is moldboard plowing and disk and tine harrowing with GHG costs of 165 kg CO_2 eq. C ha^{-1}, in heavier soils that require sub-soiling and more passes of the power harrow, this value would double.

The trial of the use of mulch film in Aberystwyth was used to test different crop establishment agronomy when combined with under-film weed control on seed, plug and rhizome plantings. The yield was measured over 2 years and compared to a control of no film for all treatments. *Mxg* was used as a comparison. The difference in yields between treated and control plots of *Mxg* were tested by ANOVA. Film costs £100 per ha and GHG emissions from its manufacture and application are 220 kg CO_2 eq. C ha^{-1}.

Rhizome Propagation

The *Mxg* rhizomes used in this experiment were produced in the United Kingdom. Producing rhizomes for propagation in the United Kingdom climate takes at least two growing season, this entails clearing the production ground of weeds, plowing in spring and tilling the ground to a fine seed bed like tilth before planting the rhizomes with a potato type planter. During the growing season weeds were controlled to ensure minimal competition using Jubilee + Starane mix. In the spring following the second growth year, the rhizomes are harvested using a modified potato harvester, hand or semi-automatically sorted and cut into viable pieces, 20–40 g. Harvested rhizomes are moved the same day to cold storage (2–5°C) before being transported to the crop planting site just before use to ensure the highest possible rhizome viability to maximize the establishment rates. This is typically 80–90% with fresh rhizomes planted within 2–3 days of harvesting or those kept in cold storage for longer periods

(Terravesta, personal communication). One ha of rhizomes produces enough material to plant 10–30 ha of crop with the same modified potato type planter. Lower quality rhizomes, tested by sprouting tests, would require 80–90 g rhizomes (private communication, M. Mos). The above ground biomass of the first growing season is mulched in the following spring and left as a soil amendment and for the second growing season is either harvested or mulched prior to rhizome harvesting. The economic and GHG cost of each component of production were calculated using the methods in "Crop Establishment: Soil Preparation, Weed Control, and Mulch Film" Section. If the rhizomes are produced in an environment where plant establishment is faster such as Poland, then the rhizomes can be harvested after the first growing season reducing the cost and improving the propagation rate. Here, the costs of United Kingdom rhizome production are considered.

In Vitro Micro Propagation

In vitro propagation is a skilled and labor intensive activity where clone growth is achieved by *in vitro* tillering on a suitable sterile medium (Lewandowski and Kahnt, 1993). *In vitro* tillers are split approximately monthly by hand under sterile conditions (private communication, K.-U. Schwarz). When the required numbers of clones are reached, the tillers are transferred out of sterile conditions into peat soil and grown in a glasshouse for 8 weeks until viable rooted plantlet plugs are achieved. This method can also be used to produce parent plants for seed production. The costs considered include the laboratory manipulation space, equipment and human resources and the greenhouse space and heating. The plugs are planted either by hand or using a standard Checchi and Magli Trium plug planting machine.

Seed Production, Direct Seeding, and Seed-Plug Propagation

The GIANT-LINK project funded by UK's DEFRA and BBSRC (2011–2016) in collaboration with CERES Inc. has successfully bred scalable seed propagated interspecies hybrids since 2013. Agronomic trials have shown, while successful establishment by direct sowing is possible, current methods waste seed and are often unreliable. To reduce the risks, the strategic emphasis has been on planting seeded hybrids via plug plants into the field (Clifton-Brown et al., 2016).

Seed production has to be conducted in climatic environments where the parental lines flower, cross pollinate and produce seed each year. Seed used in the Blankney large scale trial planted in 2012 was produced through open pollination of selected breeder's lines flowering in Braunschweig (Germany). Seeds from controlled field pollination from specifically planted 'crossing blocks' in Texas, (United States) and Sicily (Italy) were produced from 2013 onward. Seed production requires intensive management. The pollen and seed parents are cloned from 'mother plants' either by splitting rhizomes or *in vitro* tillering. The parental cloning rate depends largely on the parental species in question. In dry periods irrigation management is the key to successful seed set. Seed from ripe panicles in autumn is threshed and cold stored. Seed germination rates vary due to

many factors including ripeness at harvest and dormancy (Awty-Carroll, 2017).

Our work is showing, depending on the hybrid type, one ha of seed production can produce enough seed for ~1000–2000 ha of planting, depending on parental combinations, two orders of magnitude greater than rhizome propagation. The economic and GHG costs for all of the operations required for seed production added together are high due to the labor intensity of the agronomy. However, the cost of production is divided by the number of ha to be planted.

Trials with direct drilled *Miscanthus* seed trials are ongoing in the United Kingdom with an adapted Agricola Italiana precision pneumatic seed drill [35010 Massanzago, (PD), Italy] and have been shown to be a viable option of propagation. The longer term objective is to make *Miscanthus* seed drilling routine, though many barriers still exist (Ashman and Awty-Carroll, personal communication). Here, the GHG and economic costs of direct seeding *Miscanthus* have been estimated using current protocols for farm operation with direct seeding based upon a seed drill being pulled by a tractor with a driver and one other operator.

Technology for the plug production from seeds has been developed by Bell Brothers Nurseries Ltd. (United Kingdom), employing techniques used in the horticulture of vegetables and in field establishment agronomy using plug planters and film developed by IBERS/Terravesta Ltd. (United Kingdom) so that an 85–95% establishment rate is achieved. The seeds are planted in modules in a glasshouse around 8 weeks before field planting. Timing of the planting date affects the energy used in the greenhouse. Earlier sowings in January require more glasshouse heating than later sowings in early March (**Figure 1**). The cold hardened plugs are planted into a fine tilth to ensure good plug to soil hydraulic contact by a standard Checchi and Magli Trium plug planting machine. Economic and GHG costs were calculated using time and space estimates from the nurseries and the costs of standard farm machinery. This requires a tractor pulled planter with one operator per two rows planted. Currently, as is common practice in the horticultural industry, following personnel (one per four rows) heel in any missed plants.

Harvesting Tests

In the spring following the third growing season after planting, direct harvesting with a forage harvester was compared with the indirect harvest method using a mower and baler at the Blankney site. Biomass from both methods was used to make 6 mm pellets (Farm Feed System, United Kingdom). Direct chipping was also used at the Penglais site. The choice between chipping and baling will depend on the end use required, the storage available and the transportation distance to the end user. Both methods were evaluated at the Lincolnshire (United Kingdom) site to determine and compare the timing of each operation, the fuel consumption and the cost.

Direct chipping was evaluated on the 2015 harvest of three replicate plots of an open pollinated *M. sinensis* hybrid (OPM12) at Blankney in Lincolnshire on a scale which is representative of commercial fields. Three plots were mown with a forage harvester fitted with a 7.5 m wide cutter and chipped into a following trailer. The plots were 54 m long and mown in 7.5 m passes. The time to

FIGURE 1 | Eight-week-old seed established plug plants produced in peat soil in multi-trays in the glasshouse, hardening pre-planting. Inset shows a single plug ready for planting. Main picture of the multi-trays was provided by Dr. Michal Mos who features in the picture and has consented to his picture being published, inset picture of the plug was provided by John Clifton-Brown.

cut and chip each of several passes for each replicate was recorded as well as the fuel consumption and the biomass harvested. Machinery used was a Claas Jaguar 859 with a 7.5 m Claas Orbis header, a Claas Arion 650 tractor (184 hp) with a Baily silage trailer, this was operated by two staff. For commercial operations on large fields at least two tractors with silage trailers operated by an additional person would be required for continuous operation. The fuel consumption, timing and cost of each operation were recorded. From this the GHG cost was estimated.

Cutting to swath and baling was evaluated on the 2015 harvest of three replicates plots of three open pollinated breeder's lines (OPM52, OPM53, and OPM54) and *Mxg* (OPM9) at Blankney in Lincolnshire. These hybrids differ in leaf share and stem diameter, with the classic antagonistic relationship between stem counts per plant and height (Kalinina et al., 2017). The plots were cut to a swath using a 4.5 m mower using three 54 m runs. The time to cut a swath for each of several passes for each replicate was recorded as well as the fuel consumption and the biomass harvested and the results aggregated to hybrid means. The machinery used for mowing to a swath was a Claas Jaguar 859 with a 4.5 m Claas RU450 header (Claas, Harsewinkel, Ostwestfalen-Lippe, Germany); as the crop was sufficiently dry this was immediately followed by a Fendt 720 tractor (184 hp) with a Massey Ferguson MF2290 120 x 120 x 240 Hesston baler and chased by a JCB Loadall 531-70 telehandler (J C Bamford, Rocester, Staffordshire, ST14 5JP) and a Claas Arion 650 tractor with a Baily flat-bed trailer to transport to the store. This was operated by four staff. For continuous operation on a large field at least two tractors with

flat-bed trailers operated by an additional person are required. If turning of the swath on the field is required to dry the crop it can achieved at the rate of 2 ha h^{-1} with a 150 horse power tractor and a hay turner. The crop is normally dried in the swath until the moisture is below 14%. The fuel consumption, timing and cost of each operation were recorded. From this the GHG cost was estimated.

Pelleting

Pelleting *Miscanthus* biomass involves taking the feedstock, either from bales or chips and chipping it to <100 mm and then grinding it to <5 mm before pelletization. In this experiment, a Timberwolf chipper (TWSX200DHB, Stowmarket, United Kingdom), knife mill (SM 2000, Retsch, Haan, Germany) and MiniPress Pellet Mill (Farm Feed System, Cinderford, United Kingdom) were used to compare the 'pellet-ability' of a variety of *Miscanthus* genotypes and to estimate the energy required and conditions required to achieve useable pellet fuel.

The hybrids chosen for this pelletization experiment covered the range of plant morphologies observed in the *Miscanthus* hybrids. The energy to mill and pelletize was recorded and the GHG cost estimated from the energy consumption (United Kingdom grid electricity at 31.9 g CO_2 eq. C MJ^{-1}). It is important to note that as cost and energy-use is scaled with the size of the pellet mill, this experiment can only be used to compare the differences between hybrids. The economic costs and energy-use of pelleting commercial *Mxg* was obtained from commercial pelleting mills of differing sizes [e.g., La Meccanica

CLM200, 15 kW, Italy, Pellet Mill in Condex Ltd. (Lancaster, United Kingdom)].

Transport Costs

Using standard United Kingdom costs of truck transportation and normalized fuel consumption for the types of vehicle used (Department for Transport, 2014), the GHG and economic costs of transporting *Miscanthus* chips, bales and pellets was calculated. This was used along with the costs of chipping, baling and pelletizing to build a model to estimate the optimum distance between field, pellet mill and end user for each feedstock to minimize cost and GHG emissions. It was also used to optimize the trade-offs of transport costs with feedstock type for pelleting.

Farm Profitability

A farm economic model was constructed in Microsoft Excel to estimate the relative profitability of *Miscanthus* crops for different yields and establishment rates grown with various crop establishment, management, and harvest methodologies to estimate their impact on the return on investment to the farm.

The analysis is based on a 150 ha farm with 10% *Miscanthus*. The model assumes that *Miscanthus* reaches peak yield after x years (x variable in the model) and is productive for up to 20 years. The establishment rates and harvest yields were taken from the OPTIMISC multi-hybrid trials (Kalinina et al., 2017; Nunn et al., in press), where peak-yield took between 1 to 4 years, depending on soil and climatic conditions. The costs of establishment, crop management, and harvesting are from the experiments reported here. Yield evolution assumes that peak production continues until year 15 after which it declines by 5% per year until year 20 (Lesur et al., 2013; Arundale et al., 2014a).

The model uses an amortization period of 20 years to coincide with the economic life cycle of *Miscanthus* and discount rate of 6% (variable in the model) is assumed for the comparisons. A *Miscanthus* feedstock farm gate selling price of £88 Mg^{-1} DM was used to calculate crop income, which was based on the current United Kingdom price for bales with 15% moisture of £75 Mg^{-1}. All these values can be varied in the model to test sensitivities and to compare to other economic scenarios, however, the values used in our example reflect United Kingdom economic conditions and crop management in 2016. Land and buildings value was not considered in this study as it is site specific.

Scenarios tested were a comparison of rhizome and seed establishment and harvesting using either chipping or baling in Aberystwyth (United Kingdom), Potash (Ukraine), and Stuttgart (Germany). For each we calculated the gross margin and cumulative gross margin or net present value (NPV). Cumulative gross margins at zero indicates the break-even year on the graphs. Results for these scenarios are tabulated (**Table 9**).

RESULTS

Crop Establishment Costs

Of the four components of crop establishment mentioned earlier, soil preparation and weed control are site specific, determining
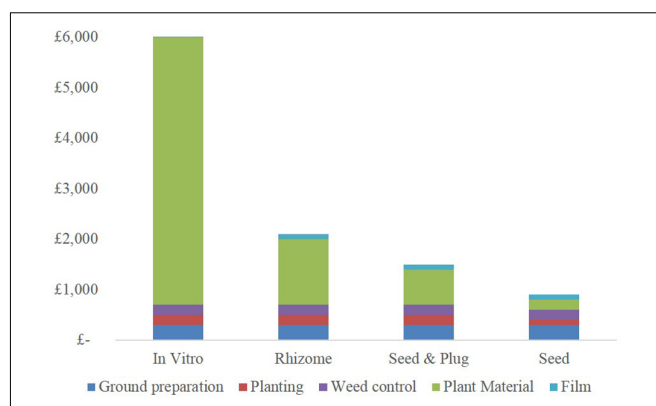
FIGURE 2 | Estimated components of economic cost of establishing one ha of *Miscanthus* using *in vitro*, rhizome, plugs from seed and direct sown seed propagation. Components include ground preparation, planting, weed control, planting material, mulch film. Here only a single pass of the power harrow is considered to produce a fine soil tilth (*in vitro* projects the cloning of 1 hectare's worth of material from a single clone which is being used as a parent for seed production).

the types of machinery, fuel and herbicides used. **Figure 2** shows the base case of light soil with moderate weed control. The ground preparation, weed control and use of film is the same for each propagation method. The main establishment cost variable is the type of material planted as shown in **Figure 2**. *In vitro* is the most expensive followed by rhizome, seed and plug and the lowest is direct seed drilling. The specific cost of rhizome and plug planting are similar as they are relatively labor intensive whereas seed drilling, is predicted to halve the cost. The overall cost of plug propagation is 2/3 that of rhizome due mainly due to the higher multiplication factor of ~2,000 to 1 compared to rhizome of 10–30 to 1. Direct seed drilling halves the cost of *Miscanthus* establishment (compared to rhizomes) to below £900 as well an increasing the ability to ramp up planted acreage. Even greater ramp ups can also be achieved by seed-plug propagation because less seed is wasted.

Greenhouse gas cost is broken down into the economic categories plus machinery manufacture as shown in **Table 2**.

TABLE 2 | Establishment greenhouse gas costs per hectare, to be amortized over total *Miscanthus* yield over the crop lifetime yield.

	GHG cost kg CO_2 eq. C ha^{-1}			
	*In vitro**	Rhizome	Seed to plug	Seed to soil
Plant material	18,905	49	1,264	0.1
Ground preparation	165	165	165	165
Machinery manufacture	13	13	13	13
Planting	233	265	233	233**
Weed control	7	7	7	7
Total	19,323	499	1,682	418

*Refers to providing 1 ha of plug plantlets from one plant.
**Assumes use of the same horsepower tractor as the plug planter.

TABLE 3 | Two-year dry matter (DM) yield comparison of _Mxg_ with/without film in Aberystwyth film effect plot trial.

Treatment	Replicates	2-year DM yield (Mg ha^{-1})		Tukey group
		mean	SD	
Film	9	7.31	2.36	a
No film	9	3.96	1.13	b

Weed control assumes only one application in the first year at 7 kg CO_2 eq. C ha^{-1}, and the base case of moldboard plow and disk and tine harrowing and costs 165 kg CO_2 eq. C ha^{-1}. Planting material has the largest variation. _In vitro_ costs are much higher due to the intensive use of controlled environments in the early stages of cloning. Rhizome costs are a little higher than seed but seed-plugs are 4× that of rhizomes due to the use of greenhouse space for their production.

Mulch Film Trial

The mulch film trial in Aberystwyth showed a significant ($P < 0.05$) difference between establishment rates for varying plant densities with the cumulative first 2-year mean yield almost doubling under film as shown in **Table 3**. Using film adds £100 per ha and 220 kg CO_2 eq. C ha^{-1}, to the cost of establishment. The effect of this increase is to reduce the establishment period of the crop by 1-year in Aberystwyth environmental conditions, similar reduction in establishment times were observed at the other trial sites and also in Ireland (O'Loughlin et al., 2017).

Harvesting by Chipping

Direct chipping results are tabulated in **Table 4**. The fuel consumption was 26 l ha^{-1} and with an average yield of 5.7 Mg DM ha^{-1}, the diesel consumption was 4.56 l Mg^{-1}. The rate of harvesting with this technique averaged 4.1 ha h^{-1} or 28 Mg h^{-1}. In this experiment, the moisture content was 15% and the density of the chipped material was estimated to be 80–100 kg m^{-3}. As the yield of this genotype was low and chipping rate is a function of crop throughput, the cost was calculated on a per Mg basis. The cost of this operation for large fields using two tractors and silage trailers is £28 Mg^{-1}. The GHG emissions including fuel use and carbon (C) embedded in the machinery (which is 7.27 kg CO_2 eq. C Mg^{-1}). This estimate is for a yield of 5.7 Mg (DM) ha^{-1} which will change if the chopper has to work harder with thicker stems or a heavier (taller) crop.

Harvesting by Cutting to Swath and Baling

The time to cut to a swath for each of several passes for each replicate was recorded as well as the fuel consumption and the biomass harvested. The mean results for each hybrid are tabulated in **Table 5**. The time to cut each swath run varied by 37% with the yield and hybrid (stem thickness), but at the slowest rate, a harvest rate of 23.3 Mg DM h^{-1} could be achieved on a thick stemmed hybrid like _Mxg_. The fuel consumption was estimated to be 10 l ha^{-1} with the 4.5 m cutter. The yield varied between 6.3 and 12.8 Mg DM ha^{-1}, so the diesel consumption varied between 1.59 and 0.79 l Mg^{-1}. The rate of cutting with this technique averaged 2 ha h^{-1} or 12.1 to 23.3 Mg h^{-1}. This mowing speed variation, both in terms of time taken to cut each hectare and time taken to cut each Mg within that hectare, was significantly different between genotypes ($P < 0.05$); particularly between _Mxg_ and the other, thinner stemmed varieties. The most important parameter is Mg DM cut h^{-1}, OPM 52 and OPM 53 were similar, however, it took 19% less time to cut each Mg of OPM 54 compared to the average of these two and 84% less to cut each Mg of _Mxg_ (see **Table 5**).

Baling was performed immediately after cutting as the biomass moisture content was below the 15% moisture level to ensure safe storage and enhance biomass fuel quality. In the case of _Mxg_, which does not flower in the United Kingdom in mild winters, it may not be fully senesced in spring and typically has a moisture content of up to 45% before February cutting. Experience has shown that the 15% moisture level can be achieved by merely drying in the swath in the field (Terravesta Ltd., personal communication). If turning is required to dry the crop further it can be achieved at the rate of 2 ha h^{-1} with a 150 horse power tractor and a hay turner. This has the added advantage of reducing the amount of leaf, which reduces ash content and leaches further Cl, N, P, and K from the material to reduce boiler corrosion and ash sintering, detrimental to combustion quality (Iqbal et al., 2017). These losses are accounted for in this study as the actual harvested yield is determined by the total weight of the baled material.

Baling speed with the large 120 × 120 × 240 Hesston baler depends on the quantity of material baled, normally around 35–40 bales h^{-1} in good ground conditions. Straw bales have a density of 140–180 kg m^{-3}, with average bale weights of 540 kg. The weight of _Miscanthus_ bales varied with genotype with the thinner stemmed genotype being around 580 kg (density = 171 kg m^{-3}) and the thicker stemmed _Mxg_ 530 kg (density = 157 kg m^{-3}), due to energy required to compact the stiffer material. Thus the rate of baling is ∼3 min Mg^{-1} or for the _Mxg_ crop with 12.7 Mg (DM) ha^{-1}, a rate of 44 min ha^{-1}.

The cost for this operation on an _Mxg_ crop with a harvest yield of 12.7 Mg (DM) ha^{-1} for large fields using two tractors and flatbed trailers would be £40.68 Mg^{-1}. The GHG emission, including fuel use and C embedded in the machinery, is 4.97 kg CO_2 eq. C Mg^{-1} (**Table 6**).

TABLE 4 | Harvesting _Miscanthus_ (hybrid OPM-12) using direct chipping.

Number of 54 m x 7.5 m cutting 'runs'	Average time taken per 'run' (s)	Standard deviation time taken per 'run' (s)	Sum area of runs = total sampled area (ha)	Diesel used for sampled area (l)	Mass from the total sampled area (Mg)	Harvest speed (ha h^{-1})	Harvest speed @15% moisture (Mg h^{-1})
12	35.4	2.7	0.49	12.6	3.3	4.1	28.0

TABLE 5 | Cutting to a swath and baling _Miscanthus_ open pollinated _Miscanthus sinensis_ (OPM 52, 53, 54) and _Mxg_ in the Blankney large scale trial, Lincoln, United Kingdom in spring 2015.

OPM*	Average time per 54 m cut run (s)	Standard deviation of time/run (s)	Harvest rate (s Mg⁻¹)	Standard deviation rate (s Mg⁻¹)	Tukey comparison group for harvest rate ($p < 0.001$)	Area of one run (ha)	Harvest speed (ha h⁻¹)	Yield (t ha⁻¹)	harvest rate (Mg h⁻¹)	Mean bale weight (kg)
OPM-52	45	4.8	295	31.2	a	0.0243	0.52	6.3	12.1	590
OPM-53	42	3.4	273	21.9	a	0.0243	0.48	6.4	13.2	580
OPM-54	42	3.8	237	21.8	b	0.0243	0.48	7.2	15.1	580
Mxg	48	5.2	166	16.7	c	0.0243	0.55	12.8	23.3	530

*Stem diameters for OPM 12, 52, 53, 54 are approximately half those of Mxg but with high stem counts m^{-2}.

TABLE 6 | Economic and greenhouse gas costs for harvesting pelletizing and transport per Mg _Miscanthus_ biomass.

Harvesting and transport option	Cost per Mg	GHG per Mg
	£	kg CO$_2$ eq. C Mg⁻¹
Chipping	£28.00	7.27
Baling	£40.68	4.97
Pelletizing (small scale)	£65.00	45.10
Pelletizing (large scale)	£19.50	13.60
	£ Mg⁻¹ mile⁻¹	g CO$_2$ eq. C Mg⁻¹ mile⁻¹
Transport chips	£0.12	35.45
Transport bales	£0.07	18.51
Transport pellets	£0.04	11.36

Pelleting

The energy to mill and pelletize the _Miscanthus_ varied between 1.33 and 0.55 kWh kg⁻¹, or between 4.79 and 1.98 MJ kg⁻¹. This experiment demonstrated that stiffer, thick stemmed genotypes had higher biomass yields and had a higher pellet density but required more energy to pelletize, in particular _Mxg_ (OPM-9). _Mxg_ required 1.1 kWh kg⁻¹ (3.96 MJ) to mill and pelletize, with a pellet density of 650 kg m⁻³ and a moisture content of 6%. The energy used in this lab scale equipment to pelletize _Mxg_ represented 22% of the energy content of the pellets, well above the normal 3–10% of commercial systems (Personal communication from Terravesta Ltd. and Blankney Estates Ltd.). Therefore the data produced in our tests is only useful as a relative comparison between hybrids with different stem properties.

The cost of pelletizing _Mxg_ in this experiment at current electricity prices in United Kingdom at £0.13 kWh is £143 Mg, for a small scale commercial plant it would be £65 Mg and for a large scale commercial plant is would be £19.5 Mg. If the pelletizing mills use electricity for grinding, which has a C. intensity of 31.9 g CO$_2$ eq. C MJ⁻¹ (year 2015 average[5]). The C. cost per Mg of _Mxg_ pellets for this test is 99 kg CO$_2$ eq. C Mg⁻¹. For a small scale commercial pelleting plant it is 45.1 kg CO$_2$ eq. C Mg⁻¹ and for a large scale plant is 13.6 kg CO$_2$ eq. C Mg⁻¹ (**Table 6**).

Transport Costs

In order to store heaped biomass fuel or transport it in enclosures it must be dry to avoid degradation and its volume must be reduced to minimize storage housing required. In addition this densification is necessary for efficient transportation. Chipped _Miscanthus_ has a density in kg m⁻³ of 80–100, bales 140–180 and pellets 650–675. Each format limits the quantity of material that can be carried on a truck – trailer in the United Kingdom by volume to a maximum of 38 bales which is ~21.5 Mg for _Mxg_, whereas in pellet form a maximum legal load of around 35 Mg could be achieved with a 44 Mg gross weight truck. Chips can only be transported a short distance as even the largest bulk carrier would only be able to transport around 11 Mg. Pellets are

[5]http://gridwatch.co.uk/co2-emissions

a preferred fuel format because they are convenient for storage and transport and comply with fuel feeders, burners, and boilers designed for wood pellets with little modification.

In the United Kingdom, a 44 Mg truck costs ~£1.46 mile to run including fuels costs at the current rate (2016) for an average annual mileage with a GHG emissions cost of 398 g CO_2 eq. C mile^{-1} considering an average fuel consumption of 8 miles per gallon of diesel. A full load of pellets would be 35 Mg with a transport cost of £0.041 Mg^{-1} mile^{-1} and a GHG cost of 11.36 g CO_2 eq. C Mg^{-1} mile^{-1}. A full load of 38 *Mxg* bales would be 21.5 Mg with a transport cost of £0.068 Mg^{-1} mile^{-1} and a GHG cost of 18.51 g CO_2 eq. C Mg^{-1} mile^{-1}. A full load of chips would be 11 Mg with a transport cost of £0.133 Mg^{-1} mile^{-1} and a GHG cost of 35.45 g CO_2 eq. C Mg^{-1} mile^{-1}. The harvesting, pelletizing and transport costs are summarized in **Table 6**.

A comparison of the economic cost and GHG cost of harvesting by chipping or baling shows that for both a large and small pelleting plant it is cheaper to transport chips but costs more in GHG emissions (**Table 7**). Analysing the distance that it becomes cheaper to transport pellets rather than bales by road shows that up to 400 miles bales are cheaper and have a much lower overall GHG cost (**Table 8**).

Seed Based Yield Trials

The GIANT Elite seed trials results are not reported here in detail but preliminary results show that all the seed based hybrids, produced by the breeding operations at Aberystwyth (Private communication R. Shafei, Aberystwyth), had yields after 2 years growth that were significantly (ANOVA Tukey test $P < 0.05$) greater than *Mxg* in both Oxford and JKI (**Figure 3B**). The hybrid yields at year 2 are at the level of *Mxg* yield normally reached by year 3 as shown in the OPTIMISC trial (Kalinina et al., 2017). However, the *Mxg* yields in both trials were similar in year 2. The ratio of the seed hybrid yields to *Mxg* yield show mean ratio of 1.9 (SD = 0.4) for JKI and 6.3 (SD = 3.2) for Oxford (**Figure 3A**), indicating that seed hybrids could also reduce establishment time. These results enabled a farm profitability estimation with the assumption that seed propagated hybrids have yields greater than or equal to *Mxg* yields to estimate the profitability of seed-plug propagation.

Farm Profitability

The longest break-even period and highest cost analyzed here (in Aberystwyth with the lowest yield, slowest establishment, using the most expensive establishment and cut and bale harvesting) was 6 years with a NPV per hectare of £1,331.00 (**Figure 4**). In Aberystwyth film reduces the pay-back time by 1 year and increases the NPV by 12% as the crop achieved maximum

TABLE 8 | Cost of bales and pellets for different transport distances.

| Distance	£ Mg^{-1}		kg CO_2 eq. C Mg^{-1}	
Miles	Bale	Pellet	Bale	Pellet
0	40.46	56.81	5.0	21.6
50	43.86	58.86	5.9	22.2
100	47.26	60.91	6.8	22.7
150	50.66	62.96	7.7	23.3
200	54.06	65.01	8.7	23.9
250	57.46	67.06	9.6	24.4
300	60.86	69.11	10.5	25.0
350	64.26	71.16	11.4	25.6
400	67.66	73.21	12.4	26.1

yield 1 year earlier. NPV rises to £4,238 with rhizome and film establishment and chip harvesting (**Table 9**). At all locations seed-plug establishment increases NPV by 15% and decreases the payback time by 1 year. Cutting and baling reduces the NPV and increased the payback time by 1 year compared to chipping. In this study, we have considered the impact of crop establishment rates observed in the multi-site, multi-hybrid trials at Aberystwyth, Potash, and Stuttgart which range from 2 to 4 years. The first year crop is mulched and not sold. The plateau yield is estimated as the average yield observed in year 3 and 4 of the trials. Scenarios are summarized in **Table 9** with NPV and break-even year.

DISCUSSION

This paper reports on measurements of the energy-use and costs involved in the cultivation of *Miscanthus* measured on plot and commercial-scale trials for the first time. These provide inputs for scalable economic models and life cycle assessments of GHG emissions. The models show that at current prices of £75 Mg^{-1} (Bales at <15% moisture) *Mxg* from rhizome with slow establishment rates and current United Kingdom yields of 12–14 Mg ha^{-1}, the breakeven payback time is 4 years for chipped harvesting and 6 years with bale harvesting. The worst case scenario of NPV in the United Kingdom is competitive with arable rotations. In continental climates with warmer summers, in this study exemplified by Potash in the Ukraine, yields reach 16 Mg ha^{-1} by the third year and breakeven payback time reduces to the third year including the costs of mulch film and seed-plug establishment. Further reductions in establishment costs are needed to increase farmer acceptance of the crop. Technological developments such as direct seeding, the use of

TABLE 7 | Relative economic and GHG costs of chips and bales of *Mxg* for different scales of pelleting facilities.

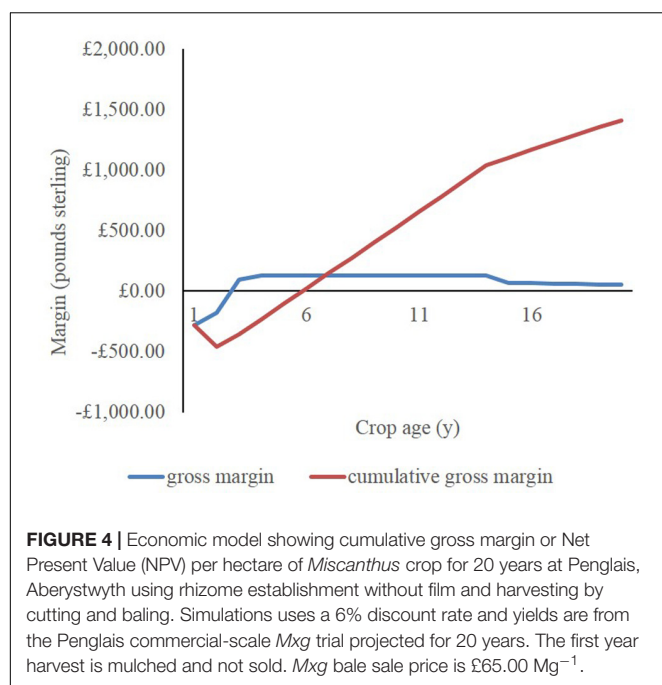|	Throughput	Crop	Land area	Catchment		Cost bales		Cost chips	
	Gg y^{-1}	ha	%	km^2	miles	£ Mg^{-1}	kg CO_2 eq. C Mg^{-1}	£ Mg^{-1}	kg CO_2 eq. C Mg^{-1}
Small scale pelletizing	5	5,000	10	500	4.6	£105.99	50	£93.55	53
Large scale pelleting	1000	100,000	10	10000	20.6	£61.58	19	£49.98	22
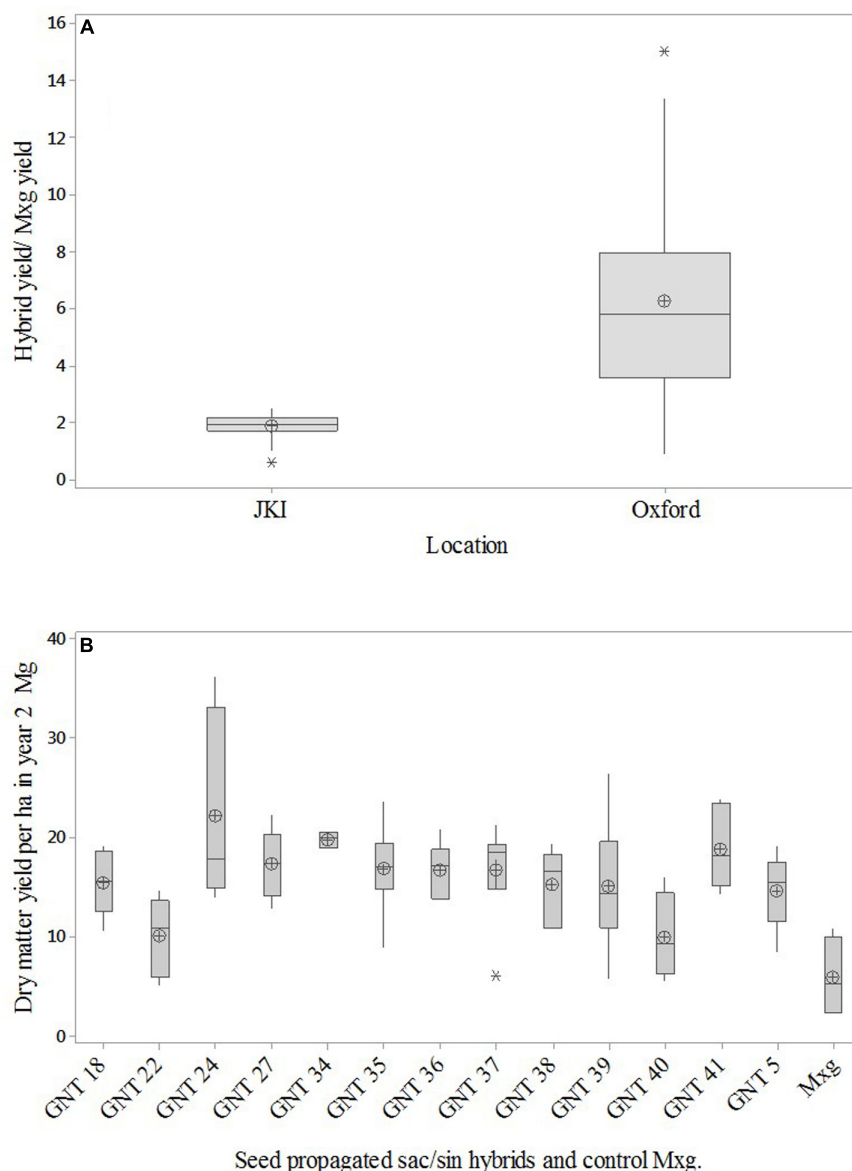
FIGURE 3 | Analysis of second year yield of Elite *Miscanthus sinensis – Miscanthus sacchariflorus* (GNT.xx) seed propagated hybrids compared to *Miscanthus x giganteus* (*Mxg*) rhizome propagated plant in Oxford and Germany (JKI). Box plots of the ratio of GNT yield/*Mxg* yield in year 2 is shown in **(A)** for both locations with the mean (⊕). The individual second year GNTxx and *Mxg* yields are shown in box plot **(B)** with the mean (⊕).

film to speed establishment and the development of higher yielding, faster establishing genotypes are all part of an ongoing research program. For our analysis, it should be noted, that we have compiled parallel advances in breeding, agronomy, and fuel processing. The particular hybrids in this study were chosen as the best material practically available from the Aberystwyth breeding program at the time when the trials were set up. The large scale trial in Blankney set-up in 2012 necessarily used open pollinated nursery seed, selected from good parents, as the production of F1 seed was insufficient in 2011. Methods to scale up seed production of F1 seed have developed year on year, and multi-location trials planted 2014 are based on scalable seed

produced in field crossing blocks (Clifton-Brown et al., 2016). **Figure 3** shows the significant improvements in establishment rates and early yields in these newer hybrids, which will reduce financial and C. costs in the future.

Currently, the commercial crop of *Mxg* is already economically viable, though it should be noted that the £75 Mg^{-1} price is supported by the CfD that subsidizes biomass used for electricity generation (Department of Energy and Climate Change [DECC], 2013). Our work shows that crop establishment, yield and harvesting method affect the C. cost of *Miscanthus* solid fuel which for baled harvesting is 0.4 g CO_2 eq. C MJ^{-1} for rhizome establishment and 0.74 g CO_2 eq. C MJ^{-1}

FIGURE 4 | Economic model showing cumulative gross margin or Net Present Value (NPV) per hectare of *Miscanthus* crop for 20 years at Penglais, Aberystwyth using rhizome establishment without film and harvesting by cutting and baling. Simulations uses a 6% discount rate and yields are from the Penglais commercial-scale *Mxg* trial projected for 20 years. The first year harvest is mulched and not sold. *Mxg* bale sale price is £65.00 Mg^{-1}.

annual crops (Heaton et al., 2004, 2008; Clifton-Brown et al., 2008; Gelfand et al., 2013; McCalmont et al., 2015a; Milner et al., 2015). In this analysis, we did not consider the GHG flux of soil which was shown to sequester on average in the United Kingdom 0.5 g of C per MJ of Miscanthus derived fuel by McCalmont et al. (2015a). Changes in SOC resulting from the cultivation of *Miscanthus* depend on the previous land use and associated initial SOC. If high carbon soils such as peatland, permanent grassland, and mature forest are avoided and only arable and rotational grassland with mineral soil is used for *Miscanthus* then the mean increase in SOC for the first 20-year crop rotation in the United Kingdom is ∼ 1–1.4 Mg C ha^{-1} y^{-1} (Milner et al., 2015). In spite of ignoring this additional benefit, these GHG cost estimates compare very favorably with coal (33 g CO_2 eq. C MJ^{-1}), North Sea Gas (16), liquefied natural gas (22), and wood chips imported from the United States (4). In addition, although *Miscanthus* production C. cost is only < 1/16 of the GHG cost of natural gas as a fuel (16–22 g CO_2 eq. C MJ^{-1}), it is mostly due to the carbon embedded in the machinery, chemicals and fossil fuel used in its production. As the economy moves away from dependence on these fossil fuels for temperature regulation (heat for glasshouse temperature control or chilling for rhizome storage) or transport, then these GHG costs begin to fall away from bioenergy production. It should be noted, the estimates in this paper do not consider either the potential to sequester C. in the soil nor any impact or ILUC (Hastings et al., 2009).

This work has shown that most genotypes of *Miscanthus* can be pelleted. Variation in stem morphology influences the energy required and the cost of pellet production. Even though pellets are more expensive to produce than bales, they are still a low C. fuel in a convenient format. Pellets require little site management in storage, unlike bales and chips, which require moisture management and between four and five times as much on-site storage and loading space (even for short term storage). The use of *Miscanthus* fuel in bale format is limited as it requires custom made facilities of at least 40 MW for heat, electricity

for seed plug establishment. If the harvested biomass is chipped and pelletized, then the emissions rise to 1.2 and 1.6 g CO_2 eq. C MJ^{-1}, respectively. The energy requirements for harvesting and chipping from this study that were used to estimate the GHG emissions are in line with the findings of Meehan et al. (2013). These estimates of GHG emissions for *Miscanthus* fuel confirm the findings of other Life Cycle Assessment (LCA) studies (e.g., Styles and Jones, 2008) and spatial estimates of GHG savings using *Miscanthus* fuel (Hastings et al., 2009). They also confirm that *Miscanthus* has a comparatively small GHG footprint due to its perennial nature, nutrient recycling efficiency and need for less chemical input and soil tillage over its 20-year life-cycle than

TABLE 9 | Net present value (NPV) and break-even year of a *Miscanthus* crop per hectare with 20-year crop life, 6% discount rate for different management options, using the costs determined from this study and using a farm gate sale price of £75.0 Mg^{-1} *Miscanthus* crop harvest (moisture < 14%).

Location	Yield establishment ramp				Establishment		Film	Harvesting		NPV	Breakeven
	Year 1	Year 2	Year 3	Year 4+	Rhizome	Seed-plug		Chipping	Baling	£	Year
Aberystwyth	0.3	5.3	12.4	12.4	×			×		£4,238	4
	0.3	5.3	12.4	12.4	×				×	£1,331	6
	0.3	5.3	12.4	12.4		×		×		£5,110	4
	0.3	5.3	12.4	12.4		×			×	£2,533	5
	0.6	9.5	12.4	12.4	×		×	×		£5,229	3
Potash	3.0	9.5	16.0	16.0	×		×	×		£6,469	3
	3.0	9.5	16.0	16.0	×		×		×	£3,096	4
	3.0	9.5	16.0	16.0		×	×	×		£7,515	3
	3.0	9.5	16.0	16.0		×	×		×	£4,142	3
Stuttgart	1.0	12.5	12.5	12.5	×		×	×		£4,148	3
	1.0	12.5	12.5	12.5	×		×		×	£1,716	5
	1.0	12.5	12.5	12.5		×	×	×		£5,464	3
	1.0	12.5	12.5	12.5		×	×		×	£2,763	4

generation or CHP, which are close to the biomass producing areas. Pellets on the other hand are versatile for automatic feeding of both domestic and commercial-scale burners and boilers because they can be remotely stored and blown by vacuum/airstream or augured. In addition these systems can be easily incorporated into existing site infrastructures. Pellets used for heating are currently subsidized in the United Kingdom by the Renewable Heat Initiative (Department of Energy and Climate Change [DECC], 2013). However, a new fuel and boiler standard is required for *Miscanthus* pellets to be used for domestic heat and concerns about air quality due to emissions from biomass boilers need to be addressed by clean burn, filtration and scrubbing technology.

Our programs have developed technology to propagate *Miscanthus* on a commercial-scale by seed sown plugs which enables ramp up rates of planting areas of around 2,000:1, meaning that a hectare of seed production can produce enough seed to plant ~2,000 ha. This is two orders of magnitude higher than with rhizomes where 1 ha or rhizome production can plant 10–30 ha. We have quantified the economic and practical benefits of using biodegradable mulch films which reduce the risk of crop establishment failure and accelerate the time to economically viable yields by about 1 year. The economic impact of different harvesting methods indicate that the costs vary from £28 to £40 per ton of biomass harvested in the United Kingdom and are similar to those estimated by Lin et al. (2016) in the United States. These harvesting costs are viable with the current farm gate price of £75 ton. However, as the harvesting of *Miscanthus* is in the spring, it can make use of harvesting equipment used for other crops in summer and autumn. There are certainly savings that can be made with the optimization of the utilization of personnel and equipment, especially on large arable farms with a cereal crop – *Miscanthus* mix. It is also worth noting that in this paper we have only considered costs of contract equipment, large farms and or groups of smaller farms cooperating on a regional basis can reduce costs through machinery ownership or sharing.

In this analysis of economic and GHG cost of *Miscanthus* crops, we have not included the cost of fertilization as it not used in current commercial planting. Most European long term trials of up to 10 years have shown little response to N fertilization except in light sandy soils (Clifton-Brown et al., 2008, 2015; Shield et al., 2014), however, Arundale et al. (2014b) showed that N applications on 5-year-old *Mxg* stands increased yields significantly. The application of N and K to replace nutrients exported at harvest is expected, but there is not enough evidence that these are limiting in the United Kingdom, possibly as a result of processes such as N fixation by endophytic bacteria (Farrar et al., 2014) or atmospheric deposition of transport/other pollution (Goulding et al., 1998). More research is required to determine the optimum rates and at that time the economic and GHG costs can be revised spatially at different scales using models and GIS.

Nodal propagation, where sections are cut from green canes and allowed to root, are not considered in this study. This is the standard method to propagate sugarcane and direct stem transplanting of activated stem buds of *Mxg* was successfully tested, although a question remains on the effect of transplanting

time and stem density optimization (Scordia et al., 2015), but it was not explicitly tested in this study. Costs for this method can be estimated from the literature from sugarcane (Xue et al., 2015). The GHG emissions for this method were not estimated.

The invasive potential of seed propagated *Miscanthus* hybrids is often raised as a potential issue. In the OPTIMISC trial fertile flowering hybrids were included. All sites were monitored and found little evidence of spread of *Miscanthus* by seed in the area surrounding areas (Kalinina et al., 2017) because volunteer seedlings rarely establish and successfully overwinter. Nonetheless, for the main biomass production regions of northern and continental Europe, we have concentrated recently on non-flowering hybrids for upscaling because these reach higher yields. While the breeding of sterile triploid seeded hybrids remains a long term goal for *Miscanthus* breeders which would completely eliminate any invasive risk in any environment, current low seed set rates need to be overcome by further research into breeding triploid hybrids.

The experience presented here has highlighted areas for continuing improvement including: further development of bespoke farm machinery for direct sowing, plug planting, harvesting *Miscanthus* and its associated agronomy. Critical foci for further research effort to make biomass systems an economic and environmentally sustainable alternative to fossil fuel energy systems include the breeding of faster-establishing high-yielding seed-propagated genotypes that are suitable for different environments. Preliminary results from on-going work in several projects are making further significant improvements through both breeding and novel agronomies. Optimizing machinery to work specifically with *Miscanthus,* optimizing weed control and crop management to reduce inputs will further reduce costs and GHG input. Economies of scale, with a larger cropped area, will create a competitive market for the machinery and products. In an ideal world, a significant proportion of the embedded fossil fuel GHG cost of this production would itself be replaced by renewable sources, further cutting GHG costs of energy crop production.

Finally it is important to note the influence of policy on the rate of acceptance of use of the crop, both from the demand side and from the supply side. The current level of support in the United Kingdom through the RHI and CfD is sufficient to justify a price of £75 per ton at the farm gate, which enables a farmer to make profit. A commensurate demand-side pull is required through a continuation of these or similar policy measures to ensure that the crops, once established, will have a market for their 15 to 20-year life. The United Kingdom government approval in 2016 for the Sustainable Fuel Register[6] to certify non-wood biomass fuels as suitable for the RHI is perhaps the most recent positive step in this direction.

CONCLUSION

- With mulch film agronomy the latest seeded hybrids establish far more quickly with significantly higher early yields (years 1

---

[6]http://www.sfregister.org/

and 2) compared to commercial *Mxg* in the United Kingdom delivering a breakeven return on investment at least a year earlier.

- *Miscanthus* crop establishment with seeded hybrids via plugs was found to be more GHG intensive than clonal rhizomes where fossil fuels are used to heat glasshouses but even then this cost is small compared to the gains in yield and scalability.
- High multiplication rates (~×2000) and lower establishment costs (~75% of rhizome costs) of seed based hybrids remove a significant barrier to producer and market uptake.
- Further optimization of crop establishment with seeds through plugs are ongoing, including breeding improved hybrids leading to higher yields which will improve profitability and reduce GHG emissions per hectare of production.
- As the growing renewable energy sector contributes more to total energy use, the embedded fossil fuel derived GHG costs in feedstock production and transport will be further reduced overall.

ETHICS STATEMENT

This statement applies to the study as the focus is reducing the GHG emissions and mitigation of climate change by reducing the GHG emissions of bioenergy feedstocks.

AUTHOR CONTRIBUTIONS

ACKNOWLEDGMENTS

REFERENCES

Arundale, R., Dohleman, F., Heaton, E., Voicht, T., and Long, S. (2014a). Yield of *Miscanthus x giganteus* and *Panicum virgatum* decline with stand and in Midwestern USA. *GCB Bioenergy* 6, 1–13. doi: 10.1111/gcbb.12077

Arundale, R., Dohleman, F., Voicht, T., and Long, S. (2014b). Nitrogen fertilization does significantly increase yields of stands of *Miscanthus x giganteus* and *Panicum virgatum* in multi-year trials in Illinois. *Bioenergy Res.* 7, 408–416. doi: 10.1007/s12155-013-9385-5

Awty-Carroll, D. (2017). *Understanding Germination for Improved Propagation and Field Establishment of the Bioenergy Crop Miscanthus*. Ph.D. thesis, Institute of Biological, Environmental and Rural Sciences, Aberystwyth University, Aberystwyth.

Clifton-Brown, J., Hastings, A., Mos, M., McCalmont, J. P., Ashman, C., Awty-Carroll, D., et al. (2016). Progress in upscaling Miscanthus biomass production for the European bio-economy with seed based hybrids. *GCB Bioenergy* 9, 6–17. doi: 10.1111/gcbb.12357

Clifton-Brown, J., Hastings, A., Smith, P., Valentine, J., Jones, M., and Donnison, I. (2008). Bioenergy technology: balancing energy outputs and environmental benefits. *Comp. Biochem. Physiol.* 150, 180–196. doi: 10.1016/j.cbpa.2008.04.464

Clifton-Brown, J., Schwartz, K.-U., and Hastings, A. (2015). History of the development of Miscanthus as a bioenergy crop: from small beginnings to potential realization. *Biol. Environ.* 11, 45–57.

Clifton-Brown, J. C., Breuer, J., and Jones, M. B. (2007). Carbon mitigation by the energy crop, Miscanthus. *Global Change Biol.* 13, 2296–2307. doi: 10.1111/j.1365-2486.2007.01438.x

Davis, S. C., Parton, W. J., Dohleman, F. G., Smith, C. M., Del Grosso, S., Kent, A. D., et al. (2010). Comparative biogeochemical cycles of bioenergy crops reveal nitrogen-fixation and low greenhouse gas emissions in a *Miscanthus x giganteus* agro-ecosystem. *Ecosystems* 13, 144–156. doi: 10.1007/s10021-009-9306-9

Department for Transport (2014). *Statistics at DFT - Department for Transport*. Available at: https://www.gov.uk/government/organisations/department-for-transport/about/statistics [accessed May 29, 2016].

Department of Energy and Climate Change [DECC] (2013). *Investing in Renewable Technologies – CfD Contract Terms and Prices*. Available at: https://www.gov.uk/government/uploads/system/uploads/attachment_data/file/263937/Final_Document_-_Investing_in_renewable_technologies_-_CfD_contract_terms_and_strike_prices_UPDATED_6_DEC.pdf [accessed November 18, 2016].

Digest of UK Energy Statistics, and Electricity Statistics [DUKES] (2016). *Chapter 5 – Electricity*. Newport: UK National Statistics. [accessed September 9, 2016].

Dondini, M., Hastings, A., Saiz, G., Jones, M., and Smith, P. (2009). The potential of Miscanthus to sequester carbon in soils; comparing field measurements in Carlow, Ireland to model predictions. *GCB Bioenergy* 1, 413–425. doi: 10.1111/j.1757-1707.2010.01033.x

Dondini, M., Richard, M., Pogson, M., McCalmont, J., Drewer, J., Marshall, R., et al. (2016). Simulation of greenhouse gasses following land-use chage to bioenergy crops using the ECOSSE model: a comparison between site measurements and model predictions. *GCB Bioenergy* 8, 925–940. doi: 10.1111/gcbb.12298

Farmers weekly (2016). Available at: http://www.fwi.co.uk/arable/drax-ends-miscanthus-contracts-and-reviews-straw-supply.htm [accessed November 2016].

Farrar, K., Bryant, D., and Cope-Selby, N. (2014). Understanding and engineering beneficial plant-microbe interactions: plant growth promotion in energy crops. *Plant Biotechnol. J.* 12, 1193–1206. doi: 10.1111/pbi.12279

Gelfand, I., Sahajpal, R., Zhang, X., Izaurralde, C., Gross, K., and Robertson, G. (2013). Sustainable bioenergy production from marginal lands in the US Midwest. *Nature* 493, 514–517. doi: 10.1038/nature11811

Goulding, K. W. T., Bailey, N. J., Bradbury, N. J., Hargreaves, P., Howe, M., Murphy, D. V., et al. (1998). Nitrogen deposition and its contribution to nitrogen cycling and associated soil processes. *New Phytol.* 139, 49–58. doi: 10.1046/j.1469-8137.1998.00182.x

Harris, L., Jones, P. D., Osbourne, T. J., and Lister, D. H. (2014). Updated high-resolution grids of monthly climatic observations – the CRU TS 3.10 Dataset. *Int. J. Climatol.* 34, 623–642.

Hastings, A., Clifton-Brown, J., Wattenbach, M., Mitchell, C. P., and Smith, P. (2009). The development of MISCANFOR, a new *Miscanthus* crop growth model: towards more robust yield predictions under different climatic and soil conditions. *Global Change Biol. Bioenergy* 1, 154–170. doi: 10.1111/j.1757-1707.2009.01007.x

Hastings, A., Clifton-Brown, J., Wattenbach, M., Mitchell, C. P., Stampfl, P., and Smith, P. (2009). Future energy potential of Miscanthus in Europe. *Global Change Biol. Bioenergy.* 1, 180–196. doi: 10.1111/j.1757-1707.2009.01012.x

Hastings, A., Tallis, M., Casella, E., Matthews, R., Milner, S., Smith, P., et al. (2013). The technical potential of Great Britain to produce lingo-cellulosic biomass for bioenergy in current and future climates. *Global Change Biol. Bioenergy* 6, 108–122. doi: 10.1111/gcbb.12103

Hastings, A., Yeluripati, J., Hillier, J., and Smith, P. (2012). "Chapter 12 – Biofuel crops and greenhouse gasses," in *Biofuel Crop Production*, ed. B. P. Singh (Hoboken, NJ: Wiley Blackwell).

Heaton, E., Clifton-Brown, J., Voight, T., Jones, M., and Long, S. (2004). Miscanthus for renewable energy generation: European Union experience and projection for Illinois. *Mitig. Adapt. Strat. Global Change* 9, 433–451. doi: 10.1023/B:MITI.0000038848.94134.be

Heaton, E., Dohleman, F., and Long, S. (2008). Meeting US biofuel goals with less land: the potential of Miscanthus. *Global Change Biol.* 14, 2000–2014. doi: 10.1111/j.1365-2486.2008.01662.x

Intergovernmental Panel on Climate Change [IPCC] (2014a). *Climate Change 2014: Synthesis Report. Contribution of Working Groups I, II and III to the Fifth Assessment Report of the Intergovernmental Panel on Climate Change.* Geneva: IPCC.

Intergovernmental Panel on Climate Change [IPCC] (2014b). "Summary for policymakers," in *Climate Change 2014: Impacts, Adaptation, and Vulnerability. Part A: Global and Sectoral Aspects. Contribution of Working Group II to the Fifth Assessment Reportof the Intergovernmental Panel on Climate Change*, eds C. B. Field, V. R. Barros, D. J. Dokken, K. J. Mach, M. D. Mastrandrea, T. E. Bilir, et al. (Cambridge: Cambridge University Press), 1–32.

Iqbal, Y., Kiesel, A., Wagner, M., Nunn, C., Kalinina, C., Hastings, A., et al. (2017). Harvest time optimization for combustion quality of different Miscanthus genotype across Europe. *Front. Plant Sci.* 8:727. doi: 10.3389/fpls.2017.00727

Kalinina, O., Nunn, C., van der Weijde, T., Ozguven, M., Tarakanov, I., and Schüle, H. (2017). Extending Miscanthus cultivation with novel germplasm at six contrasting sites. *Front. Plant Sci.* 8:563. doi: 10.3389/fpls.2017.00563

Lesur, C., Jeuffroy, M. H., Makowski, D., Riche, A. B., Shield, I., Yates, M., et al. (2013). Modelling long-term yield trends of *Miscanthus x giganteus* using experimental data across Europe. *Field Crop Res.* 149, 252–260. doi: 10.1016/j.fcr.2013.05.004

Lewandowski, I., Clifton-Brown, J., Trindade, L. M., van der Linden, G. C., Schwarz, K. U., Müller-Sämann, K., et al. (2016). Progress on optimizing miscanthus biomass production for the European bioeconomy: results of the FP7 project OPTIMISC. *Front. Plant Sci.* 7:1620. doi: 10.3389/fpls.2016.01620

Lewandowski, I., and Kahnt, G. (1993). Development of a tissue culture system with unemerged inflorescences of Miscanthus 'Giganteus' for the Induction and Regeneration of Somatic Embryoids. *Beitr. Biol. Pflanzen* 67, 439–451.

Lin, T., Mathanker, S., Rodriguez, L., Hansen, A., and Ting, K. (2016). Impact of harvesting operations on miscanthus provision costs. *Trans. ASABE* 59, 1031–1039. doi: 10.13031/trans.59.11178

McCalmont, J. P., Hastings, A., Robson, P., Donnison, I., Richter, G., McNamara, N., et al. (2015a). The environmental credentials of Miscanthus as a bio-energy crop in the UK. *GCB Bioenergy* 9, 489–507. doi: 10.1111/gcbb.12294

McCalmont, J. P., McNamara, N. P., Donnison, I. S., Farrar, K., and Clifton-Brown, J. C. (2015b). An inter-year comparison of CO2 flux and carbon budget at a commercial scale land-use transition from semi-improved grassland to *Miscanthus x giganteus. GCB Bioenergy* 9, 229–245. doi: 10.1111/gcbb.12323

Meehan, P., Finnan, J., and McDonnell, K. (2013). A comparison of the energy yield at the end use for *M.x.giganteus* using two different harvesting systems. *Bioenergy Res.* 6, 813–821. doi: 10.1007/s12155-013-9307-6

Milner, S., Lovett, A., Holland, R., Sunnenberg, G., Hastings, A., Smith, P., et al. (2015). A preliminary assessment of the ecosystem service impacts of bioenergy in GB to 2050. *Global Change Biol. Bioenergy.* 8, 317–333. doi: 10.1007/s12155-013-9307-6

Nunn, C., Kalinina, O., Hastings, A., Khokhlov, N., Mc Calmont, J. P., Meyer, H., et al. (in press). Growing season end time and ripening in diverse Miscanthus germplasm grown in Aberystwyth, Adana, Moscow, Kiev, Stuttgart and Wageningen. *Front. Plant Sci.*

Ofgem. (2016). *Wholesale Energy Market in (2016).* Available at: https://www.ofgem.gov.uk/system/files/docs/2016/08/wholesale_energy_markets_in_2016.pdf [accessed November 18, 2016].

O'Loughlin, J., Finnan, J., and McDonnel, K. (2017). Accelerating early growth in Miscanthus with the application of plastic mulch film. *Biomass Bioenergy* 100, 52–61. doi: 10.1016/j.biombioe.2017.03.003

Pogson, M., Richards, M., Dondini, M., Jones, E. O., Hastings, A., and Smith, P. (2016). ELUM: a spatial modelling tool to predict soil greenhouse gas changes from land conversion to bioenergy in the UK. *Environ. Model. Softw.* 84, 458–466. doi: 10.1016/j.envsoft.2016.07.011

Richards, M., Pogson, M., Dondini, M., Jones, E. O., Hastings, A., Henner, D. N., et al. (2016). High-resolution spatial modelling of greenhouse gas emissions from land-use change to energy crops in the United Kingdom. *GCB Bioenergy* 9, 627–644. doi: 10.1111/gcbb.12360

Scordia, D., Zanetti, F., Varga, S. S., Alexopoulou, E., Cavallaro, V., Copani, V., et al. (2015). New insights into the propagation methods of switchgrass, miscanthus and giant reed. *Bioenergy Res.* 8, 1480–1491. doi: 10.1007/s12155-015-9682-2

Searchinger, T., Heimlich, R., Houghton, R. A., Dong, F., Elobeid, A., Fabiosa, J., et al. (2008). Use of U.S. Croplands for Biofuels Increases Greenhouse Gases Through Emissions from Land Use Change. *Science* 319, 1238–1240. doi: 10.1126/science.1151861

Shield, I. F., Barradough, T. J. P., Riche, A. B., and Yates, N. E. (2014). The yield and quality response of the energy grass *Miscanthus x giganteus* to fertiliser applications of nitrogen, potassium and sulphur. *Biomass Bioenergy* 68, 185–194. doi: 10.1016/j.biombioe.2014.06.007

Sims, R., Hastings, A., Schlamadinger, B., Taylor, G., and Smith, P. (2006). Energy Crops: current status and future prospects. *Global Change Biol.* 12, 2054–2076. doi: 10.1111/j.1365-2486.2006.01163.x

St. Clair, S., Hillier, J., and Smith, P. (2008). Calculating the pre-harvest greenhouse gas costs of Energy Crops. *Biomass Bioenergy* 32, 442–452. doi: 10.1016/j.biombioe.2007.11.001

Styles, D., and Jones, M. B. (2008). Miscanthus and willow heat production - an effective land-use strategy for GHG emission avoidance in Ireland. *Energy Policy* 36, 97–107. doi: 10.1016/j.enpol.2007.08.030

Valentine, J., Clifton-Brown, J., Hastings, A., Robson, P., Allison, G., and Smith, P. (2011). Food vs. fuel: the use of land for lignocellulosic 'next generation' energy crops that minimise competition with primary food production. *Global Change Biol. Bioenergy* 4, 1–19. doi: 10.1111/j.1757-1707.2011.01111.x

World Bank (2015). Available at: http://documents.worldbank.org/curated/en/961661467990086330/pdf/WPS7220.pdf [accessed November 2016].

Xue, S., Kalinina, O., and Lewandowski, I. (2015). Present and future options for Miscanthus propagation and establishment. *Renew. Sustain. Energy Rev.* 49, 1233–1246. doi: 10.1016/j.rser.2015.04.168

Zimmerman, J., Styles, D., Hastings, A., Dauber, J., and Jones, M. B. (2013). Assessing the impact of within crop heterogeneity ("patchiness") in young *Miscanthus x giganteus* fields on economic feasibility and soil carbon sequestration. *Global Change Biol. Bioenergy* 6, 566–576. doi: 10.1111/gcbb.12084

Novel Miscanthus Germplasm-Based Value Chains: A Life Cycle Assessment

Moritz Wagner[1]*, Andreas Kiesel[1], Astley Hastings[2], Yasir Iqbal[1] and Iris Lewandowski[1]

[1] Department Biobased Products and Energy Crops, Institute of Crop Science, University of Hohenheim, Stuttgart, Germany,
[2] The School of Biological Sciences, University of Aberdeen, Aberdeen, United Kingdom

In recent years, considerable progress has been made in miscanthus research: improvement of management practices, breeding of new genotypes, especially for marginal conditions, and development of novel utilization options. The purpose of the current study was a holistic analysis of the environmental performance of such novel miscanthus-based value chains. In addition, the relevance of the analyzed environmental impact categories was assessed. A Life Cycle Assessment was conducted to analyse the environmental performance of the miscanthus-based value chains in 18 impact categories. In order to include the substitution of a reference product, a system expansion approach was used. In addition, a normalization step was applied. This allowed the relevance of these impact categories to be evaluated for each utilization pathway. The miscanthus was cultivated on six sites in Europe (Aberystwyth, Adana, Moscow, Potash, Stuttgart and Wageningen) and the biomass was utilized in the following six pathways: (1) small-scale combustion (heat)—chips; (2) small-scale combustion (heat)—pellets; (3) large-scale combustion (CHP)—biomass baled for transport and storage; (4) large-scale combustion (CHP)—pellets; (5) medium-scale biogas plant—ensiled miscanthus biomass; and (6) large-scale production of insulation material. Thus, in total, the environmental performance of 36 site × pathway combinations was assessed. The comparatively high normalized results of human toxicity, marine, and freshwater ecotoxicity, and freshwater eutrophication indicate the relevance of these impact categories in the assessment of miscanthus-based value chains. Differences between the six sites can almost entirely be attributed to variations in biomass yield. However, the environmental performance of the utilization pathways analyzed varied widely. The largest differences were shown for freshwater and marine ecotoxicity, and freshwater eutrophication. The production of insulation material had the lowest impact on the environment, with net benefits in all impact categories expect three (marine eutrophication, human toxicity, agricultural land occupation). This performance can be explained by the multiple use of the biomass, first as material and subsequently as an energy carrier, and by the substitution of an emission-intensive reference product. The results of this study emphasize the importance of assessing all environmental impacts when selecting appropriate utilization pathways.

Keywords: miscanthus, biobased value chains, LCA, environmental performance, normalization, impact categories

INTRODUCTION

The developing European bioeconomy will lead to an increasing demand for sustainably produced biomass in the near future. Miscanthus is one of the leading candidate biomass crops and has the advantage that it can also grow under marginal site conditions (Lewandowski et al., 2016). It is a perennial rhizomatous C4 grass originating from Southeast Asia, where it shows large genetic diversity. Miscanthus was introduced into Europe in 1935, where the genotype *Miscanthus × giganteus* is predominately cultivated (Clifton-Brown et al., 2015). It is a resource-efficient, low-input crop, which can achieve yields of well above 20 Mg ha^{-1} a^{-1} (dry matter) in Central Europe (Lewandowski and Schmidt, 2006; Iqbal et al., 2015) and more than 30 Mg ha^{-1} a^{-1} (dry matter) in southern Europe under irrigated conditions (Lewandowski et al., 2000). As a perennial crop, miscanthus can be harvested over a 15–20-year cultivation period (Lewandowski et al., 2000; Christian et al., 2008). Due to its perennial nature and its high nitrogen- and water-use efficiency, miscanthus has a comparatively low impact on the environment as a biomass crop (Lewandowski et al., 2000; Voigt, 2015; McCalmont et al., 2017).

Miscanthus biomass can be used in several different utilization pathways. When harvested green in the period September to October, it can be used as a biogas substrate (Whittaker et al., 2016; Kiesel and Lewandowski, 2017). When harvested in early spring, it is suitable for combustion (Dahl and Obernberger, 2004; Iqbal and Lewandowski, 2014), as a late harvest leads to a lower water and mineral content (Lewandowski et al., 2000). In addition, miscanthus biomass can be fermented to ethanol (van der Weijde et al., 2016) or used as a raw material for the production of insulation material (Uihlein et al., 2008) or bio-composites (Muthuraj et al., 2015).

However, despite these diverse potential applications, there is currently low implementation of miscanthus cultivation as several major barriers hinder its utilization in practice (Clifton-Brown et al., 2016). To overcome these barriers, considerable efforts have been made in the last years in (a) development of new genotypes, tailored to different, especially marginal, site conditions in Europe, and different biomass uses; (b) the optimization of miscanthus management (Clifton-Brown et al., 2016; Lewandowski et al., 2016).

The objective of this study is to assess the environmental performance of various miscanthus-based energetic and material value chains using the most up-to-date genotype as well as management options. Most previous studies used cultivation and yield data from the standard genotype *Miscanthus × giganteus* to analyse environmental performance. However, as explained above, in the last years there have been substantial efforts especially in the breeding of new genotypes. The inclusion of this progress in the current study will allow a more realistic assessment of the environmental impact and mitigation possibilities of miscanthus-based value chains.

Several studies have already evaluated the environmental performance of miscanthus-based value chains in different impact categories. These studies encompass the utilization of miscanthus as a biogas substrate (Kiesel et al., 2016), for electricity generation (Sanscartier et al., 2014), as feedstock for

bioethanol (Jeswani et al., 2015), and as fuel for heat generation (Wagner and Lewandowski, 2017). However, most of these studies examine only one single utilization pathway or assess only a few impact categories (Meyer et al., 2016).

The various assumptions, system boundaries and methodologies used in these studies makes a comparison of the results very difficult. Therefore, the second objective of the current study is to assess the environmental sustainability of different miscanthus utilization pathways in several impact categories under the same assumptions and underlying conditions. This is done in order to enable the comparison of the environmental performance of different miscanthus-based value chains.

For this purpose, an attributional Life Cycle Assessment (LCA) was conducted according to the ISO standards 14040 and 14044 (ISO, 2006a,b). The energetic and material utilization pathways assessed in this study are: (1) small-scale combustion (heat)—chips; (2) small-scale combustion (heat)—pellets; (3) large-scale combustion (CHP)—biomass baled for transport and storage; (4) large-scale combustion (CHP)—pellets; (5) medium-scale biogas plant—biomass ensiled; and (6) large-scale production of insulation material—biomass baled for transport and storage. These pathways were assessed for miscanthus biomass cultivated from different genotypes on six climatically different sites across Europe: Aberystwyth (UK), Adana (Turkey), Moscow (Russia), Potash (Ukraine), Stuttgart (Germany), and Wageningen (Netherlands). Data for the cultivation of the biomass were provided through the EU-funded research project OPTIMISC (Optimizing Miscanthus Biomass Production) (Lewandowski et al., 2016). The environmental performance of each of the six utilization pathways was assessed for each site in 18 impact categories using the life-cycle impact assessment methodology ReCiPe (Goedkoop et al., 2008). To assess the mitigation potential of the analyzed pathways in the different impact categories, a system expansion approach was chosen. This approach enabled the assessment of the net benefits and impacts of the different pathways on the environment through the substitution of a chiefly fossil-based reference product with a miscanthus-based one.

In addition, a normalization step was applied. This allows the relevance of the analyzed impact categories for each utilization pathway to be assessed (Wagner and Lewandowski, 2017). The normalization factors used in this study were taken from the ReCiPe methodology (Goedkoop et al., 2008).

MATERIALS AND METHODS

Scope and Boundaries

The scope of this study is a cradle-to-grave analysis of the environmental performance of miscanthus cultivation at six sites in Europe and the subsequent utilization in six pathways. In total, 36 site × pathway combinations were assessed. In order to include the substitution of a reference product, a system expansion approach was applied. This allows the impact of the substitution of a reference product (e.g., heat produced by the combustion of natural gas) through the utilization of 1 ha

miscanthus (e.g., heat produced by the combustion of miscanthus chips) to be included in the assessment for each value chain. Thus, negative values represent burdens avoided by such a substitution, while positive values represent an additional impact through the use of miscanthus biomass. This is the case when the production and utilization of the reference products emits less than the substituting miscanthus-based product.

The functional unit (FU) as well as main and co-products for the six utilization pathways are shown in **Table 1**. In addition, for each product, the substituted reference product is indicated. One hectare was chosen as functional unit to assess the annual net benefit or impact of substituting a reference product by the energetic or material utilization of miscanthus. On the cultivation sites Aberystwyth (UK), Moscow (Russia), Potash (Ukraine), Stuttgart (Germany), and Wageningen (Netherlands), the genotype OPM-06 was used, a *M. sinensis* × *M. sacchariflorus* hybrid. On the Adana site in Turkey, the genotype *M* × *giganteus* (OPM-09) was used. These two were preselected from 15 assessed genotypes, because they were the most suitable for the location and utilization pathway in terms of biomass quality and yield. The data on the cultivation process and choice of genotypes are based on multi-location field trials described in Lewandowski et al. (2016). The sites in Adana, Potash, Stuttgart and Wageningen are mostly on land previously used as agricultural land, whereas the sites in Aberystwyth and Moscow are on marginal land. In Aberystwyth, the miscanthus was cultivated on land which was previously low-quality grassland. At the Moscow site, harsh winters lead to non-ideal growing conditions (Lewandowski et al., 2016).

The agricultural system is described in **Figure 1**. The system boundaries include the production of input substrates (e.g., fertilizers, propagation material) and the whole cultivation process (from soil preparation through planting and establishment to harvest over a twenty-year cultivation period) to subsequent recultivation. For all utilization pathways, the miscanthus is mulched in the first year and harvested from the second year onwards. In pathways 2, 3, 4, and 6, it is mowed and then pressed into bales; in 1 and 5 it is harvested with a

self-propelled forage harvester in the form of chips. For the combustion pathways 2 and 4, the miscanthus bales are then further processed to pellets.

The utilization pathways 1 to 5 are shown in **Figure 2**. In all four combustion pathways (1, 2, 3, and 4), the handling of the ash is the same. It is assumed that both the fly and bottom ash is disposed of in landfill. The fly ash in particular has high levels of heavy metals. In utilization pathway 1, the miscanthus biomass is used on-farm in a small combustion unit to generate heat. In utilization pathway 2, miscanthus biomass in the form of pellets instead of chips is utilized in a small combustion unit to generate heat. The reference product of the utilization pathways 1 and 2 is heat produced by combustion of light fuel oil. This reference product was chosen, because it is produced in a comparable small-scale combustion unit. A sensitivity analysis was performed with heat produced by combustion of natural gas as a reference product to analyse the impact of this assumption.
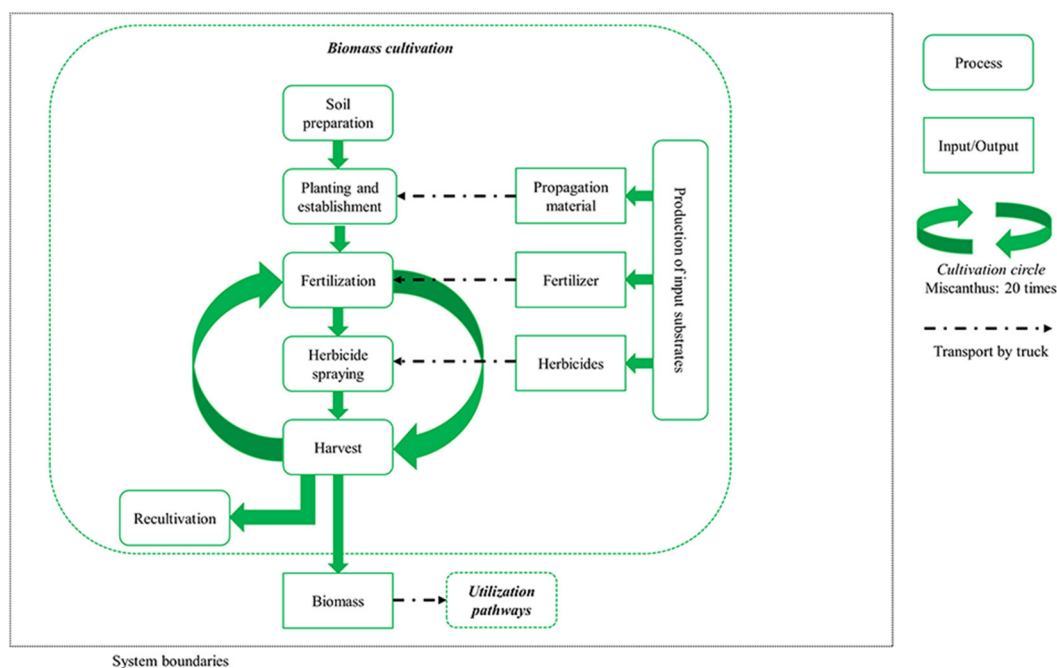
In utilization pathway 3, miscanthus bales are combusted in a combined heat and power unit (CHP) to generate heat, with electricity as a co-product. In pathway 4, miscanthus pellets are utilized in the CHP instead of bales. Heat was specified as the main and electricity as the co-product in accordance with the description in the ecoinvent database (Weidema et al., 2013). The electricity produced is assumed to substitute the European electricity mix. The heat generated substitutes heat produced by the combustion of natural gas in a CHP. Natural gas was chosen in this case as a reference product, because it is a relative clean energy source (May and Brennan, 2006). This assumption reduces the risk of overestimating the net environmental benefit of the miscanthus-based alternative.

Utilization pathway 5 includes the fermentation of green-harvested miscanthus biomass to biogas and subsequent combustion to generate electricity, with heat as a co-product. Electricity was selected as main product in accordance with Bacenetti et al. (2016) and the European electricity mix was chosen as reference product. The heat generated as co-product substitutes heat produced by the combustion of natural gas in a CHP. The residues of the fermentation process are rich in

TABLE 1 | Utilization pathways assessed in this study, the functional unit, their outputs and the reference products.

No.	Utilization pathway	Biomass used	FU	Output	Main product	Co-product	Reference product
1	Small-scale combustion	Chips	1 ha	Heat	*		Heat produced by combustion of light fuel oil
2	Small-scale combustion	Pellets	1 ha	Heat	*		Heat produced by combustion of light fuel oil
3	Large-scale combustion (CHP)	Bales	1 ha	Heat	*		Heat produced by combustion of natural gas in a CHP
				Electricity		*	European electricity mix
4	Large-scale combustion (CHP)	Pellets	1 ha	Heat	*		Heat produced by combustion of natural gas in a CHP
				Electricity		*	European electricity mix
5	Biogas plant	Silage	1 ha	Electricity	*		European electricity mix
				Heat		*	Heat produced by combustion of natural gas in a CHP
6	Production of insulation material	Bales	1 ha	Insulation material	*		Glass wool

Indicates if the product is the main- or the co-product.

FIGURE 1 | System description and boundaries for miscanthus biomass cultivation.
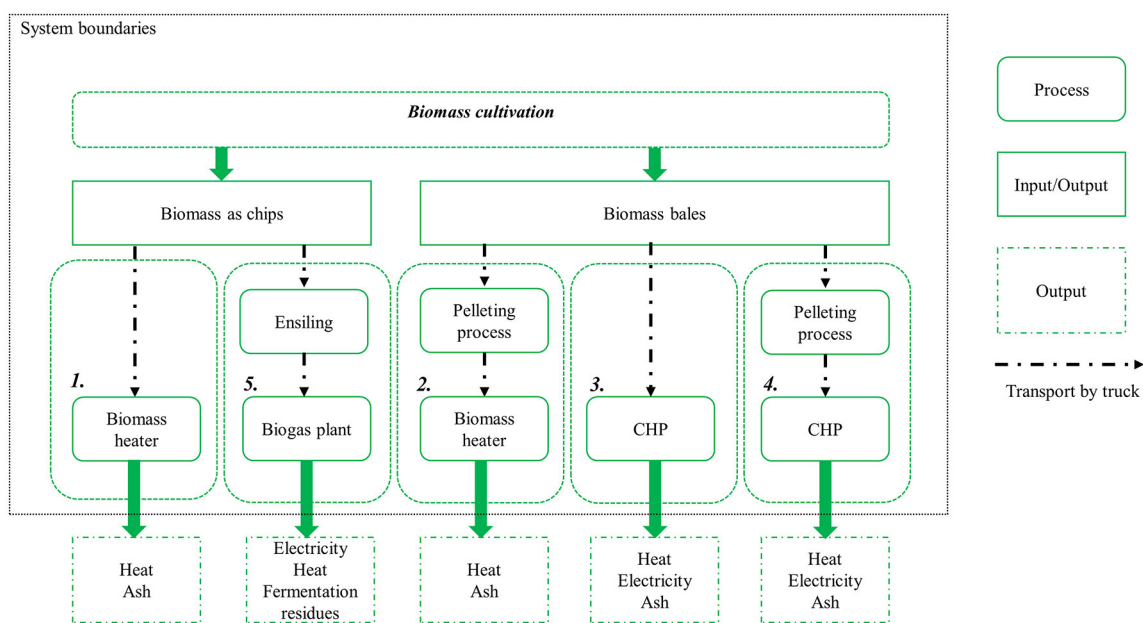
FIGURE 2 | System description and boundaries for the energetic utilization pathways 1–5.

nutrients (see Table S1) and can be used to substitute mineral fertilizer.

Utilization pathway 6, which is displayed in **Figure 3**, is the production of insulation material from miscanthus biomass. The miscanthus fibers are separated via steam explosion,

dried, and mixed with additives. Insulation material is then produced through hot pressing. The reference product for 1 m³ miscanthus-based insulation material is 110 kg glass wool mats with comparable characteristics (Meyer et al., 2016). The End-of-Life of the miscanthus- and the fossil-based pathways are

FIGURE 3 | System description and boundaries for the material utilization pathway 6.
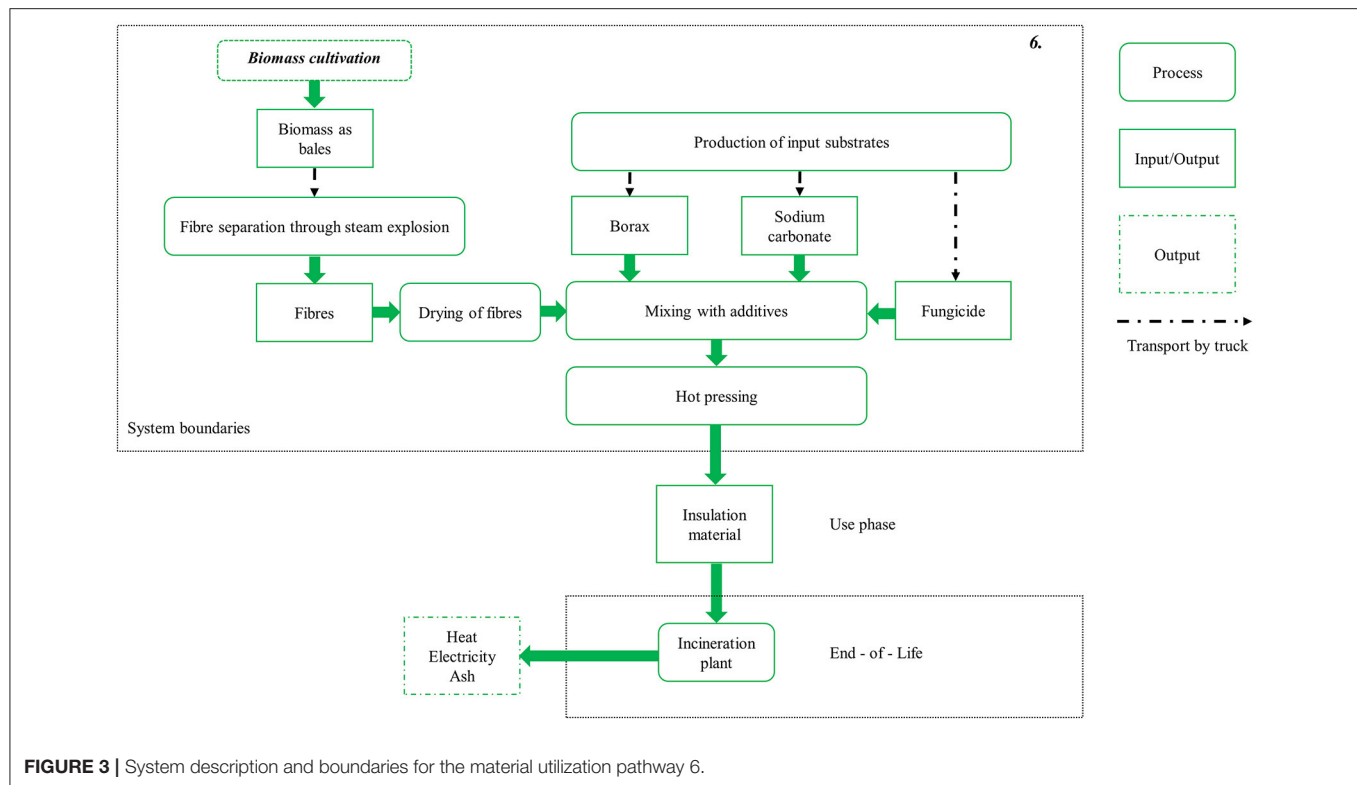
included in the assessment. The glass wool is treated as inert waste and disposed of to landfill. After its use phase, it is assumed that the miscanthus-based insulation material is incinerated, generating heat and electricity (see **Figure 3**). The electrical and thermal efficiencies of the incineration plant are comparable to the CHP plant used in the utilization pathways 3 and 4.

Life Cycle Inventory
Agricultural System

The data used in this Life Cycle Assessment for the cultivation phase of miscanthus were obtained from multi-location field trials conducted within the OPTIMISC project (Lewandowski et al., 2016). **Table 2** shows the main inputs and outputs at the different sites for the pathways using biomass harvested in spring (combustion, production of insulation material), or autumn (biogas substrate). Field data for pathway 5 was only available for the Adana, Moscow and Stuttgart sites (see **Table 2**).

In addition to the inputs shown in **Table 2**, the field trials in Adana were irrigated with 976.75 m³ water per hectare and year, independent of harvest date.

Nitrogen was applied as calcium ammonium nitrate, potassium as potassium sulfate and phosphate as triple superphosphate. Herbicides are only necessary in miscanthus cultivation in the preparation of the sites, in the first two cultivation years, when miscanthus is unable to compete with weeds, and in the recultivation process. Over the twenty-year cultivation period, a total application of 16.2 l herbicides ha^{-1} were applied: 10 l ha^{-1} Round up (Monsanto, active ingredient 360 g l^{-1} glyphosate); 3.5 l ha^{-1} Stomp Aqua (BASF,

active ingredient 455 g l^{-1} pendimethalin); 1.5 l ha^{-1} Calisto (Syngenta, active ingredient 100 g l^{-1} mesotrione); 0.2 l ha^{-1} Arrat (BASF, active ingredient 100 g l^{-1} tritosulfuron and 500 g l^{-1} dicamba); and 1 l ha^{-1} Dash, (BASF, an emulsifiable concentrate). This corresponds to an average of 0.81 l or 0.93 kg ha^{-1} yr^{-1} herbicides.

The yield data in **Table 2** is shown per year. However, these yield data are based on the whole cultivation period including the establishment phase. In the first year, the biomass is not harvested but mulched, and the full yield is only achieved from the third year onwards (Lewandowski et al., 2003). The calculation for the early spring harvest is given in Equation 1 and for the autumn harvest in Equation 2.

$$Mean\ yield\ spring\ \left[t\ DM\ ha^{-1}yr^{-1}\right]$$
$$= \frac{yield\ (2.\ year\_spring\ +\ 3.year\_spring*18)}{20} \quad (1)$$
$$Mean\ yield\ autumn\ \left[t\ DM\ ha^{-1}yr^{-1}\right]$$
$$= \frac{yield\ (2.\ year\_autumn\ +\ 3.year\_autumn*18)}{20} \quad (2)$$

Table 3 shows the agricultural operations applied during miscanthus cultivation including frequency. These are shown for two harvest procedures: in the chopping line, the biomass is processed to chips to be used in the utilization pathways 1 and 5; and in the baling line, it is baled (utilization pathways 2, 3, 4, and 6).

The background data for the environmental impacts associated with the cultivation processes (e.g., plowing, mowing)

TABLE 2 | Summary of the main inputs and outputs of the spring and the autumn harvests.

Values in kg yr^{-1} ha^{-1}	Adana	Aberystwyth	Moscow	Potash	Stuttgart	Wageningen
			Harvest Feb./Mar.			
N	60	60	60	60	60	60
K$_2$O	120	120	120	120	120	120
P$_2$O$_5$	30	30	30	30	30	30
Herbicides	0.93	0.93	0.93	0.93	0.93	0.93
Dry matter yield	12,600	9,745	9,734	16,065	15,316	10,320
			Harvest Sept./Oct.			
N	140	n.a.	140	n.a.	140	n.a.
K$_2$O	200	n.a.	200	n.a.	200	n.a.
P$_2$O$_5$	30	n.a.	30	n.a.	30	n.a.
Herbicides	0.93	n.a.	0.93	n.a.	0.93	n.a.
Dry matter yield	19,365	n.a.	15,568	n.a.	23,624	n.a.

TABLE 3 | Agricultural operations applied during 20 years of miscanthus cultivation with frequency.

Agricultural operations	Frequency per cultivation period	
	Chopping line	**Baling line**
Rotary harrow	2	2
Plowing	1	1
Planting	1	1
Mulching—first year	1	1
Spraying	5	5
Fertilizing	19	19
Mowing	0	18
Swath	0	18
Chipping	18	0
Baling	0	18
Mulching—final year	1	1
Chisel plow	1	1

and the production of the input substrates were taken from the ecoinvent database version 3.3 (cut-off system model) (Weidema et al., 2013). The energy demands of the harvesting processes (chopping and baling) and the pelleting process are based on Hastings et al. (under review).

N$_2$O emissions from harvest residues and indirect N$_2$O emissions from nitrogen fertilizer were estimated using emission factors based on IPCC (2006). Direct N$_2$O and NO emissions from nitrogen fertilizer were calculated according to Bouwman et al. (2002). Ammonia emissions were calculated using emission factors from EMEP/CORINAIR (2001). Phosphate and phosphorus emissions to surface and groundwater, and heavy metal emissions to agricultural soil were estimated based on Nemecek and Kägi (2007). Nitrate leaching to groundwater was calculated according to the SQCB—NO$_3$ model described in Faist Emmenegger et al. (2009). All pesticide applied have been modeled completely as emission to agricultural soil in accordance to Nemecek and Schnetzer (2011). The ecotoxicity values of this emission are based on the ecoinvent database (Weidema et al., 2013).

Several recent publication have demonstrated the ability of miscanthus to sequester CO$_2$ in the soil through an increase in soil organic carbon, especially in comparison to annual plants (Gauder et al., 2016; McCalmont et al., 2017). However, these changes in soil organic carbon are highly dependent on the previous crop and thus contain a high degree of uncertainty (Harris et al., 2015). Because of this, carbon sequestration in the soil was not included this assessment.

Table 4 gives the farm-to-field distances and truck transport distances for the different utilization pathways. No data were available for the transport distances of input substrates (e.g., fertilizer) or propagation material. Therefore, a transport distance of 150 km for the input material by a EUR5 truck was assumed. The background data associated with the transportation of the input material and biomass were taken from the ecoinvent database (Weidema et al., 2013).

There are considerable differences in transport density between chips, bales and pellets. To account for these differences, the emission data from the ecoinvent database used for the transport process (Weidema et al., 2013) was adapted in accordance with Hastings et al. (under review).

Utilization Pathways

The following section describes the life cycle inventories for the different utilization pathways. The modeling of the pathways included the emissions associated with the construction of the conversion plants (e.g., CHP unit, biogas plant) and necessary infrastructure, based on background data from the ecoinvent database (Weidema et al., 2013).

The biomass heater used for utilization pathways 1 and 2 is a furnace with a heat generation capacity of 300 kW. The background data for the emissions associated with combustion is taken from the ecoinvent database. This data is based on a Froling Turbomat 320 kW woodchip boiler with a thermal efficiency of 75%. This is lower than in the technical specification, because it represents the average annual operation, which includes start and stop phases (Weidema et al., 2013).

The background emission data for utilization pathways 3 and 4 [combined heat and power unit (CHP)] are based on

Process	Unit	Utilization pathways					
		(1)	(2)	(3)	(4)	(5)	(6)
Truck transport of input substrates	km	150	150	150	150	150	150
Farm-field distance	km	2	2	2	2	15	2
Truck transport of bales	km	–	100	400	100	–	400
Truck transport of pellets	km	–	400	–	400	–	–

Technical characteristics		Unit
Full load hours	7,800	H
Plant output electrical	500	kWh_{el}
Plant output total	1,351	kWh
Electrical efficiency	37	% of plant total output
Thermal efficiency	53	% of plant total output
Inherent heat demand	20	% of total heat production
Inherent power consumption	12	% of total power production

the ecoinvent process *"heat and power co-generation, wood chips, 6,667 kW, state-of-the-art 2014."* According to the process description in the ecoinvent database, an organic rankine cycle (ORC) steam generator with an electrical efficiency of 15% and a thermal efficiency of 45% is used (Weidema et al., 2013).

As there is insufficient specific information available on emissions from miscanthus combustion, all four utilization pathways are based on wood combustion processes. Miscanthus-specific emission factors for carbon monoxide, sulfur dioxide, hydrogen chloride, nitrogen oxides, and particulates were taken from Dahl and Obernberger (2004). At the time of harvest, miscanthus biomass has a water content of around 15% (Lewandowski et al., 2016). A further drying process is therefore not necessary. A mean calorific value of 4.3 kWh kg^{-1} fresh biomass was calculated based on the model of Jiménez and González (1991).

The miscanthus biomass used in the biogas plant is harvested in autumn and then ensiled. Dry matter losses of 12% were assumed during the ensilage process. The silage is subsequently fermented to biogas. The methane hectare yield [m^3 CH$_4$ yr^{-1} ha^{-1}] for the Adana site was 4,676, for the Moscow site 4,194, and for the Stuttgart site 6,495 (Kiesel et al., 2017). The methane yield was measured as described in Kiesel and Lewandowski (2017). A biogas batch test was performed for 35 days in mesophilic conditions (39°C) according to VDI guideline 4,630. The approach of the biogas batch test was certified by the KTBL and VDLUFA interlaboratory comparison test 2014 and 2015. Each sample was assessed in four technical replicates. Methane losses of 1% were assumed in the biogas plant based on Börjesson and Berglund (2007). The biogas is combusted in a CHP unit to generate heat and power. The electricity is fed into the grid. Twenty percent of the heat produced is used internally for the heating of the fermenter. In this study, it was assumed that 50% of the remaining heat (that is 40% of the total heat produced) is used to heat nearby residential buildings and so substitute heat produced from fossil sources. The other 50% of the remaining heat is not used and thus is excess heat that escapes into the atmosphere. The technical characteristics of the CHP used in this study are shown in **Table 5** (Uihlein et al., 2008). Both the emissions associated with biogas combustion in the CHP unit and the construction of the biogas plant are based on the ecoinvent database (Weidema et al., 2013).

To produce 1 m^3 of insulation material, 194.3 kg dry-matter miscanthus biomass is required. This corresponds to 228.6 kg fresh biomass at a moisture content of 15%. The additives consist of 3.85 kg borax, 3.85 kg sodium carbonate and 1.1 kg of the

fungicide thiocarbamate (Velásquez et al., 2003). The energy required for the production process is shown in **Table 6**.

Choice of Impact Categories

The life cycle impact assessment methodology ReCiPe was used in this LCA study (Goedkoop et al., 2008). All 18 mid-point indicators described in this methodology were included: climate change (CC), which corresponds to global warming potential (GWP); ozone depletion (OD); terrestrial acidification (TA); freshwater eutrophication (FE); marine eutrophication (ME); human toxicity (HT); photochemical oxidant formation (POF); particulate matter formation (PMF); terrestrial ecotoxicity (TET); freshwater ecotoxicity (FET); marine ecotoxicity (MET); ionizing radiation (IR); agricultural land occupation (ALO); urban land occupation (ULO); natural land transformation (NLT); mineral resource depletion (MRD); fossil fuel depletion (FFD); and water depletion (WD). The results are shown as normalized values. This means, that the results of each impact category are divided by the respective emissions caused by an average European in the year 2000. The resulting values show the calculated impact as a proportion of the emissions of an average European citizen. The characterization and normalization factors are based on Goedkoop et al. (2008). No normalized values are given for the impact category "water depletion," as no normalization factor is available in the ReCiPe methodology for this impact category (Goedkoop et al., 2008).

RESULTS

The results are presented as normalized values. These show the net benefits and impacts of the utilization of 1 ha miscanthus for all six sites and for all six utilization pathways (see **Figures 4–9**). The absolute values per ha for all utilization pathways on all sites analyzed are given in the Supplementary Material (Tables S2–S7). In addition, they are shown per MJ$_{th}$ for the utilization pathways 1, 2, 3, and 4 (Tables S2–S5), in MJ$_{el}$ for utilization pathway 5 (Table S6) and in m^3 insulation material for utilization pathway 6 (Table S7).

The normalized net benefits and impacts per ha in the impact categories TA, FE, and ME, MRD and FFD, and CC are shown in **Figure 4** for the sites Adana, Stuttgart and Moscow and in **Figure 5** for the sites Aberystwyth, Potash, and Wageningen. Utilization pathway 6 (production of insulation material) has the largest net benefits in the categories TA, FE, MRD, and CC on all

TABLE 6 | Energy consumption for the production of miscanthus-based insulation material.

Energy consumption	Unit	Per kg dry-matter miscanthus biomass	Per m³ insulation material
Steam explosion	MJ$_{th}$	1.452	282.085
	MJ$_{el}$	0.073	14.104
Drying of fibers	MJ$_{th}$	1.493	290.111
	MJ$_{el}$	0.075	14.506
Mixing and hot pressing	MJ$_{th}$	0.824	160.103
	MJ$_{el}$	0.042	8.161
Total	MJ$_{th}$	3.769	732.299
	Mj$_{el}$	0.19	36.771

sites. This is due to the substitution of the reference product glass wool, which has a very emission-intensive production process. All utilization pathways perform negatively in the category ME. This is largely caused by nitrogen-fertilizer-induced nitrate emissions in the miscanthus cultivation process. Utilization pathways 1 and 2 (both small-scale combustion) also have a negative impact in FE, which is mainly caused by phosphate-fertilizer-induced emissions. The production process of the reference product of utilization pathways 1 and 2 (heat generated through the combustion of light fuel oil) has a low FE. For this reason, the substitution caused a net negative impact on the environment in this category. Differences between the utilization pathways 1 and 2, as well as 3 and 4 are due to differences in transport distance and the additional pelleting process. As a result, pathway 1 has lower environmental impacts than pathway 2, and pathway 3 lower environmental impacts than pathway 4. This applies to all impact categories.

The normalized net benefits and impacts per ha in the impact categories PMF, HT, MET, FET, and TET for the sites Adana, Stuttgart and Moscow are shown in **Figure 6**, and for the sites Aberystwyth, Potash and Wageningen in **Figure 7**. The utilization pathway 5 (medium-scale biogas plant) had relatively high environmental benefits in HT, MET, and FET (see **Figure 6**). These can be explained by the emission-intensive production process of the substituted reference product, the European electricity mix. Utilization pathway 6 showed low environmental impacts in the category PMF compared with the other utilization options. This is due to the high impact of the substituted reference product glass wool in this impact category, in particular its production process. All other utilization pathways had a comparatively negative performance in all impact categories depicted in **Figures 6**, **7**. The net impacts in ME, FE and especially HT in the utilization pathways 1 to 4 result from the treatment of the bottom and fly ash, which incur in the combustion process.

The normalized net benefits and impacts per ha in the impact categories IR, POF, OD, ALO, and ULO are shown in **Figure 8** for the sites Adana, Stuttgart, and Moscow, and in **Figure 9** for the sites Aberystwyth, Potash, and Wageningen. Naturally, all biomass-based utilization pathways perform negatively in the category ALO. Utilization pathway 6 shows a comparatively

large net benefit in the category POF. This is again caused by the substitution of the reference product. The net benefit of utilization pathways 1 and 2 in the category OD result from the emission-intensive generation of the reference product (heat generated by the combustion of light fuel oil). All utilization pathways had a comparatively large net benefit in the impact category natural land transformation (data not shown). The normalized results range from −6.15 for utilization pathway 5, to −42.86 for utilization pathway 1. In all utilization pathways, this is caused by the substituted reference products, which have a strong negative impact in this category. For clarity of presentation, these results are not included in **Figures 8**, **9** due to their considerably higher values.

DISCUSSION

The first part of the discussion focuses on the normalized values shown in **Figures 4**–**9**, including a critical reflection on the influence on the final results of reference product selection and credits given for co-products. In addition, the impact of the End-of-Life phase of the products is elaborated. The second part discusses the relevance of the impact categories for the various utilization pathways analyzed in this study. The final part gives recommendations for improving the environmental performance of the biobased value chains and considers the implications of the results for future biomass use.

Determinants of Environmental Benefits and Impacts

Figures 4–**9** show the normalized values for the environmental benefits and impacts per hectare (including the cultivation of the biomass and subsequent utilization) minus the substitution of a reference product and the credits given for co-products.

A comparison of the normalized results from this study with results from reference literature is only partially possible due to different assumptions, system boundaries and methodologies used. Wagner and Lewandowski (2017) analyzed the relevance of various impact categories for a small-scale combustion chain using miscanthus and willow cultivated under three nitrogen fertilizer regimes. The results of their study show strong similarities with those of the current assessment, in particular with regard to the question of which impact categories are relevant and which not.

In general, the utilization pathways 5 (fermentation of miscanthus in a biogas plant and subsequent utilization in a CHP) and 6 (production of insulation material) had the lowest impacts on the environment. They had considerably larger net benefits, especially in the impact categories MET and FET, and FE. The results of the small-scale combustion chains again emphasized the necessity of including more impact categories than just climate change when analyzing and comparing the environmental performance of biobased utilization pathways (Jeswani et al., 2015; Wagner and Lewandowski, 2017). The small-scale combustion chains had advantages in the impact categories OD and FFD, and achieved the highest climate change saving potential of all energetic value chains (1, 2, 3, 4,
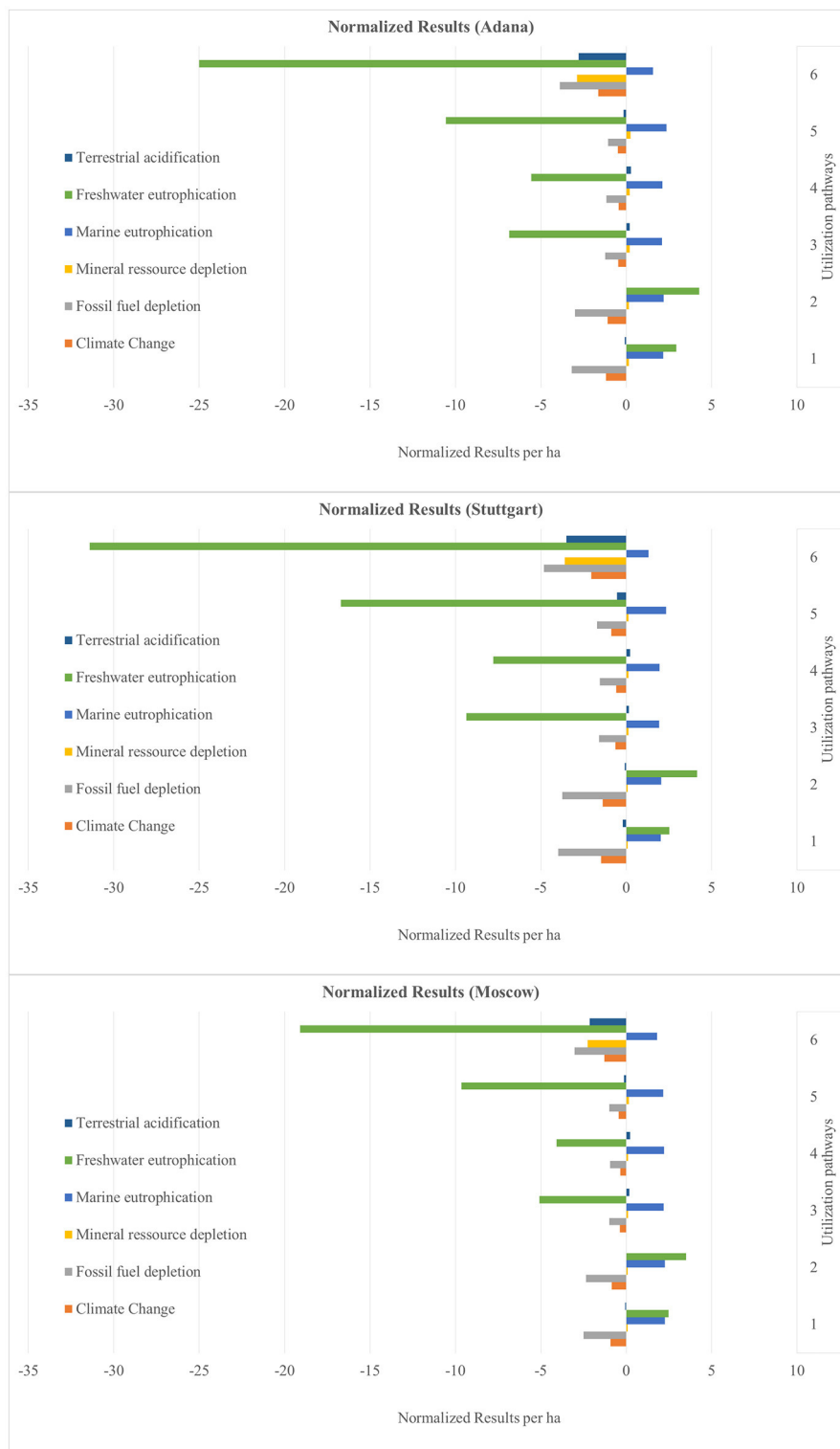
FIGURE 4 | Normalized results per ha for the sites Adana, Stuttgart, and Moscow—Part 1. Utilization pathways: 1. Small-scale combustion—chips; 2. Small-scale combustion—pellets; 3. Large-scale combustion—biomass baled for transport and storage; 4. Large-scale combustion—pellets; 5. Medium-scale biogas plant—biomass ensiled; and 6. Large-scale production of insulation material—biomass baled for transport and storage.
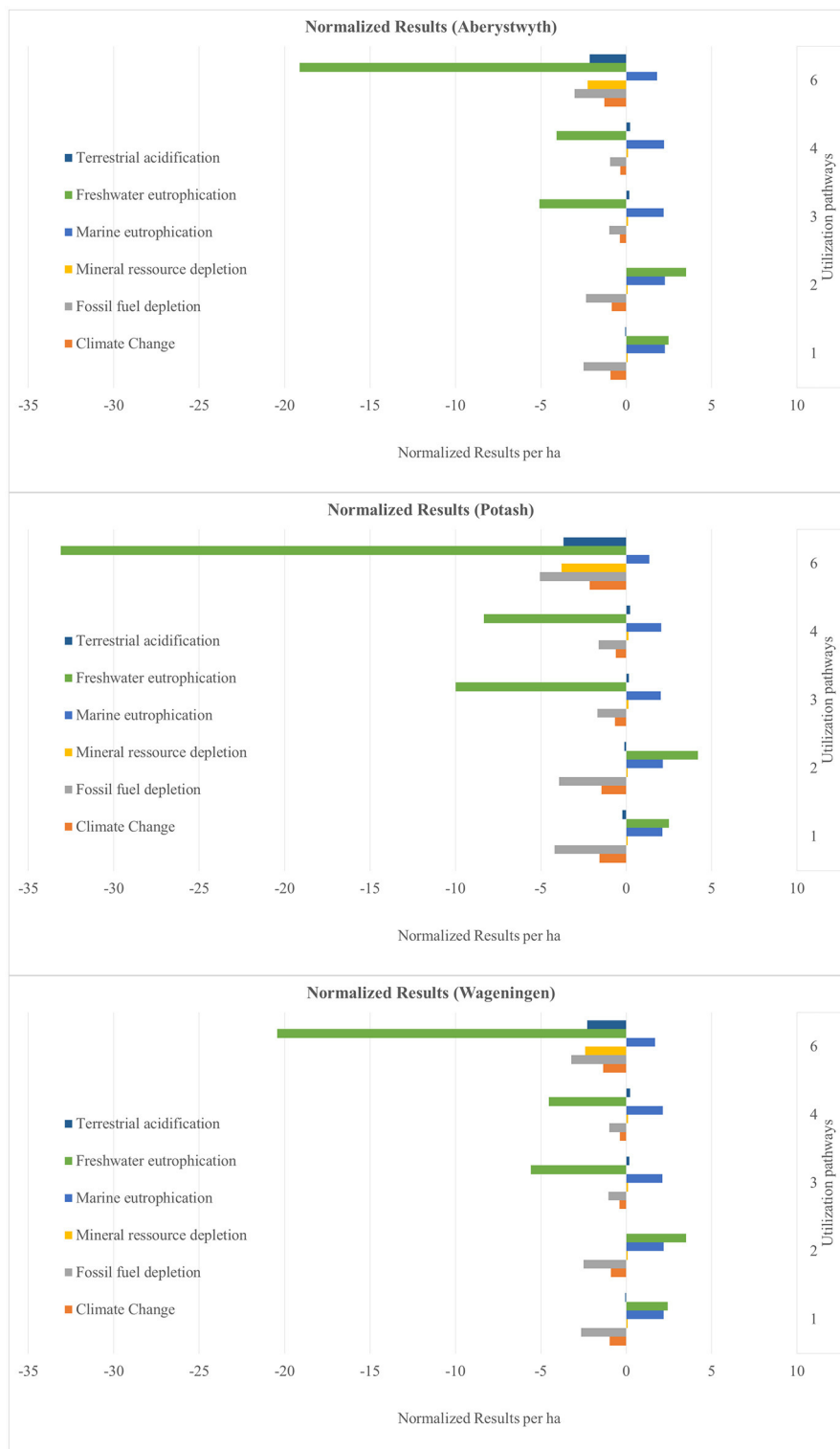
FIGURE 5 | Normalized results per ha for the sites Aberystwyth, Potash, and Wageningen–Part 1. Utilization pathways: 1. Small-scale combustion—chips; 2. Small-scale combustion—pellets; 3. Large-scale combustion—biomass baled for transport and storage; 4. Large-scale combustion—pellets; and 6. Large-scale production of insulation material—biomass baled for transport and storage.
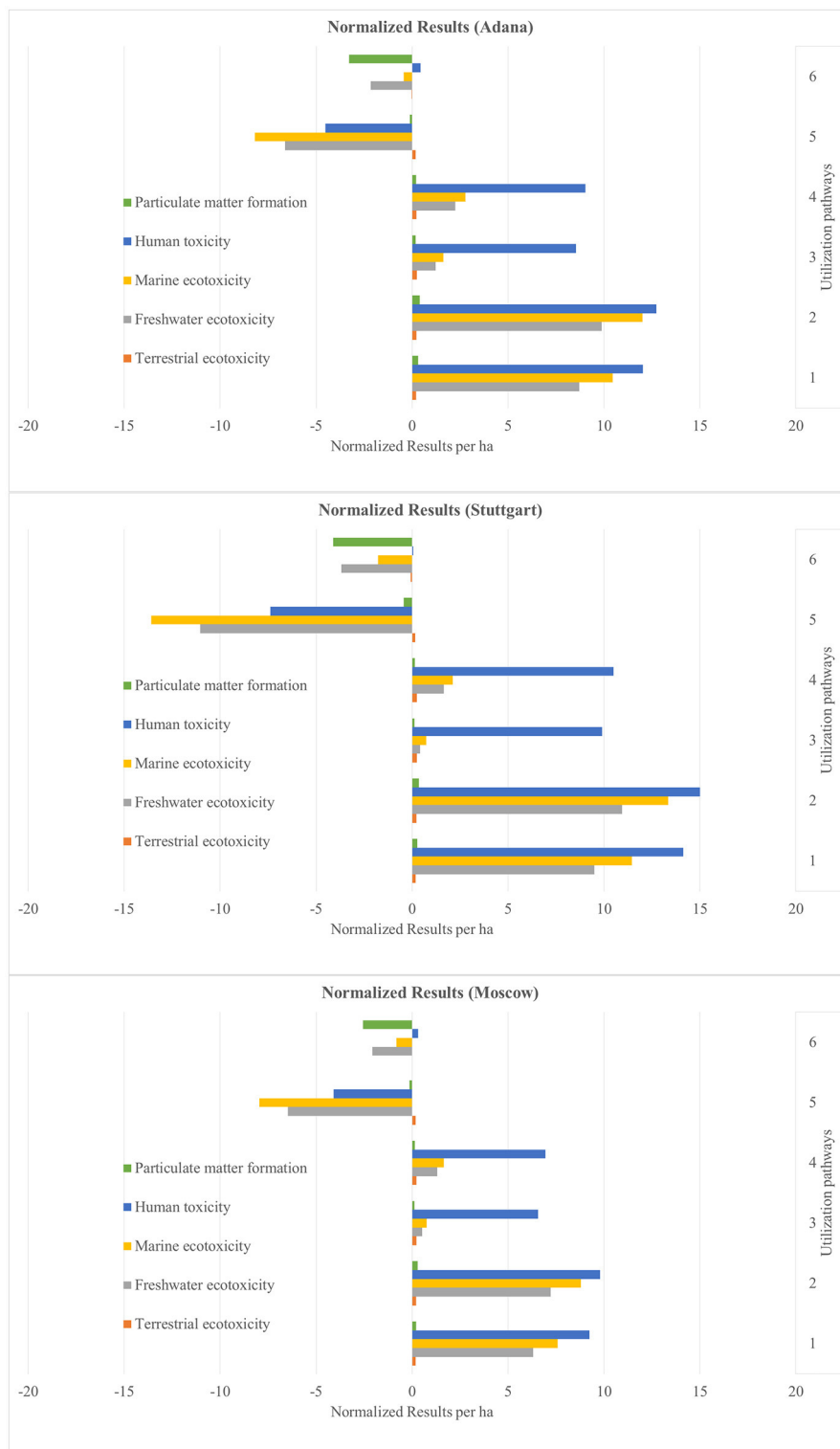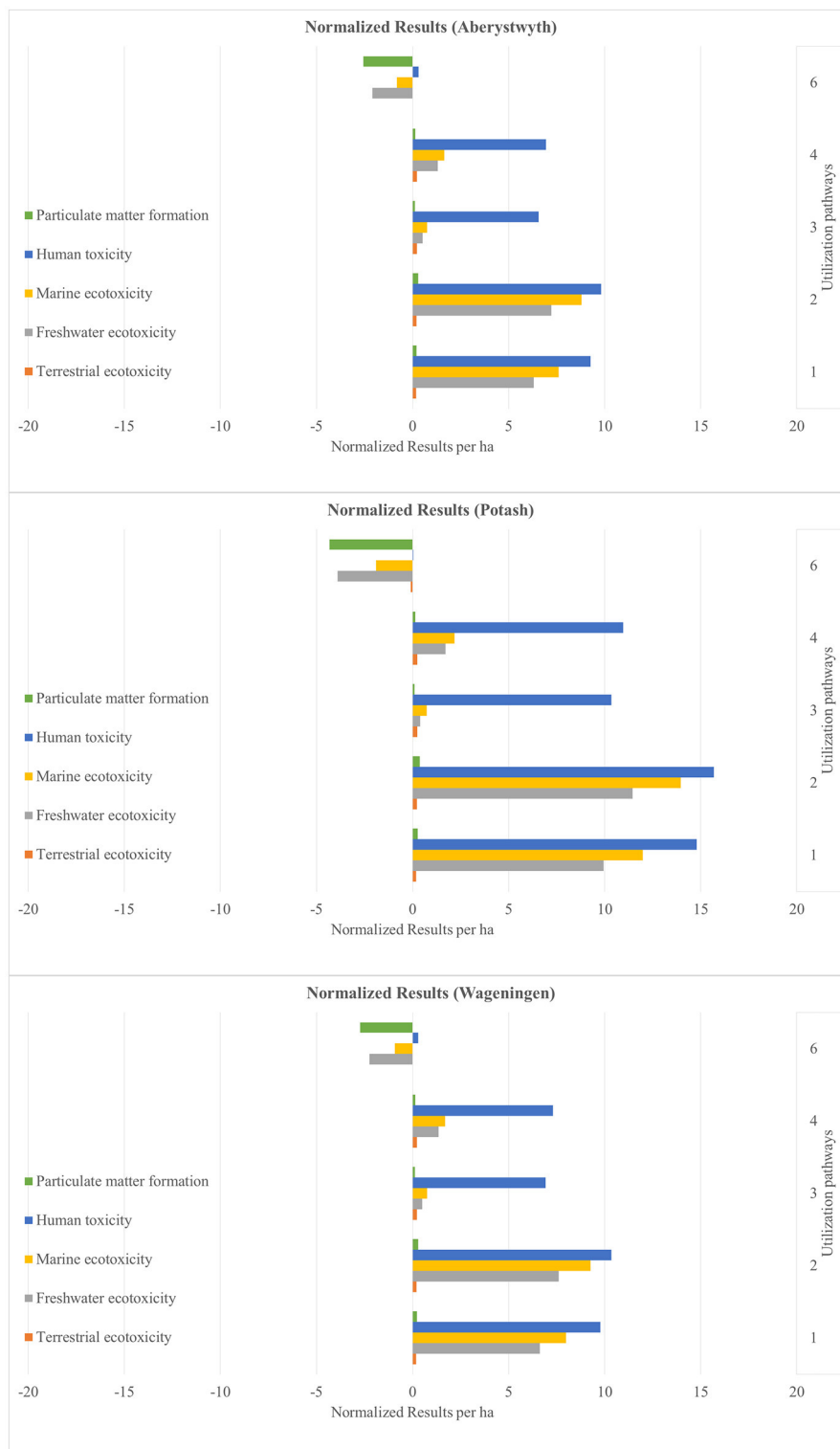
FIGURE 6 | Normalized results per ha for the sites Adana, Stuttgart, and Moscow—Part 2. Utilization pathways: 1. Small-scale combustion—chips; 2. Small-scale combustion—pellets; 3. Large-scale combustion—biomass baled for transport and storage; 4. Large-scale combustion—pellets; 5. Medium-scale biogas plant—biomass ensiled; and 6. Large-scale production of insulation material—biomass baled for transport and storage.

FIGURE 7 | Normalized results per ha for the sites Aberystwyth, Potash, and Wageningen—Part 2. Utilization pathways: 1. Small-scale combustion—chips; 2. Small-scale combustion—pellets; 3. Large-scale combustion—biomass baled for transport and storage; 4. Large-scale combustion—pellets; and 6. Large-scale production of insulation material—biomass baled for transport and storage.
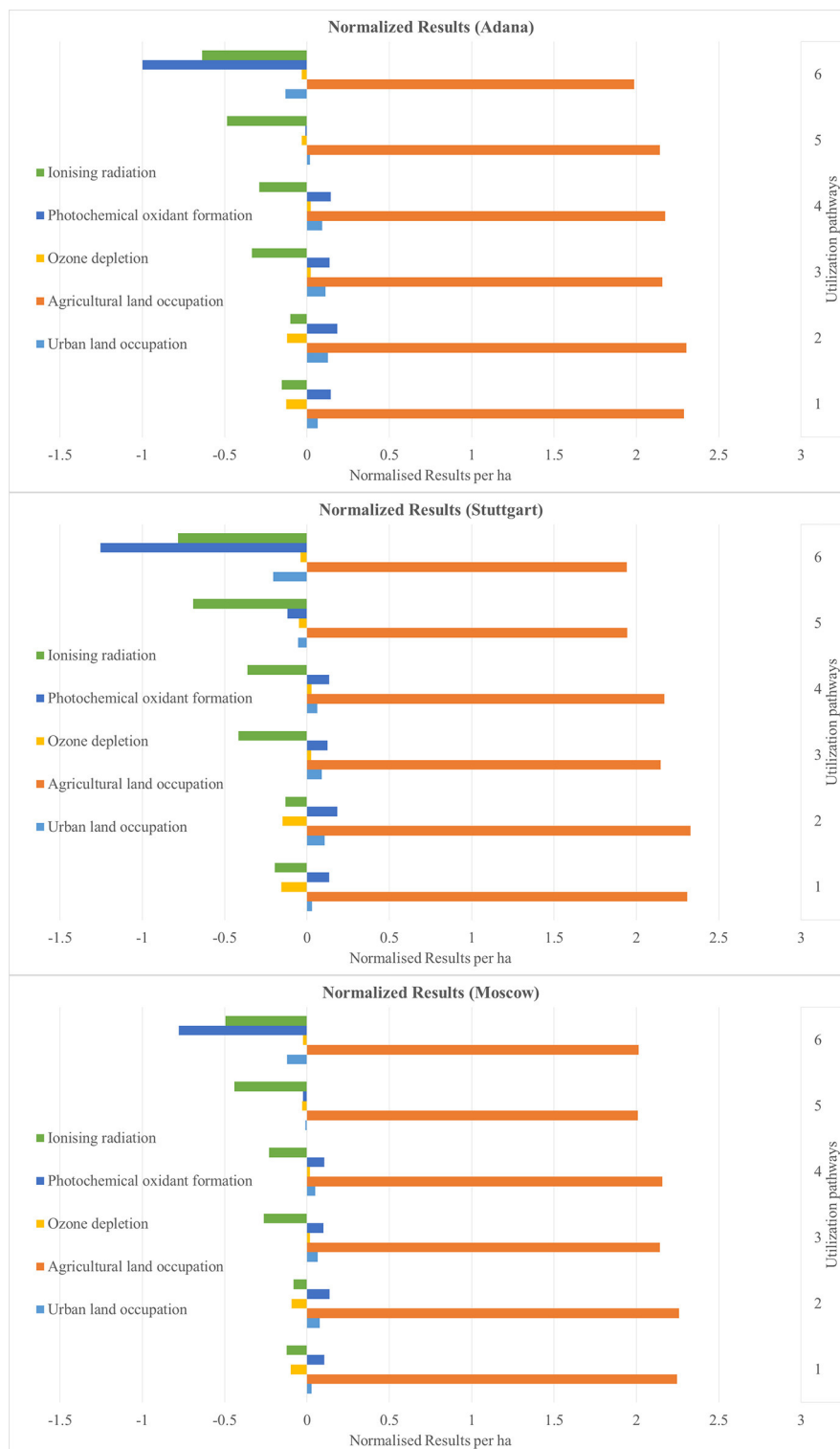
FIGURE 8 | Normalized results per ha for the sites Adana, Stuttgart, and Moscow—Part 3. Utilization pathways: 1. Small-scale combustion—chips; 2. Small-scale combustion—pellets; 3. Large-scale combustion—biomass baled for transport and storage; 4. Large-scale combustion—pellets; 5. Medium-scale biogas plant—biomass ensiled; and 6. Large-scale production of insulation material—biomass baled for transport and storage.

FIGURE 9 | Normalized results per ha for the sites Aberystwyth, Potash, and Wageningen—Part 3. Utilization pathways: 1. Small-scale combustion—chips; 2. Small-scale combustion—pellets; 3. Large-scale combustion—biomass baled for transport and storage; 4. Large-scale combustion—pellets; and 6. Large-scale production of insulation material—biomass baled for transport and storage.
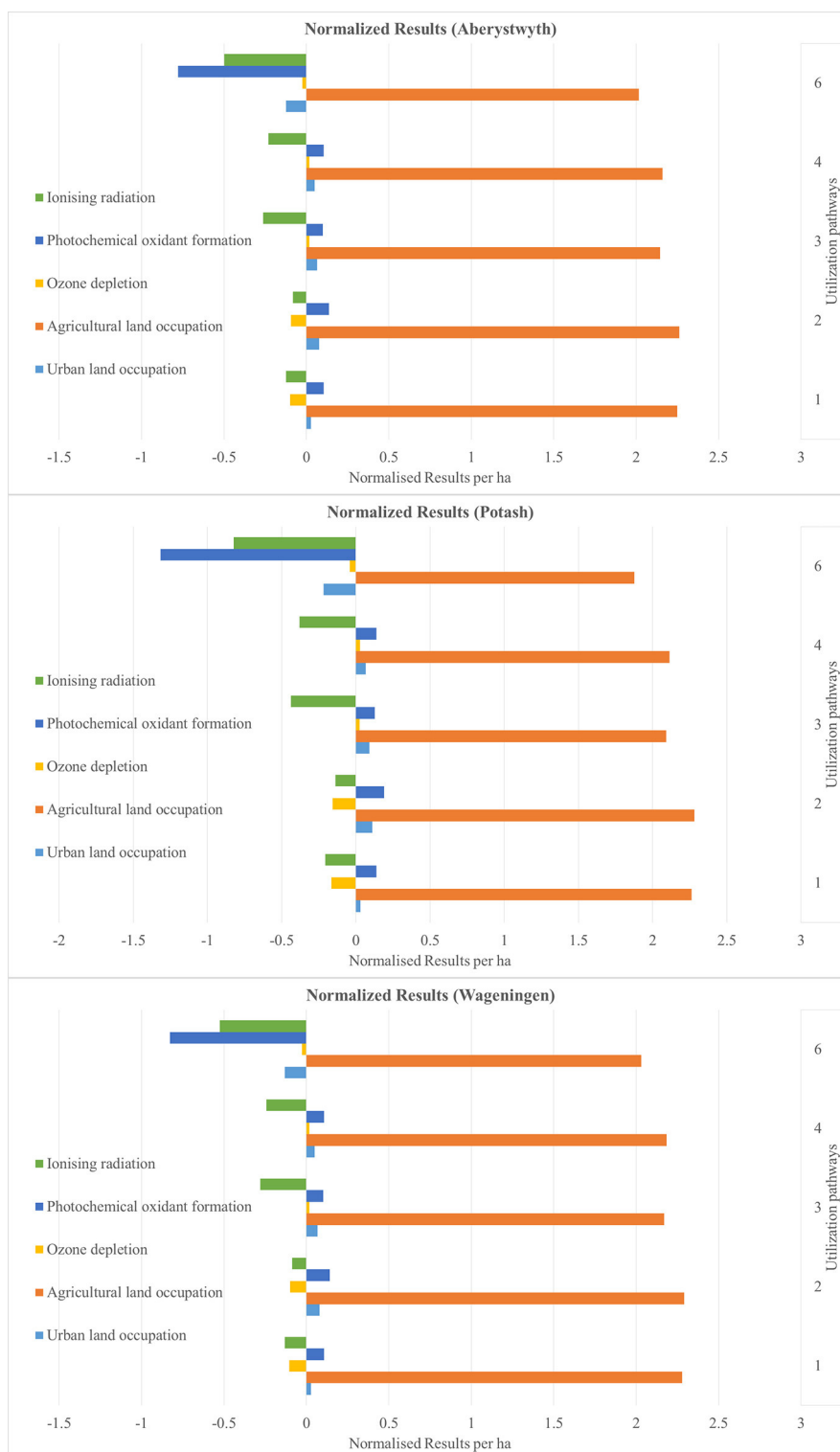
and 5). However, they scored worse in most of the other impact categories. This also emphasizes the difficulty of determining the most sustainable utilization option from an environmental point of view. One way of resolving this issue is to combine the results of several impact categories into a single score for the total environmental sustainability (Rajagopalan et al., 2017). However, such an aggregation reduces the overall transparency of the results (Bare et al., 2000).

There is a large variation in the results between the six sites and between the six utilization pathways. The site differences are chiefly caused by variations in yield. The differences between the utilization pathways have several causes: the reference products have the largest impact, but the credits given for co-products and the effect of End-of-Life phase also play an important role. These four factors with a strong influence on the environmental benefits and impacts are discussed in the following sub-sections.

Influence of the Variability of the Biomass Yield

The average yields used in this assessment are based on the yield measured in the third year and are at the lower end of those of other studies (Christian et al., 2008; Iqbal et al., 2015). In this study, it was assumed that full yields are reached from the third year onwards. However, other studies analyzing long-term field trials suggest that full yields are only achieved from the fourth year onwards (Christian et al., 2008; Iqbal et al., 2015). That would mean that the yields used in this study are conservative assumptions and could be higher over the whole cultivation period.

The differences between the six sites for the same utilization pathways seen in **Figures 4–9** can be attributed to differences in yield. Sites on which significantly higher yields were achieved (e.g., Potash and Stuttgart) showed a better environmental performance. Other studies also emphasize the importance of yield for environmental performance (Meyer et al., 2016). However, it is worth mentioning that the influence of yield variation only changed an impact into a benefit, or vice versa, in very few impact categories, independent of utilization pathway (see **Figures 4–9**). Aberystwyth was a particularly interesting site; the values for the environmental benefits here were low compared to the other sites. The reason for that is that, in Aberystwyth, the yield was lower because the miscanthus was grown on marginal land. However, some utilization pathways, such as production of insulation material, still achieved comparatively low impacts on the environment even though the miscanthus was cultivated under marginal conditions.

Influence of the Selection of the Reference Product

The selection of an appropriate reference product is essential for the accuracy of the assessment, especially in the case of the heat-producing value chains 1–4 (Wolf et al., 2016). For the utilization pathways 1 and 2 (small-scale combustion), heat produced by combustion of light fuel oil was substituted. Changing the reference product to natural gas alters the results substantially. The net impact for the category MRD increases by 231%, for PMF by 220%, and for POF by 220%. In addition, the climate change saving potential is reduced by 77% and the benefit in the impact category fossil fuel depletion is reduced by 66%. This sensitivity

analysis clearly shows the influence of the selection of the reference product on the result of the assessment. Furthermore, it emphasizes how crucial it is in practice to first phase out emission-intensive power plants based on coal and fuel oil, rather than those based on natural gas. However, the change of the reference product in utilization pathways 1 and 2 only turns a net benefit into an impact in the impact categories ionizing radiation and terrestrial acidification. The results of this sensitivity analysis are shown in the Supplementary Material (Table S8).

Heat generated by the combustion of natural gas was selected as reference product for the utilization pathways 3 and 4. Natural gas is a fossil energy carrier with comparatively low environmental impacts (May and Brennan, 2006), thus reducing the risk of overestimating the benefits of substitution by miscanthus-based heat. However, this also means that the environmental performance of the utilization pathways 3 and 4 can be improved considerably if heat generated by the combustion of fuel oil or coal is substituted.

The European electricity mix was used as reference product for the energetic utilization pathway 5. The choice of this reference is one reason for the low impacts on the environment of this utilization pathway. As electricity is an energy form with higher emissions per MJ than heat generation, the net benefits of its substitution are also higher. It should be noted that in this study an electricity mix was used as a reference product, which also includes electricity from renewable sources (Weidema et al., 2013). If only electricity generated by fossil sources is substituted, the environmental performance can be further improved.

Influence of Credits Given for Co-products

For those utilization pathways with more than one product, credits were given for the co-products. This was the case for the electricity produced as co-product in the CHP unit in the utilization pathways 3 and 4. The CHP produced 0.3 MJ of electricity for every MJ heat and it was assumed that this electricity substituted a European electricity mix. As already mentioned above, electricity has higher negative impacts on the environment than heat. That is why, in most impact categories, the credits given for the co-product were higher than the effect of substituting the reference product (see Table S9). The utilization pathway 5 produces heat as a co-product, which is partly utilized to heat nearby buildings, thus substituting fossil-based heat. In addition, the fermentation residues are rich in nutrients and can be used to substitute mineral fertilizers. These residues are a particularly valuable resource and the credits given for their utilization improve the environmental performance of this pathway considerably. The values used for these credits are displayed in Table S10.

Influence of the Inclusion of the End-of-Life Phase

The inclusion of the End-of-Life of biobased products is also an important point with a strong influence on their environmental performance. The insulation material produced in pathway 6 is first used as a biobased construction material and after the use phase incinerated in a CHP. The positive influence of this multiple use is important for the relatively low impacts on the environment of miscanthus-based insulation

material. For example, the production of this insulation material (including the cultivation phase on the Stuttgart site and the truck transport of the biomass) causes around 124 kg CO_2 eq. per m^3. Of this, around 117 kg CO_2 eq. can be recovered through its incineration, generating heat and power which substitute conventionally produced energy. In the impact category terrestrial acidification, 0.58 kg SO_2 eq. per m^3 are saved through this energy recovery, which is more than are emitted in the whole value-chain including the production process (0.42 kg SO_2 eq.). These advantages of multiple use in comparison to single use have also been shown in other studies (Höglmeier et al., 2014, 2015). Another advantage of material use is the temporal storage of carbon in the product (Sikkema et al., 2013). This storage function can help decelerate climate change.

Relevance of Different Impact Categories

The normalization step applied enables the assessment of the relevance of the different impact categories for the environmental performance of each utilization pathway (Wagner and Lewandowski, 2017). There are large variations in relevance within the utilization pathways and within the impact categories analyzed. Once the relevance of an impact category has been established, it becomes evident which need to be included in a holistic analysis of the environmental performance of miscanthus-based value chains. The relevance of the impact categories should not only be evaluated in general but also for each specific utilization pathway. This knowledge assists the selection of the impact categories that require further improvement in each pathway.

The following section classifies the impact categories according to their normalized values into three groups: impact categories of (1) low relevance; (2) average relevance and (3) high relevance.

Several impact categories have comparatively low normalized impacts or benefits on the environment in most pathways and are therefore deemed of low relevance. These include: terrestrial acidification (TA), mineral resource depletion (MRD), particulate matter formation (PMF), ionizing radiation (IR), ozone depletion (OD), urban land occupation (ULO), photochemical oxidant formation (POF), and terrestrial ecotoxicity (TET). In addition, as the model and the LCI data used contain some uncertainties, small differences of ± 2 in normalized values are not considered significantly different.

The impact categories marine eutrophication (ME) and fossil fuel depletion (FFD) are deemed of average relevance. They should be included in the assessment, if the utilization pathways analyzed are expected to have a substantial impact in these categories. This is the case for ME, when higher amounts of nitrogen fertilizer are applied. The ME then increases considerably because higher nitrogen fertilizer application leads to an increase in nitrate leaching, the main cause of ME. As the production process of mineral nitrogen fertilizer is quite energy-intensive, FFD should also be included, when higher amounts of nitrogen fertilizer are applied. The FFD should also be assessed if the production phase of the utilization pathways analyzed requires large amounts of energy.

On the basis of the comparatively high normalized results, the impact categories human toxicity (HT), marine (MET), and freshwater ecotoxicity (FET) and freshwater eutrophication (FE) are considered very relevant for the assessment of miscanthus-based value chains. These results usually represent a substantial net impact for the combustion chains and a considerable net benefit for utilization in a biogas plant and production of insulation material.

The impact categories climate change (CC) and agricultural land occupation (ALO) are both deemed of high relevance, even if they have comparably low normalized impacts or benefits. This is due to the related environmental and social problems, which are of high interest to society in general. Climate change, for example, is presently one of the most urgent environmental problems and, as a result, this impact category is included in virtually every study which assesses the environmental performance of miscanthus-based value chains (Godard et al., 2013; Parajuli et al., 2015; Roy et al., 2015). The ALO can be a problem if the utilization of land for biomass production leads to land-use competition and thus hinders the production of food crops.

Although the normalization of the results allows the evaluation of the relevance of different impact categories, this method has its limitations. For example, it does not consider social preferences. In addition, the preload of the environment is not taken into account. For this reason, the results of the relevance assessment always need to be adapted according to the goal and scope of the respective study.

How to Improve the Environmental Performance

The relevance of the different impact categories also helps to identify potential for improvement by starting the focus on the categories with the highest normalized scores. The high values of the combustion chains for HT are caused by the treatment of the ash, which is rich in heavy metals. In this study the entire ash was disposed of to sanitary landfill. A separation into fly ash and coarse ash could improve the environmental performance. In this case, only the fly ash, which contains most of the heavy metals, would be disposed of to landfill and the coarse ash, which is rich in phosphate and potassium, could be used as fertilizer (Pitman, 2006). Performance in MET and FET is also problematic, especially for the combustion chains. The combustion process of the miscanthus biomass is responsible for the largest share of the emissions in these impact categories. Improvements in the emission control systems of the combustion unit would be one possibility to decrease the impacts in these categories. Another could be adaption of the harvest date and selection of the genotype in order to utilize biomass that contains less elements which lead to harmful emissions in the combustion process (Iqbal and Lewandowski, 2014).

The impact category ALO chiefly describes the area of agricultural land needed to produce the amount of biomass required for each utilization pathway. If it is possible to obtain higher yields per hectare, less land would be needed to produce

the same amount of biomass and thus the ALO would decrease. Another possibility would be to increase the use efficiency of the biomass utilization pathways, so that less biomass is needed to produce the same amount of products.

The ME is mostly caused by nitrate leaching through the use of nitrogen fertilizers. Nitrogen-fertilizer-induced emissions in form of N_2O are also a main hot spot in the impact category CC. Thus, a decrease in the amount of nitrogen fertilizer used would decrease the impact in these categories. Another possibility for improvement would be the use of nitrification inhibitors (Akiyama et al., 2010). In the impact category FFD, there is a clear distinction between the energetic (1, 2, 3, 4, 5) and the material (6) utilization pathways. The hot spots in the energetic pathways are the harvest, biomass transport to the conversion plant and pelleting process (where applicable). In utilization pathway 6 (insulation material), the production process is the main hot spot and has the largest potential for improvement, for example, through the use of renewable instead of fossil-based energy forms.

Outlook

The utilization pathways modeled in this assessment are all based on novel genotypes, except at the Adana site. These novel genotypes were more suitable than the standard genotype *Miscanthus × giganteus* for the utilization pathways analyzed, based on yield and quality parameters (Lewandowski et al., 2016). Thus, the environmental performance assessed in this study reflects the advances made in recent years in both agricultural management and miscanthus breeding. The results reveal substantial differences in environmental performance between the various utilization pathways. Furthermore, they emphasize the advantages of the multiple use of biomass (as in the case of insulation material) compared to single use as an energy carrier. In order to increase the environmental benefits of biomass-based value chains, in future the material use of biomass should be favored.

Another relevant outcome of this study was the demonstration of the positive environmental performance of marginal land for miscanthus biomass production and utilization. In a developing European bioeconomy with a steadily increasing demand for biomass, this is a promising opportunity to boost biomass production without competing with food crops.

AUTHOR CONTRIBUTIONS

MW was performing the LCA modeling and was leading the writing process. AK, AH, and YI provided data and contributed to the material and method parts and thus supporting the creation of the Life cycle inventory. Furthermore AH supported the modeling process and AK the discussion of the results. IL added valuable contribution to each chapter and in manifold discussions.

SUPPLEMENTARY MATERIAL

The Supplementary Material for this article can be found online at: http://journal.frontiersin.org/article/10.3389/fpls.2017. 00990/full#supplementary-material

REFERENCES

Akiyama, H., Yan, X., and Yagi, K. (2010). Evaluation of effectiveness of enhanced-efficiency fertilizers as mitigation options for N2O and NO emissions from agricultural soils: meta-analysis. *Glob. Chang. Biol.* 16, 1837–1846. doi: 10.1111/j.1365-2486.2009.02031.x

Bacenetti, J., Sala, C., Fusi, A., and Fiala, M. (2016). Agricultural anaerobic digestion plants: what LCA studies pointed out and what can be done to make them more environmentally sustainable. *Appl. Energy* 179, 669–686. doi: 10.1016/j.apenergy.2016.07.029

Bare, J. C., Hofstetter, P., Pennington, D. W., and Udo de Haes, H. A. (2000). Midpoints versus endpoints: the sacrifices and benefits. *Int. J. Life Cycle Assess.* 5, 319–326. doi: 10.1007/BF02978665

Börjesson, P., and Berglund, M. (2007). Environmental systems analysis of biogas systems—Part II: the environmental impact of replacing various reference systems. *Biomass Bioenergy* 31, 326–344. doi: 10.1016/j.biombioe.2007.01.004

Bouwman, A. F., Boumans, L. J. M., and Batjes, N. H. (2002). Modeling global annual N2O and NO emissions from fertilized fields. *Glob. Biogeochem. Cycles* 16, 28-1-28-9. doi: 10.1029/2001GB001812

Christian, D. G., Riche, A. B., and Yates, N. E. (2008). Growth, yield and mineral content of *Miscanthus × giganteus* grown as a biofuel for 14 successive harvests. *Ind. Crops Prod.* 28, 320–327. doi: 10.1016/j.indcrop.2008.02.009

Clifton-Brown, J., Hastings, A., Mos, M., McCalmont, J. P., Ashman, C., Awty-Carroll, D., et al. (2016). Progress in upscaling Miscanthus biomass production for the European bio- economy with seed based hybrids. *Glob. Change Biol. Bioenergy* 9, 6–17. doi: 10.1111/gcbb.12357

Clifton-Brown, J., Schwarz, K.-U., and Hastings, A. (2015). History of the development of Miscanthus as a bioenergy crop: from small beginnings to potential realisation. *Biol. Environ. Proc. R. Irish Acad.* 115B, 1–13. doi: 10.3318/BIOE.2015.05

Dahl, J., and Obernberger, I. (2004). "Evaluation of the combustion characteristics of four perennial energy crops (*Arundo donax, Cynara cardunculus, Miscanthus x giganteus* and *Panicum virgatum*)," in *2nd World Conference on Biomass for Energy, Industry and Climate Protection*, Rome.

EMEP/CORINAIR (2001). *Joint EMEP/CORINAIR Atmospheric Emission Inventory Guidebook, 3rd Edn*. Copenhagen: European Environment Agency.

Faist Emmenegger, M., Reinhard, J., and Zah, R. (2009). *Sustainability Quick Check for Biofuels – Intermediate Background Report*. Agroscope Reckenholz-Tänikon Research Station ART, Dübendorf.

Gauder, M., Billen, N., Zikeli, S., Laub, M., Graeff-Hönninger, S., and Claupein, W. (2016). Soil carbon stocks in different bioenergy cropping systems including subsoil. *Soil Tillage Res.* 155, 308–317. doi: 10.1016/j.still.2015.09.005

Godard, C., Boissy, J., and Gabrielle, B. (2013). Life-cycle *Glob. Change Biol. Bioenergy* 5, 16–29. doi: 10.1111/j.1757-1707.2012.01187.x

Goedkoop, M., Heijungs, R., Huijbregts, M., De, S. A., Struijs, J., and Van, Z. R. (2008). *ReCiPe 2008. A Life Cycle Impact Assessment Method which Comprises Harmonised Category Indicators at the Midpoint and the endpoint level; First edition Report I. Characterisation*. VROM, Den Haag.

Harris, Z. M., Spake, R., and Taylor, G. (2015). Land use change to bioenergy: a meta-analysis of soil carbon and GHG emissions. *Biomass Bioenergy* 82, 27–39. doi: 10.1016/j.biombioe.2015.05.008

Höglmeier, K., Steubing, B., Weber-Blaschke, G., and Richter, K. (2015). LCA-based optimization of wood utilization under special consideration of a cascading use of wood. *J. Environ. Manage.* 152, 158–170. doi: 10.1016/j.jenvman.2015.01.018

Höglmeier, K., Weber-Blaschke, G., and Richter, K. (2014). Utilization of recovered wood in cascades versus utilization of primary wood—a comparison with life cycle assessment using system expansion. *Int. J. Life Cycle Assess.* 19, 1755–1766. doi: 10.1007/s11367-014-0774-6

IPCC (2006). "Guidelines for national greenhouse gas inventories," in *Prepared by the National Greenhouse Gas Inventories Programme,* eds H. S. Eggleston, L. Buendia, K. Miwa, T. Ngara, and K. Tanabe (Hayama: IGES), 11.1–11.54.

Iqbal, Y., Gauder, M., Claupein, W., Graeff-Hönninger, S., and Lewandowski, I. (2015). Yield and quality development comparison between miscanthus and switchgrass over a period of 10 years. *Energy* 89, 268–276. doi: 10.1016/j.energy.2015.05.134

Iqbal, Y., and Lewandowski, I. (2014). Inter-annual variation in biomass combustion quality traits over five years in fifteen Miscanthus genotypes in south Germany. *Fuel Process. Technol.* 121, 47–55. doi: 10.1016/j.fuproc2014.01.003

ISO (2006a). *ISO 14040: Environmental Management — Life Cycle Assessment — Principles and Framework, 2nd Edn.* Geneva: ISO.

ISO (2006b). *ISO 14044: Environmental Management — Life Cycle Assessment — Requirements and Guidelines.* Geneva: ISO.

Jeswani, H. K., Falano, T., and Azapagic, A. (2015). Life cycle environmental sustainability of lignocellulosic ethanol produced in integrated thermo-chemical biorefineries. *Biofuels Bioprod. Bioref.* 9, 661–676. doi: 10.1002/bbb.1558

Jiménez, L., and González, F. (1991). Study of the physical and chemical properties of lignocellulosic residues with a view to the production of fuels. *Fuel* 70, 947–950. doi: 10.1016/0016-2361(91)90049-G

Kiesel, A., and Lewandowski, I. (2017). Miscanthus as biogas substrate - Cutting tolerance and potential for anaerobic digestion. *Glob. Change Biol. Bioenergy* 9, 153–167. doi: 10.1111/gcbb.12330

Kiesel, A., Nunn, C., Iqbal, Y., van der Weijde, T., Wagner, M., Özgüven, M., et al. (2017). Site-specific management of miscanthus genotypes for combustion and anaerobic digestion: a comparison of energy yields. *Front. Plant Sci.* 8:347. doi: 10.3389/fpls.2017.00347

Kiesel, A., Wagner, M., and Lewandowski, I. (2016). Environmental performance of miscanthus, switchgrass and maize: can C4 perennials increase the sustainability of biogas production? *Sustainability* 9:5. doi: 10.3390/su9010005

Lewandowski, I., Clifton-Brown, J. C., Scurlock, J., and Huisman, W. (2000). Miscanthus: European experience with a novel energy crop. *Biomass Bioenergy* 19, 209–227. doi: 10.1016/S0961-9534(00)00032-5

Lewandowski, I., Clifton-Brown, J., Trindade, L. M., van der Linden, G. C., Schwarz, K.-U., Müller-Sämann, K., et al. (2016). Progress on optimizing miscanthus biomass production for the european bioeconomy: results of the EU FP7 project OPTIMISC. *Front. Plant Sci.* 7:2202. doi: 10.3389/fpls.2016.01620

Lewandowski, I., and Schmidt, U. (2006). Nitrogen, energy and land use efficiencies of miscanthus, reed canary grass and triticale as determined by the boundary line approach. *Agric. Ecosyst. Environ.* 112, 335–346. doi: 10.1016/j.agee.2005.08.003

Lewandowski, I., Scurlock, J. M., Lindvall, E., and Christou, M. (2003). The development and current status of perennial rhizomatous grasses as energy crops in the US and Europe. *Biomass Bioenergy* 25, 335–361. doi: 10.1016/S0961-9534(03)00030-8

May, J. R., and Brennan, D. J. (2006). Sustainability assessment of Australian electricity generation. *Process Safety Environ. Prot.* 84, 131–142. doi: 10.1205/psep.04265

McCalmont, J. P., Hastings, A., McNamara, N. P., Richter, G. M., Robson, P., Donnison, I. S., et al. (2017). Environmental costs and benefits of growing Miscanthus for bioenergy in the UK. *Glob. Change Biol. Bioenergy* 9, 489–507. doi: 10.1111/gcbb.12294

Meyer, F., Wagner, M., and Lewandowski, I. (2016). Optimizing GHG emission and energy-saving performance of miscanthus-based value chains. *Biomass Conv. Bioref.* 7, 139. doi: 10.1007/s13399-016-0219-5

Muthuraj, R., Misra, M., and Mohanty, A. K. (2015). Injection molded sustainable biocomposites from poly(butylene succinate) bioplastic

and perennial grass. *ACS Sustainable Chem. Eng.* 3, 2767–2776. doi: 10.1021/acssuschemeng.5b00646

Nemecek, T., and Kägi, T. (2007). *Life Cycle Inventories of Agricultural Production Systems: Data v2.0.* Amersfoort; Zürich: Agroscope Reckenholz-Tänikon Research Station ART; Dübendorf: Swiss Centre for Life Cycle Inventories.

Nemecek, T., and Schnetzer, J. (2011). *Methods of Assessment of Direct Field Emissions for LCIs of Agricultural Production Systems: Data v3.0.* Zürich: Agroscope Reckenholz-Tänikon Research Station ART.

Parajuli, R., Sperling, K., and Dalgaard, T. (2015). Environmental performance of Miscanthus as a fuel alternative for district heat production. *Biomass Bioenergy* 72, 104–116. doi: 10.1016/j.biombioe.2014.11.011

Pitman, R. M. (2006). Wood ash use in forestry - a review of the environmental impacts. *Forestry* 79, 563–588. doi: 10.1093/forestry/cpl041

Rajagopalan, N., Venditti, R., Kelley, S., and Daystar, J. (2017). Multi-attribute uncertainty analysis of the life cycle of lignocellulosic feedstock for biofuel production. *Biofuels Bioprod. Bioref.* 11, 269–280. doi: 10.1002/bbb.1737

Roy, P., Dutta, A., and Deen, B. (2015). Greenhouse gas emissions and production cost of ethanol produced from biosyngas fermentation process. *Bioresour. Technol.* 192, 185–191. doi: 10.1016/j.biortech.2015.05.056

Sanscartier, D., Deen, B., Dias, G., MacLean, H. L., Dadfar, H., McDonald, I., et al. (2014). Implications of land class and environmental factors on life cycle GHG emissions of Miscanthus as a bioenergy feedstock. *Glob. Change Biol. Bioenergy* 6, 401–413. doi: 10.1111/gcbb.12062

Sikkema, R., Junginger, M., McFarlane, P., and Faaij, A. (2013). The GHG contribution of the cascaded use of harvested wood products in comparison with the use of wood for energy—A case study on available forest resources in Canada. *Environ. Sci. Policy* 31, 96–108. doi: 10.1016/j.envsci.2013.03.007

Uihlein, A., Ehrenberger, S., and Schebek, L. (2008). Utilisation options of renewable resources: a life cycle assessment of selected products. *J. Clean. Prod.* 16, 1306–1320. doi: 10.1016/j.jclepro.2007.06.009

van der Weijde, T., Kiesel, A., Iqbal, Y., Muylle, H., Dolstra, O., Visser, R. G. F., et al. (2016). Evaluation of *Miscanthus sinensis* biomass quality as feedstock for conversion into different bioenergy products. *Glob. Change Biol. Bioenergy* 9, 176–190. doi: 10.1111/gcbb.12355

Velásquez, J. A., Ferrando, F., Farriol, X., and Salvadó, J. (2003). Binderless fiberboard from steam exploded *Miscanthus sinensis*. *Wood Sci. Technol.* 37, 269–278. doi: 10.1007/s00226-003-0182-8

Voigt, T. B. (2015). Are the environmental benefits of Miscanthus × giganteus suggested by early studies of this crop supported by the broader and longer-term contemporary studies? *Glob. Change Biol. Bioenergy* 7, 567–569. doi: 10.1111/gcbb.12150

Wagner, M., and Lewandowski, I. (2017). Relevance of environmental impact categories for perennial biomass production. *Glob. Change Biol. Bioenergy* 9, 215–228. doi: 10.1111/gcbb.12372

Weidema, B. P., Bauer, C., and Hischier, R. (2013). *The Ecoinvent Database: Overview and Methodology. Data Quality Guideline for the Ecoinvent Database Version 3.* Dübendorf: Swiss Centre for Life Cycle Inventories.

Whittaker, C., Hunt, J., Misselbrook, T., and Shield, I. (2016). How well does Miscanthus ensile for use in an anaerobic digestion plant? *Biomass Bioenergy* 88, 24–34. doi: 10.1016/j.biombioe.2016.03.018

Wolf, C., Klein, D., Richter, K., and Weber-Blaschke, G. (2016). Mitigating environmental impacts through the energetic use of wood: regional displacement factors generated by means of substituting non-wood heating systems. *Sci. Total Environ.* 569–570, 395–403. doi: 10.1016/j.scitotenv.2016.06.021

Progress on Optimizing Miscanthus Biomass Production for the European Bioeconomy: Results of the EU FP7 Project OPTIMISC

Iris Lewandowski[1]*, John Clifton-Brown[2], Luisa M. Trindade[3], Gerard C. van der Linden[4], Kai-Uwe Schwarz[5], Karl Müller-Sämann[6], Alexander Anisimov[7], C.-L. Chen[3], Oene Dolstra[3], Iain S. Donnison[2], Kerrie Farrar[2], Simon Fonteyne[8], Graham Harding[9], Astley Hastings[10], Laurie M. Huxley[2], Yasir Iqbal[1], Nikolay Khokhlov[7], Andreas Kiesel[1], Peter Lootens[8], Heike Meyer[5], Michal Mos[9], Hilde Muylle[8], Chris Nunn[2], Mensure Özgüven[11], Isabel Roldán-Ruiz[8], Heinrich Schüle[12], Ivan Tarakanov[7], Tim van der Weijde[3], Moritz Wagner[1], Qingguo Xi[13] and Olena Kalinina[1]

[1] Department of Biobased Products and Energy Crops, Institute of Crop Science, University of Hohenheim, Stuttgart, Germany, [2] Institute of Biological, Environmental and Rural Sciences, Aberystwyth University, Aberystwyth, UK, [3] Department of Plant Breeding, Wageningen University, Wageningen, Netherlands, [4] Dienst Landbouwkundig Onderzoek, Wageningen UR Plant Breeding, Wageningen, Netherlands, [5] Julius Kühn-Institut, Braunschweig, Germany, [6] ANNA - The Agency for Sustainable Management of Agricultural Landscape, Freiburg, Germany, [7] Department of Plant Physiology, Russian State Agrarian University–Moscow Timiryazev Agricultural Academy, Moscow, Russia, [8] Plant Sciences Unit, Institute for Agricultural and Fisheries Research, Melle, Belgium, [9] Blankney Estates, Blankney, UK, [10] The Institute of Biological and Environmental Sciences, University of Aberdeen, Aberdeen, UK, [11] Faculty of Agriculture and Natural Sciences, Konya Food and Agriculture University, Konya, Turkey, [12] German Agrarian Centre, Potash, Ukraine, [13] Dongying Agricultural Institute, Dongying, China

This paper describes the complete findings of the EU-funded research project OPTIMISC, which investigated methods to optimize the production and use of miscanthus biomass. Miscanthus bioenergy and bioproduct chains were investigated by trialing 15 diverse germplasm types in a range of climatic and soil environments across central Europe, Ukraine, Russia, and China. The abiotic stress tolerances of a wider panel of 100 germplasm types to drought, salinity, and low temperatures were measured in the laboratory and a field trial in Belgium. A small selection of germplasm types was evaluated for performance in grasslands on marginal sites in Germany and the UK. The growth traits underlying biomass yield and quality were measured to improve regional estimates of feedstock availability. Several potential high-value bioproducts were identified. The combined results provide recommendations to policymakers, growers and industry. The major technical advances in miscanthus production achieved by OPTIMISC include: (1) demonstration that novel hybrids can out-yield the standard commercially grown genotype *Miscanthus x giganteus;* (2) characterization of the interactions of physiological growth responses with environmental variation within and between sites; (3) quantification of biomass-quality-relevant traits; (4) abiotic stress tolerances of miscanthus genotypes; (5) selections suitable for production on marginal land; (6) field establishment methods for seeds using plugs; (7) evaluation of harvesting methods; and (8) quantification of energy used in densification (pellet) technologies with a range of hybrids with differences in stem wall properties. End-user needs were addressed by demonstrating the potential of optimizing miscanthus biomass composition for the production of ethanol and biogas

as well as for combustion. The costs and life-cycle assessment of seven miscanthus-based value chains, including small- and large-scale heat and power, ethanol, biogas, and insulation material production, revealed GHG-emission- and fossil-energy-saving potentials of up to 30.6 t CO_{2eq} C ha^{-1}y^{-1} and 429 GJ ha^{-1}y^{-1}, respectively. Transport distance was identified as an important cost factor. Negative carbon mitigation costs of −78€ t^{-1} CO_{2eq} C were recorded for local biomass use. The OPTIMISC results demonstrate the potential of miscanthus as a crop for marginal sites and provide information and technologies for the commercial implementation of miscanthus-based value chains.

INTRODUCTION

Miscanthus is a C4 perennial rhizomatous grass native to East Asia. The genus *Miscanthus* has its origins in the tropics and subtropics, but its various species are found over a wide climatic range throughout East Asia (Greef and Deuter, 1993). The remarkable ability of miscanthus to adapt to different environments (Numata, 1974) makes this novel crop suitable for production over a range of European and North American climatic conditions. Miscanthus was first cultivated in Europe in the 1930s, when it was introduced from Japan. Today it has become a leading candidate crop for production of lignocellulosic feedstocks for both bioenergy and material uses, thanks to its rapid biomass accumulation in temperate climates (Clifton-Brown et al., 2017).

Field experiments with the only genotype currently commercially available, *Miscanthus x giganteus*, a clone-based interspecies hybrid, have revealed its great photosynthetic efficiency, high biomass yield capacity, low input demands and good tolerance of temperate climates, and many of the characteristics that make miscanthus an ideal biomass crop (Lewandowski et al., 2000; Dohleman and Long, 2009; Heaton et al., 2010; van der Weijde et al., 2013; Davey et al., 2016). Analyses of the environmental impacts of miscanthus cultivation on a range of factors, including greenhouse gas mitigation, show that the benefits outweigh the costs in most cases (McCalmont et al., 2015). At present, only about 20,000 ha of miscanthus are commercially grown in the EU, mostly in the UK (10,000 ha), France (4000 ha), Germany (4000 ha), Switzerland (500 ha), and Poland (500 ha). There are several reasons for the low implementation and even decreasing cultivation area of miscanthus in Europe (Lewandowski, 2016).

Biomass production costs for miscanthus are presently too high to compete commercially with fossil fuels on an energy basis. The high biomass production costs for miscanthus result from insufficient development of agricultural production technology, accompanied by additional costs for agricultural inputs, land and labor for a relatively low-value biomass. Although they are amortized over a production period of 10–25 years, initial establishment costs for miscanthus are still comparatively high. This is because the only commercially available genotype *Miscanthus × giganteus* is a triploid hybrid that does not produce viable seeds. Consequently, costly establishment via

rhizome or *in vitro* propagation has to be performed (Xue et al., 2015). Miscanthus is also new to farmers and they have neither the knowledge nor the technical equipment to cultivate it. Thus, inefficient production technology is currently limiting its widespread uptake as a biomass crop.

There are no stable markets for miscanthus biomass and relevant applications are low-value. Farmers are hesitant to cultivate miscanthus because it involves dedicating their fields to long-term biomass production. They will only be willing to do this once biomass markets are stable or if long-term contracts are available (Wilson et al., 2014). The main use of lignocellulosic biomass from perennial crops is as a solid fuel for heat and power generation—a comparatively low-value use, its profitability being ultimately determined by the price of fossil fuels. In Europe, subsidies are generally necessary for bioenergy products to be able to compete in retail energy markets—with the notable exception of forest wood and forestry by-products that cannot be used for wood material products. Therefore, also higher-value applications for miscanthus biomass are required in order to provide attractive market options.

There are no miscanthus varieties adapted to different site characteristics and biomass use options. In Europe, *Miscanthus × giganteus* is the only genotype commercially available. Major barriers to the breeding of miscanthus varieties are the high costs involved and the long breeding periods, necessary because most yield- and quality-relevant parameters are not quantifiable until after the establishment phase of 2–3 years.

The EU project OPTIMISC (Optimizing Miscanthus Biomass Production) was initiated in 2012 with the objective of providing solutions to remove some of these barriers to miscanthus production. More specifically, the following research goals were the starting point for the OPTIMISC R&D activities (see also **Table 5**).

– Identification of novel miscanthus genotypes adapted to different climatic conditions and to adverse and marginal site conditions, such as cold, drought, and salinity;
– Improvement of productivity and yield stability of miscanthus;
– Reduction of biomass production and supply costs by demonstrating large-scale field production based on seeded hybrids and by optimizing harvesting regime and logistics;
– Improving marketing opportunities for miscanthus biomass by assessing genetic determinants of biomass quality,

identifying novel value chains and developing logistic technology;

– Optimization of miscanthus-based product supply chains in terms of costs and environmental performance.

To address these objectives, miscanthus bioenergy and bioproduct chains were optimized by trialing diverse germplasm types over a range of sites across central Europe, Ukraine, Russia, and China. The key traits that currently limit the potential of miscanthus were analyzed, high-value bioproducts identified and the combined results modeled to provide recommendations to policy makers, growers, and industry.

Here we provide a summary of the OPTIMISC project's achievements and discuss their relevance for the advancement of miscanthus development and its implementation.

MATERIALS AND METHODS

Figure 1 gives an overview of the organization of the research and development activities of the OPTIMISC project in different

work packages (WP). The overall project co-ordination was performed in WP1. Diverse miscanthus germplasm (provided by IBERS from Aberystwyth University, the Department of Plant Breeding from Wageningen University (WU), ILVO, Schwarz and the Dongying Agricultural Institute) was propagated (Work package 2; WP2) and experiments were conducted on different scales in laboratories, glasshouses, field plots and in pre-commercial scale field trials. About 100 genotypes were studied under controlled conditions to obtain insights into the available genetic variation in the miscanthus genepool for traits such as growth under low water input, saline conditions and low temperatures (WP3). Fifteen genotypes were screened on field sites in the UK, Germany, the Netherlands, Turkey, Ukraine, Russia, and China (WP4). Harvest systems designed to optimize biomass quality and costs were applied on large-scale farm demonstration trials with one to three genotypes (WP5). The composition of the biomass was investigated with regard to its quality for various energy supply chains and material uses (WP6). Yields and miscanthus-based value chains were modeled with the objective of identifying the best options for different climatic
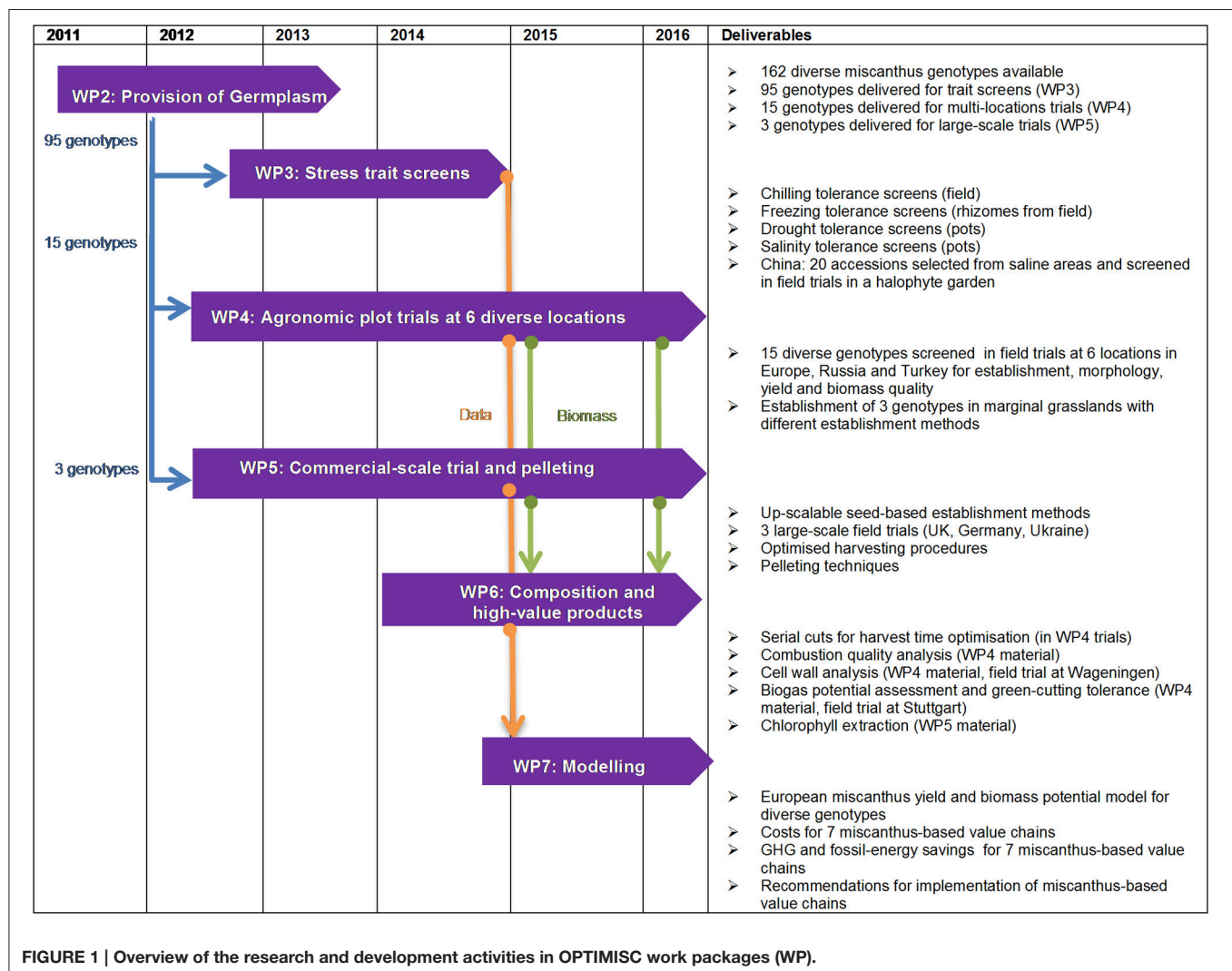
FIGURE 1 | Overview of the research and development activities in OPTIMISC work packages (WP).

settings and biomass uses (WP7). The following sections give a more detailed description of the methods of the experimental work packages.

Work Package 2: Provision of Germplasm and Plant Material

The objective of WP2 was to provide novel miscanthus germplasm to be screened in laboratory, glasshouse and field trials in WPs3, 4, and 5 (**Figure 1**).

Miscanthus germplasm was provided by several partners from the UK, the Netherlands, Germany, Belgium and China. **Table 1** summarizes the germplasm used by species and provider.

By 2013, about 95 miscanthus genotypes had been successfully transferred to *in vitro* culture, mostly from rhizome buds. However, several tests had to be performed to find the appropriate source material (rhizome pieces, stem segments, immature inflorescences, and seeds) and media compositions for all genotypes. The standard medium used for the storage of the plants was made by stirring a ready-mixed basic MS-medium, saccharose and the phytohormone BAP in distilled water. Clones were supplied as *in vitro* cultures by partner Schwarz to WP3-participating partners who then propagated them further *in vitro* to use in the trait screens in controlled environments in WP3.

A subset of 15 germplasm types (11 genotypes by clones, and 4 seed populations—a total of 22,200 plants) were produced for the WP4 multi-location trials. The clone-based genotypes were transferred from *in vitro* vessels to soil in multi-trays. These were covered with film for approximately 10 days to increase air humidity and to keep leaf transpiration low. High temperature (25°C) in the glasshouse in that period was also advantageous for root growth. The multi-trays were kept in the glasshouse for 3 weeks before the plants were sent to the WP4 partner locations. For the propagation of seed-based populations, seeds were sown

TABLE 1 | Miscanthus germplasm investigated in OPTIMISC and its origin.

Germplasm	Total	Provider*	Number of genotypes
Miscanthus × giganteus	1	Schwarz	1
Miscanthus sinensis	111	IBERS	6
		WU	100
		Schwarz	4
		ILVO	1
Miscanthus sacchariflorus	35	IBERS	15
		Dongying	20
Miscanthus hybrids (novel breeds)	16	IBERS	16
Total number of genotypes investigated	163		

*IBERS, Aberythwyth University (UK); WU, Department of Plant Breeding, Wageningen University (the Netherlands); Schwarz, Schwarz, Braunschweig (Germany), ILVO, Institute for Agricultural and Fisheries Research (Belgium); Dongying, Dongying Agricultural Institute (China).

into multi-trays and kept for 6 weeks in the glasshouse at 25°C before being sent to the WP4 partners.

In WP5, seed-based hybrids were sown in plugs under glasshouse conditions and planted at the sites in Blankney (UK) in 2012, and in Stuttgart (Germany) and Potash (Ukraine) in 2013. They were produced through a close collaboration between the OPTIMISC commercial partner Blankney Estates and Bell's nurseries in Lincoln, UK. Bell used vacuum sowing for the modules, which were then raised for 6 weeks in the glasshouse at 25°C. The seeds for plug plantings in 2013 were produced in German breeding nursery trials. Plug plants with 2–5 stems and about 20–30 cm height were transplanted using hand and mechanical planting systems.

Work Package 3: Stress Trait Screen in Controlled Environments and in the Field

The objective of WP3 was to identify miscanthus genotypes tolerant to abiotic stresses by performing screening for cold, drought, and salinity tolerance. Combining resilience traits through breeding is expected to result in future hybrids better suited to marginal conditions than the standard genotype *Miscanthus × giganteus* (*M. × giganteus*) (Fonteyne et al., 2016c). Trait screens were performed in controlled environments on chilling tolerance by the partner ILVO in Belgium, on drought by the partner IBERS in the UK, and on salinity by the partner DLO in the Netherlands. Chilling tolerance was screened in field trials and in a saline field by the partner ILVO in Belgium, and salinity tolerance in a saline environment in China by the partner Dongying.

Quantifying Variation in Low-Temperature Tolerance of (i) the Overwintering Rhizome (ii) Spring Growth

Ninety-five of 162 genotypes were successfully *in vitro* cloned for use in the abiotic stress experiments. Chilling and winter frost tolerance were tested by planting clones in the field (**Table 2**). In the first winter after planting, rhizomes were dug out and cleaned, cut into 10-cm lengths with at least one viable bud, and exposed to different freezing temperatures in a temperature-controlled bath. The rhizomes were left to thaw and then allowed to grow in optimal conditions. Frost tolerance was quantified by determining the temperature at which 50% of the rhizomes of each genotype were killed (LT_{50}). A total of 95 genotypes were tested for this trait. Shoot frost tolerance and winter survival were evaluated in field trials. Chilling tolerance (102 genotypes) was investigated by studying early vigor at the beginning of the growing season in field trials and by measuring growth under chilling stress in growth chambers. From these experiments, a number of growth traits were calculated (including longest shoot, no. of leaves and shoots, growth rate, leaf formation rate) and these traits were analyzed to determine which can best be used to describe early vigor and chilling tolerance, and which are most reproducible and useful to breeders.

Screens on Drought and Salinity Tolerance under Controlled Conditions

For the preferred protocol for screening for drought tolerance, *in vitro*-grown plants were transferred and established in soil

TABLE 2 | Overview of trait screen experiments.

Trait	No of genotypes screened	Method's	Location*	References
Chilling	56	Growth chambers	ILVO	Fonteyne et al., 2016a
Chilling—early vigor	102	Field trial (chilling tolerance trial)	ILVO, WP4 partners	
Frost—winter survival—shoot frost tolerance	102	Field trial (chilling tolerance trial, mini-plots trial, multi-location trial)	ILVO, WP4 partners	Fonteyne et al., 2016b
Frost—rhizomes	95	Rhizomes pieces temperature-controlled bath	ILVO	Fonteyne et al., 2016b
Drought	87	Greenhouse, pots and 1-m long plastic tubes	IBERS	van der Weijde et al., 2016b
Salinity	70	Greenhouse, hydroponics system	DLO	

*IBERS, University of Aberythwyth (UK); DLO, Wageningen University and Research Centre, Plant Research International (the Netherlands); ILVO, Institute for Agricultural and Fisheries Research (Belgium).

conditions (**Table 2**). After 1 year of establishment in soil, the senesced year-1 biomass was harvested in the spring. Like-sized, newly emerged tillers were subsequently selected per genotype ($n = 20$) once emerged, and grown in 5-inch pots (37 genotypes) and 1-m long pipes (50 genotypes), where water was withheld for 12 and 28 days, respectively. Half the plants were harvested at the end of the drought treatment. For the other half watering was resumed for a period of recovery. Growth measurements included leaf elongation of the newest emerging leaf, number of tillers, and fresh and dry weight of leaves, stems, and roots at the time of harvest. A subsequent similar evaluation of six selected genotypes exhibiting a variety of responses to drought stress included additional physiological traits: Stomatal conductance, stomata count, and maximum efficiency of photosystem II (Fv/Fm).

For evaluation of salt tolerance, 70 *in vitro*-grown genotypes were transferred to a hydroponics system in the greenhouse and grown under normal conditions as well as saline conditions (150 mM NaCl added to the growth medium) (**Table 2**). The salt treatment was continued for 3 weeks. During the stress period, tiller number, leaf elongation and leaf elongation rate, plant height, and chlorophyll content were measured, and senescence was visually assessed. At the end of the stress period, the plants were harvested and shoot and root fresh and dry weight determined. The dried samples were used for determination of ion contents (Na^+, K^+, Ca^{2+}, Cl^-, Mg^{2+}, SO_4^{2-}, PO_4^{3-}). A selected set of genotypes was further evaluated in pots. These included *in vitro*- and hydroponics-propagated plants, as well as plants started from rhizomes (collected in the field). Rhizomes were cut into pieces of similar size. The plants were subjected to normal conditions (no added salt), 150 and 250 mM NaCl salinity after 3 weeks of acclimation. The salt treatment was continued for 6 weeks, after which the plants were harvested. Leaves, stems, and root fresh and dry weights were determined at harvest, and the dry material was used for determination of ion contents (Na^+, K^+, Ca^{2+}, Cl^-, Mg^{2+}, SO_4^{2-}, PO_4^{3-}).

Field Trials in Halophyte Gardens in China

Twenty novel natural miscanthus germplasm types, selected under saline conditions in China and grown in pots from seeds, were planted in the field at Dongying in China in 2013. The field trials were designed as fully randomized blocks with three replicates. There were two trials at different sites, one with almost normal soil and the other with saline soil. The salinity levels, measured by electrical conductivity (EC), were 1–2 S/m at site A, and 2–8 S/m at site B. Growth parameters were measured throughout 2014.

Work Package 4: Multi-Location Agronomic Plot Trials

The objectives of WP4 were to screen novel miscanthus germplasm under field conditions in diverse European climates, and to establish miscanthus into marginal grasslands. Assessments were performed on the productivity and yield stability of these genotypes and to identify those that yield higher than the standard genotype *M. × giganteus*. Further, biomass samples for quality analysis were delivered to WP6 and data for yield modeling and cost and life cycle assessment to WP7.

Agronomic Plot Trials at 6 Locations in Europe, Turkey, and Russia

In 2012, 15 miscanthus types (see **Table 4** for description) were provided through WP2 for plot trials in Turkey near Adana, in Germany near Stuttgart, in Ukraine near Potash, in the Netherlands at Wageningen, in the United Kingdom near Aberystwyth, and in Russia near Moscow. At each site, three replicate 25 m² plots were planted with 49 plants (plugs) per plot (resulting in a density close to 2 plants per m²) in randomized blocks. For the remainder of this paper, the sites are referred to by the name of the nearest town. The six trial sites cover a wide range of climate and soil conditions (**Table 3**). The field trials were established mostly on arable or horticultural land except in Aberystwyth, where the trial was set up on marginal (low-quality) grassland.

Before planting out the plugs, the ground was prepared as follows: Weeds were removed with glyphosate or by mechanical methods, inversion plowed and harrowed or rotivated to produce a fine tilth. The plugs were planted between 15 and 25 May 2012 at all sites and watered to provide a good hydraulic

TABLE 3 | Location characteristics and previous land use of the six OPTIMISC field trials established in May 2012.

Country	Location name	Latitude	Longitude	Altitude (m)	Previous land use	Annual air temperature,°C	Annual rainfall, mm
Turkey	Adana	37.00	35.00	27	Arable	19.0	575.2
Germany	Stuttgart	48.74	8.93	463	Arable	9.8	725.4
Ukraine	Potash	48.89	30.44	237	Arable	8.9	537.2
Netherlands	Wageningen	51.59	5.39	10	Horticultural	10.3	826.4
UK	Aberystwyth	52.43	−4.01	39	Grassland	9.7	1038.1
Russia	Moscow	55.50	37.33	140	Arable	4.1	644.0

TABLE 4 | Miscanthus genotypes used in plot-based field trials.

Genotype ID	Provider	Species	Propagation Method
OPM-01	IBERS	*Miscanthus*	*In vitro tillering to*
OPM-02	IBERS	*sacchariflorus*	*produce plug plants*
OPM-03	IBERS		
OPM-04	IBERS		
OPM-05	IBERS	*M. sinensis × M.*	*In vitro tillering to*
OPM-06	IBERS	*sacchariflorus* hybrids,	*produce plug plants*
OPM-07	IBERS		
OPM-08	IBERS		
OPM-09	IBERS	*Miscanthus ×*	
		giganteus	
OPM-10	Schwarz	*M. sinensis × M.*	
		sacchariflorus hybrids	
OPM-11	IBERS	*Miscanthus sinensis.*	*In vitro*
OPM-12	IBERS		Seedlings raised in
OPM-13	WUR		plugs
OPM-14	WUR		
OPM-15	IBERS		

contact between the soil and plug. Post-planting herbicide was not applied in the first year, and weeds were controlled mechanically.

In the first year (2012), fertilizer was applied at all the sites at rates of 44 and 110 kg ha^{-1} phosphorus (P) and potassium (K), respectively. No nitrogen (N) fertilizer was applied that year to avoid stimulating weed growth. In the following year, fertilizer was applied at a rate of 100 kg ha^{-1} P, 140 kg ha^{-1} K and 60 kg ha^{-1} N to ensure non-limiting crop nutrition at all sites.

A drip irrigation system was installed in Turkey. Irrigation amounts in years 1 and 2 (2012 and 2013) were 75% of evapotranspiration (ETp). In years 3 and 4, irrigation levels were lowered to 25% of ETp, to help identify the most drought-tolerant germplasm.

Yields were estimated in the spring following the growing season by harvesting nine plants in the middle of the plots (4.6 m^2) at a cutting height of 5 cm above the soil surface. Subsamples were weighed and oven-dried to calculate yield as tons of dry matter per hectare.

Establishment of Miscanthus in C3 Grasslands

The effects of different planting and mowing regimes on miscanthus establishment in grassland and yields in the mixed grassland/miscanthus production systems were assessed in trials established on marginal land near Stuttgart, Germany.

Two field trials were established in May 2012. One on high-productivity (nitrogen-rich) grassland and the other on low-productivity grassland (marginal land, nitrogen-poor soil). A split-split-plot design with four block-replicates was adopted. Each main plot occupied 30.6 m2 and was treated by one of the two establishment regimes (Er1 = cutting the existing grassland vegetation to a height of 5 cm; Er4 = Er1 + spraying herbicide in strips of 20-cm width with a distance of 0.71 m between strips). The secondary treatments consisted of three different cutting frequencies (one, two or three biomass harvests per growing season), which were applied to the 10.2 m^2 sub-plots within each main plot, starting from the second growing season. In each sub-plot, three different genotypes of *Miscanthus sacchariflorus* (*M. sacchariflorus*) were planted. Additionally, in each treatment, one sub-sub-plot of grassland without miscanthus planted was used as a control for biomass yield comparisons. In addition to these three main genotypes, one standard *Miscanthus sinensis* (*M. sinensis*) clone "Goliath" and one more *M. sacchariflorus* genotype were included in the trials.

The following factors were assessed: Miscanthus plant mortality; miscanthus and grass biomass yield; and a number of phenotypic traits reflecting miscanthus growth and development.

To address biodiversity issues, a vegetation analysis was performed in the two trials established at the university's experimental station: In 2012, before planting the miscanthus, and in 2016, 4 years after planting. In particular, species abundance (according to a multilevel cover-abundance scale; van der Maarel, 2007), species richness (the number of species present) and total canopy cover were recorded for every sub-sub-plot.

Work Package 5: Commercial-Scale Trial and Pelleting

The objective of WP5 was to provide data on large-scale miscanthus production for cost assessment and LCA in WP7, to demonstrate large-scale establishment of seed-derived plugs and to identify optimized harvesting and pelleting technologies.

In UK, a large-scale trial was established in 2012 in a marginal field at Blankney, Lincoln. Four replicate plots of 0.25 ha were planted with four seed-based hybrids and the clone *M. ×*

giganteus (resulting in 20 plots, with an area of 5 ha). Over-winter survival rates were 97% for the plug plants, higher than for rhizome-propagated *M. × giganteus*. In the second and third years, subplots (sets of rows) were used to investigate herbicide treatments for weed control.

In Germany, a large-scale trial was planted in 2013 at Ihinger Hof field station near Stuttgart with 0.6 ha of the *M. sinensis* population hybrid OPM-111, using the "Checci & Magli" four-row plug planter. Strip plots were used to assess herbicide treatments to improve weed control in miscanthus.

In Ukraine, a large-scale trial was established in 2013 at German Agrarian Center (DAZ) in Potash with three replicates using plugs of OPM-111 and OPM-112 and rhizomes of *M. x giganteus*. In total 23,593 seedlings and rhizomes were planted on a total area of 1.26 ha. Plant losses after transplanting and in first winter were less than 5%.

Yield and quality traits were determined at each site and in the spring following the previous growing season. Additionally, in the UK harvesting techniques (direct chipping and mowing and baling) were compared for speed, yield and quality parameters in the spring following the third growing season. Harvested samples were used for pelleting trials to measure energy requirements at each biomass-formatting step needed to create pellets.

Data from these large-scale trials, combined with commercial knowledge of *M. × giganteus* from the company Terravesta, were used to assess the costs and benefits of these methods on the environment and economics of growing the crop (WP7).

Work Package 6: Composition and High-Value Products

The main goal of WP6 was to identify high-yielding miscanthus genotypes with biomass qualities suited to different biobased products. End-use applications assessed included bioethanol, biogas, combustion, and fibreboards.

Data from sequential harvests in the multiple-locations trials in Germany, Russia, and Turkey (WP4) were used to model the quality and yield development of different genotypes at different harvest times.

Analysis of Combustion Quality

The autumn and spring harvests of the third and fourth year stands of the multi-location trials (WP4), as well as the biomass from sequential harvests from the multiple-locations trials in Germany, Russia, and Turkey (WP4) were analyzed for quality parameters relevant for combustion. These include the contents of ash, potassium (K), chloride (Cl), phosphorus (P), and nitrogen (N). Analytical methods are described by Iqbal and Lewandowski (2016).

Cell Wall Analysis and Biogas Potential

The plant cell wall composition of all genotypes used in OPTIMISC was analyzed in various experiments and correlations with the quality for different biobased applications were evaluated. Three new field trials were established to study the interplay between cell wall composition and saccharification yield as a measure of bioethanol production (van der Weijde et al., 2016a, 2017), combustion quality (van der Weijde et al., 2017),

biogas yield (Kiesel and Lewandowski, 2017; van der Weijde et al., 2017), and cutting tolerance of the different miscanthus genotypes (Kiesel and Lewandowski, 2017). Additionally the effects of abiotic stresses and geographic location on biomass quality were studied using the material harvested in the multi-location trials (WP4) and the abiotic stress tests (WP3) (van der Weijde et al., 2016b).

Chlorophyll and Protein Extraction

The chlorophyll and protein production potential of the stay-green OPM-111 *M. sinensis* hybrid planted at all three large-scale trial locations (WP5) was quantified for in-season and end-season harvests. Chlorophyll was extracted using the Soxhlet method. Total protein analysis was performed according to the Kjeldahl protocol.

Work Package 7: Modelling (Yield, LCA, Costs)

In this work package, the MiscanFor model was extended to create a European miscanthus yield and biomass potential model for diverse genotypes. The MiscanFor model was originally developed using experimental data available in 2008 from multi-location trials with the only commercially planted miscanthus clone *M. × giganteus*. In the third and fourth growing seasons after planting the WP4 multi-location trials, regular measurements were taken to quantify "in season" growth curves for green leaf area index, radiation intercepted by the canopy and standing biomass. New parameters for process descriptions between thermal time (degree days) and green leaf area index; and accumulated radiation intercepted and yield were derived from ten genotypes from 4 out of the 6 locations. These new growth and climate data sets expand those currently available for *M. x giganteus*. These data improve the model parametrization for *M. × giganteus* over a wider climatic range and extend the model to include a range of germplasm types and novel hybrids with commercially relevant traits.

A cost and life cycle assessment (LCA) was performed for seven selected miscanthus-based product chains. For this purpose, data from field trials in WP4 and 5 were used. The LCA was performed using the Gabi 5 Software. The overall biomass transport distance was assumed to be 400 km when bales were transported to the bioethanol plant or to the plant producing insulation material as well as in the value chain "Combined heat and power (CHP) bales." For the value chains "CHP pellets" and "Heat pellets" the bales were transported 100 km to a pelleting plant and from there the pellets were transported 400 km to the power plants. The average farm-to-field distance was assumed to be 2 km. This transport distance is also assumed for the value chain "heat chips" in which a utilization of the chips as a biomass fuel on the producing farm was assumed. Because of the higher biomass requirements of the biogas plant an average transport distance of 15 km from field to plant was assumed.

RESULTS AND DISCUSSION

The results of the various research activities are summarized in **Table 5**. These are then discussed, focusing on their relevance

TABLE 5 | Overview of development needs for miscanthus, how these were approached and relevant results.

	Development need	Development approaches	Main results
Growing the crop	Adaptation to different climatic conditions and to adverse and marginal site conditions	Provision (WP2) and evaluation of new breeding material (WP3, 4, 5, 6)	More than 160 miscanthus genotypes were provided for screening under field and controlled conditions. *M. sinensis* is more difficult to *in vitro* culture than *M. sacchariflorus* and their hybrids. Improvements in *in vitro* tillering methods included new surface sterilization approaches for a rhizome, node and flower meristems. Protocol adaptation and persistence achieved > 70% success rate for transfer of germplasm to *in vitro*.
		Better understanding of genotype x environment interactions (WP4, 5)	Recommendations for optimal choice of genotypes for all European regions.
			Northern Europe: OPM-08, -06, -10, -09
			Central Europe: OPM-09, -10, -06, -03
			Southern Europe: OPM-11, -14, -02, -03
		Develop chilling and frost tolerant genotypes (WP3) to: a) Extend productive range of miscanthus to the north and east b) Improve establishment and overwintering success c) Breed genotypes with a longer growing season	Genotypes identified with relative tolerance to chilling and frost and with high early vigor, which have potential for cultivation in regions further north and east and as starting material for breeding.
			M. sinensis and *M. sinensis x sacchariflorus* hybrid genotypes were more frost tolerant than *M. sacchariflorus* genotypes and *M. x giganteus*.
		Develop water-use efficient and water-stress tolerant genotypes (WP3) to: a) Extend the productive range for miscanthus further south b) Provide genotypes for marginal land	*M. × giganteus* has medium tolerance in terms of maintaining biomass production under drought, but recovers well when water is re-applied.
			Several genotypes were identified with improved yield compared to *M. × giganteus* under water-limiting conditions and with improved recovery potential after drought.
			A few genotypes are very high yielding under drought conditions despite only having medium drought tolerance. These genotypes may not perform so well under continuous drought. Of 7 genotypes with drought yields significantly higher than *M. x giganteus,* only 3 are in the top 10 in terms of drought tolerance. These may be suited to more southerly locations.
			Drought tolerance mechanisms include reduced water loss, such as leaf rolling, and water seeking strategies such as increased root to shoot ratio.
		Develop salinity-tolerant genotypes (WP3) for marginal land	Genotypes identified with high yields under both optimal and saline conditions.
			Starting material for breeding for salt tolerance through improved ion-exclusion activity.
			M. sacchariflorus and *M. sinensis* genotypes show salinity tolerance through mechanism of salt exclusion.
			Land areas with soil electric conductivity (EC) up 2.5 S/m suitable for miscanthus production.
		Develop establishment methods for marginal land and grasslands	In Germany, 80% establishment success rate for miscanthus into C3 grassland was achieved with both a no-till method and conventional pre-planting disturbance (i.e. mowing or herbicide spraying applied before planting miscanthus).
			Competitive miscanthus genotypes with tall, thick shoots to be chosen for establishment in grassland.

(Continued)

TABLE 5 | Continued

	Development need	Development approaches	Main results
	Reduction of biomass production costs	Target the development of genotypes that can be established via seeds (WP2, WP5)	Commercially scalable protocols for plug planting seed-based hybrids were developed. (The project produced 100,000 plants needed for large-scale trials in three locations: UK, Germany and Ukraine).
		Identify more winter-hardy genotypes to reduce or avoid over-winter losses (WP3)	See above
		Reduce the input demands, e.g. nitrogen fertilization, of biomass production	As expected, significantly lower nutrient offtake in early senescing genotypes. This reduces the fertilizer offtake and increases biomass quality when used for heat production. Unexpectedly, leaf share not always linked to offtakes at harvest.
	Improvement of yield and biomass supply stability	Identify high-yielding genotypes adapted to different climatic conditions (WP4)	Several genotypes were identified with high yields (exceeding that of *M.* × *giganteus*) under different climatic conditions. In particular, OPTIMISC has helped identify genotypes suitable for cultivation in climatic extremes: in colder climates (Moscow), in hot climates with low water availability (Adana) and on marginal land (Aberystwyth).
		Increase yields of valuable biomass co-products (WP5, 6)	Chlorophyll and protein can be extracted before biomass goes to biogas production.
Harvesting	Reduction of harvest and logistic costs	Reduce harvest, logistic and drying costs by selection of genotypes with dry biomass at harvest (WP4, 5). Reduce pre- and post-harvest losses (WP 5)	Direct chipping with a 7.5-m cutter on a self-propelled forage harvester was the most time-efficient cutting method. However, in climates with mild winters and inadequate senescence, the indirect mowing and baling methods are more scalable due to more efficient transport and storage.
	Optimization of harvest time in terms of quality and reduction of harvest losses	Select genotypes with improved senescence patterns for dry harvestable biomass (WP4, 6)	Significant GxE (Genetic x Environment) interaction for senescence was observed. The interspecies hybrids tested senesced earlier than wild types.
Connecting to market	Biomass quality suitable for purpose of user	Understand genetic variation and effect of drought on biomass quality performance (WP 3, 6)	GxE interaction for biomass quality relevant for combustion and production of ethanol and biogas.
			Drought has a negative effect on yield but a positive effect on biomass quality. Developing drought resistant genotypes would create opportunities for growing high-quality miscanthus biomass on marginal soils (in particular dry areas).
		Diversity in biomass quality of miscanthus genotypes	There are large differences in biomass quality, and consequently performance in different chains, e.g. bioethanol and biogas, among miscanthus genotypes.
			Many genotypes have been identified with better biomass quality than *M.* × *giganteus*.
	Development of novel value chains	Biogas production was identified as a promising value chain for miscanthus biomass (WP6). *Miscanthus* × *giganteus* and novel genotypes showed high and promising potential.	October was identified as optimum biomass harvest date for Central Europe due to a very high biogas potential and sufficient cutting tolerance.
			Novel genotypes showed significantly higher specific biogas/methane yield (up to 520 ml/g DM) than *M.* × *giganteus*.
	Optimization of biomass supply chain	Develop logistics for the supply of transportable, storable and tradeable biomass (WP5)	Shorter hybrids with thinner stems had the benefits of lower moisture content (13%), higher bale weights (500 kg for *M.* × *giganteus*, vs. 650 kg) with less string breakages and ca. 20% power to pellet. However, compared to *M.* × *giganteus*, lower yielding and the pellets are 5% less dense.

(Continued)

Development need	Development approaches	Main results
		Pellets: highest bulk density for _M. × giganteus_ biomass (OPM-09) at 810 g/l and the lowest for OPM-12 at 664 g/l.
		All miscanthus genotypes can be pelleted. _M. × giganteus_ most difficult to pellet due to hard, stiff stems. _M. sinensis_ OPM-12 best to pellet genotype.
		Pelleting costs 40–80 Euro/ton pellets.
Optimization of miscanthus-based product chains	Identify cost-optimized and environmentally benign miscanthus-based product chains (WP7).	Up to 25 t (small-scale combustion, chips) and 31 t (insulation material) CO_{2eq}./ha*a savings.
		In Central Europe cost of fuel for domestic small-scale combustion ($\leq$ 2 ct/kWth) compete well with other fuels.
		Lowest carbon mitigation costs of -78 Euro/t CO_{2eq}. avoided for local small-scale combustion of chips.

These are listed from top to bottom along the production to utilization chain.

for the advancement of miscanthus and implementation of miscanthus-based value chains.

Options for Producing Miscanthus in Different Climates and on Marginal Land

This section presents the results of testing novel miscanthus germplasm in comparison to _M. × giganteus_ over a wide range of European climates and also recommendations for miscanthus production on marginal land.

Yield Performance of Novel Miscanthus Genotypes over a Wide Range of Climatic Conditions in Europe, Ukraine, Russia, and Turkey

Some of the trial locations represented marginal (limiting) growth conditions for miscanthus. In particular, the field trial in Adana (Turkey) exhibited the highest air temperature and driest soil conditions among the OPTIMISC experiments, and the trial in Moscow (Russia) represented the coldest location with cold winter temperatures, late spring frosts and longer summer photoperiod than at the other sites. The Moscow site also suffered a summer drought in 2014.

As part of the OPTIMISC multi-location trial (WP4), 15 genotypes were planted on a marginal land site at Aberystwyth (UK). This field site was formally grassland, with low nutrient levels and shallow soils. Additionally, the growing season temperatures and radiation levels in cool wet summers here delay establishment rates. The shallow soils lead to rapid changes in soil moisture levels, with flooding conditions after rainfall and drought stress in summer. The high stone content of the soil made miscanthus establishment difficult.

The more challenging growth conditions at these sites resulted in lower miscanthus yields at Aberystwyth and Moscow than at the other four locations. The drought at the Mediterranean site Adana caused the miscanthus to start senescing in July and therefore only dry matter (DM) yields of up to 15 t/ha*a could be harvested here. The highest DM yields (up to 20 t/ha*a harvestable biomass in early spring) were achieved at Potash/Ukraine, where good clay-rich soils and good water supply prevailed. The south German site Stuttgart is characterized by low soil depth (on average 60 cm soil horizon) and encountered a drought in summer 2015. It was only possible to harvest up to 18 t DM/ha*a here.

Apart from the Ukrainian site Potash, miscanthus genotypes with yields exceeding that of _M. × giganteus_ (OPM-09) were identified at all sites. These were either other _M. sinensis × M. sacchariflorus_ hybrids (Moscow, Aberythwyth, Wageningen, Stuttgart), _M. sacchariflorus_ (OPM-02, Stuttgart) or _M. sinensis_ (Adana).

We therefore conclude that new genotypes are available that can out-perform _M. × giganteus_, especially on marginal lands.

Table 6 gives a ranking of genotypes according to yield and yield stability. Both absolute yield (top panel) and yield stability (lower panel) are important factors in selection.

Table 7 gives recommendations for the use of different genotypes, with reasons, based on field observation. _M. sacchariflorus_ types are characterized by spreading rhizomes, which can lead to escape of the crop. Overall, _M. sacchariflorus_ types tested here are only recommended for southern European sites with irrigation or no susceptibility to drought. _M. sinensis × M. sacchariflorus_ hybrids, including _M. × giganteus_, are recommended for most areas of Europe (OPM-09, OPM-10) or northern Europe (OPM-08), mainly on account of their high yields.

The _M. sinensis_ type OPM-11 is recommended here for Mediterranean areas, where it can make best use of the spring period before the onset of summer droughts (**Table 7**).

The potential miscanthus growing area for Europe was modeled based on measurements of field performance of the genotypes OPM-01 to OPM-15. Compared to a scenario where only the genotype _M. × giganteus_ is available (**Figure 2A**), a large potential expansion of the miscanthus growing area to the east, south and north of Europe is predicted for a scenario where the genotypes screened in OPTIMISC can be grown commercially (**Figure 2B**).

TABLE 6 | Yield ranking across the six sites, in the first 3 years (spring harvest years) after planting miscanthus.

Largest biomass yield (mean yield across three plots)	2013	2014	2015
Best Yield	OPM-09	OMP-06	OPM-06
Second Best Yield	OMP-06	OPM-09	OPM-09
Best Yield Adana	OPM-09	OPM-09	OPM-09
Best Yield Stuttgart	OPM-01	OPM-03	OPM-06
Best Yield Potash	OPM-06	OPM-06	OPM-02
Best Yield Wageningen	OPM-06	OPM-09	OPM-08
Best Yield Aberystwyth	OPM-08	OPM-08	OPM-08
Best Yield Moscow	OPM-06	OPM-06	OPM-06
Least yield variability (Coefficient of Variablility)	**2013**	**2014**	**2015**
Best CoV	OPM-11	OPM-06	OPM-10
Second Best CoV	OPM-06	OPM-10	OPM-06
Best CoV Adana	OPM-09	OPM-09	OPM-10
Best CoV Stuttgart	OPM-02	OPM-07	OPM-05
Best CoV Potash	OPM-12	OPM-01	OPM-04
Best CoV Wageningen	OPM-04	OPM-15	OPM-13
Best CoV Aberystwyth	OPM-15	OPM-11	OPM-08
Best CoV Moscow	OPM-12	OPM-13	OPM-02

TABLE 7 | Recommendations for the choice of miscanthus genotypes for different European regions.

Genotype ID	Recommended	Reason
OPM-01 (*M. sac*)	No	Poor yields, spreading (creeping) rhizome.
OPM-02 (*M. sac*)	Sometimes	Only in southern Europe with irrigation where drought possible. Excellent yield but requires high temperatures and susceptible to drought. Has spreading rhizome but can be managed by mowing field plot borders once or twice mid-season.
OPM-03 (*M. sac*)	Sometimes	Mainly in southern Europe with irrigation where drought is possible; also possible for Central Europe. High yielding in some locations. It has a spreading rhizome but can be managed by mowing field plot borders once or twice mid-season.
OPM-4 (*M. sac*)	No	Poor yields and a spreading rhizome.
OPM-05 (*M. sac* × *M. sin*)	No	Acceptable yield but out-performed by similar hybrids.
OPM-06 (*M. sac* × *M. sin*)	Yes	Central and eastern parts of northern Europe. Excellent yields but lodging crop not acceptable to farmers.
OPM-07 (*M. sac* × *M. sin*)	No	Poor yields.
OPM-08 (*M. sac* × *M. sin*)	Yes	Northern Europe. Excellent yields at the cooler sites.
OPM-09 (*M. x gig*)	Yes	Most of Europe. Excellent yields generally sufficient for large areas of Europe, especially with the projected climate changes of warmer wetter winters, which is consistent with the years these trials were conducted. Limited by clonal propagation.
OPM-10 (*M. sac* × *M. sin*)	Yes	Most of Europe. Excellent yields and low moisture content at harvest on account of early senescence.
OPM-11 (*M. sin*)	Yes	Southern Europe. Good yields at the locations with warm summers and frequent droughts (this clone did not perform well in Aberystwyth or Moscow).
OPM-12 (*M. sin*)	No	This seeded germplasm entry is heterogeneous. It flowers too early to attain high yields. It produces viable seeds. (In the WP4 trials, establishment problems were largely linked to logistical issues around planting, rather than being a reflection of germplasm establishment ability.)
OPM-13 (*M. sin*)	Yes	Potential in areas with warm summers and drought. Advantages: seed-based and non-creeping. More homogeneous than OPM-12 and OPM-15. Generally lower yielding than interspecies hybrids. It was less susceptible to drought conditions in Turkey.
OPM-14 (*M. sin*)	Yes	Southern Europe. Similar to OPM-13, but on average slightly lower yielding.
OPM-15 (*M. sin*)	No	As for OPM-12. This seeded germplasm entry is heterogeneous. It flowers too early to attain high yields. It produces viable seeds.
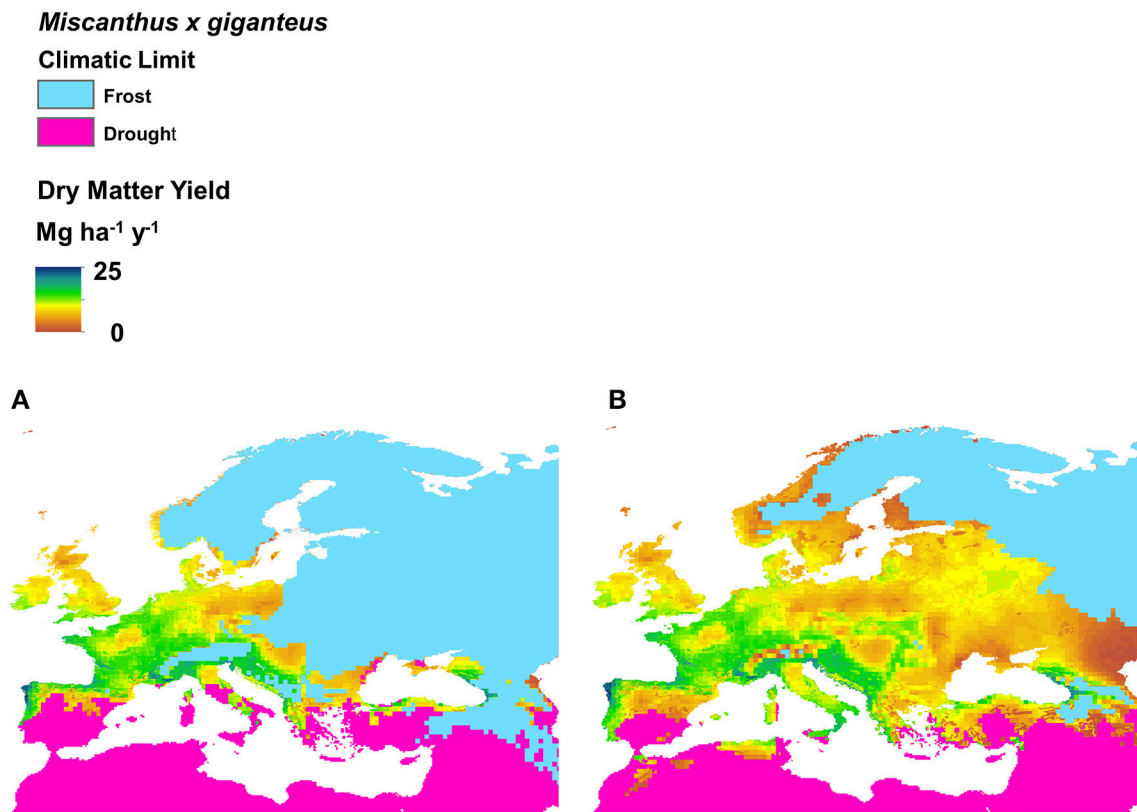
FIGURE 2 | Bioclimatic envelope of *Miscanthus* × *giganteus* showing limit of frost and drought tolerance. Excluded area is shown in light gray. Left **(A)** shows the original Hastings et al. (2009) bioclimatic envelope and right **(B)** shows the revised estimation of the bioclimatic envelope for *M.* × *giganteus* and the new trialed hybrids resulting from the research in this project. The crop yield prediction for *M.* × *giganteus* is displayed on a scale from 41 Mg ha^{-1} (black) to 0 Mg ha^{-1} (gray). Both bioclimatic envelopes are based on recent climate data (2000 to 2009) and FAO/IGBP plant-available water estimates on a 5-min grid. The new cold limit considers the data from in-field soil temperature measurements and the overwinter survival success. The new drought limit is based on observed in-field drought responses and water balances with estimates of plant-available water derived from depth and soil textures measurements. This high-level analysis does not identify the marginal lands within the grids where the yields may be lower than those indicated.

Identification of Stress-Tolerant Miscanthus Genotypes

One important result from the OPTIMISC project is the expansion of the potential miscanthus production area in Europe (as shown in **Figure 2**). This is achieved mainly by the successful identification of stress-tolerant genotypes for biophysically marginal cultivation conditions in WP3. Biophysical marginality is often caused by the abiotic stresses of water shortage, unfavorable temperature or poor soil conditions, including salinity.

The evaluation of stress tolerance in plants is not straightforward, as it is strongly affected by environmental conditions. Therefore, we focused on finding relevant traits and mechanisms for four abiotic stressors that are relevant to miscanthus cultivation (drought, salinity, chilling, and frost), assessing genetic diversity in a range of cultivars and breeding material, and identifying traits that can be used for selection and improvement of miscanthus cultivation on marginal lands. At the same time, genotypes were selected that are expected to have a relatively high production under marginal conditions where they experience drought, salt, chilling, and/or frost stress.

Drought

The response to drought and recovery after drought differs between and within species. Recovery potential is likely to be of critical importance for yield under conditions with regular drought spells. As this is a likely climate-change scenario, recovery should be part of any drought tolerance evaluation for miscanthus.

Among the genotypes tested, some produced high biomass yield under both well-watered and drought conditions. Other genotypes were not high yielding under well-watered conditions, but showed only a small reduction in yield under limited water availability. While it is tempting to speculate that these would be potential sources of drought-tolerance traits to be utilized in breeding programs, it is important to exclude genotypes that require less water simply due to their small size and slow growth.

Several of the genotypes screened demonstrated a harvestable biomass yield greater than that of the standard *M.* × *giganteus* (OPM-09). Four of the genotypes that produced more biomass than *M.* × *giganteus* under control conditions were also among the most drought-tolerant genotypes (maintaining a high

percentage biomass under drought): OPM-06 (hybrid), OPM-25 (*M. sacchariflorus*), OPM-77 (*M. sinensis*), and OPM-27 (*M. sacchariflorus*). A further 10 genotypes showed medium tolerance (OPM-05 (hybrid), OPM-86 (*M. sinensis*), OPM-38 (*M. sinensis*), OPM-69 (*M. sinensis*), OPM-02 (*M. sacchariflorus*), OPM-19 (*M. sacchariflorus*), OPM-20 (hybrid), OPM-23 (*M. sacchariflorus*), OPM-07 (hybrid), and OPM-39 (*M. sinensis*) and also exceeded *M. × giganteus* yield under control conditions. These 14 genotypes had higher yields than *M. × giganteus* in both drought and well-watered conditions. A single drought-susceptible genotype [OPM-50 (*M. sinensis*)] yielded more than *M. × giganteus* when watered but not under drought, emphasizing the importance of biomass yield *per se* as opposed to maintaining biomass yield in a smaller plant. Of the 10 highly tolerant genotypes (in terms of maintained biomass yield), 5 also demonstrated relatively high maintained soil moisture. This indicates that these plants are water-use efficient and are able to maintain biomass production without depleting soil moisture. Of the 14 genotypes that outperformed *M. × giganteus* under control and drought conditions, five were *M. sacchariflorus*, five were *M. sinensis* and four were hybrids (van der Weijde et al., 2016b).

It should be noted that different traits may be of more or less importance depending on the timing and severity of the drought stress, and that it is a combination of traits that provided tolerance under the conditions applied in this experiment. While growth cessation and damage protection may be good strategies to withstand the adverse effects of a relatively short but severe drought, long-term mild droughts were not tested in this study. It remains to be seen whether the same genotypes are productive under such conditions, or whether traits enabling the maintenance of growth may be more favorable.

Salinity

Saline soils affect crops in two ways: It induces water shortage due to osmotic stress and accumulation of salt in the plant can have toxic effects.

In our screen, we found indications that miscanthus uses two mechanisms to mitigate the effects of salinity. The best performing genotype (OPM-56, *M. sinensis*) utilizes a mechanism that actively keeps the ions from accumulating in the leaves, thus minimizing damage to essential physiological processes like photosynthesis. This mechanism is known as salt exclusion, and is known to be able to confer salt tolerance to rice and wheat (Munns et al., 2012). The causal gene in these two cereal crops is HKT1; 5, an ion transporter that takes Na^+ out of the xylem and into the parenchyma cells in the roots, avoiding Na^+ accumulation in the leaves. This is a strategy that can be effectively selected for by measuring ion contents in the leaves of plants. In addition, it would be interesting to target the HKT1; 5 gene in miscanthus as the causal gene for this mechanism. Further exploration in miscanthus germplasm to identify the most effective alleles of this gene and for the Na^+ exclusion mechanism is therefore recommended. In view of the quality of harvestable yield, the salt exclusion mechanism may also be preferred. High concentrations of ions are known to interfere with combustion quality, and may be a problem for

saline cultivation of miscanthus. Improving salinity tolerance by improving salt exclusion properties enhances yield under saline conditions, and at the same time improves product quality.

Field trials were performed with the genotypes *M. × giganteus* (OPM-09), OPM-01, -03, -06, -08, and several *M. sacchariflorus* genotypes, selected from marginal and saline land in North-East China. The trials revealed that *M. × giganteus* is not suitable for saline land. Different *M. sacchariflorus* genotypes proved salinity-tolerant. The yield declined with increasing soil salt electrical conductivity (EC) values. A soil EC value under 2.5 had little effect on yield, but at a soil EC above 3 yields decline dramatically. Compared to slightly saline land (average EC of 1.10) the yields of the most salinity- tolerant genotypes on the heavily saline site (average EC of 3.85) declined by 30–55% in the second stand year.

In conclusion, the highest-yielding genotypes under controlled conditions (especially *M. sinensis* OPM-56) have potential to grow in saline soils, and should be tested under field conditions. In addition, several of the *M. sacchariflorus* genotypes tested in the field can be recommended for growth under saline soil. Land areas with a soil EC value up to 2.5 are suitable for miscanthus production.

Low Temperature

A small number of genotypes were analyzed for photosynthetic and biochemical traits, which are likely to be linked to chilling tolerance. These revealed large variations for both trait types (Mortaignie, 2014; Fonteyne et al., 2016a). This indicates that a combination of these traits may in fact enhance chilling tolerance and can be targeted for combined selection (Fonteyne et al., 2016a). Outdoor evaluation of chilling tolerance indicated a wide variation in the germplasm and that emergence of first shoots, time to reach 50 cm shoot length and early growth rate are good parameters for large-scale chilling tolerance evaluation.

Frost tolerance evaluation of a set of miscanthus genotypes was performed using potential marker traits such as moisture content, ion leakage and phenological characteristics. None of these markers was strongly correlated to frost tolerance. The best marker trait to determine frost tolerance turned out to be the LT_{50} in artificial rhizome freezing tests. The LT_{50} can be directly related to winter survival (Clifton-Brown and Lewandowski, 2000). Mechanisms underlying freezing tolerance in miscanthus are still elusive, but may be linked to production of specific metabolites and molecules that stabilize cell structures, most notably membranes, under freezing conditions (Thomashow, 1999).

In general, the hybrid genotypes were more frost-tolerant and the *M. sacchariflorus* and *M. × giganteus* genotypes were less frost-tolerant. On average, the *M. sacchariflorus* genotypes had a significantly higher LT_{50} than the hybrids, while the *M. sinensis* genotypes were not different from either group, but genotypes with higher frost tolerance than *M. × giganteus* were found in all species groups.

Stress-Tolerant Genotypes in the Wider Context

Based on our observations, the miscanthus genotypes tested under various conditions display a wide range of variation in response to abiotic stresses, but this may not be the

full range of tolerance to stresses that can be exploited in miscanthus germplasm. For instance, the salinity field trial in Dongying showed that several of the newly collected Chinese *M. sacchariflorus* genotypes were relatively tolerant to saline conditions (with CN32 being most tolerant), although its tolerance was not much higher than some of the genotypes tested under controlled conditions. Further collection of miscanthus material growing on marginal soils is required, and this should be tested using the screening procedures developed within this project as well as in the field, alongside the best performers selected in this project.

Predicting how tolerant to stresses the selected genotypes will be in terms of water requirements and temperature is not straightforward. The field trials indicate that some genotypes perform better in relatively hot climates, while others thrive even after cold winters. However, the set of genotypes tested in the multi-location trials was too small and not enough of the best-performing genotypes were tested under field conditions. Thus, the logical next step would be to test the top performers from the controlled condition evaluations in different climatic regions to establish whether these selections are also relatively tolerant under varying field conditions.

For salinity at least, it can be deduced that the best-performing miscanthus genotypes' tolerance of saline soils is higher than in cereals, even barley (considered to be a salt-tolerant cereal). This offers opportunities for miscanthus cultivation in marginal, saline areas.

We would recommend that genotypes with extreme traits are crossed into highly productive parental lines, and the progeny are evaluated for resilience in further laboratory screens and field trials. Identification of the trait variation is an important step, but only one of many steps necessary for genetic improvement. This is part of a longer-term program of breeding and evaluation, which needs ongoing public support to deliver the resilient hybrids required to drive the feedstock supply for the bioeconomy.

Methods for the Establishment of Miscanthus on Marginal Land

Challenging establishment conditions, including drought, stoniness, and low temperature, present a major barrier to miscanthus production on marginal land (Xue et al., 2016). The OPTIMISC project developed technical approaches for the establishment of miscanthus under marginal soil conditions (WP5) and on grassland (WP4).

The planting of seed-derived plugs proved to be most successful method for miscanthus establishment on marginal soils. Covering the plants with a plastic film accelerates their growth. The film keeps the humidity in the topsoil and increases the temperature. This is beneficial for the plants, especially on light soils with a higher risk for drought stress and in cool temperatures.

In Europe, there are large areas of marginal land covered by grassland. The OPTIMISC project performed field trials for the establishment of miscanthus into grassland (WP4). The hypothesis was that the inclusion of miscanthus (high-yielding C4 grass species) into C3 grasslands could be beneficial for

biomass yield, given that suitable miscanthus genotypes are to be carefully selected for this purpose. Examples of yield increase in C3/C4 mixed grasslands compared to pure C3 grasslands can be found in the scientific literature (Adler and Sanderson, 2009). Growth patterns of C3 and C4 grasses are often complementary and lead to higher total annual harvestable yield (Thumm et al., 2012). Addition of miscanthus into C3 grasslands in temperate climates could also improve biomass quality for certain purposes, such as combustion.

The establishment of miscanthus on grassland proved successful with two propagation techniques: (1) direct planting of rhizomes in the soil and (2) transplanting of pre-grown, rhizome-derived plantlets. The second technique appeared to lead to better establishment success, although this depended on the genotype.

Pre-treatment of the existing vegetation is important to ensure good establishment of the introduced miscanthus plants. Cutting the existing vegetation and spraying herbicide in narrow strips (defined as intermediate in severity) appears to be the most advantageous pre-treatment of the grassland. This improves miscanthus establishment without negatively impacting on the productivity and existing vegetation of the C3 grassland itself.

Strong, competitive miscanthus genotypes with tall, thick shoots seem to be a better choice for establishment on grassland than genotypes with short, thin shoots, regardless of the species.

The C3/C4 grasslands can and should be managed by multiple in-season mowing of green biomass, as is usually performed on European grasslands. Our results demonstrated that a mowing regime with two harvests per year (spring and autumn) is most suitable to achieve good biomass yields from these mixed grasslands. Harvesting once per season in autumn leads to a higher proportion of miscanthus biomass but to a lower biomass gain from the C3 grassland due to its natural senescence early in summer.

Meeting Biodiversity Concerns

Biodiversity issues need to be considered when planting miscanthus into C3 grasslands. In our trials, vegetation analyses performed before and 3 years after the establishment of miscanthus revealed that the species richness and abundance did not change significantly with this addition. However, the miscanthus was planted at a relatively low density and remained only a small contributor to the plant canopy and biomass (3–6%) due to high competition. Planting at higher densities or development of the miscanthus over time could potentially bring about changes in the existing plant communities.

As miscanthus is a not native to Europe, there are also concerns about uncontrolled spreading of this crop. There are two potentially relevant pathways for such spreading: (1) via creeping rhizomes and (2) via seed.

Creeping rhizomes were observed in several *M. sacchariflorus* genotypes, one of which was strongly creeping. We therefore recommend excluding genotypes with this feature from commercialization (see **Table 7**).

Germination tests carried out under controlled conditions showed that 10 of the 15 miscanthus genotypes tested in the OPTIMISC multi-location trials produced viable seeds. All these genotypes belonged either to *M. sinensis* species or *M. sinensis*

x *M. sacchariflorus* hybrids. The highest seed germination rates were observed in Germany and the Netherlands and the lowest in the most southerly trial location of Turkey and two more northerly (colder) sites in Russia and Ukraine. The germination rate was especially low (on average 0.2 ± 0.13 seeds per panicle in 2014) in Russia (Moscow area), where long-day conditions retarded the transition to flowering and the vegetation period is short, preventing complete seed ripening (plant senescence occurs earlier). Strong genotypic differences were observed for seed germination. Two *M. sinensis* genotypes/accessions (OPM-12 and OPM-13) showed particularly high numbers of viable seeds per panicle (on average 150 ± 38 and 123 ± 34 seeds per panicle, respectively, in 2014). The *M. sacchariflorus* genotypes produced no viable seeds at all six trial locations. The *M. sinensis x sacchariflorus* hybrids (OPM-05–OPM-10) showed an average (six locations pooled, 2014) of 38% lower seed germination per panicle than the *M. sinensis* accessions. This ratio varied however between locations and genotypes. In the UK for example, the number of germinating seeds per panicle was approximately 50% higher in the hybrids than in the *M. sinensis* accessions. By contrast, in Germany, Ukraine and Turkey, this number was much lower in the hybrids than in *M. sinensis*. The highest number of geminating seeds per panicle was observed for the genotypes OPM-05 and OPM-10 (all locations pooled, in 2014).

Spreading via seeds was carefully monitored in the OPTIMISC trials. Volunteer miscanthus seedlings were found at two of the six locations of multi-location trials (WP4), the Netherlands and Germany. These seedlings were found outside the planted plots but within the plantation borders. No accidental spreading via seeds was observed at any of the more southerly or more northerly locations. In the south, seed germination in the field was possibly prevented by drought conditions, in the north by low temperatures and a shorter vegetation period. No volunteer miscanthus seedlings were found outside the plantation borders.

From these observations, we conclude that spreading via seeds in miscanthus—relevant for *M. sinensis* and *M. sinensis × M. sacchariflorus* hybrids—can be prevented by careful choice of genotype. Therefore, genotypes should be recommended that either do not form fertile seeds or that are unable to establish via seed due to the climatic conditions of a specific site.

Another biodiversity concern is that miscanthus, as a perennial crop with tall and dense stands, may give rise to a monoculture, which supports only low species diversity.

Our results show that young miscanthus stands sustain high plant species diversity before the canopy closure. Species richness was found to correlate negatively with the density of the stands and to be lower in mature plantations. However, even the 16-year-old, dense miscanthus plantations supported up to 16 different weed species per 25-m² plot, accounting for up to 12% of the plantation. The literature data support this finding: Miscanthus stands are usually reported to support farm biodiversity, providing habitat for birds, insects, and small mammals (Semere and Slater, 2007a; Bellamy et al., 2009). Studies by Semere and Slater (2007b) have shown biodiversity in miscanthus to be higher than in other crop stands, but still lower than in open field margins.

Scaling Up Miscanthus Production and Connecting to Markets

The results of the OPTMISC project can contribute to the fulfillment of requirements for scaling up miscanthus production by:

- Providing seed-based, low-cost, and safe establishment methods;
- Providing germplasm for the development of stress-tolerant miscanthus varieties, adapted to a wide range of climatic conditions in Europe;
- Providing higher and more stable-yielding miscanthus genotypes that can also be produced economically on marginal lands;
- Developing genotypes that are optimally suited to harvesting, processing and biomass user requirements;
- Developing harvesting and densification technologies;
- Improving the marketability of miscanthus biomass by assessing new miscanthus-based value chains and demonstrating how the biomass can be suited to user requirements.

Seed-Based Establishment Methods

Cloning is expensive and the process of upscaling to the large areas necessary to deliver sufficient biomass for a future European bioeconomy would be too slow. For this reason, four seeded hybrids were included in the WP4 and WP5 trials. Although these were not as productive as the interspecific hybrids [including *M. × giganteus* (OPM-9)] and therefore not commercially "recommended," we have pioneered the upscaling of the planting of seed-based hybrids using plugs. These plugs are also called "modules" and were originally developed for the vegetable industry. Seeds are sown by machine and raised in the greenhouse (**Figure 3A**) before being planted out in the field (**Figure 3B**). It is anticipated that seed-based establishment methods will prove most effective for the scaling up of miscanthus production because they have the following advantages:

➢ With increasing market demand, large quantities can easily be provided, once seed production has been well developed
➢ Short growing period for plantlets: Only 8–10 weeks from seed to final product (plugs)
➢ Plug production is energy efficient (no need for refrigerators)
➢ Low establishment costs

When establishing miscanthus via seed in temperate climates, it is recommended that newly planted stands are protected with plastic film (**Figure 3C**) as this increases establishment success and it is anticipated that it can reduce the length of the establishment period so that an economic biomass yield is produced earlier.

However, if seeds cross out or are not genetically uniform, inhomogeneous field stands are possible.

During the term of the OPTIMISC project, major advances in breeding interspecific hybrids have been made in the UK (Clifton-Brown et al., 2017). The next steps in this development include determining how to: (1) increase the seed production potential of elite interspecific crosses; 2) optimize

FIGURE 3 | (A) Miscanthus establishment starting with seeds sown in modules (plugs) and grown in the greenhouse. **(B)** A Checci & Magli planter in action and planted field. **(C)** Film technology protects modules from drying out and provides them with extra heat units.

planting density; (3) maintain effective weed control during establishment—especially where the crop is to be established on marginal land.

If investment in breeding and trialing is sustained, we expect to be able to apply the knowledge gained from these parallel roads of development to achieve commercial upscaling by about 2020.

Genotypes Suitable for Processing and Use—Biomass Quality

The properties of miscanthus biomass determine its harvestability, transportability, marketability, and usability. Moisture content must be appropriate for harvest technology and storage. If the moisture content exceeds 20%, there is a danger of self-ignition of the biomass during storage. For ensiling, the water content should ideally be in the range of 65–72%. The combustion quality of biomass is determined by both water content and the concentration of elements that cause corrosion and reduce the ash melting point, mainly chloride (Cl), potassium (K), and nitrogen (N) (Lewandowski and Kauter, 2003). Densification of biomass, for example in the form of bales or pellets, is often necessary for storage or long-distance transport. (The economic relevance of this is discussed in Section Miscanthus value chains—options and implementation). The organic composition of the cell walls affects the digestibility of the biomass and therefore determines its usability in ethanol or methane (biogas) production.

The OPTIMISC project found in WP6 that the different miscanthus genotypes exhibit extensive variation in both biomass composition and characteristics relevant for energy use and that these are affected by their growing environment and crop management (mainly harvest).

Genotypic Differences in Biomass Composition and Properties

The moisture content of miscanthus biomass is mainly determined by harvest date (see **Figure 4**), but is also affected by genotypic variation resulting from morphological differences and senescence patterns. Data from the Blankney Estate large-scale (5-ha) trial in WP5 show that shorter-growing hybrids with thinner stems had lower moisture content (below 13% in the standing crop in 2015), significantly higher bale weight (650 kg vs. 500 kg for $M. \times giganteus$, with less string breakages) and require about 20% less power for pelleting. However, short-statured types were lower-yielding than $M. \times giganteus$ and the pellets were ∼5% less dense.

A trade-off between biomass yield and quality was also observed for the production of biomass for combustion. The concentration of combustion-critical elements declines over winter, as does the biomass yield (**Figure 4**). Therefore, for combustion purposes, we recommend genotypes with the best combination of good combustion qualities and relatively low biomass losses (and high biomass potential) such as OPM-11 for Adana/Turkey, OPM-03, OPM-06 and OPM-09 for Stuttgart/Germany and OPM-06, and OPM-09 for Moscow/Russia.

Of the eight compositionally diverse *M. sinensis* genotypes evaluated in a field trial in Wageningen, biogas yield ranged from 441 to 520 ml/g dry matter and glucose yield for fermentation
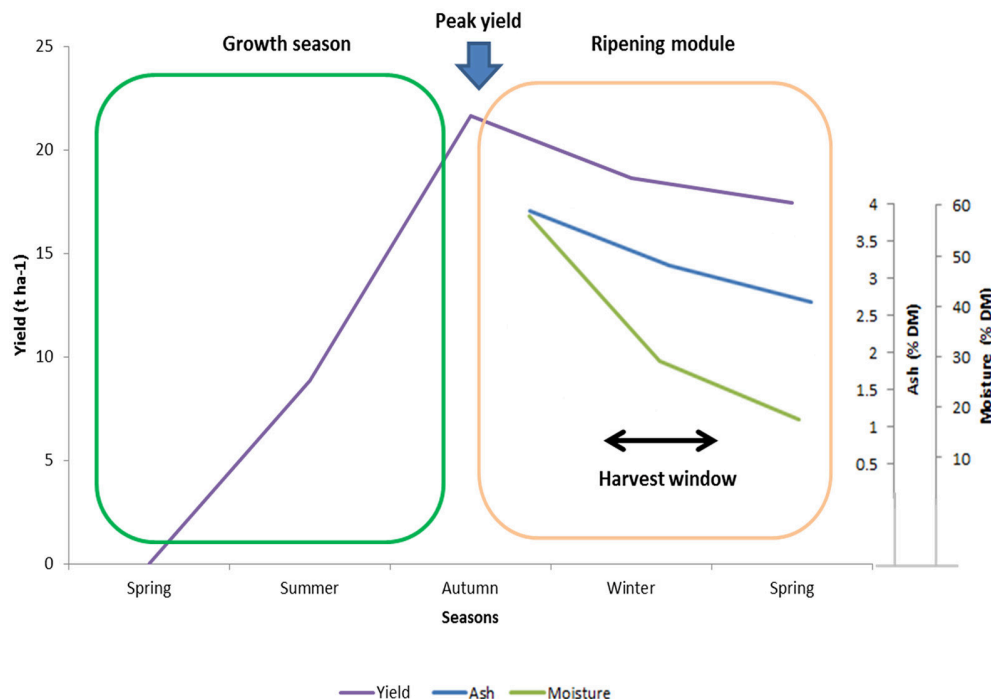
FIGURE 4 | Average yield accumulation during the growing season and changes in combustion-quality-relevant traits (moisture and ash content) from autumn to spring for the leading clone OPM-06 grown in Stuttgart in the third and fourth year after establishment.

ranged from 146 to 208 g/kg dry matter (in very mild processing conditions). Furthermore, variation in genotype performance for these value chains was found to correlate strongly with cell wall compositional characteristics, such as contents of lignin, hemicellulosic polysaccharides, arabinose, *trans*-ferulic acid, *para*-coumaric acid and ratios of these cell wall components. Biogas yield and saccharification efficiency were not highly correlated to each other, although they were both influenced by some of the above compositional characteristics. Nonetheless, some genotypes performed relatively well in both value chains. Unfortunately, these genotypes were not the best-performing genotypes in terms of yield. Thus, one of the challenges for the future is the crossbreeding of biomass-quality and biomass-yield-related traits.

The large variations observed in genotype performance indicate that, by developing and utilizing higher-quality feedstocks, vast improvements could be made in processing efficiency for these value chains.

Effect of Environmental Factors, Especially Abiotic Stress, on Cell Wall Composition

Variation in biomass composition was also shown to be highly influenced by environmental factors. Location accounted for a large part of the variation in cell wall composition in 15 genotypes that were evaluated across six locations in Europe and Russia. Some of this environmental influence can be explained by differences in relative stand maturity during the establishment phase of the trials, but it was still significant after the third

growing season. Stand maturity was also found to affect cell wall composition. The cell wall composition in the first growing season had a low predictive value of that in the third growing season. However, cell wall composition in the second year was predictive of that in the third year with reasonable accuracy across all locations. Significant genotype-by-location interaction was seen for cell wall, cellulose, hemicellulose, and lignin contents, indicating that the ranking of genotypes in terms of cell wall components varied across locations. Some genotypes showed considerably more sensitivity to environmental factors than other more stable genotypes. The environmental influence on biomass quality is substantial and should be taken into account when matching genotype, location and end-use of miscanthus.

As lignocellulosic feedstocks are low-value, high-volume commodities, most scenarios consider their cultivation on low-quality/marginal land where the occurrence of various abiotic stresses is highly probable. The fact that agricultural inputs need to be minimized on such land may lead to additional stresses. As miscanthus is seen as a robust perennial crop with high potential for low-quality/marginal soils (Quinn et al., 2015), it is very likely to experience abiotic stresses during its cultivation. Apart from the adverse effects of abiotic stresses on plant growth, another challenge is the fact that abiotic stresses result in changes in cell wall architecture and that in some cases these can lead to a reduction in the industrial quality of the biomass. It has been shown that subjecting plants to abiotic stress treatments often results in cell wall biosynthesis genes being

differentially expressed (Moura et al., 2010; Frei, 2013; Le Gall et al., 2015; Tenhaken, 2015). However, there have not been many investigations into the specific effects of the various abiotic stresses on cell wall composition and biomass quality (Tenhaken, 2015).

The OPTIMISC project assessed the effects of the abiotic stresses drought, salinity and cold on miscanthus biomass quality (WP3, WP4, WP6). The abiotic stress treatments were found to lead to substantial changes in biomass composition. Drought stress caused significant reductions in cell wall and cellulose content and a significant increase in hemicellulosic polysaccharides. However, it had only a small effect on lignin content. However, this effect can hardly be separated from the effect of increasing lignin content with maturity of the crop. It was hypothesized that the reduction in cellulose is the result of an increase in osmolyte production at the expense of cellulose as a strategy for maintaining turgor at a lower water potential. Cold stress caused a significant decrease in cell wall, cellulose, and lignin content, again with a significant increase in hemicellulosic polysaccharides. The same trends were observed in response to salt stress, but the effects were smaller.

Overall, the main response observed to all of these abiotic stresses was a decrease in cellulose content and a concomitant increase in hemicellulosic polysaccharides. The reduction in cellulose content has a negative impact on the industrial quality of the biomass for biofuel production, as it implicates a reduction in the main source of fermentable sugars. However, as also seen in the drought-treated samples, the increase in hemicellulosic polysaccharides led to a substantial increase in saccharification efficiency of the biomass. There is often a positive correlation between hemicellulosic polysaccharides and increased cell wall degradability, as an increase in these highly branched polysaccharides is associated with a reduction in crystallinity (Xu et al., 2012). Thus, although the stressed samples contain a lower amount of fermentable sugars, they are more easily extracted. This could potentially reduce processing costs for many potential value chains, including biofuel production. The higher degradability of plants experiencing abiotic stresses makes miscanthus an interesting crop for exploitation of marginal soils for the production of second-generation biofuel.

Harvest Regime

Several of the OPTIMISC trials (WP4, WP5) included evaluations of the effects of different harvest regimes on miscanthus biomass yields. As **Figure 4** shows, the yield reaches a peak in autumn and then decreases, mainly due to leaf loss. The assessments concentrated on the effect of harvest time on biomass yield and quality and investigated whether multiple cutting systems could improve yield performance.

For *M. sinensis*, a double-cut harvest (summer cut in July, winter cut in February) was shown to yield significantly less biomass than a single-cut harvest in February. Averaged over eight genotypes, the double-cut regime yielded an annual biomass of ∼2.4 t DM/ha while the single-cut regime yielded ∼6.3 t DM/ha for the first complete growing season after establishment. The weather conditions in summer 2015 favored a higher biomass quality for ethanol and biogas value chains, but

the yield penalty of an early cut was too substantial to recommend a summer cut for any of the miscanthus value chains considered.

Similar results were observed in a cutting tolerance trial using *M. × giganteus* (Kiesel and Lewandowski, 2017). In this trial, a double-cut harvest regime (first green cut in July, second green cut in October) and two single-cut harvest regimes (early harvest in August and late harvest in October) were compared with a conventional spring harvest. The double-cut and the early single-cut harvest regime showed serious yield decline the following year, indicating that both regimes were not tolerated by the crop and are not sustainable in terms of yield formation. The harvest in late October delivered very high and stable yields of 25–28 t DM ha^{-1}, suggesting that *M. × giganteus* can tolerate a green harvest at this time. Relocation of carbohydrates was identified as an important factor influencing the cutting tolerance. Our hypothesis is that the autumn-harvested crop had enough time to relocate sufficient carbohydrate reserves to the rhizome before the harvest in late October (Kiesel and Lewandowski, 2017).

The biomass quality of green-harvested miscanthus for biogas production and consequently substrate-specific biogas yield declined with later harvest dates. October was identified as the most promising and cutting-tolerant harvest date for biogas production. On average it delivered a 45% higher methane yield than the conventional winter harvest, due to higher biomass yield and improved biomass quality.

However, the early green harvest led to a biomass yield decline the following year due to insufficient cutting tolerance. This lower biomass yield was not compensated by the higher substrate-specific biogas yield. Therefore, cutting tolerance was identified as a crucial factor for the long-term productivity of green-harvested miscanthus.

Cutting tolerance is also relevant for the use of miscanthus biomass for protein and chlorophyll production. These can be extracted from the biomass prior to its processing for bioenergy or other applications. Chlorophyll is used as a food additive, whereas protein is used as a feed additive. As such, both are important added-value bioproducts and can contribute to the value of miscanthus biomass in the biorefinery chain. In the large-scale field trials at Blankney and Stuttgart, it was found that harvesting the stay-green OPM-111 (*M. sinensis*) later than early July resulted in a significant decrease in both chlorophyll and protein content. At harvest earlier than July, the protein content of leaves and stems were about 12 and 11% of DM, respectively. At Blankney, the chlorophyll content reached up to 3.5% of DM in leaves and 2.8% of DM in stems. At Stuttgart however, leaf and stem chlorophyll contents only reached about 2.5 and 1.8% of DM, respectively. We concluded that miscanthus can probably hardly compete with the existing methods for chlorophyll extraction from perennial ryegrass.

Technologies for Harvesting and Logistics

Harvesting miscanthus is a fuel- and labor-intensive process (depending on harvest procedures), and has the largest cost and environmental impact (in terms of fuel usage) for a producer. For this reason, it is important to gather data that can help growers make use of methods best suited to their existing equipment and facilities. In addition, data is required that take the variation

in harvest efficiencies of the different genotypes into account to allow farmers to cultivate the genotype best suited to their harvesting needs, thus maximizing profitability in the biomass value chain.

Harvesting techniques, climatic conditions and plant morphology all interact to affect biomass quantity and quality and the resultant options for downstream biomass utilization (see Section Genotypes suitable for processing and use—biomass quality). Self-propelled forage harvesters (normally used for maize) have been successfully used to produce chips from *M. × giganteus* in the UK, France and Germany following cold winters, which force the crop to ripen with a moisture content below 25%. This direct chipping approach results in biomass losses of only 5% (Meehan et al., 2013). The chips dry well in covered storage. However, miscanthus chips have a number of drawbacks. Firstly, they have a low bulk density (150 kg m^{-3}), which leads to high storage costs and limits the location of markets to within the proximity of the available crop. Secondly, the low bulk density reduces the fuel mass in the combustion chamber, which lowers the thermal output of most boilers. Thirdly, unless the chips have been produced using a high-precision chop forage harvester, bridging, and clogging can be a problem with automated feed systems.

The harvesting experiments at Blankney in WP5 led to the following conclusions:

– Large self-propelled direct chipping harvesters with 7.5-m cutting widths have high throughputs and are potentially more fuel (3%) and time (~10%) efficient than machines with a 4.5-m cutting width.
– Farmers (or machine rings) will most probably harvest with the locally available technology in order to minimize additional capital costs. Therefore, it is likely that smaller harvesting machines will be used. Harvesting speed and efficiencies do not represent a bottleneck to deployment. As the scale of planting increases, the machinery will develop to match demands.
– Moisture content of the different hybrid types harvested at Blankney ranged from 13 to 20% of DM in April 2015. The hybrids with low moisture content are the most amenable to harvest by self-propelled direct chipping harvesters, since no degradation of the biomass occurs during storage at these low moisture levels.
– In mild winters, where senescence is incomplete in non-flowering genotypes such as *M. × giganteus*, mowing and then windrowing before baling will remain an important harvest method even though harvest losses are higher.

OPTIMISC also investigated the pelleting of miscanthus biomass. All the pellets produced are described as "good, hard, and durable." The highest bulk density (810 g/l) was achieved using *M. × giganteus* (OPM-09) biomass and the lowest (664 g/l) was observed for OPM-12. The highest percentage of fines (small particles of un-pelleted material) occurred in OPM-52 (25%) and the lowest in OPM-12 (16%).

Large-scale commercial pelleting tests showed that all miscanthus hybrids could be successfully pelleted. Slight adjustments to the machinery normally used for wood pellets are needed with *M. × giganteus* to avoid overheating of the press. All the new (softer-stemmed) hybrids tested had lower pressing resistances and therefore lower die temperatures and power requirements.

The different miscanthus hybrids tested showed significant variation in pelletability. As was expected, *M. × giganteus*, with its hard, stiff stems, was the most difficult to pellet, but it gave the highest pellet bulk density.

The energy costs of large-scale pellet production can vary from 40 to 80€/t pelleted biomass, at a capacity of approximately 3 t/h. The final cost of production also depends on the wear and tear of pellet press parts (die and rollers), and there is a significant correlation between this wear and tear and biomass composition and structure.

The calorific values of the pellets from the different hybrids varied slightly, but there was wide variation in ash and chloride contents. The biomass of the softer-stemmed hybrids had both a lower moisture content at harvest and also lower levels of ash and chlorine after pelleting than that of *M. × giganteus*.

Miscanthus Value Chains—Options and Implementation

In OPTIMISC, the economics as well as GHG- and fossil-fuel-saving potentials of seven miscanthus-based value chains were analyzed in detail in WP7. **Table 8** ranks the potential GHG savings by different miscanthus-based value chains for sites in north-eastern Europe (data from the Moscow/Russia site), for Central Europe (data from the Stuttgart/Germany site), and for southern Europe (data from the Adana/Turkey site).

Carbon Mitigation and Fossil-Energy Substitution Potentials

For all miscanthus energy and material applications, OPM-06 is most suitable in north-eastern and Central Europe, followed by OPM-10 and OPM-09 in north-eastern and OPM-03 and OPM-09 in Central Europe. In southern Europe, OPM-09 (*M. × giganteus*) proved most suitable for all the miscanthus-based value chains analyzed, followed by OPM-11 and OPM-14 or OPM-06 for biogas. This means that *M. × giganteus* proved a feasible choice for all locations and applications. The suitability of the genotypes was determined according to yield and quality performance with regard to anticipated use.

The optimal harvest time differs for each value chain. For combustion, a late harvest leads to low moisture content and other favorable biomass quality criteria, but also to biomass yield losses. For ethanol and biogas production, a green harvest in autumn is optimal (**Table 8**). For biogas production, high DM yield and low lignin content are important determinants for high biogas yield and can best be achieved by a green cut. A green cut is also a prerequisite for biomass ensilage.

The highest biomass yields as well as the highest GHG- and fossil-energy savings potentials (up to 30.6 t CO$_{2eq}$/ha*a and 429 GJ/ha*a, respectively) can be achieved on non-marginal sites in Central Europe. On marginal sites limited by cold (Moscow/Russia) or drought (Adana/Turkey) savings of up to 19.2 t CO$_{2eq}$/ha*a and 273 GJ/ha*a (Moscow) and 24.0 t CO$_{2eq}$/ha*a and 338 GJ/ha*a (Adana) can be achieved.

TABLE 8 | Optimized miscanthus-based value chains.

	Biomass production genotype	Harvest	Pre-treatment	Processing	End product
NORTH-EASTERN EUROPE					
Insulation	OPM-06 (10, 9)	March	Steam explosion	Mixing/pressing	Insulation material
Heat–chips	OPM-06 (10, 9)	March	Chipping	Combustion	Heat
CHP–bales	OPM-06 (10, 9)	March	Baling	Combustion	Heat + Power
CHP–pellets	OPM-06 (10, 9)	March	Pelleting	Combustion	Heat + Power
Heat–pellets	OPM-06 (10, 9)	March	Pelleting	Combustion	Heat
Biogas	OPM-06 (10, 14)	October	Ensiling	Anaerobic digestion	Heat + Power
Ethanol	OPM-06 (10, 9)	March	Thermo-chemical	Fermentation	Ethanol
CENTRAL EUROPE					
Insulation	OPM-06 (3, 10)	March	Steam explosion	Mixing/pressing	Insulation material
Heat–chips	OPM-06 (3, 9)	March	Chipping	Combustion	Heat
CHP–bales	OPM-06 (3, 9)	March	Baling	Combustion	Heat + Power
CHP–pellets	OPM-06 (3, 9)	March	Pelleting	Combustion	Heat + Power
Heat–pellets	OPM-06 (3, 9)	March	Pelleting	Combustion	Heat
Ethanol	OPM-06 (3, 10)	March	Thermo-chemical	Fermentation	Ethanol
Biogas	OPM-06 (3, 11)	October	Ensiling	Anaerobic digestion	Heat + Power
SOUTHERN EUROPE					
Insulation	OPM-09 (11, 14)	March	Steam explosion	Mixing/pressing	Insulation material
Heat–chips	OPM-09 (11, 14)	March	Chipping	Combustion	Heat
CHP–bales	OPM-09 (11, 14)	March	Baling	Combustion	Heat + Power
CHP–pellets	OPM-09 (11, 14)	March	Pelleting	Combustion	Heat + Power
Heat–pellets	OPM-09 (11, 14)	March	Pelleting	Combustion	Heat
Ethanol	OPM-09 (11, 14)	March	Thermo-chemical	Fermentation	Ethanol
Biogas	OPM-09 (11, 6)	October	Ensiling	Anaerobic digestion	Heat + Power

The GHG and fossil-energy savings are highest where miscanthus biomass is used as construction material (our analysis uses the example of insulation material). A high GHG- and fossil-energy-saving potential was also found for domestic heating on account of the short transportation distance. Pelleting is only advantageous in terms of the minimization of GHG emissions and energy consumption where biomass is transported over a long distance, for example for heat and power production in CHP. Pelleting requires additional energy, but at the same time reduces the energy required for transport due to its higher density.

The lowest GHG- and fossil-energy-saving potentials were found for power production via the biogas pathway, followed by bioethanol. However, this result is strongly influenced by the assumptions that (a) only 50% of the available heat is used and (b) transport distance from the field to the biogas plant is relatively long (15 km). A biogas chain with 100% heat utilization and lower transportation distances would perform better. It can be concluded that for power generation from miscanthus biomass, the most favorable pathway is combustion for base load power, and biogas to cover peak loads.

The economics of biomass production for different value chains are shown in **Table 9** for the example of the Stuttgart site (Germany).

Biomass supply costs are assessed here as the costs of producing, densifying, and transporting the biomass from the farm to the unit where the biomass is burned or processed into ethanol or insulation material. They range from 78€ per ton dry mass of chips (for local, small-scale production) and 79€ per ton silage (50% water) for biogas production up to about 140€ per ton dry mass of bales for the production of insulation material, ethanol, and pellets.

In a comparison with the production of energy from fossil fuels, small-scale combustion of chips proved to be highly profitable. The pelleting of biomass increases the cost by about 30%, but the cost per KWh thermal energy produced still remains comparatively low. Both options lead to negative carbon mitigation costs (**Table 9**).

When electricity is produced in a medium-scale 5 MW CHP power plant, carbon mitigation costs are about 83€ per ton avoided $CO_{2equivalents}$ for biomass supply as bales or pellets, assuming a transport distance of 400 km (**Table 9**). To make CHP electricity a viable option for electricity production from miscanthus biomass, transportation costs need to be reduced. For bioethanol, costs of about 24€ ct per liter stem from biomass supply. Here too, reduction of transport distances is an important factor in lowering biomass supply costs. For insulation material, biomass supply costs per m^3 are of the order of 28€, if a transport distance of 400 km is assumed. This can compete with the market price of glass wool. The competitiveness of

TABLE 9 | State-of-the-art biomass supply costs, allocated costs (assessed as difference between biobased and fossil resources), and carbon mitigation costs of each value chain at the Stuttgart site.

Value chain	Biomass supply costs		Allocated costs		CO_2 mitigation costs [€ (t CO_{2eq})$^{-1}$]
1) Small-scale combustion: chips	0.46	€ct (MJ$_{th.}$)$^{-1}$	−0.77	€ct (MJ$_{th.}$)$^{-1}$	−78.33
2) Small-scale combustion: pellets	0.79	€ct (MJ$_{th.}$)$^{-1}$	−0.43	€ct (MJ$_{th.}$)$^{-1}$	−49.65
3) Large-scale combustion: bales	6.25	€ct (MJ$_{el.}$)$^{-1}$	5.6	€ct (MJ$_{el.}$)$^{-1}$	82.52
4) Large-scale combustion: pellets	6.15	€ct (MJ$_{el.}$)$^{-1}$	5.5	€ct (MJ$_{el.}$)$^{-1}$	83.54
5) Large-scale bioethanol production	14.80	€ct (MJ$_{Bioethanol}$)$^{-1}$	11.52	€ct (MJ$_{Bioethanol}$)$^{-1}$	1737.56
6) Medium-scale biogas production	2.15	€ct (MJ$_{el.}$)$^{-1}$	1.47	€ct (MJ$_{el.}$)$^{-1}$	93.69
7) Large-scale insulation plant	27.69	€ (m^3)$^{-1}$	28.53	€ (m^3)$^{-1}$	70.75

miscanthus insulation can be improved by its cultivation closer to the insulation material production site.

There was a clear effect of yield level on the cost per unit of biomass. For conditions comparable to those prevailing at the Stuttgart site, the cost of bale harvest was 28.9€/t DM for a yield of 15 t/ha. This decreased to 23.5€/t DM when a higher yield of 18 t DM/ha was assumed. This example reveals the limitations of miscanthus cultivation on marginal land, where costs per unit produced are higher and not always compensated for by lower costs for lease of land. However, the results of the OPTIMISC project should lead to an increase in biomass yield of miscanthus cultivated on marginal land, as novel genotypes outyielded *M. × giganteus* at three of the five experimental sites. At the Stuttgart site, OPM-06 had a 20% higher yield than *M. × giganteus*. New hybrids from the gene pools tested and characterized in OPTIMSC are expected to become commercially available in the near future.

Another option for alleviating the problem of marginal yield levels is cultivation on larger-sized plots. Growing miscanthus for combustion on a 20-ha plot instead of a 2-ha plot can decrease biomass costs by 18% (KTBL, 2012). As cultivation on marginal land involves lower opportunity costs than on high-yielding farmland, lower economic returns are acceptable. When grown on fields where annual crops often fail, the perennial crop will always give some return and thus can be more attractive, even with moderate yield levels. In Iowa/USA, it is estimated that there are good opportunities for miscanthus cultivation on 10–20% of marginal corn land, where farmers lose money every year (Heaton, 2014).

The OPTIMISC project also created new perspectives and opportunities through the option of higher prices for miscanthus with higher added value for industry. Research on quality aspects of different genotypes for specific end uses allowed the identification of novel genotypes which can incorporate improved quality characteristics at field level. For example, it was shown that there is scope for development of new varieties with considerable potential to reduce pre-treatment costs for bioethanol production. Bioethanol yield after mild treatment of lignocellulosic biomass is a good indicator of possible savings in industrial production. At Stuttgart/Germany, hybrid OPM-06 had a 37% higher ethanol yield than *M. × giganteus* (OPM-09)

after mild treatment. This should lead to higher biomass prices due to cost reduction in industrial processes.

OUTLOOK: HOW TO SUPPORT THE IMPLEMENTATION OF MISCANTHUS PRODUCTION AND USE IN EUROPE

The two most important areas where technological advances can be made are breeding programs and development of agricultural equipment for miscanthus production. Other factors are access to markets and the development of a robust supply chain from the farmer to the end-user. The development of high-value biomass applications, such as biochemicals and biocomposites, should also be encouraged. A stronger engagement of farmers in the value chain through "on-farm biorefining" concepts would increase their income opportunities, allowing them to market high-value products instead of low-value biomass. It is also recommended that the ecological potential of miscanthus should be acknowledged in the European Common Agricultural Policy (CAP), for example by giving further consideration to the development of so-called "greening measures." These recommendations are elaborated below:

Ecological Benefits of Perennial Biomass Crops Need to be Recognized

Remuneration for non-market ecosystem services should include funding for particularly high-service provision, e.g., flood risk reduction, soil protection, nitrate mitigation etc.

Replace Less Sustainable Biomass with Perennial Biomass Crops (PBC)

About six million ha of agricultural land in the EU are used for so-called "first generation" energy and industry crops. Rapeseed and maize are the most prominent examples. The replacement of these intensively managed annual crops by perennial biomass crops could be a priority for reducing nitrate leaching, erosion and the use agrochemical use, and increasing soil carbon sequestration and biodiversity. Miscanthus could replace maize for biogas production, if fermentation techniques are adapted or the biomass pre-treated.

Support the Development of Miscanthus Varieties Adapted to Marginal Land

Miscanthus shows good potential to make use of land, which is marginal or difficult to manage, or for land restoration. However, marginal production conditions can also result in low profit margins (van Dam et al., 2005) which are not compensated for by lower land costs. Therefore, crop management systems that ensure safe establishment and optimal management in these conditions need to be developed and stress-tolerant genotypes are required.

Plant genetic improvement, even of major agricultural crops such as wheat, is subject to significant market failure (Moran et al., 2007). This leads to underinvestment in breeding on the private market, as the incentive is insufficient for the level of investment optimal for society. This failure is likely to be even greater for perennial biomass crops, particularly for adaptation to marginal land. The OPTIMISC project identified the tolerance of miscanthus to the abiotic stresses that characterize marginal land. Insights were gained into the available land resources and thus the potential market for improved planting material. These findings lead us to suggest a miscanthus strategy that includes a plan for appropriate public investment in plant breeding, also through partnerships with private-sector breeders. This should stimulate demand for "upstream" research, an area that also requires long-term support.

Technical Barriers to the Implementation of PBC on Marginal Land Need to be Overcome

The estimated area of land under miscanthus cultivation in the EU is currently about 20,000 ha and is decreasing in many regions. Insufficient development of cultivars and production technology, along with high costs for agricultural inputs, land and labor, result in high production costs for a relatively low-value biomass. Although they are amortized over a cultivation period of 4 to 25 years, establishment costs for miscanthus are high and need to be reduced.

The development of agricultural machinery, such as planting and harvesting equipment, will remain insufficient unless it finds a larger market. Today, farmers often use self-made equipment,

such as adapting potato harvesting machines for the harvest of miscanthus rhizomes. In addition, the development of service units, e.g., machinery cooperatives, will only develop once miscanthus production reaches a significant scale.

Farmers hesitate to grow miscanthus because it involves dedicating their land to long-term biomass production. They will only be willing to do this if biomass markets are reliable or if long-term contracts are available in recognized supply chains. Therefore, the development of biomass marketing structures should be supported by agricultural policies.

The main current application of miscanthus biomass is for bulk heat and power production—a comparatively low-value market whose value depends on the price of fossil fuels used in large-scale heat and for electricity generation. Complementary to these existing markets, there is a need for programs that support smaller-scale but higher-value applications of miscanthus biomass to develop new, attractive market options. These should include options for "on-farm biorefineries" that help keep a higher proportion of the value generated from biomass on the farm. The development of on-farm biorefinery concepts, which allow decentralized biomass densification and valorization, can help involve farmers in local biobased value chains.

AUTHOR CONTRIBUTIONS

The authors contributed in the following roles: IL University of Hohenheim, as corresponding author and coordinator of the project. JC as Work Package Leader. LT as Work Package Leader. GV as Work Package Leader. KS as Work Package Leader. KM as Work Package Leader. OK as Project Manager. AA, CC, OD, ID, KF, SF, GH, AH, LH, YI, NK, AK, PL, HeM, MM, HiM, CN, MÖ, IR, HS, IT, TV, MW, and QX as Project Coworkers.

ACKNOWLEDGMENTS

REFERENCES

Adler, P. R., Sanderson, M. A., Weimer, P. J., and Vogel, K. P. (2009). Plant species composition and biofuel yields of conservation grasslands. *Ecol. Appl.* 19, 2202–2209. doi: 10.1890/07-2094.1

Bellamy, P. E., Croxton, P. J., Heard, M. S., Hinsley, S. A., Hulmes, L., Hulmes, S., et al. (2009). The impact of growing miscanthus for biomass on farmland bird populations. *Biomass Bioenergy* 33, 191–199. doi: 10.1016/j.biombioe.2008.07.001

Clifton-Brown, J. C., Hastings, A., Mos, M., McCalmont, J., Ashman, C., Awty-Carroll, D., et al. (2017). Progress in upscaling Miscanthus biomass production for the European bioeconomy with seed based hybrids. *Glob. Change Biol. Bioenergy.* doi: 10.1111/gcbb.12357

Clifton-Brown, J. C., and Lewandowski, I. (2000). Overwintering problems of newly established *Miscanthus* plantations can be overcome by identifying genotypes with improved rhizome cold tolerance. *New Phytol.* 148, 287–294. doi: 10.1046/j.1469-8137.2000.00764.x

Davey, C. J., Jones, L. E., Laurence, E. J., Squance, M., Purdy, S., Maddison, A., et al. (2016). Radiation capture and conversion efficiencies of *Miscanthus sacchariflorus*, *M. sinensis* and their naturally occurring hybrid *M. x giganteus*. *Glob. Change Biol. Bioenergy.* doi: 10.1111/gcbb.12331

Dohleman, F. G., and Long, S. P. (2009). More productive than maize in the midwest: how does miscanthus do it? *Plant Physiol.* 150, 2104–2115. doi: 10.1104/pp.109.139162

Fonteyne, S., Lootens, P., Muylle, H., Van den Ende, W., De Swaef, T., Reheul, D., et al. (2016a). Chilling tolerance and early vigour related characteristics evaluated in two Miscanthus genotypes. *Photosynthetica* 54, 1–12. doi: 10.1007/s11099-016-0193-y

Fonteyne, S., Muylle, H., De Swaef, T., Reheul, D., Roldán-Ruiz, I., and Lootens, P. (2016b). How low can you go? Rhizome and shoot frost tolerance in miscanthus germplasm. *Ind. Crops Prod.* 89, 323–331. doi: 10.1016/j.indcrop.2016.05.031

Fonteyne, S., Roldán-Ruiz, I., Muylle, H., De Swaef, T., Reheul, D., and Lootens, P. (2016c). "A review of frost and chilling stress in Miscanthus and its importance to biomass yield," in *Perennial Biomass Crops for a Resource Constrained World,*

eds S. Barth, D. Murphy-Bokern, O. Kalinina, G. Taylor, and M. Jones (New York, NY: Springer).

Frei, M. (2013). Lignin: characterization of a multifaceted crop component. *Sci. World J.* 2013, 1–25. doi: 10.1155/2013/436517

Greef, J. M., and Deuter, M. (1993). Syntaxonomy of *Miscanthus × giganteus* GREEF et DEU. *Angew. Bot.* 67, 87–90.

Hastings, A., Clifton-Brown, J. C., Wattenbach, M., Mitchell, C. P., and Smith, P. (2009). The development of MISCANFOR, a new Miscanthus crop growth model: towards more robust yield predictions under different climatic and soil conditions. *Glob. Change Biol. Bioenergy* 1, 154–170. doi: 10.1111/j.1757-1707.2009.01007.x

Heaton, E. (2014). Available online at: http://www.news.iastate.edu/news/2014/07/23/miscanthus2014

Heaton, E. A., Dohleman, F. G., Miguez, A. F., Juvik, J. A., Lozovaya, V., Widholm, J., et al. (2010). Miscanthus: a promising biomass crop. *Adv. Bot. Res.* 56, 75–137. doi: 10.1016/B978-0-12-381518-7.00003-0

Iqbal, Y., and Lewandowski, I. (2016). Biomass Composition and ash melting behaviour of selected miscanthus genotypes in Sothern Germany. *Fuel* 180, 606–612. doi: 10.1016/j.fuel.2016.04.073

Kiesel, A., and Lewandowski, I. (2017). Miscanthus as biogas substrate - Cutting tolerance and potential for anaerobic digestion. *Glob. Change Biol. Bioenergy*. doi: 10.1111/gcbb.12330

KTBL (2012). *Energiepflanzen. KTBL Datensammlung. Kuratorium für Technik und Bauwesen in der Landwirtschaft e. V., 2. Aufl.*, Darmstadt, 372.

Le Gall, H., Philippe, F., Domon, J.-M., Gillet, F., Pelloux, J., and Rayon, C. (2015). Cell wall metabolism in response to abiotic stress. *Plants* 4, 112–166. doi: 10.3390/plants4010112

Lewandowski, I. (2016). "The role of perennial biomass crops in a growing bioeconomy," in *Perennial Biomass Crops for a Resource Constrained World*, eds S. Barth, D. Murphy-Bokern, O. Kalinina, G. Taylor, and M. Jones (New York, NY Springer).

Lewandowski, I., Clifton-Brown, J. C., Scurlock, J. M. O., and Huisman, W. (2000). Miscanthus: European experience with a novel energy crop. *Biomass Bioenergy* 19, 209–227. doi: 10.1016/S0961-9534(00)00032-5

Lewandowski, I., and Kauter, D. (2003). The influence of nitrogen fertilizer on the yield and combustion quality of whole grain crops for solid fuel use. *Ind. Crops Prod.* 17, 103–117. doi: 10.1016/S0926-6690(02)00090-0

McCalmont, J., Hastings, A., McNamara, N. P., Richter, G. M., Robson, P., and Clifton-Brown, J. C. (2015). Environmental costs and benefits of growing miscanthus for bioenergy in the UK. *Glob. Change Biol. Bioenergy*. doi: 10.1111/gcbb.12294

Meehan, P. G., Finnan, J. M., and McDonnell, K. P. (2013). A comparison of the energy yield at the end user for M. × giganteus using two *different harvesting and transport systems*. Bioenergy Res. 6, 813–821. doi: 10.1007/s12155-013-9307-6

Moran, D., Barnes, A., and McVittie, A. (2007). *The Rationale for Defra Investment in R&D Underpinning the Genetic Improvement of Crops and Animals*. Defra report for project IF0101. SAC Commercial Ltd, Scotland.

Mortaignie, E. (2014). *Evaluatie Van Het Effect Van koudestress op de Jeugdgroei Van Miscanthus*. Ghent: Ghent University.

Moura, J. C. M. S., Bonine, C. A. V., De Oliveira Fernandes Viana, J., Dornelas, M. C., and Mazzafera, P. (2010). Abiotic and biotic stresses and changes in the lignin content and composition in plants. *J. Integr. Plant Biol.* 52, 360–376. doi: 10.1111/j.1744-7909.2010.00892.x

Munns, R., James, R. A., Xu, B., Athman, A., Conn, S. J., Jordans, C., et al. (2012). Wheat grain yield on saline soils is improved by an ancestral Na(+) transporter gene. *Nat. Biotechnol.* 30, 360–364. doi: 10.1038/nbt.2120

Numata, M. (ed.). (1974). *Grassland Vegetation. The Flora and Vegetation of Japan.* Tokyo: Elsevier, 125–147.

Quinn, L. D., Straker, K. C., Guo, J., Kim, S., Thapa, S., Kling, G., et al. (2015). Stress-tolerant feedstocks for sustainable bioenergy production on marginal land. *Bioenergy Res.* 8, 1081–1100. doi: 10.1007/s12155-014-9557-y

Semere, T., and Slater, F. M. (2007a). Invertebrate populations in miscanthus (Miscanthus × giganteus) and reed canary-grass (*Phalaris arundinacea*) fields. *Biomass Bioenergy* 31, 30–39. doi: 10.1016/j.biombioe.2006.07.002

Semere, T., and Slater, F. M. (2007b). Ground flora, small mammal and bird species diversity in miscanthus (Miscanthus × giganteus) and reed canary-grass (*Phalaris arundinacea*) fields. *Biomass Bioenergy* 31, 20–29. doi: 10.1016/j.biombioe.2006.07.001

Tenhaken, R. (2015). Cell wall remodeling under abiotic stress. *Front. Plant Sci.* 5:771. doi: 10.3389/fpls.2014.00771

Thomashow, M. F. (1999). Plant cold acclimation: freezing tolerance genes and regulatory mechanisms. *Annu. Rev. Plant Physiol. Plant Mol. Biol.* 50, 571–599. doi: 10.1146/annurev.arplant.50.1.571

Thumm, U., Fenn, L., and Lewandowski, I. (2012). Establishment of switchgrass in permanent grassland. *Grassland Sci. Eur.* 17, 79–81.

van Dam, J. E. G., de Klerk-Engels, B., Struik, P. C., and Rabbinge, R. (2005). Securing renewable resource supplies for changing market demands in a bio-based economy. *Ind. Crops Prod.* 21, 129–144. doi: 10.1016/j.indcrop.2004.02.003

van der Maarel, E. (2007). Transformation of cover-abundance Values for appropriate numerical treatment – alternatives to the proposals by Podani. *J. Veg. Sci.* 18, 767–770. doi: 10.1111/j.1654-1103.2007.tb02592.x

van der Weijde, T., Alvim Kamei, C. L., Torres, A. F., Vermerris, W., Dolstra, O., Visser, R. G. F., et al. (2013). The potential of C4 grasses for cellulosic biofuel production. *Front. Plant Sci.* 4:107. doi: 10.3389/fpls.2013.00107

van der Weijde, T., Huxley, L., Hawkins, S., Sembiring, E. H., Farrar, K., Dolstra, O., et al. (2016b). Impact of drought stress on growth and quality of miscanthus for biofuel production. *Glob. Change Biol. Bioenergy*. doi: 10.1111/gcbb.12382

van der Weijde, T., Kiesel, A., Iqbal, Y., Muylle, H., Dolstra, O., Visser, R. G. F., et al. (2017). Evaluation of Miscanthus sinensis biomass quality as feedstock for conversion into different bioenergy products. *Glob. Change Biol. Bioenergy*. doi: 10.1111/gcbb.12355

van der Weijde, T., Torres, A. F., Dolstra, O., Visser, R. G. F., and Trindade, L. M. (2016a). Impact of different lignin fractions on saccharification efficiency in diverse species of the bioenergy crop miscanthus. *Bioenergy Res.* 9, 146–156. doi: 10.1007/s12155-015-9669-z

Wilson, P., Glithero, N. J., and Ramsden, S. J. (2014). Prospects for dedicated energy crop production and attitudes towards agricultural straw use: the case of livestock farmers. *Energy Policy* 74, 101–110. doi: 10.1016/j.enpol.2014.07.009

Xu, N., Zhang, W., Ren, S., Liu, F., Zhao, C., Liao, H., et al. (2012). Hemicelluloses negatively affect lignocellulose crystallinity for high biomass digestibility under NaOH and H2SO4 pretreatments in Miscanthus. *Biotechnol. Biofuels* 5, 1–12. doi: 10.1186/1754-6834-5-58

Xue, S., Kalinina, O., and Lewandowski, I. (2015). Present and future options for the improvement of Miscanthus propagation techniques. *Renewable Sustain. Energy Rev.* 49, 1233–1246 doi: 10.1016/j.rser.2015.04.168

Xue, S., Lewandowski, I., Wang, X., and Yi, Z. (2016). Assessment of the production potentials of Miscanthus on marginal land in China. *Renewable Sustain. Energy Rev.* 54, 932–943. doi: 10.1016/j.rser.2015.10.040

Advantages of publishing in Frontiers

OPEN ACCESS
Articles are free to read for greatest visibility and readership

FAST PUBLICATION
Around 90 days from submission to decision

HIGH QUALITY PEER-REVIEW
Rigorous, collaborative, and constructive peer-review

TRANSPARENT PEER-REVIEW
Editors and reviewers acknowledged by name on published articles

Frontiers
Avenue du Tribunal-Fédéral 34
1005 Lausanne | Switzerland

Visit us: www.frontiersin.org
Contact us: info@frontiersin.org | +41 21 510 17 00

REPRODUCIBILITY OF RESEARCH
Support open data and methods to enhance research reproducibility

DIGITAL PUBLISHING
Articles designed for optimal readership across devices

FOLLOW US
@frontiersin

IMPACT METRICS
Advanced article metrics track visibility across digital media

EXTENSIVE PROMOTION
Marketing and promotion of impactful research

LOOP RESEARCH NETWORK
Our network increases your article's readership